

UNCLASSIFIED

AD NUMBER

AD856559

LIMITATION CHANGES

TO:

Approved for public release; distribution is unlimited.

FROM:

Distribution authorized to U.S. Gov't. agencies and their contractors;
Administrative/Operational Use; MAY 1969. Other requests shall be referred to Rome Air Development Center, Griffiss AFB, NY.

AUTHORITY

RADC ltr 17 Sep 1971

THIS PAGE IS UNCLASSIFIED

AD856559

RADC-TR-68-340, Vol II
Final Technical Report
May 1969

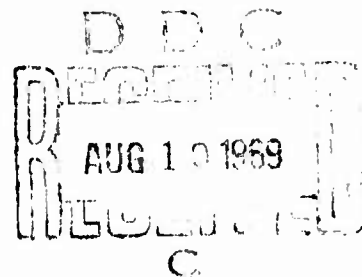


INVESTIGATION OF SCATTERING PRINCIPLES
Volume II - Scattering Matrix Measurements

Dr. George W. Gruver
General Dynamics
Fort Worth Division

This document is subject to special export controls and each transmittal to foreign governments, foreign nationals or representatives thereto may be made only with prior approval of RADC (EMASS), GAFB, NY 13440.

Rome Air Development Center
Air Force Systems Command
Griffiss Air Force Base, New York



ACCESSION FOR	
CFSTI	WHITE SECTION <input type="checkbox"/>
DOC	BUFF SECTION <input checked="" type="checkbox"/>
UNANNOUNCED	<input type="checkbox"/>
JUSTIFICATION	
BY	
DISTRIBUTION	AVAILABILITY CODES
DIST.	AVAIL. FULLY SPECIFIC
2	

When US Government drawings, specifications, or other data are used for any purpose other than a definitely related government procurement operation, the government thereby incurs no responsibility nor any obligation whatsoever; and the fact that the government may have formulated, furnished, or in any way supplied the said drawings, specifications, or other data is not to be regarded, by implication or otherwise, as in any manner licensing the holder or any other person or corporation, or conveying any rights or permission to manufacture, use, or sell any patented invention that may in any way be related thereto.

Do not return this copy. Retain or destroy.

INVESTIGATION OF SCATTERING PRINCIPLES
Volume II - Scattering Matrix Measurements

Dr. George W. Gruver
General Dynamics
Fort Worth Division

This document is subject to special export controls and each transmittal to foreign governments, foreign nationals or representatives thereto may be made only with prior approval of RADC (EMASS), GAFB, NY 13440.

FOREWORD

This report is a documentation of a measurements program designed to provide a comprehensive spectrum of scattering matrix measurements on a variety of vehicle model configurations. These measurements were subsequently used as an aid to obtaining a better understanding of the principles of radar scattering. This report is the second of four volumes which comprise the Technical Report in which the overall investigation is documented.

This work was sponsored by the Space Surveillance and Instrumentation Branch of Rome Air Development Center. The investigation was conducted by the Fort Worth Division of General Dynamics, Fort Worth, TX 76101, under contract F30602-67-C-0074. This work was conducted under the auspices of Mr. John Cleary of RADC and the report was prepared by Dr. G. W. Gruver of the Fort Worth Division. This report is General Dynamics Report No. FZE-792. The contents of this report and the abstract are unclassified. The RADC project number is 6512, Task 651207. Distribution is limited by the Mutual Security Acts of 1949.

This report has been reviewed and is approved.

ABSTRACT

This report includes the results of a measurements program conducted at the Radar Range of the Fort Worth Division of General Dynamics as a part of an experimental and analytical investigation into the principles of radar scattering. The primary purpose of this program was to provide a broad spectrum of scattering matrix measurements for use in conjunction with a number of experimental and analytical tasks.

A description of the radar range is included along with a description of the measurement procedures, vehicle models, and system measurement parameters. Scattering matrix data obtained using 70 different model configurations which were constructed from a basic set of 20 generic surfaces are presented. These included three cones, six cylinders, four frustrums, and three hemispheres. Monostatic and bistatic data obtained at S- and C-band frequencies using a coherent radar system are presented.

A computerized technique is described, the use of which allows the absolute phase center of a target to be located. This technique was applied to the data to produce analog plots of cross section and phase.

TABLE OF CONTENTS

<u>Section</u>	<u>Title</u>	<u>Page</u>
1	Introduction	1
2	System Description and Measurement Procedures	5
2.1	General	5
2.2	Ground Plane Radar Scattering Range	5
2.2.1	Electronics System	7
2.3	Scattering Matrix Measurement Procedures	9
2.3.1	Radar Range Setup Procedures	9
2.3.2	Amplitude Calibration	16
2.3.3	Absolute Phase Calibration	17
2.3.4	Bistatic Measurement Procedures	23
2.4	Editing and Magnetic Tape Format of Scattering Matrix Data	25
3	Scattering Matrix Measurements	30
3.1	General	30
3.2	Measurements Data	32
3.2.1	Generic Vehicles	35

<u>Section</u>	<u>Title</u>	<u>Page</u>
	3.2.2 Composite Generic Vehicles	150
	3.2.3 Smooth Aerospace Vehicles	257
	3.2.4 Complex Aerospace Vehicles	287
	3.2.5 Scientific Satellite Vehicles	321
4	Summary	344
	References	346

LIST OF FIGURES

<u>Number</u>	<u>Title</u>	<u>Page</u>
2-1	Radar Range at the Fort Worth Division of General Dynamics	6
2-2	Ground Plane Radar Range	7
2-3	Block Diagram of Electronics System	10
2-4	Interior of Electronic Equipment Van	11
2-5	Vertical Probe - VV Polarization	13
2-6	Background Cross Section - VV Polarization	15
2-7	Absolute Phase Location Geometry for Cylinder	19
2-8	Phase Reference Points for Composite Targets	22
2-9	Bistatic Radar Range Configuration	24
2-10	Flow Diagram for Processing Radar Signature Data	26
3-1	Construction of Composite Vehicles	31
3-2	Typical Generic Vehicles	37
3-3	Typical Composite Generic Vehicles	152
3-4	Scientific Satellite Models	323

LIST OF TABLES

<u>Number</u>	<u>Title</u>	<u>Page</u>
2-1	Magnetic Tape Format of Long Pulse Data	29
3-1	Radar Range Analog Plots	33
3-2	Generic Vehicle Measurements	36
3-3	Composite Generic Vehicle Measurements	151
3-4	Smooth Aerospace Vehicle Measurements	258
3-5	Complex Aerospace Vehicle Measurements	288
3-6	Scientific Satellite Measurements	322

SECTION I

INTRODUCTION

This document is Volume II of a set of four volumes (References 1, 2, 3) which comprise the Technical Documentary Report on the Investigation of Scattering Principles, Contract F30(602)-67-C-0074. This investigation was performed during 1967 and 1968 by the Fort Worth Division of General Dynamics under contract to Rome Air Development Center. The overall investigation is divided into the following elements:

1. An experimental investigation of the scattering matrices of a broad spectrum of target configurations and frequencies.
2. An analytical investigation of the use of the geometrical theory of diffraction (GDT) to compute the monochromatic scattering matrix of selected targets.
3. An investigation of the applicability (and limitations) of using linear superposition of target signature data to construct radar signatures of composite targets.
4. An investigation of the possibility of synthesizing the signatures of complex targets by use of targets

exhibiting various degrees of physical similitude to the target of interest.

5. An investigation of the use of long and short pulse radar signatures in inverse scattering analyses as a means of estimating target physical characteristics.

Comprehensive coverage of the spectrum of scattering mechanisms and geometries was needed to fulfill the requirements for the various investigations conducted under this contract. Consequently, the scope of the measurement program was quite large, and a wide range of different surface and body configurations had to be constructed and measured. In fact, the scope of these measurements was so extensive that the resulting data may represent a significant contribution in the field of radar signature measurements. For this reason, the results of the measurement program are published in this separate volume along with a brief but comprehensive description of the measurement system and measurement techniques utilized to obtain them.

Measurement data are presented herein in the form of analog plots of cross section and phase obtained by varying the parameters of the measurement system, including frequency, polarization, and bistatic angle. Monostatic

measurements were obtained at C-band on each vehicle measured. Bistatic measurements were made at C-band on a selected set of vehicles and S-band measurements were also made on a few vehicles. Subsections 2.1 and 2.2 respectively contain a description of the measurement system and the specific techniques which were used to ensure the quality of each measurement.

Radar signature measurements were initially recorded on punch paper tape at the same time that the analog plots of the data were obtained. However, in order to remove erroneous digital data points and provide absolute amplitude and phase calibration, these tapes were then processed by use of a computer program on an IBM 360 digital computer to produce a magnetic tape recording containing measurement data at exactly 3600 aspect orientations at 0.1-degree intervals. This processing was undertaken (1) to edit the digital data, (2) to calibrate cross section in decibels above a square meter (dBsm), (3) to calibrate phase to correspond the actual position of the target phase center on the target, and (4) to provide scattering matrix data on library tapes for use as library data with other computer processing techniques. The measurement data in Section 2 are presented in the form of analog plots of the digital data contained on the magnetic tapes. These plots were

obtained by use of a Stromberg-Carlson SC 4020 plotter in
conjunction with the IBM 360.

SECTION II

SYSTEM DESCRIPTION AND MEASUREMENT PROCEDURES

2.1 General

The radar cross section and phase measurements presented in this report were obtained through use of the Radar Range at the Fort Worth facilities of General Dynamics. Figure 2-1 is a photograph of this range showing the electronics equipment van, mobile antennas, target rotator with a mounted target, and a secondary calibration standard. A detailed description is contained in Reference 4.

2.2 Ground Plane Radar Scattering Range

The measurements acquired during this program were obtained by use of a ground plane radar scattering facility. The ground plane technique is based upon the utilization of both the direct and the indirect or ground reflected waves to illuminate the target being measured; the concept is illustrated in Figure 2-2. Reference 4 contains a detailed explanation of the salient features of the ground plane concept, including the advantages and disadvantages of the technique.



Fig. 2-1 RADAR RANGE AT THE FORT WORTH DIVISION OF GENERAL DYNAMICS

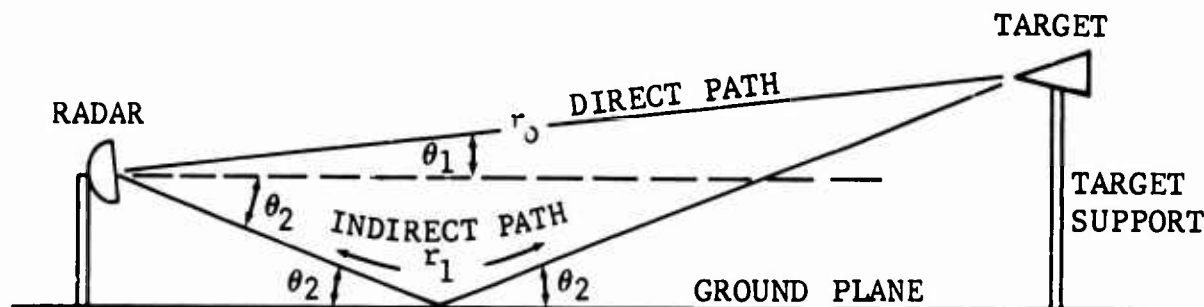


Fig. 2-2 GROUND PLANE RADAR RANGE

2.2.1 Electronics System

The radar used to obtain long pulse measurements consists of a coherent pulsed radar which incorporates a range gate to provide isolation of the target environment. A dual antenna system is used in order to allow bistatic operation. The bistatic angle is denoted by β . Both amplitude and absolute phase measurements are obtained with the same system.

The radar transmitter consists of a coherent oscillator which drives a pair of traveling wave tubes in series to provide approximately one kilowatt of output power. The receiving system is a typical superheterodyne receiver which incorporates a variable range gate that is manually controlled to gate a 60-megahertz IF amplifier on during

the time interval of the range gate. This variable range gate is controlled by the operator so that the location in space of the origin of the scattered signal can be varied between the target rotator and the secondary standard in order to calibrate the system.

Within the receiver system, a fixed range gate is utilized to turn on the receiver at a range at which no target is present in order to inject a reference signal from the transmitter. This reference signal is a 60-megahertz pulse which is injected from a pulsed coherent oscillator through a linear attenuator and a variable phase shifter. The difference between the target signal and the injected reference signal is applied to an amplitude servo and a phase servo which, if differences exist, are used to drive the calibrated attenuator and the variable phase shifter to force the two signals to correspond in both amplitude and phase. The resulting changes in the attenuator and the phase shifter are used to drive a pair of analog recorders and are also encoded to provide a digital output which is recorded on punch paper tape. During the calibration process, the outputs of the attenuator and the phase shifter are calibrated by use of a target of known cross section and location to provide radar cross section in terms of decibels above a square meter (dBsm) and absolute phase in degrees.

Figure 2-3 contains a block diagram of the electronics system. The interior of the electronic equipment van is shown in Figure 2-4.

The recording system records cross section to the nearest 0.1 dB, phase to the nearest degree (modulo 360 degrees), and aspect angle to the nearest 0.1 degree. The dynamic range of the cross section measurement system is 50 dB.

2.3 Scattering Matrix Measurement Procedures

In addition to the actual measurement run, the vehicle measurement process included initially positioning the radar beam, pre- and post-calibrating the equipment, and checking the measured analog plots for any obvious errors. These calibration and measurement techniques will be briefly described in the following paragraphs; a more detailed explanation is presented in Reference 4.

2.3.1 Radar Range Setup Procedures

The initial adjustment of the measurement system is made by varying the antenna heights of the transmitter and receiver in order to position the radar beam so that the target is located in the first lobe of the radar interference pattern. The approximate antenna height, H_A , is

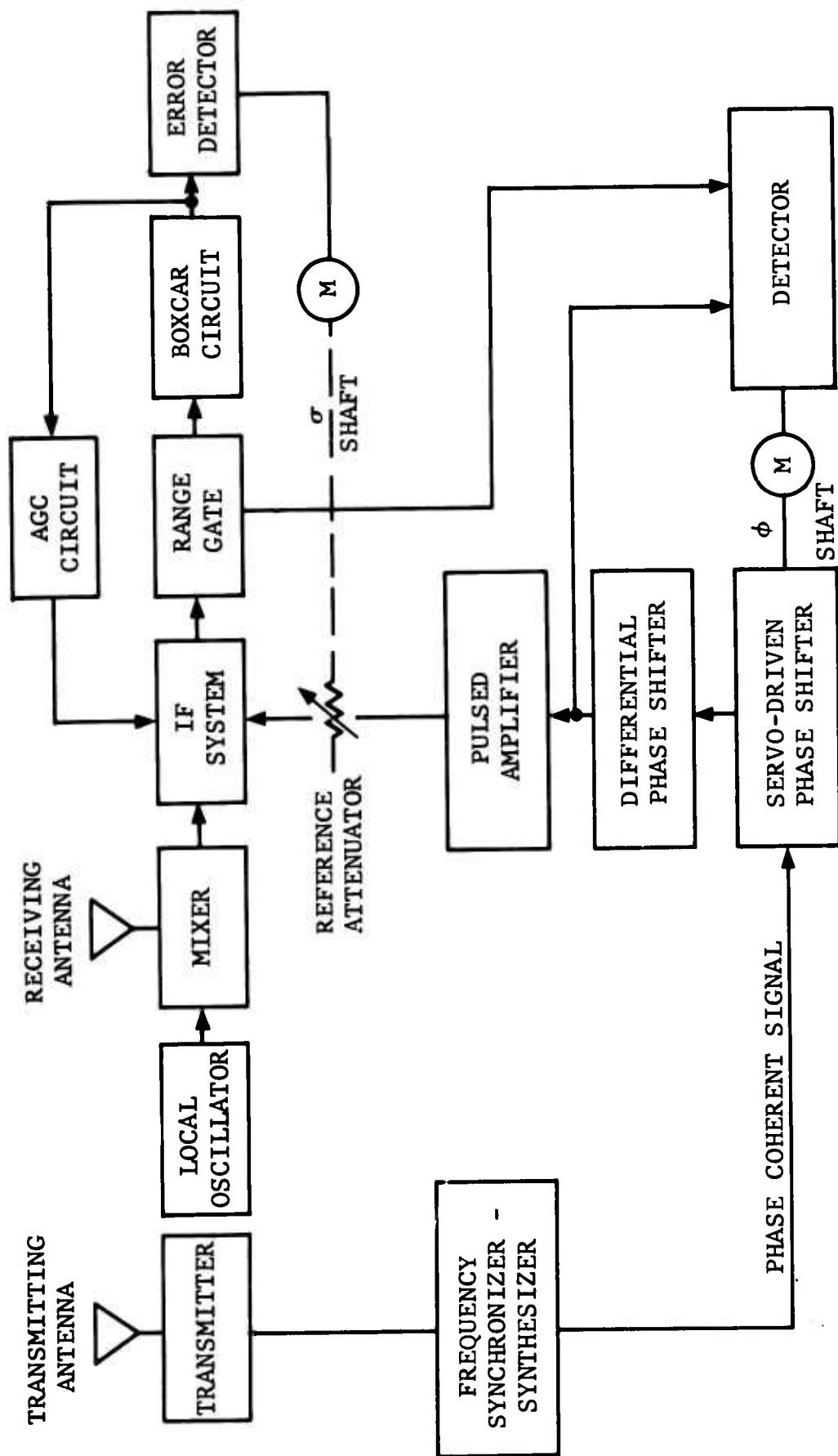


Fig. 2-3 BLOCK DIAGRAM OF ELECTRONIC SYSTEM



Fig. 2-4 INTERIOR OF ELECTRONIC EQUIPMENT VAN

determined from the wave length, λ , the target height, H_T , and the range, r , by use of the following relationship:

$$H_A = \frac{\lambda r}{4H_T} \quad (1)$$

The final height adjustment is made by maximizing the return from a calibrated target, such as a sphere of known cross section.

In the subject effort, the uniformity of the field in the target area was determined by raising a calibration probe (in this case a corner reflector) through the region to be occupied by the target and recording the signal return as a function of the height of the probe. A graph displaying the results of a primary vertical probe test is shown in Figure 2-5. A gradient of 0.5 dB per foot across the target volume was considered acceptable.

The target rotator was adjusted so that the target would rotate in the plane of the radar beam, which generally is not parallel to the ground as a result of the ground plane effect. This procedure was completed by adjusting the rotator tilt angle so that the radar cross section of each side of a flat plate was identical.

In order to determine the cross section and phase of the target accurately, the return from the rotator and other background signals must be minimized. The reduction

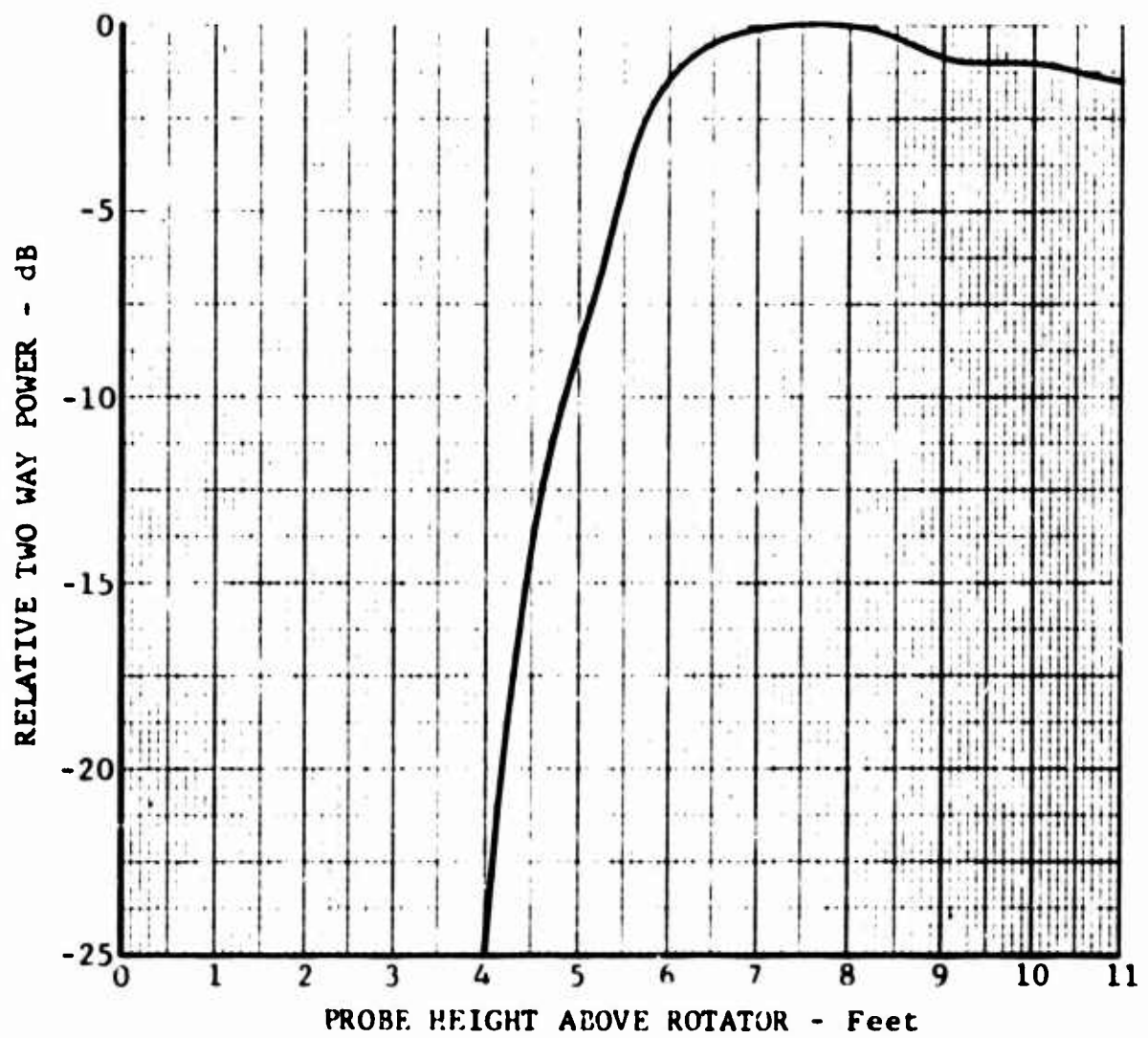


FIG. 2-5 VERTICAL PROBE - VV POLARIZATION

in the cross section of the support column was accomplished by physically changing the column size and by small adjustments in frequency. The combined effects of these two actions were used to tune the column so that the reflections from the front and back of the column tended to cancel. In some cases, it was necessary to tilt the column away from the perpendicular in order to obtain a low background level over a large angular region. Use of this tilting process essentially positioned the column so that the radar illuminated a null in the column's backscatter pattern over a large region of aspect angles; however, this result could not be achieved at all aspect angles. In such cases, the high value of background was positioned so that it coincided with a high value of target cross section in order to introduce an error as insignificant as possible.

The background levels achieved during the measurements presented in this report averaged less than -40 dBsm, well below the value of cross section of a typical target. Figure 2-6 contains an example of typical background data obtained from the support with the target removed.

In order to accurately measure the target scattering matrix, the antenna system must be capable of rejecting energy produced by undesirable polarizations. Such capability is usually expressed in terms of the dB rejection

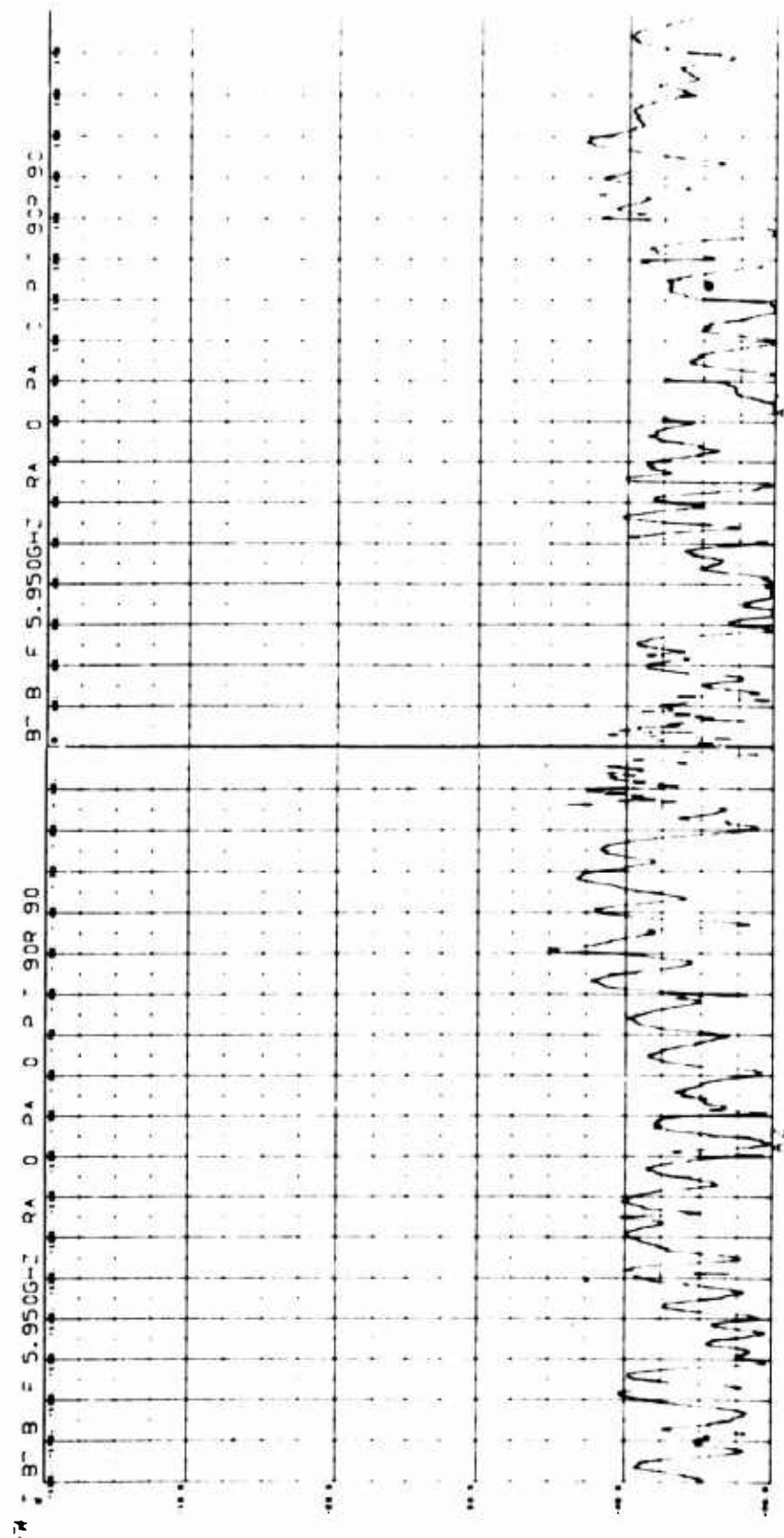


Fig. 2-6 BACKGROUND CROSS SECTION - VV POLARIZATION

obtained when an antenna is required to receive a signal whose polarization is orthogonal to that of the antenna. The total field received by a vertically polarized antenna can be expressed as the phasor sum of a vertically polarized signal, \bar{E}_V , and a horizontally polarized signal, \bar{E}_H , as expressed in Equation 2.

$$\bar{E} = \bar{E}_V + \beta_{VH}\bar{E}_H \quad (2)$$

β_{VH} represents the rejection of the antenna to horizontally polarized signals. The rejection achieved with the radar used to obtain the subject measurements was measured by use of a spherical target to be approximately 29.0 dB.

2.3.2 Amplitude Calibration

Amplitude calibration of the measured cross section data was accomplished by use of a precision sphere for a primary standard and a corner reflector which was located outside of the target range gate for a secondary standard. The radar system was initially calibrated by placing a sphere of known cross section on the target rotator and measuring its cross section. The range gate was moved to the vicinity of the corner reflector, the signal from the corner was measured, and its cross section was then calibrated in terms of the cross section of the sphere. The corner reflector was subsequently measured before and after the

measurement of each target so that system changes would be detected and corrected before the target was removed from the rotator.

2.3.3 Absolute Phase Calibration

A unique technique was used to determine the precise position in space of the instantaneous target phase center. Phase calibration was achieved by placing a cylinder with its axis vertical directly over the center of rotation of the target support column. When the rotator was turned, the analog phase recording produced a periodic plot of phase similar to a sine function of aspect angle. The amplitude of this function is related to the deviation of the center of the cylinder from the true axis of rotation of the rotator. Although knowledge of this function allows the deviation to be post-calibrated for any deviation, the reference point on the top of the rotator was generally moved so that the measured phase deviation between the reference point and the actual center of rotation was less than 360 degrees; this deviation corresponds to a maximum off-center distance of 1.0 inch. The actual equation which should be used to correctly locate the center of rotation along the radar line of sight (RLOS) is given by

$$R_e = \frac{1}{4k} \psi_e$$

where

k = wave number

ψ_e = maximum measured phase deviation in degrees

R_e = distance the cylinder axis should be moved to be
colinear with the center of rotation.

The value of 4 is necessary to account for the two-way radar path, as well as the fact that the radius R_e is half of the measured geometrical difference. The aspect angle, where ψ_e is maximum, is easily determined from the analog phase plot.

This same technique can be applied directly to a target if it possesses vertical planes of symmetry. For example, the actual center of rotation of a cylinder with its axis horizontal can be located by determining the measured phase deviation between the opposite ends of the cylinders and that between the opposite sides of the cylinder. An illustration of how a cylinder might be erroneously placed on the rotator is shown in Figure 2-7.

The objective set for these measurements was to accurately determine the position of the center of rotation of each target. Consequently, the absolute position of the target phase center was determined so that its behavior could be traced as a function of target rotation.

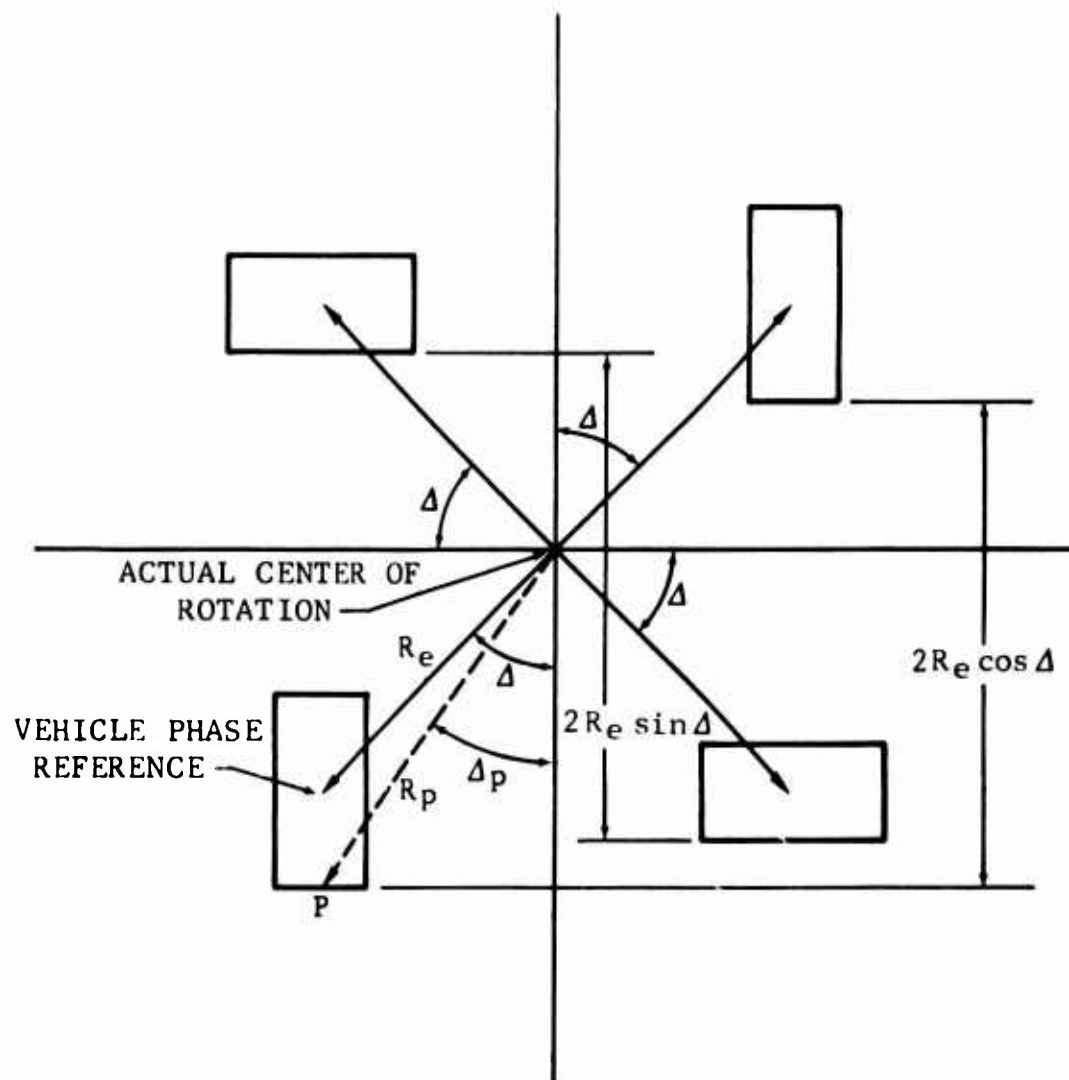


Fig. 2-7 ABSOLUTE PHASE LOCATION GEOMETRY FOR CYLINDER

The position of the center of the cylinder illustrated in Figure 2-7 can be determined from the plot of measured phase obtained when the rotator is rotated through 360 degrees in azimuth. The difference in measured phase obtained when the target presents its two end-on aspects to the radar is given by ψ_{eo} , where

$$\begin{aligned}\Delta\psi_{eo} &= 2k (2 R_e \cos \Delta) \\ &= 4K R_e \cos \Delta\end{aligned}\quad (3)$$

Similarly, the difference in measured phase obtained when the target presents its two broadside views to the RLOS (broadside is here used to indicate that the cylinder axis is perpendicular to the RLOS) is given by

$$\begin{aligned}\Delta\psi_{bs} &= 2K (2 R_e \sin \Delta) \\ &= 4K R_e \sin \Delta\end{aligned}\quad (4)$$

Equations 3 and 4 may be solved simultaneously to give the radius arm, R_e , and its position angle, Δ , which is measured relative to an end-on view. The solution of these equations gives

$$\begin{aligned}R_e &= \frac{1}{4k} (\Delta\psi_{eo})^2 + (\Delta\psi_{bs})^2 \\ \Delta &= \tan^{-1} \left[\frac{\Delta\psi_{bs}}{\Delta\psi_{eo}} \right]\end{aligned}$$

The location of points on the target other than its geometrical center may be referenced in a similar manner by

simple vector manipulations. Point P on the cylinder could be used as a reference, for example, by noting that

$$R_P = R_e^2 \sin^2 \Delta + (R_e \cos \Delta + L/2)^2$$

$$\text{and } \Delta_P = \tan^{-1} \left[\frac{R_e \sin \Delta}{R_e \cos \Delta + L/2} \right]$$

where L is the length of the cylinder.

This technique was used to locate the position of the center of rotation on the top of the target support column. Reference marks were then used to locate each target model with respect to the center of rotation. Figure 2-8 is an illustration of the method in which different target types were referenced to the center of rotation.

As mentioned in paragraph 1.2.2, the secondary standard was measured before and after each target run to detect and correct any significant changes in system operation. To insure that no measurements were omitted, each target was rotated continuously through at least 380 degrees of aspect, and the signatures were recorded through this range.

As an additional system check the raw analog data was checked for phase closure within a limit of ± 8 degrees. For use in determining accurate phase calibration, the position of the phase center of both the VV and HH terms was checked at a specular point on each target. An equation of $\psi_{VV} = \psi_{HH} \pm 8$ degrees was necessary for acceptance.

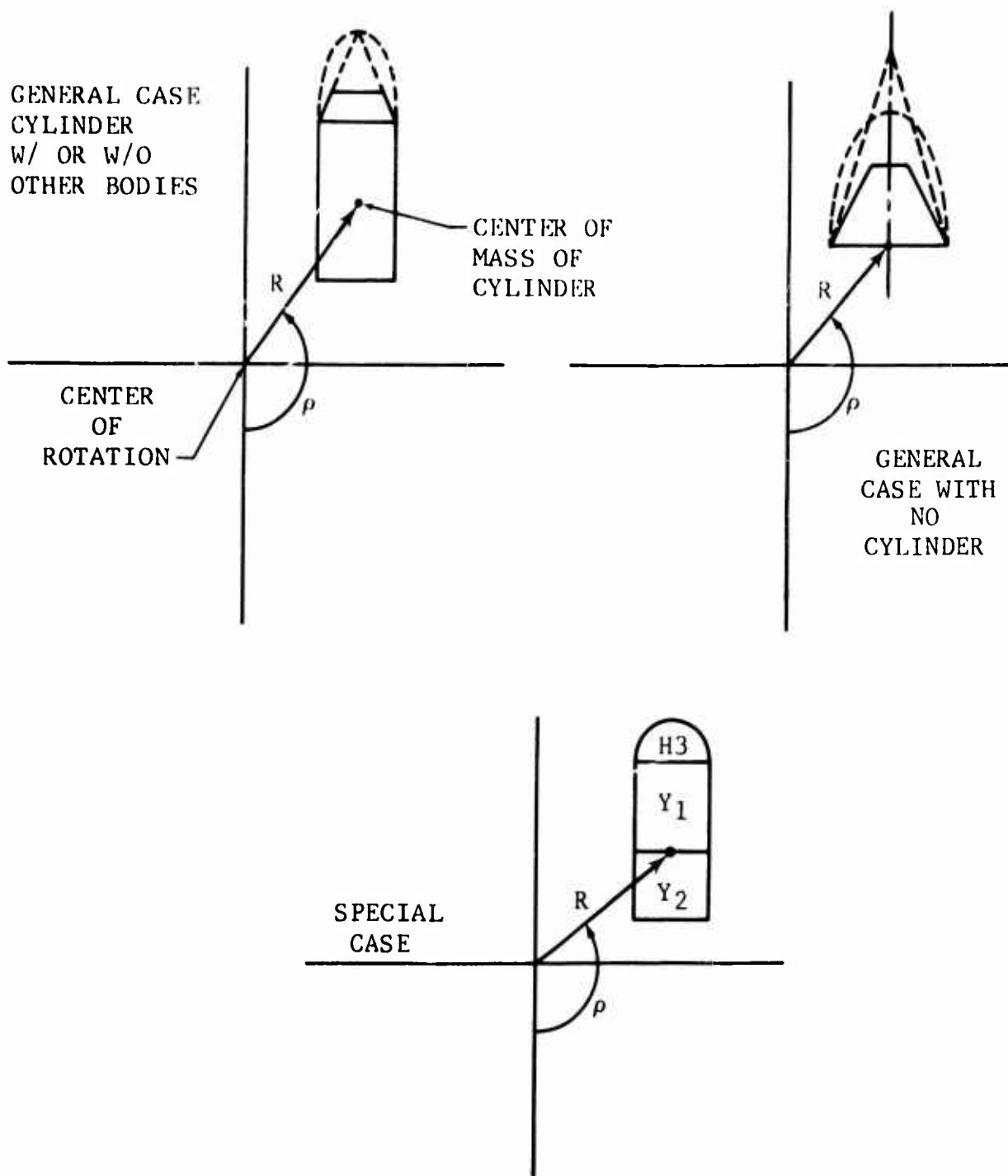


Fig. 2-8 PHASE REFERENCE POINTS FOR COMPOSITE TARGETS

Other measures taken to guarantee the validity of the data included noting the limiting values on the digital display of the digital encoding equipment before and after each measurement run. Also the generic-shape cross section measurements obtained from the range were compared with the computed values determined by use of the physical optics approximation. This comparison of computed and measured values verified the system accuracy as the values checked within ± 1 dB.

2.3.4 Bistatic Measurement Procedures

The basic range configuration used to obtain bistatic measurements is illustrated in Figure 2-9. The zero aspect angle reference coincided with the bisector of the bistatic angle.

The calibration procedures used in the bistatic measurements were identical to those used in the monostatic measurements. This approach was made possible by noting that the bistatic radar cross section of the calibration sphere was essentially the same at the bistatic angle of interest, namely 0, 10, and 30 degrees. Computed bistatic sphere data was available at the Fort Worth Division for a range of ka from 0.01 to 20 and for bistatic angles between 0 and 180 degrees.

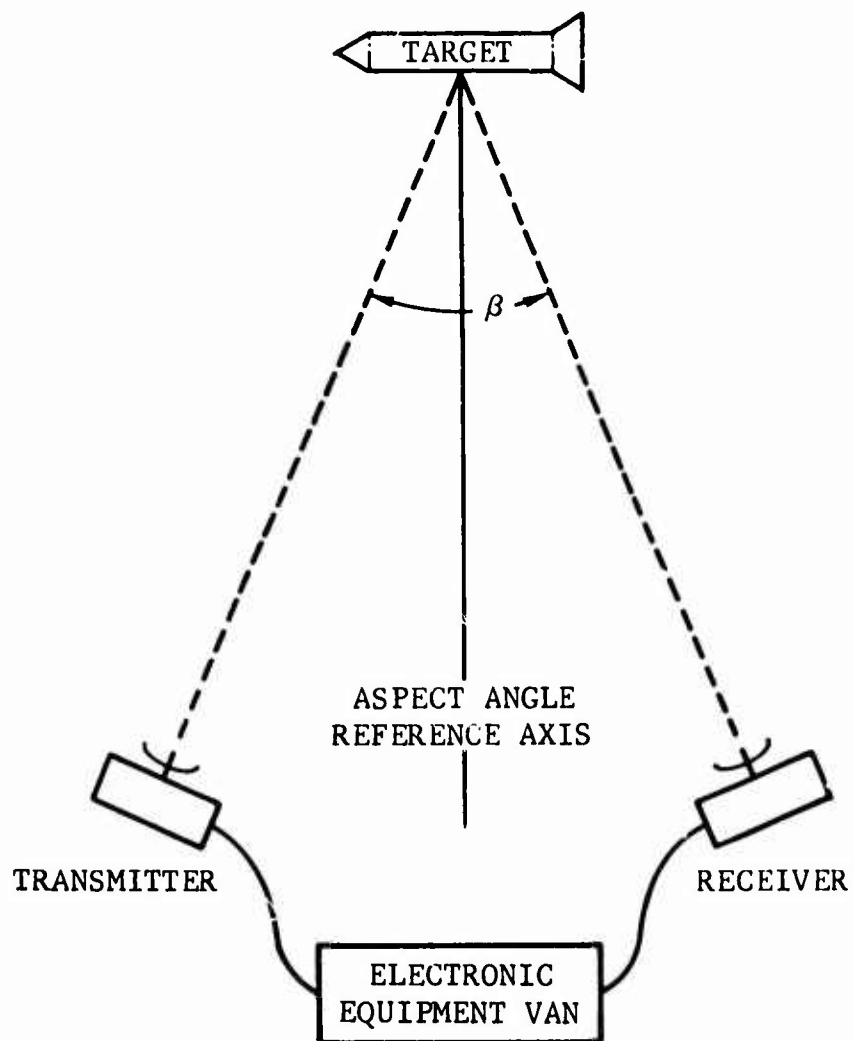


Fig. 2-9 BISTATIC RADAR RANGE CONFIGURATION

2.4 Editing and Magnetic Tape Format of Scattering Matrix Data

Scattering measurement data was prepared for use as library data by editing, calibrating, and formatting the data and then recording the processed data on magnetic library tapes. Figure 2-10 contains a flow diagram showing the evolution of scattering data from the radar range to the completed library tape.

In its final form, the long pulse cross section, phase, and aspect angle data obtained on each measurement run reflect the following processing:

1. Data on magnetic tape was recorded for exactly 3600 discrete aspect angles beginning with $\theta = -180.0$ degrees, increasing to $\theta = 0.0$ degree, and then increasing to $\theta = 179.9$ degrees in increments of 0.1 degree. Aspect angle data was multiplied times 10 and recorded on tape in an integer mode for $\theta = -180.0$ through 0 degree to $\theta = 179.9$ degrees.
2. Aspect angle data was calibrated from knowledge of the orientation of specular returns. This calibration assured, for example, that the specular returns from the end-on aspects of a cylinder would occur at $\theta = 0.0$ degree and $\theta = 180.0$ degrees.

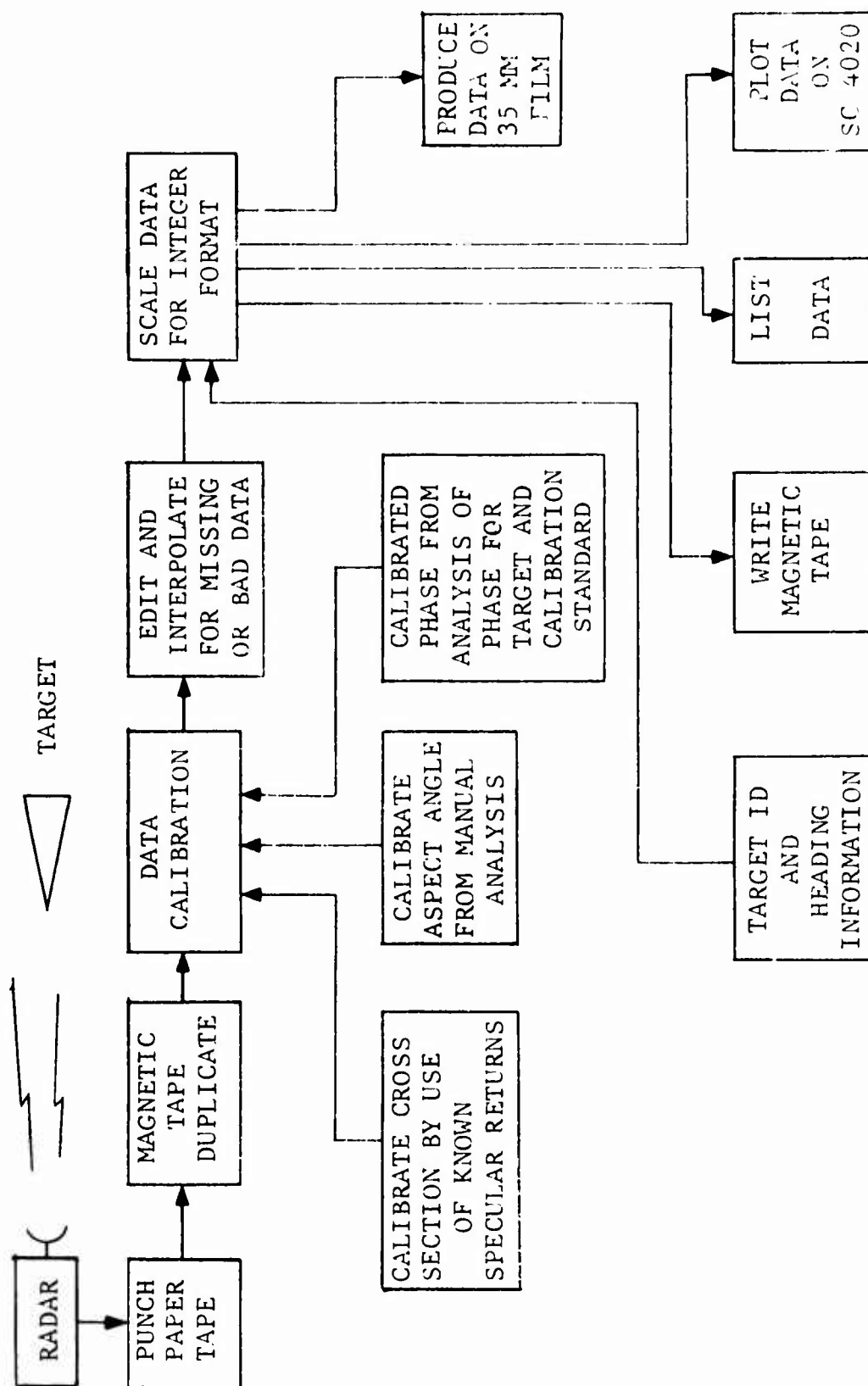


Fig. 2-10 FLOW DIAGRAM FOR PROCESSING
RADAR SIGNATURE DATA

3. In some instances, cross section data was post-calibrated (1) in accordance with post-calibration radar range data or (2) by use of computed cross section values obtained from the physical optics expressions of cross section at specular points for cones, frustra and cylinders.
4. If a phase bias error was detected, a fixed bias value was added to the measured phase as a correction.

The target model data indicates the value of the residual radius arm, R , and the position angle, ρ , which remains in the final library data after it is formatted on magnetic tape. The position vector determined by R and ρ indicates the position of the target phase reference with respect to the actual axis of rotation of the turntable.

Scattering measurement data were recorded on magnetic tape as BCD information in the following manner. Each file on a tape consists of 903 records or card images and an end-of-file mark. Each record consists of 14 words and represents one 80-column card. The first two records contain alphanumeric information identifying the target and the parameters of the radar range used for that sequence of measurements. These two records are followed by 900 records which contain measured data. Each of these records contains

a set of four values of aspect angle, cross section, and phase. The last record of each file consists of an end-of-file mark. The format of a typical data file is illustrated in Table 2-1 in detail.

Table 2-1
MAGNETIC TAPE FORMAT FOR LONG PULSE DATA

Card #1	Alphanumeric Heading Information
Card #2	Alphanumeric Heading Information
Card #3	-1800, $\sigma(-1800)$, $\emptyset(-1800)$; -1799, $\sigma(-1799)$, $\emptyset(-1799)$; -1798, $\sigma(-1798)$, $\emptyset(-1798)$; -1797, $\sigma(-1797)$, $\emptyset(-1797)$
Card #453	-0, $\sigma(-0)$, $\emptyset(-0)$; 1, $\sigma(1)$, $\emptyset(1)$; 2, $\sigma(2)$, $\emptyset(2)$; 3, $\sigma(3)$, $\emptyset(3)$
Card #902	1796, $\sigma(1796)$, $\emptyset(1796)$; 1797, $\sigma(1797)$, $\emptyset(1797)$; 1798, $\sigma(1798)$, $\emptyset(1798)$; 1799, $\sigma(1799)$, $\emptyset(1799)$
Card #903	End of File

SECTION III

SCATTERING MATRIX MEASUREMENTS

3.1 General

This section contains all of the analog plots of cross section and phase of the different vehicles measured during this program. Data are presented according to the degree of physical complexity of the target shapes, i.e., simple generic, composite generic, smooth aerospace, complex aerospace, and scientific satellites. Pictures of most of the models are displayed and a brief description of their composition and construction is presented.

All of the models measured in this project were fabricated from solid aluminum. The physical dimensions of the models are presented in subsection 3.2, preceding relevant analog plots. The generic targets were constructed so that they could be interconnected in order to produce composite bodies and to simulate aerospace vehicles. The method of connecting the generic shapes to form composite models is indicated in Figure 3-1 for the case of the cone-cylinder. The tolerance on the model dimensions was 0.002 inch, which corresponds to less than one electrical degree in terms of a two-way path. This is a significantly greater

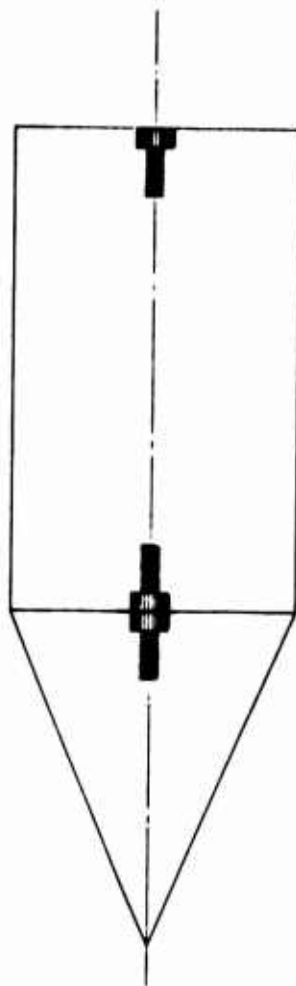


Fig. 3-1 CONSTRUCTION OF COMPOSITE VFICLES

constraint than that placed on the measurement accuracy of the phase measurement system.

3.2 Measurements Data

The following pages contain the analog plots of the cross section and phase measurements. With a few exceptions, these plots are reproductions of the output of plots obtained by use of the SC 4020 plotter.

These data have been edited and corrected so that the cross section measurements are made with the axis of each target aligned with the radar line of sight when the zero-degree aspect is recorded. The analog plots for the measurements are presented in this section.

Unedited analog measurements are presented in Table 3-1, along with those printed by the SC 4020 in the cases of a very few targets. Subsequent to the original measurements, the data for the measurement runs listed in Table 3-1 were rendered unacceptable for automatic plotting. A table of target dimensions and measurements and an illustration of some typical targets are presented for each target classification. All targets were measured by using VV and HH polarizations, and both cross section and phase were recorded. In addition, the measurements of the asymmetrical targets included the cross section and phase obtained by use of VH polarizations.

Table 3-1
RADAR RANGE ANALOG PLOTS

Vehicle	Designation	Measurement Frequency (GHz)	Polarization	Bistatic Angle
Cylinder 1	CY1	6.0	HH	0°
Frustrum 5	F5	6.05	VV	30°
Hemisphere 2 Cylinder 4	H2Y4	5.975	VV	0°
Smooth Aerospace Vehicle A2	C1Y3F3Y5F2Y1F1	3.0	HH	0°

Each analog plot printed by the SC 4020 contains a heading across the top of the plot giving the vehicle symbol, frequency (F) in GHz, target roll angle (RA), target pitch angle (PA), transmitter polarization (T), and receiver polarization (R). Roll and pitch angles were zero in the case of all measurements contained in this document. The bistatic angle of each measurement is recorded beneath the plots in the case of non-zero bistatic angles. Tables 3-2 through 3-6 contain the pertinent target dimensions for each surface classification.

3.2.1 Generic Vehicles

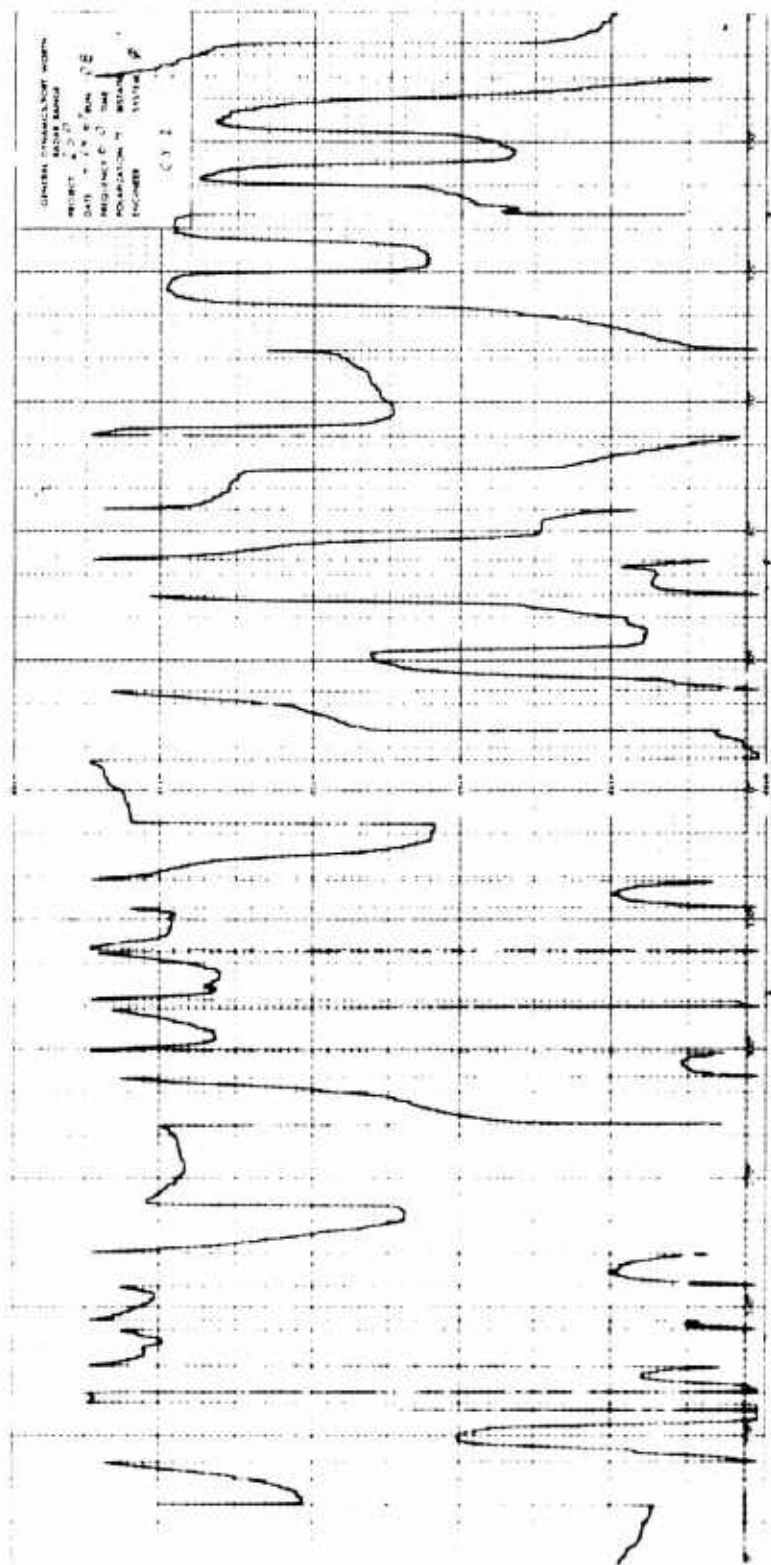
The data contained in this paragraph are described in Table 3-2 in terms of vehicle designation and dimensions, radar system parameters, and the residual error in the location of the vehicle reference with respect to the axis of the rotation. Figure 3-2 contains actual photographs of typical models used to make these measurements.

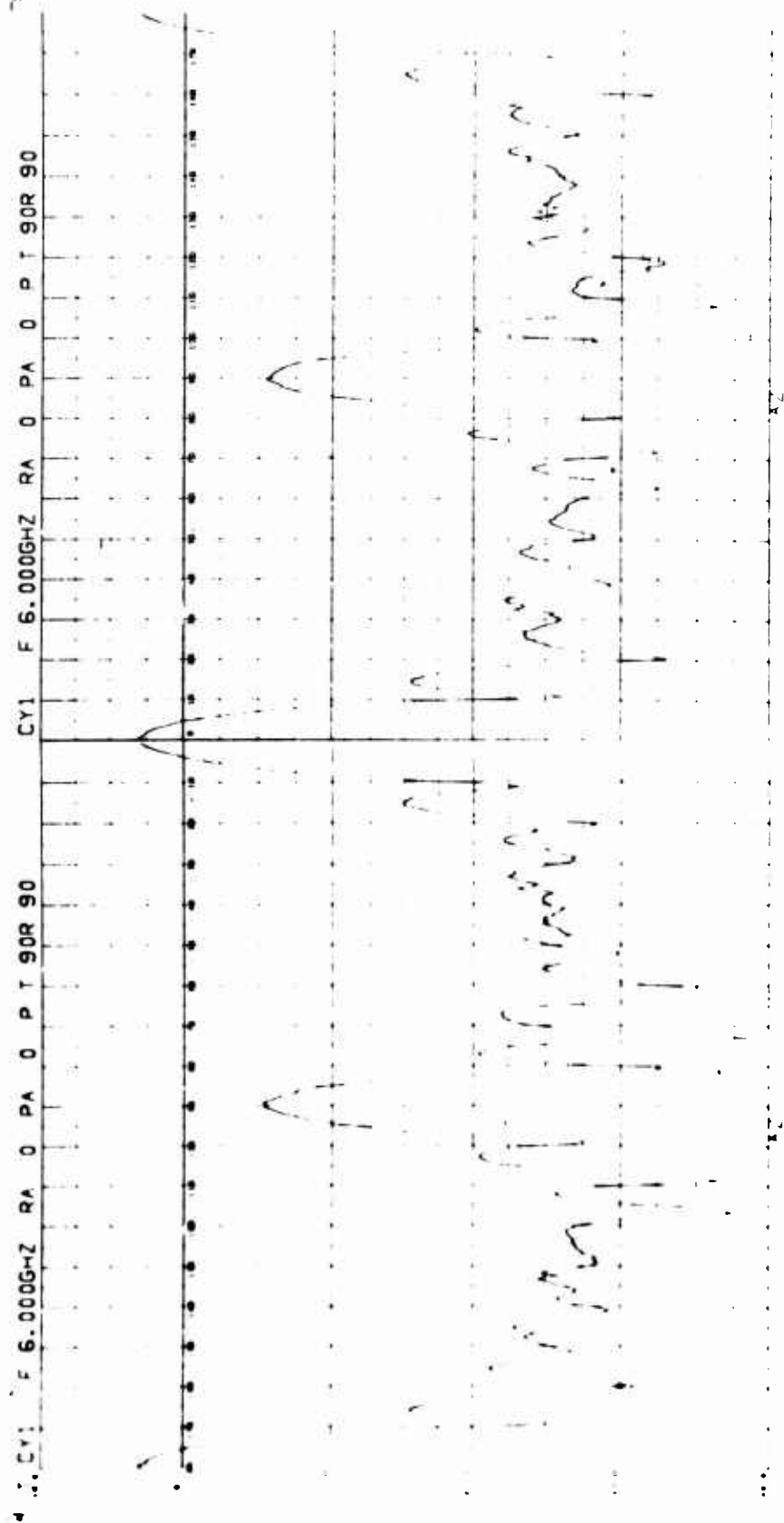
Table 3-2 GENERIC VEHICLE MEASUREMENTS

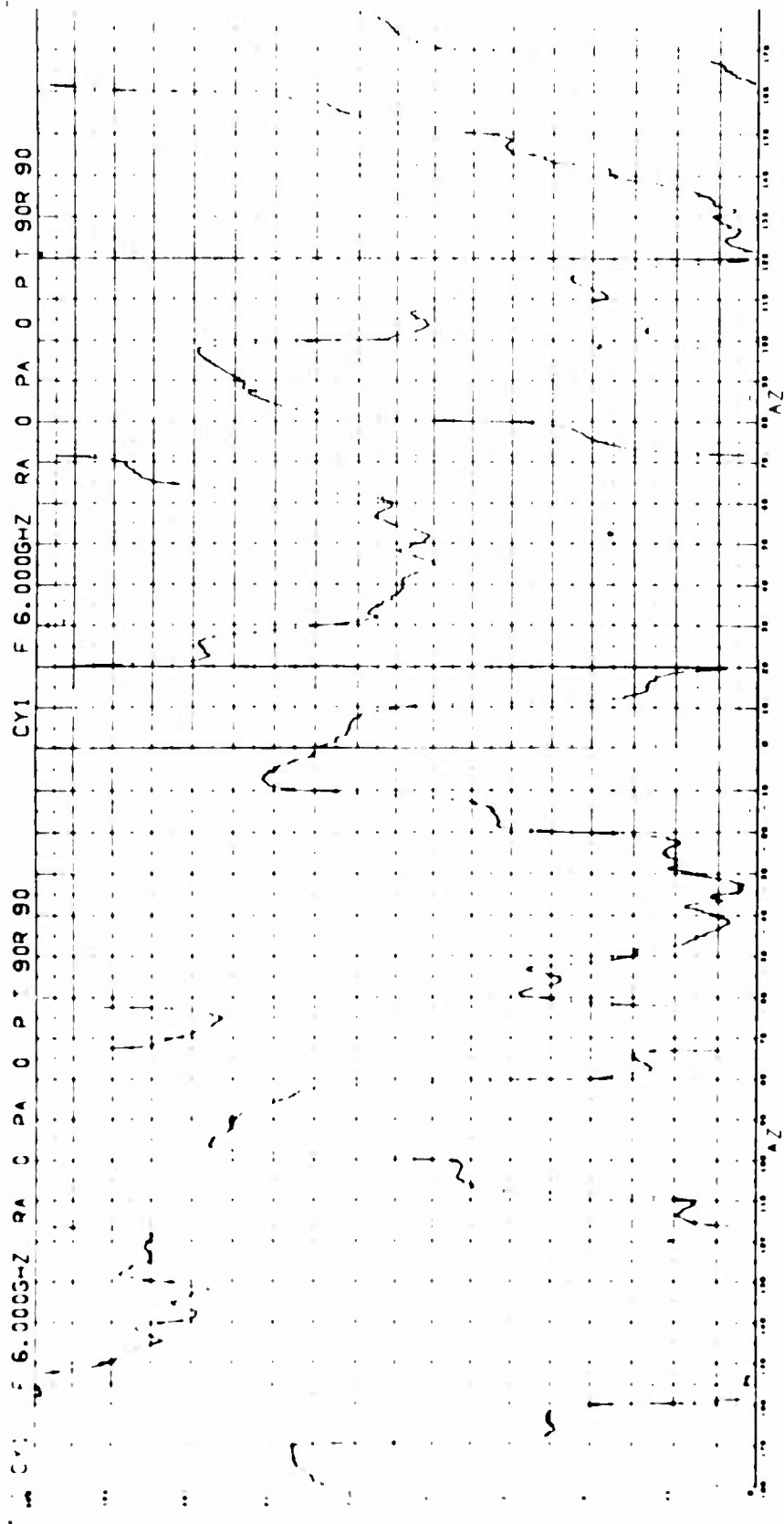
VEHICLE	SYMBOL	MAXIMUM DIAMETER INCHES	MINIMUM DIAMETER INCHES	MAXIMUM LENGTH INCHES	FREQUENCY GHZ	BISTATIC ANGLE DEGREES	ρ DEGREES	R DEGREES
CYLINDER 1	CY1	6.320	-	6.344	6.0	0	223.9	0.688
CYLINDER 2	CY2	6.320	-	8.313	5.975	0	0.0	0.000
CYLINDER 3	CY3	6.320	-	10.513	5.975	0	138.5	0.206
CYLINDER 5	CY5	7.500	-	17.260	6.0	0	234.5	0.678
					5.885	10	97.8	0.226
					6.050	30	245.3	0.020
CYLINDER 6	CY6	15.736	-	44.320	6.0	0	339.4	0.661
					5.885	10	162.5	0.226
					6.050	30	76.9	0.371
CONE 1	C1	6.320	0	11.783	6.0	0	2.414	0.806
CONE 2	C2	6.320	0	15.814	6.0	0	2.4	1.620
CONE 4	C4	7.500	0	13.983	5.975	0	177.4	2.302
FRUSTRUM 1	F1	6.316	2.000	4.030	5.975	0	183.4	0.365
FRUSTRUM 2	F2	7.500	6.320	2.200	6.0	0	0.0	1.150
FRUSTRUM 3	F3	7.500	6.320	3.358	6.0	0	116.5	0.505
FRUSTRUM 4	F4	6.312	4.892	4.063	6.0	0	31.4	0.902
					5.885	10	37.0	0.187
					6.050	30	65.0	0.179
FRUSTRUM 5	F5	7.500	4.892	7.421	6.0	0	4.5	4.313
					5.885	10	163.9	0.487
					6.050	30	216.4	0.049
HEMISPHERE 2	H2	4.892	-	2.446	5.975	0	90.0	0.004
HEMISPHERE 3	H3	6.320	-	3.160	5.975	0	239.6	0.027
CONNECTING ROD 1	CR1	1.500	-	6.000	5.975	0	0.0	0.494
CONNECTING ROD 2	CR2	1.500	-	12.000	5.975	0	180.0	0.077
CONNECTING ROD 3	CR3	1.500	-	24.000	5.975	0	180.0	0.016
PARABOLOID	P1	4.892	-	3.50	5.975	0	0.0	0.000
DIPLANE 1	D1	10.000	-	10.000	5.975	0	135.6	8.486

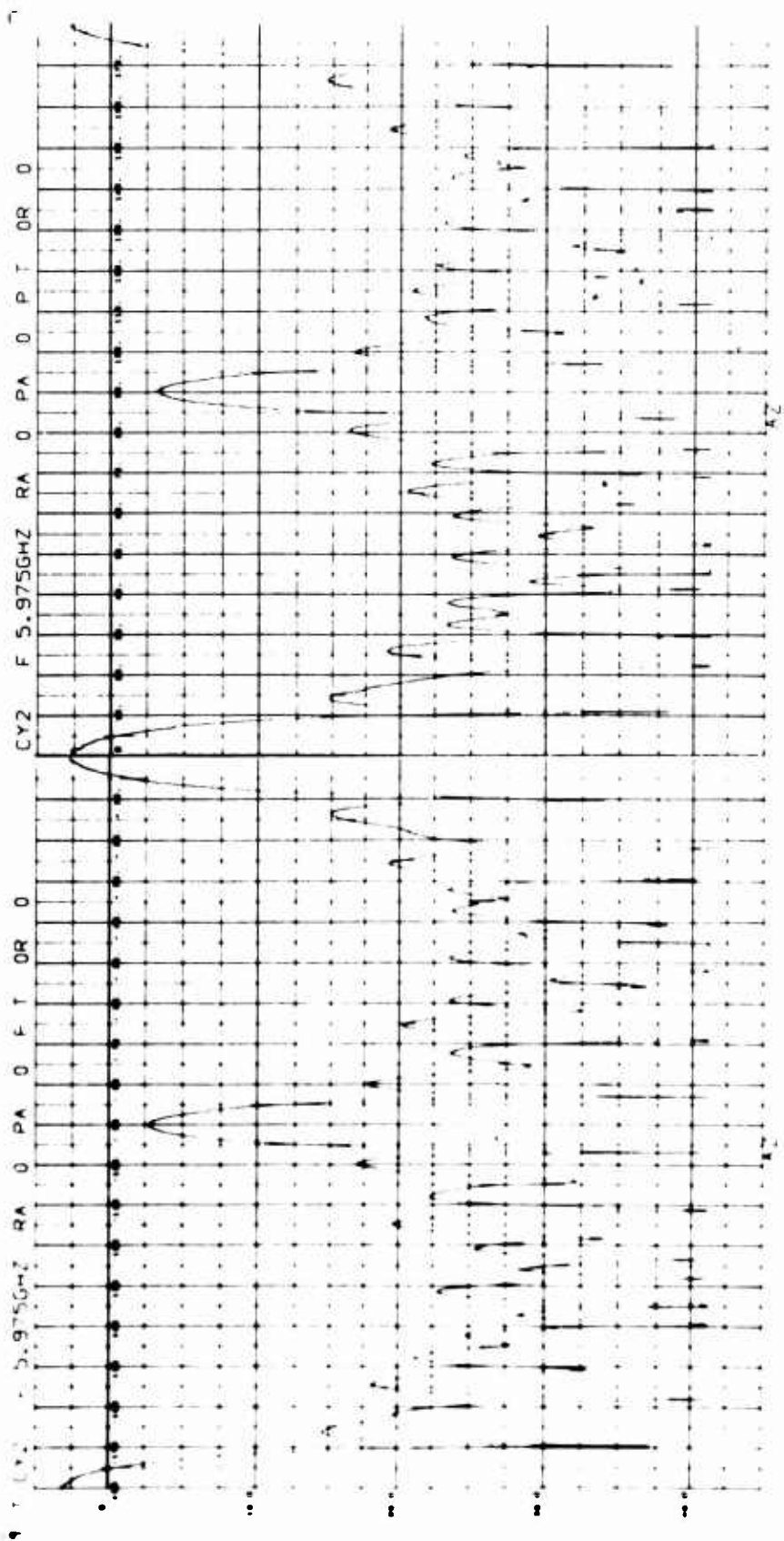


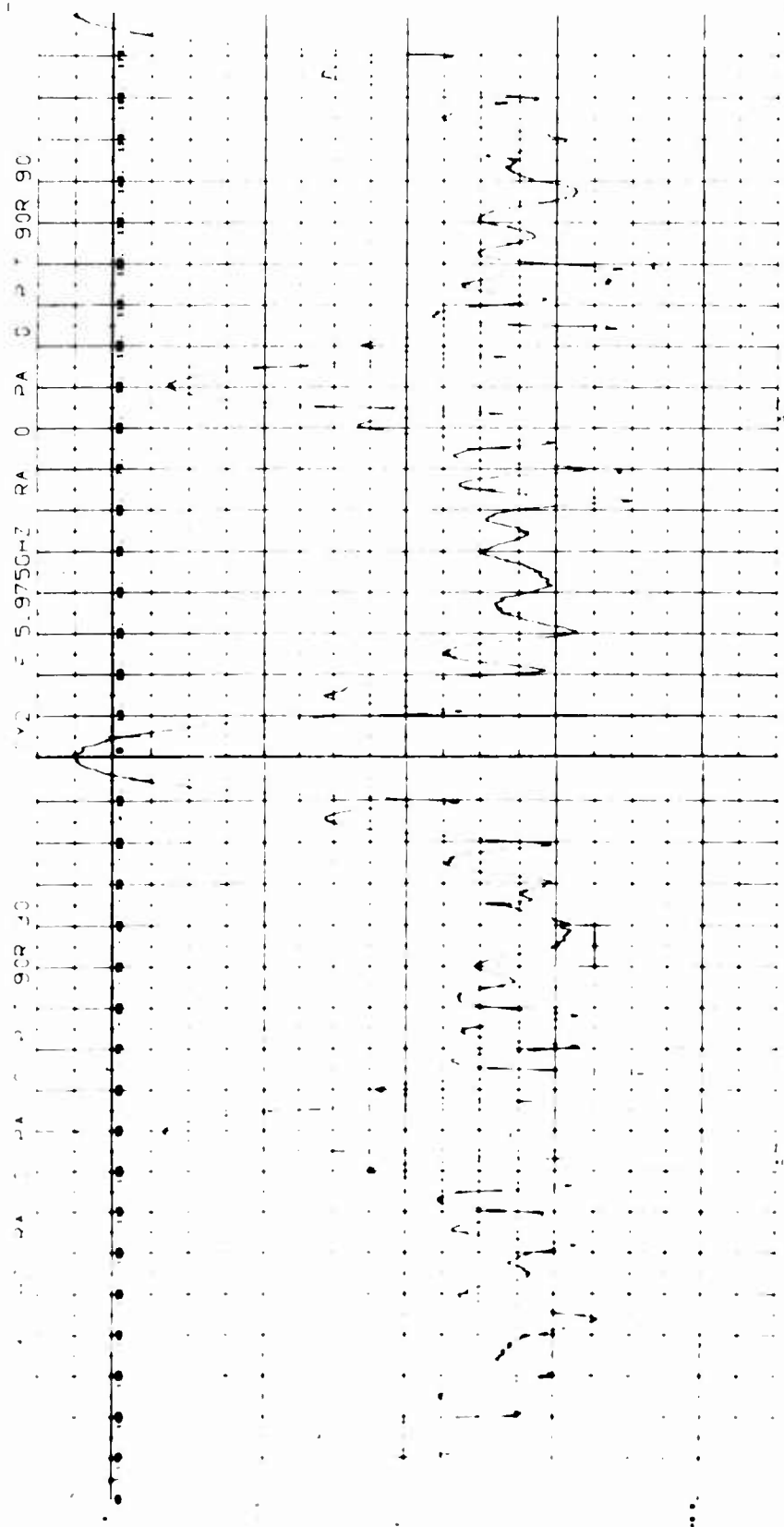
Fig. 3-2 TYPICAL GENERIC VEHICLES

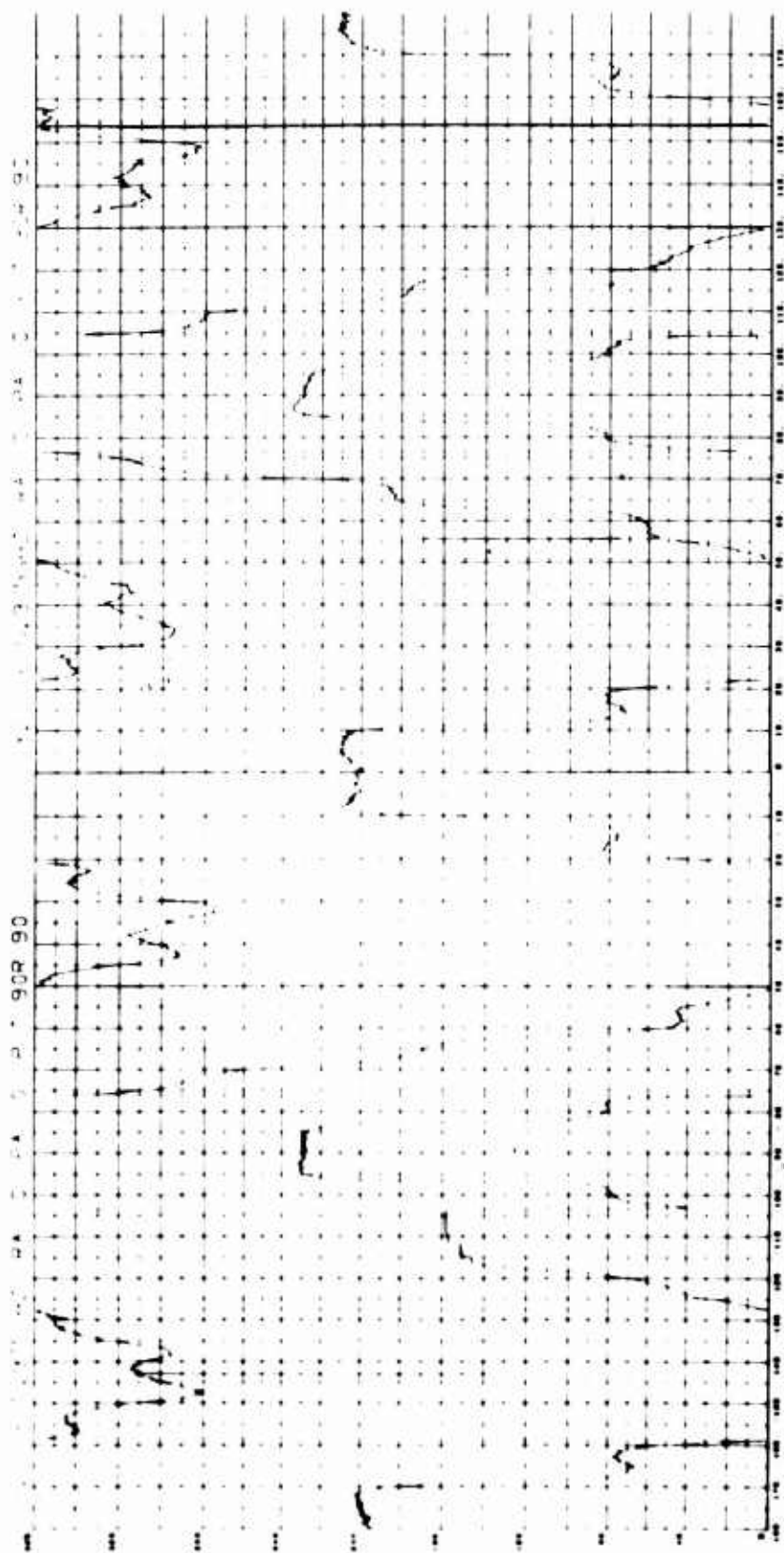


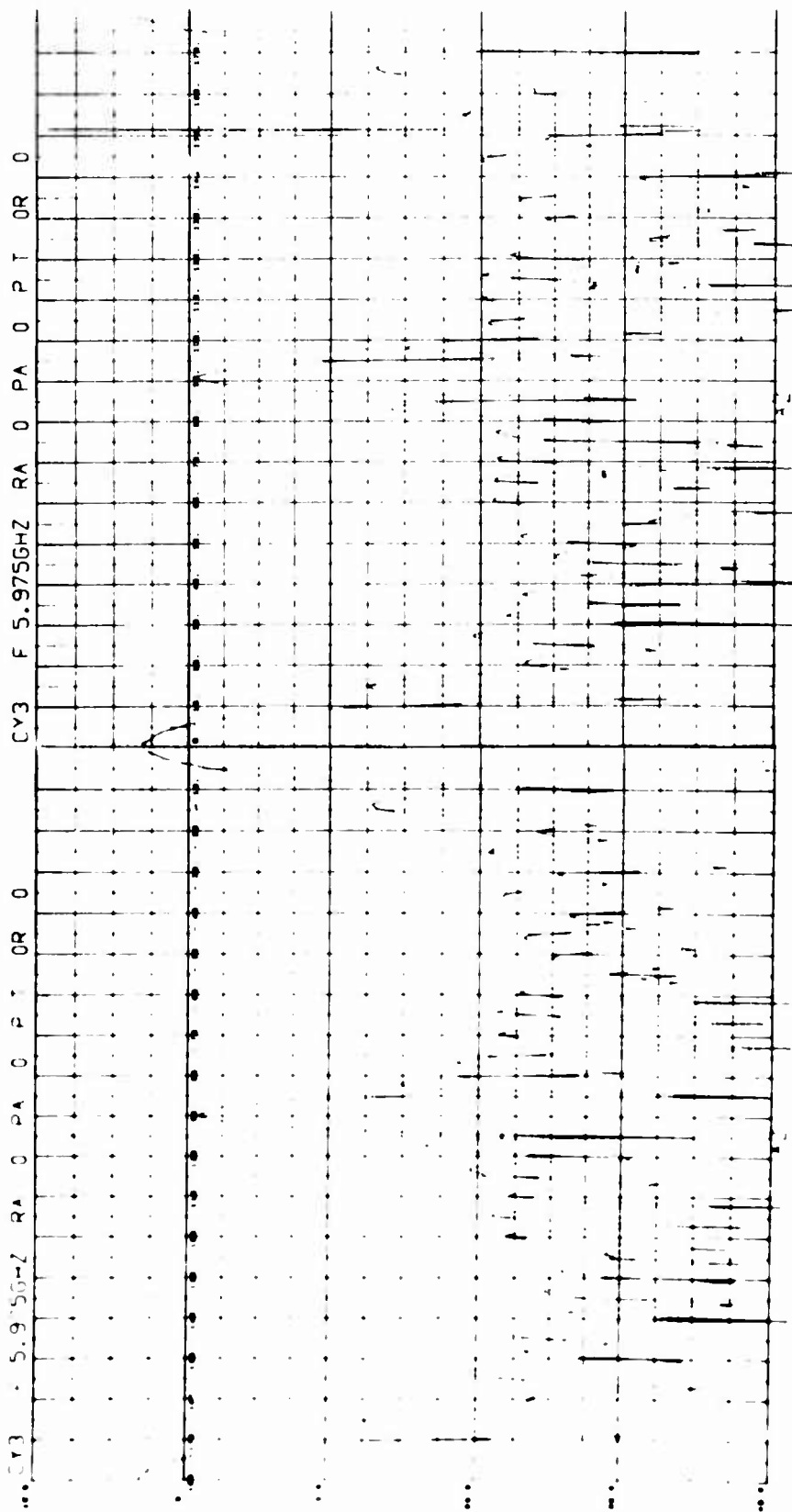


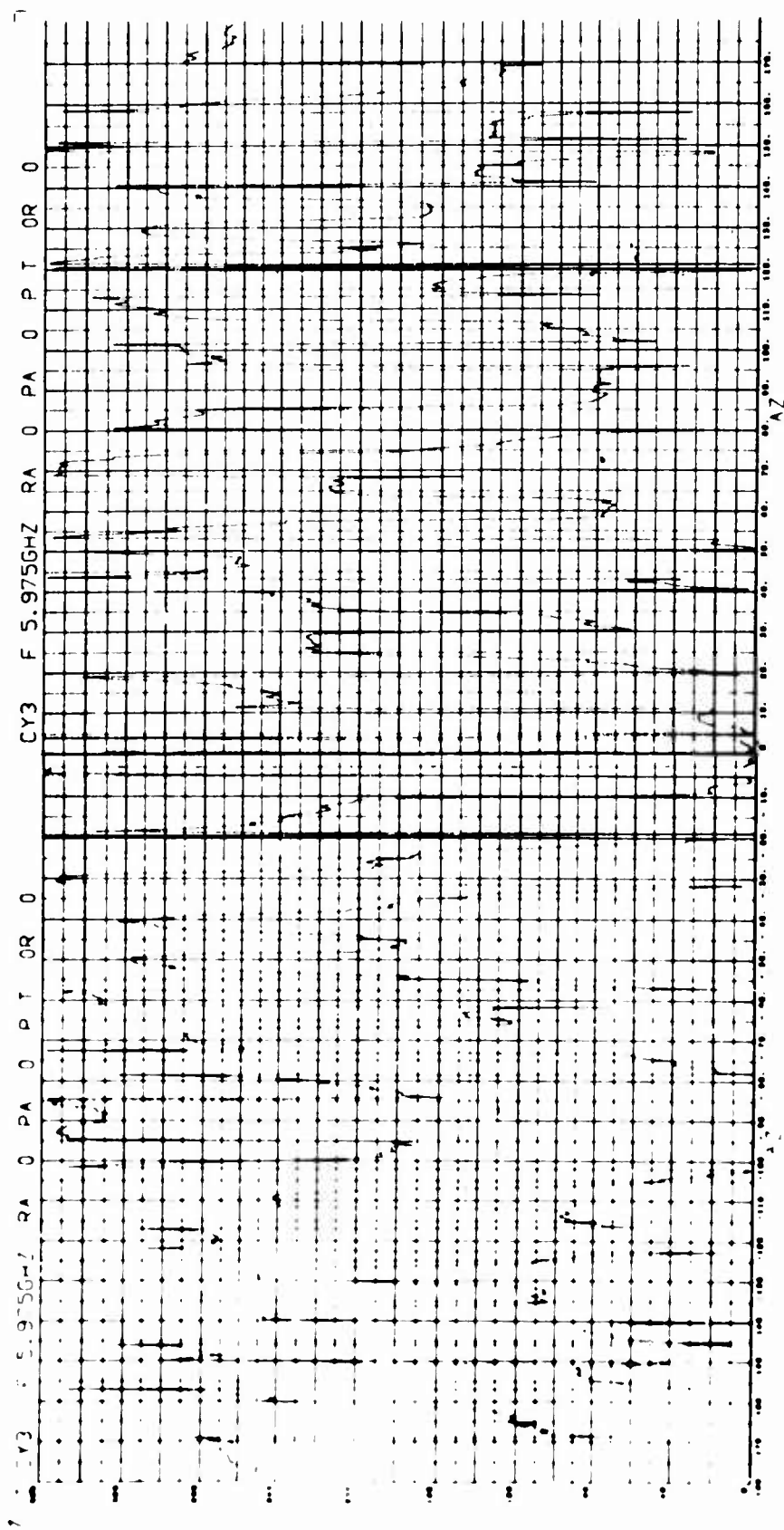


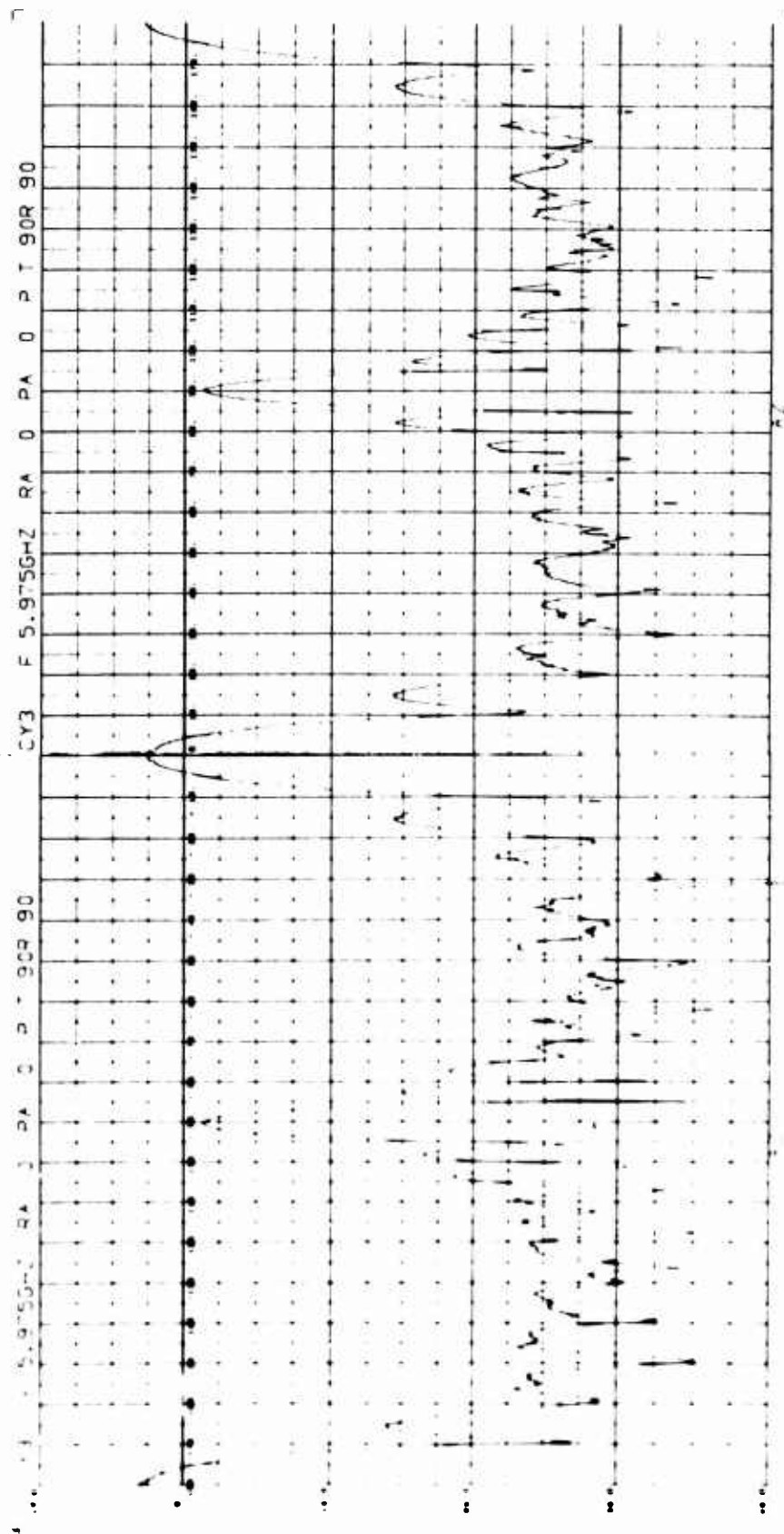


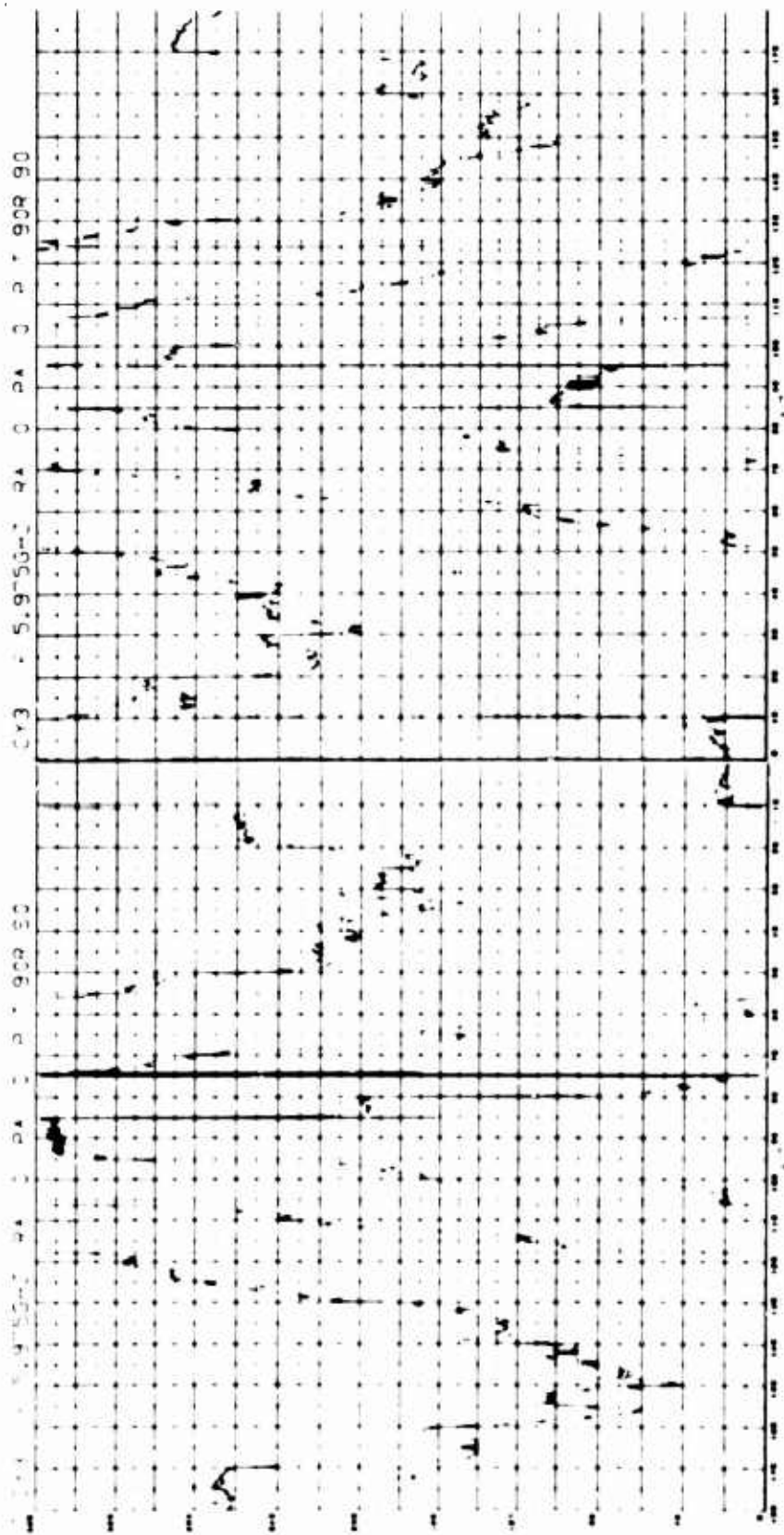


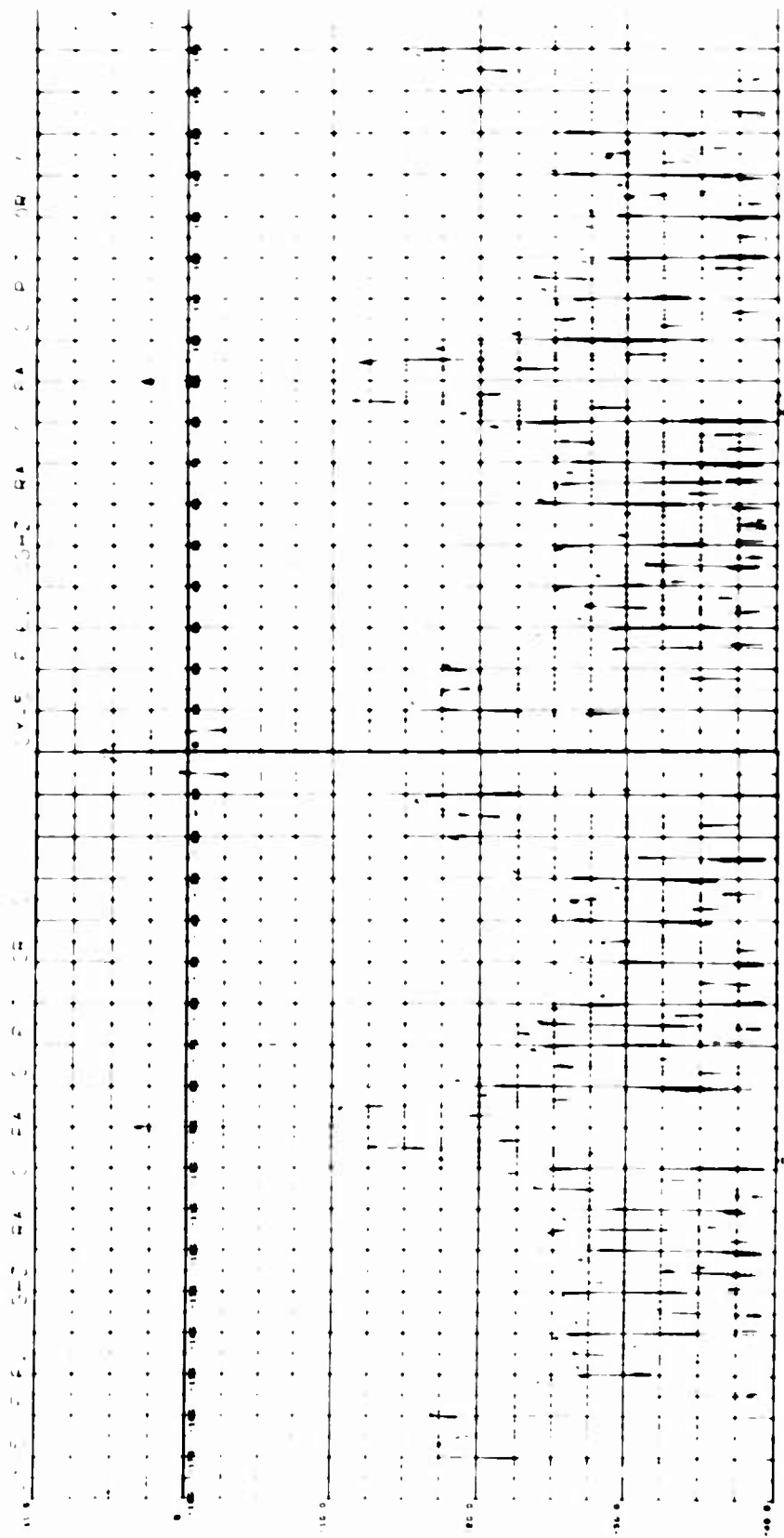


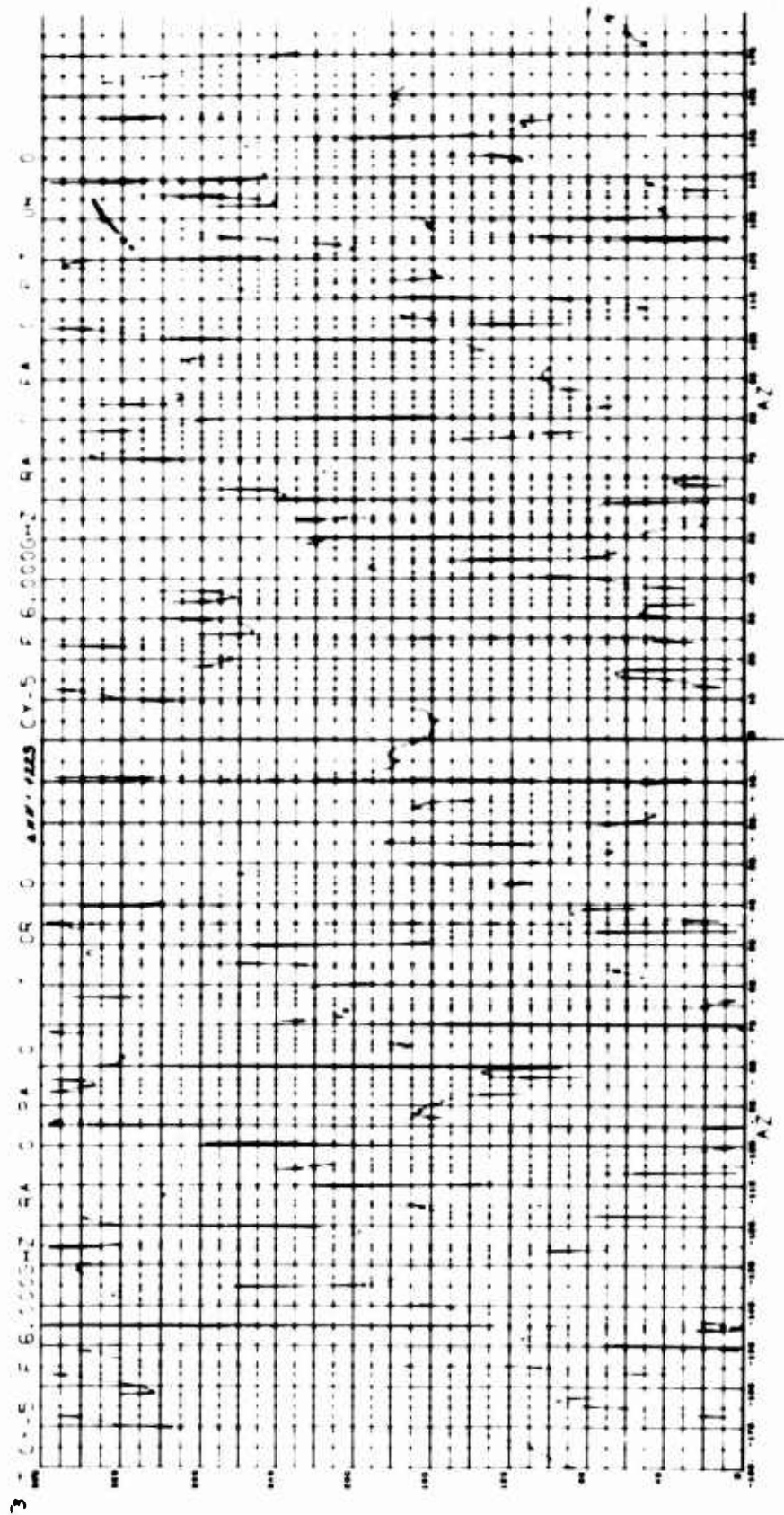


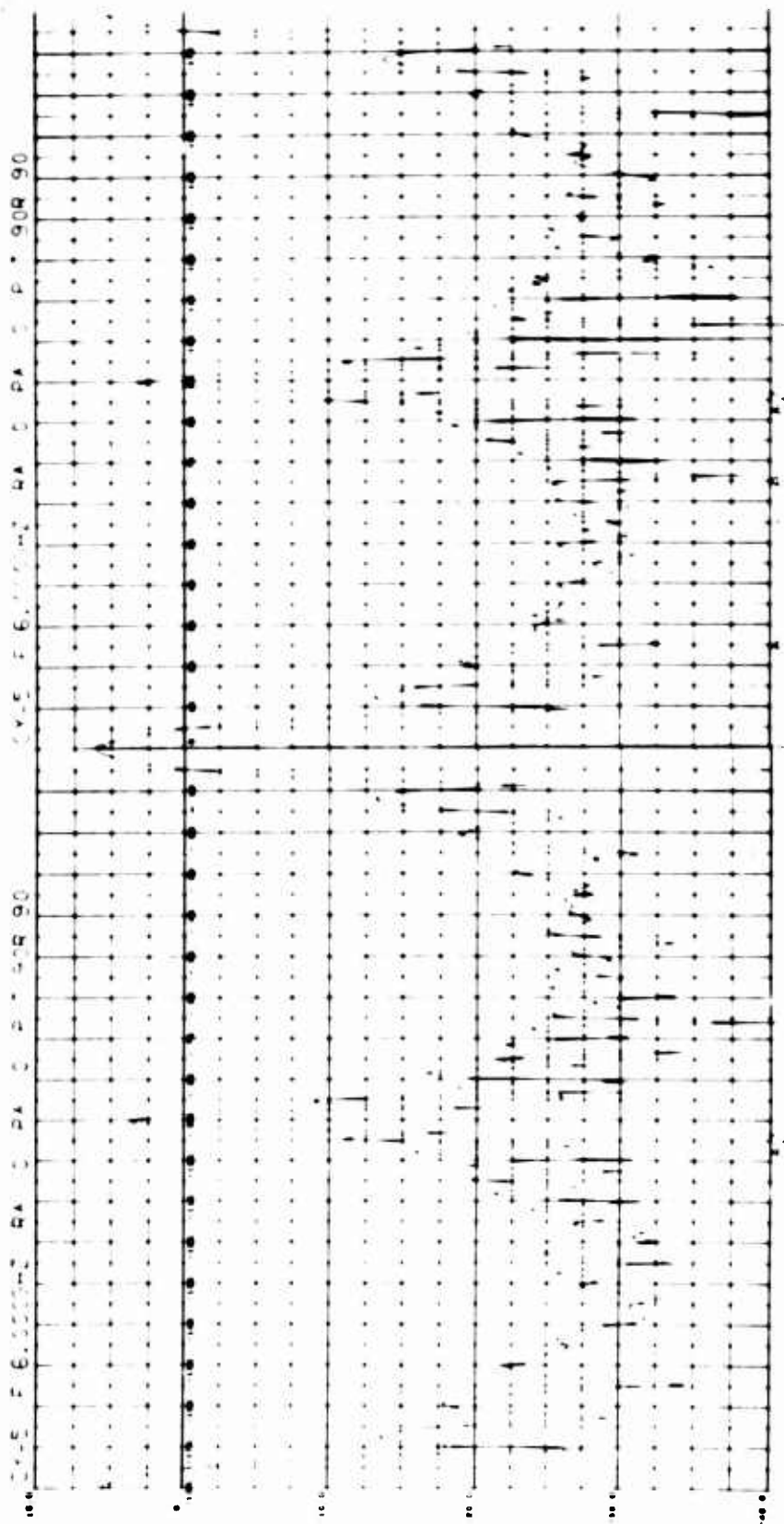


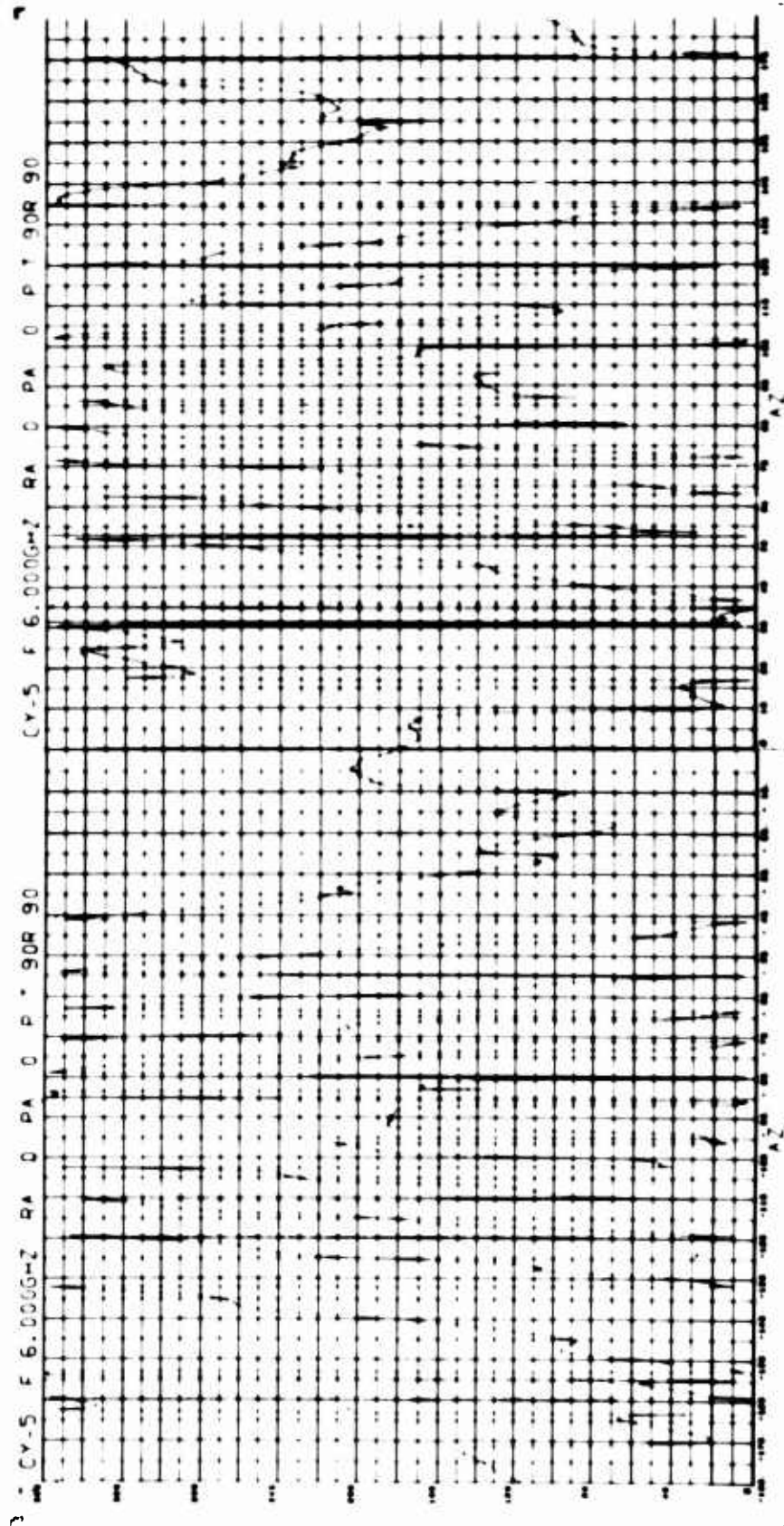


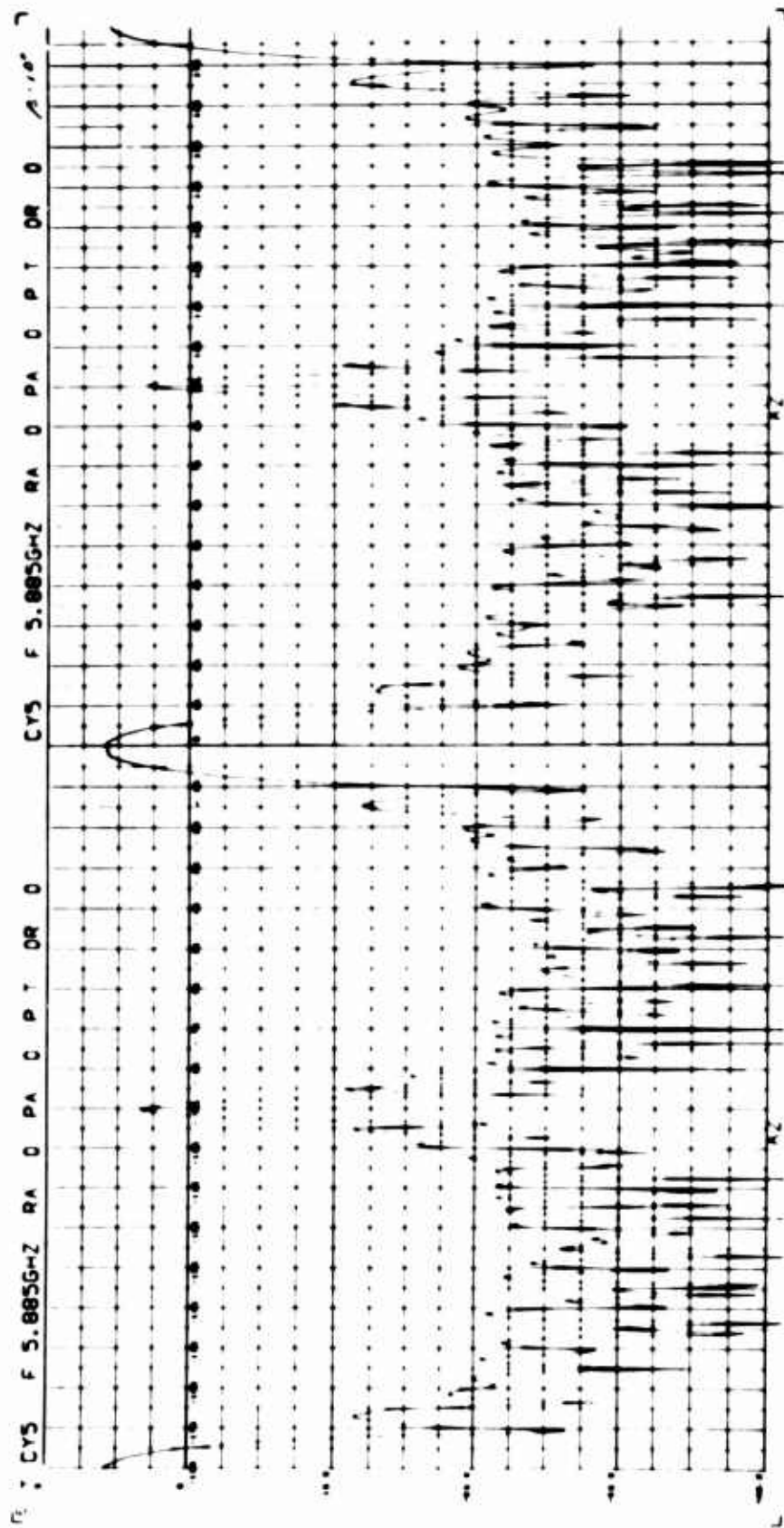




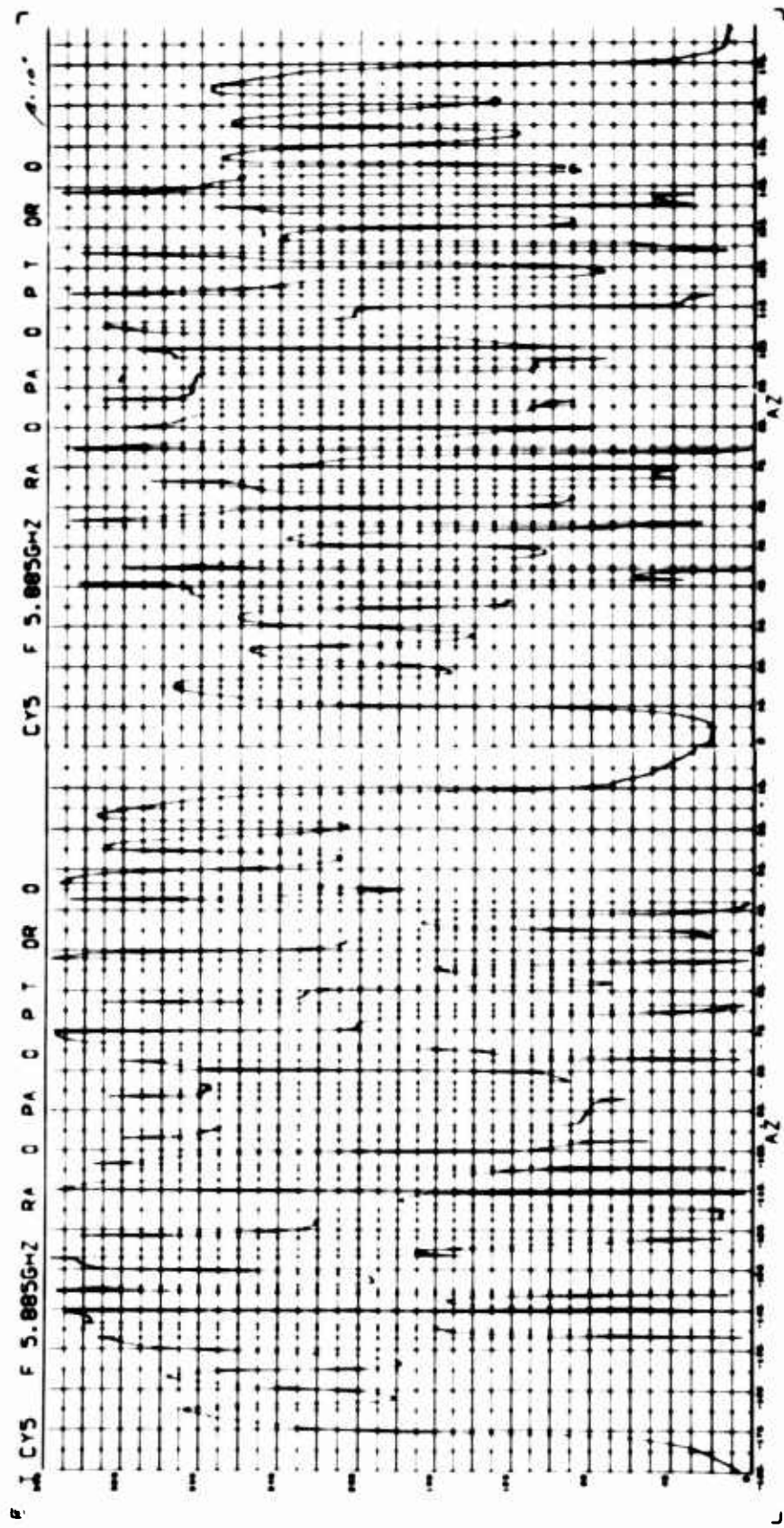




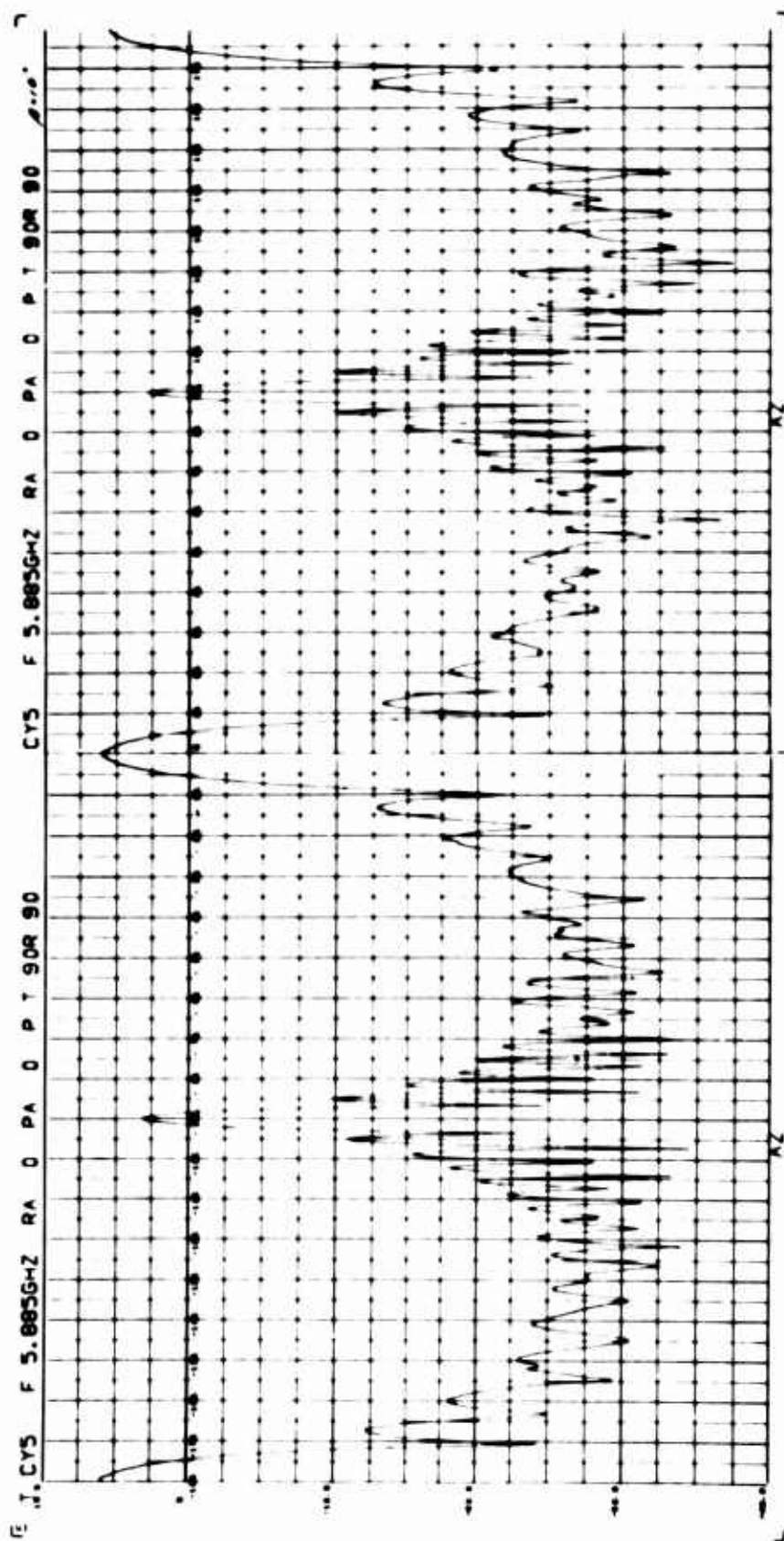




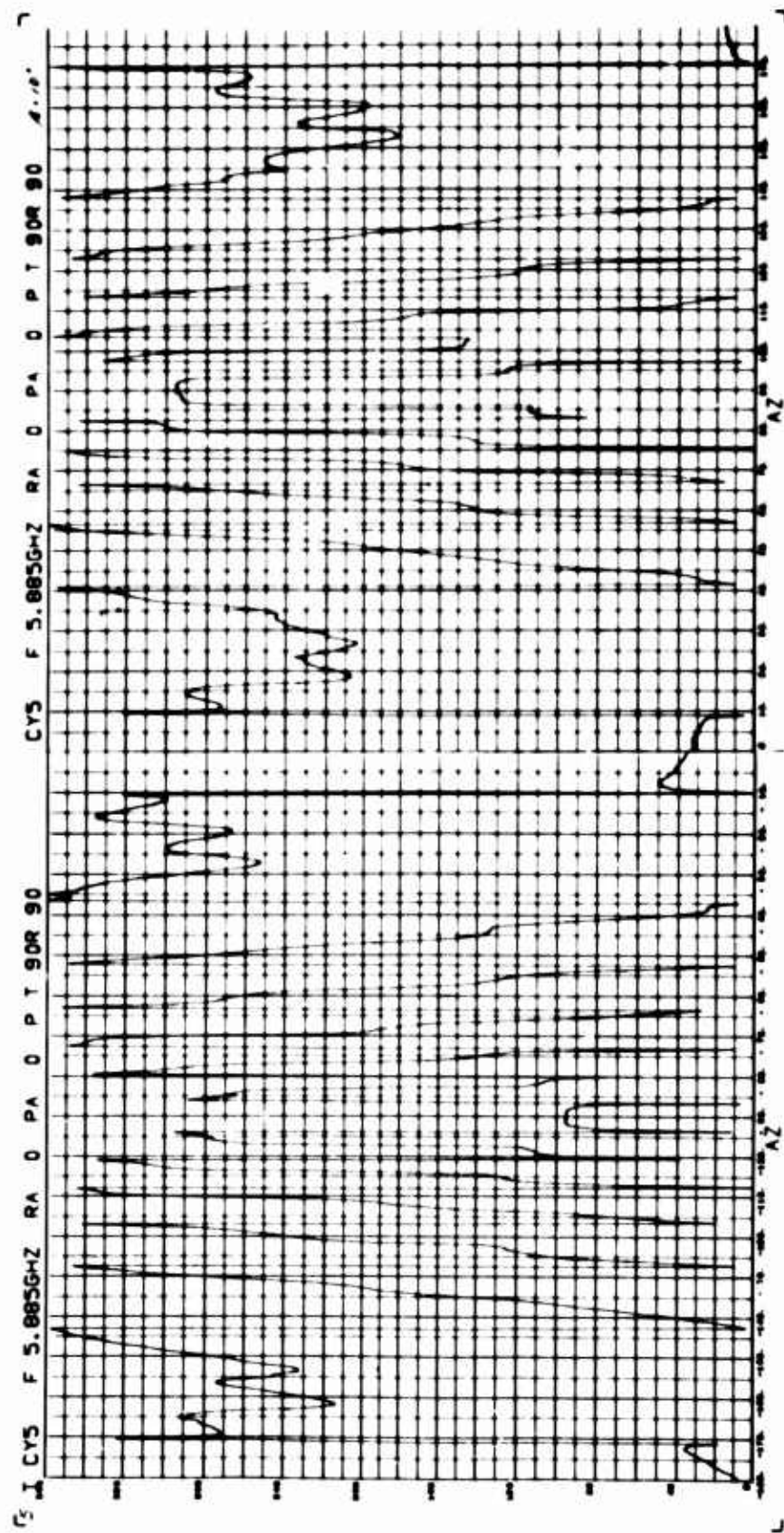
BISTATIC ANGLE = 10.25 DEGREES



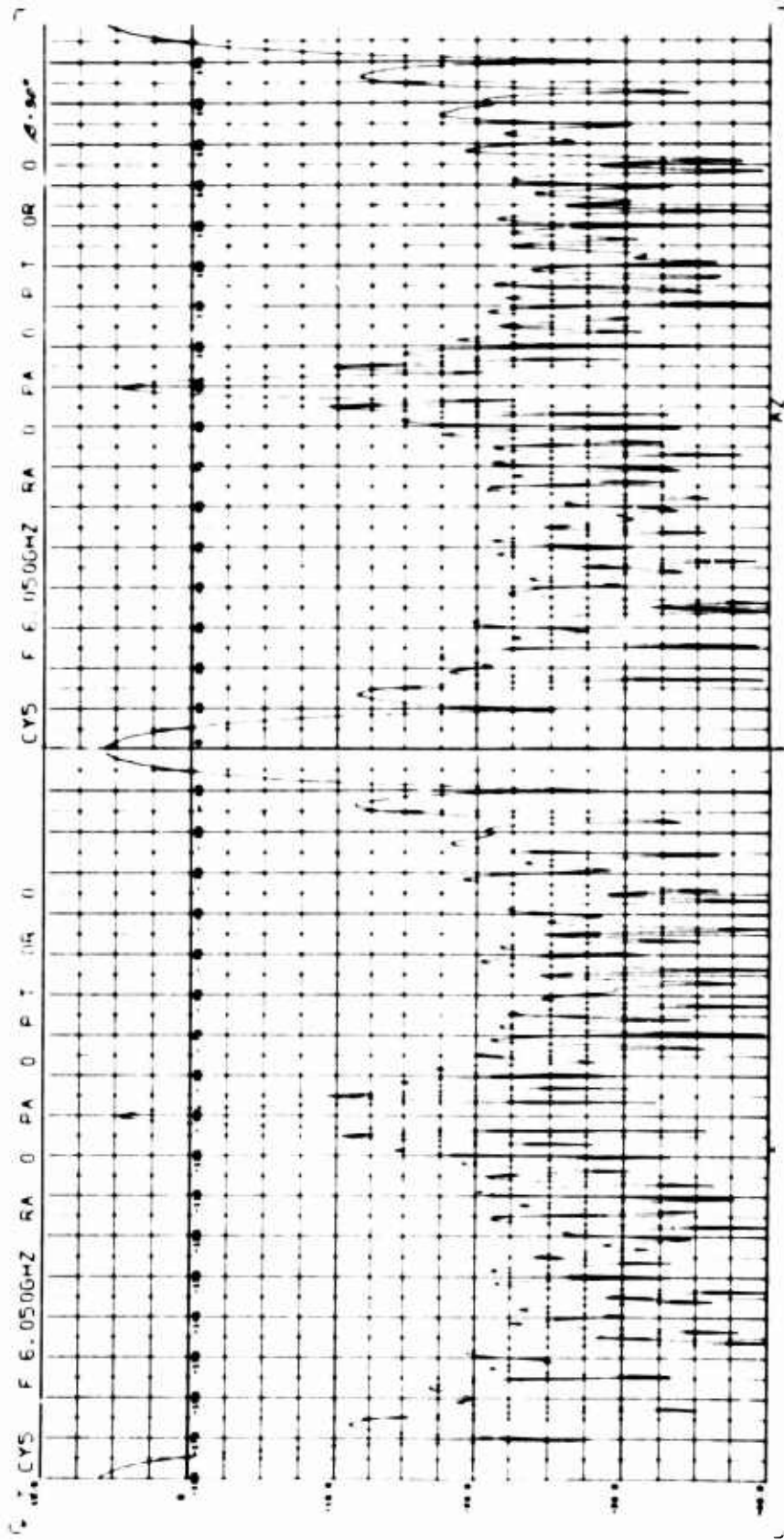
BISTATIC ANGLE = 10.25 DEGREES



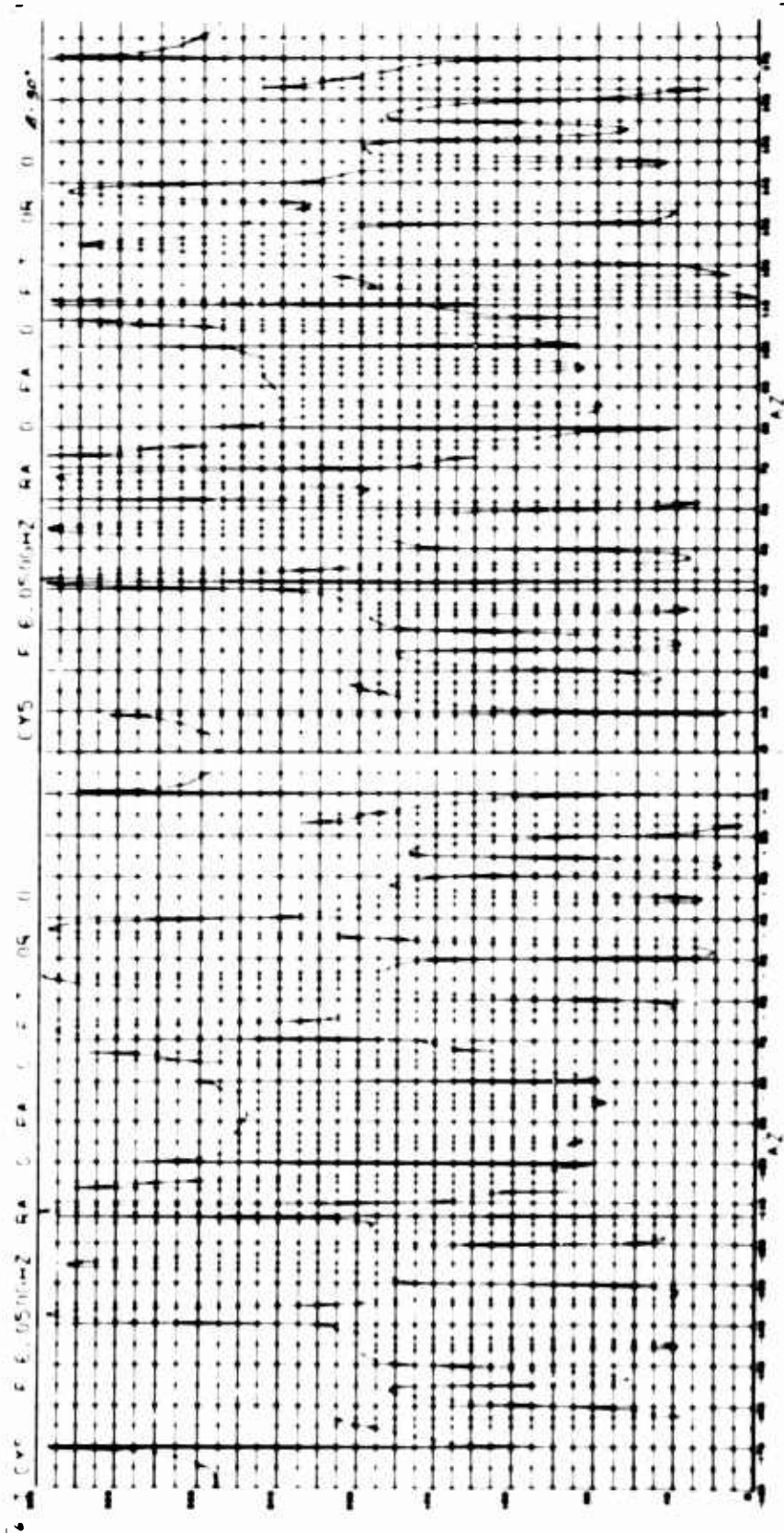
BISTATIC ANGLE = 10.25 DEGREES



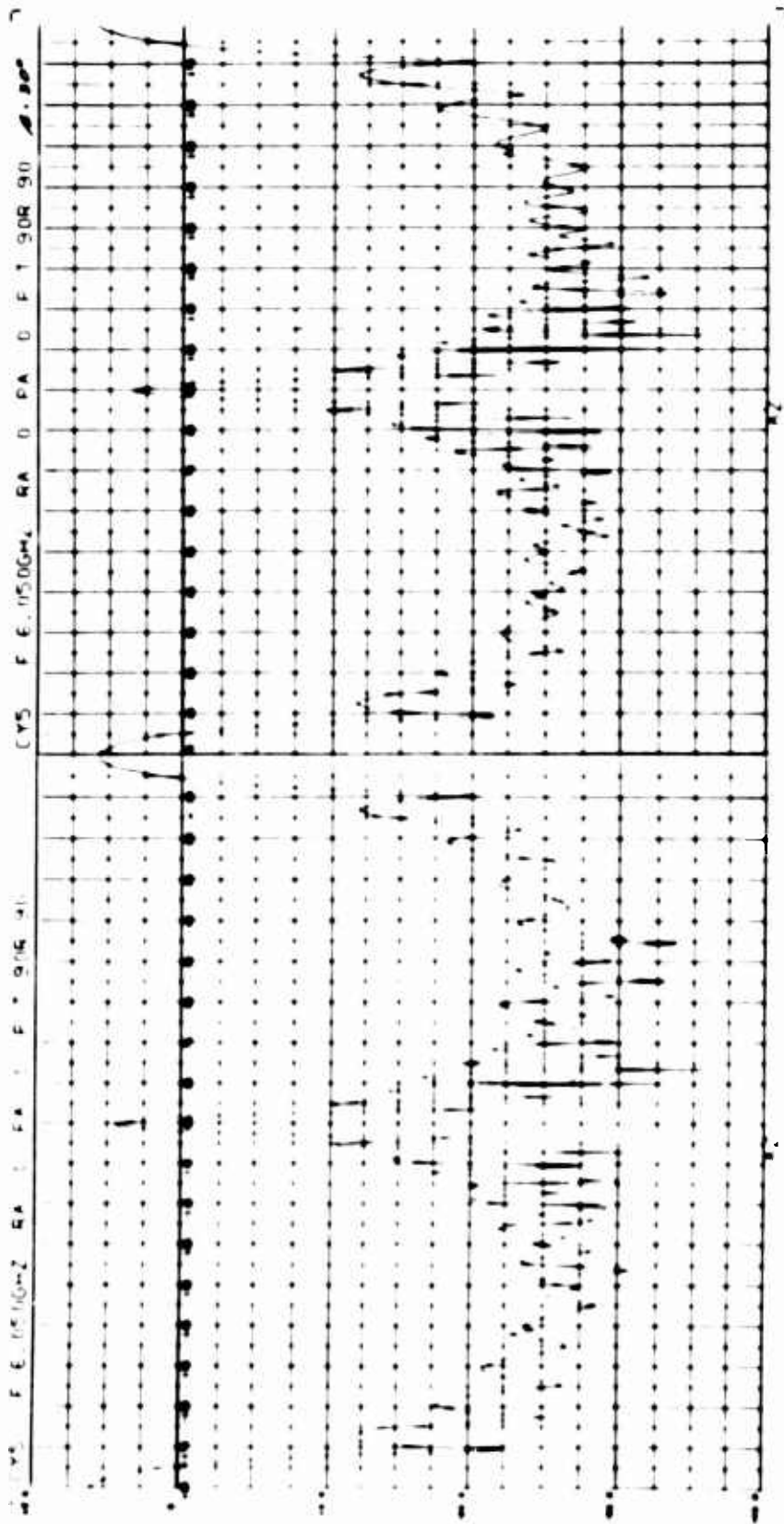
BISTATIC ANGLE = 10.25 DEGREES



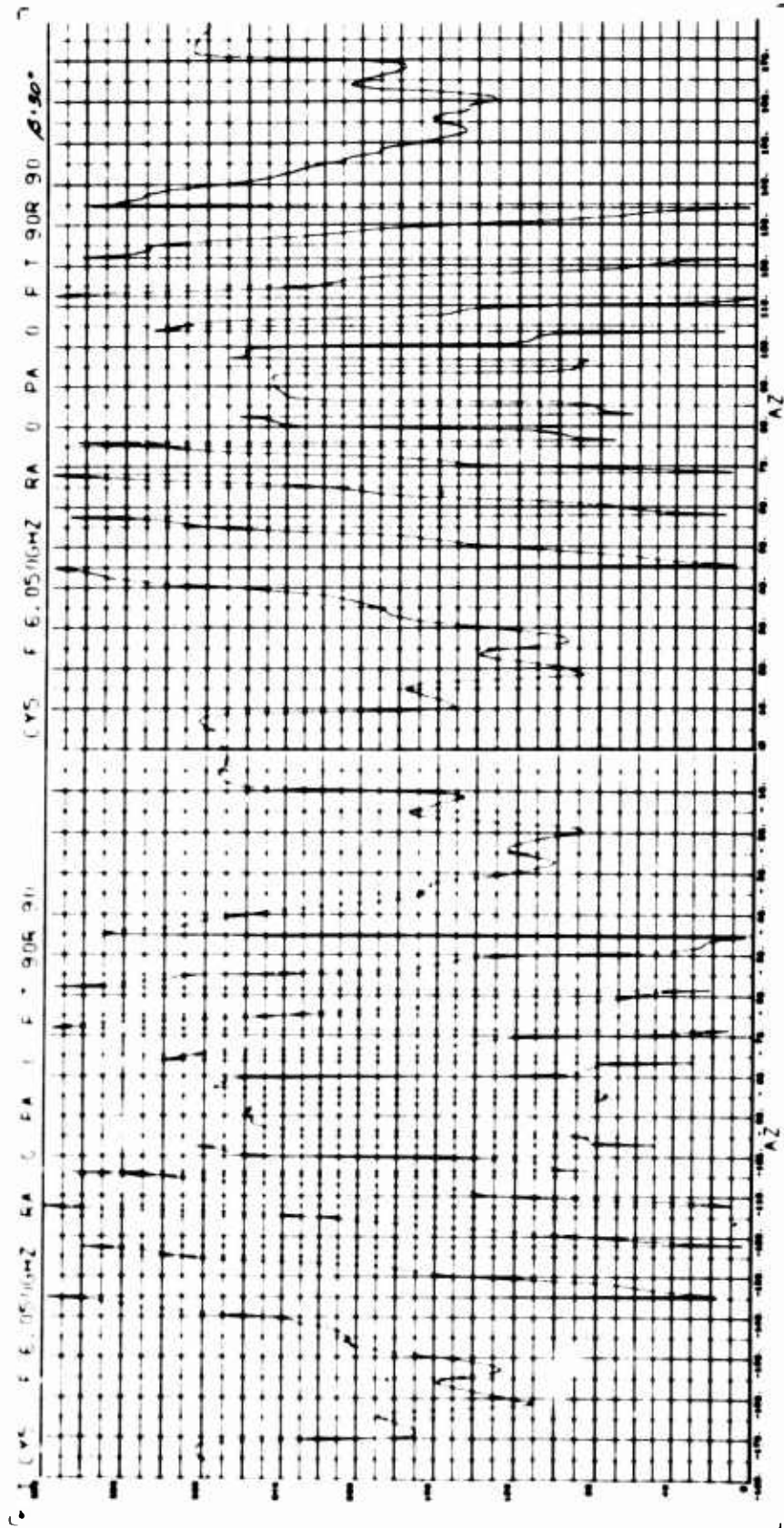
BISTATIC ANGLE = 30.0 DEGREES



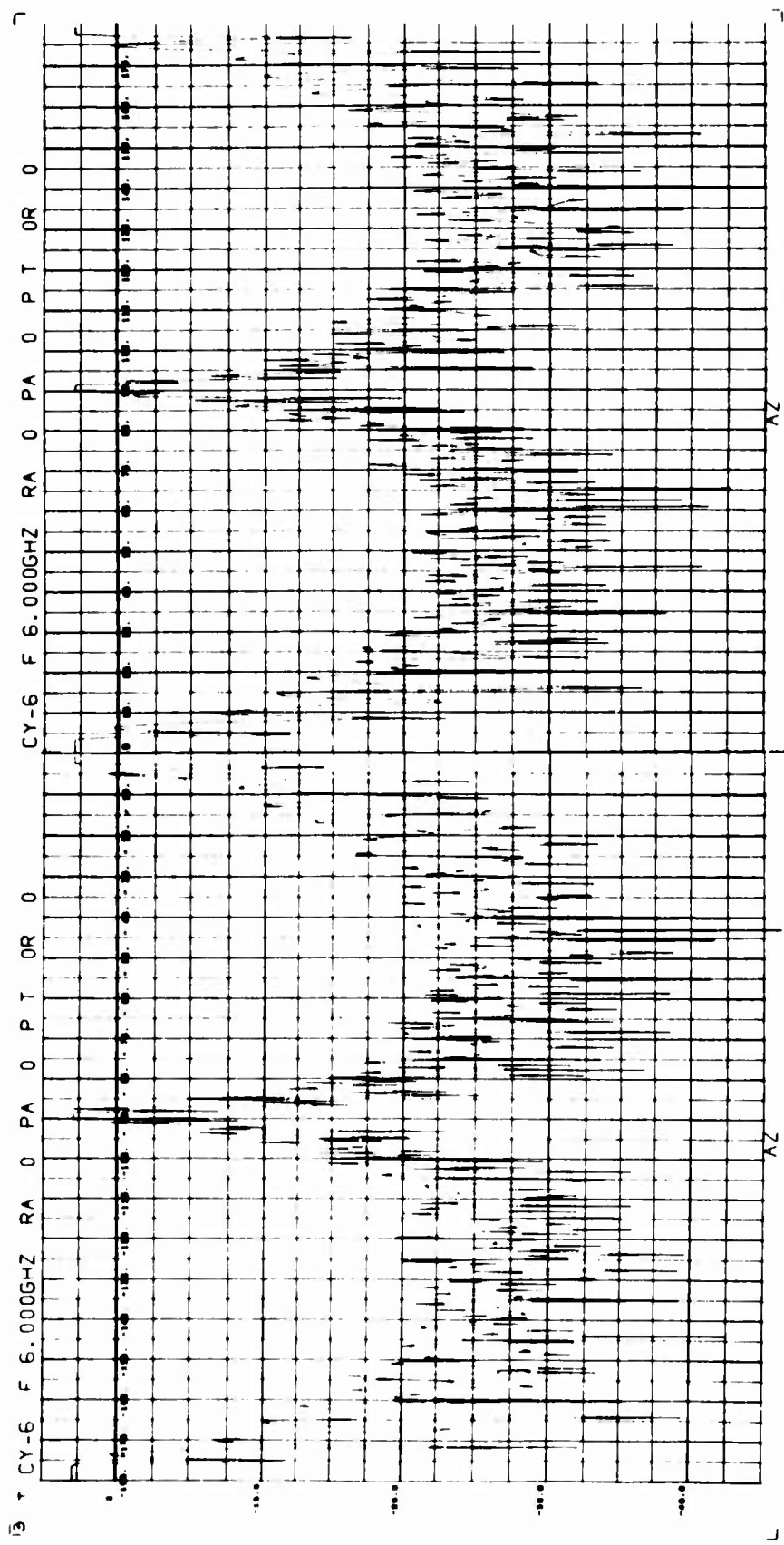
BISTATIC ANGLE - 30.0 DEGREES

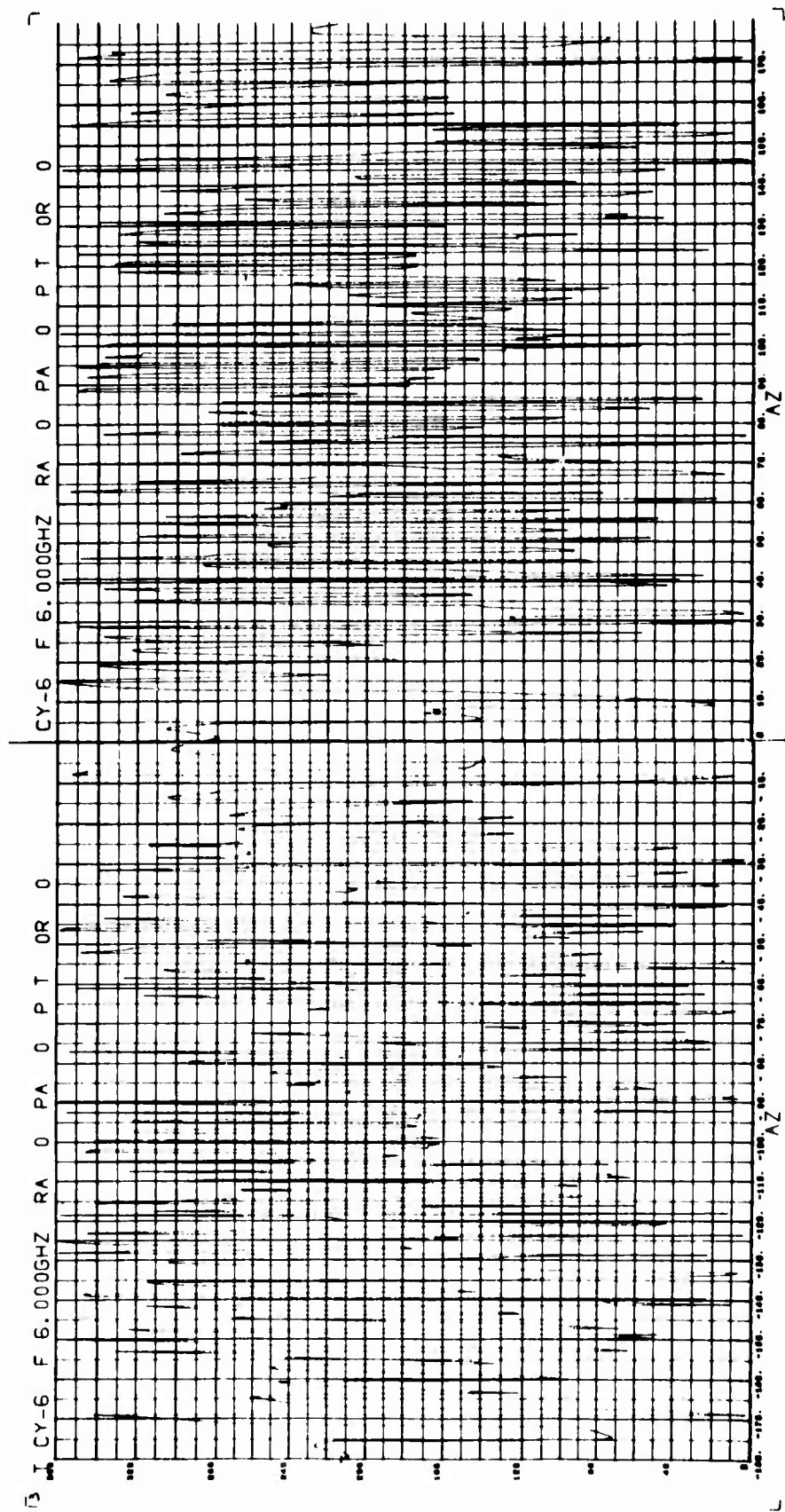


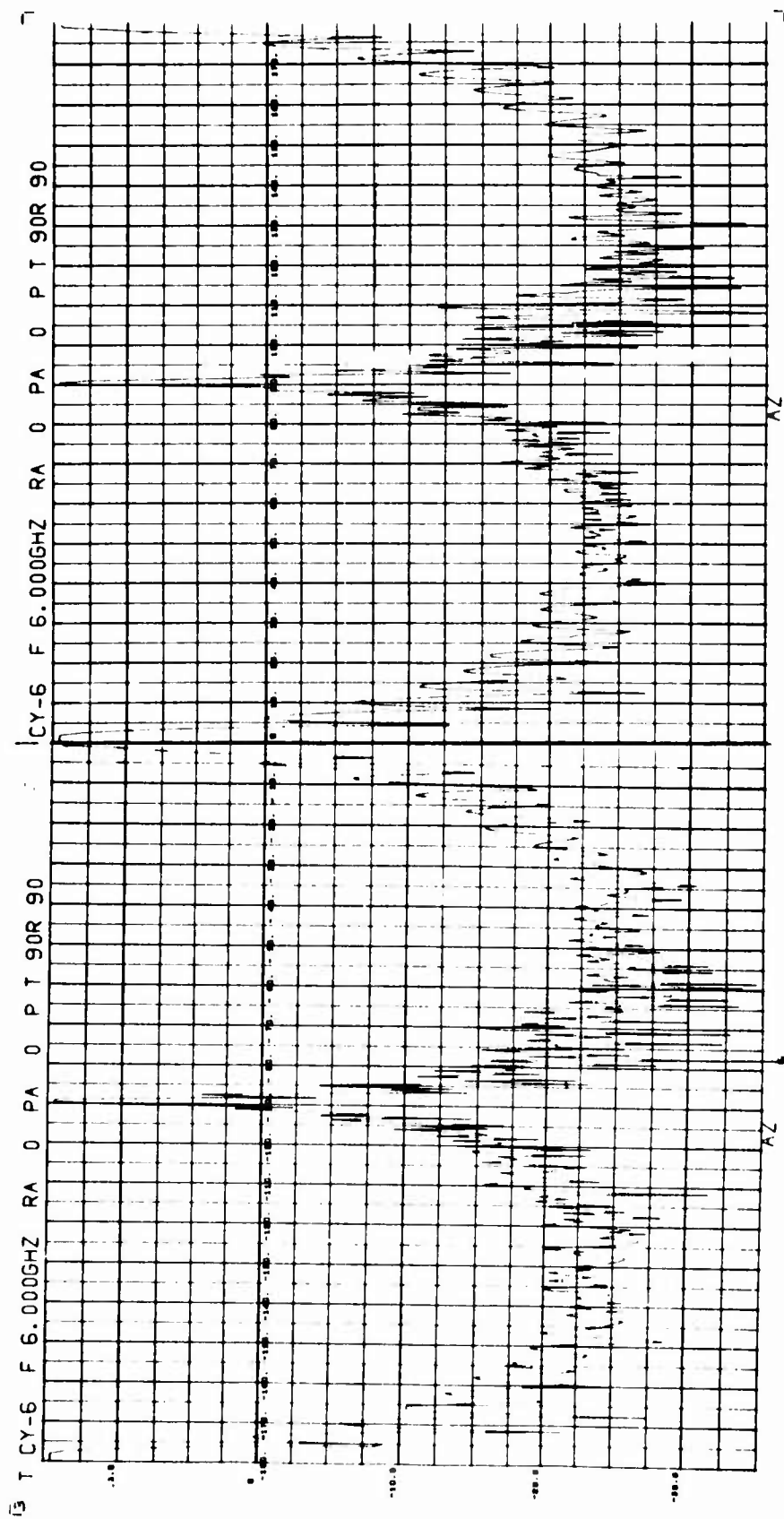
BISTATIC ANGLE - 30.0 DEGREES

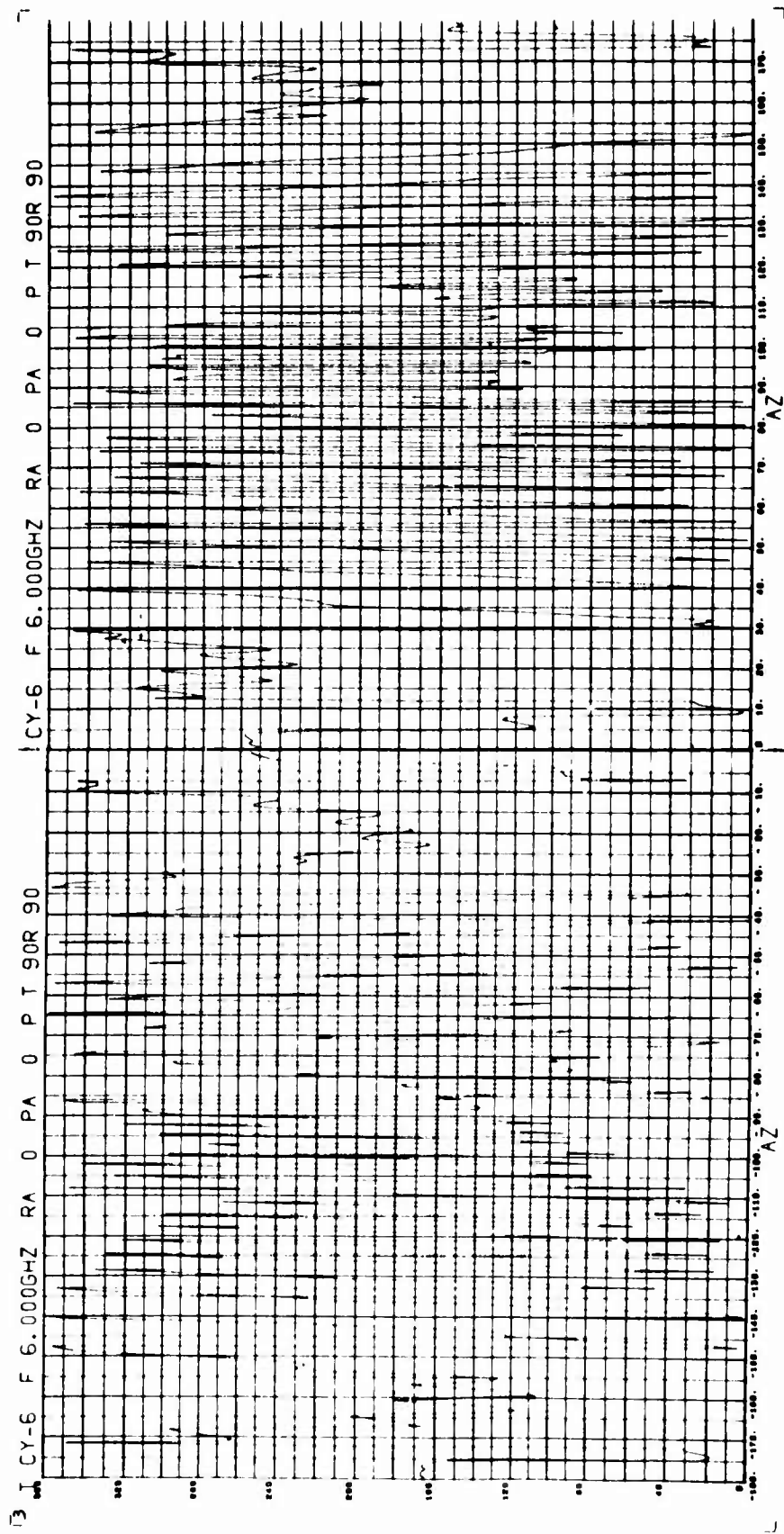


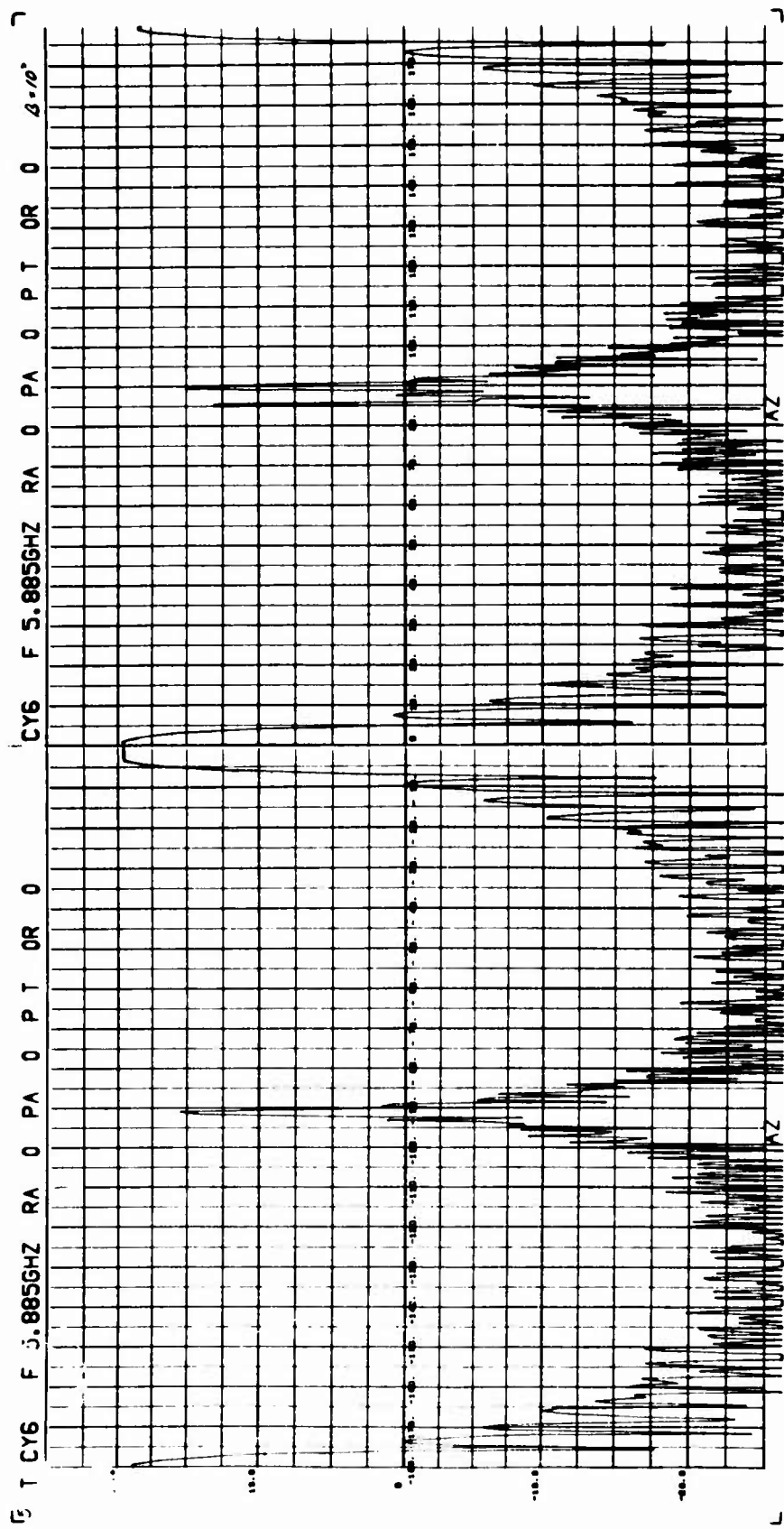
BISTATIC ANGLE = 30.0 DEGREES



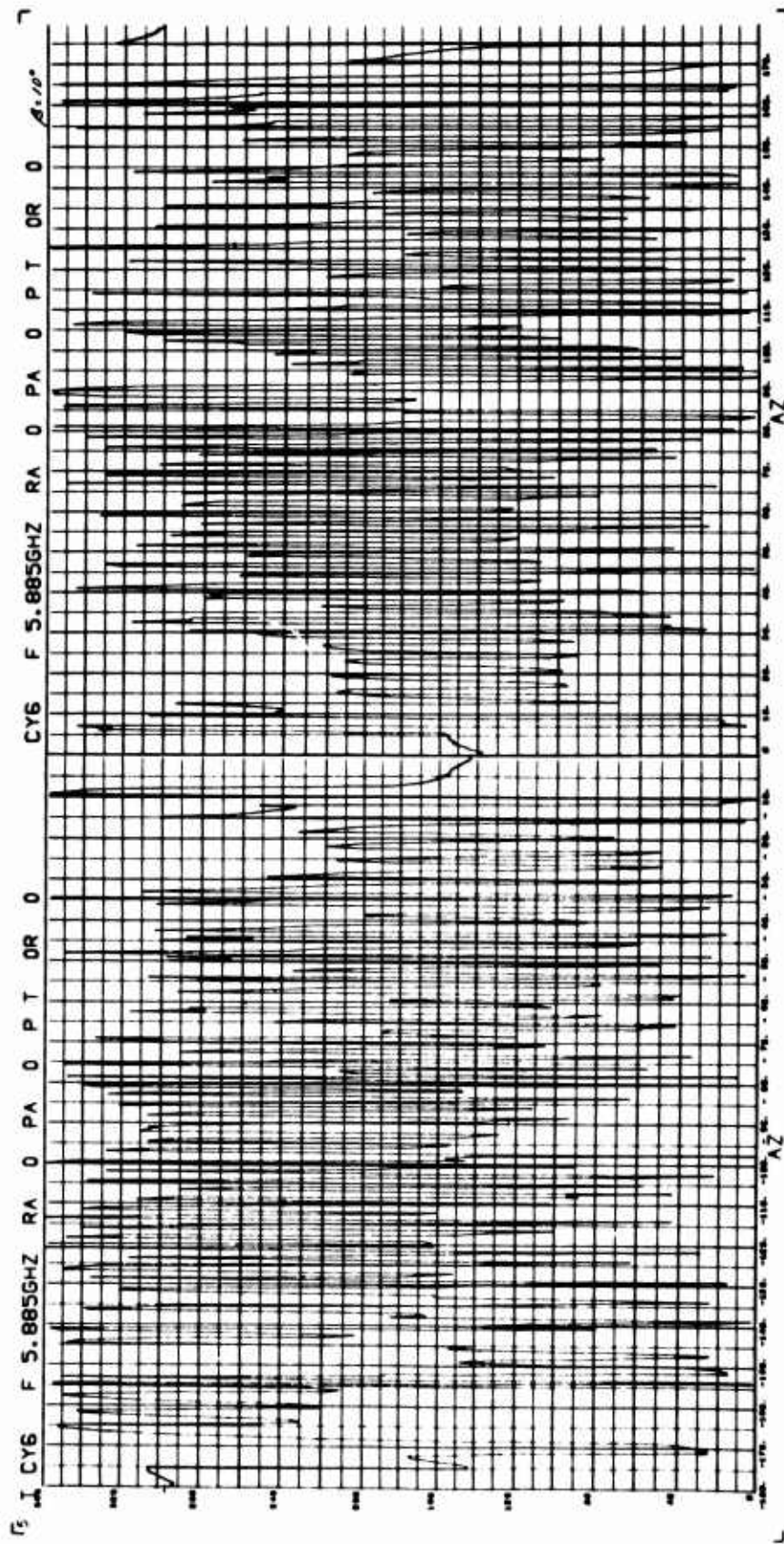




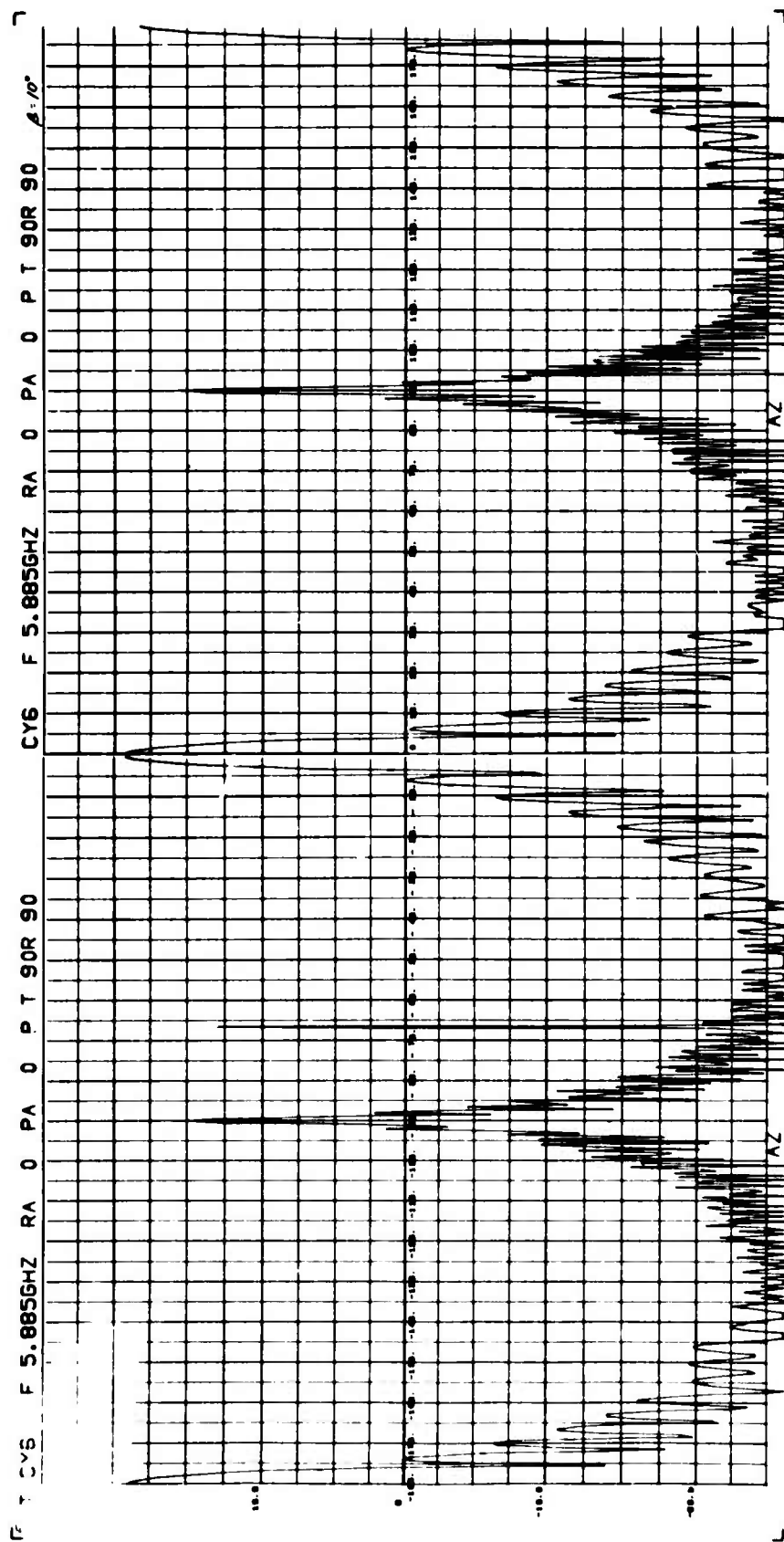




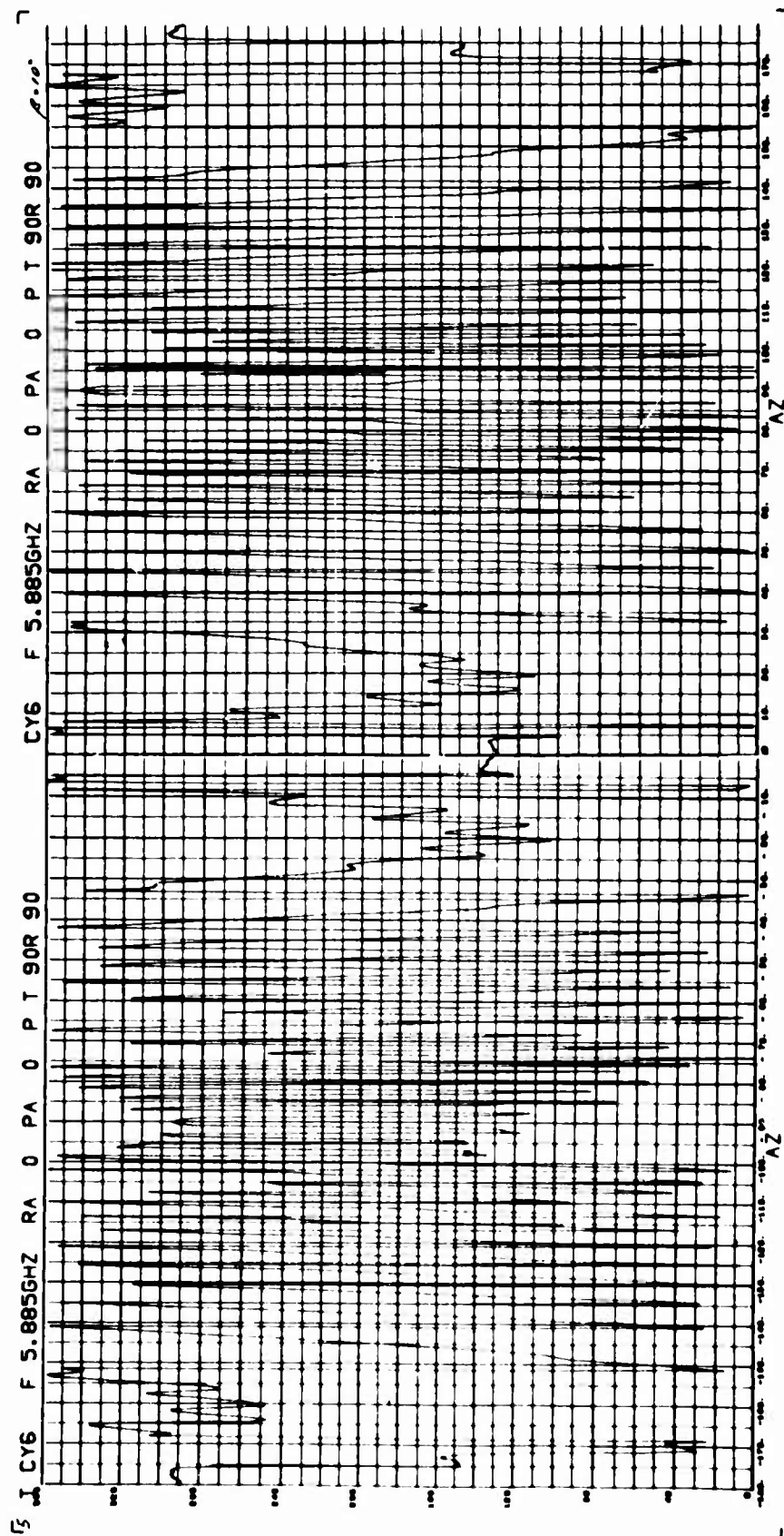
BISTATIC ANGLE = 10.25 DEGREES



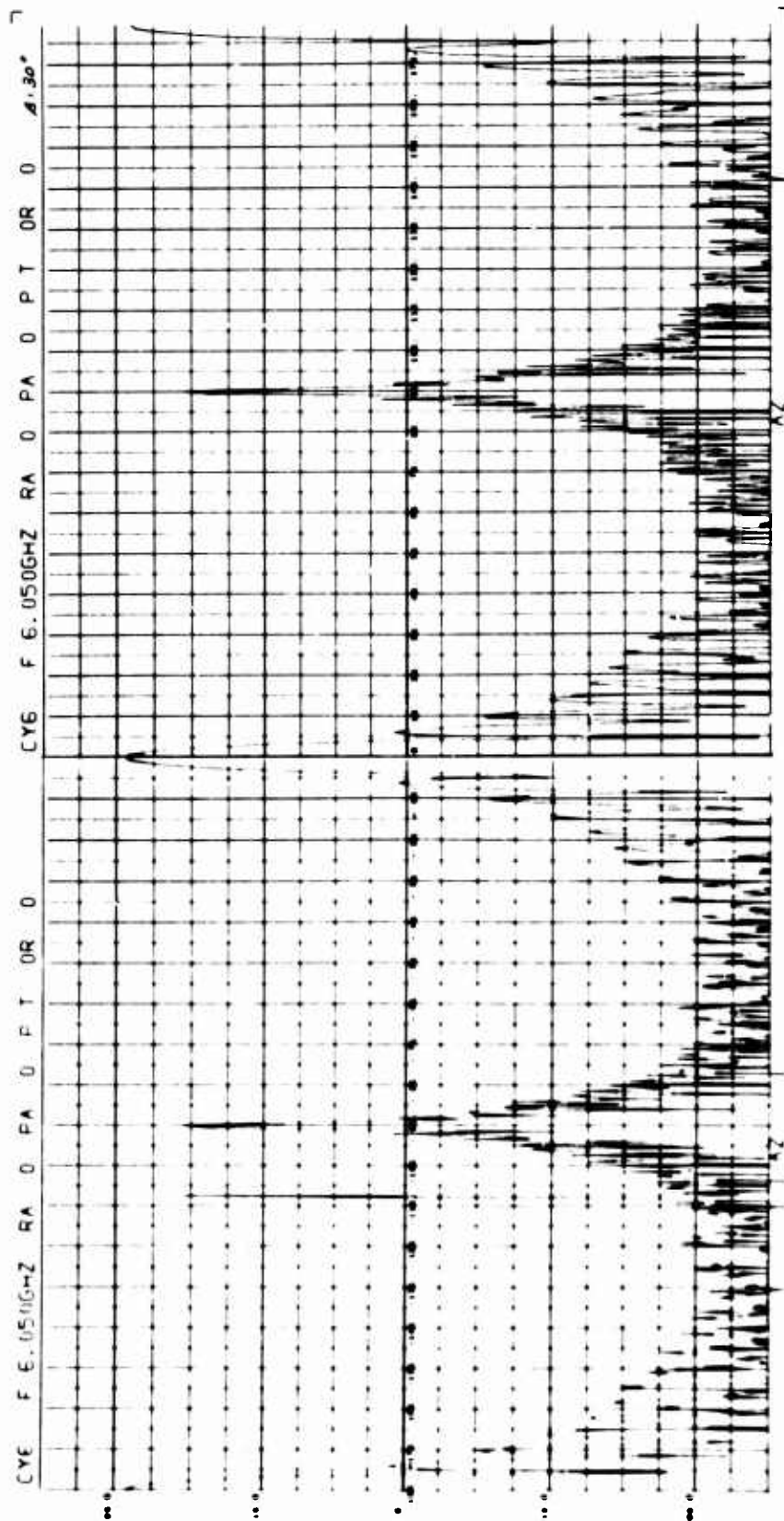
BISTATIC ANGLE = 10.25 DEGREES



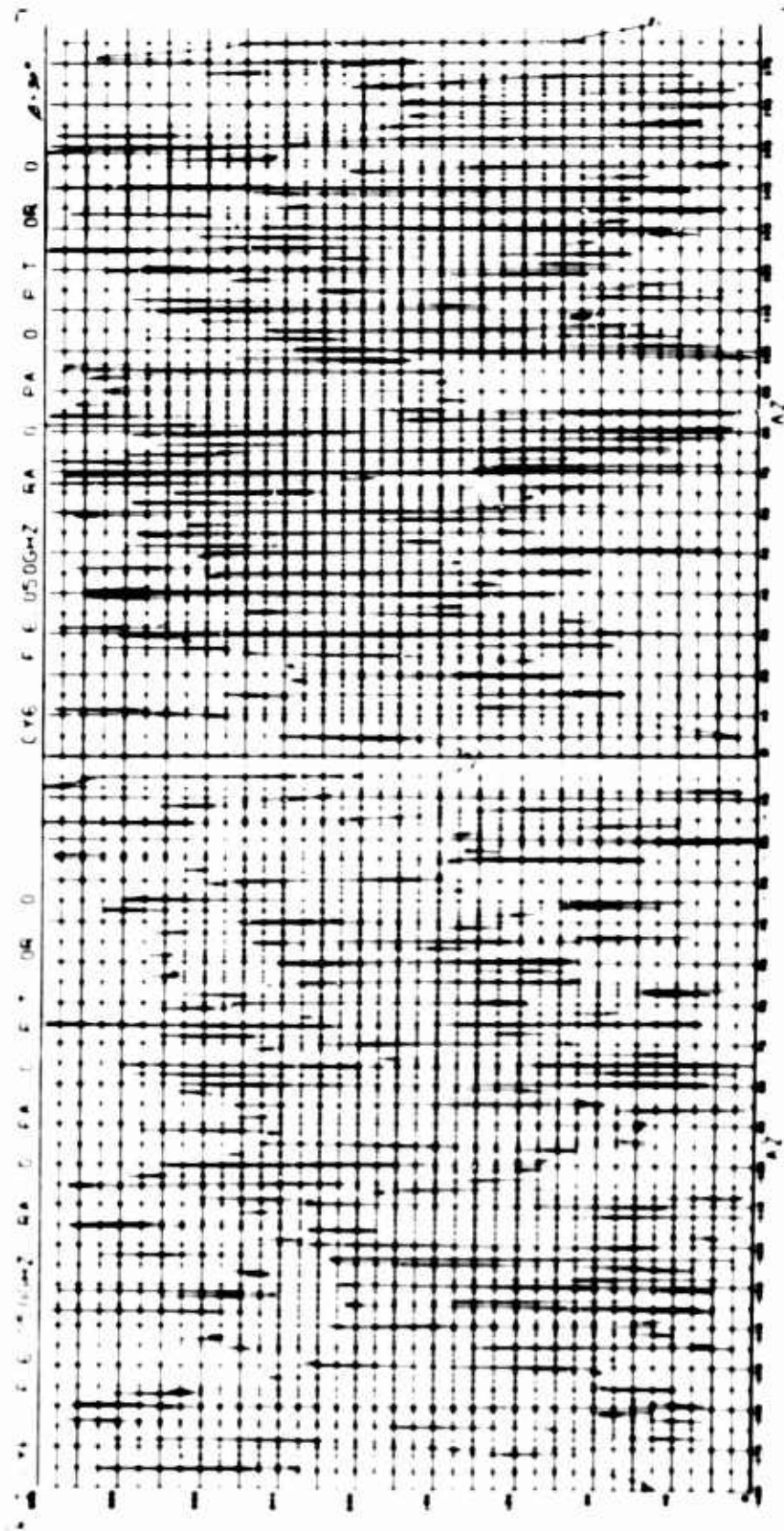
BISTATIC ANGLE = 10.25 DEGREES



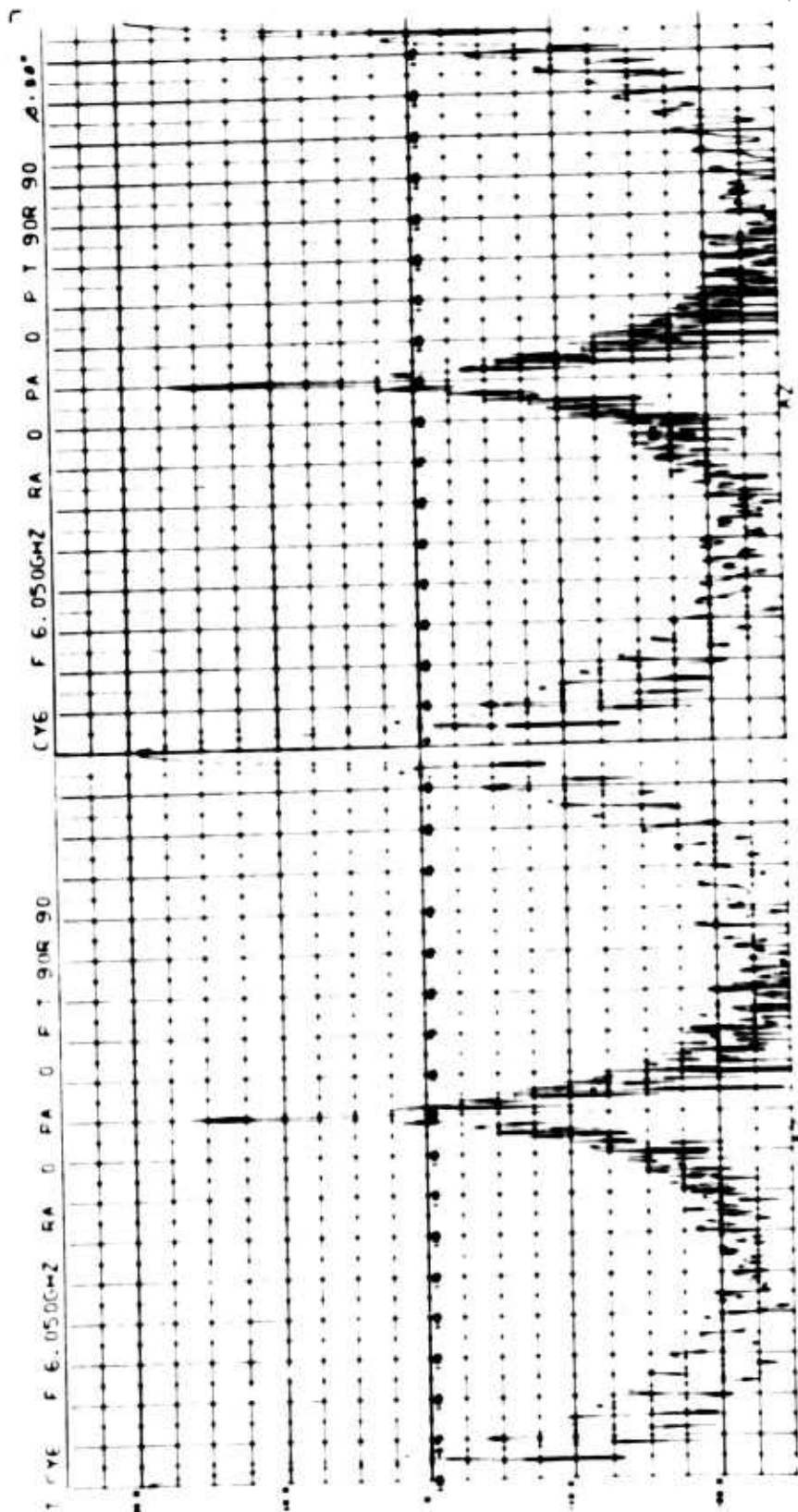
BISTATIC ANGLE = 10.25 DEGREES



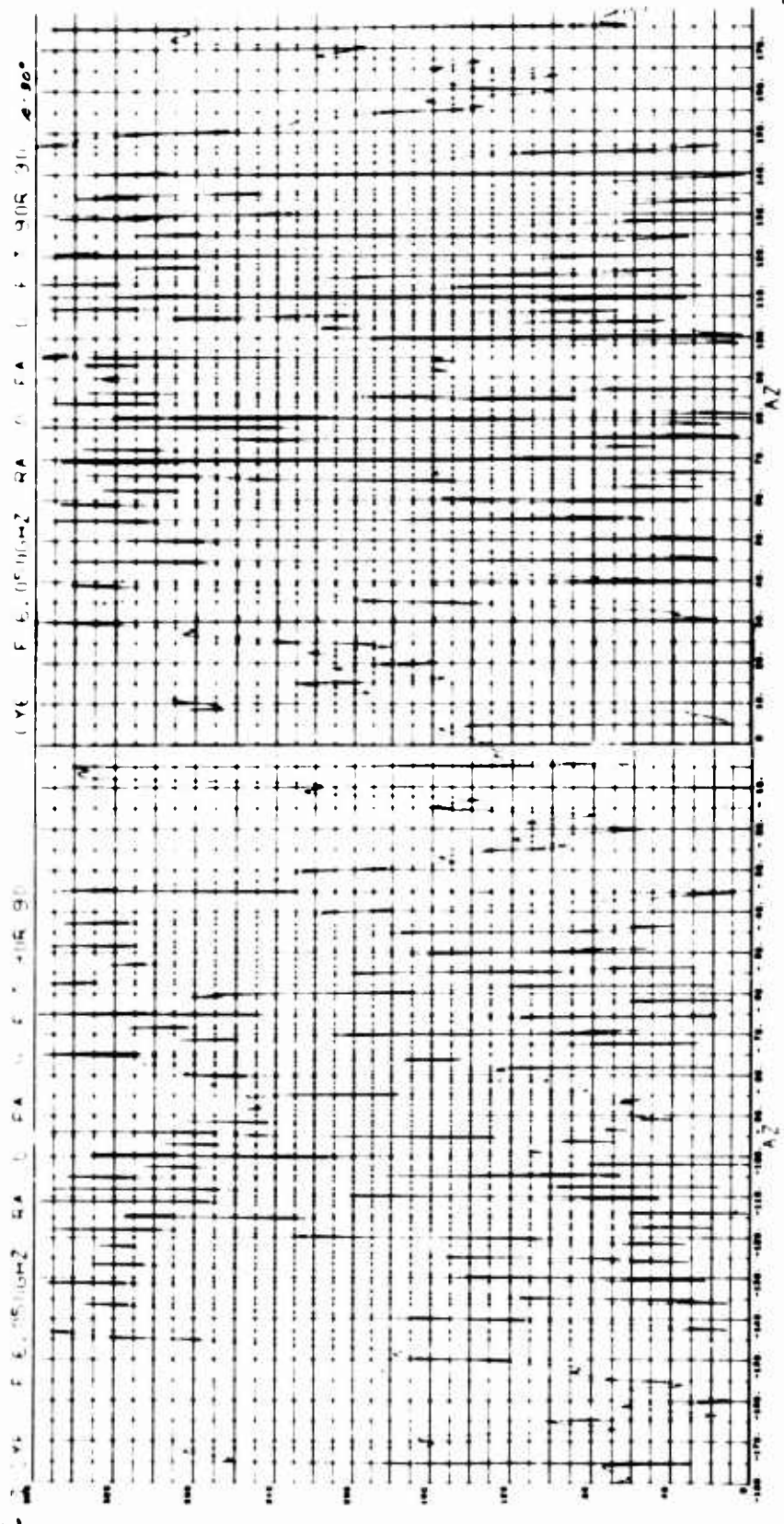
BISTATIC ANGLE = 30.0 DEGREES



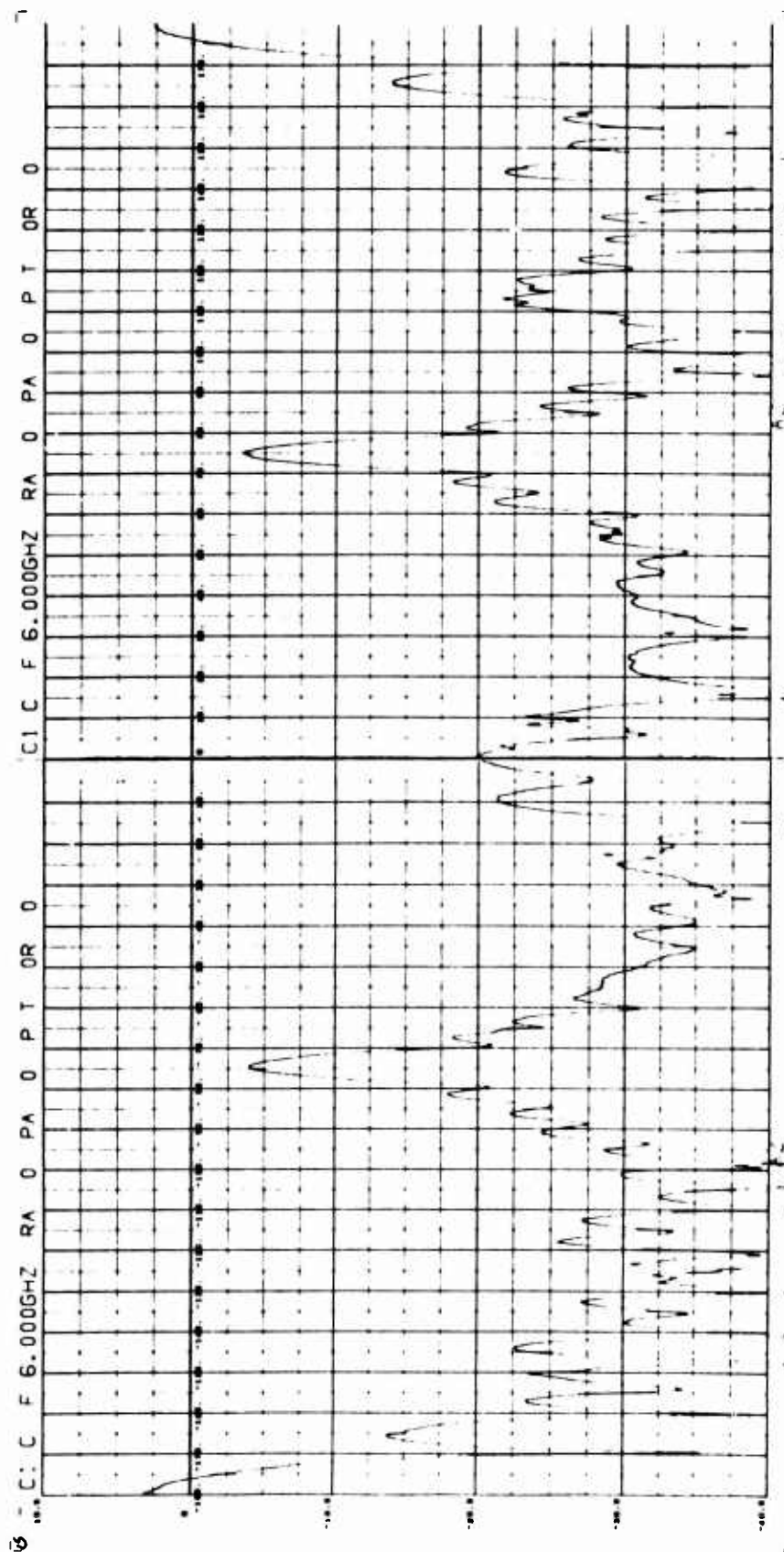
BISTATIC ANGLE - 30.0 DEGREES

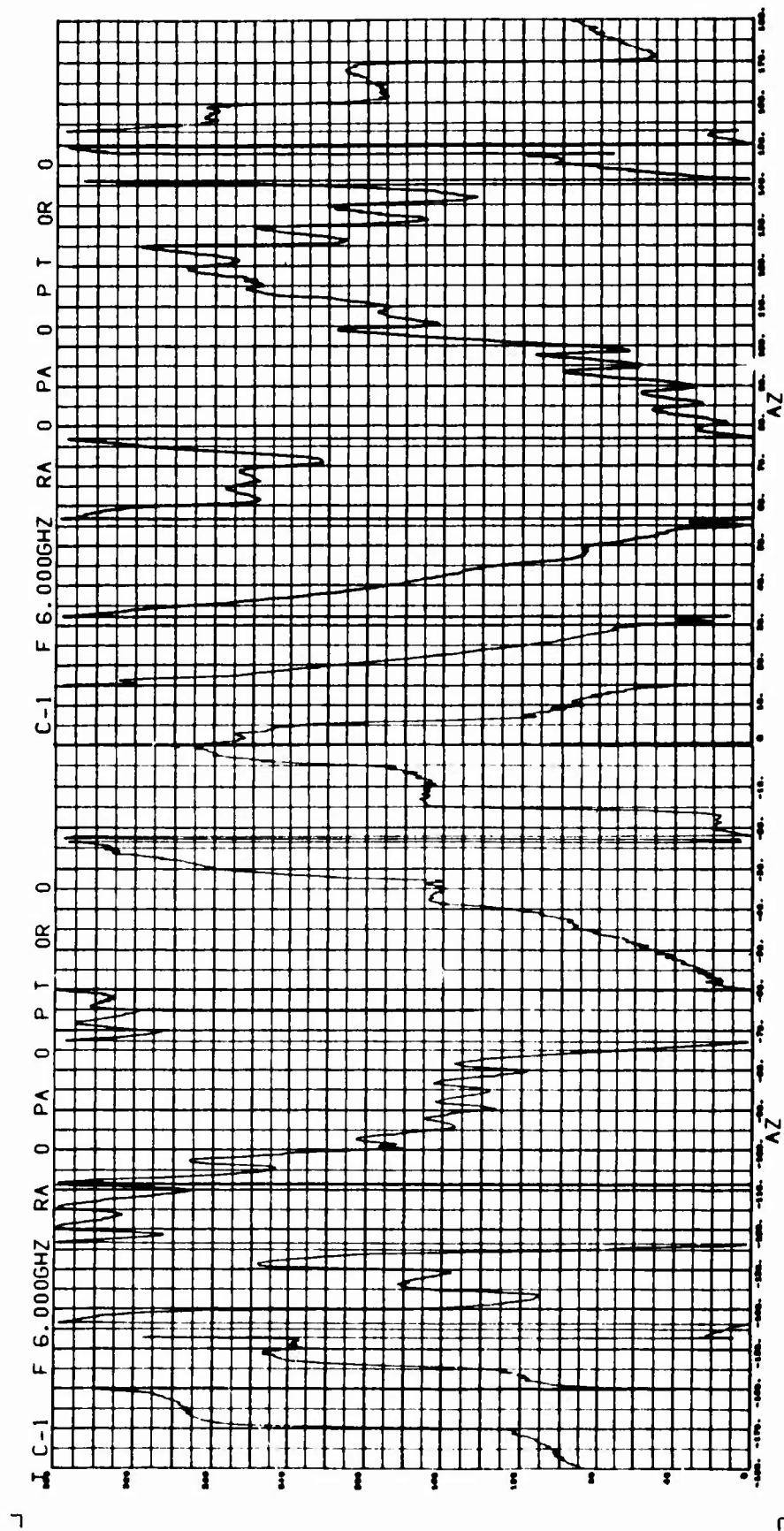


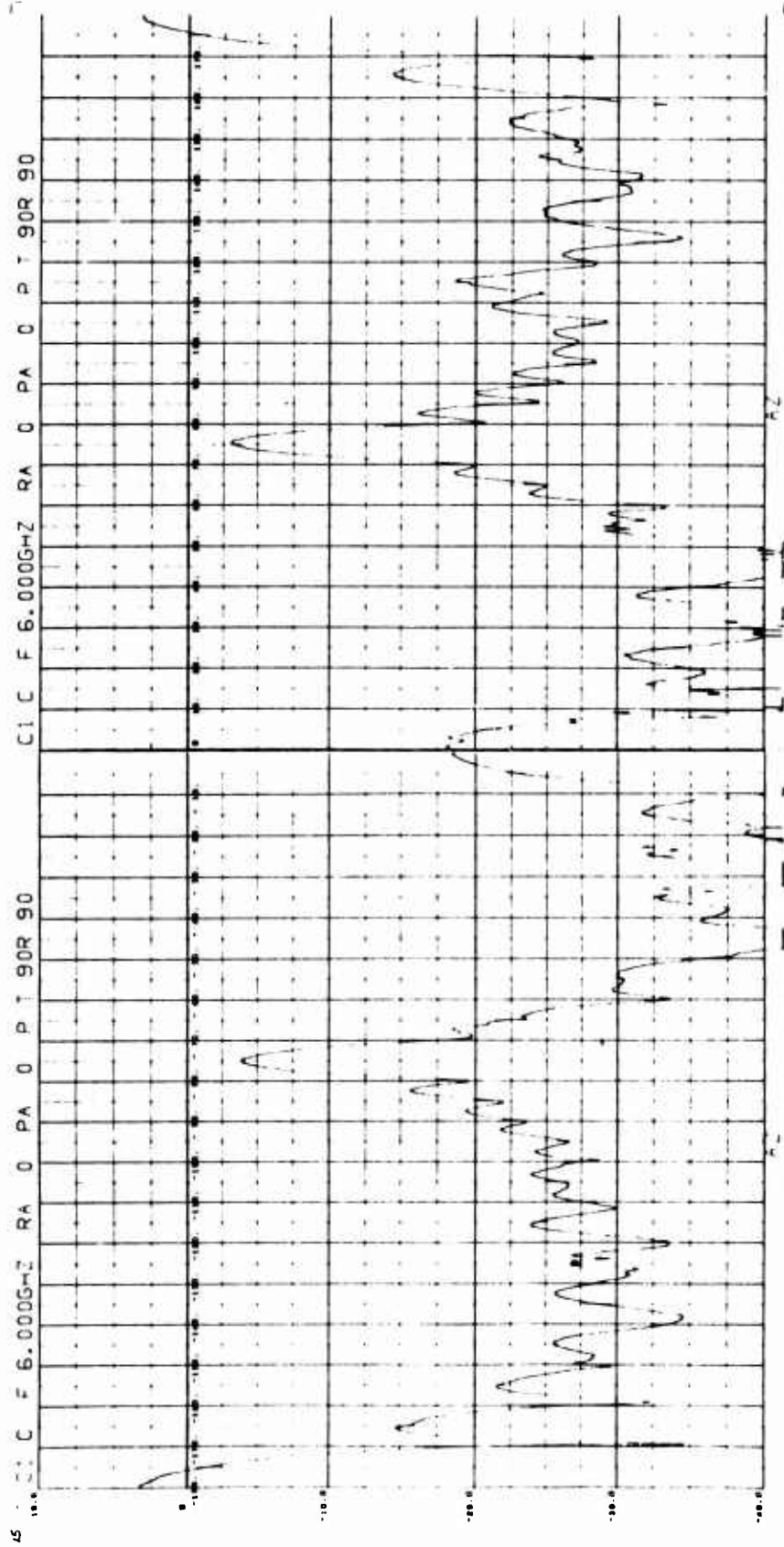
BISTATIC ANGLE - 30.0 DEGREES

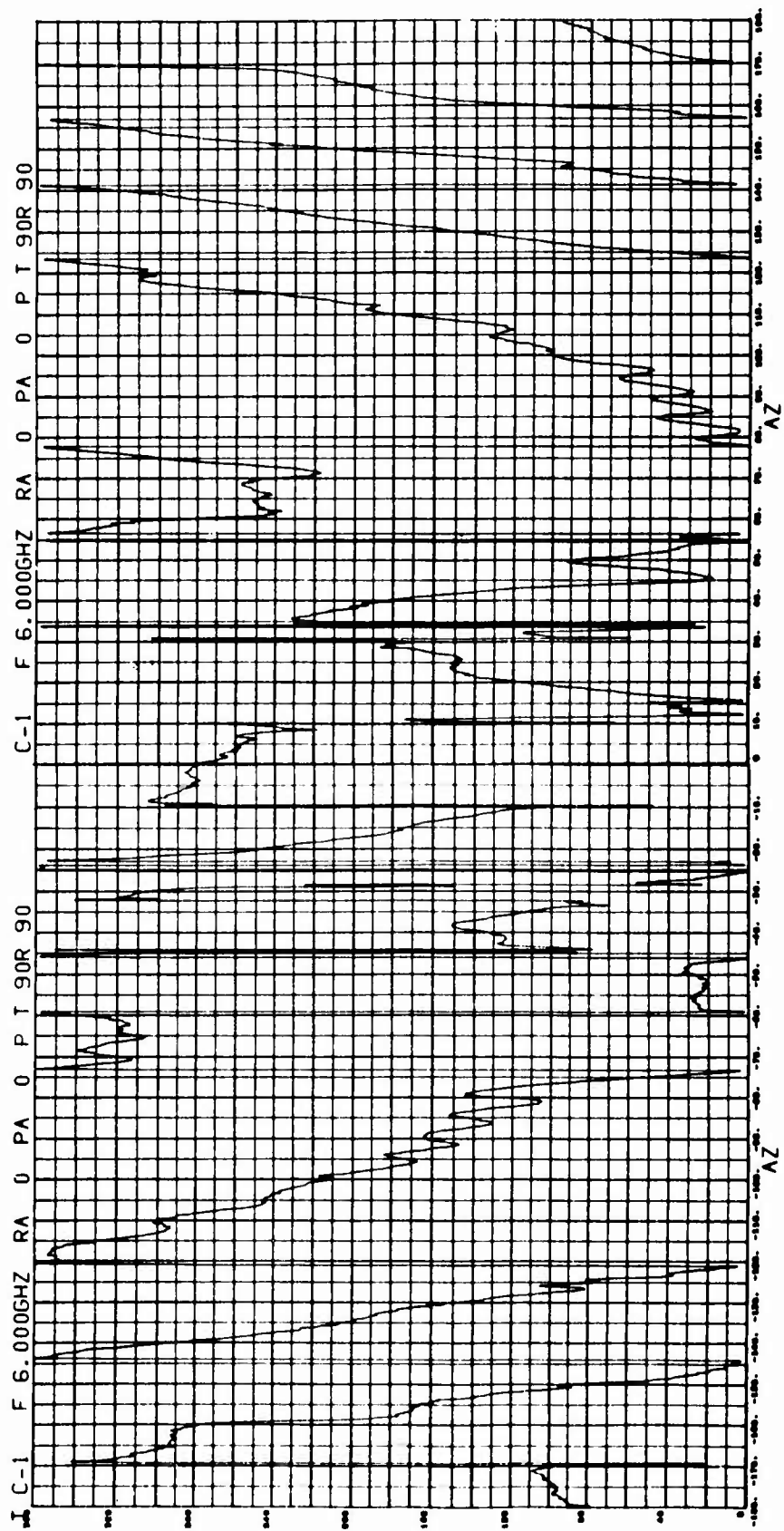


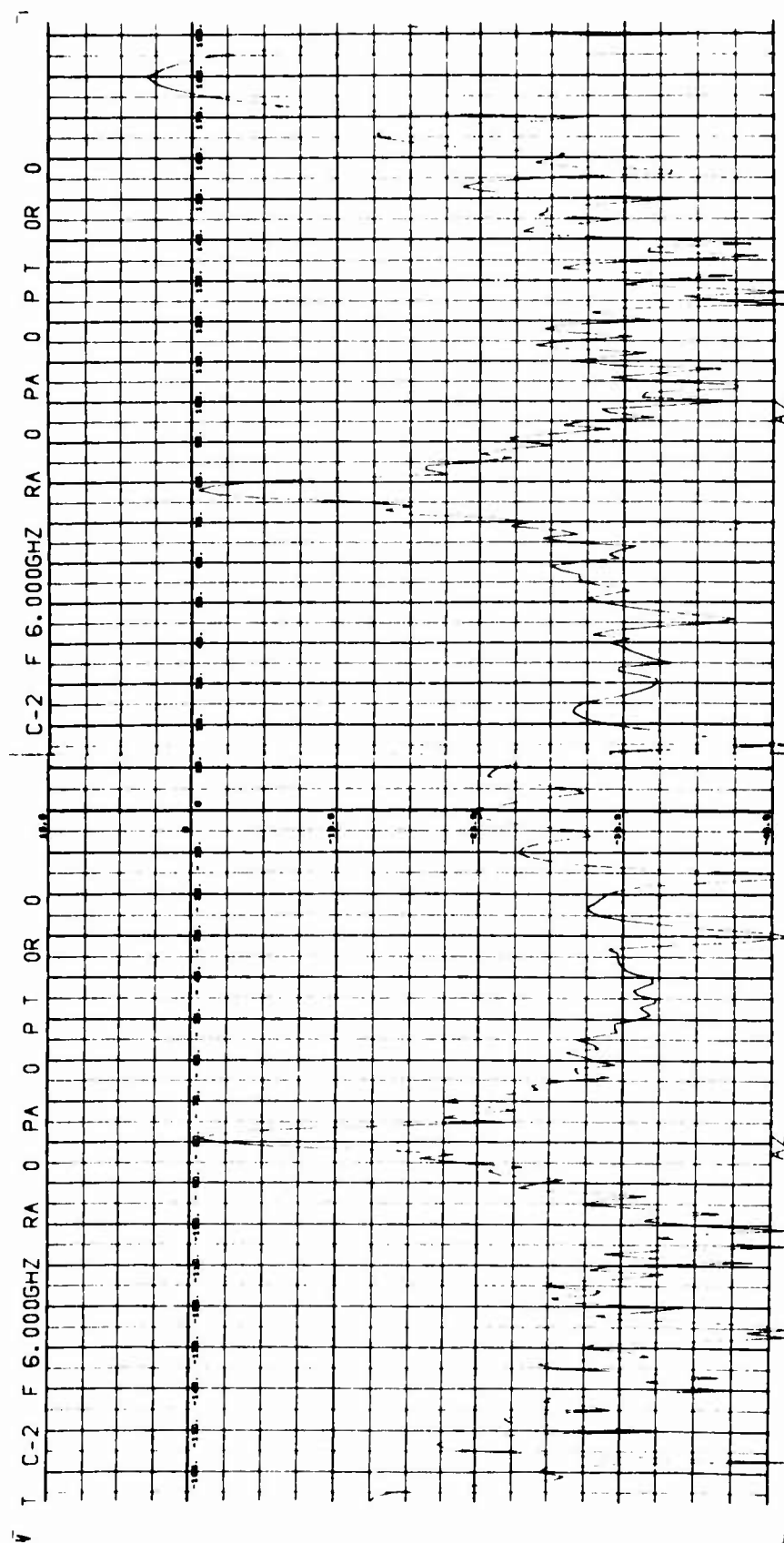
BISTATIC ANGLE = 30.0 DEGREES

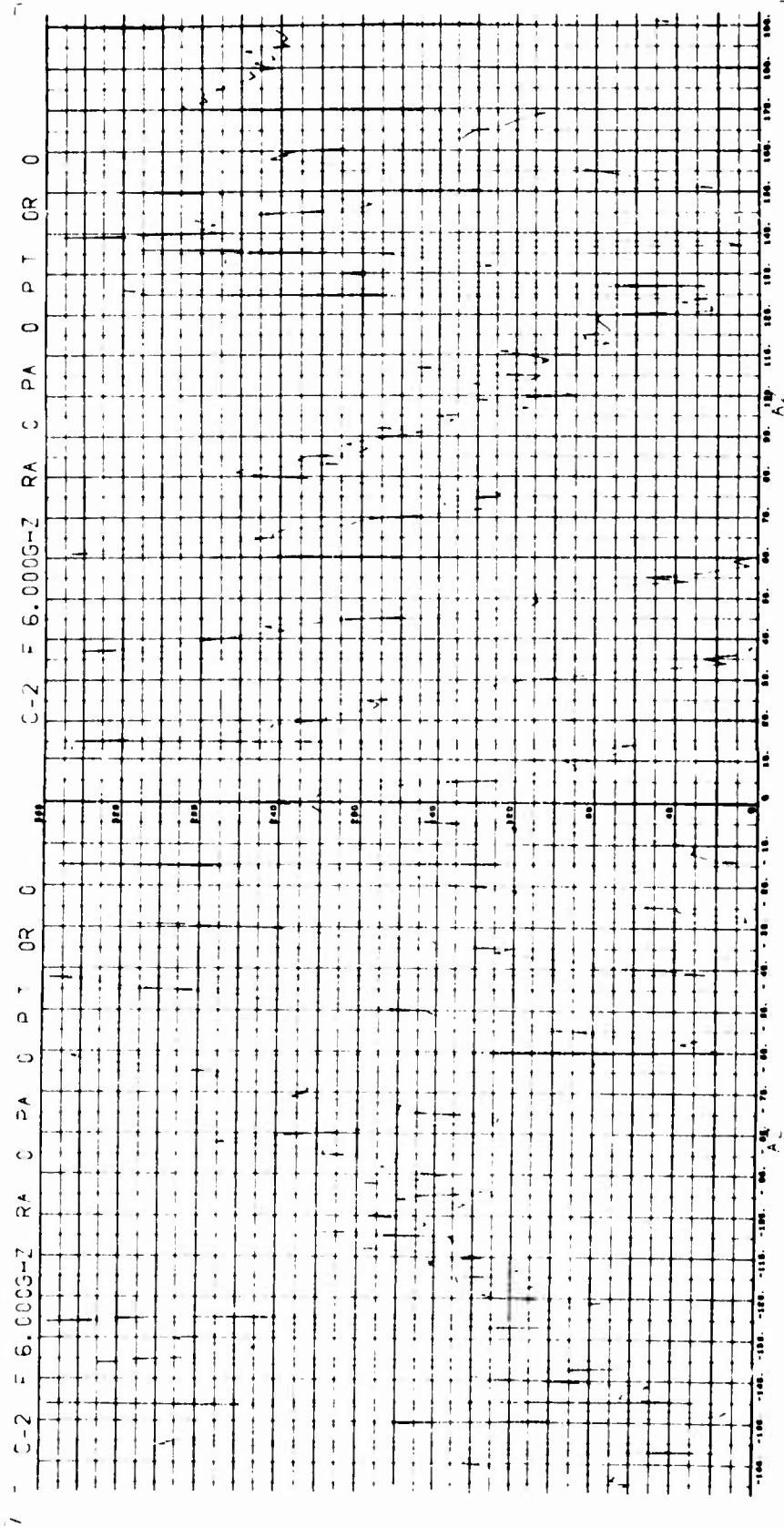


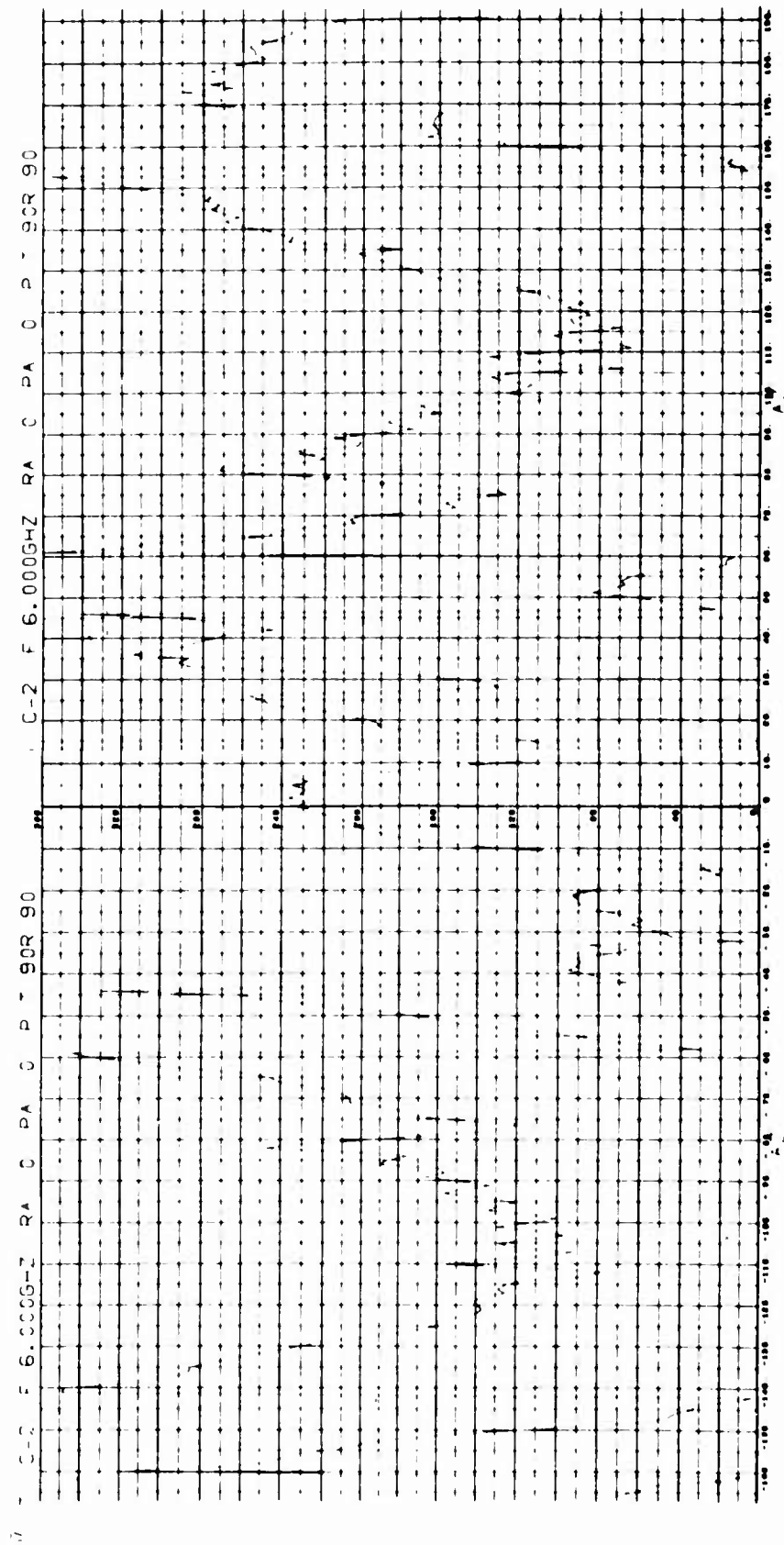


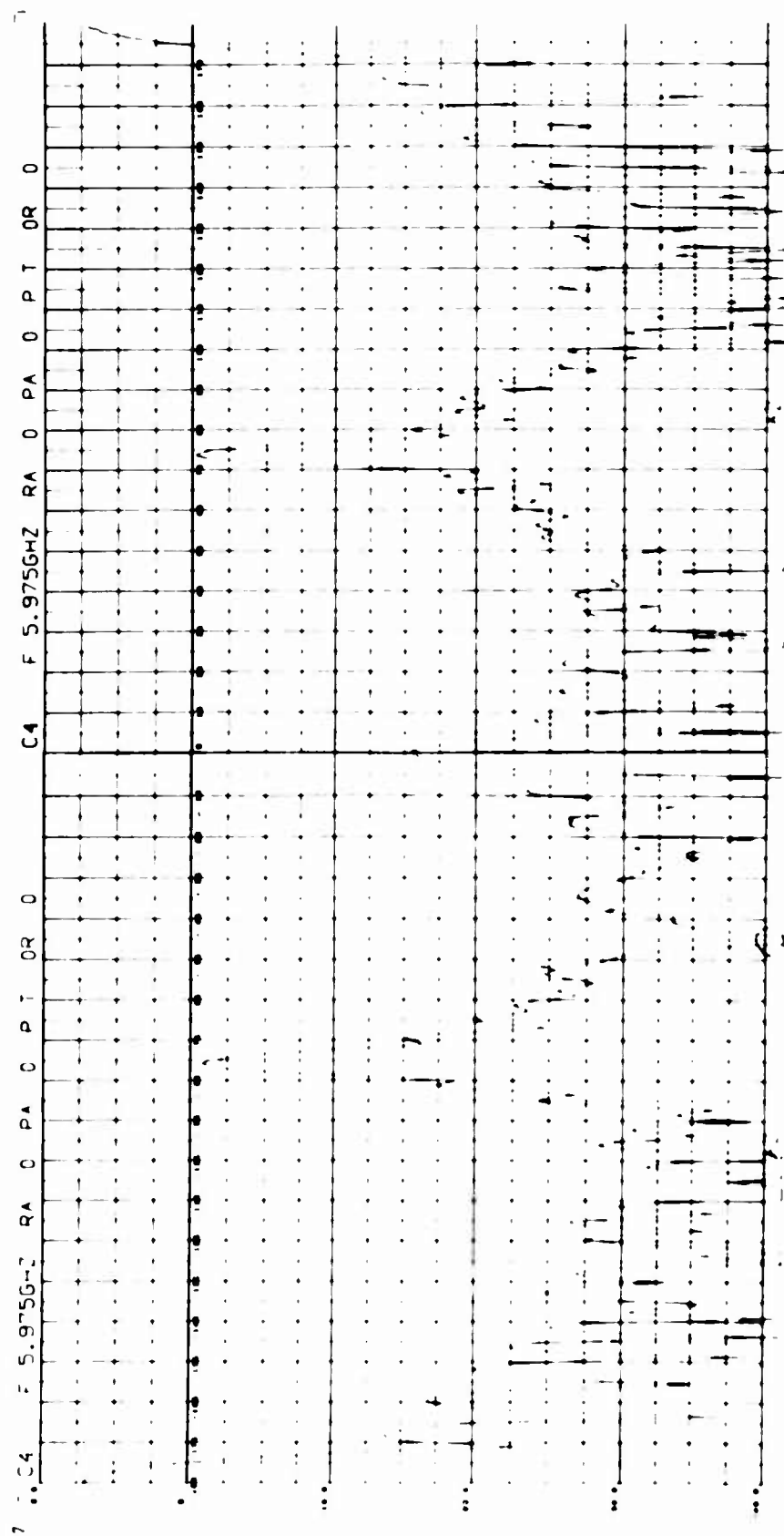


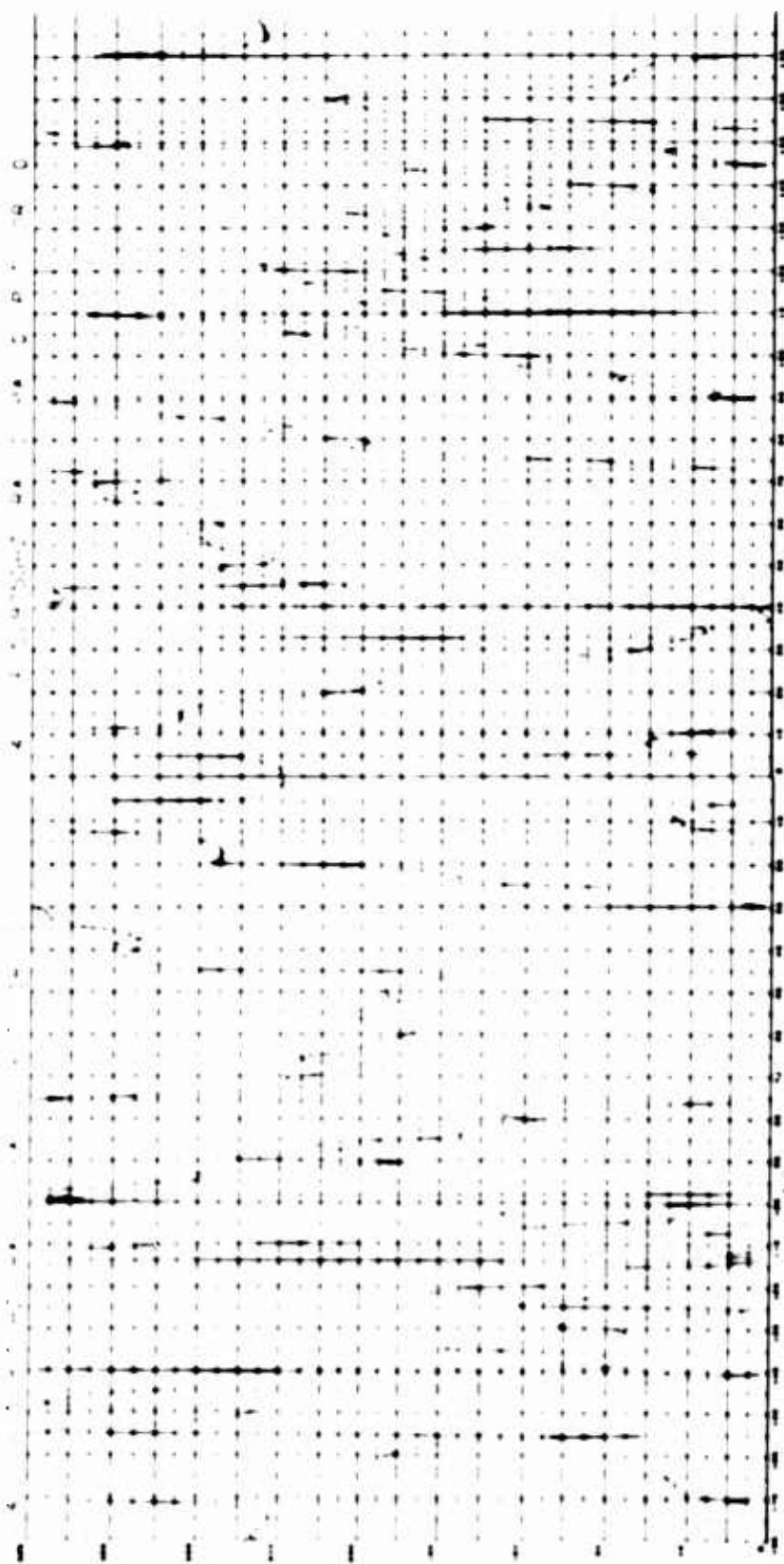


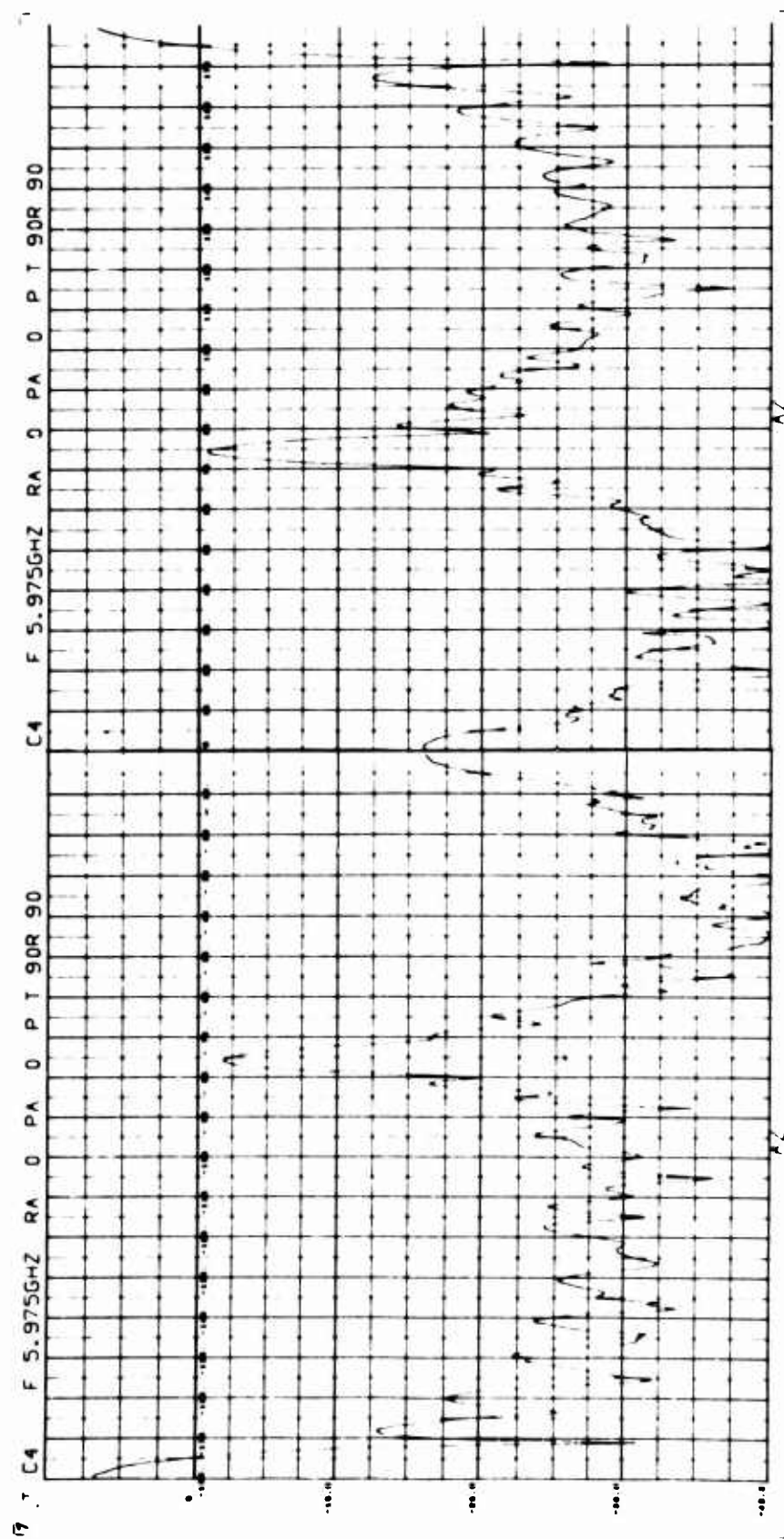


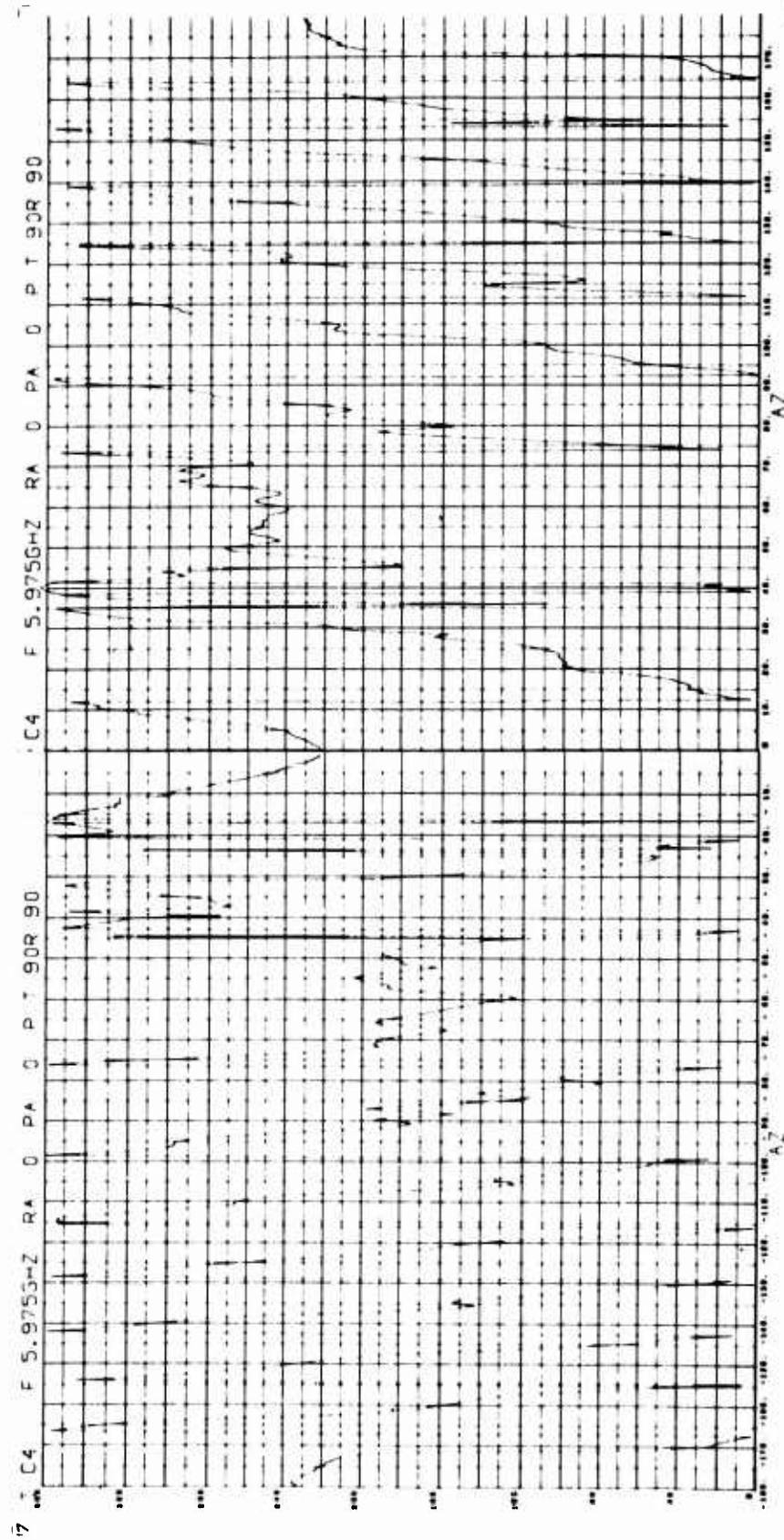


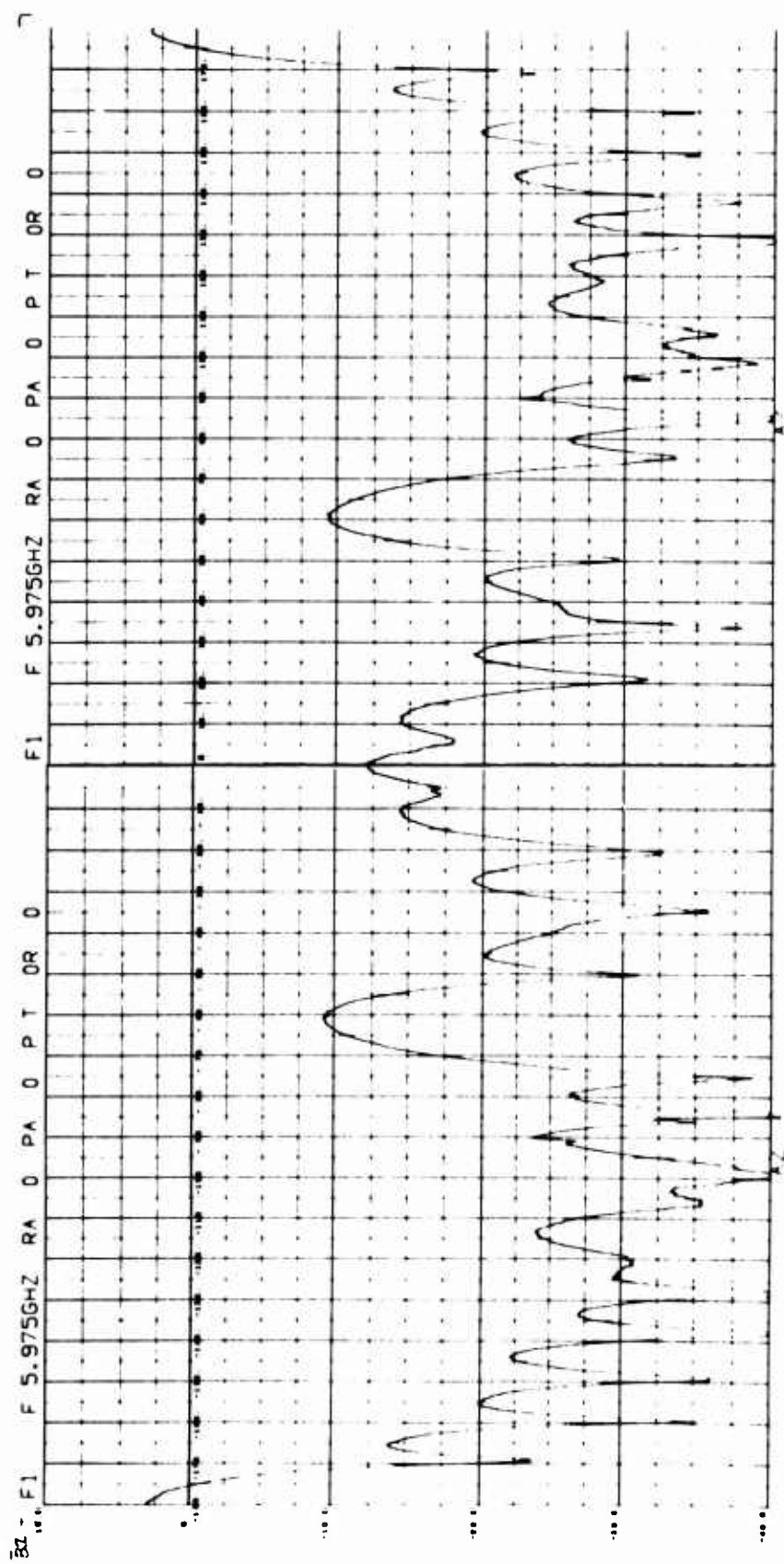


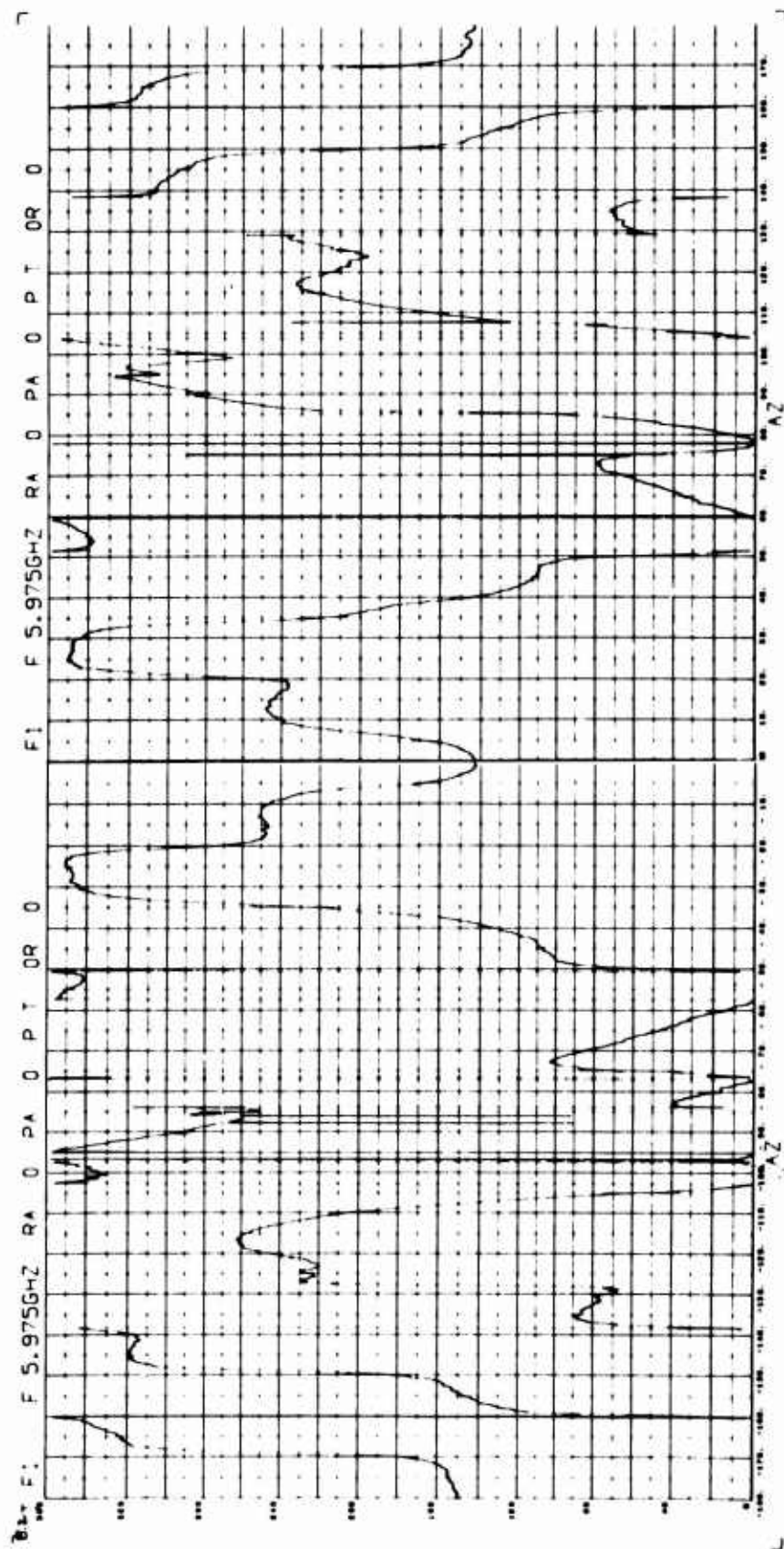


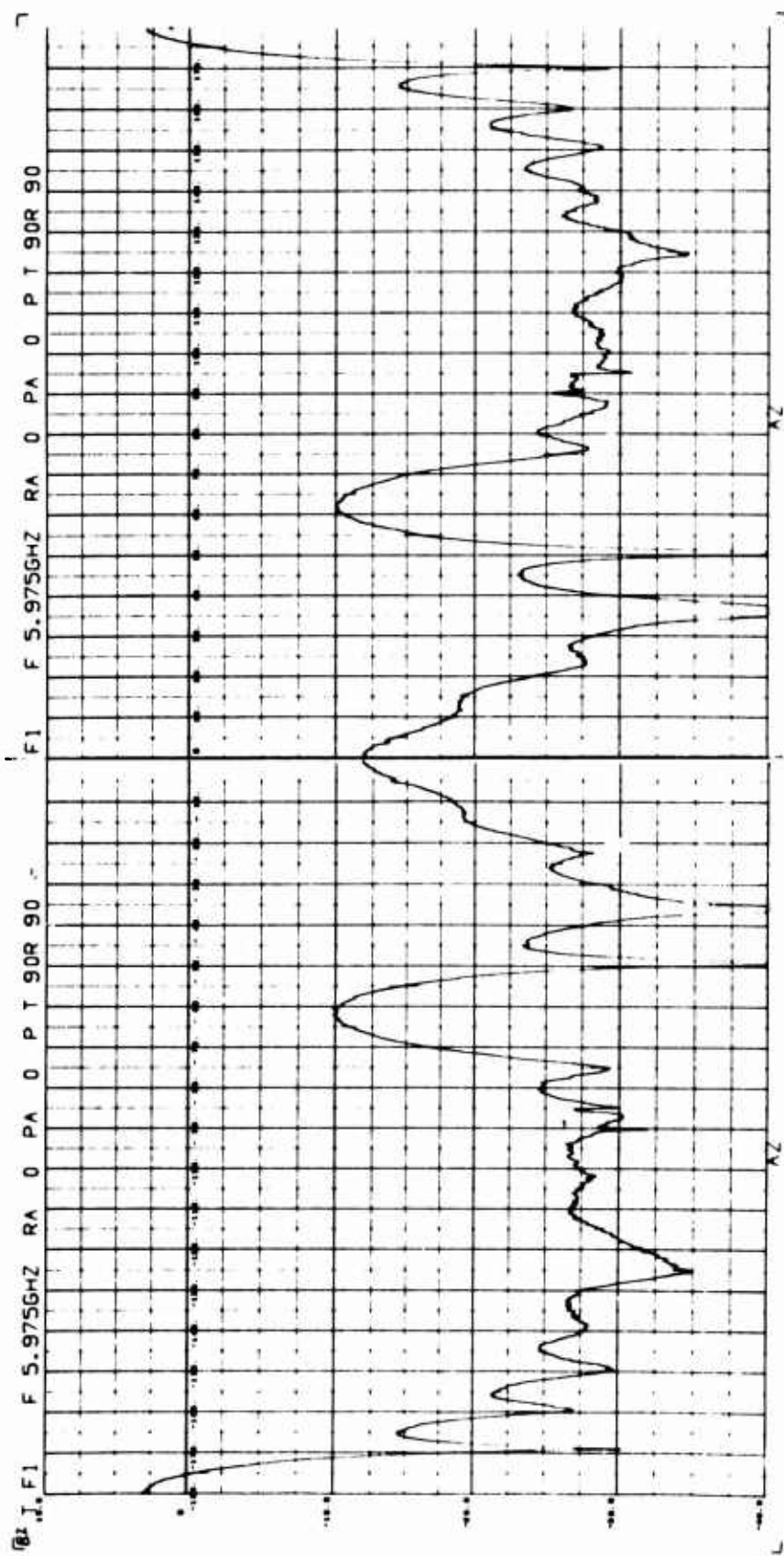


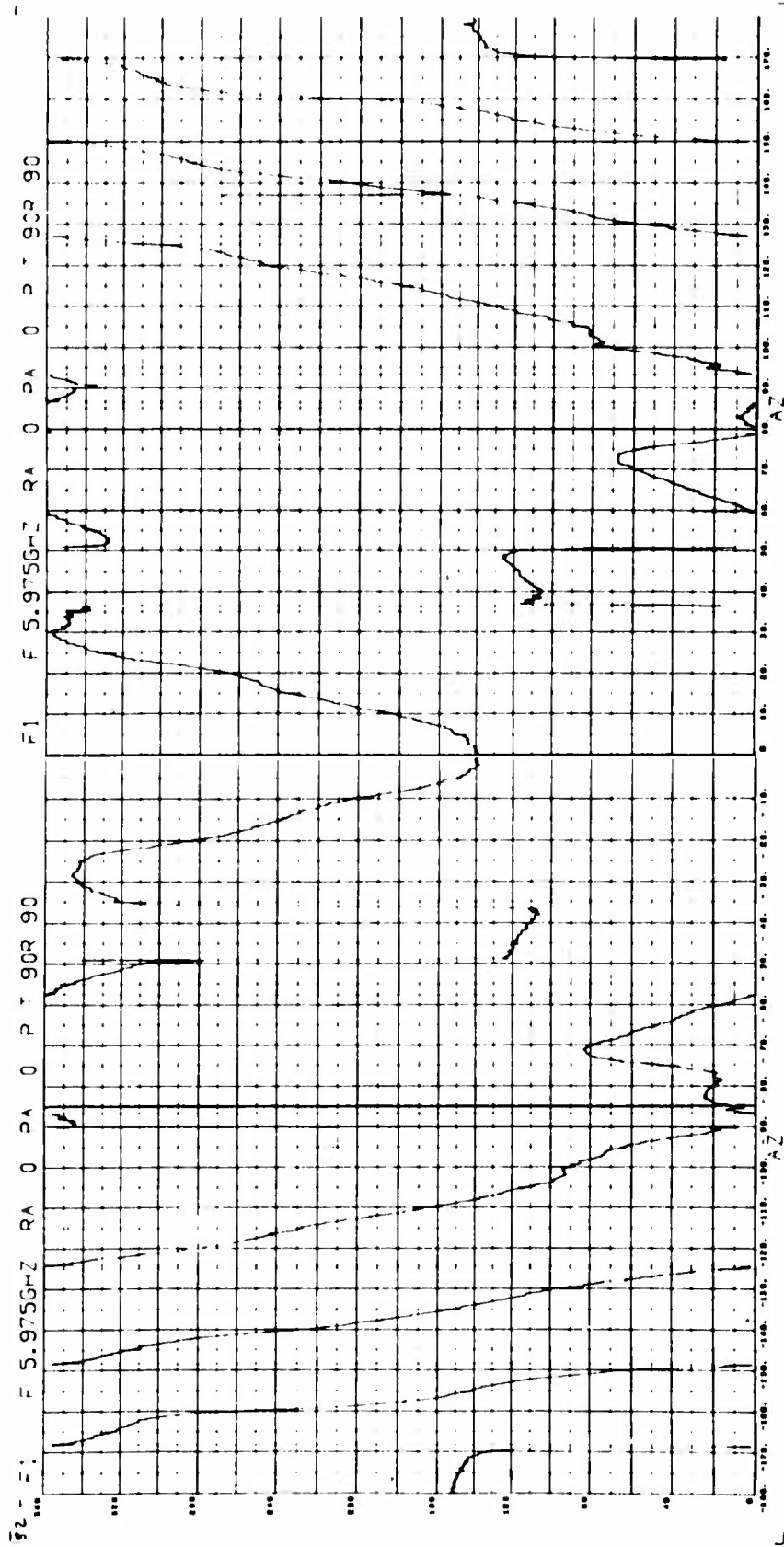


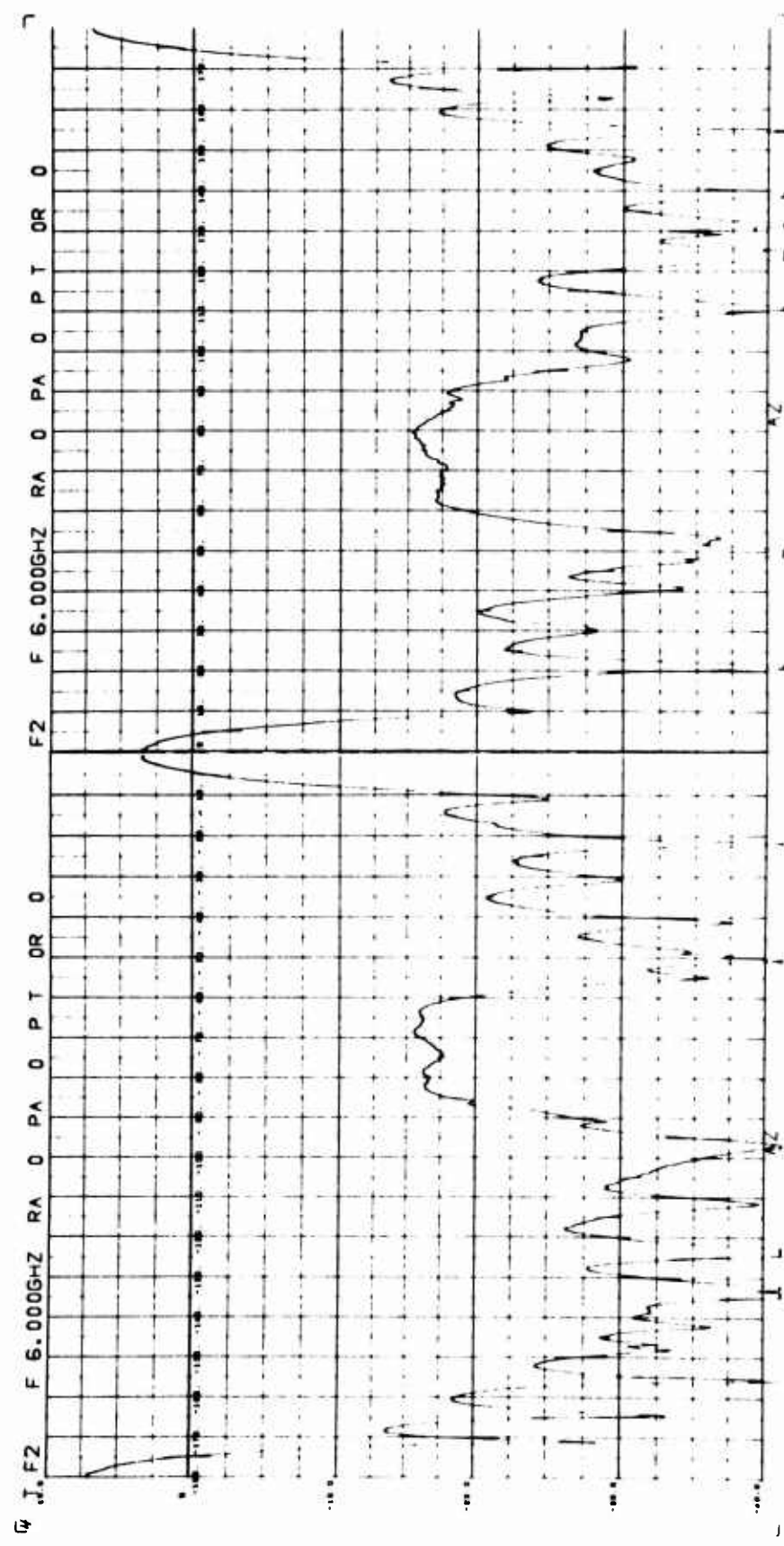


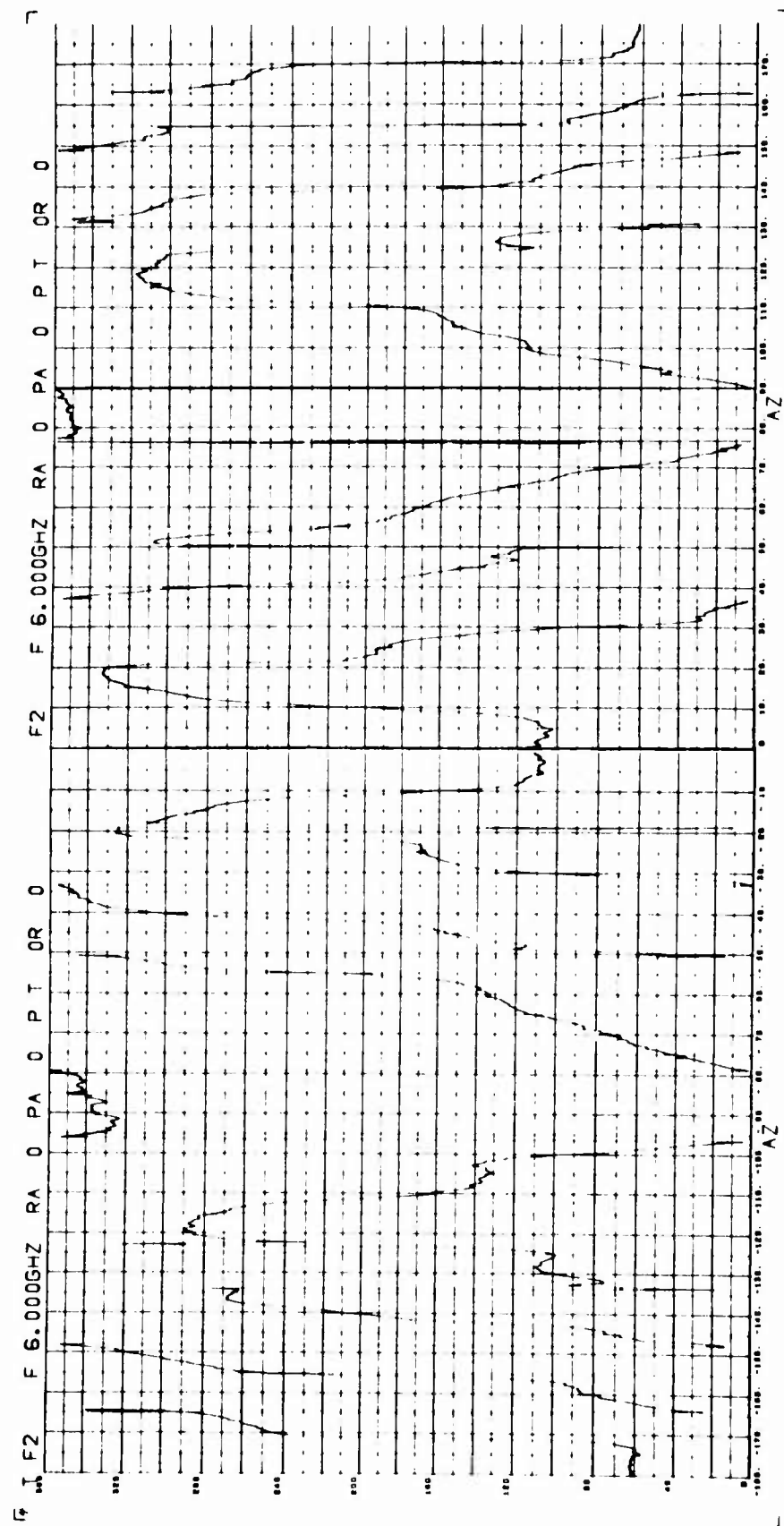


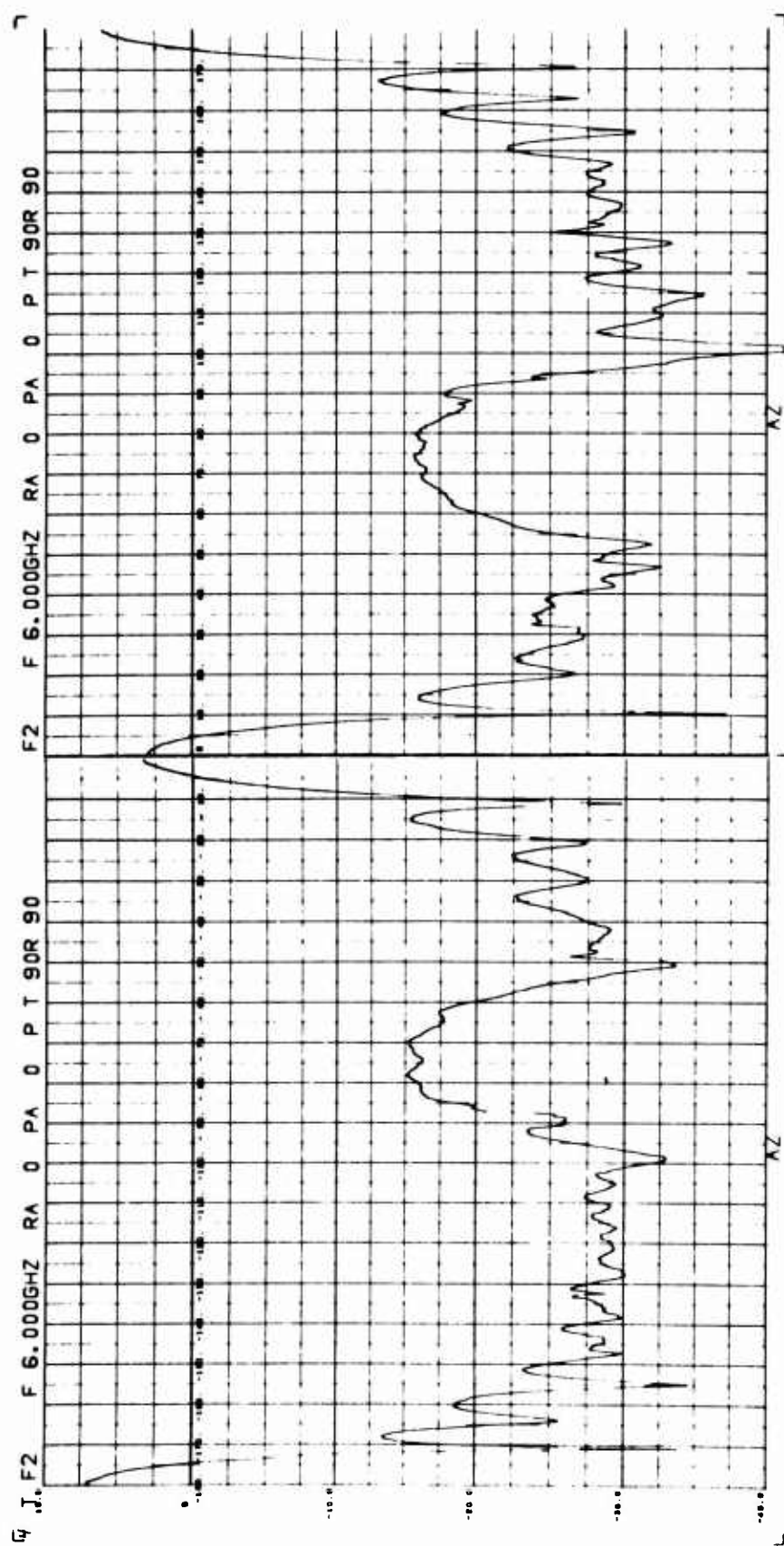


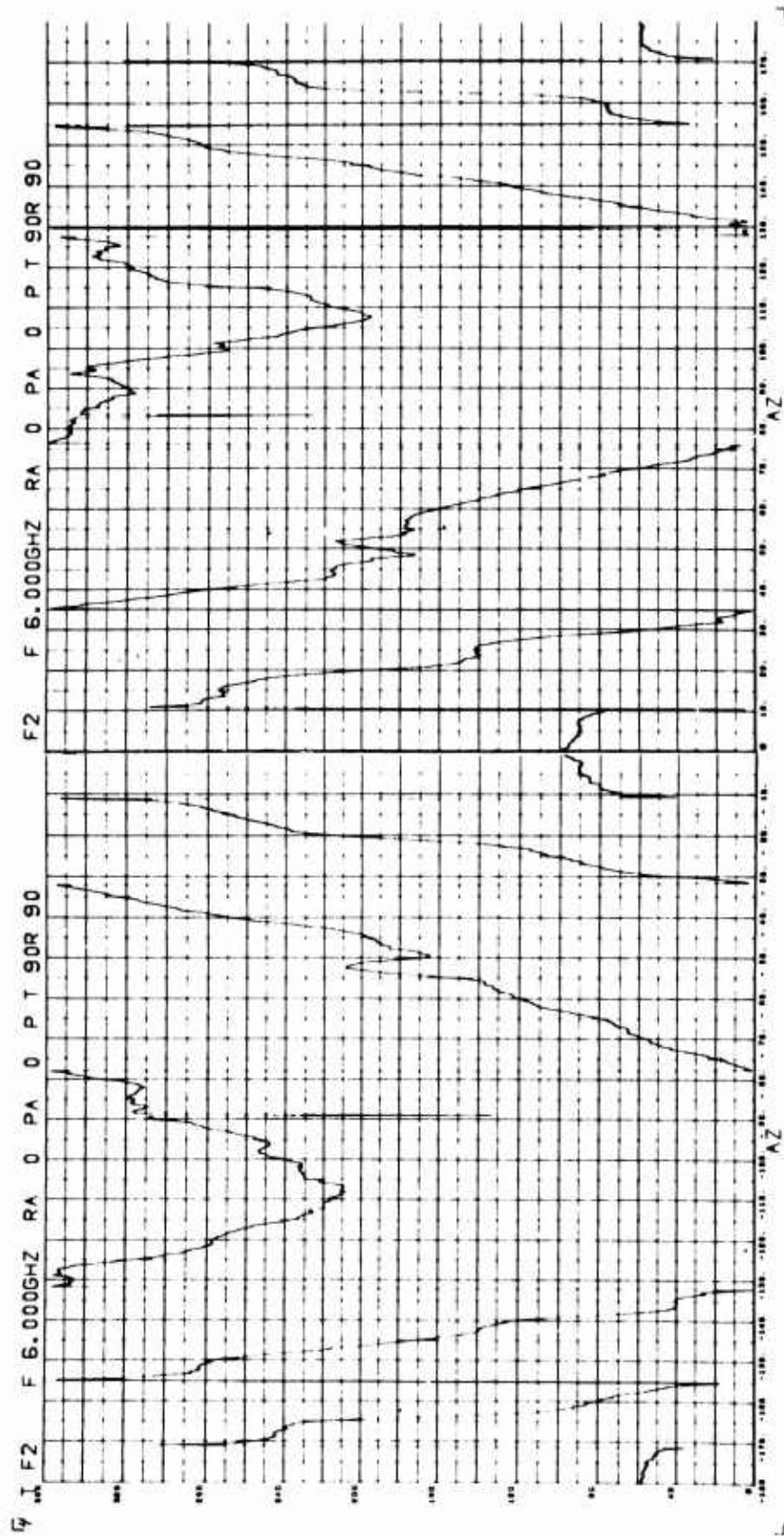


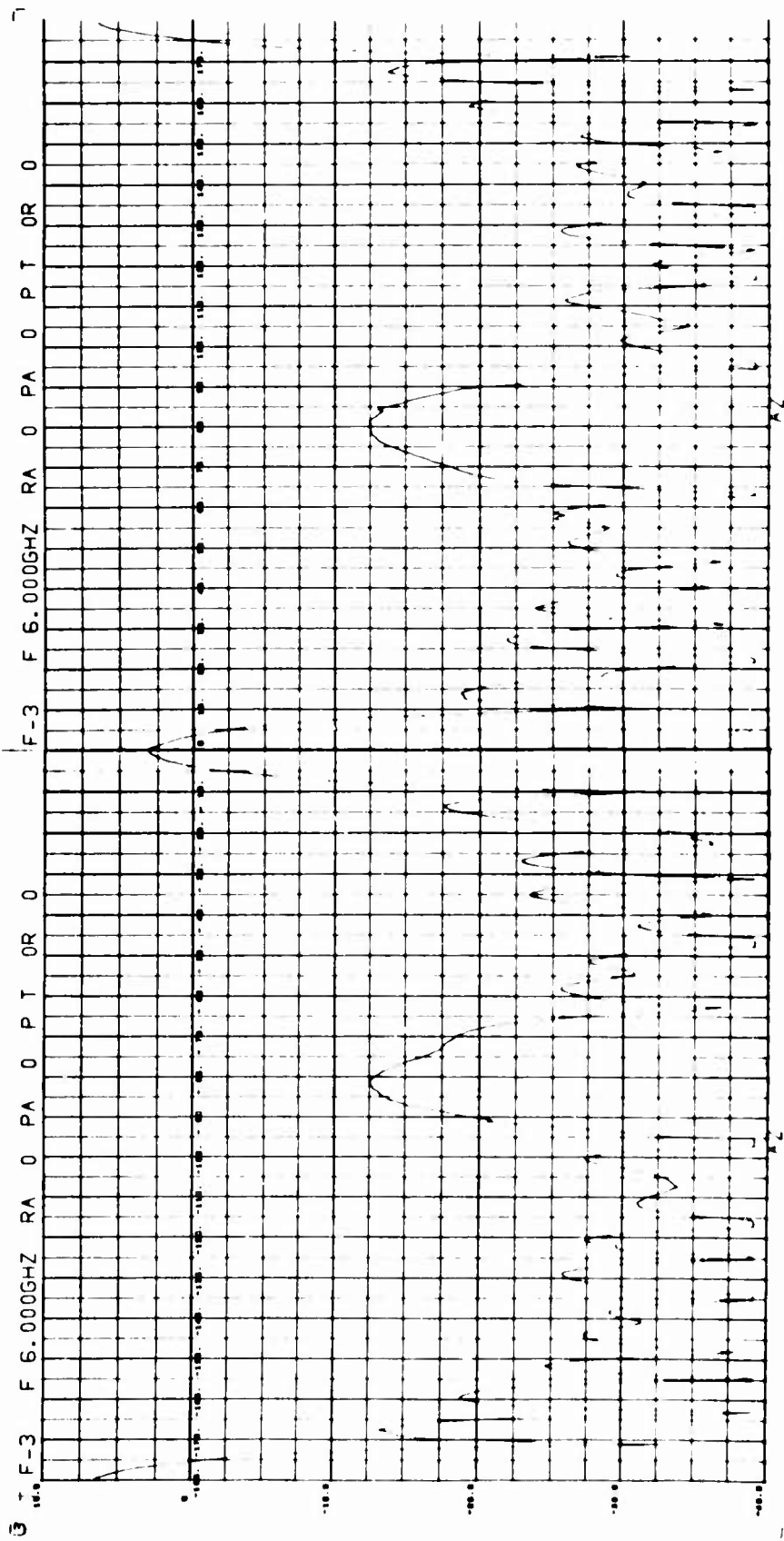


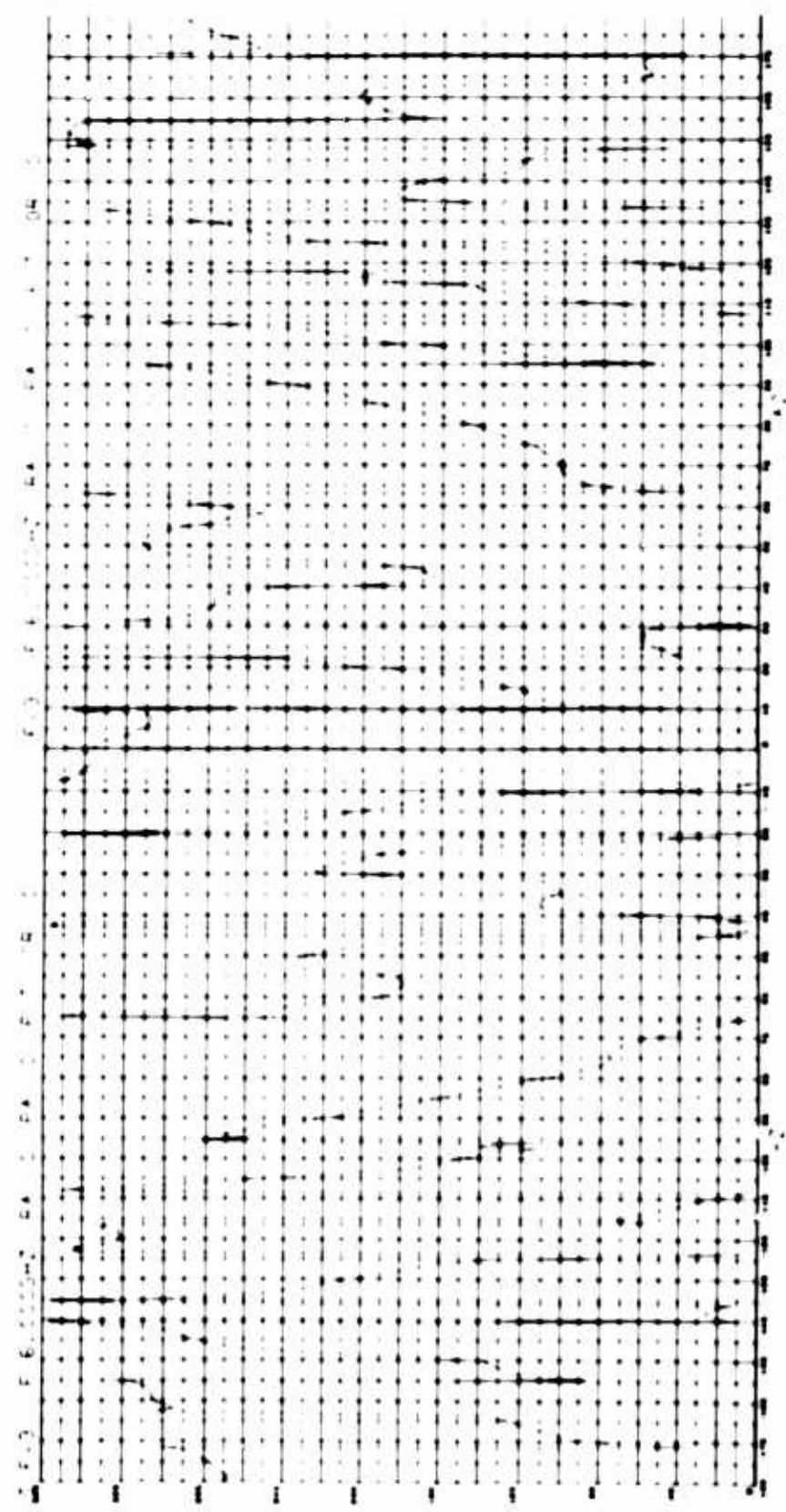


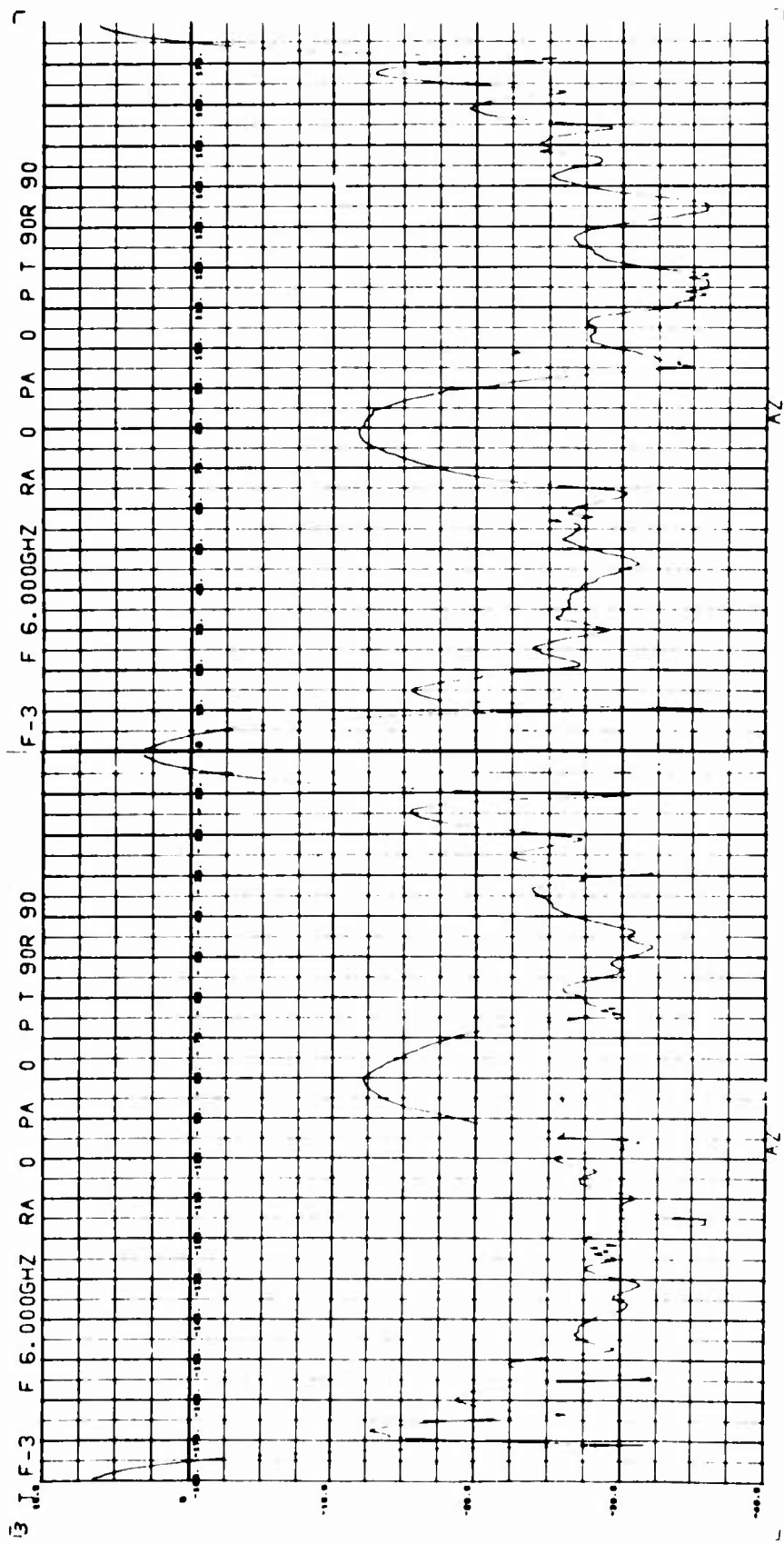


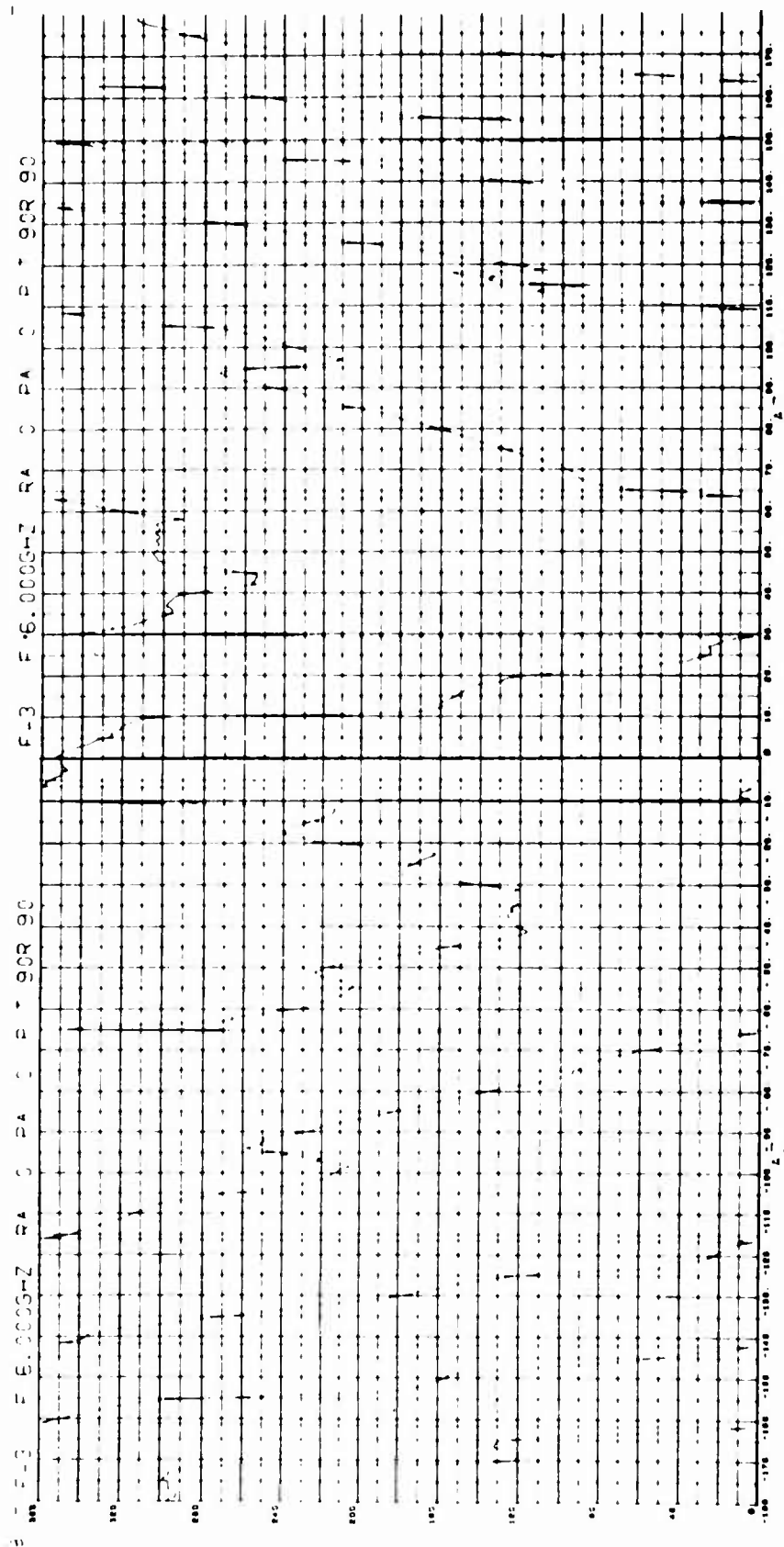


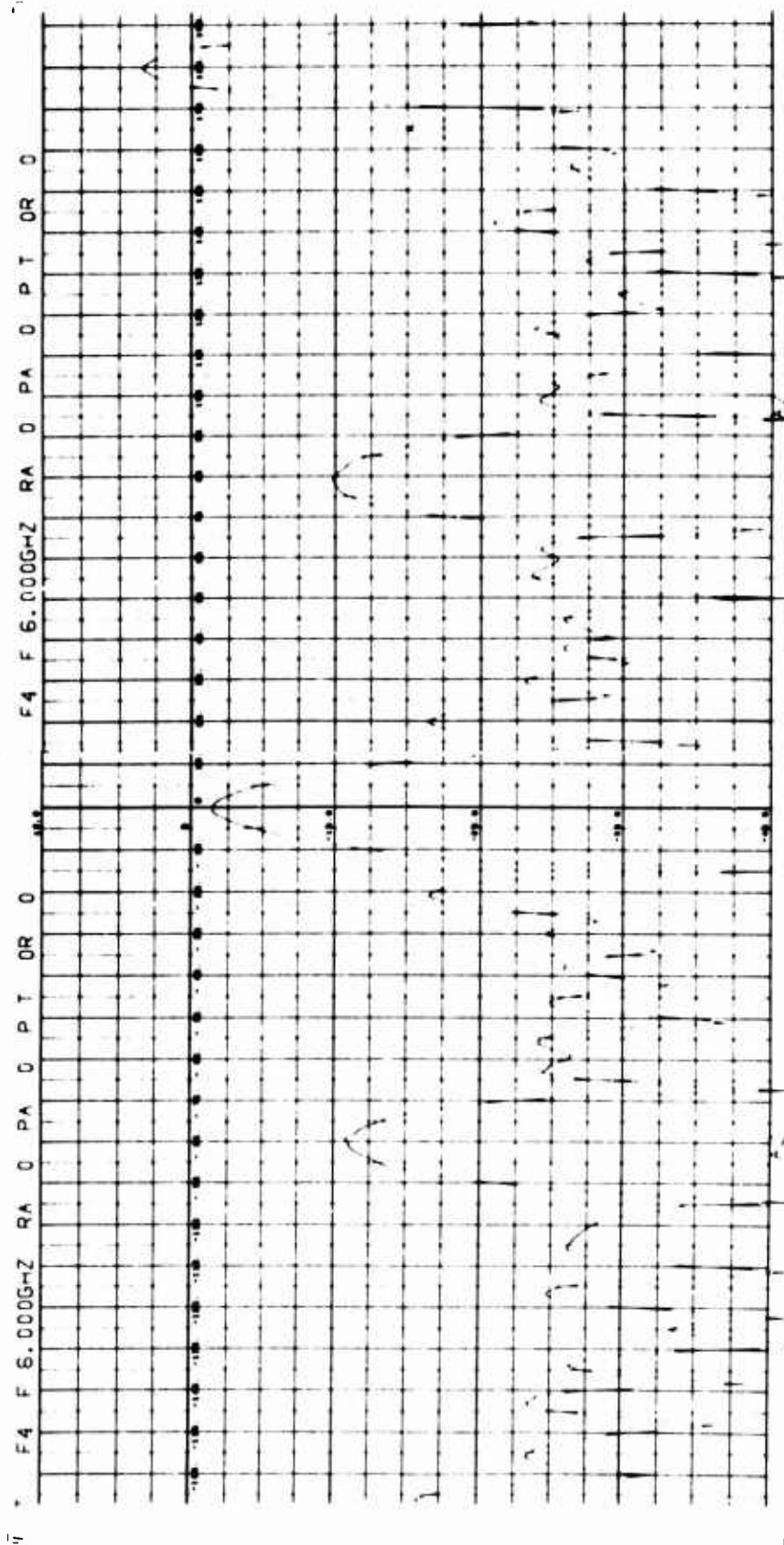


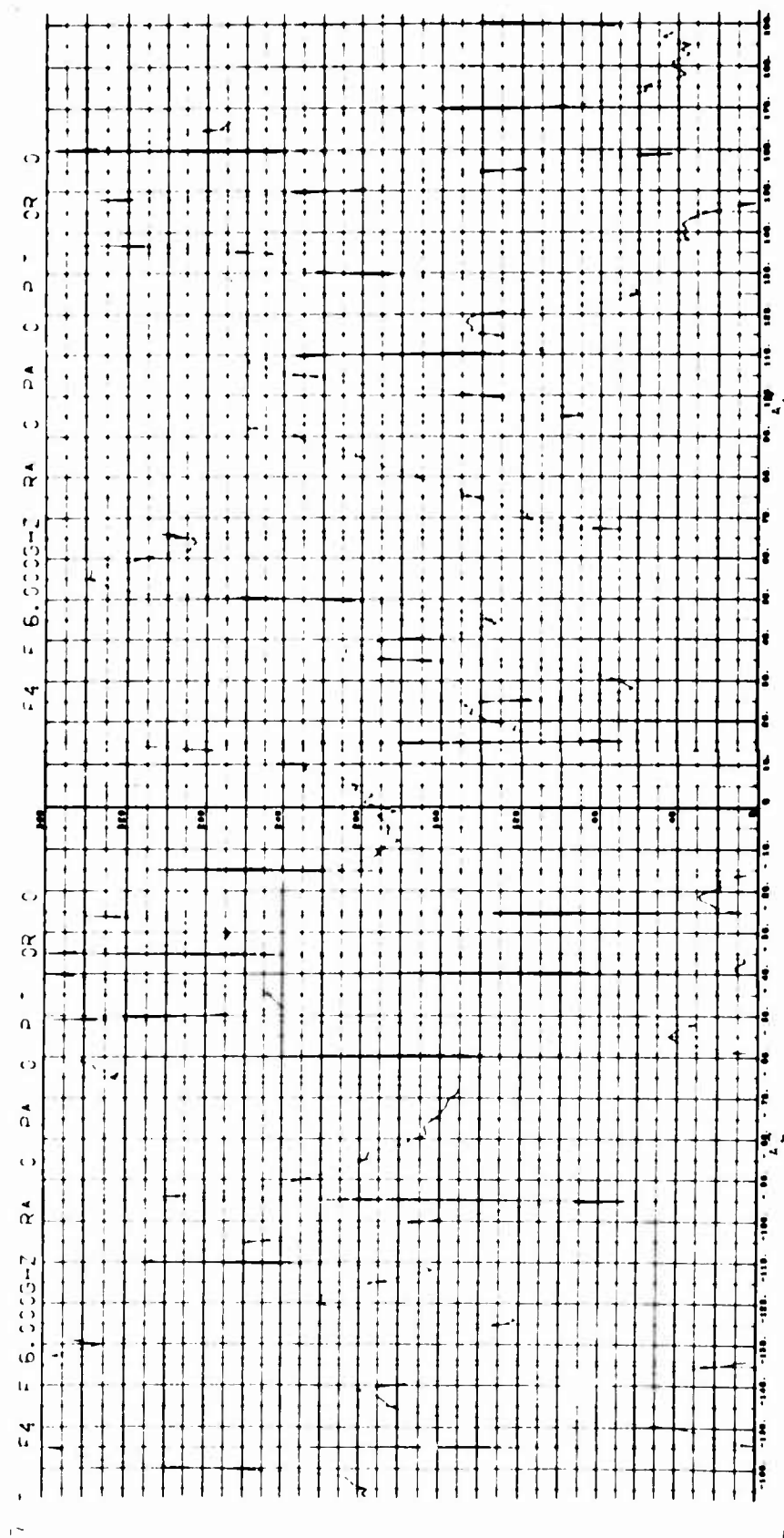


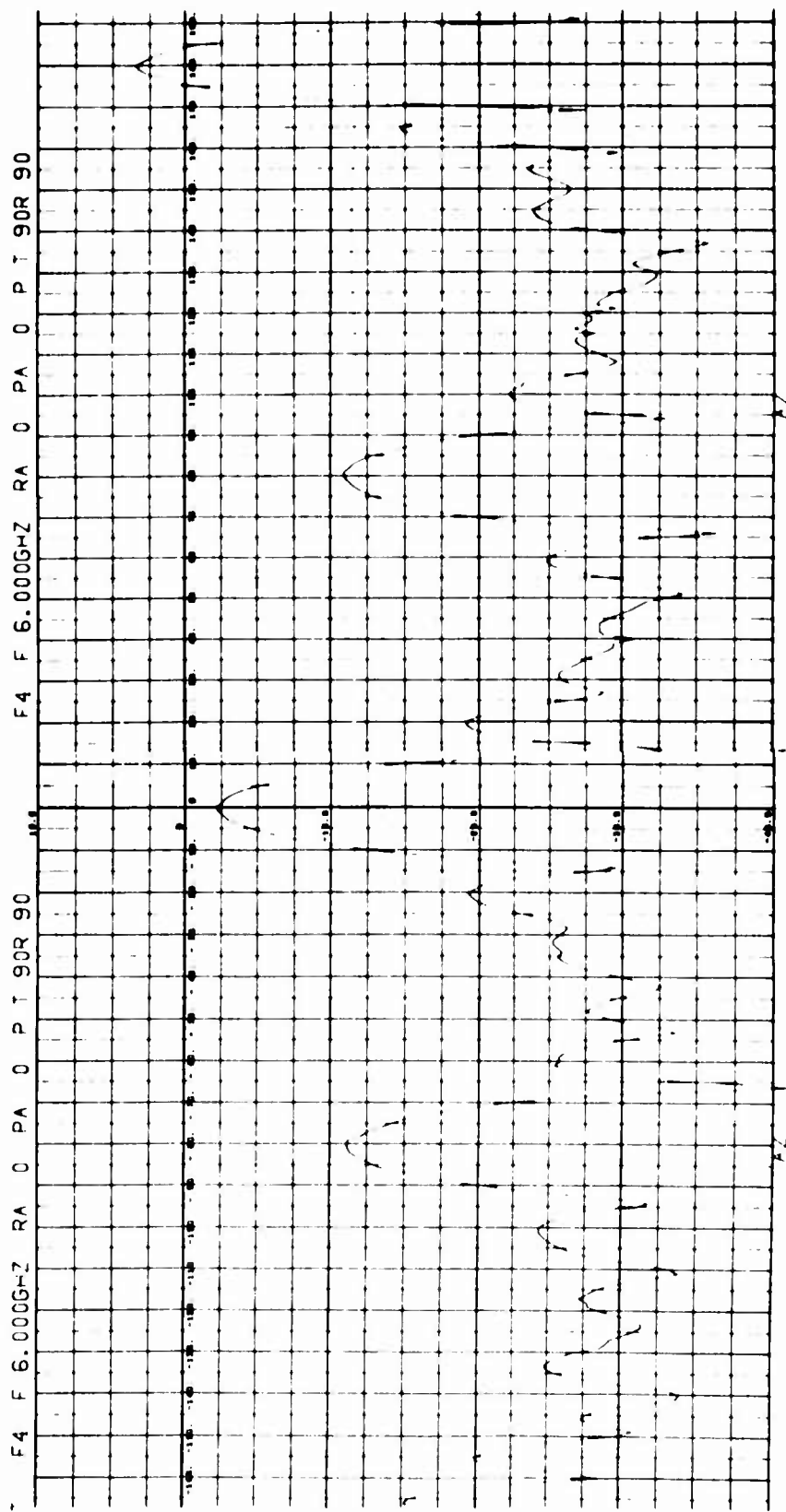


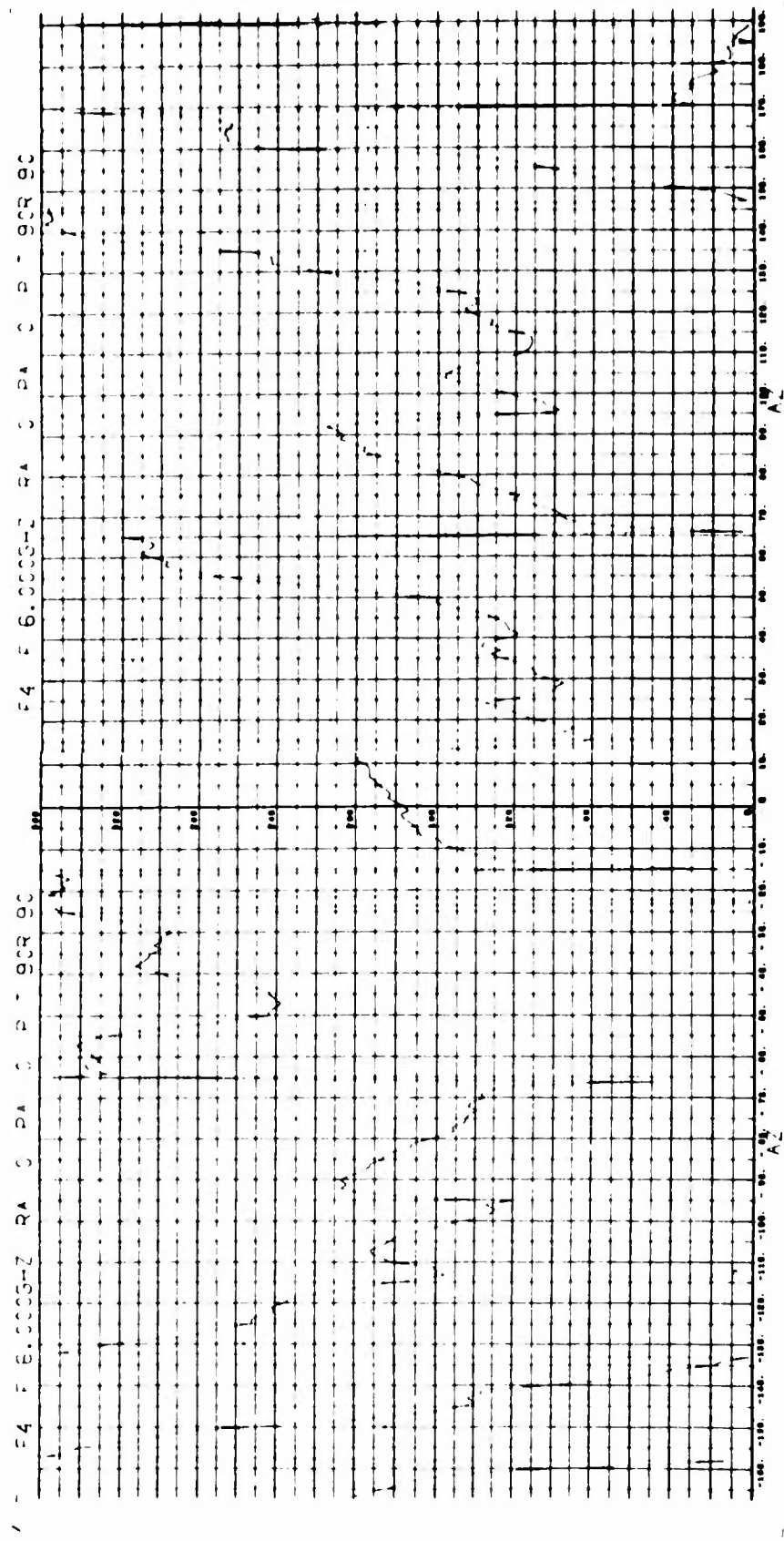


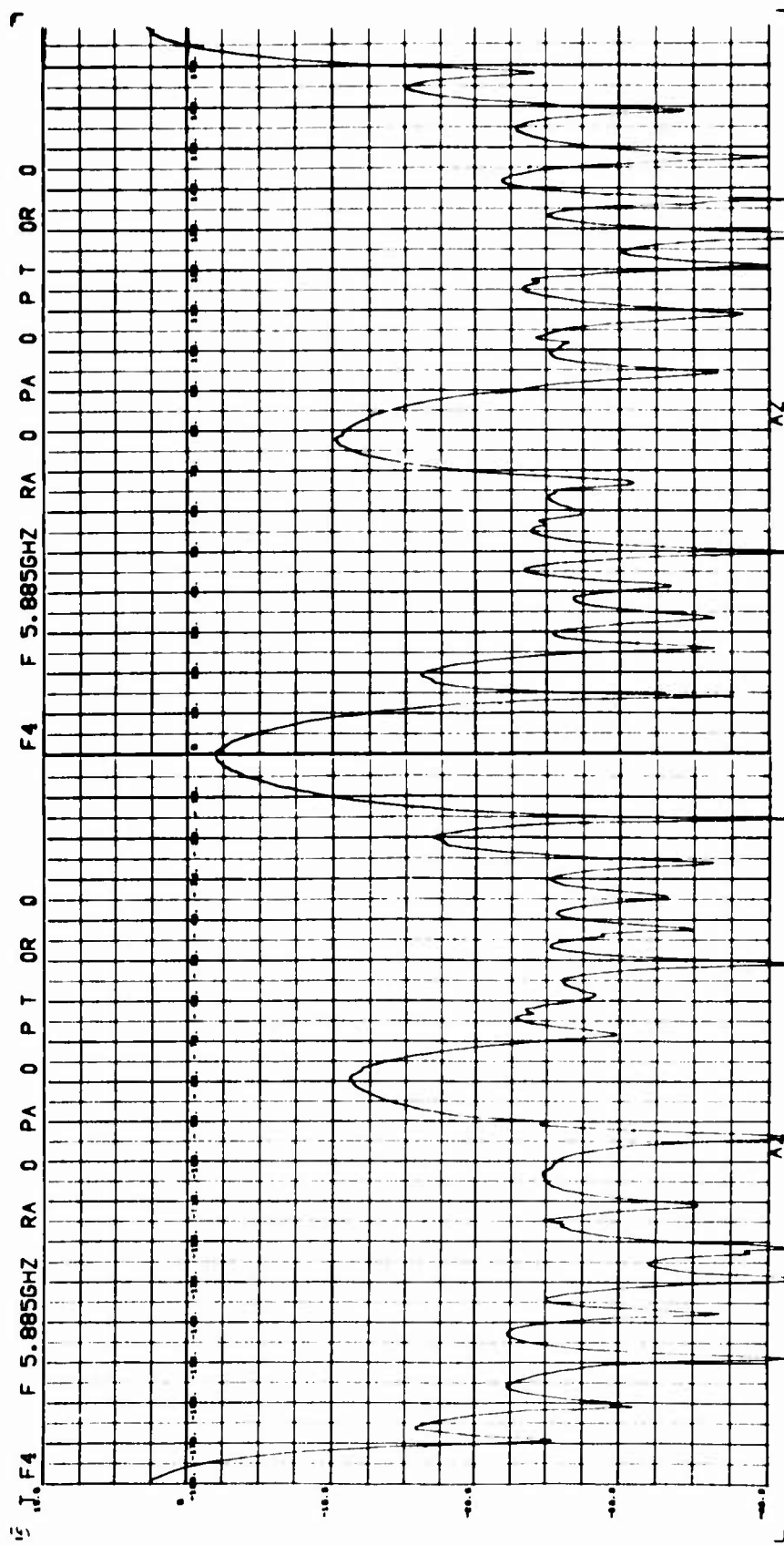




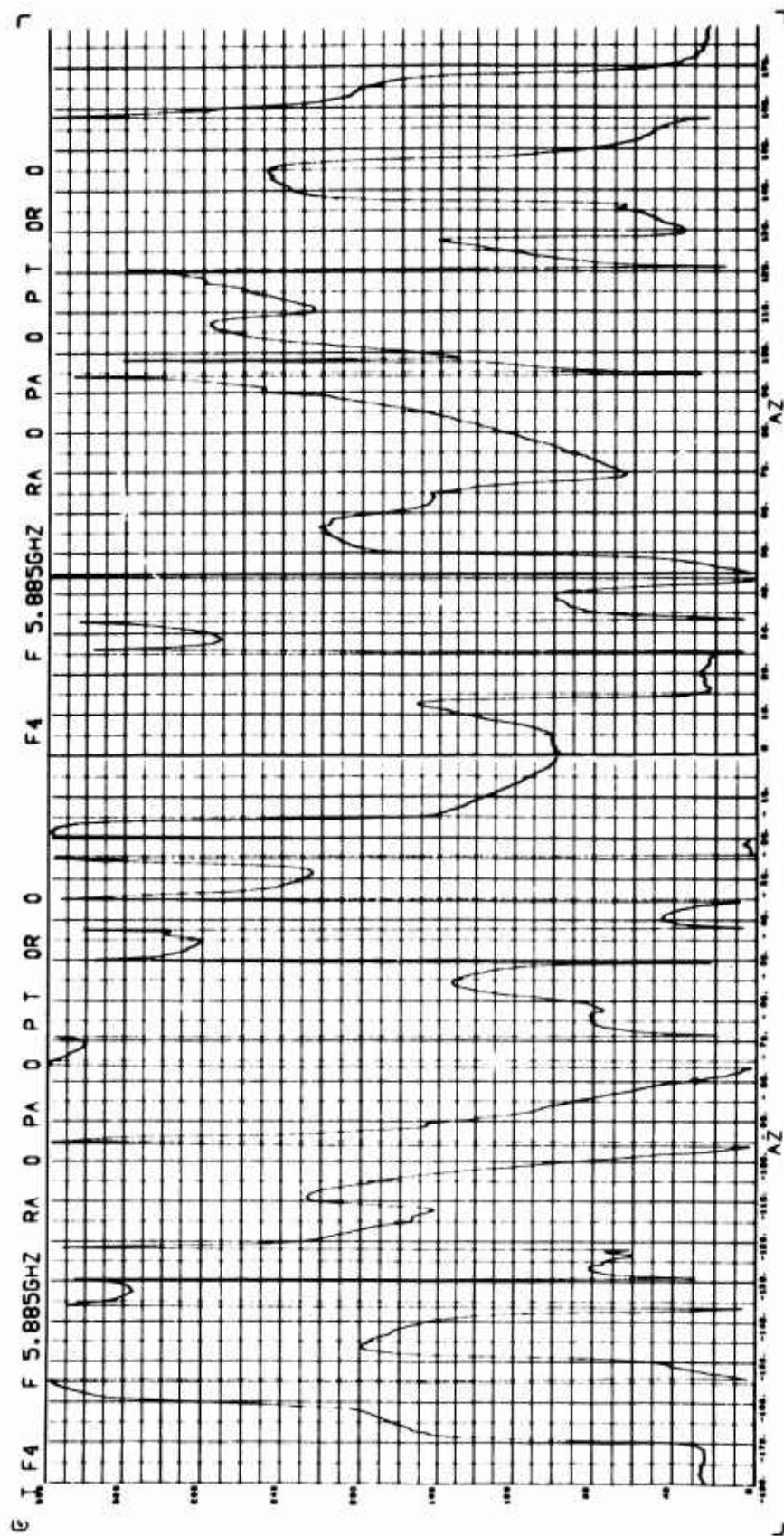




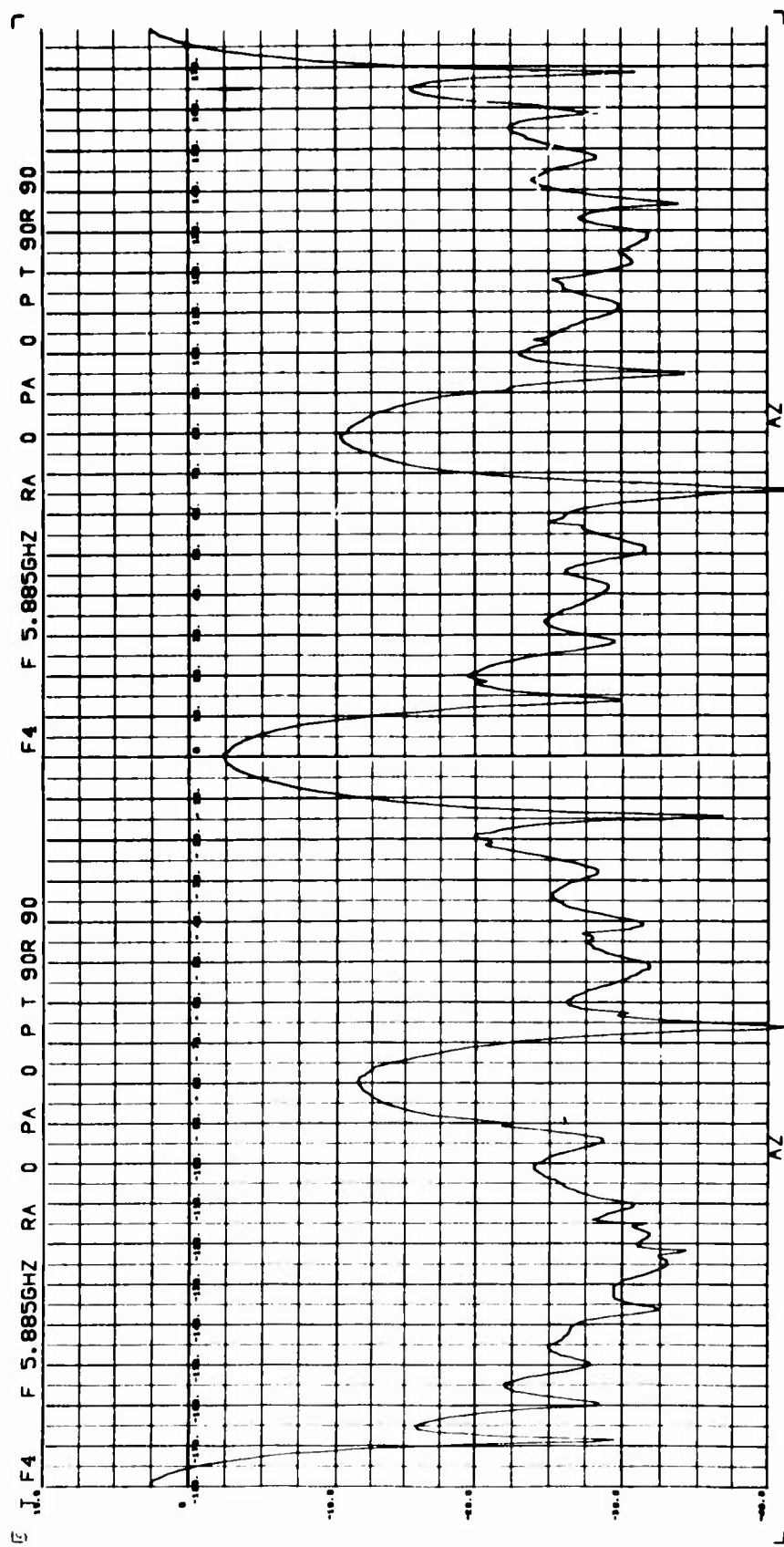




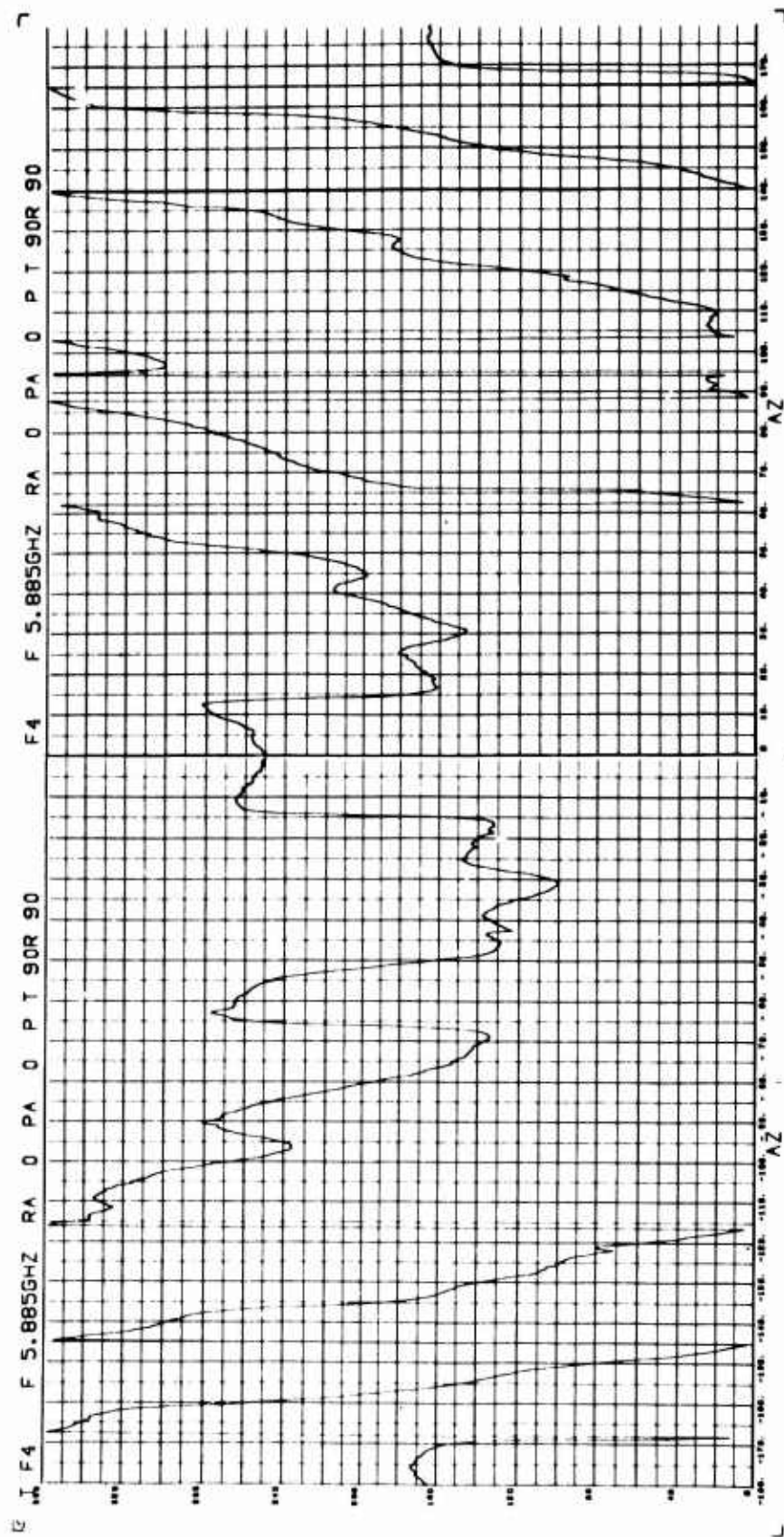
BISTATIC ANGLE = 10.25 DEGREES



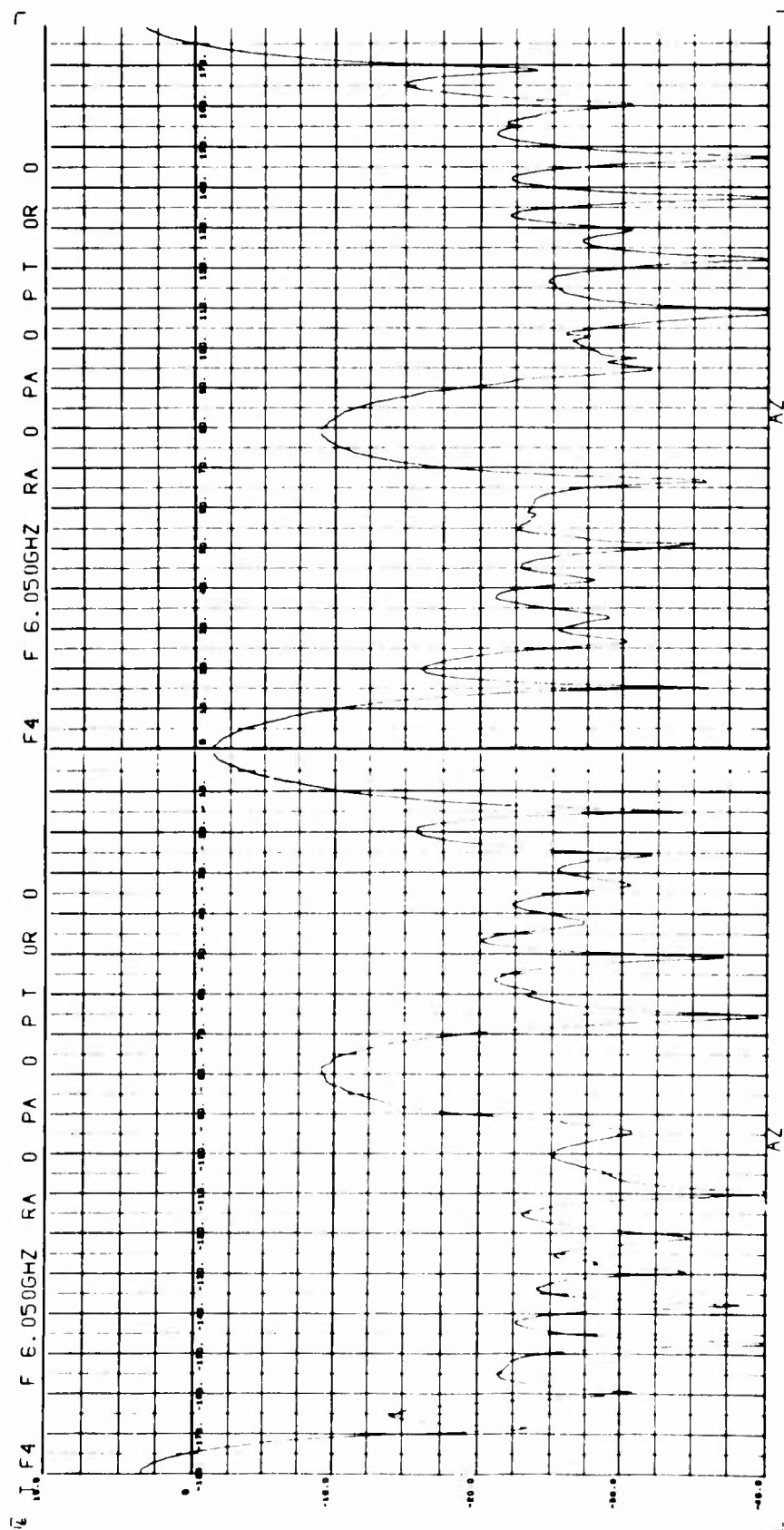
BISTATIC ANGLE = 10.25 DEGREES



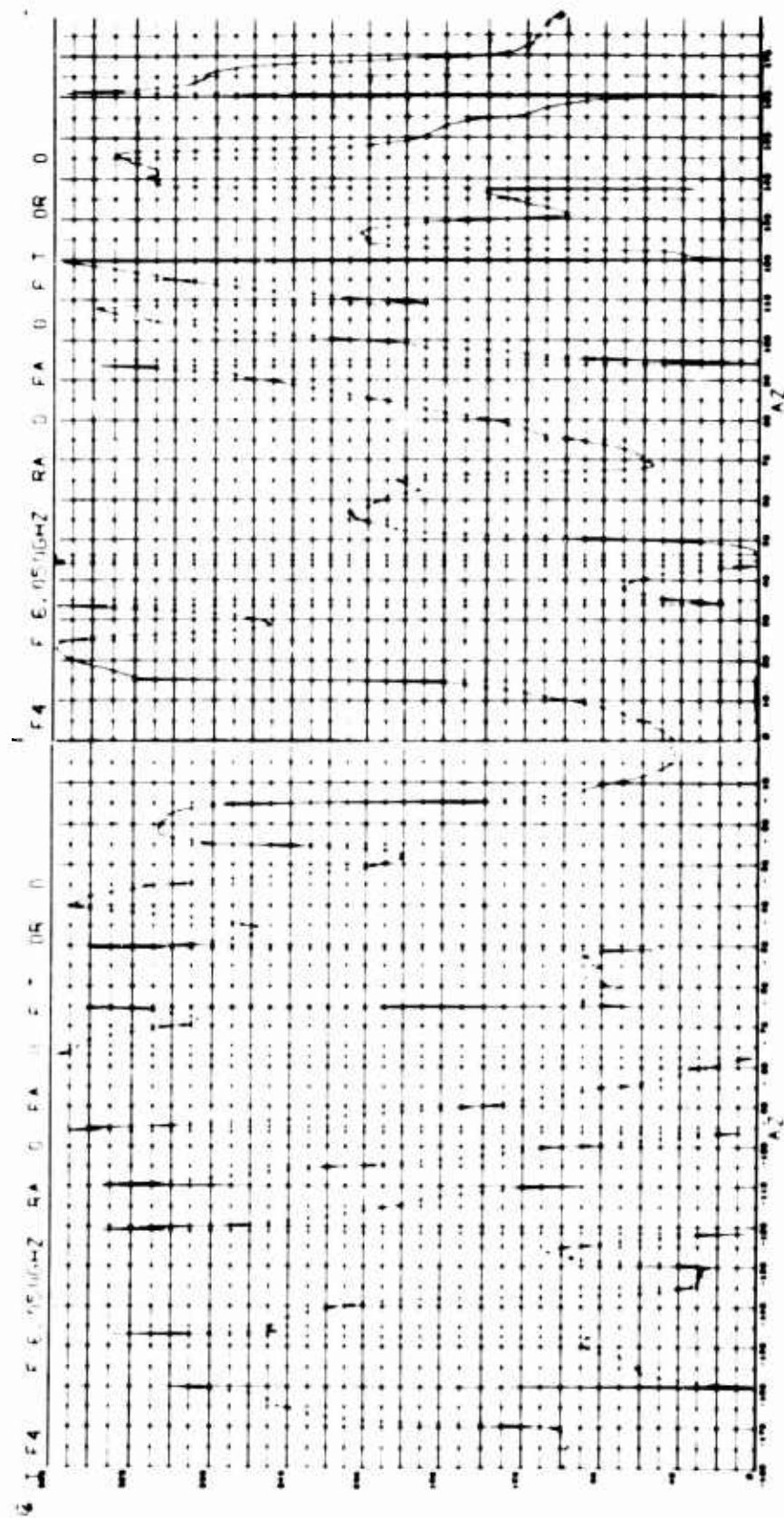
BISTATIC ANGLE = 10.25 DEGREES



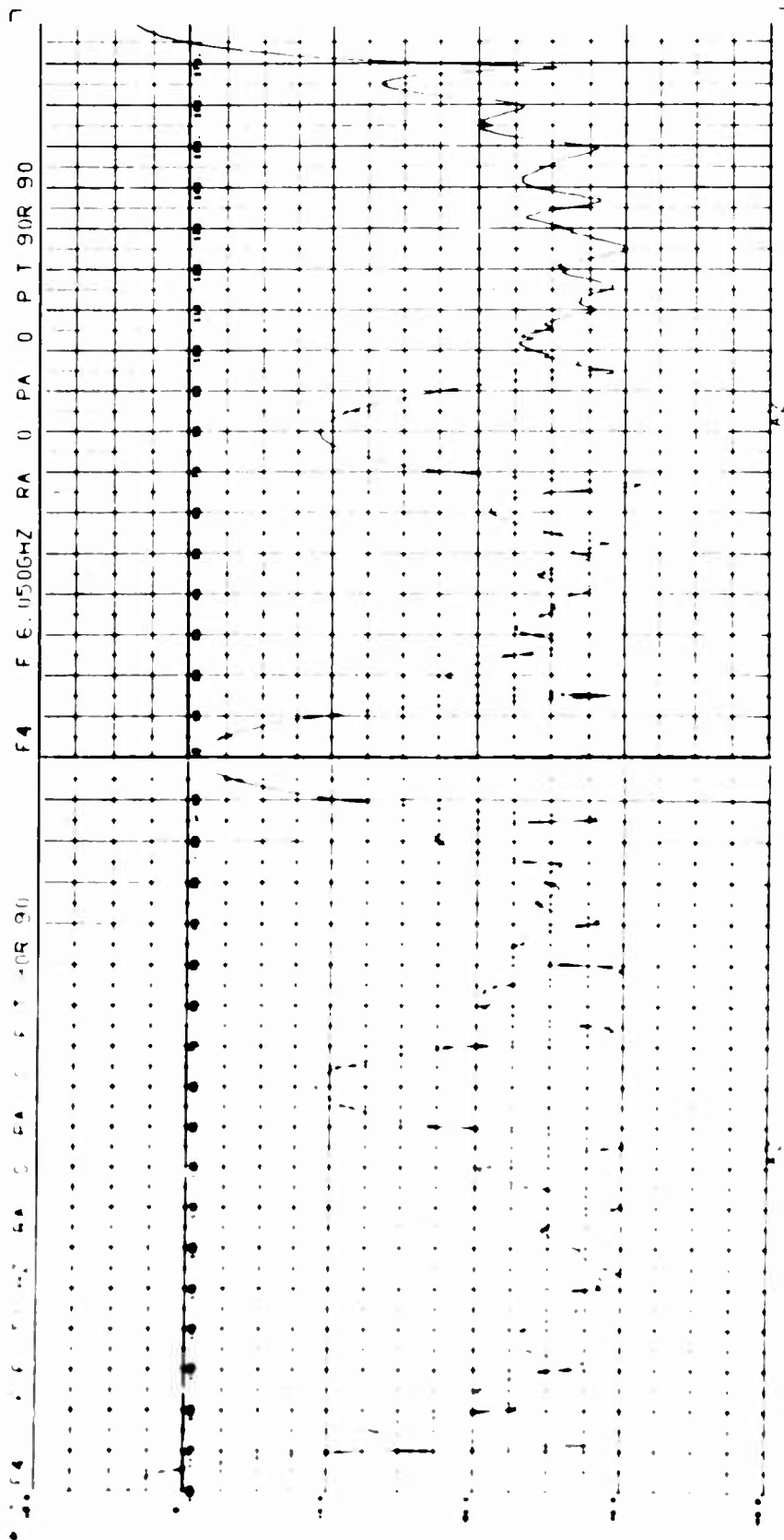
BISTATIC ANGLE = 10.25 DEGREES



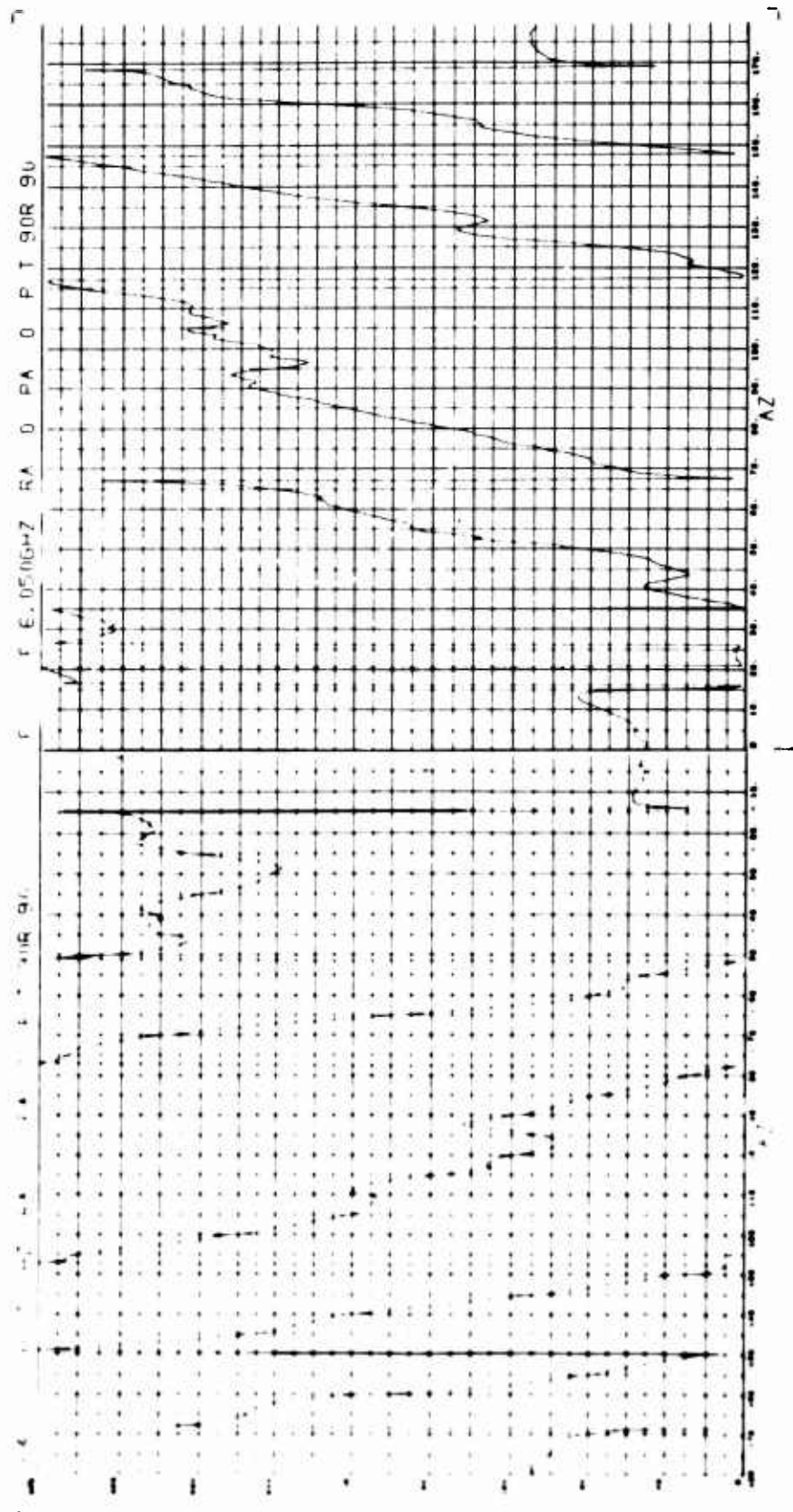
BISTATIC ANGLE = 30.0 DEGREES



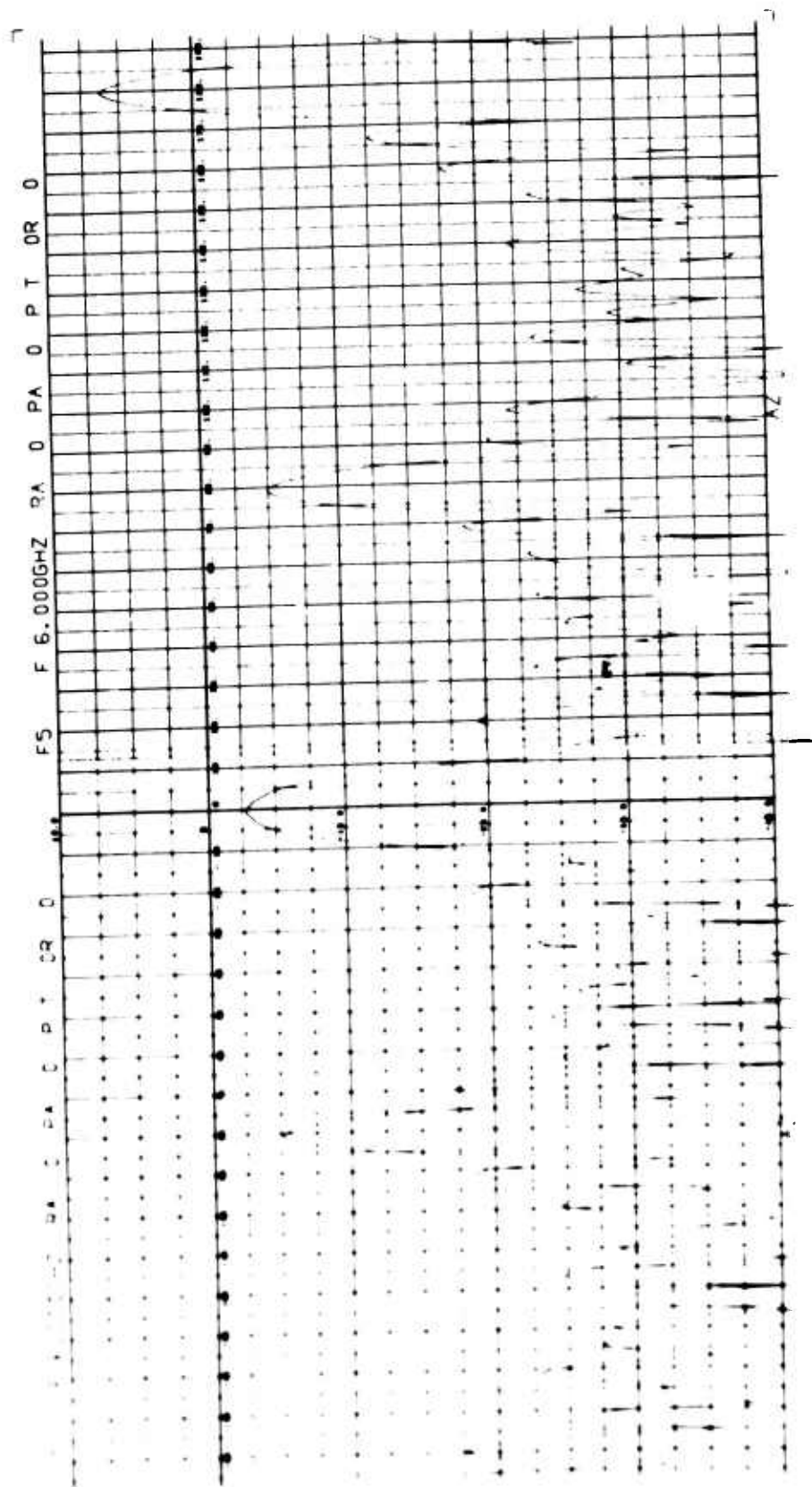
BISTATIC ANGLE = 30.0 DEGREES

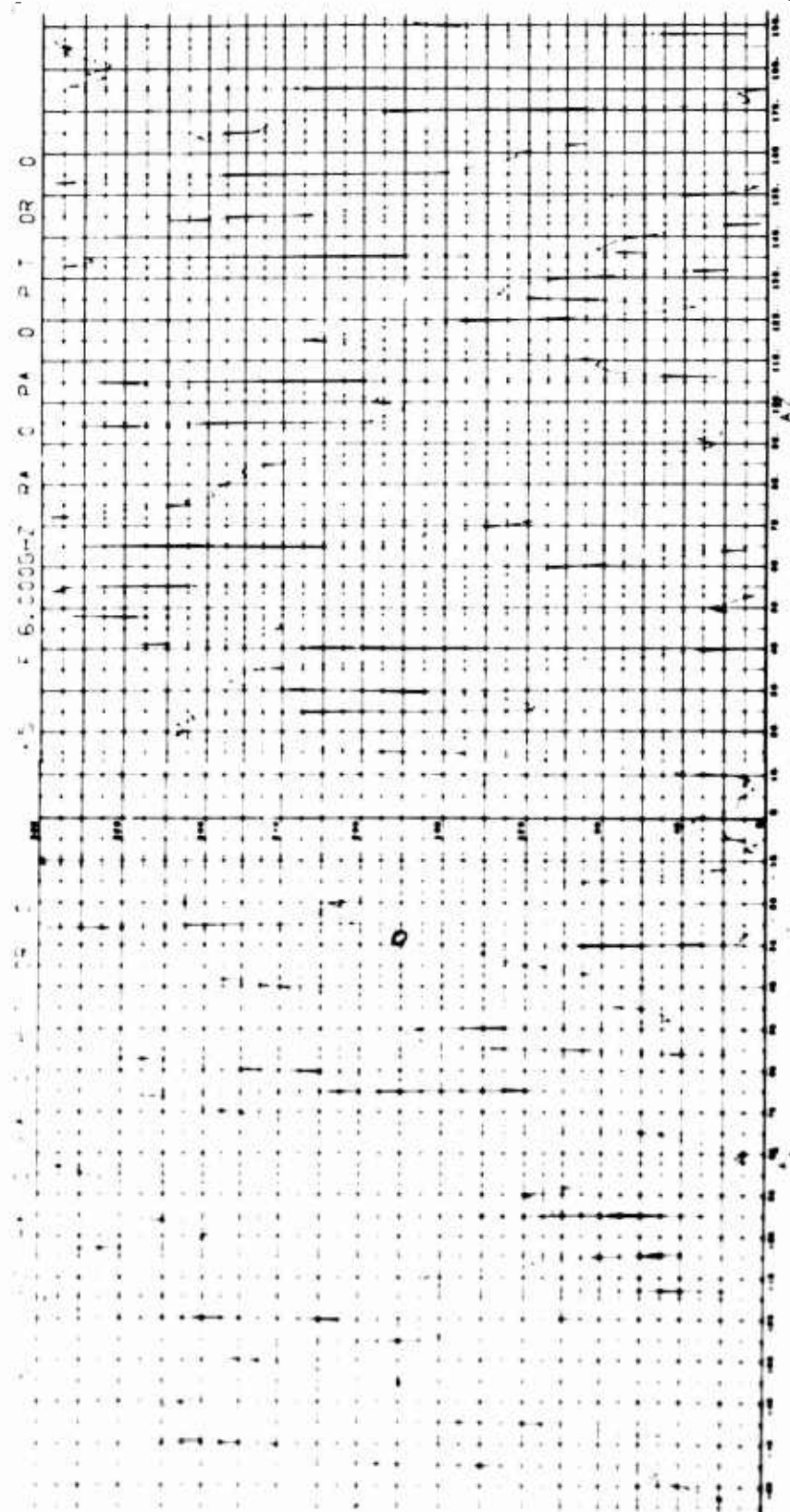


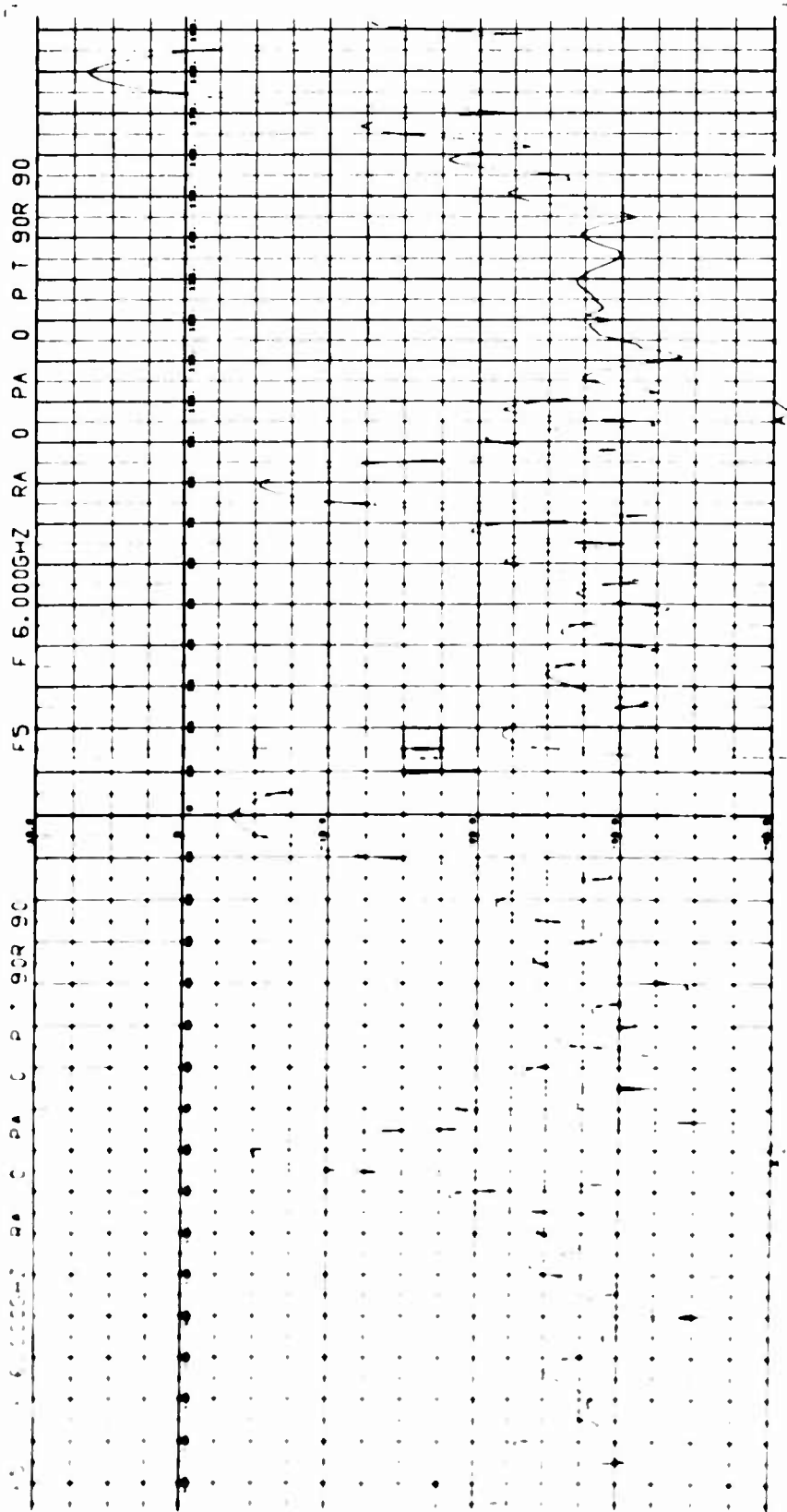
BISTATIC ANGLE = 30.0 DEGREES

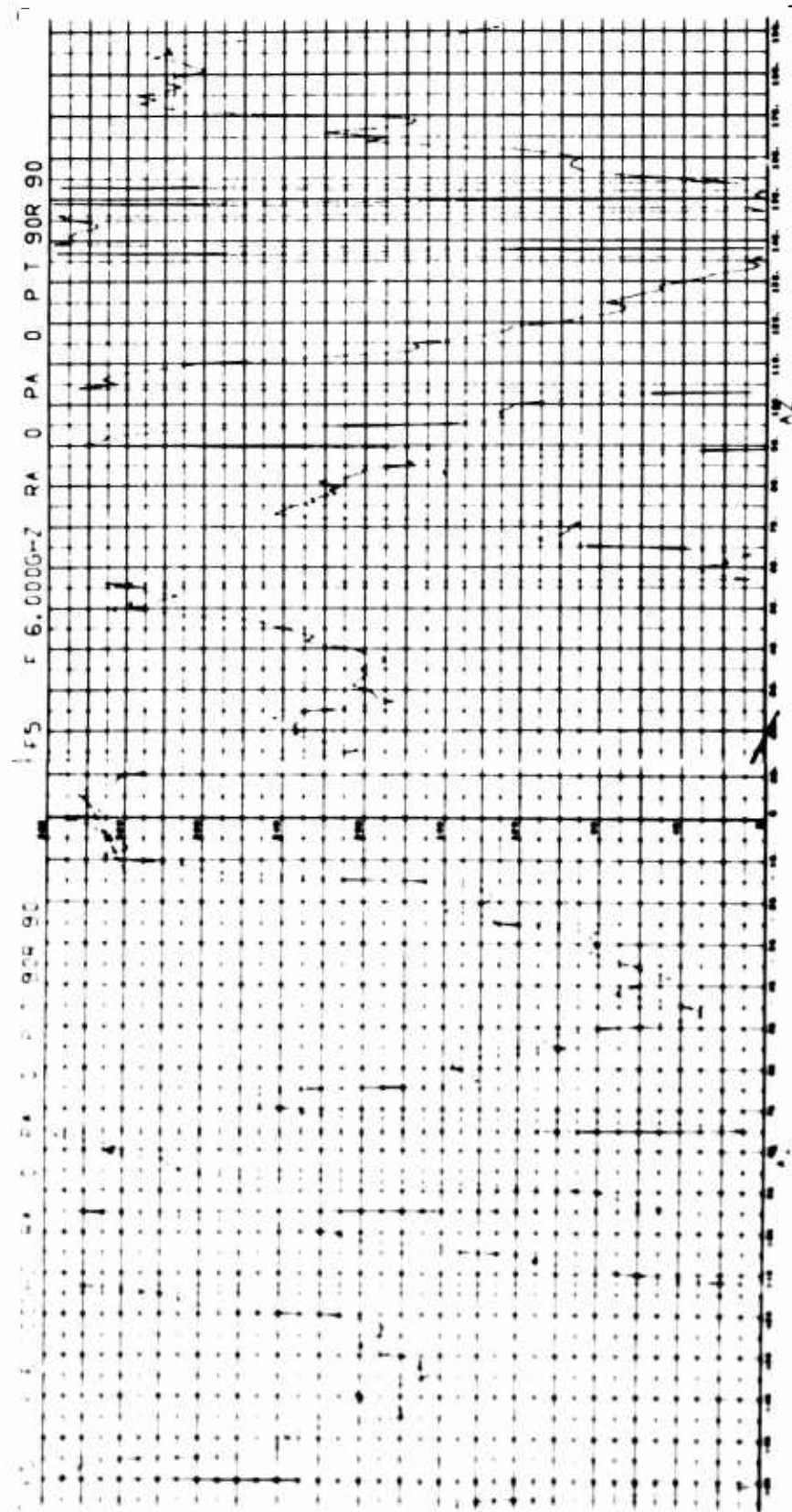


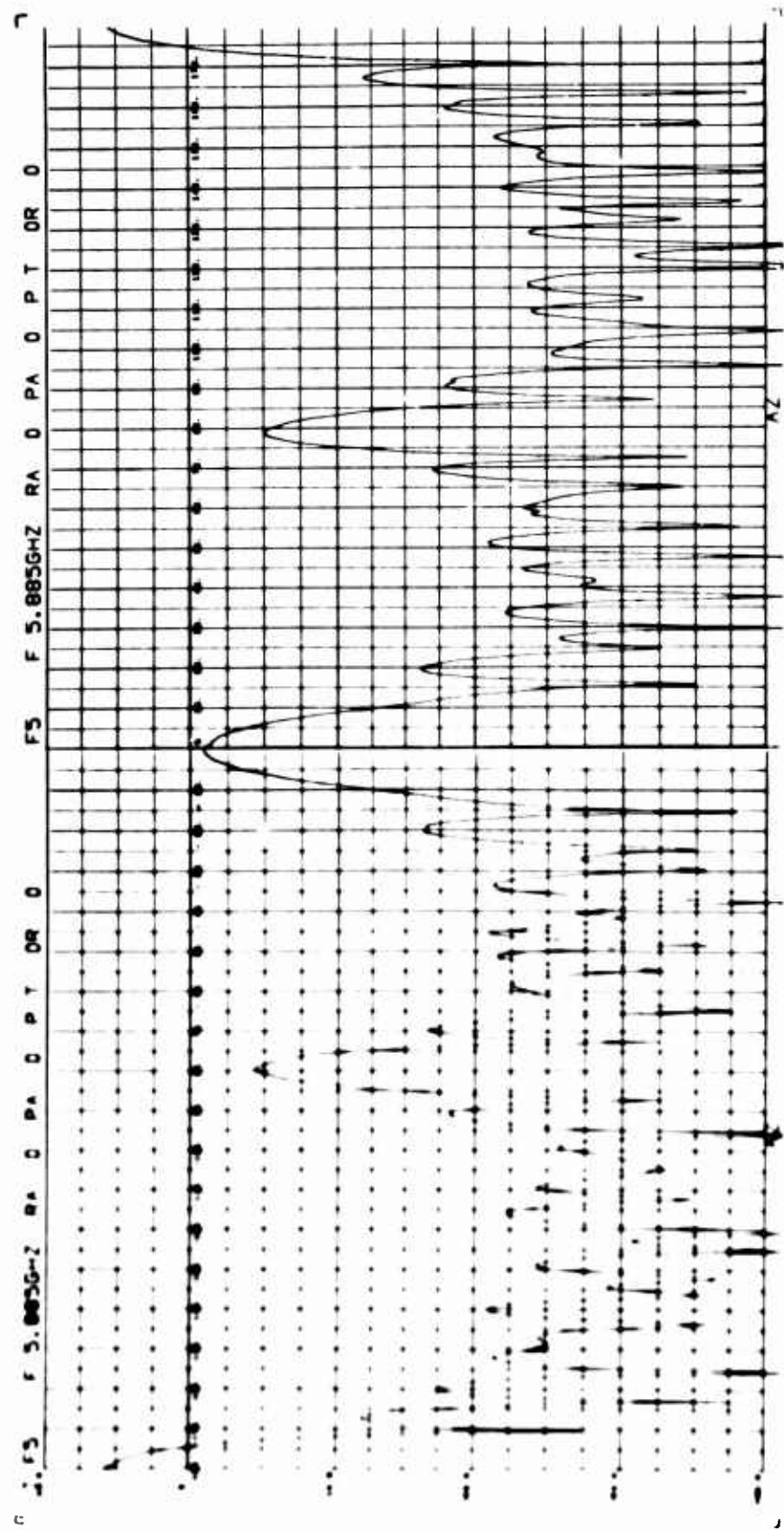
BISTATIC ANGLE = 30.0 DEGREES



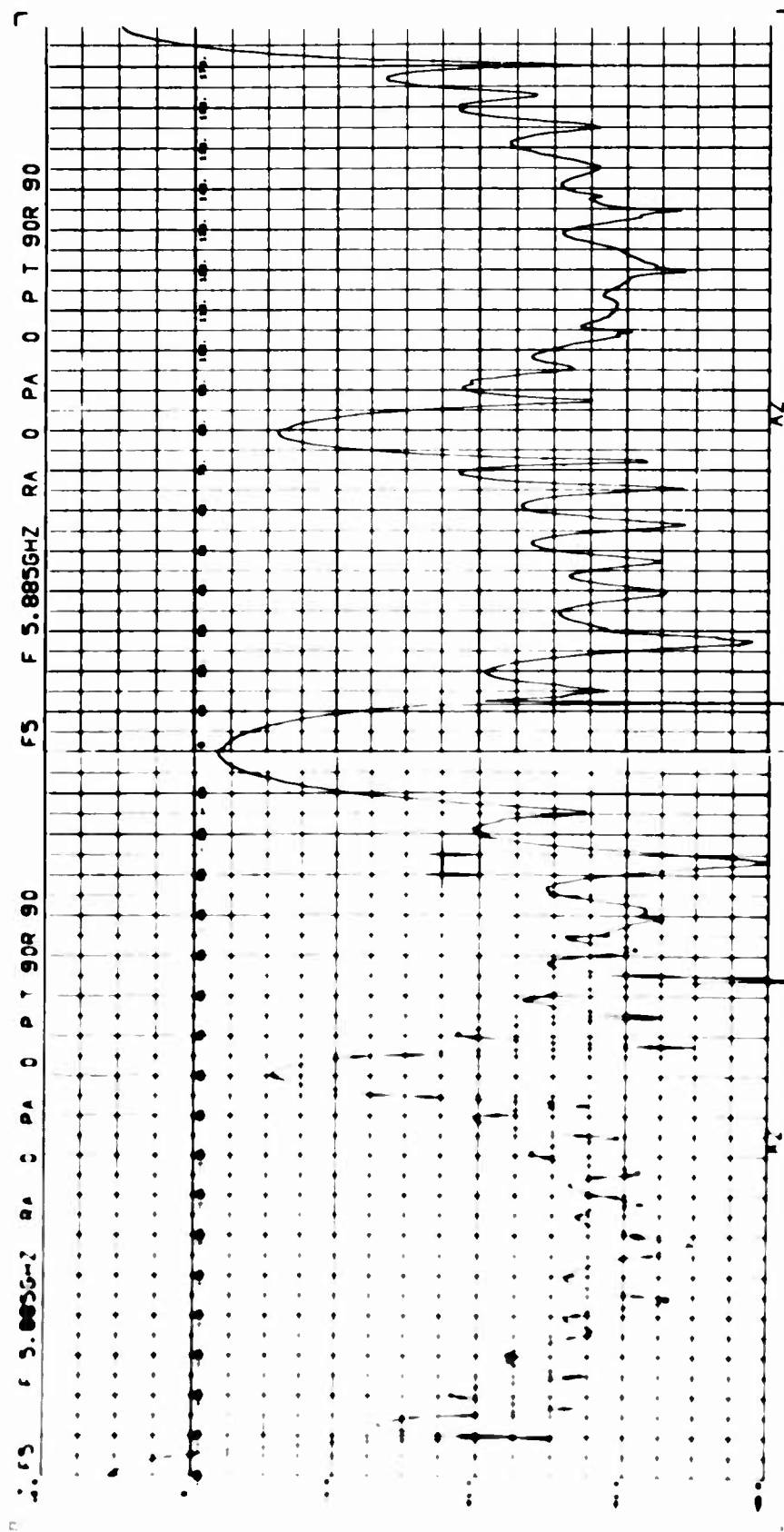




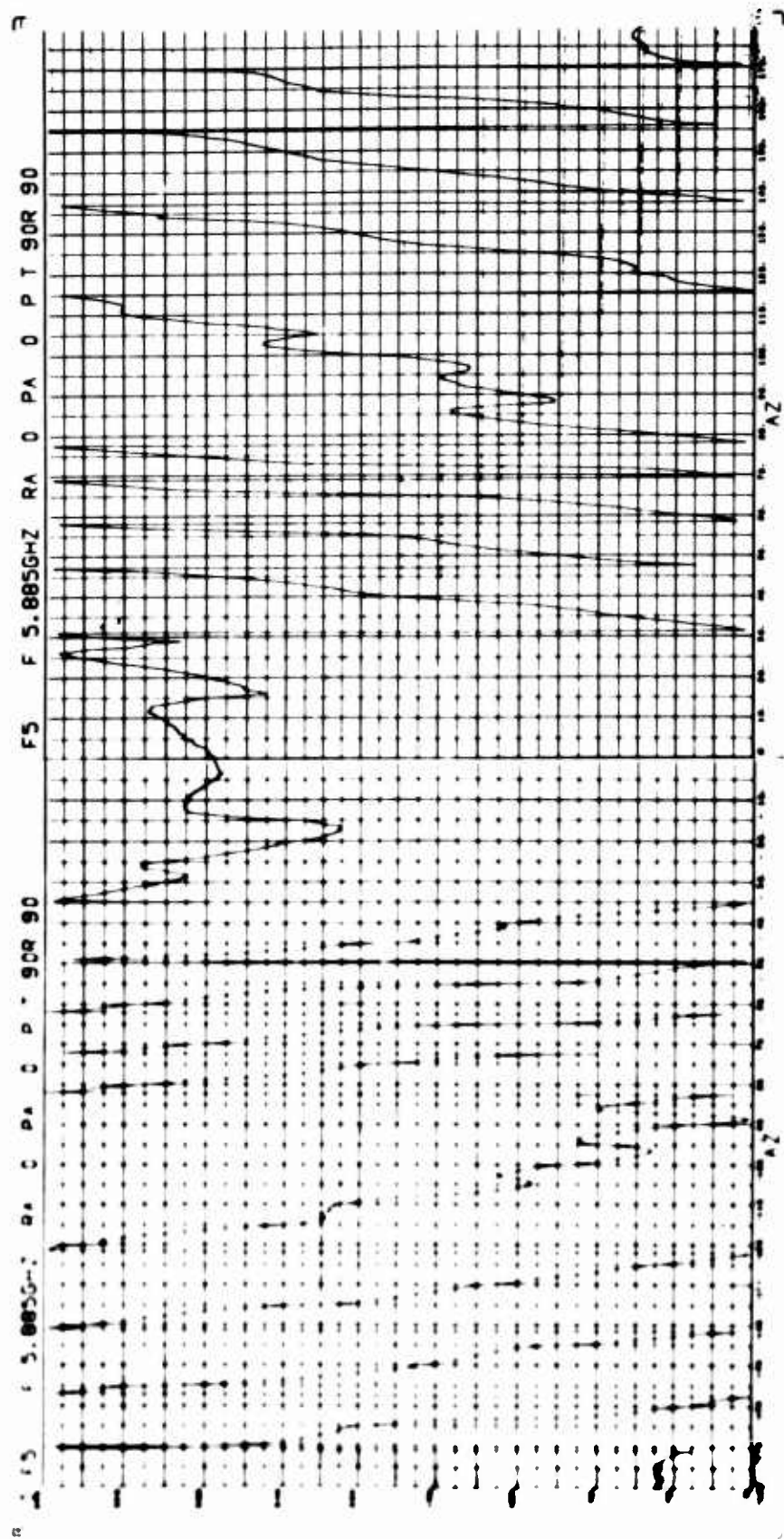




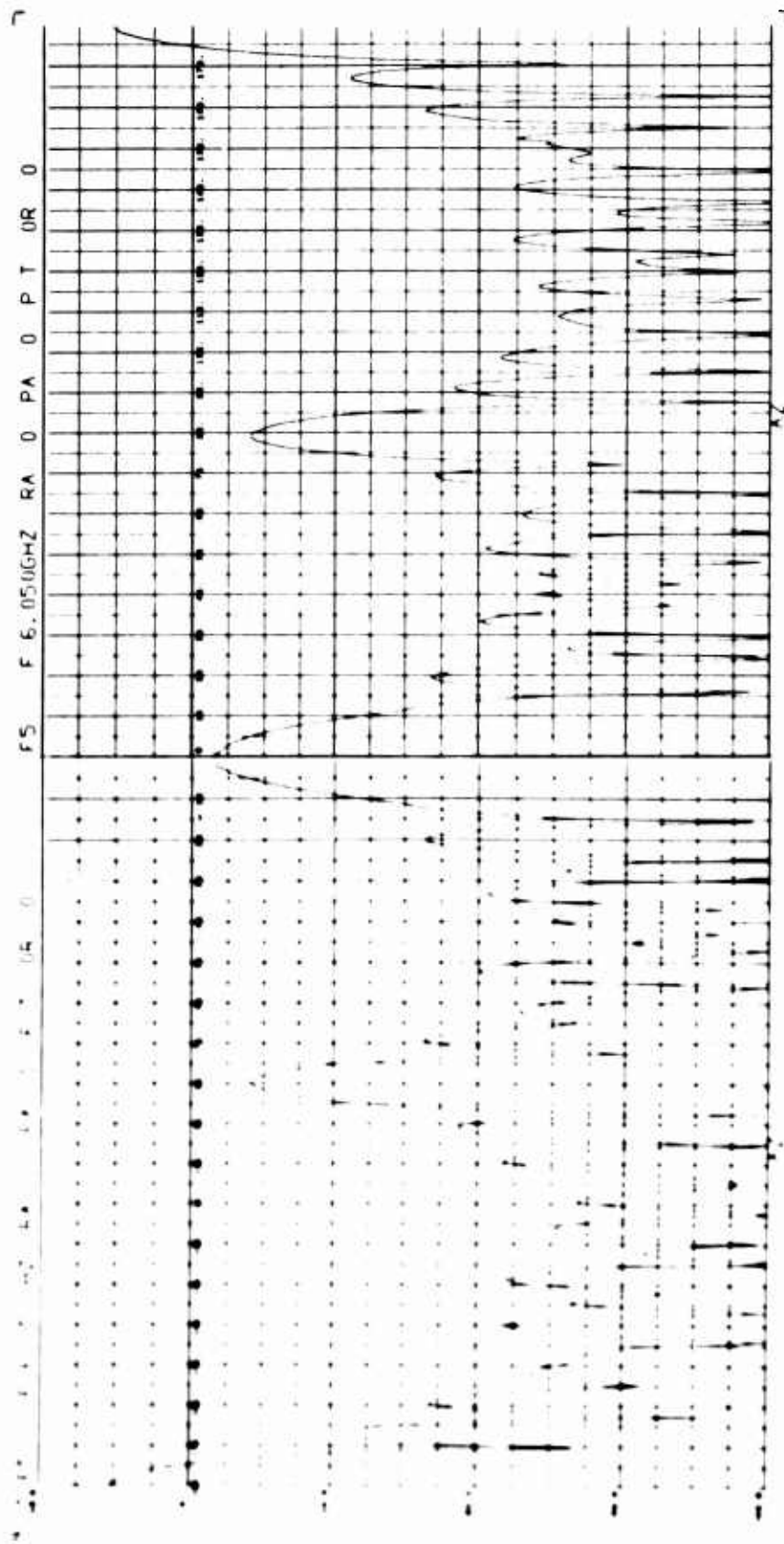
BISTATIC ANGLE = 10.25 DEGREES



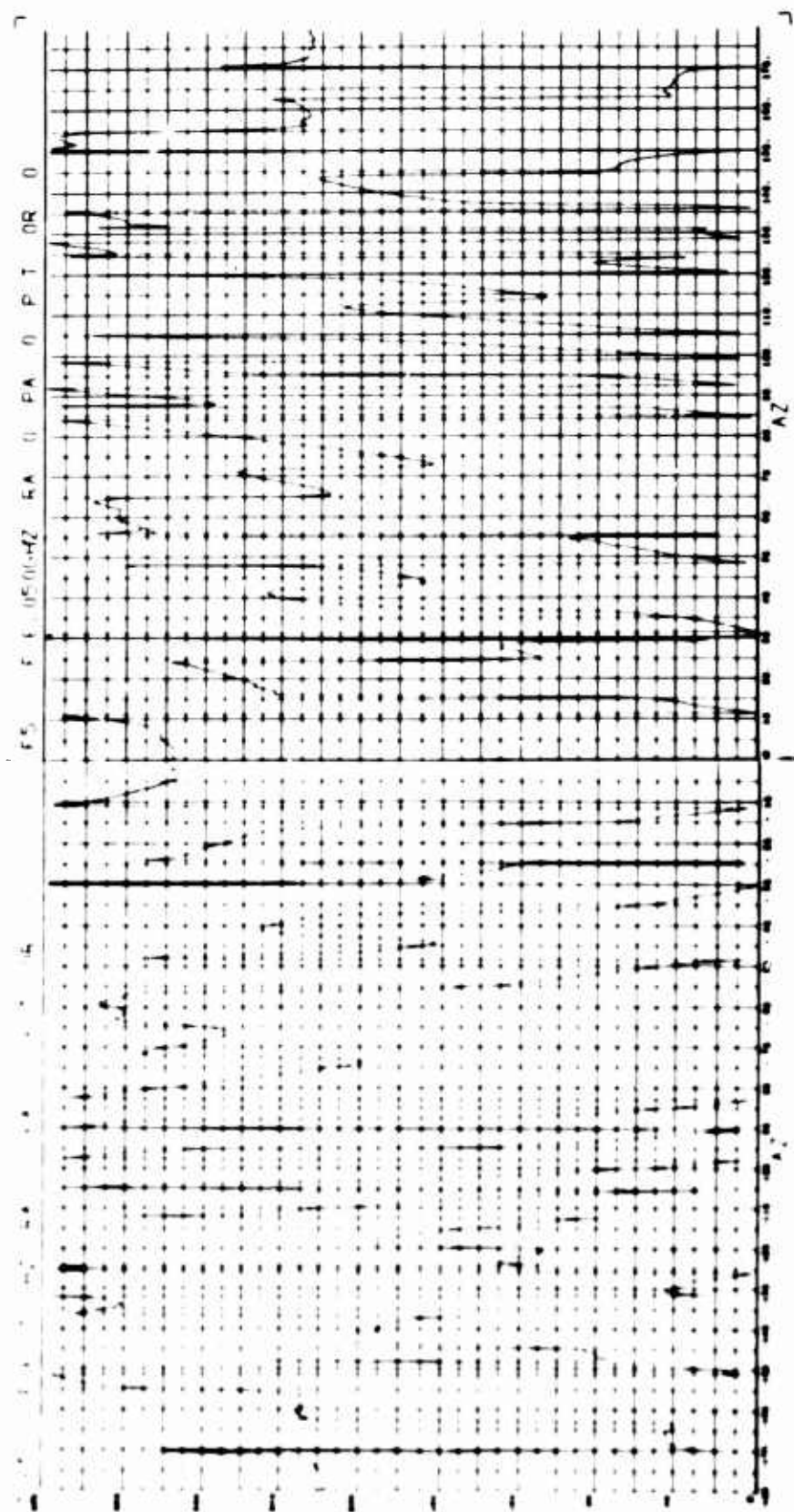
BISTATIC ANGLE = 10.25 DEGREES



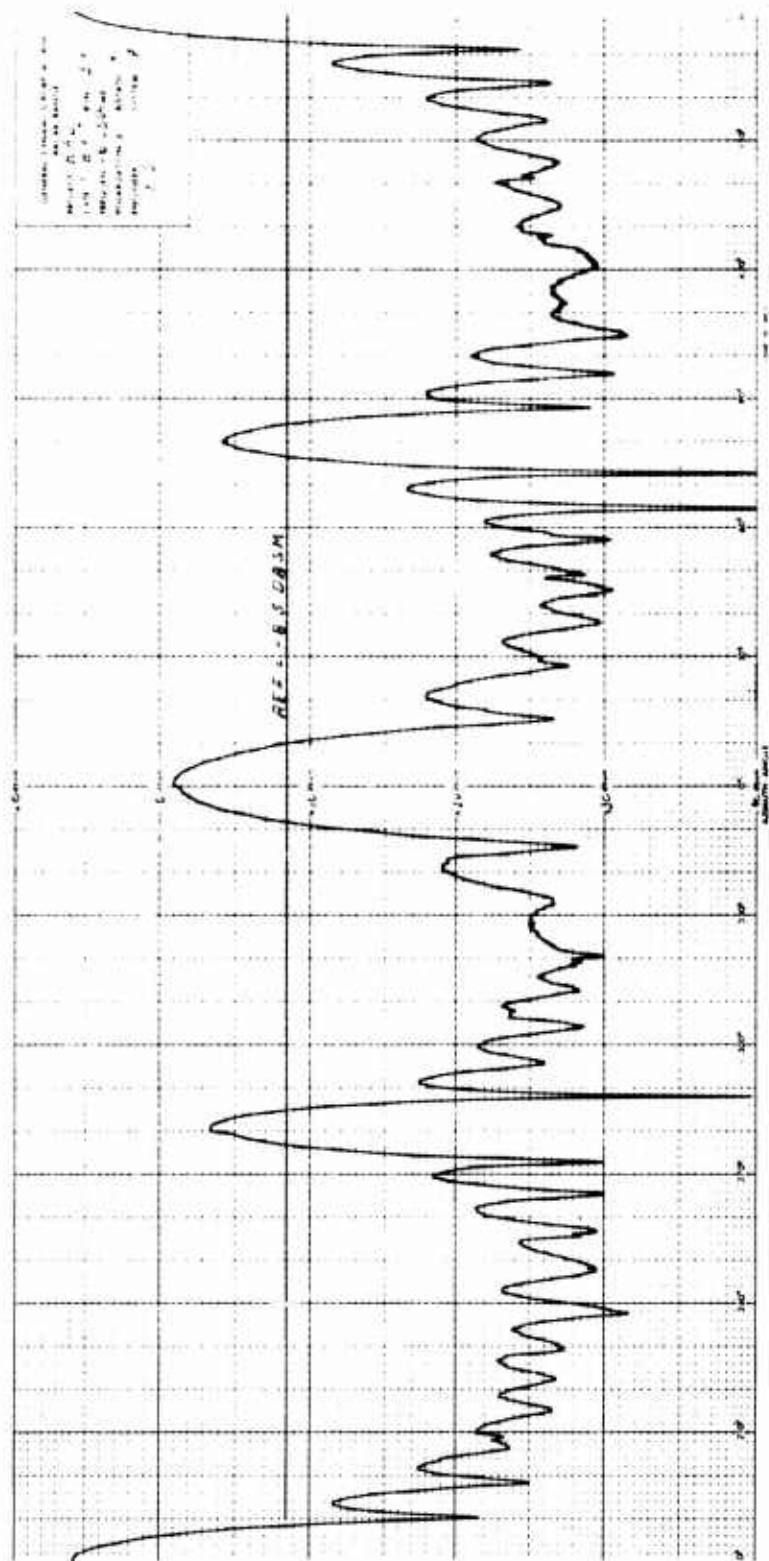
BISTATIC ANGLE = 10.25 DEGREES



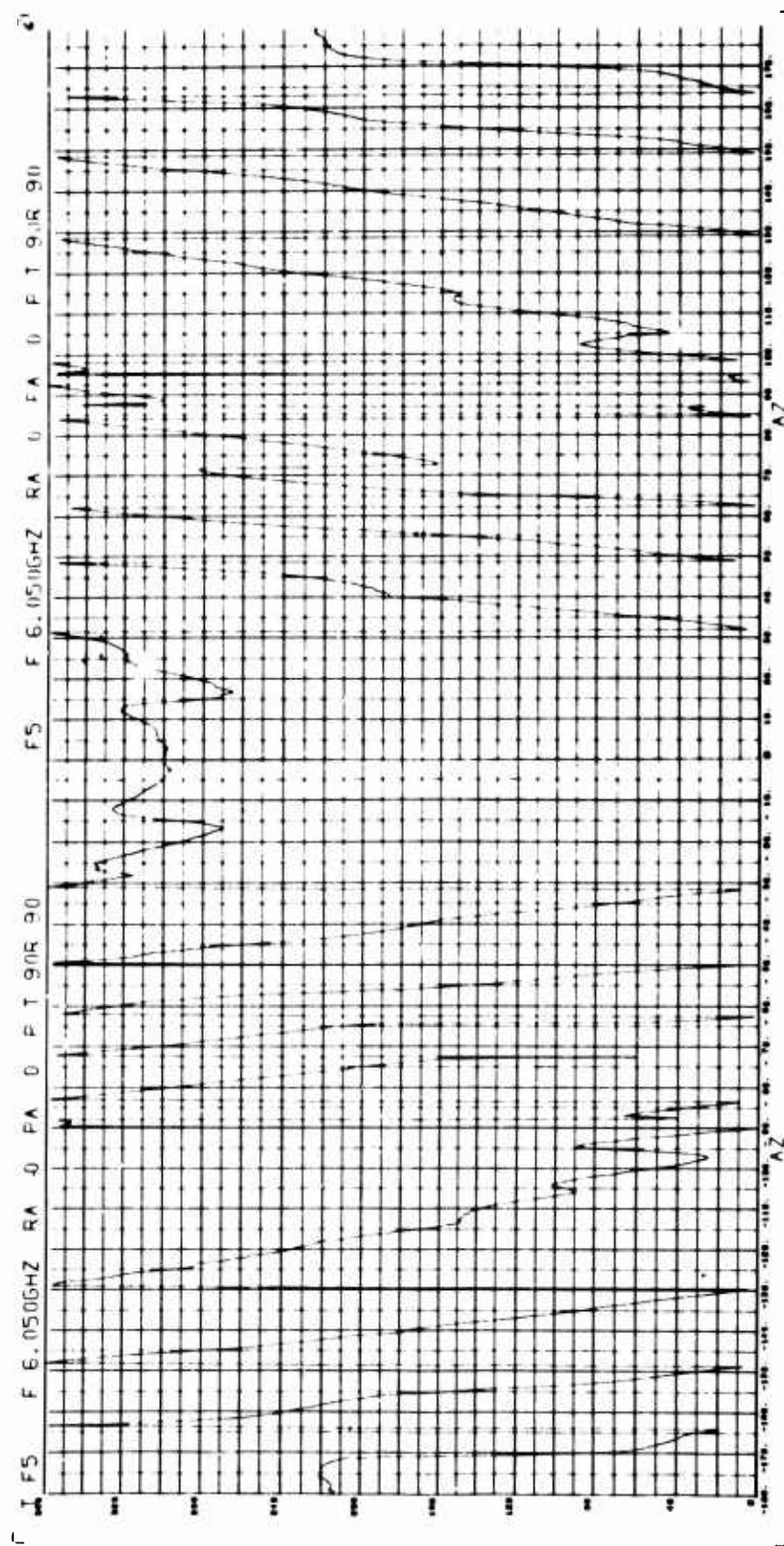
BISTATIC ANGLE = 30.0 DEGREES



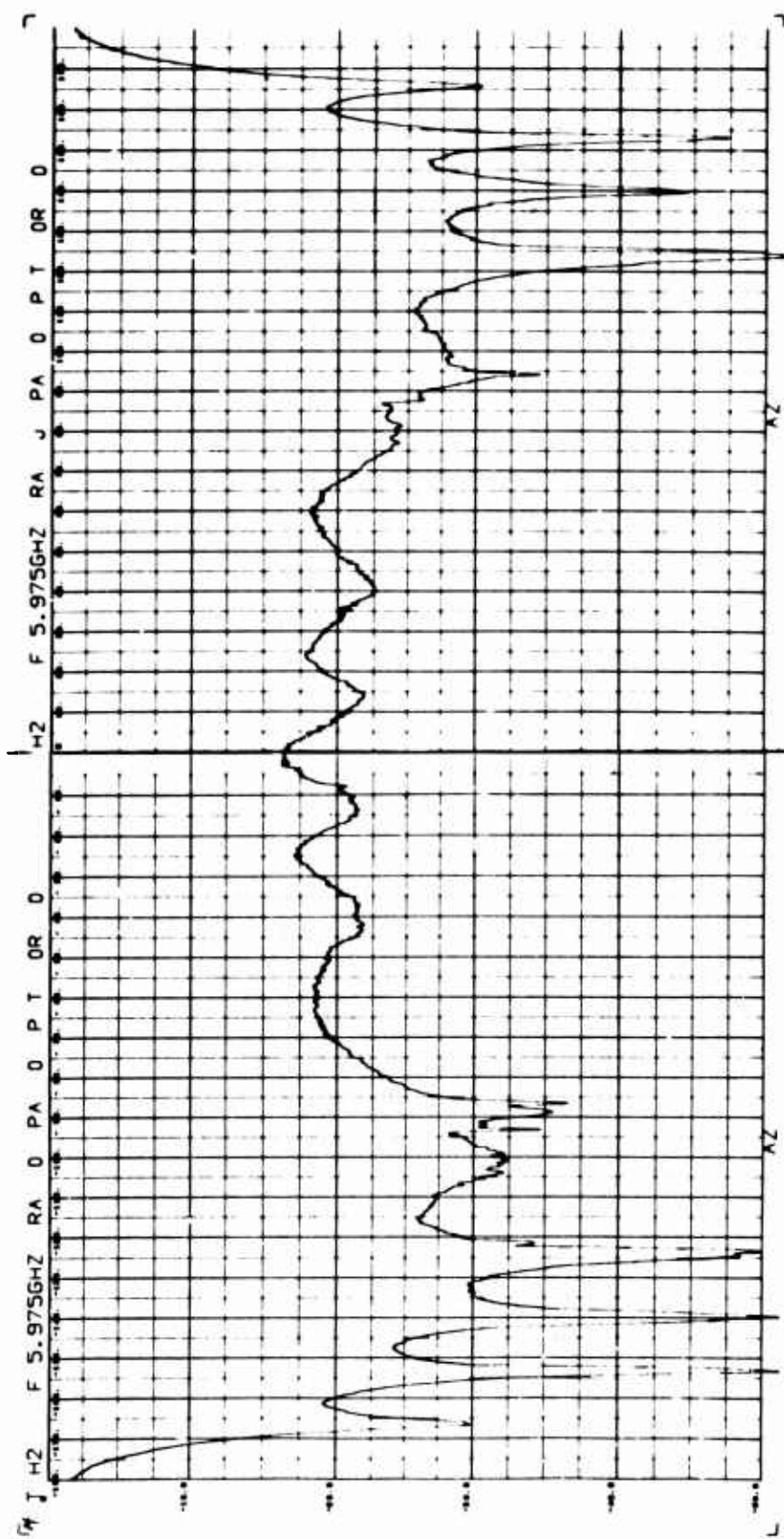
BISTATIC ANGLE = 30.0 DEGREES

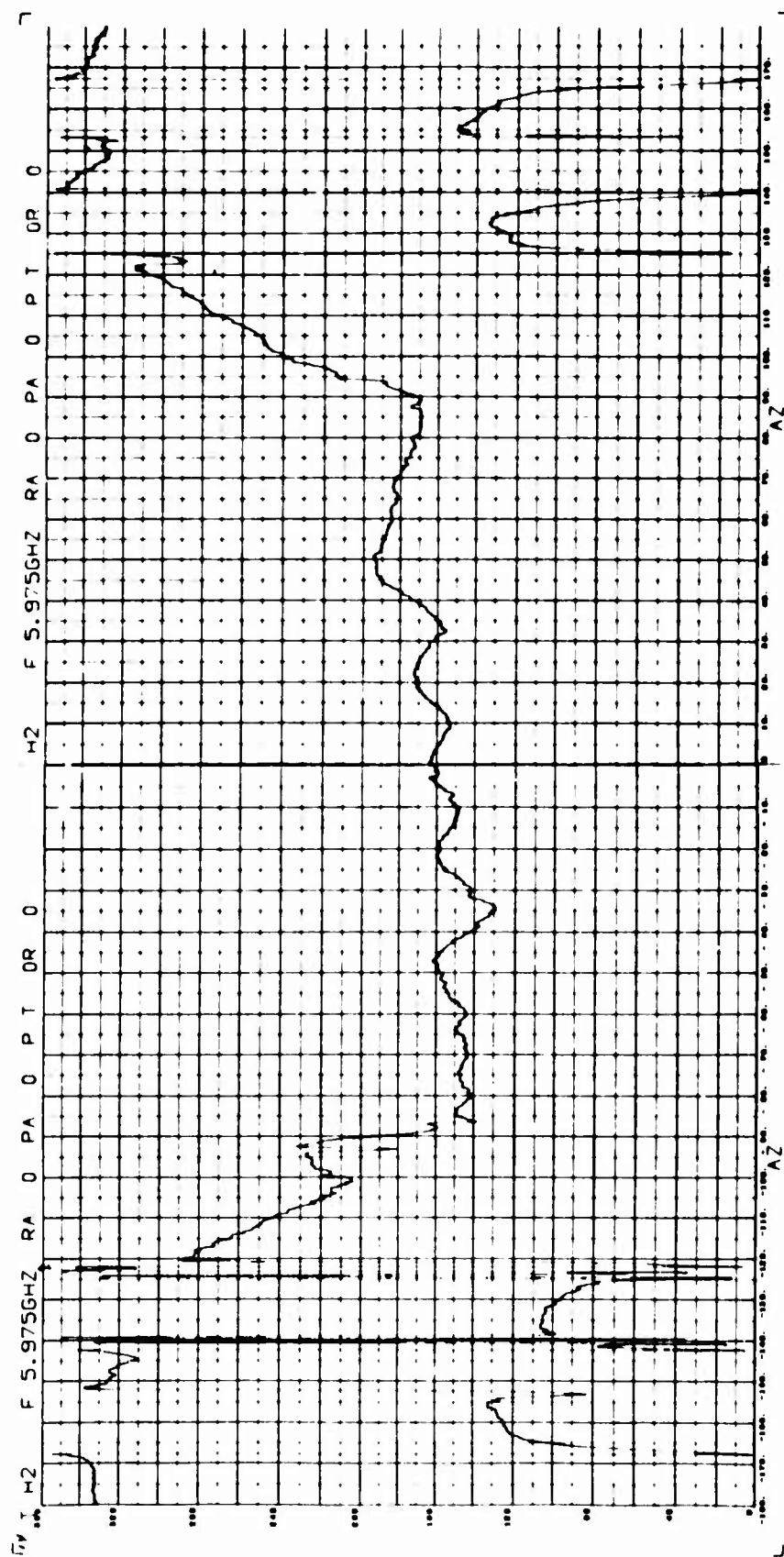


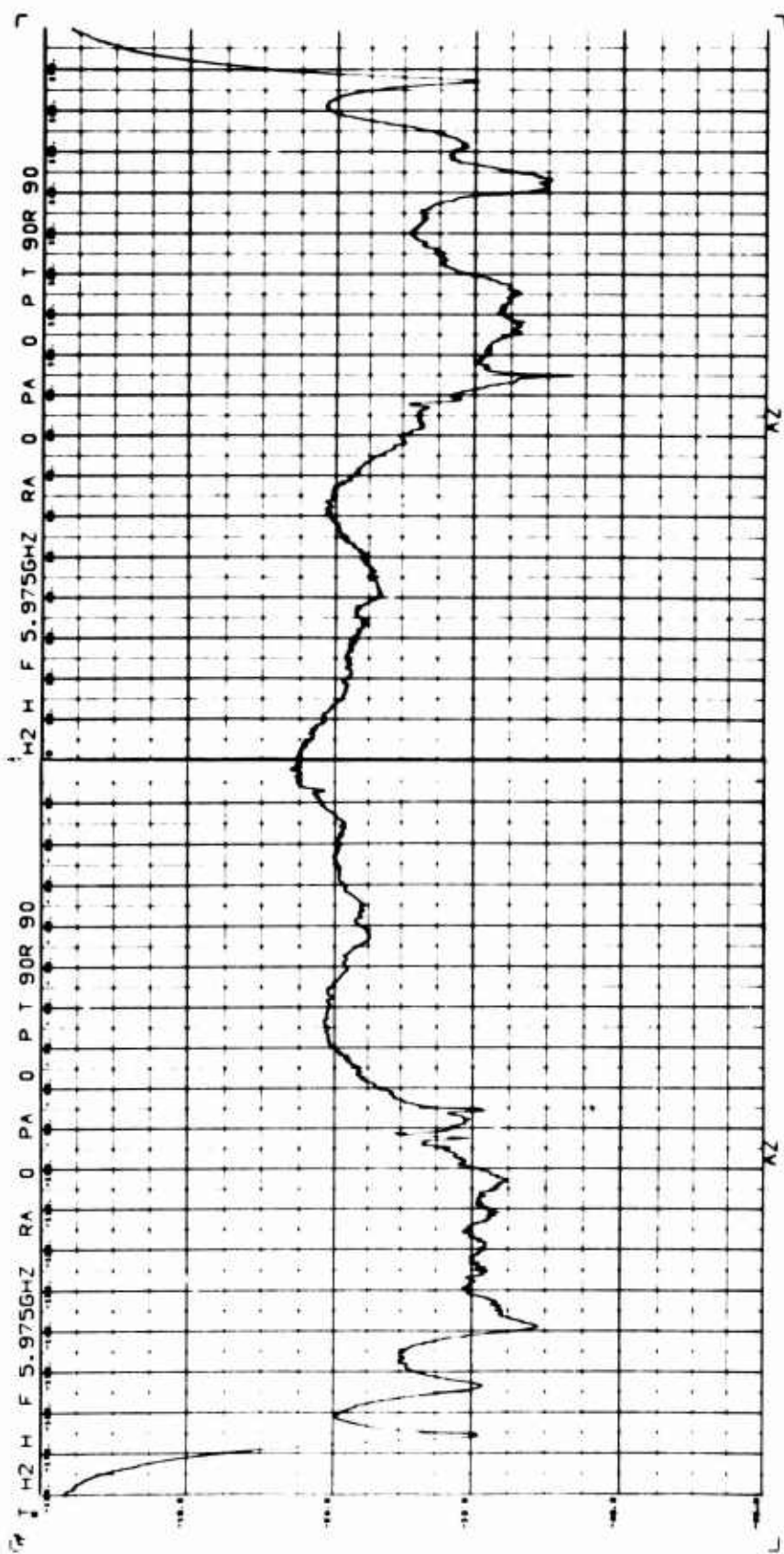
BISTATIC ANGLE = 30.0 DEGREES

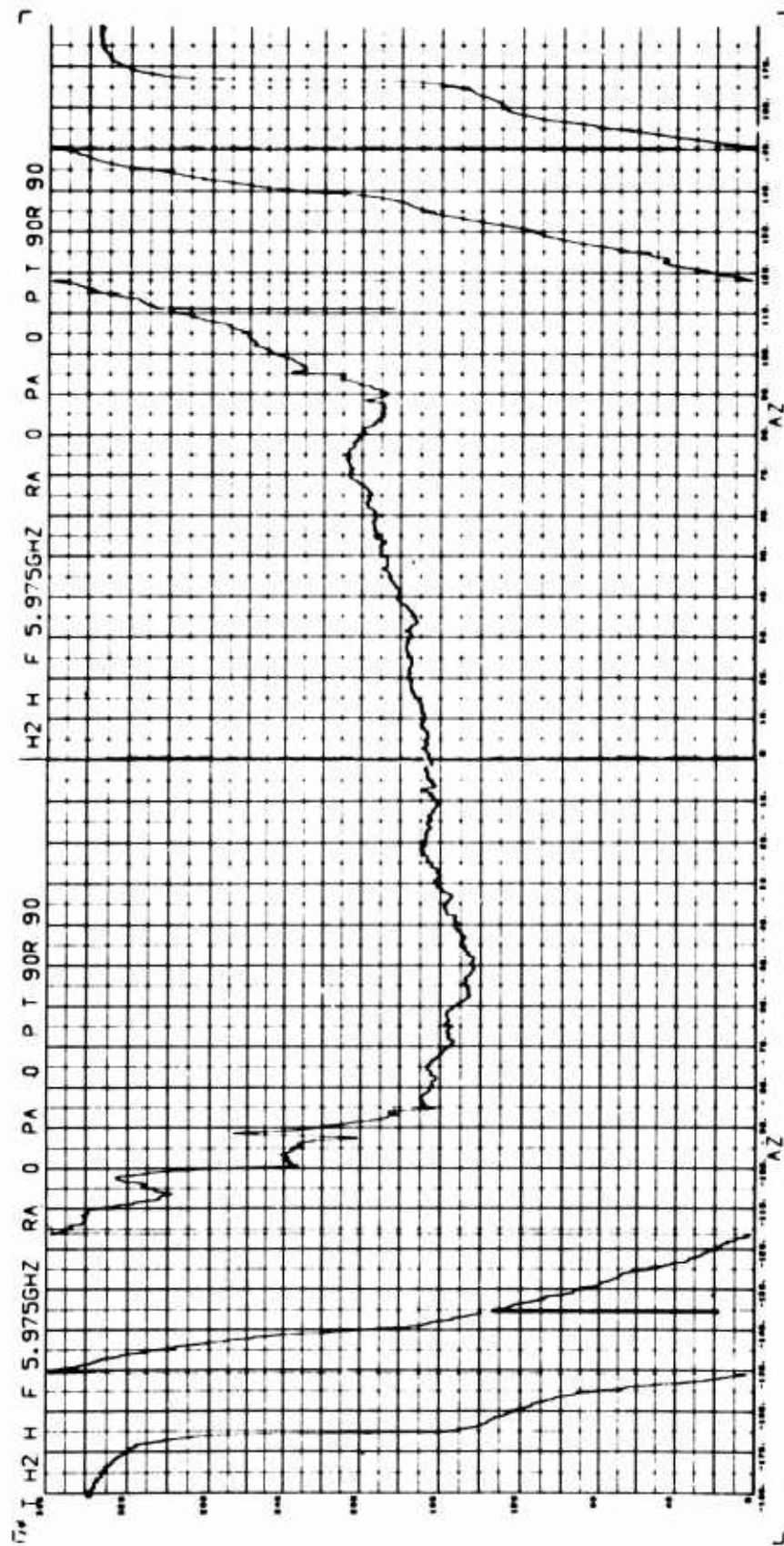


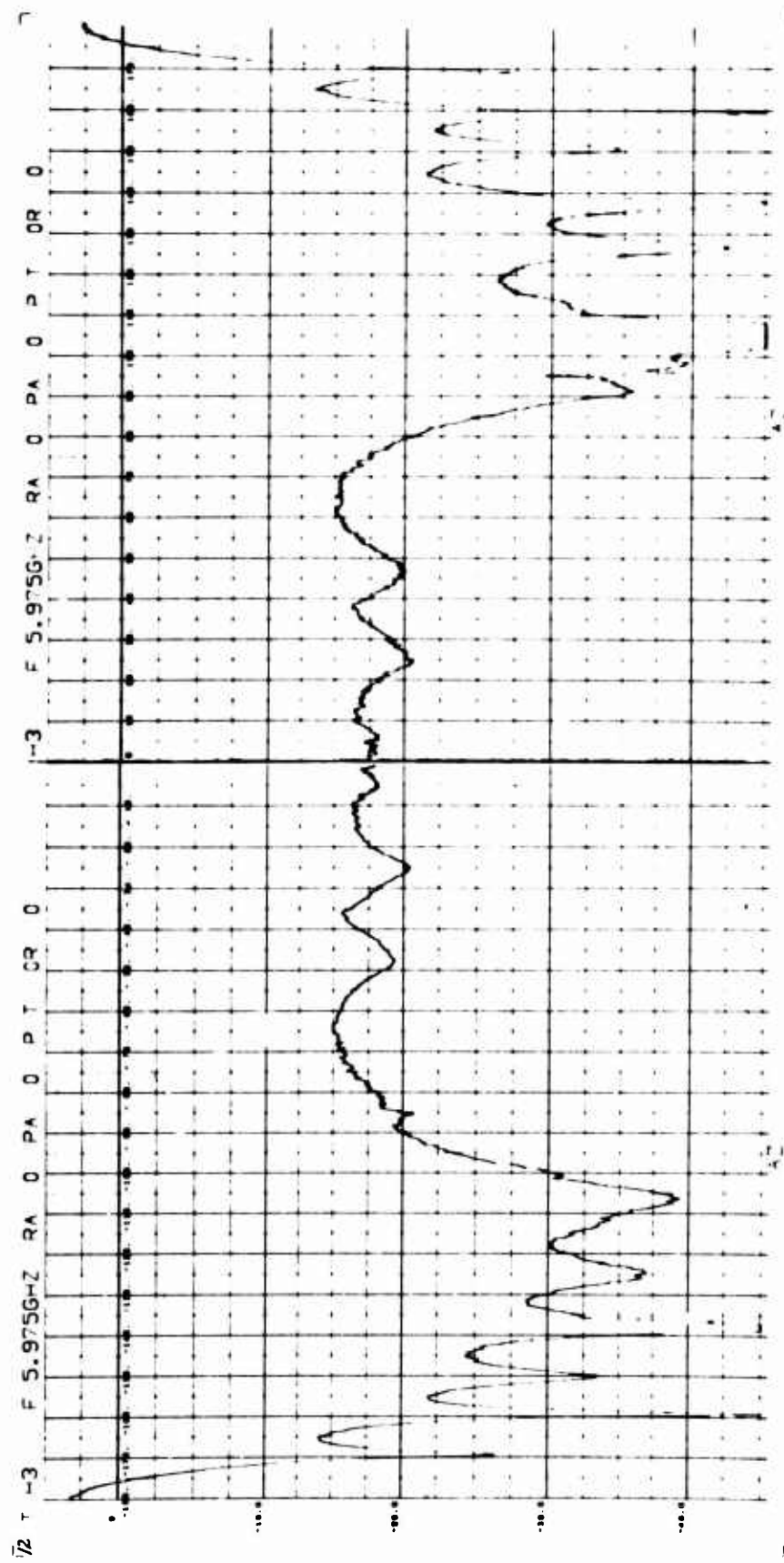
BISTATIC ANGLE = 30.0 DEGREES

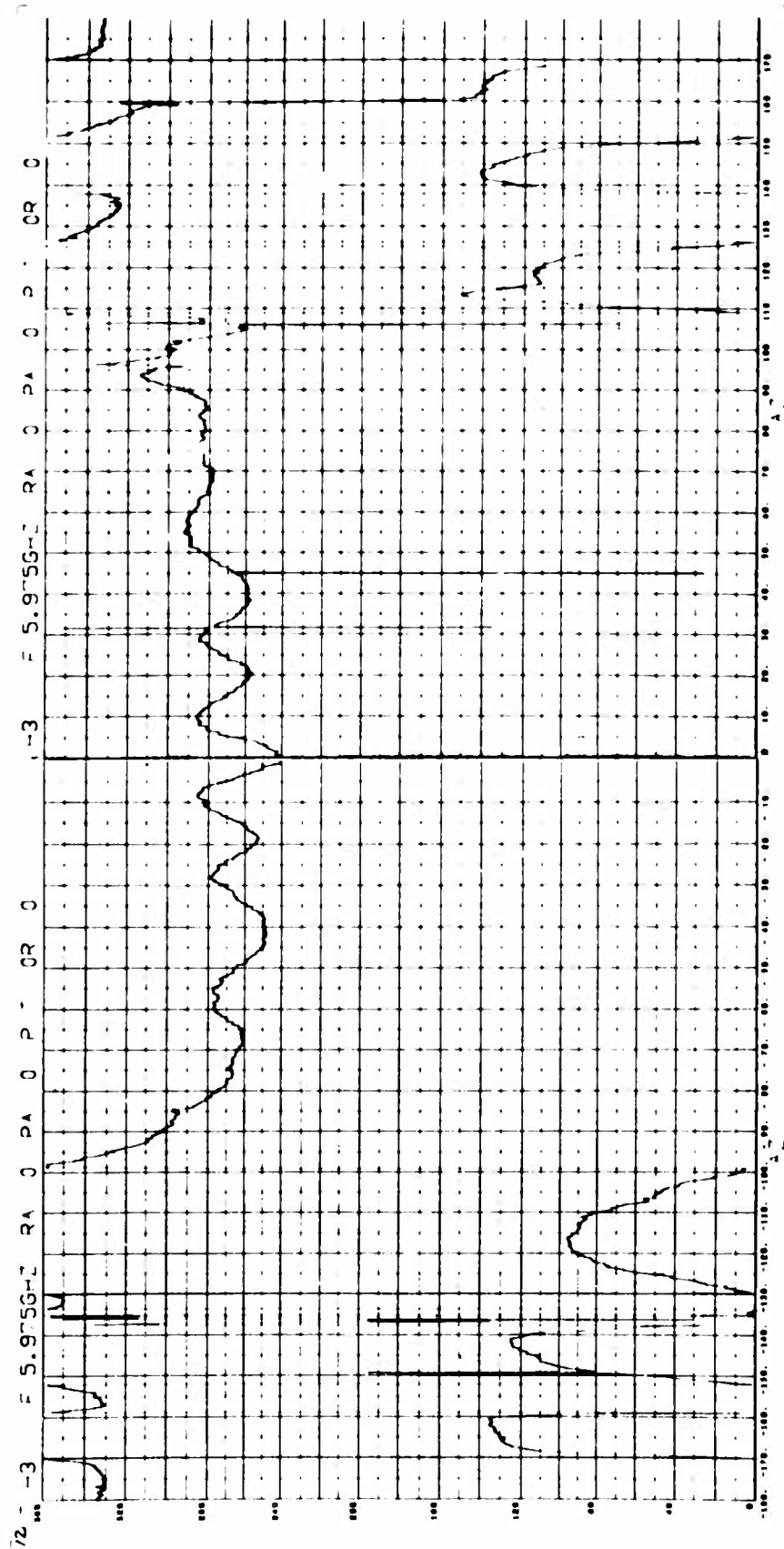


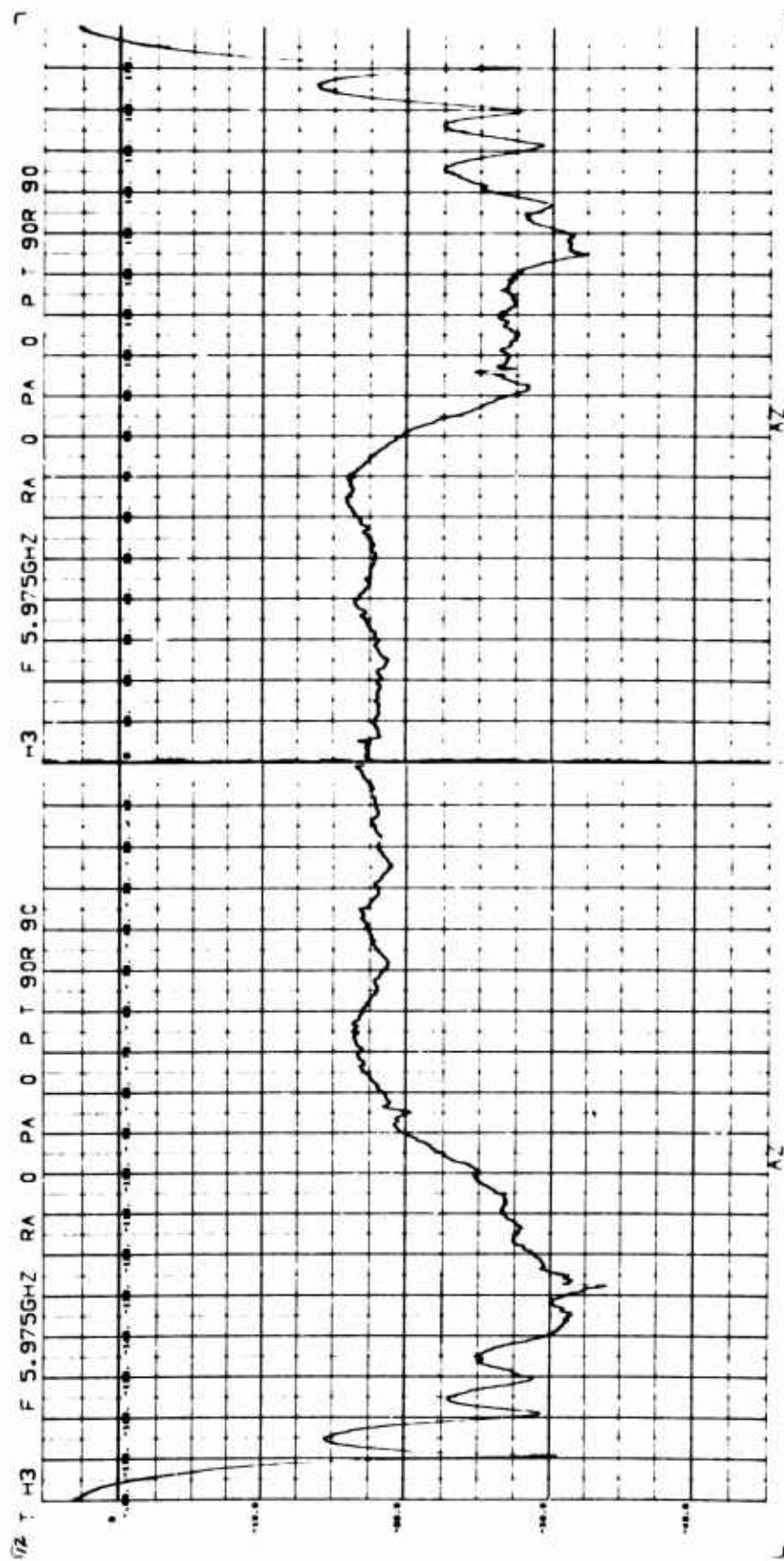


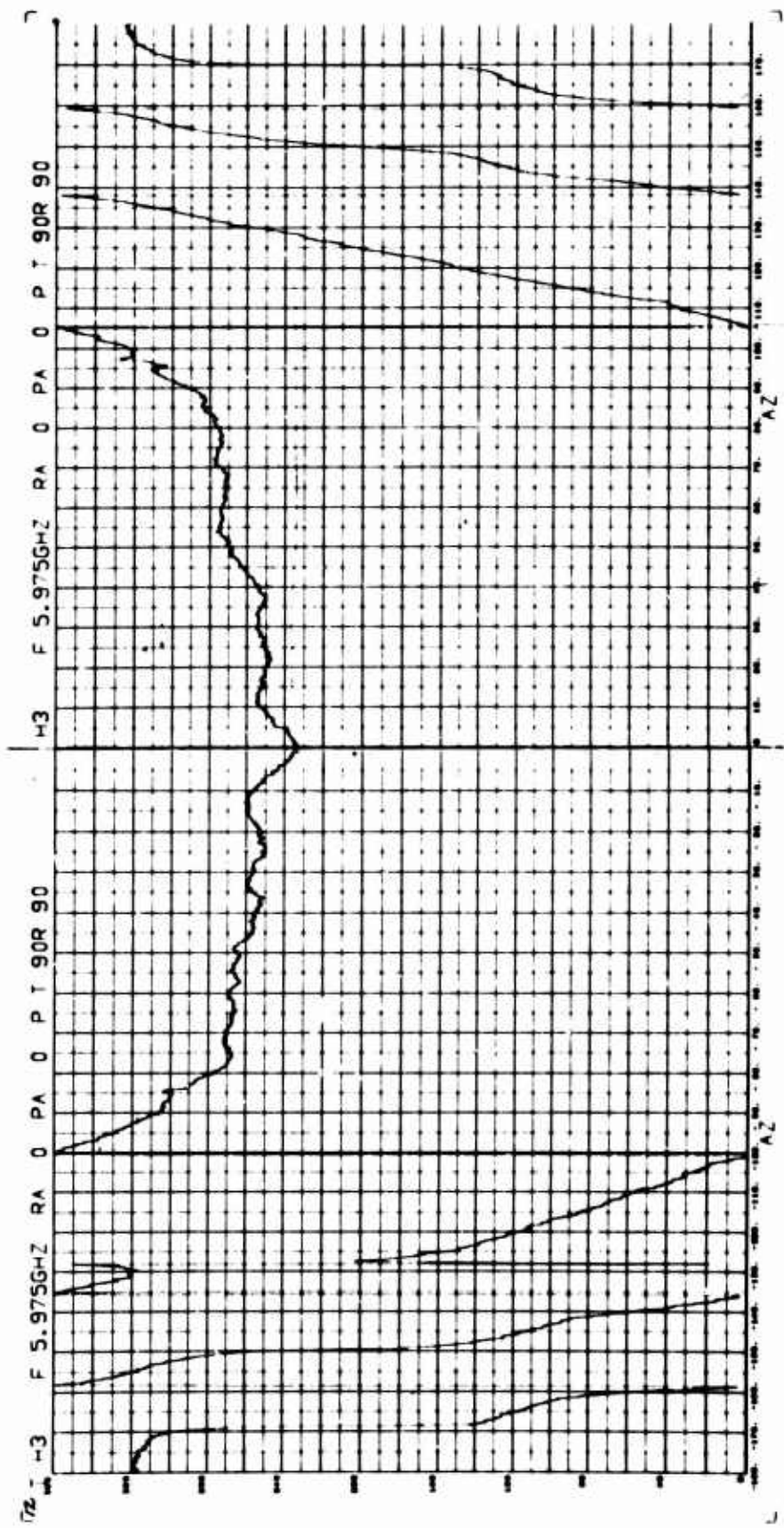


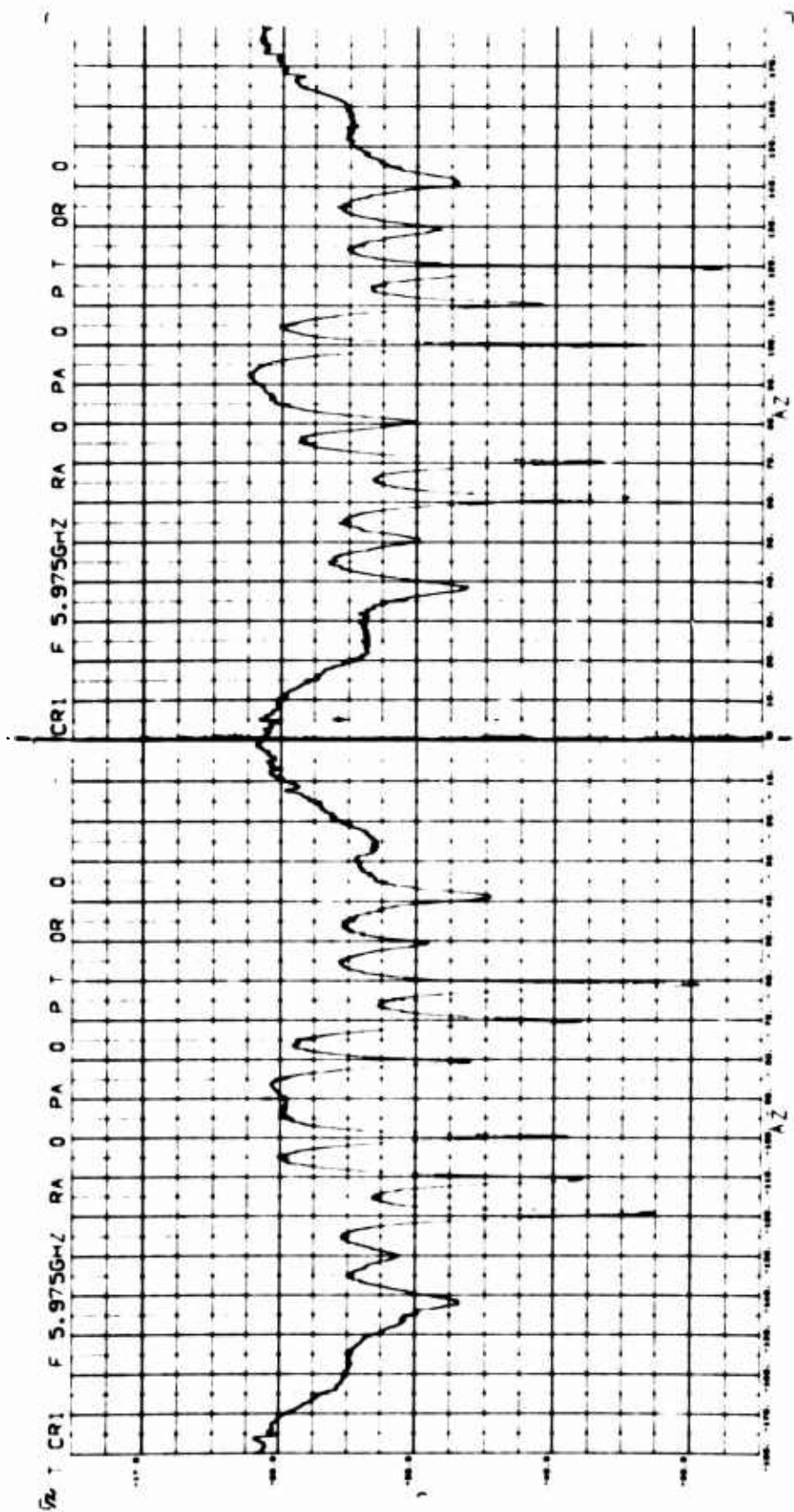


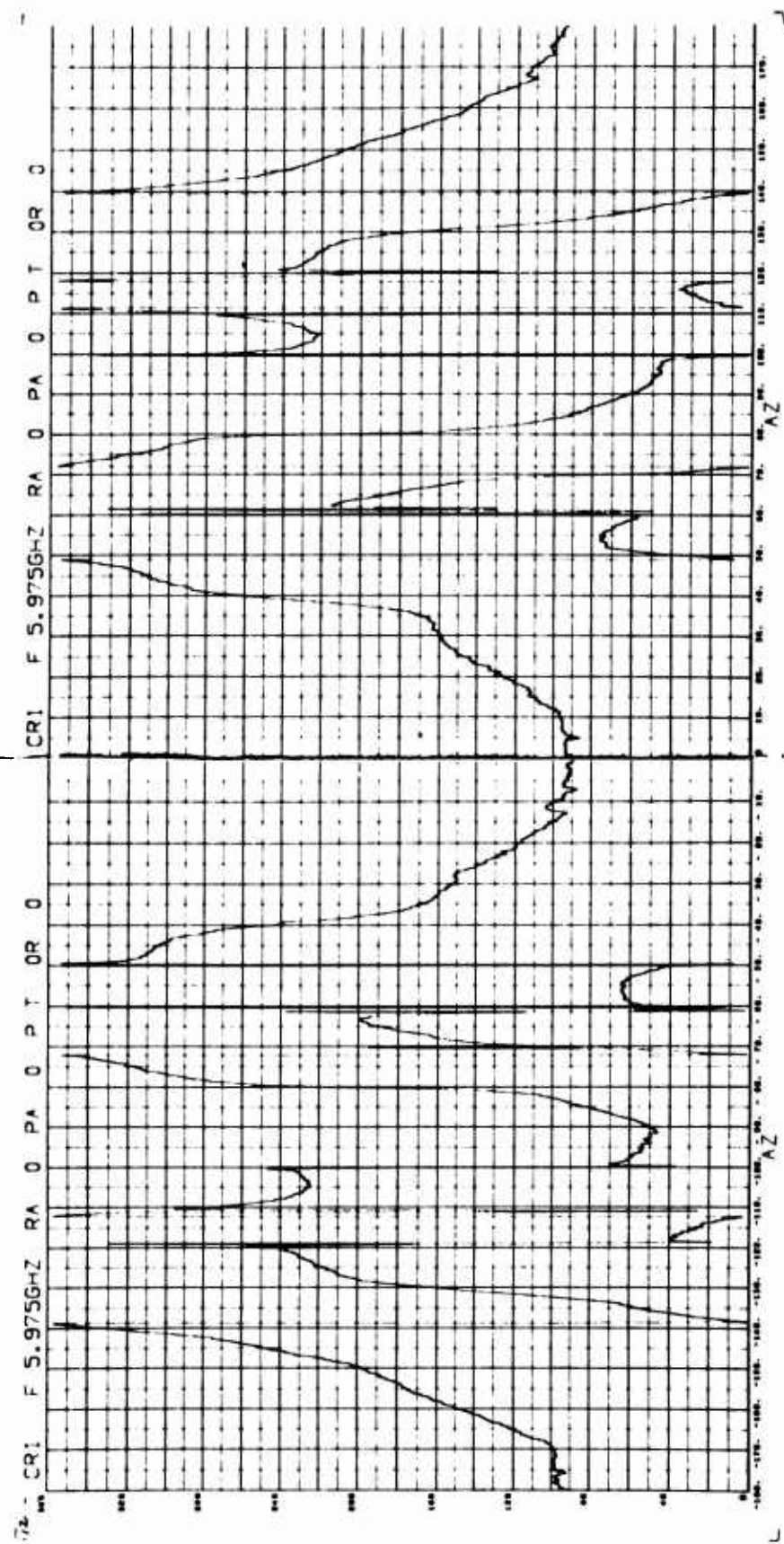


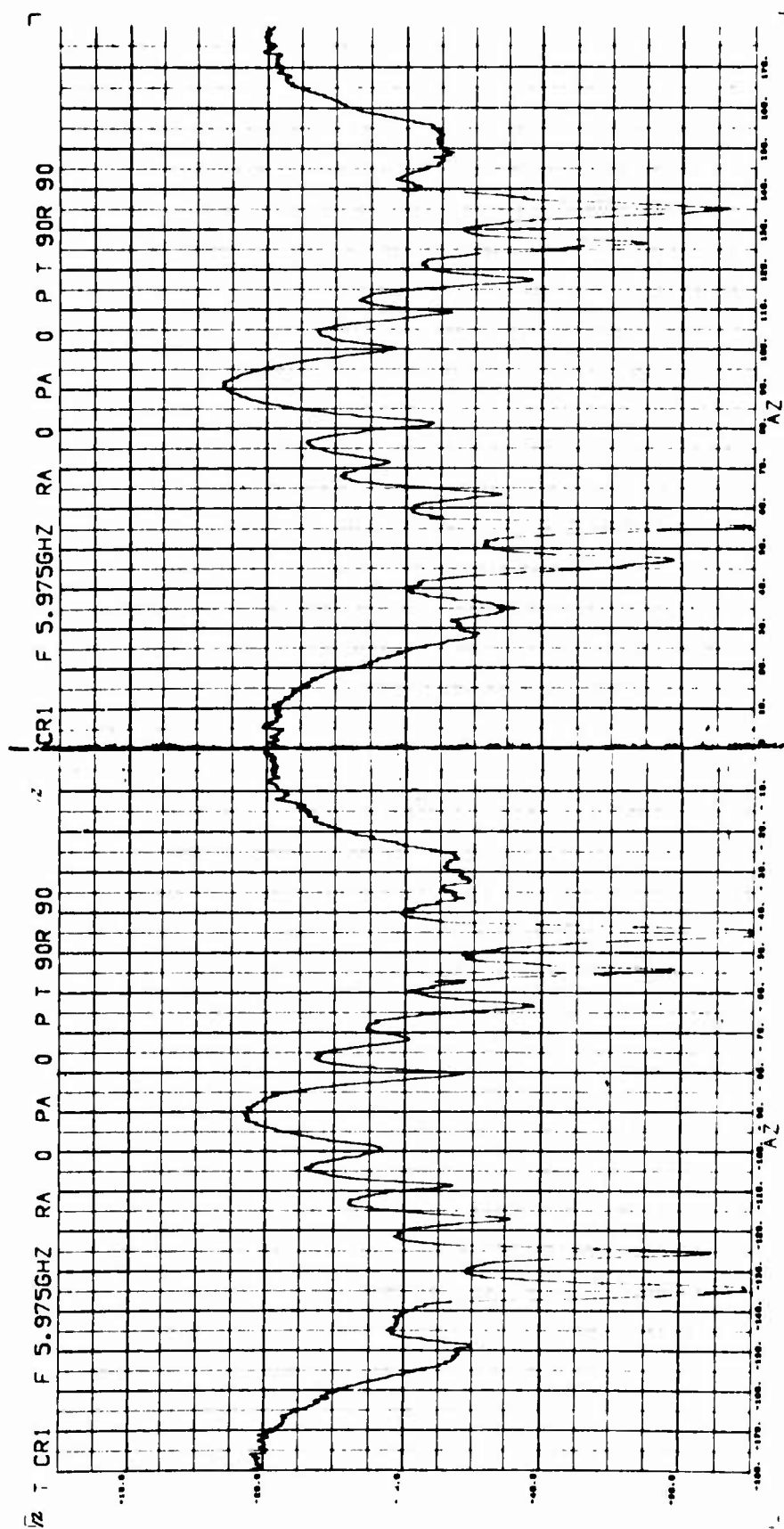


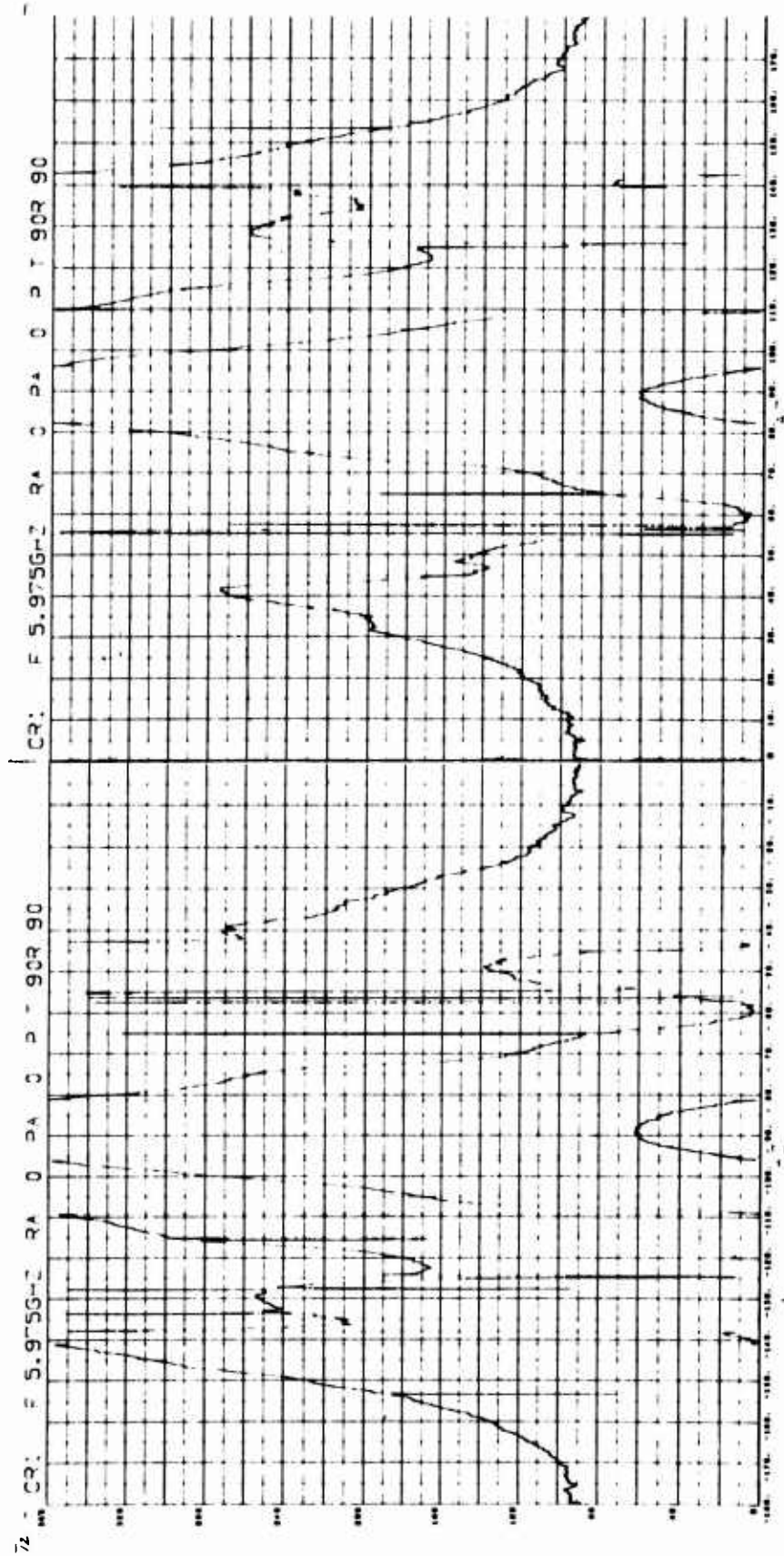


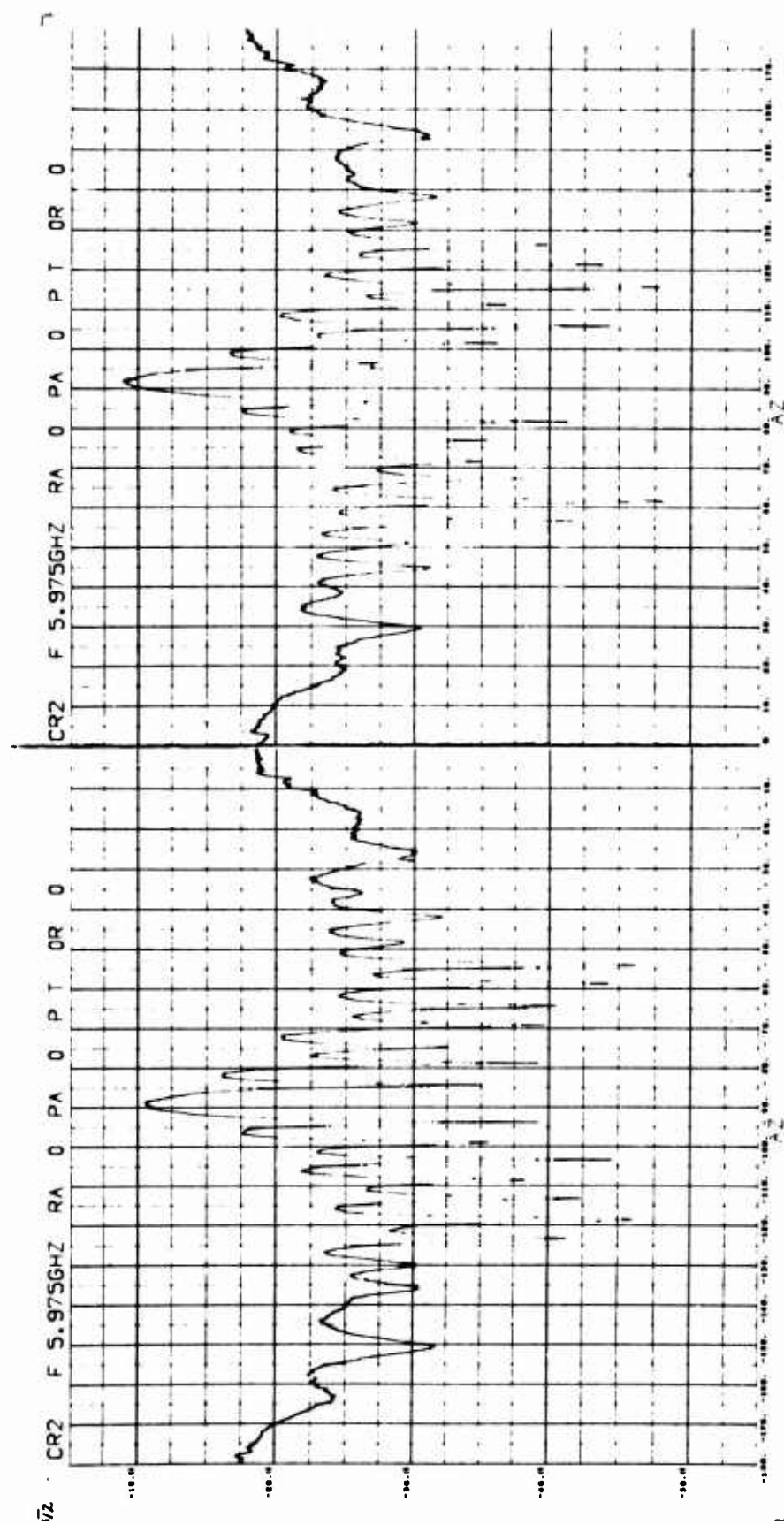


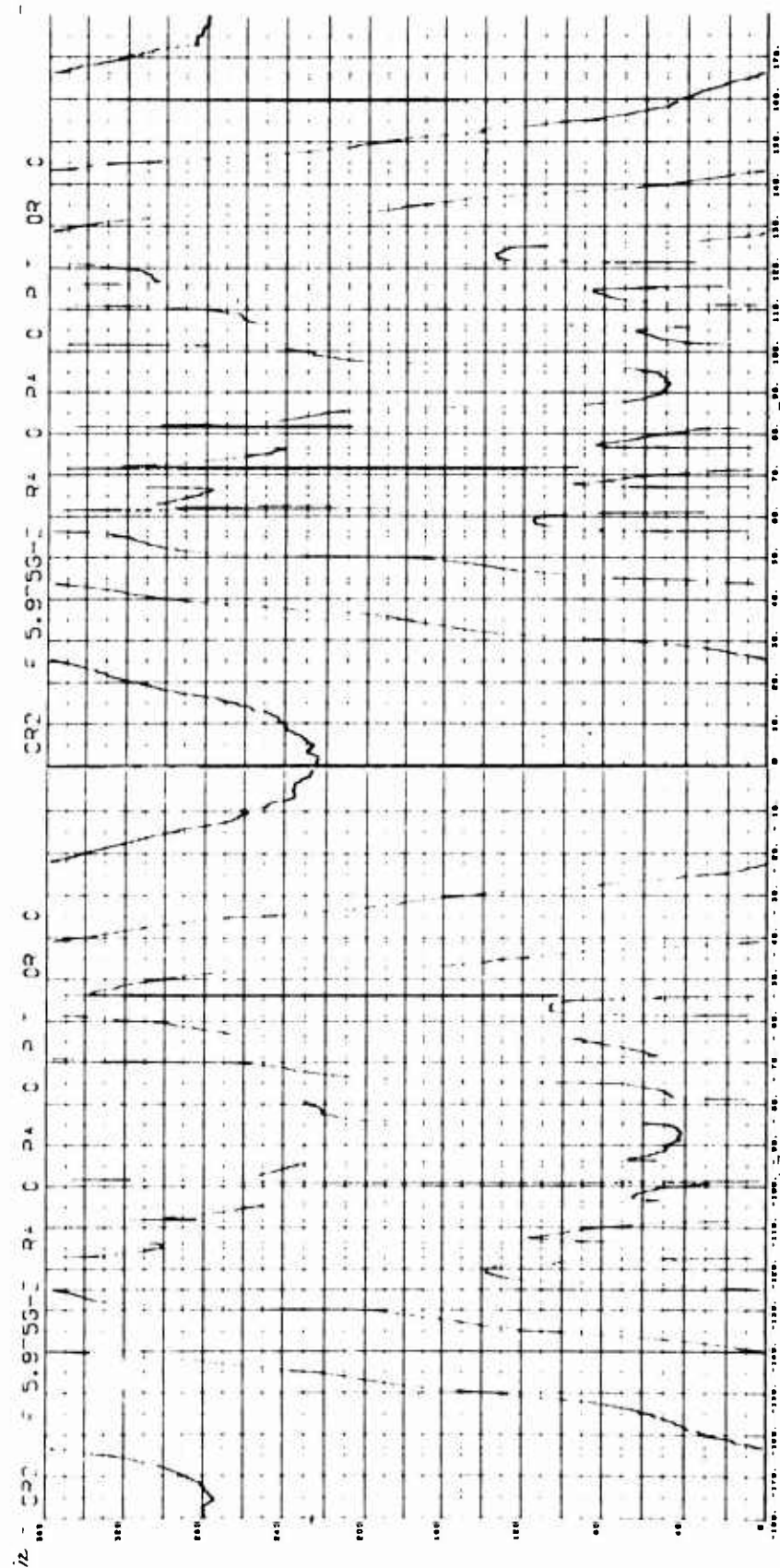


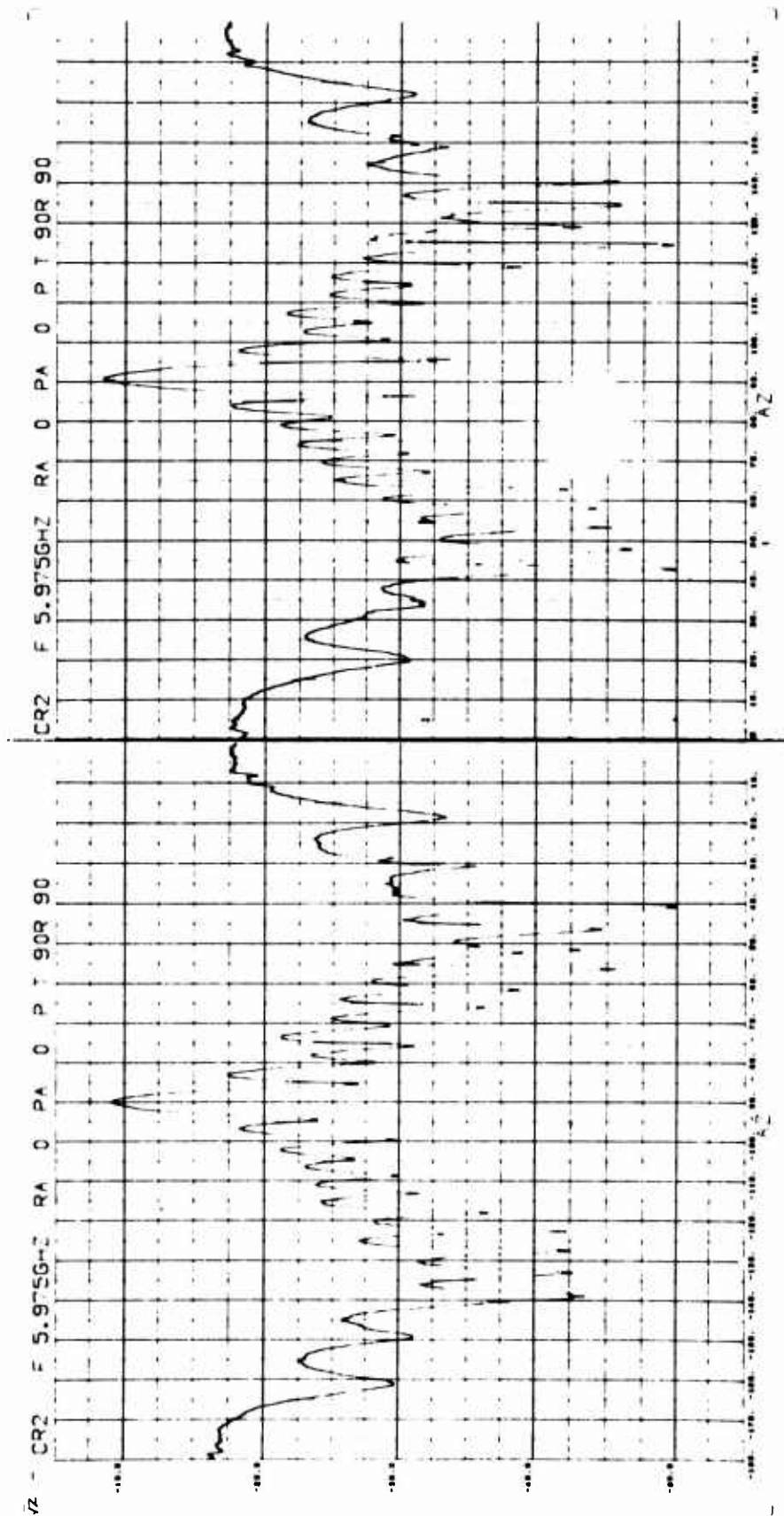


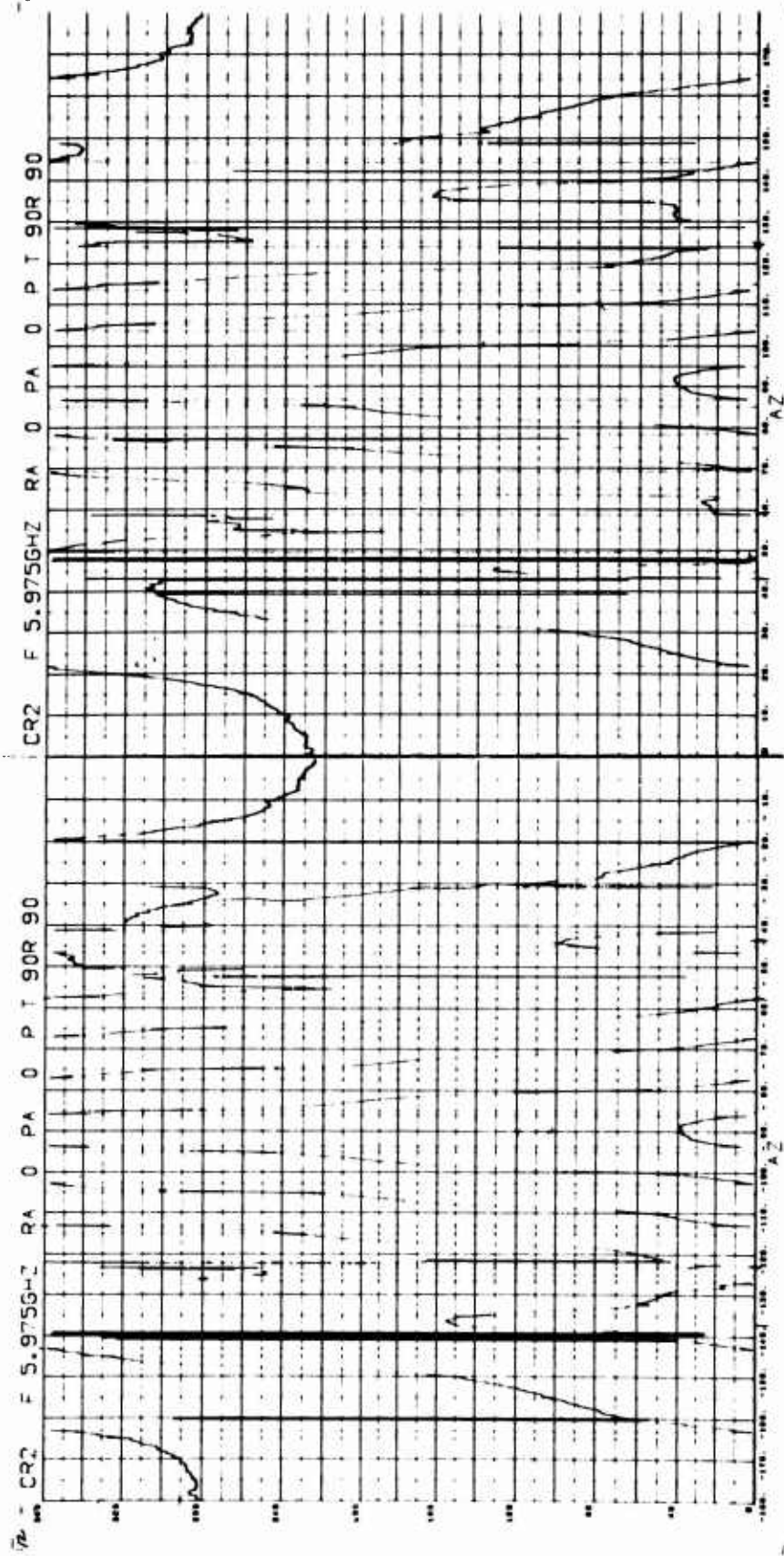


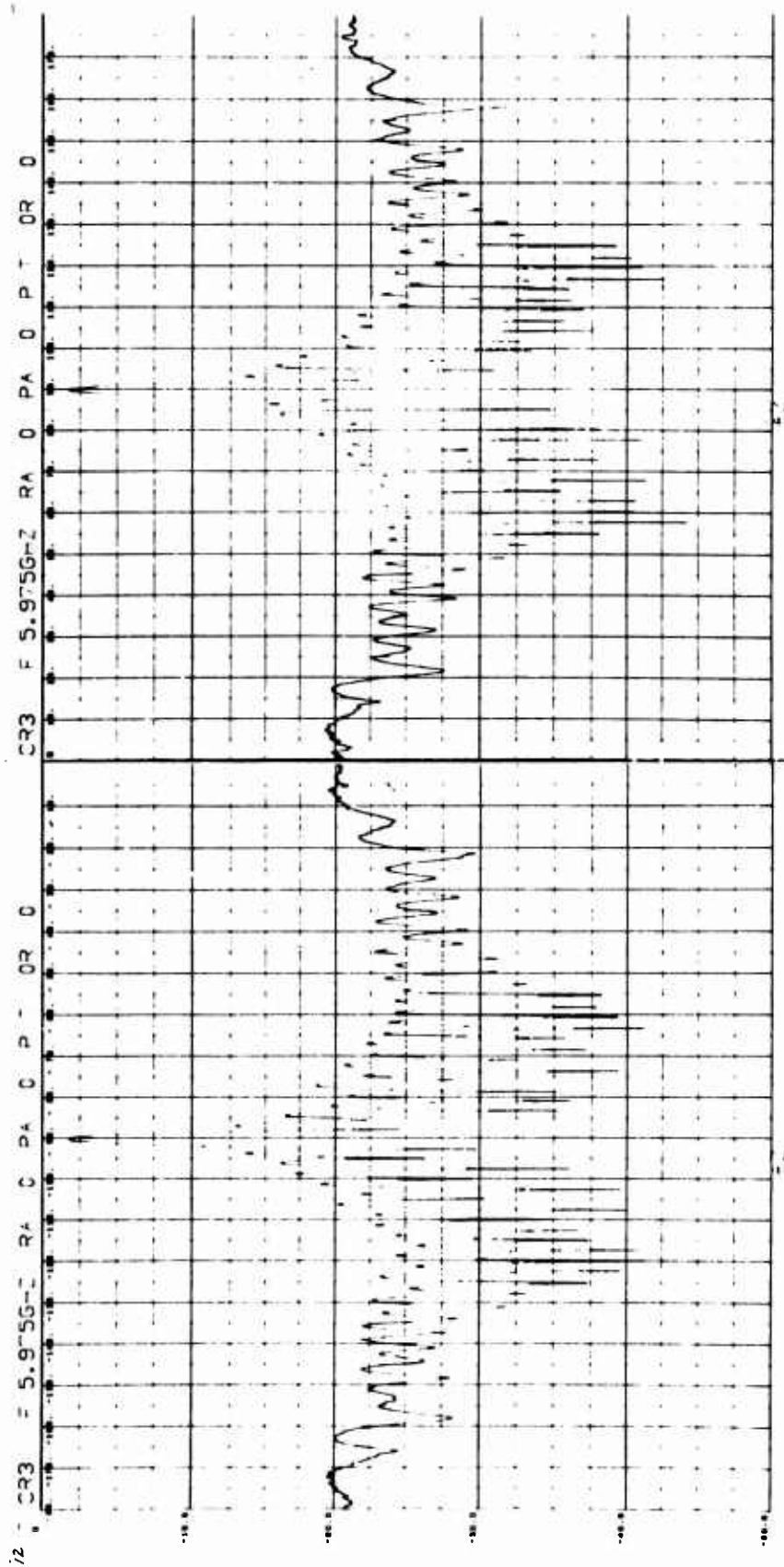


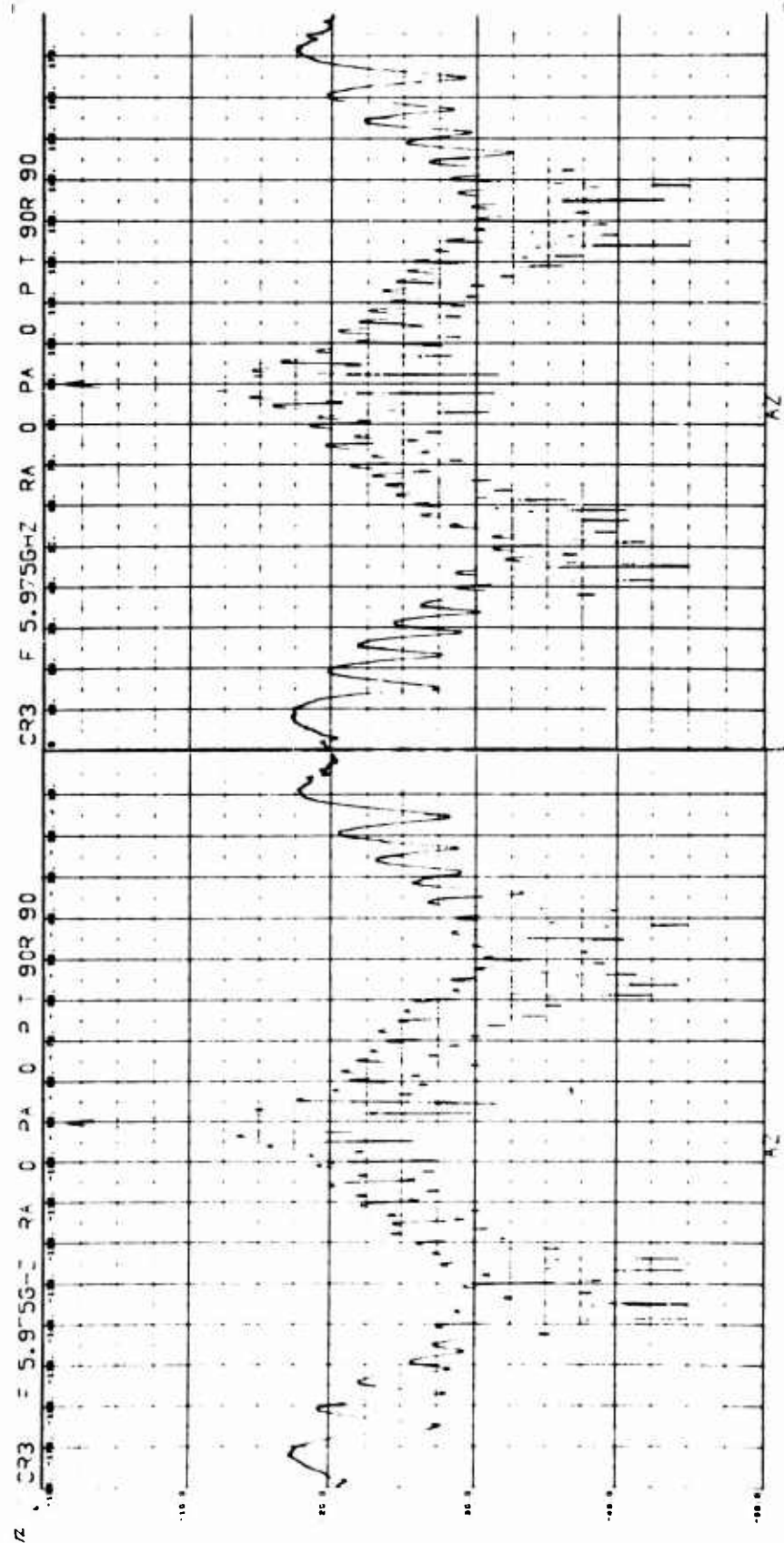


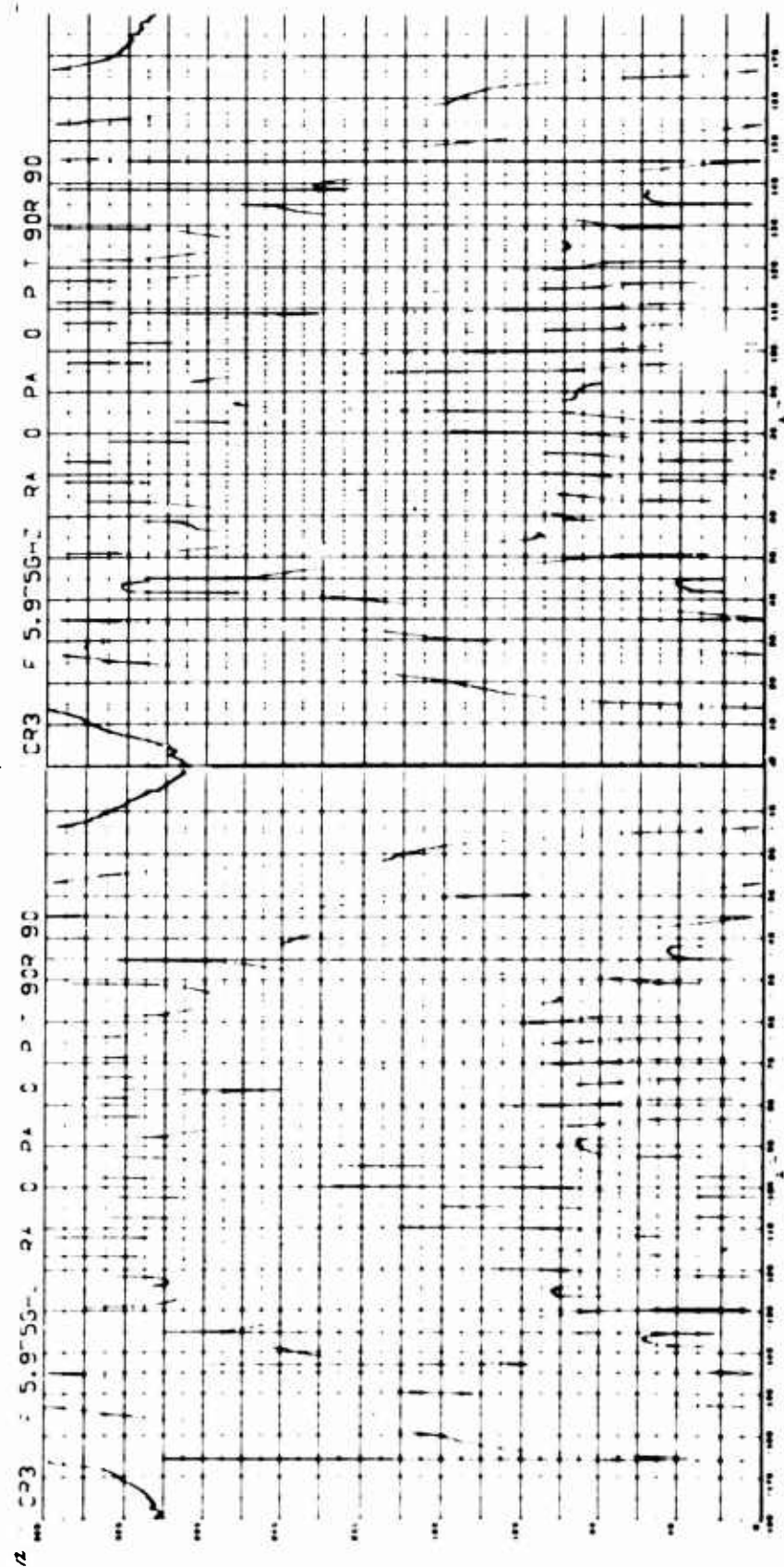


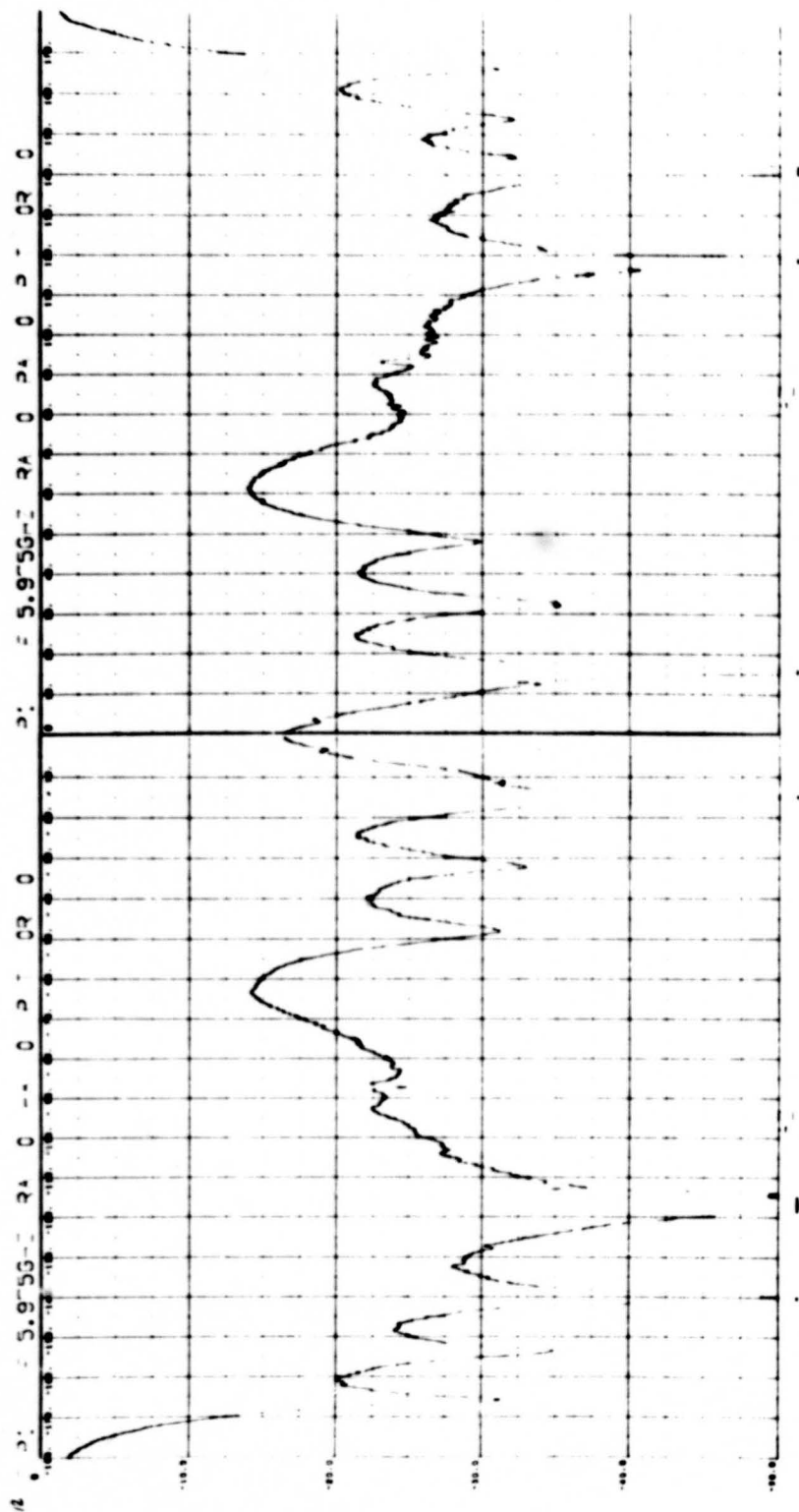


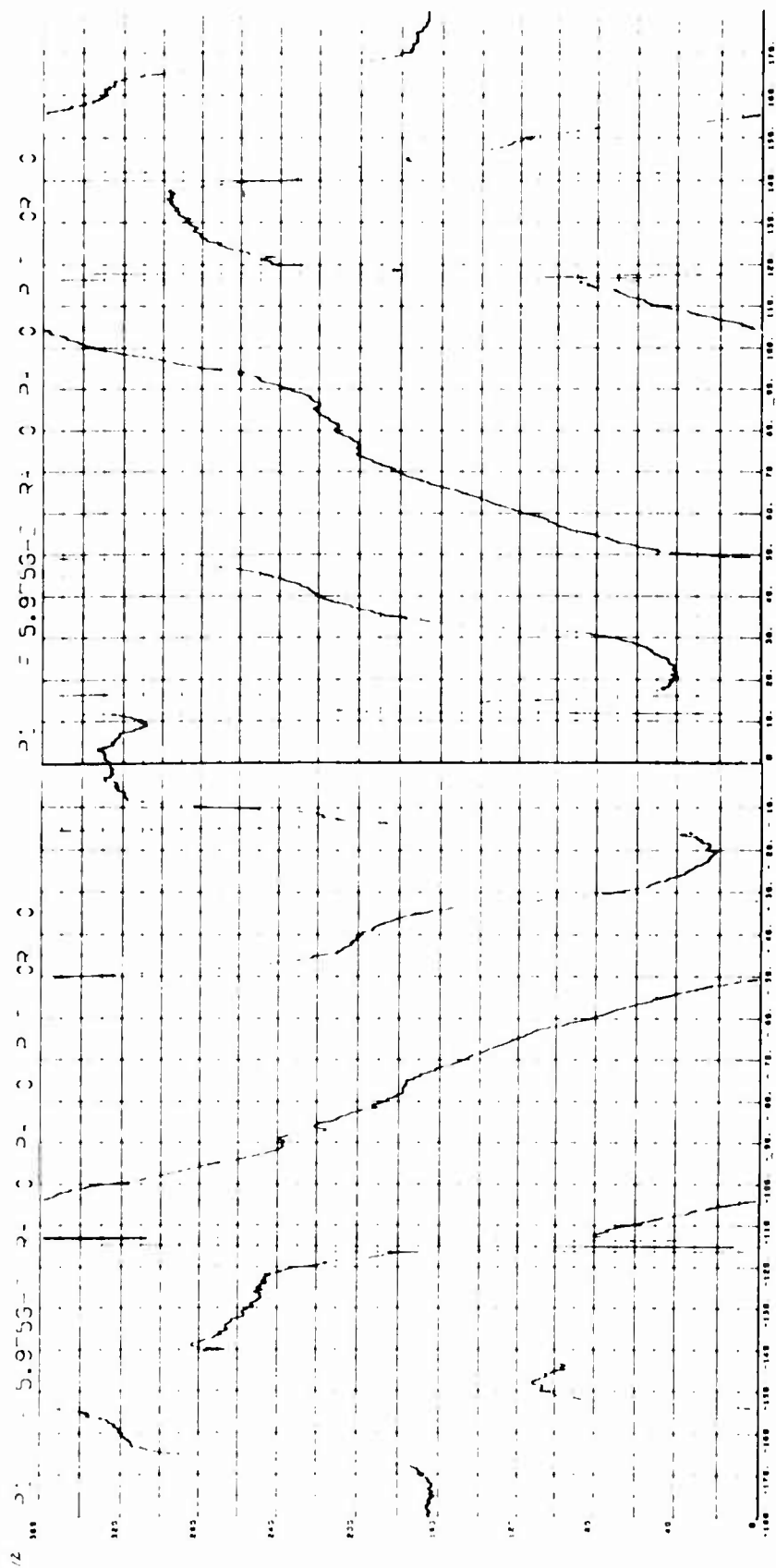


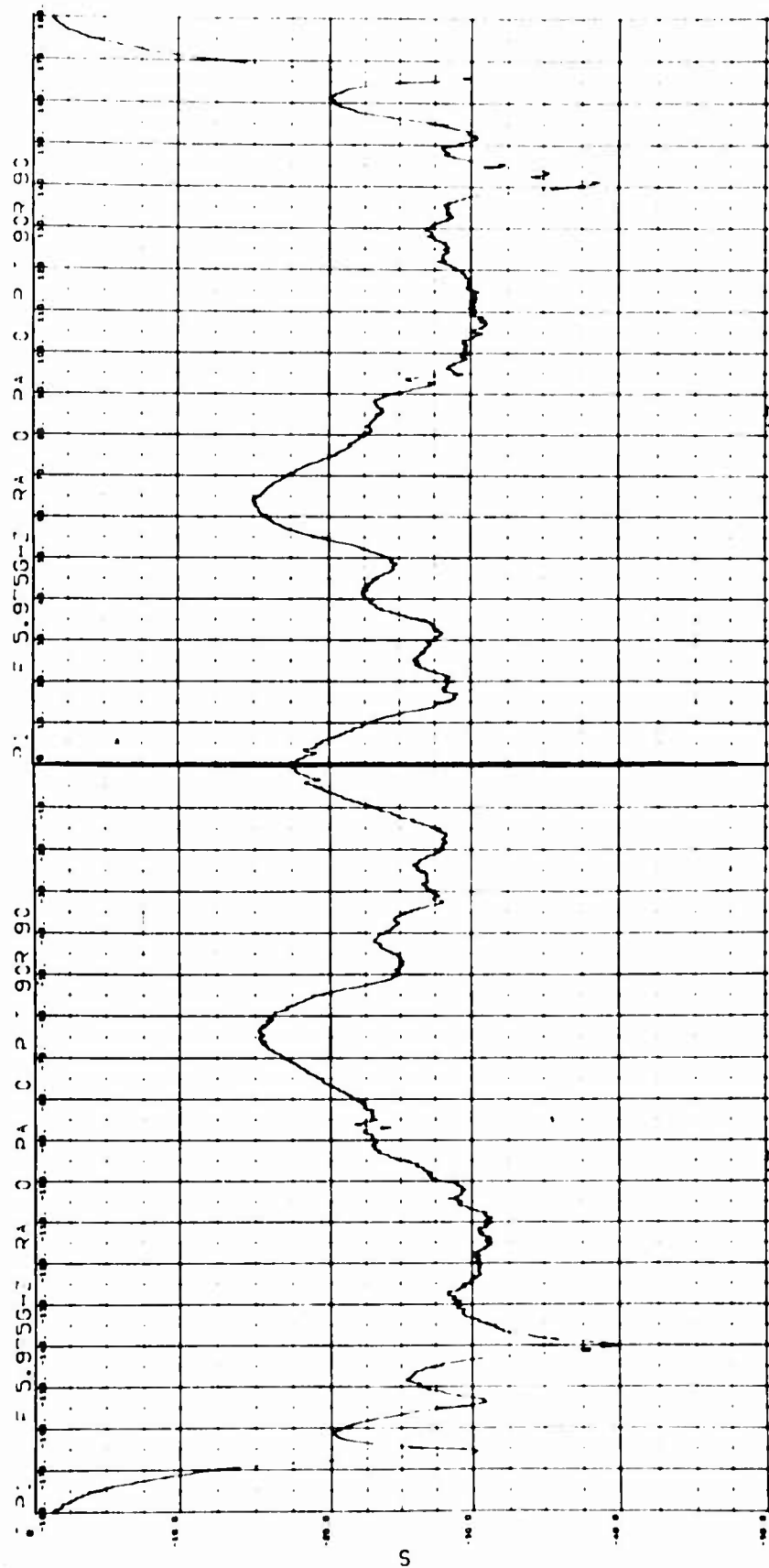


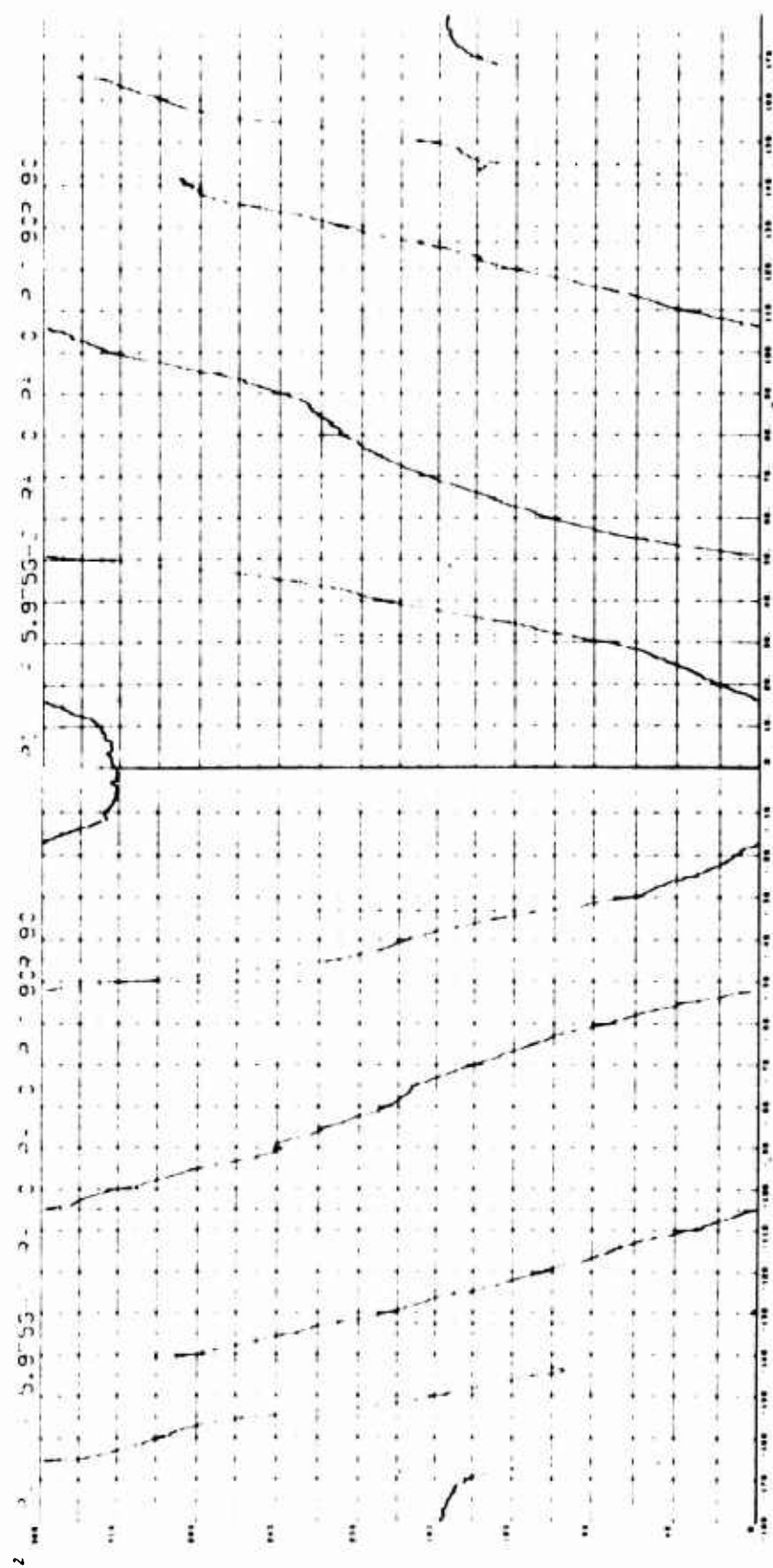


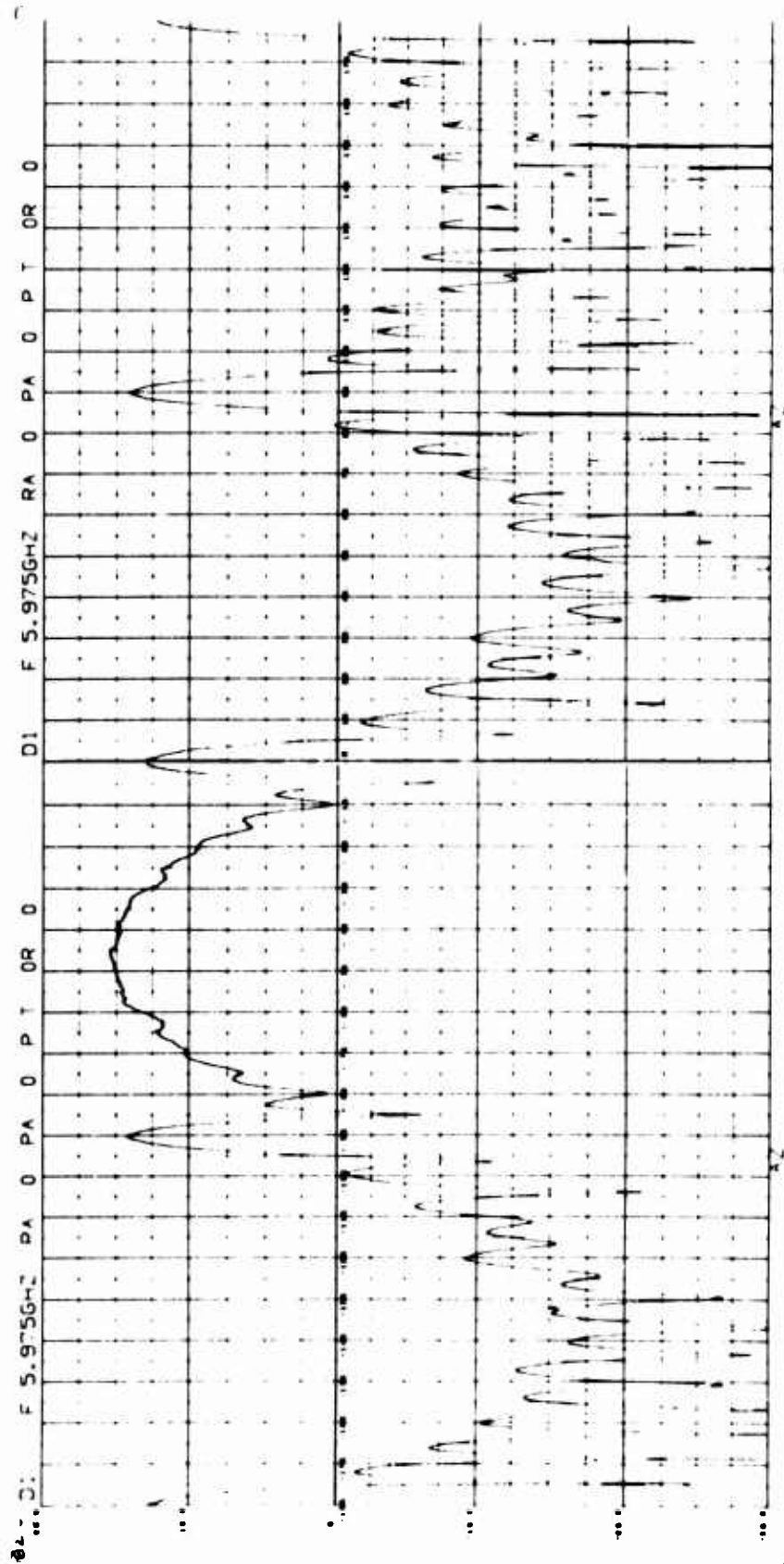


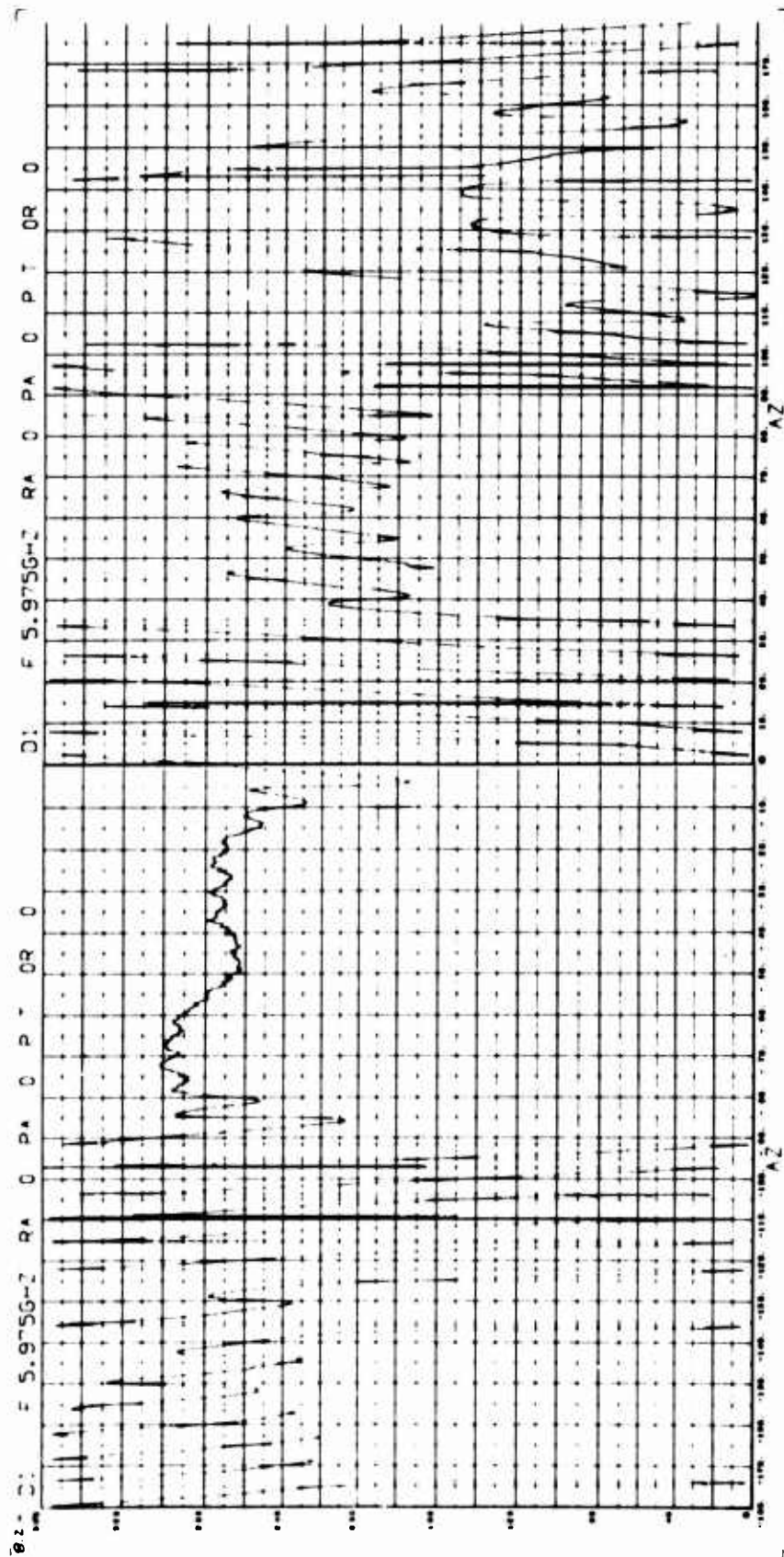


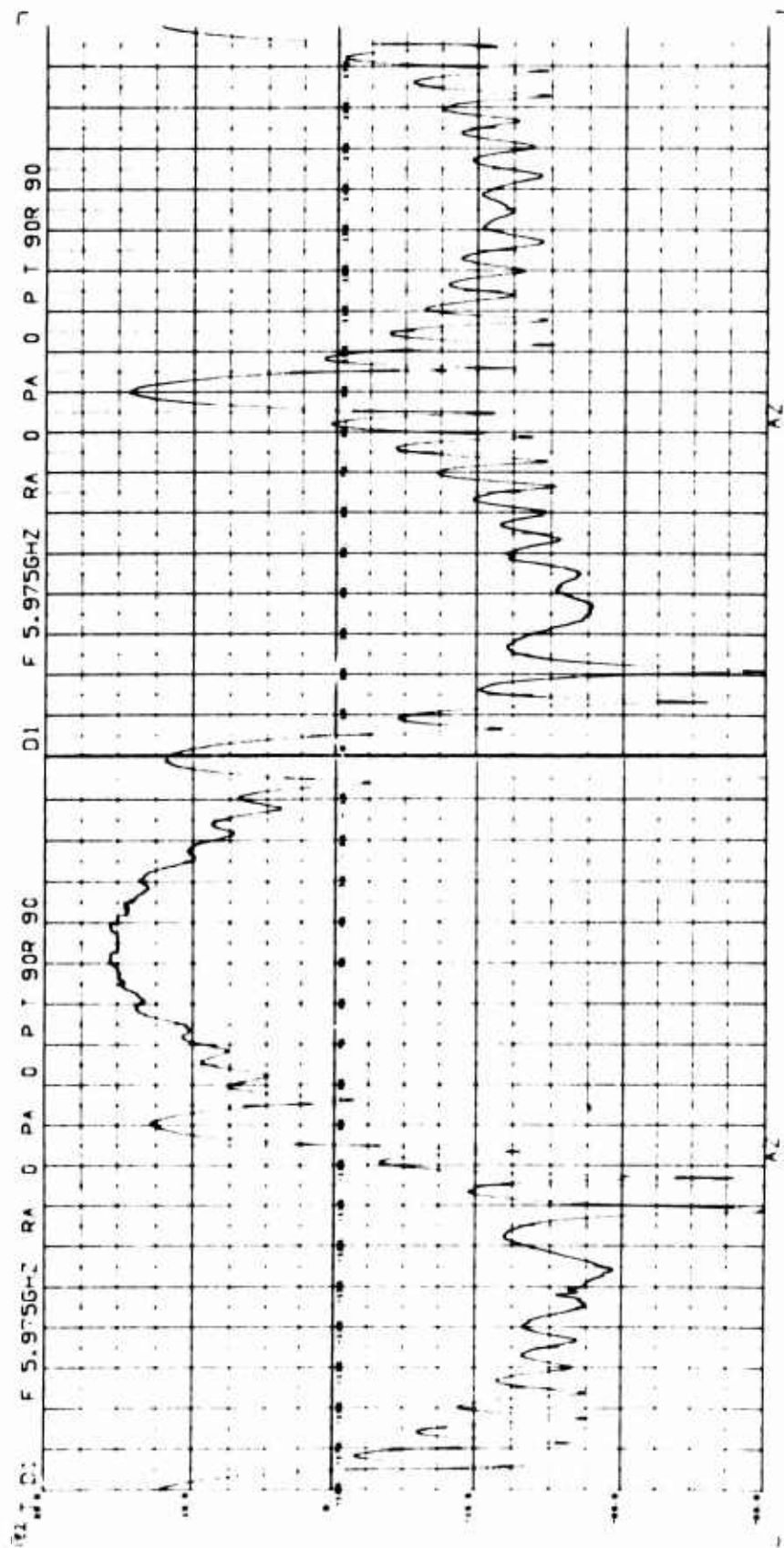


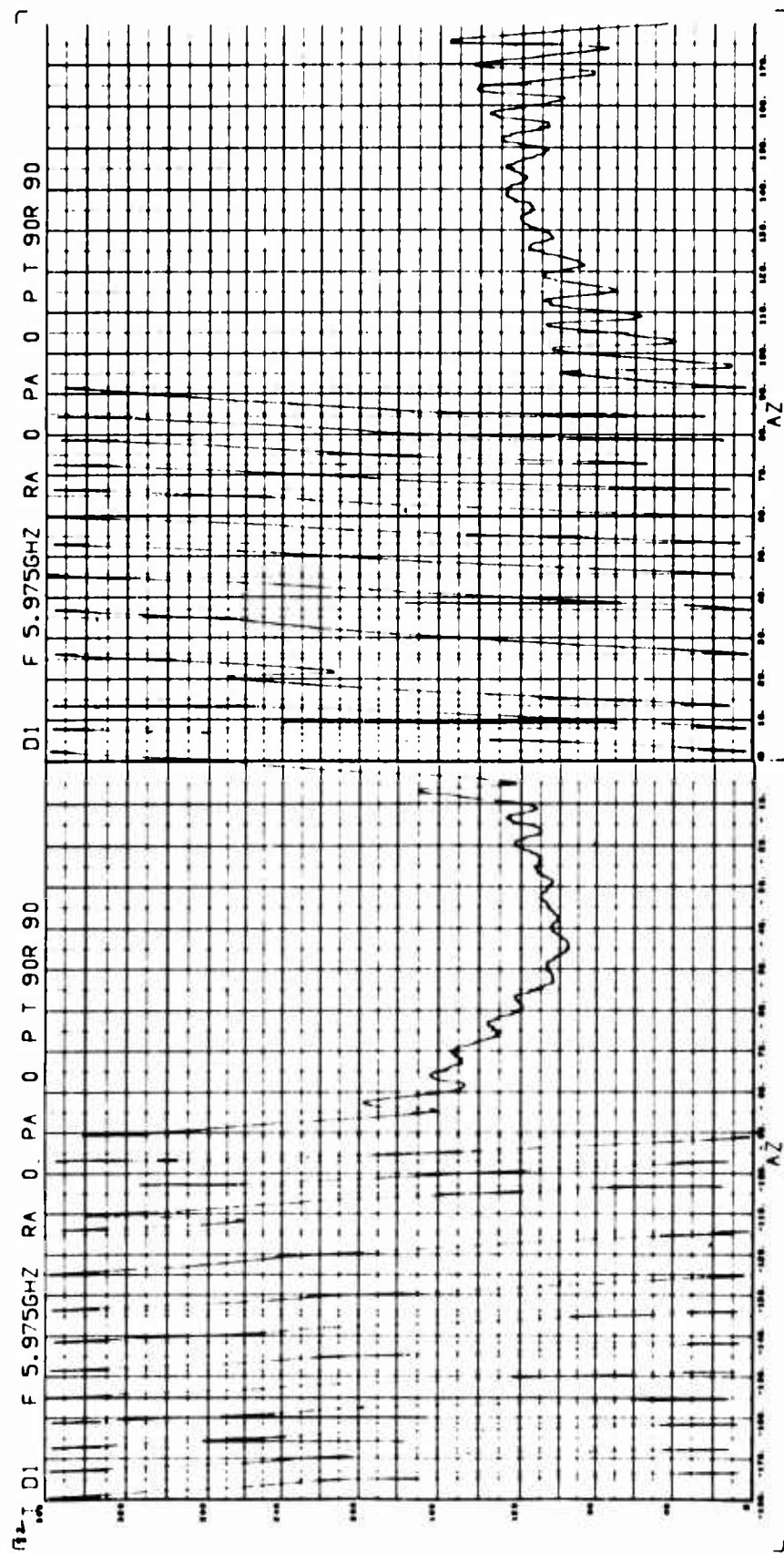












3.2.2 Composite Generic Vehicles

As an aid in the analysis of radar target signatures, the generic shapes were assembled in various configurations to produce composite generic shapes. The similarity of the composite target signatures to those of the generic shapes is evidenced by comparing the plots presented in this paragraph with those in paragraph 3.2.1. The composite generic target measurements are listed in Table 3-3 and some of the configurations are shown in Figure 3-3.

Table 3-3 COMPOSITE GENERIC VEHICLE MEASUREMENTS

VEHICLE	SYMBOL	MAXIMUM DIAMETER INCHES	MINIMUM DIAMETER INCHES	MAXIMUM LENGTH INCHES	FREQUENCY GHZ	BISTATIC ANGLE DEGREES	ρ DEGREES	R INCHES
FRUSTRUM 2 CYLINDER 5 FRUSTRUM 4 CYLINDER 3 FRUSTRUM 5 CYLINDER 5	F2Y5	7.500	6.320	19.460	5.975	0	180.0	0.530
	F4Y3	6.320	4.892	14.576	5.975	0	97.3	0.228
	F5Y5	7.500	4.892	24.680	5.975	0	00.0	0.000
CYLINDER 4 FRUSTRUM 4	Y4F4	6.312	4.892	12.063	5.885	10	232.9	0.114
					6.050	30	230.6	0.317
					5.975	0	204.3	0.047
FRUSTRUM 2 CYLINDER 5 FRUSTRUM 3	F2Y5F3	7.500	6.320	22.818	5.975	0	180.0	0.012
CONE 1 CYLINDER 3 CONE 2 CYLINDER 3 CONE 3 CYLINDER 3 CONE 4 CYLINDER 5 CONE 2 FRUSTRUM 2 CONE 1 CYLINDER 1 FRUSTRUM 3 CONE 2 CYLINDER 3 FRUSTRUM 3 CONE 4 CYLINDER 3 FRUSTRUM 3	C1Y3	6.320	0.000	22.246	5.975	0	0.0	0.000
	C2Y3	6.320	0.000	26.327	5.975	0	37.8	0.343
	C3Y3	6.320	0.000	12.543	5.975	0	215.8	0.019
	C4Y5	7.500	0.000	31.243	6.0	0	225.8	0.571
	C2F2	7.500	0.000	18.014	6.0	0	24.5	0.525
	C1Y1F3	7.500	0.000	21.485	6.0	0	279.0	2.554
	C1Y3F3	7.500	0.000	25.654	5.975	0	193.9	1.202
	C1Y5F3	7.500	0.000	34.601	5.975	0	18.4	0.096
HEMISPHERE 2 CYLINDER 4 HEMISPHERE 3 CYLINDER 1 CYLINDER 2 HEMISPHERE 3 CYLINDER 3	H2Y4	4.892	-	10.446	5.975	0	239.6	0.027
	H3Y1Y2	6.320	-	17.817	5.975	0	173.8	0.963
	H3Y3	6.320	-	13.673	5.975	0	107.8	0.259
PARABOLOID 1 FRUSTRUM 4 PARABOLOID 1 FRUSTRUM 4 CYLINDER 3	P1F4 P1F4Y3	6.314 6.320	- -	7.563 18.076	5.975 5.975	0 0	182.8 180.0	0.329 0.134
AFT RACK 1 AFT RACK 2 AFT RACK 3	AR1 AR2 AR3	6.320 6.320 6.320	5.500 5.500 5.500	8.000 8.000 8.00	5.975 5.975 5.975	0 0 0	0.0 0.0 0.0	0.00 0.00 0.00

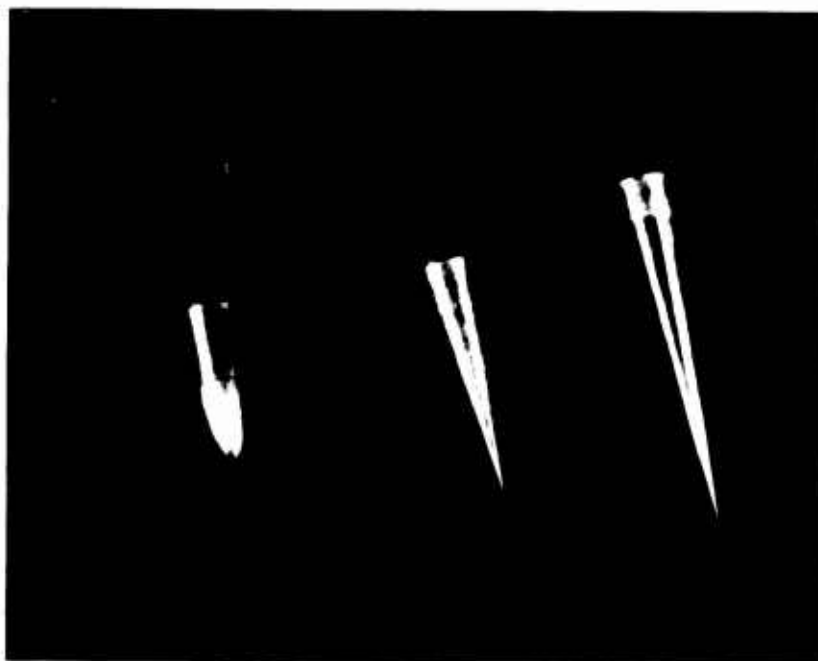
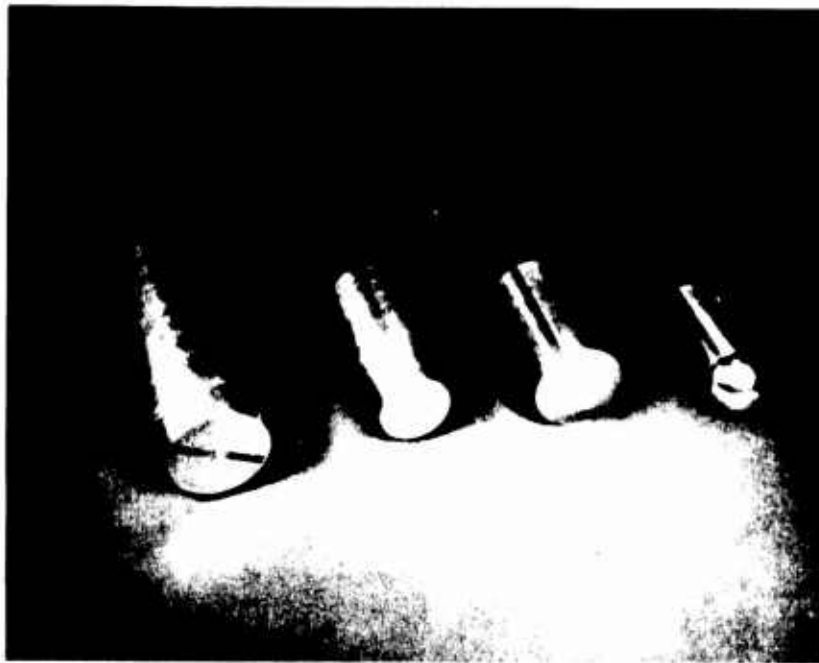
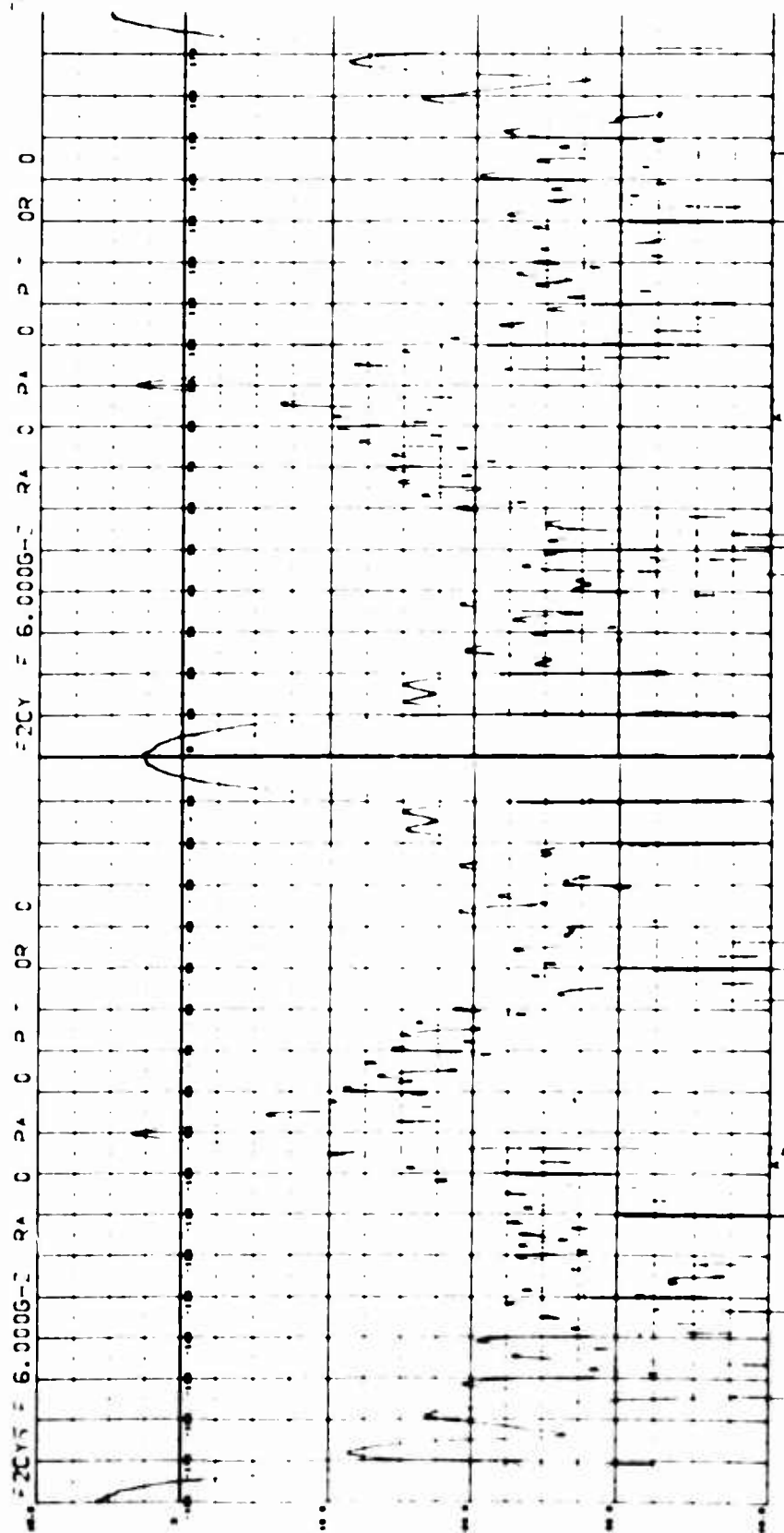
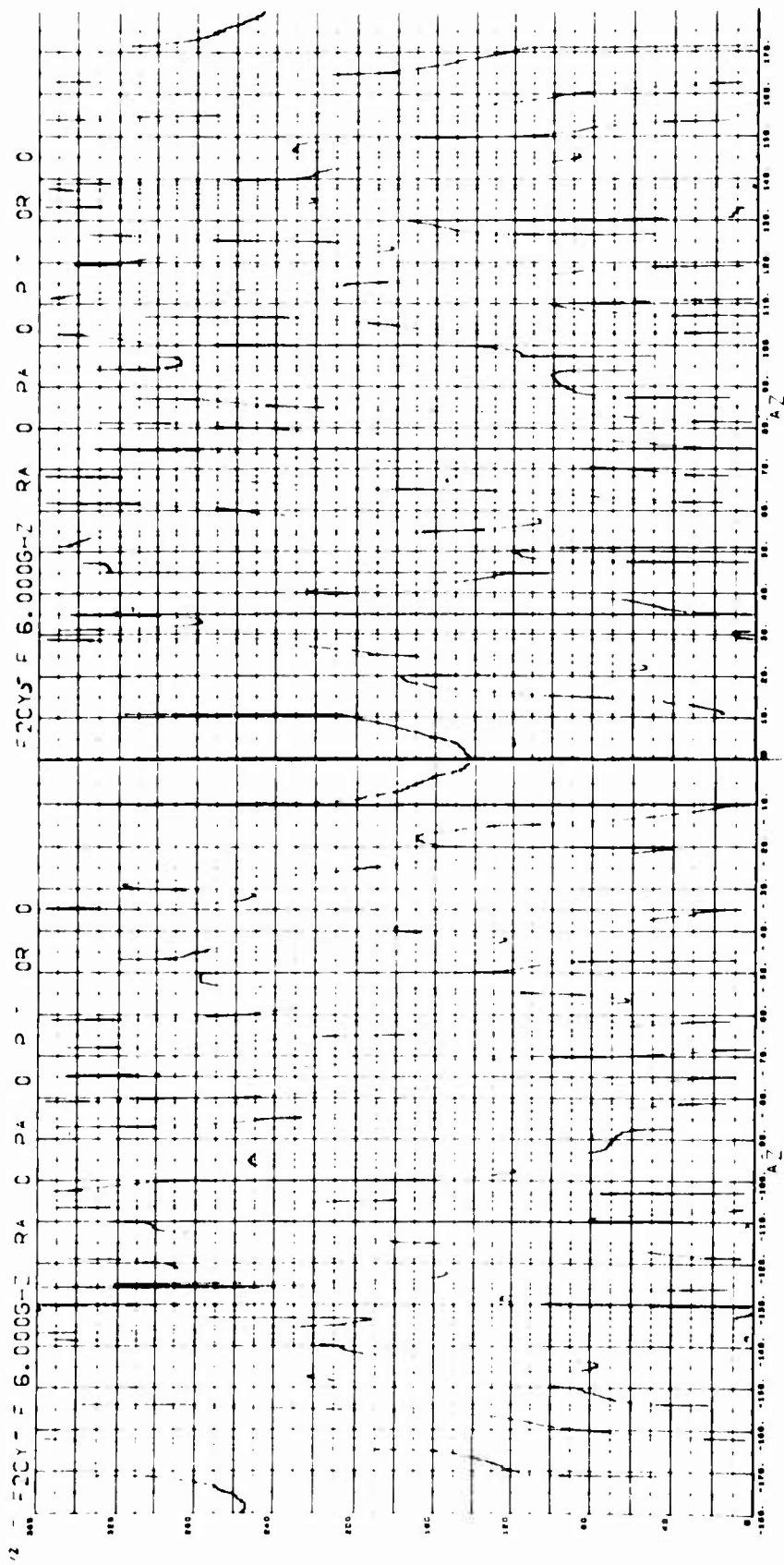
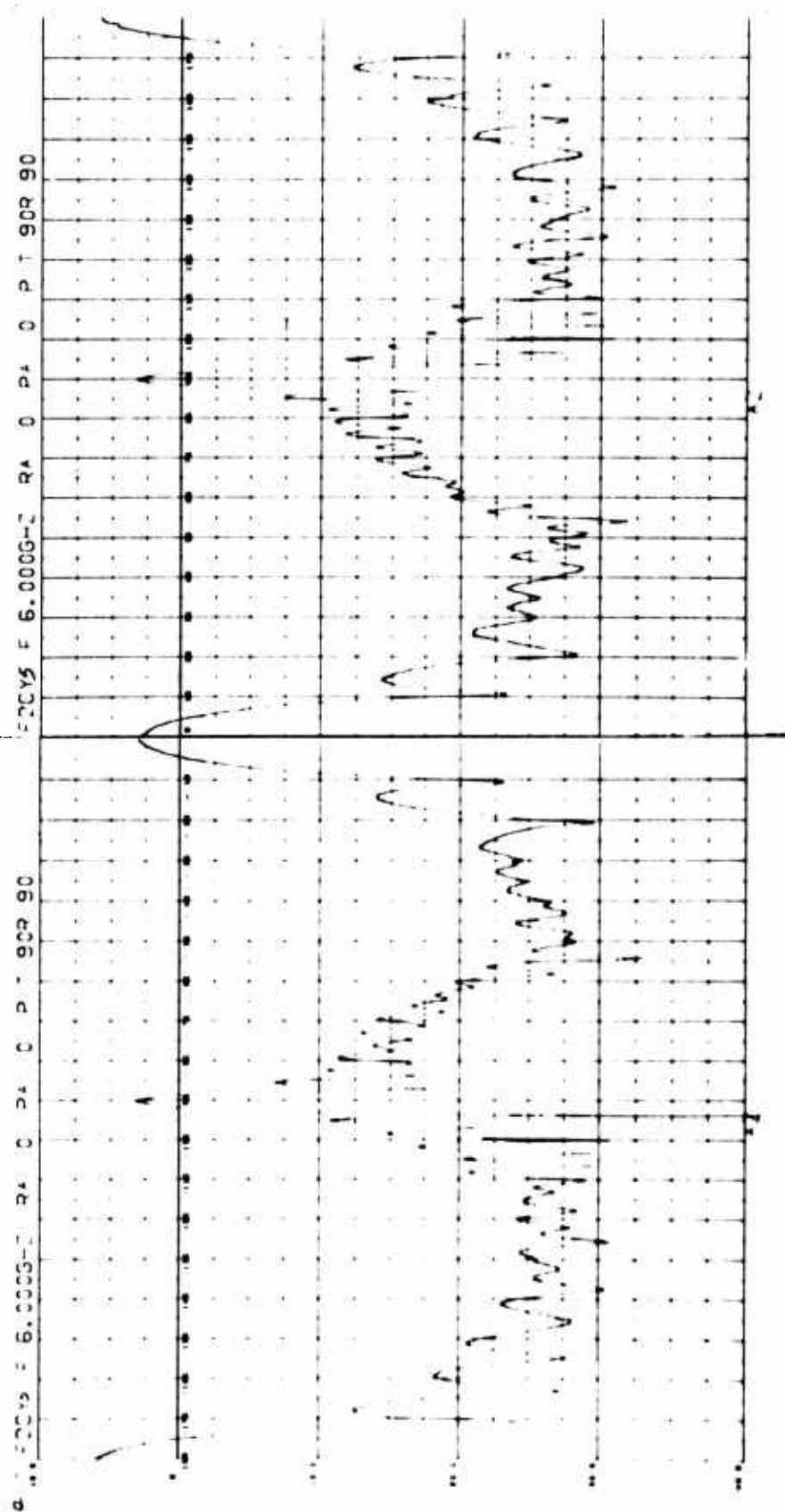
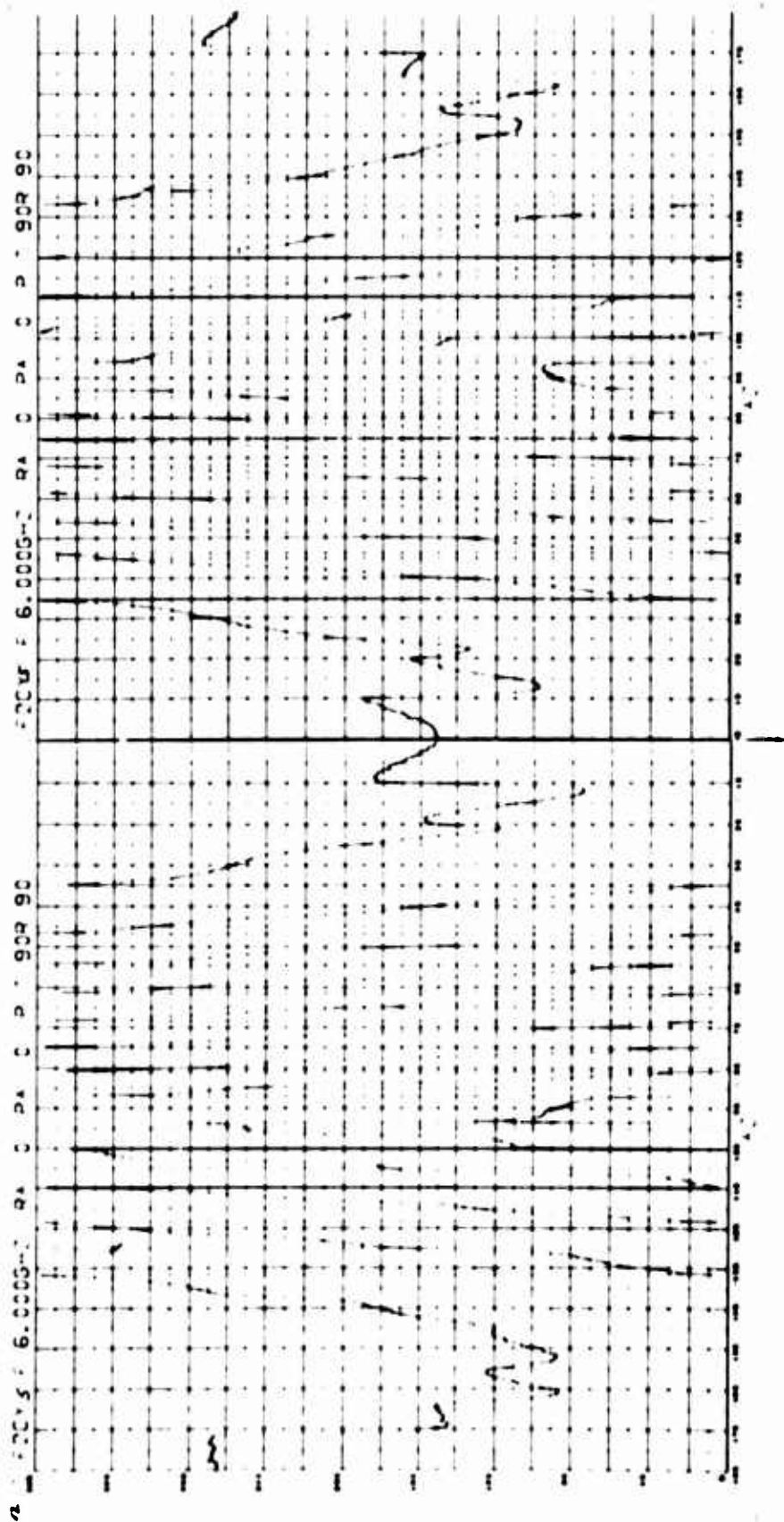


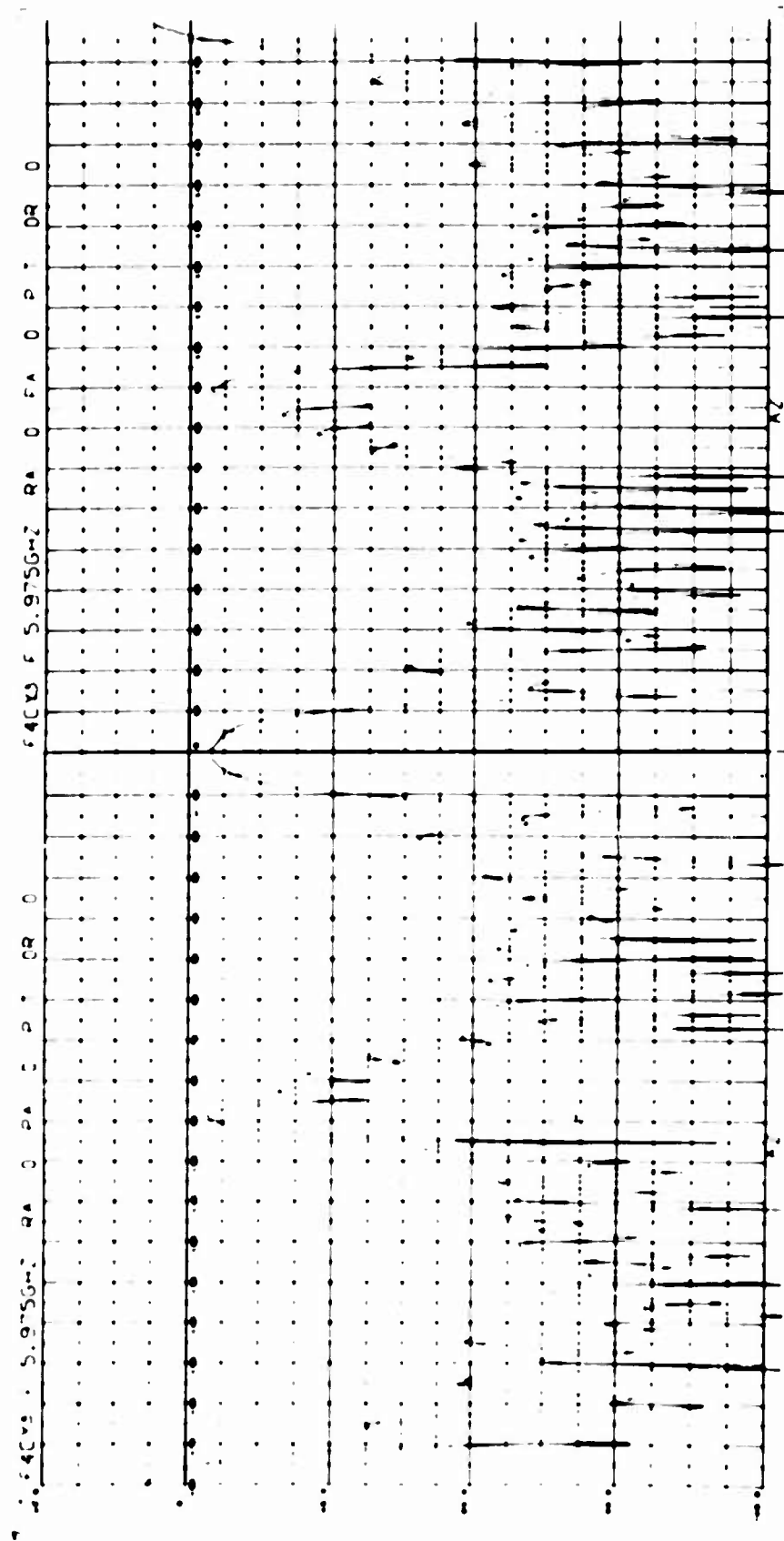
Fig. 3-3 COMPOSITE GENERIC VEHICLES

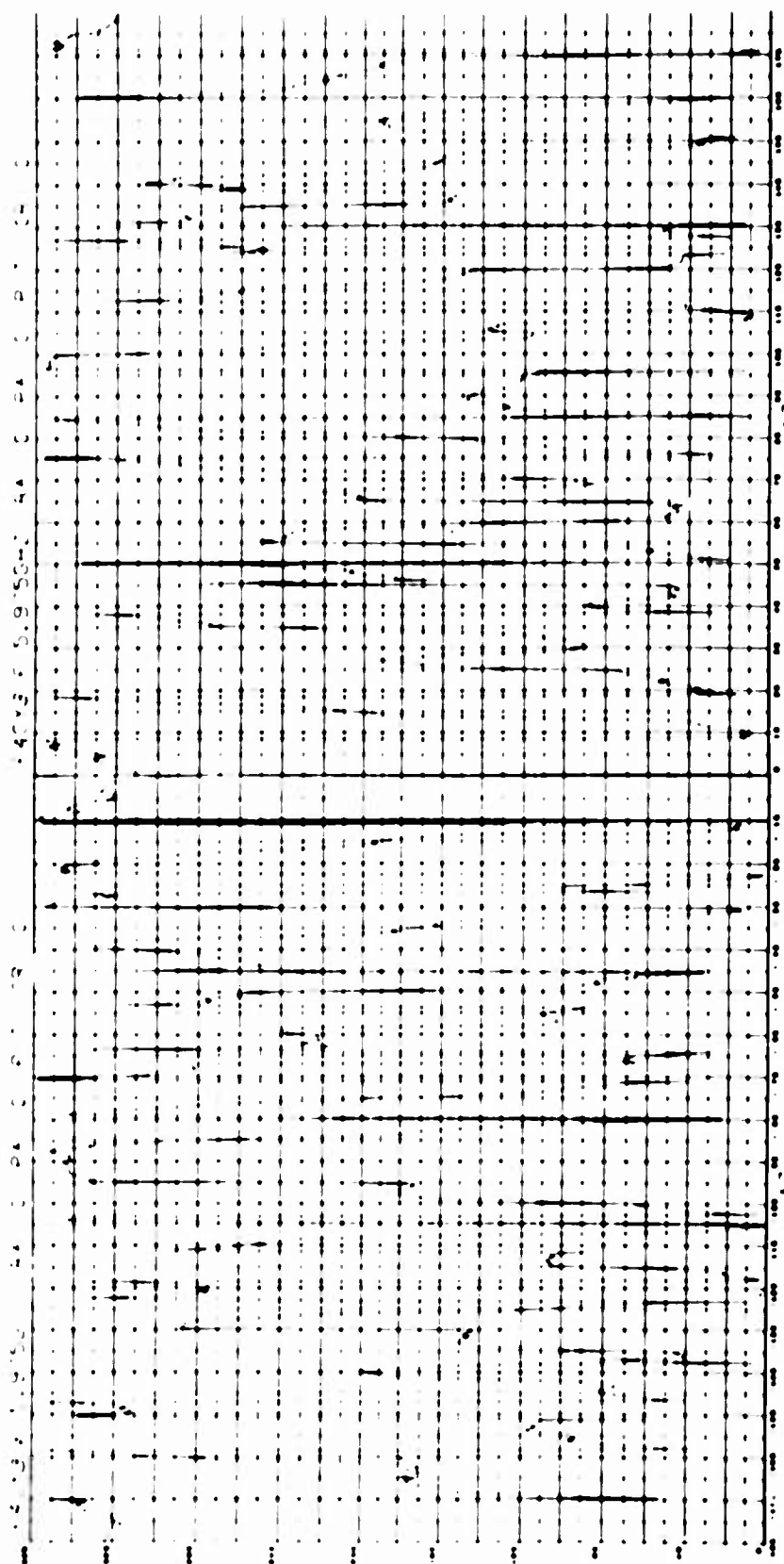


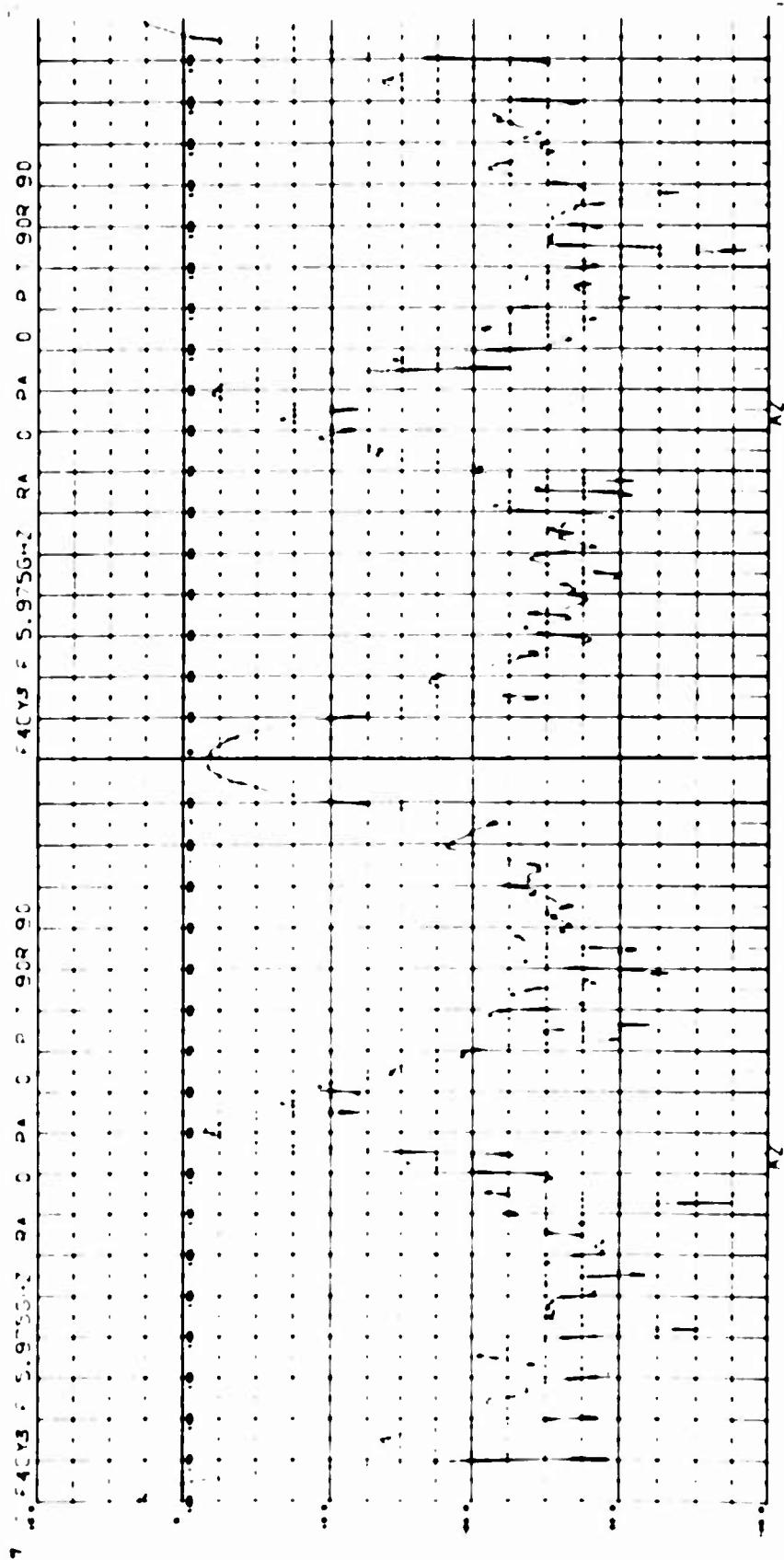


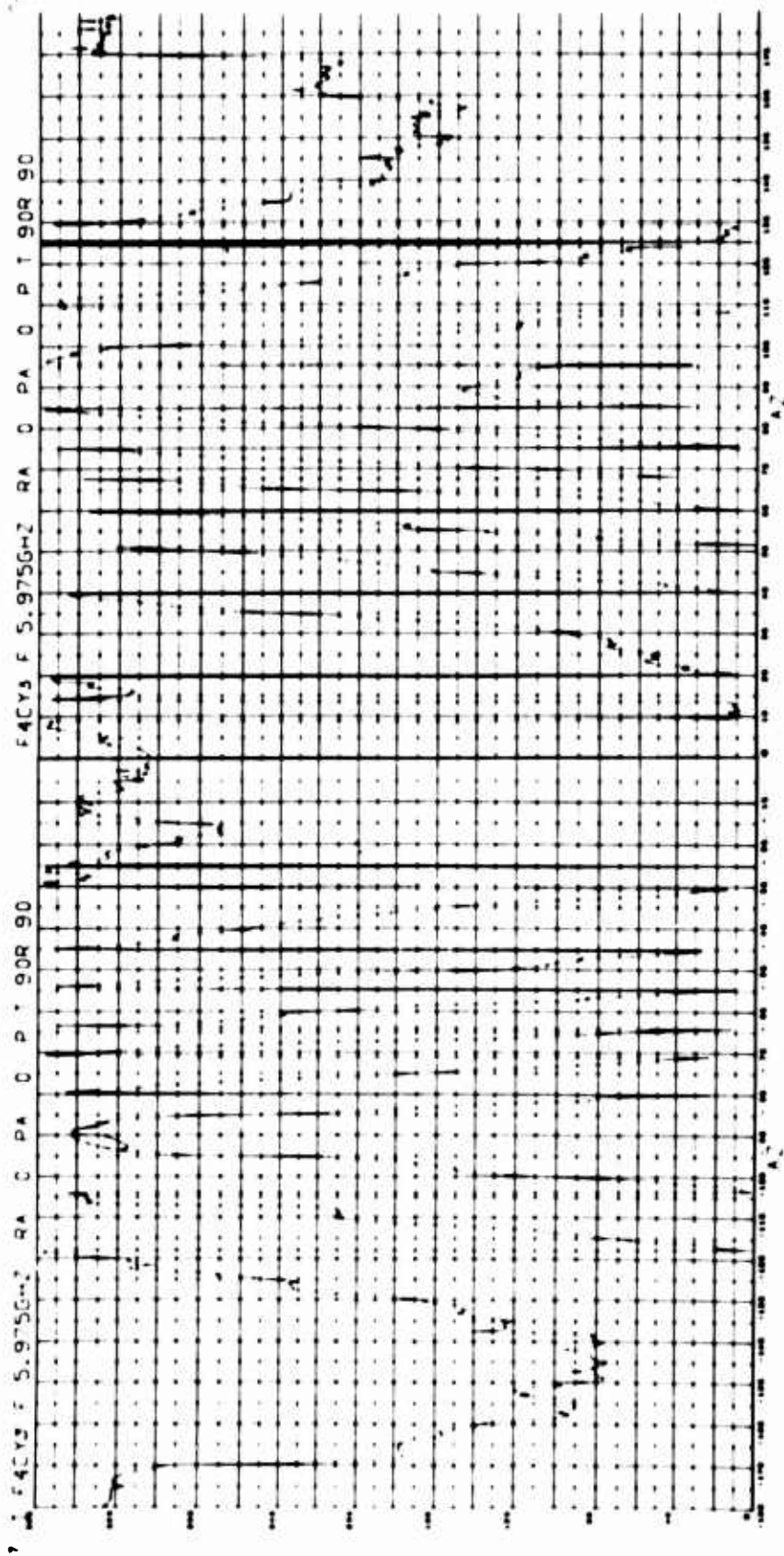


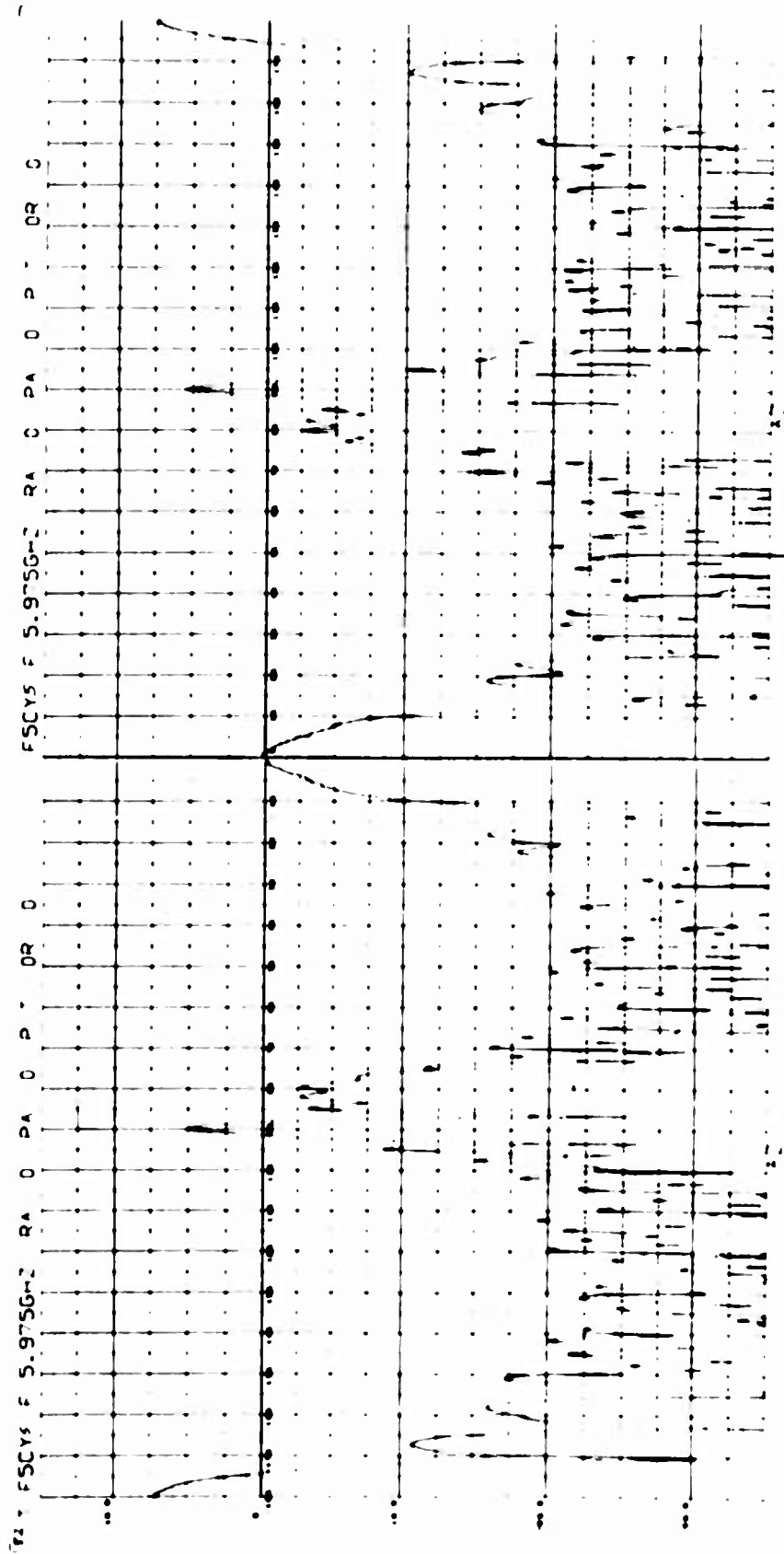


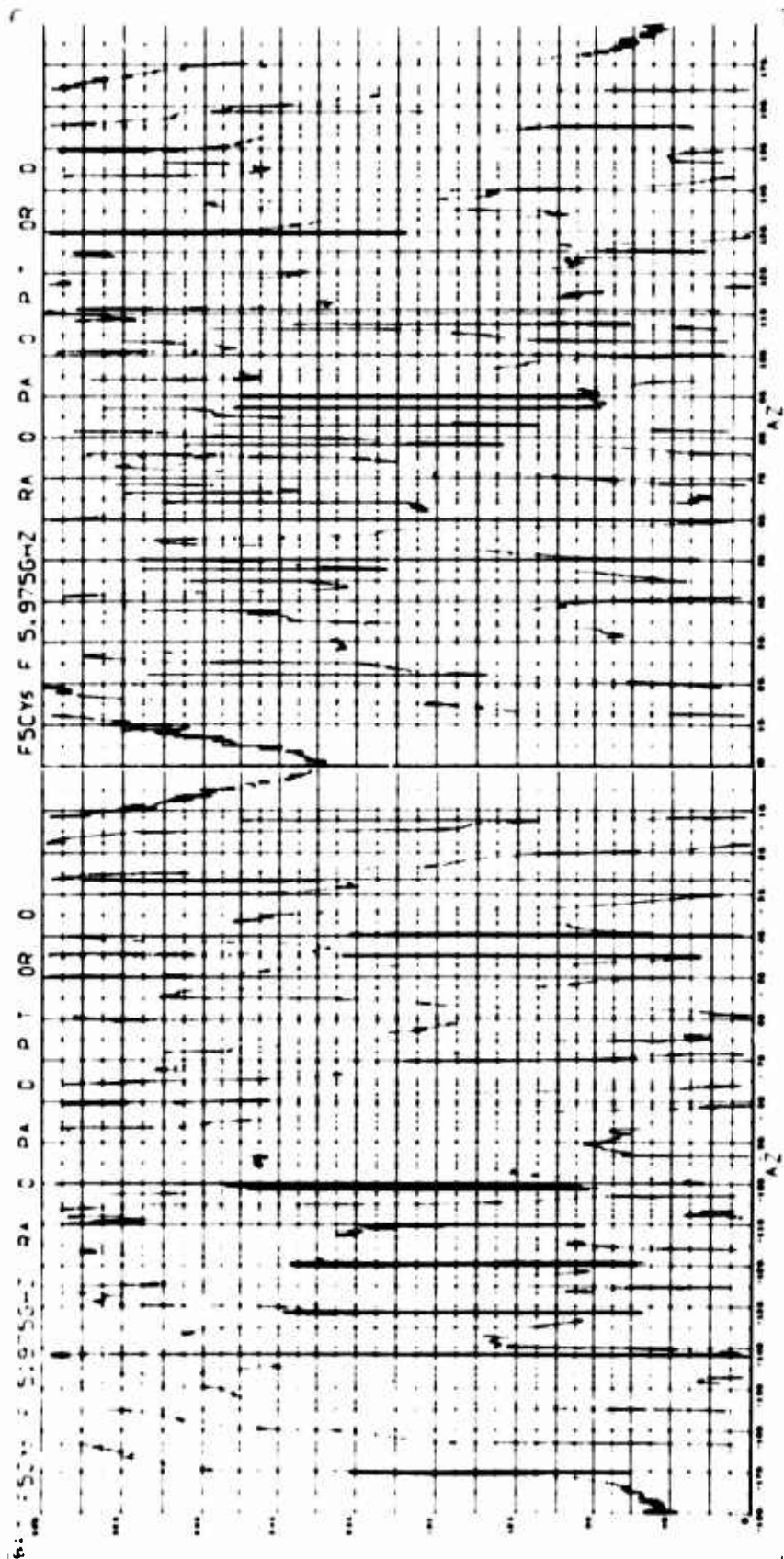


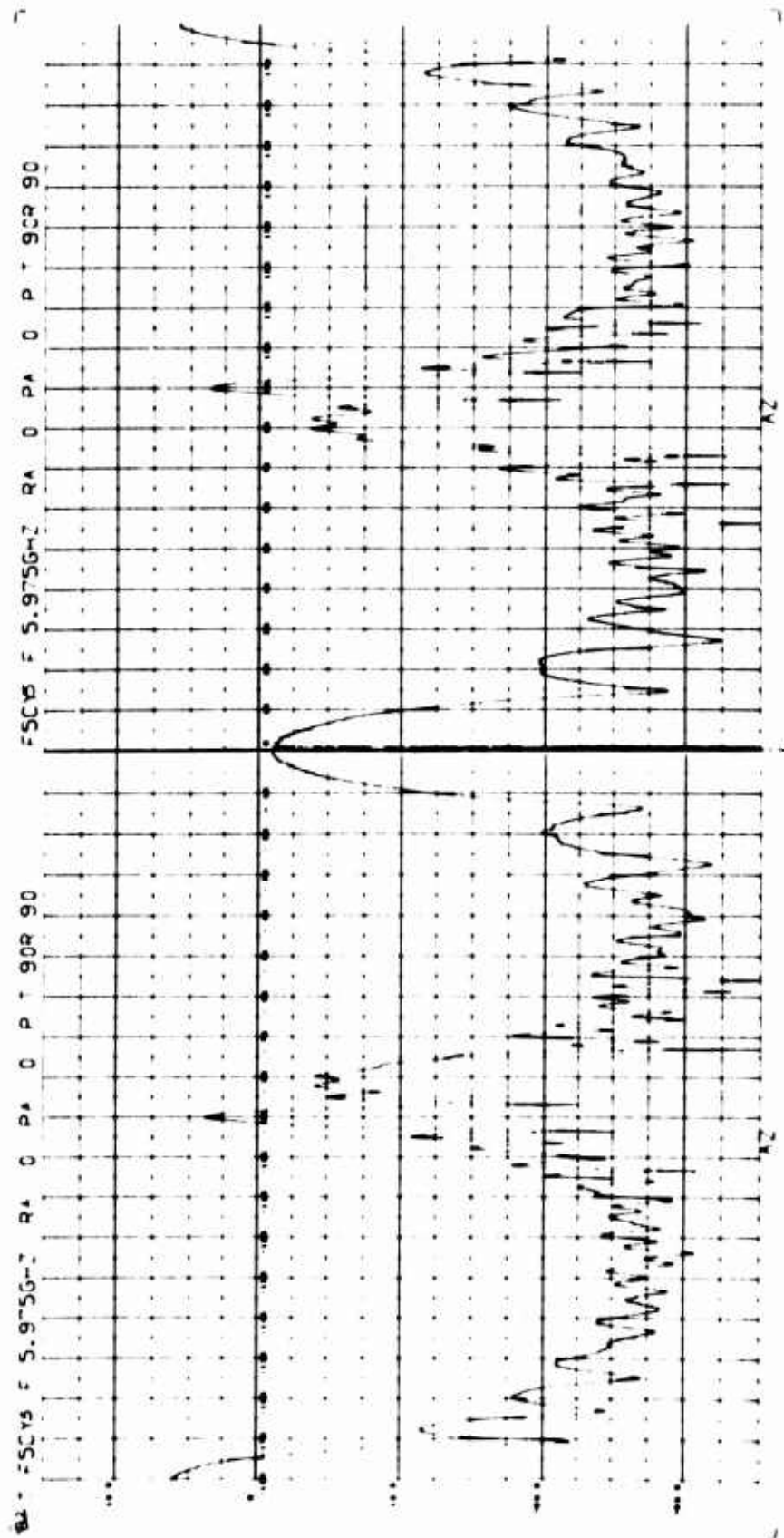


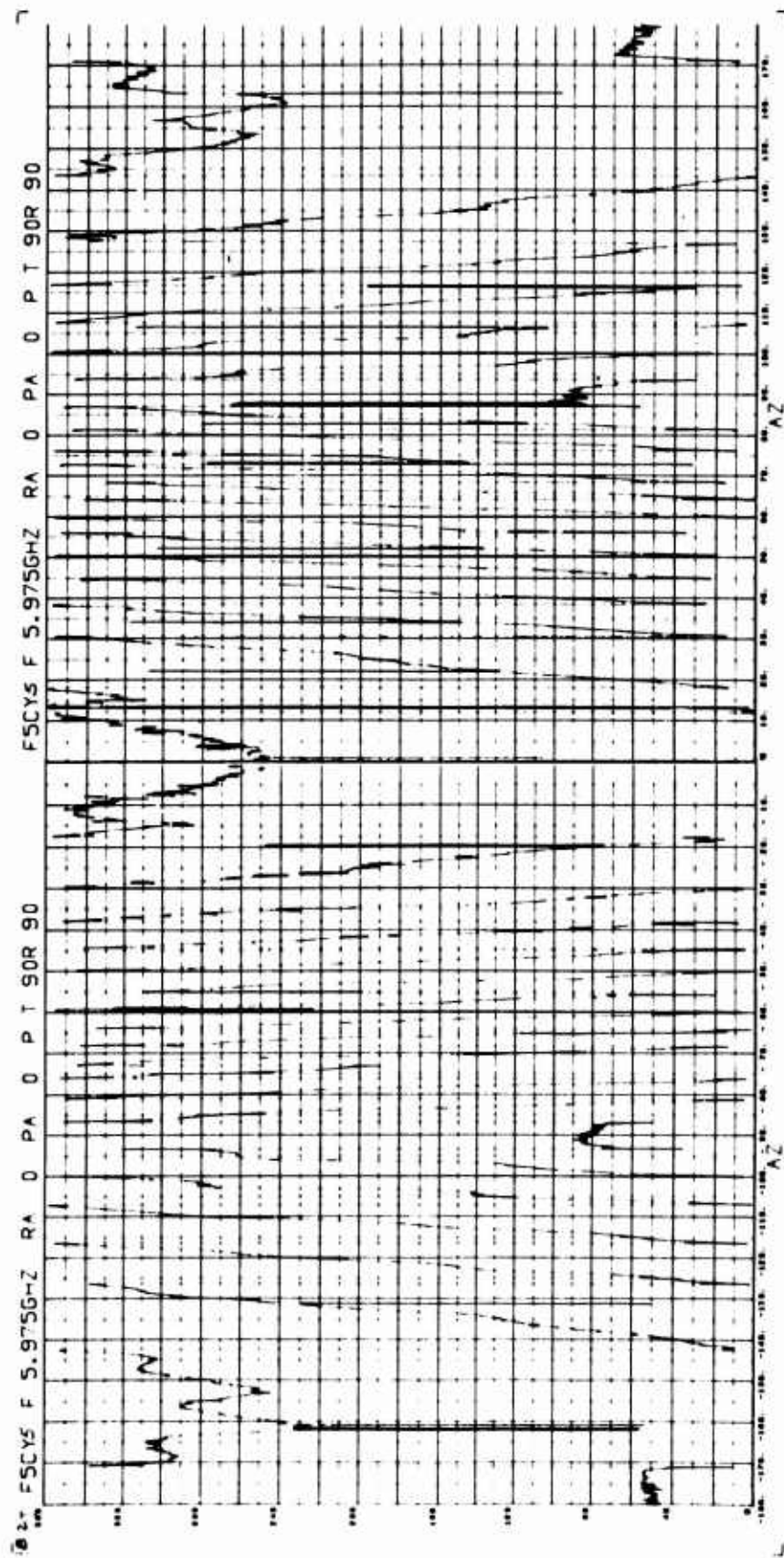


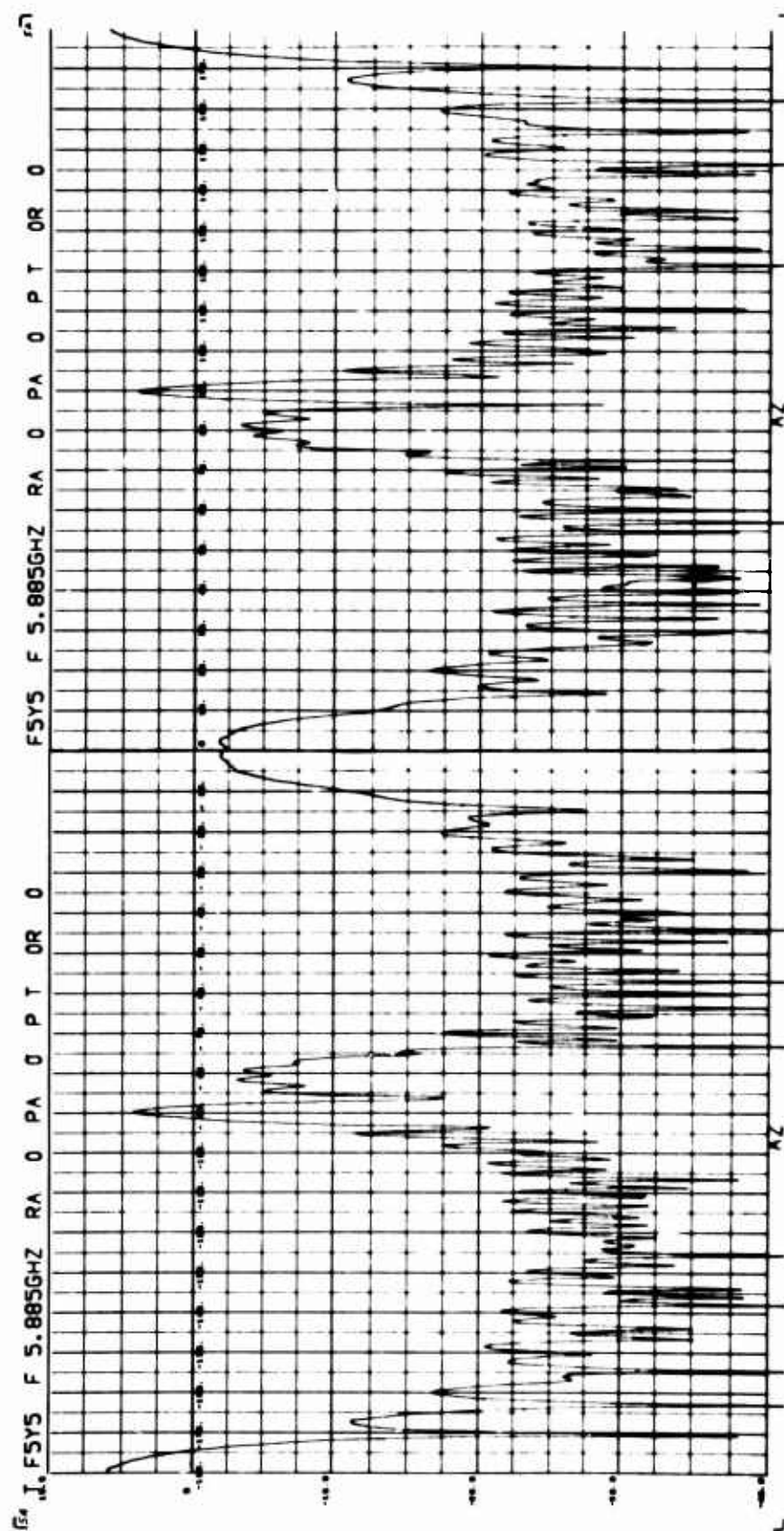




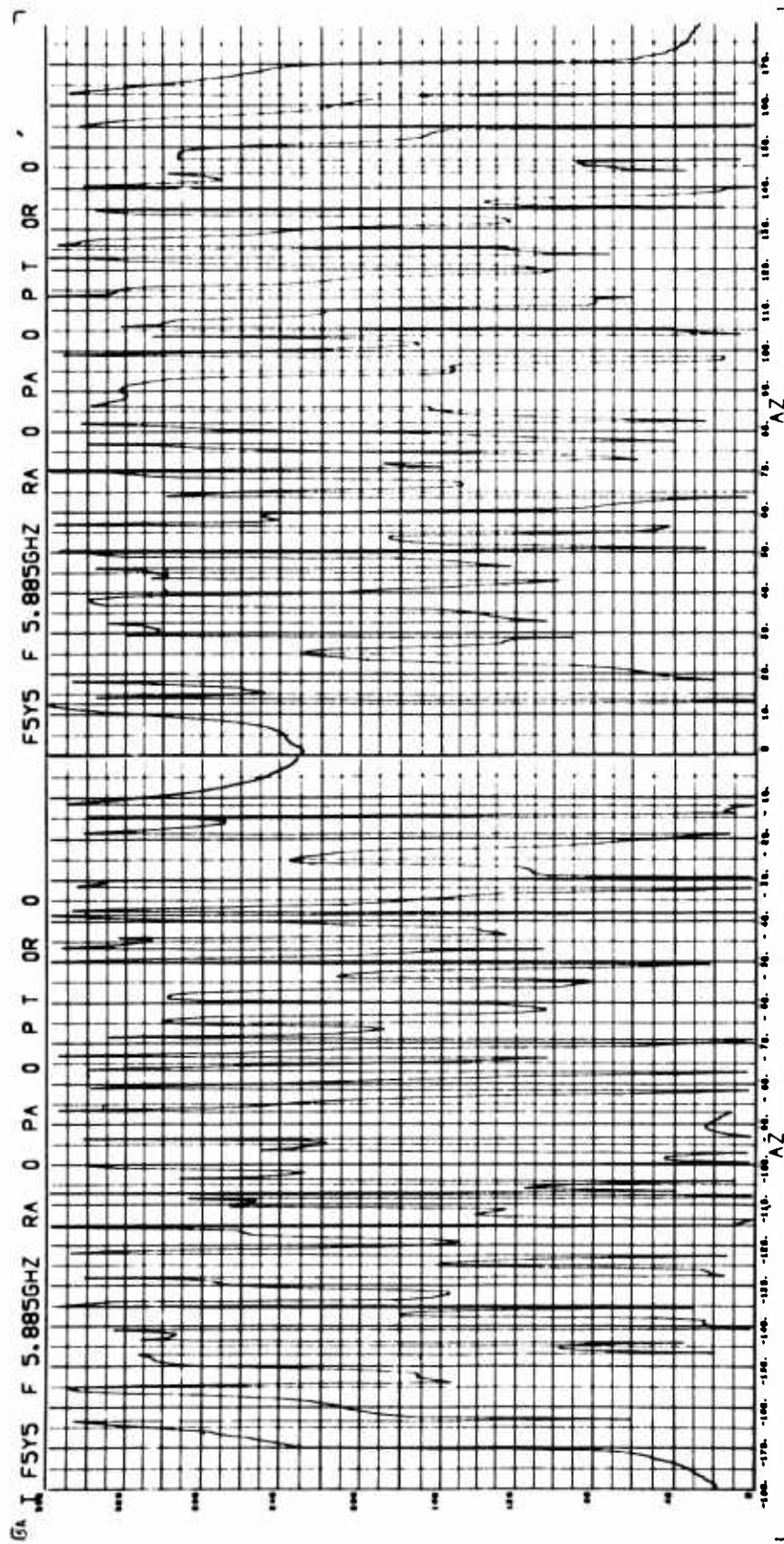




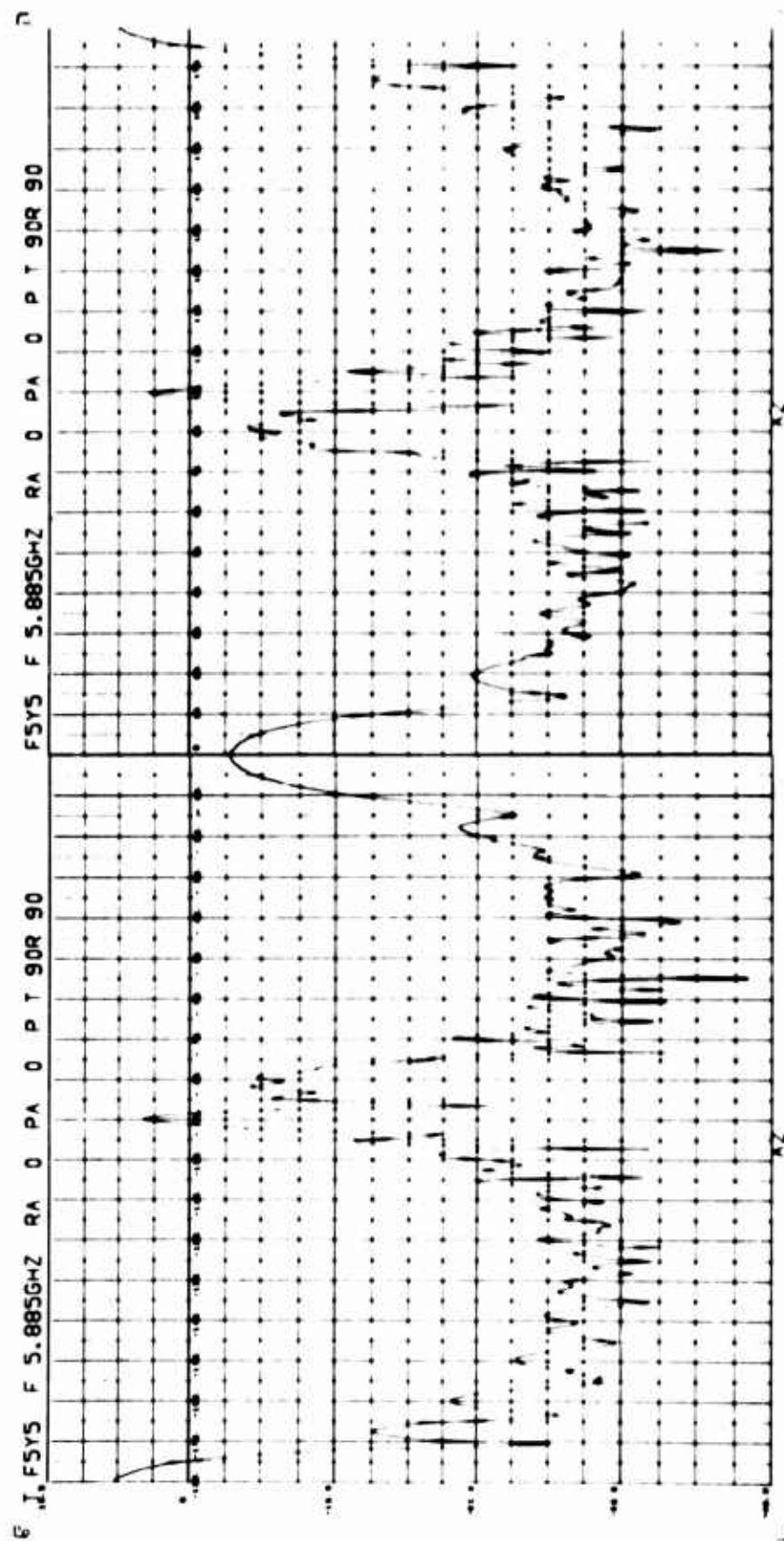




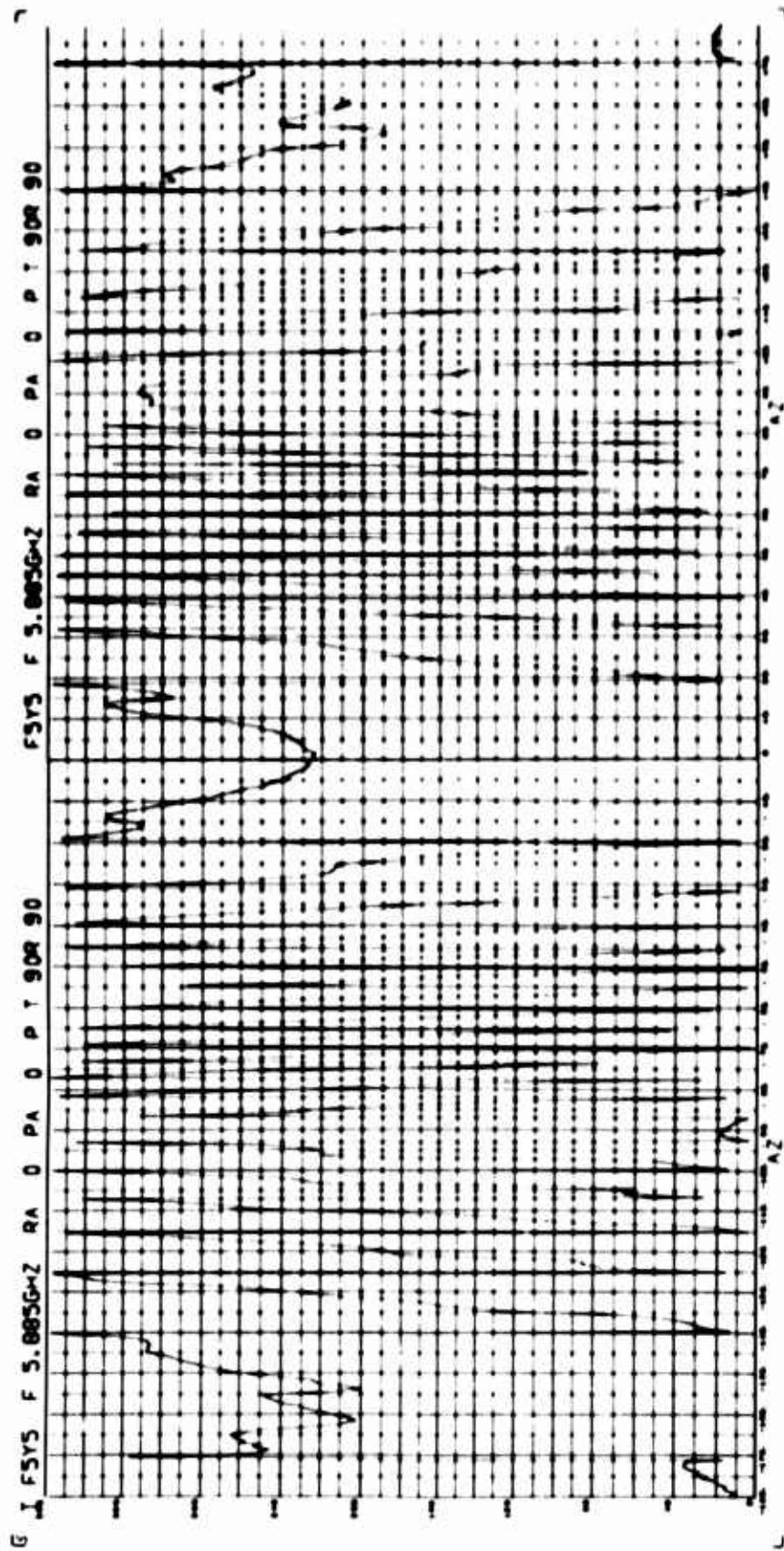
BISTATIC ANGLE = 10.25 DEGREES



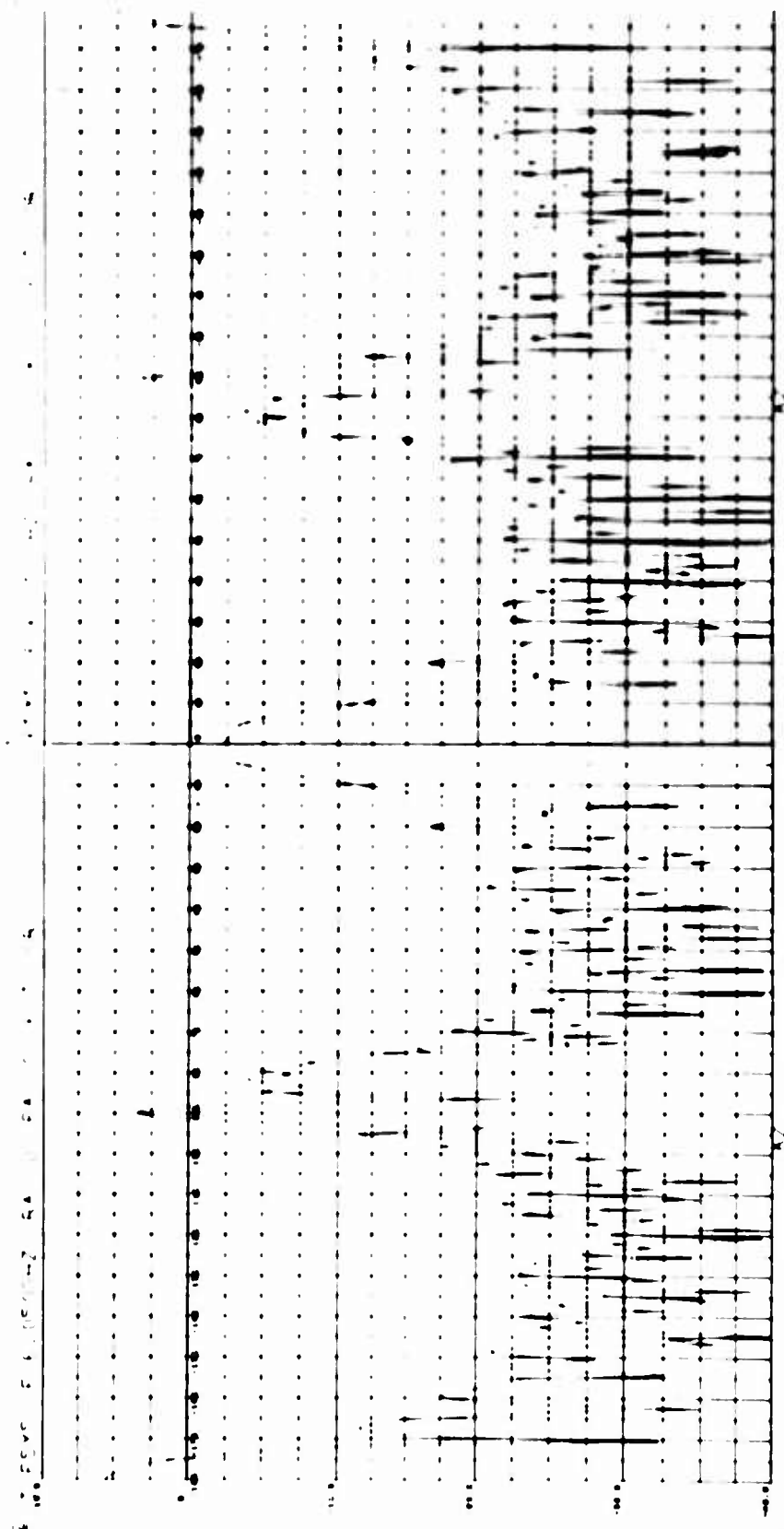
BISTATIC ANGLE = 10.25 DEGREES



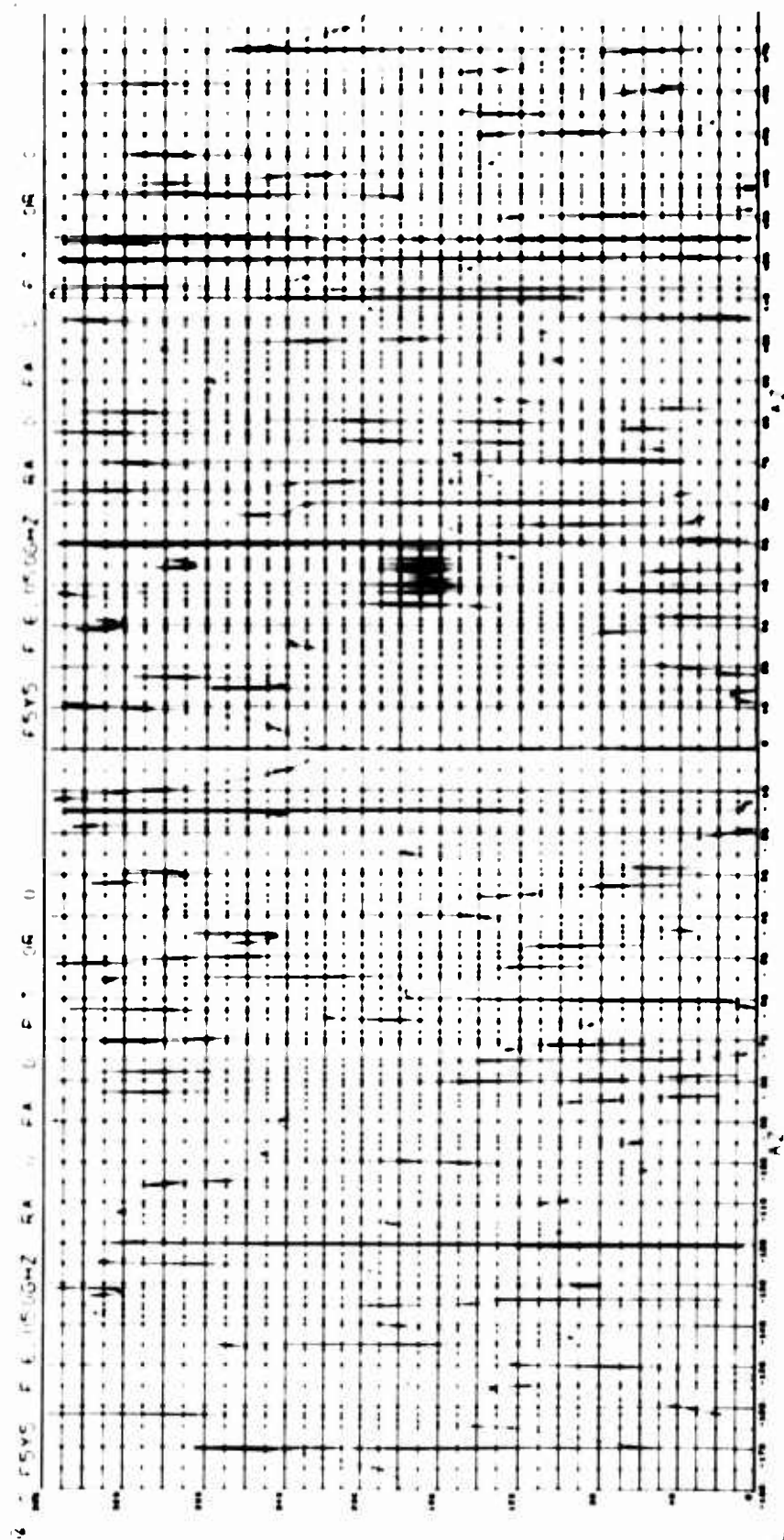
BISTATIC ANGLE - 10.25 DEGREES



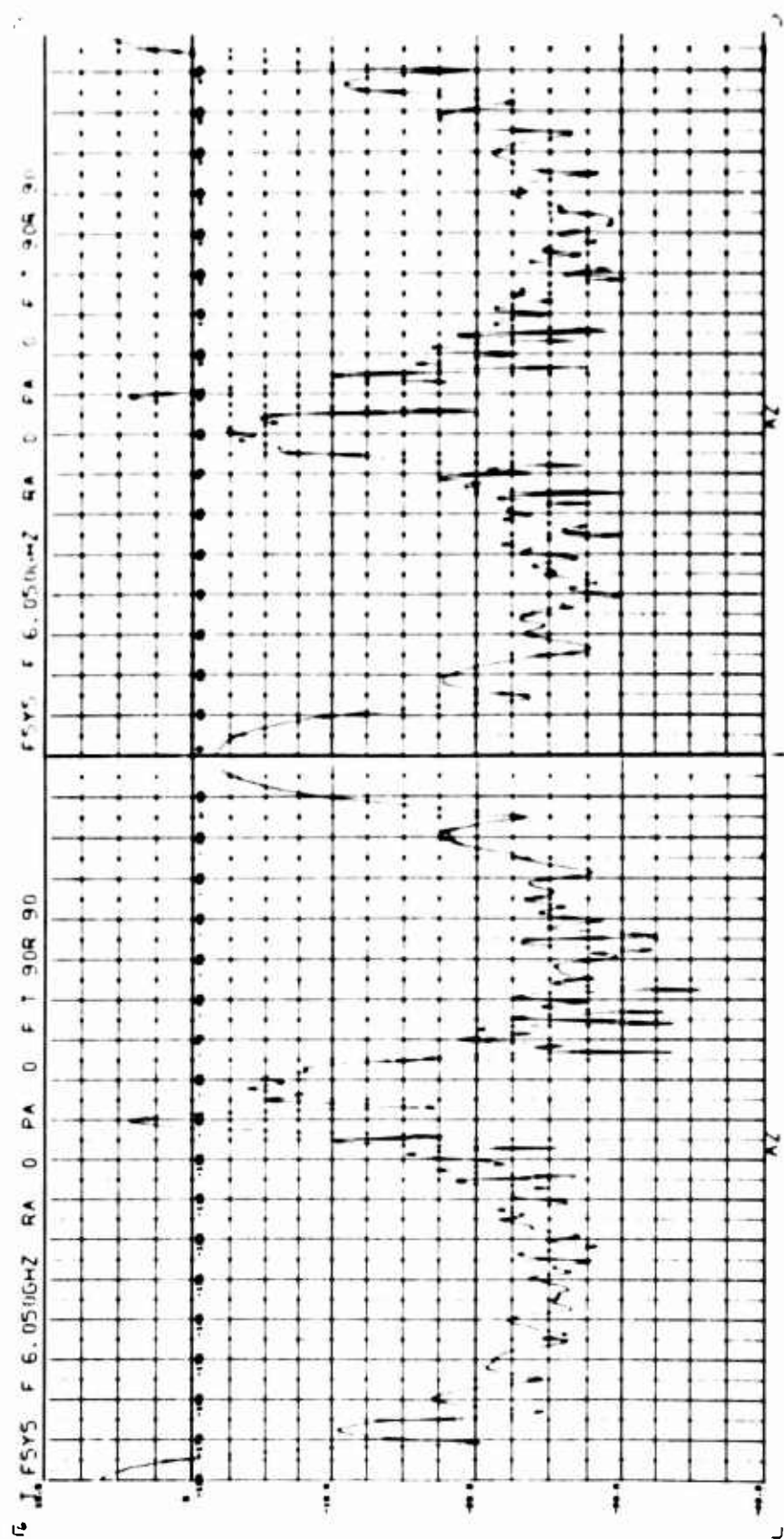
BISTATIC ANGLE = 10.25 DEGREES



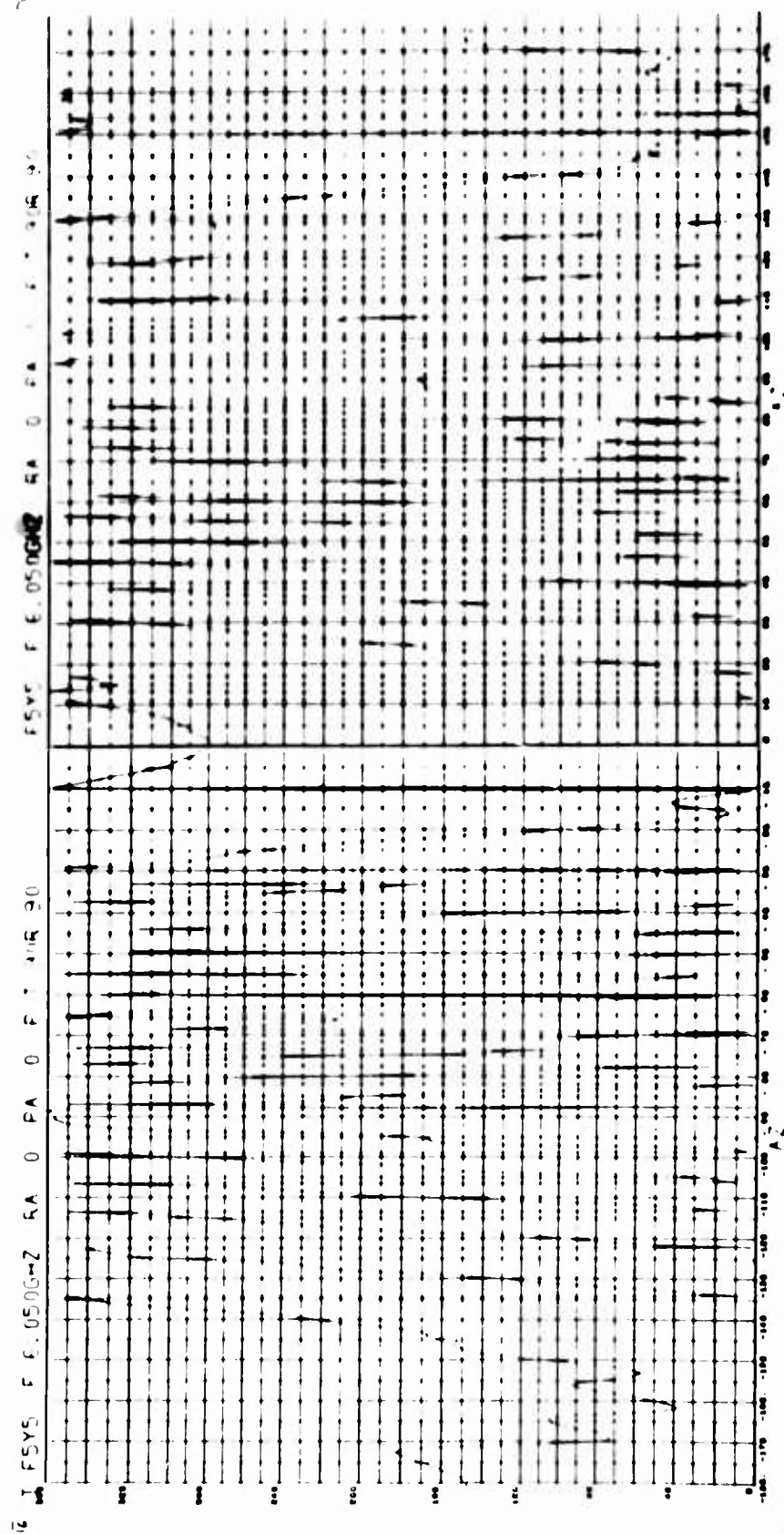
BISTATIC ANGLE = 30.0 DEGREES



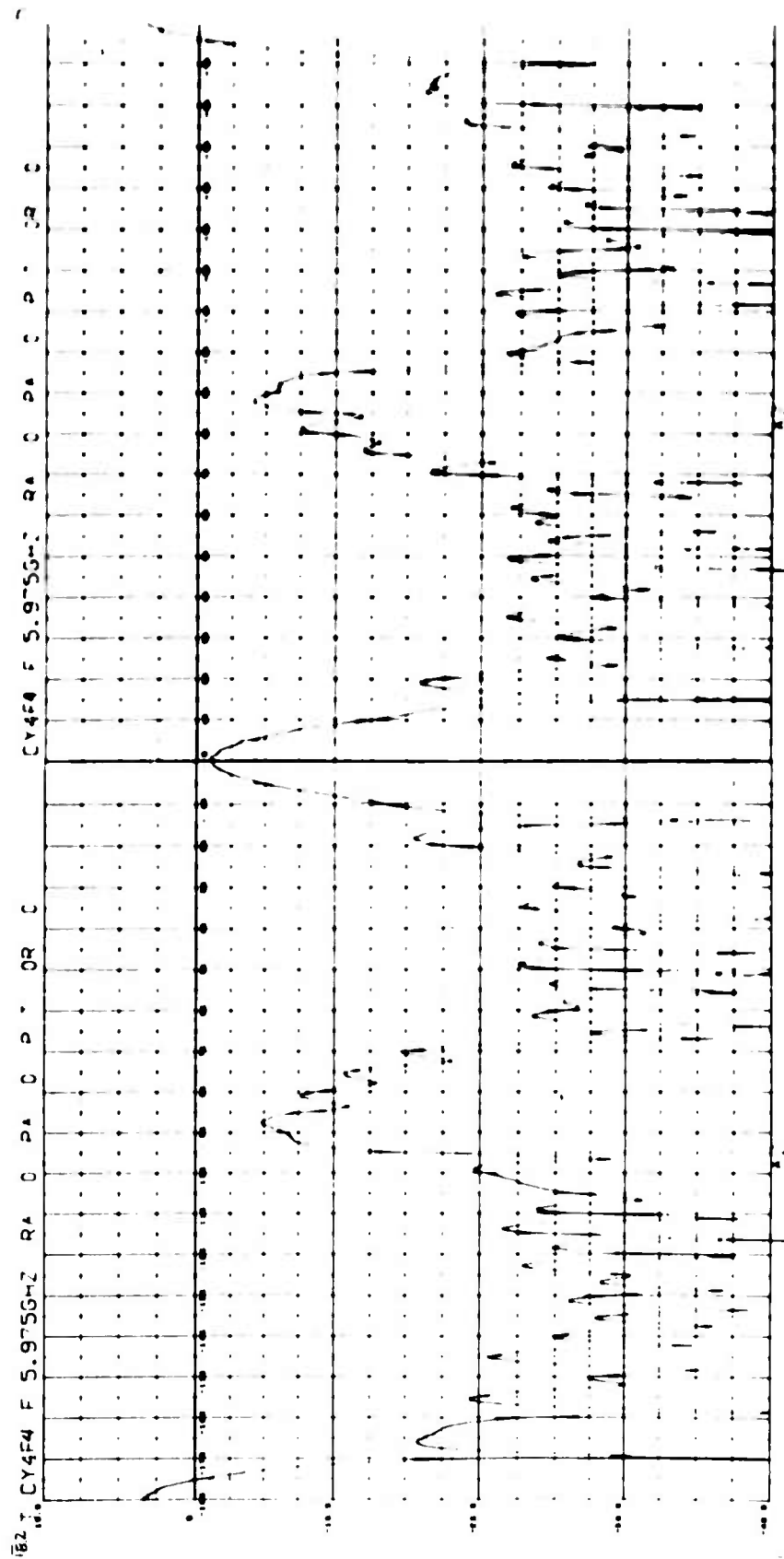
BISTATIC ANGLE = 30.0 DEGREES

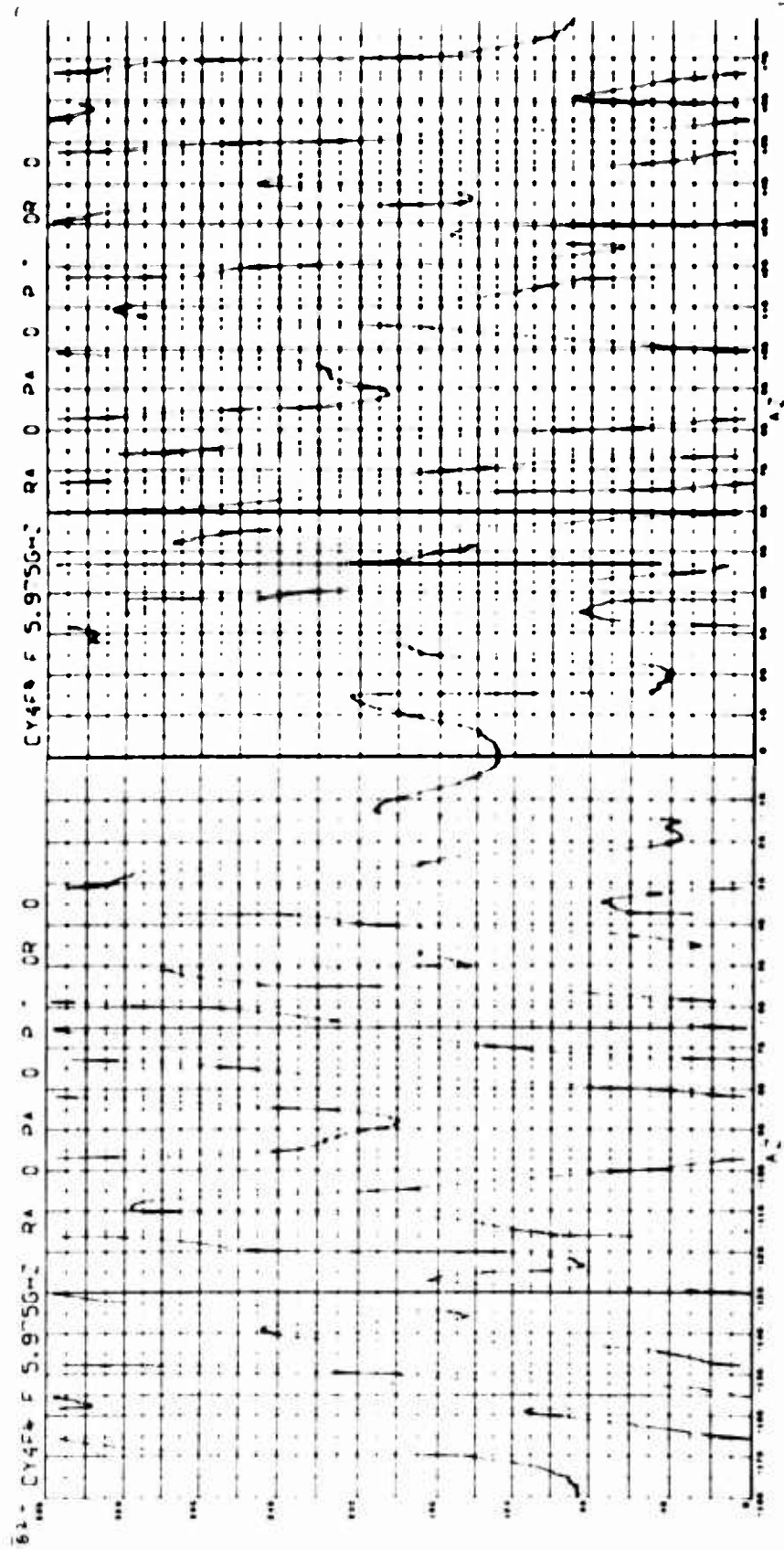


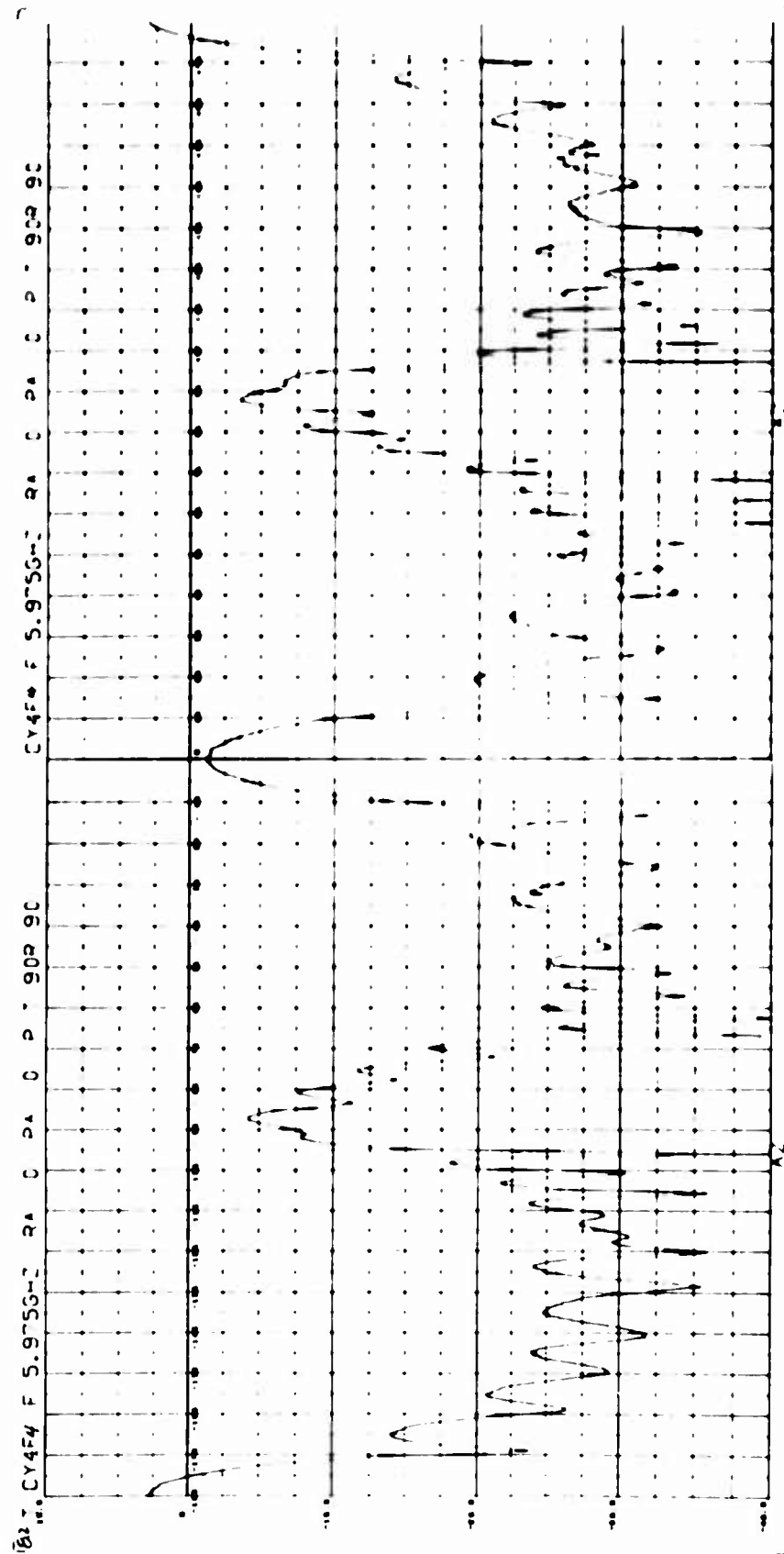
BISTATIC ANGLE = 30.0 DEGREES

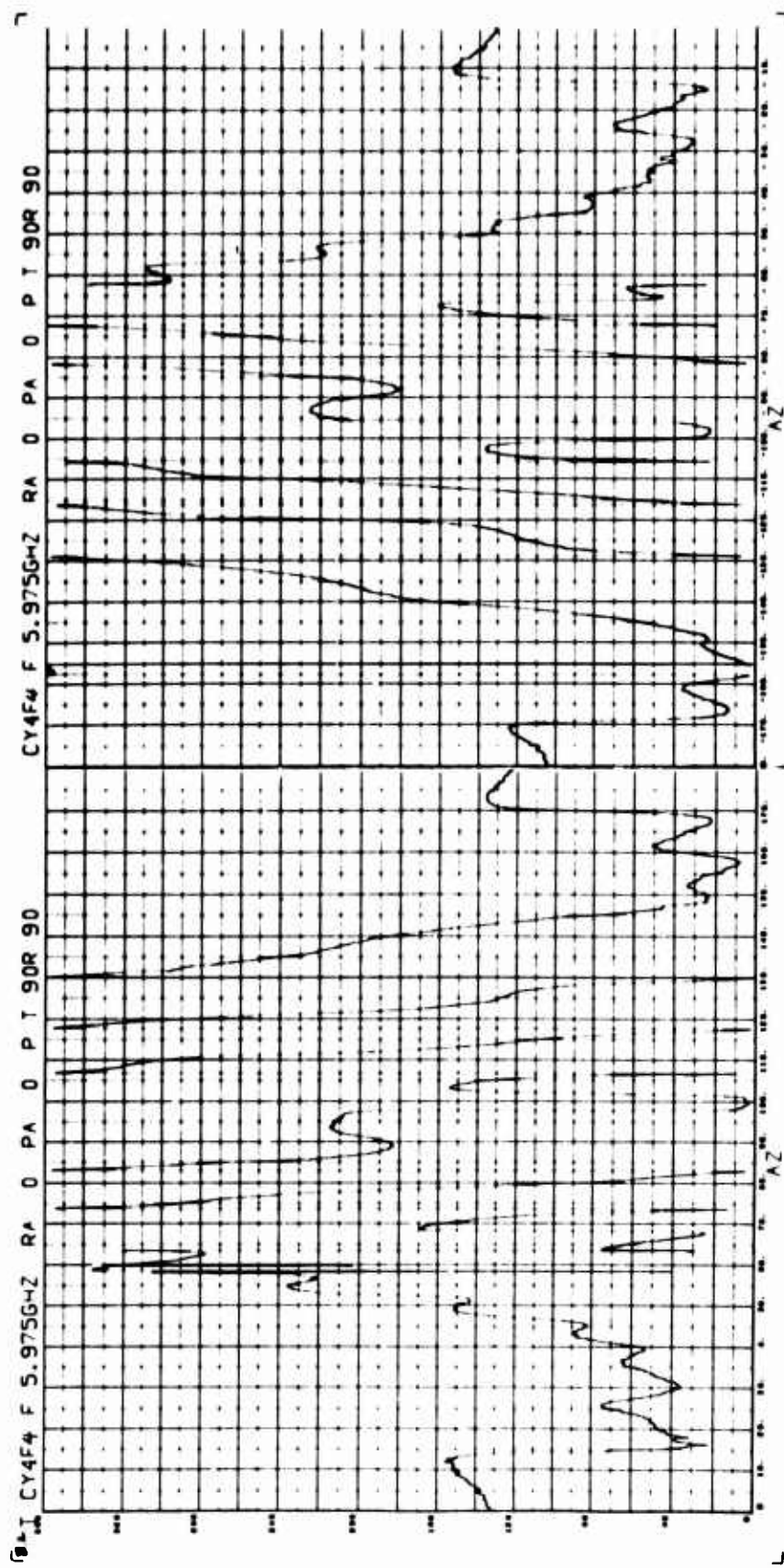


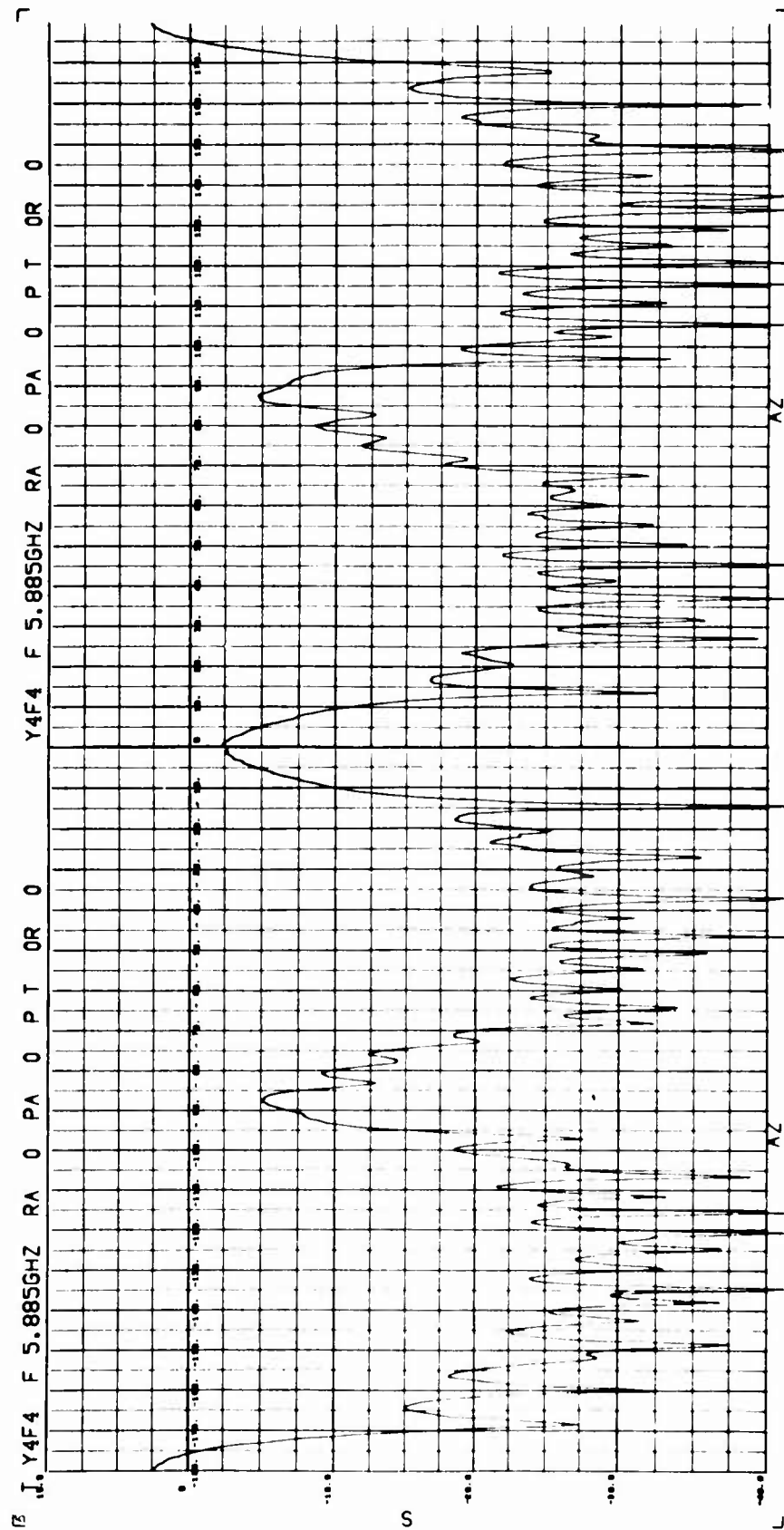
BISTATIC ANGLE = 30.0 DEGREES



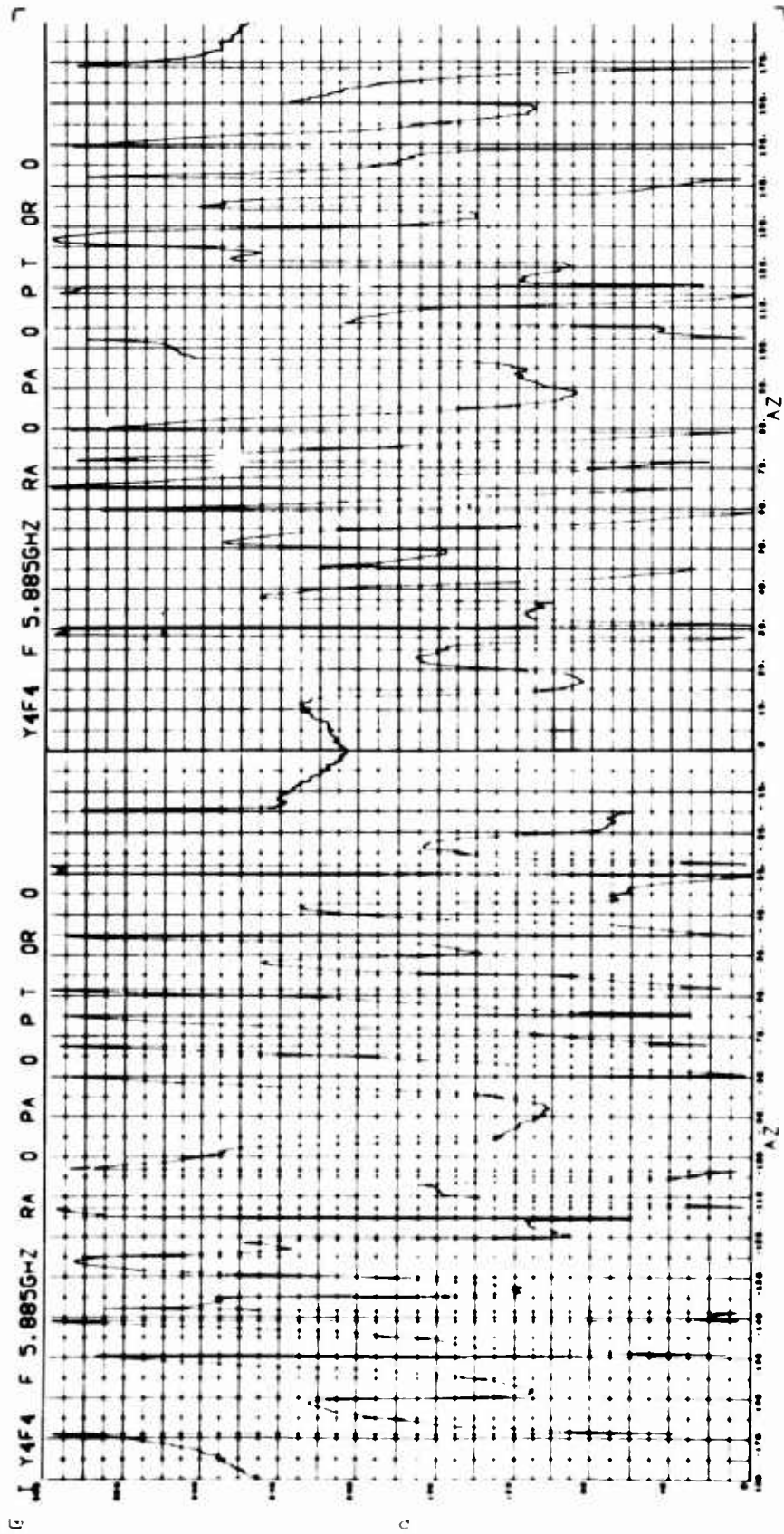




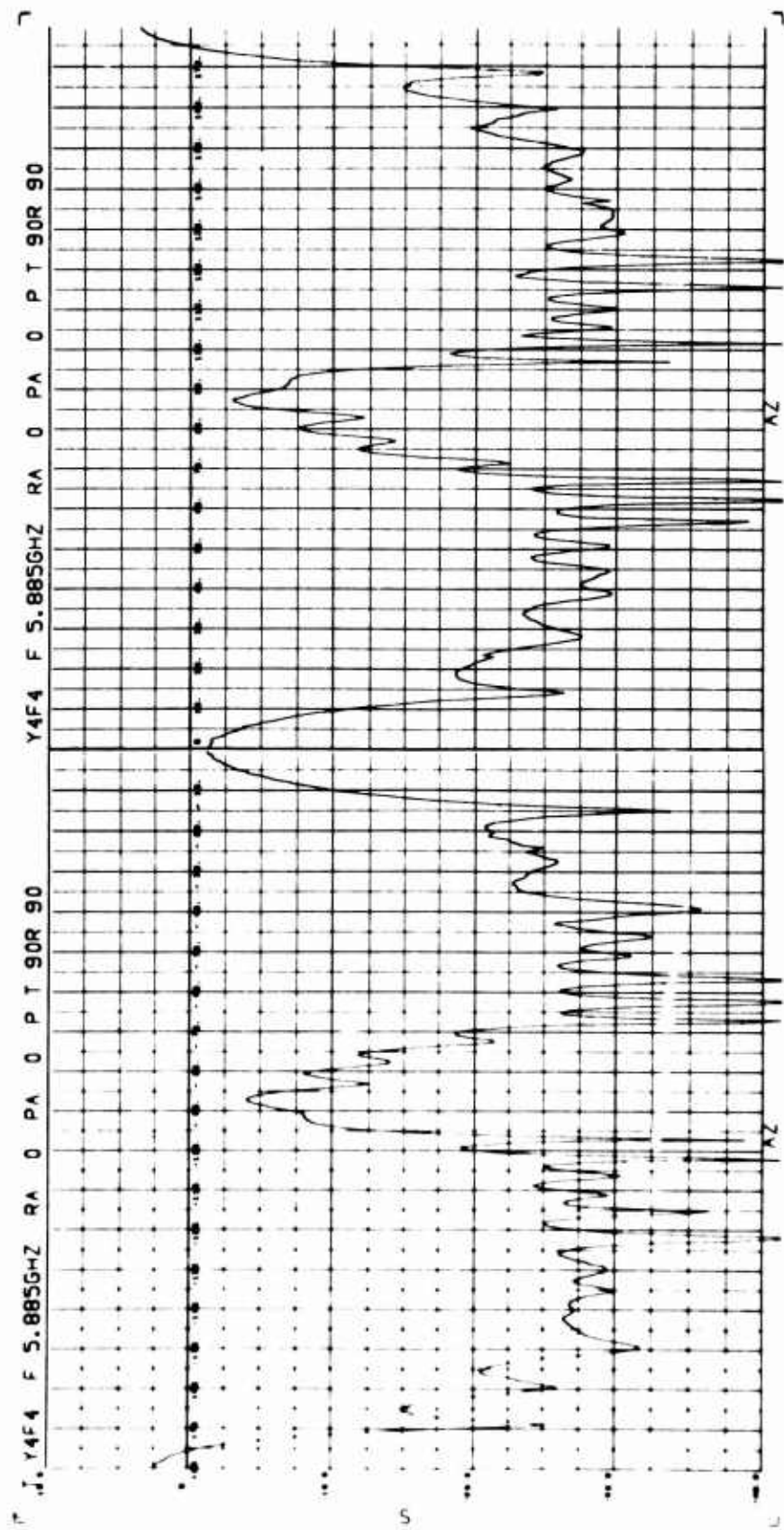




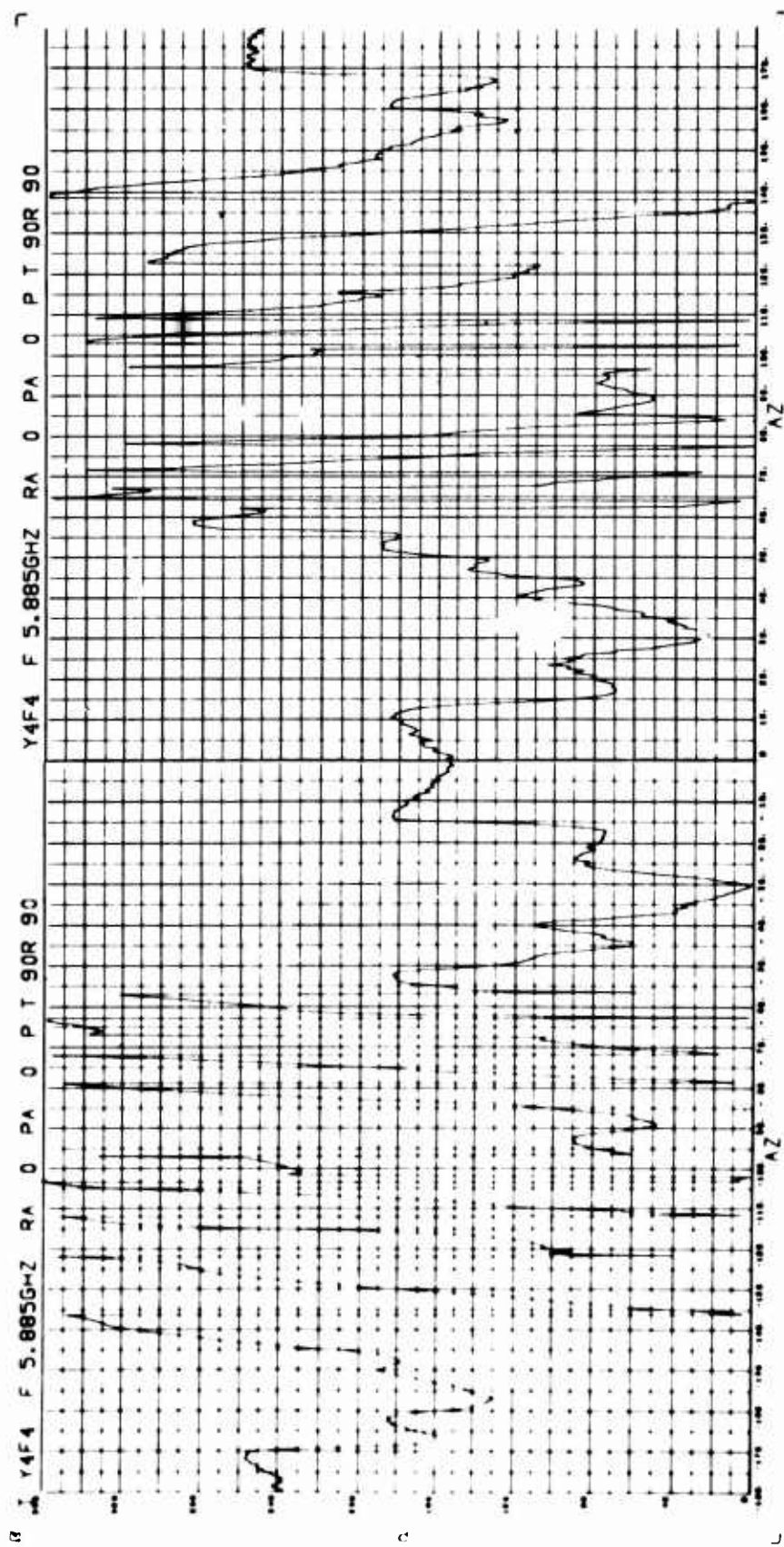
RISTATIC ANGLE = 10.25 DEGREES



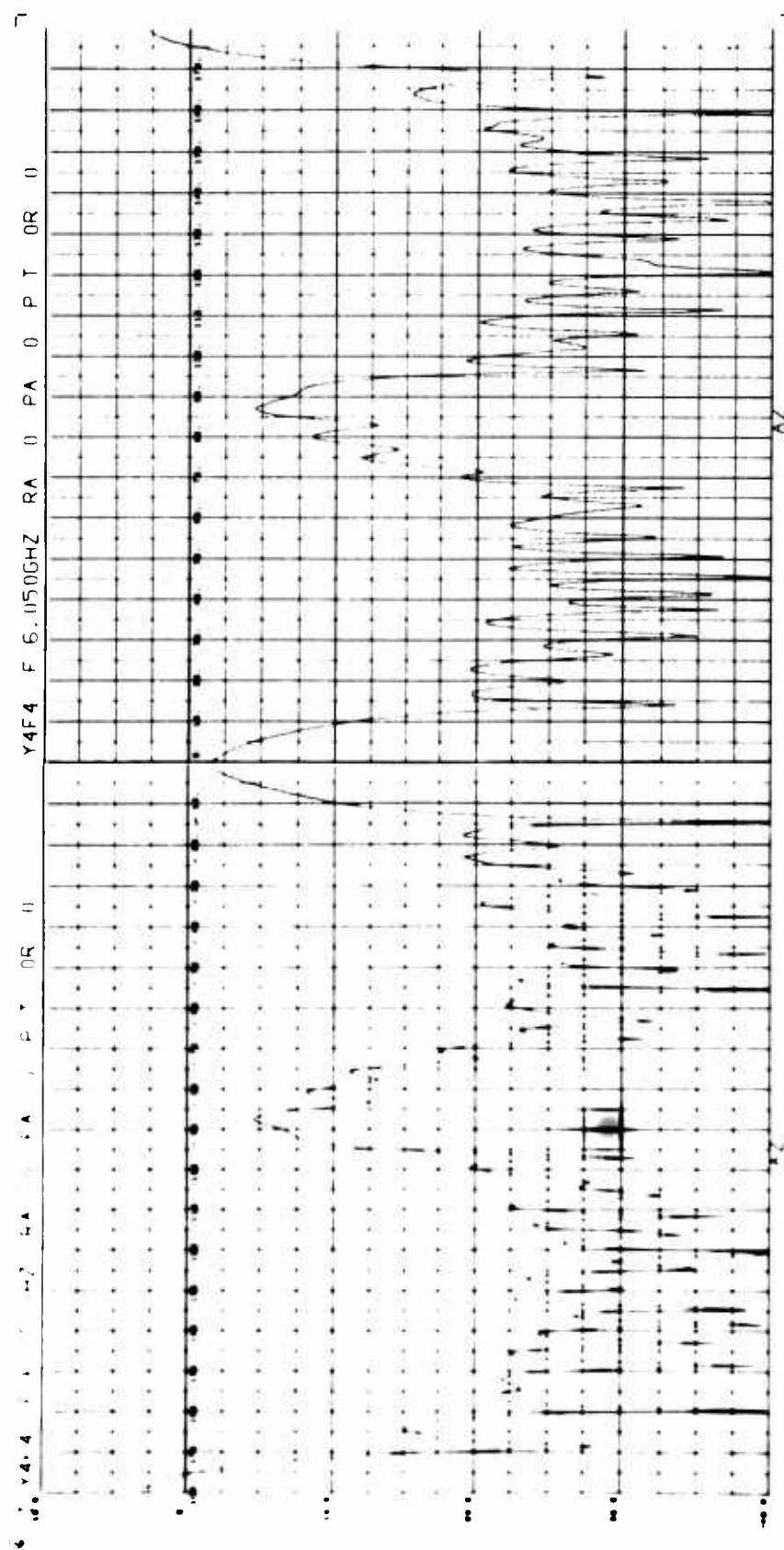
BISTATIC ANGLE = 10.25 DEGREES



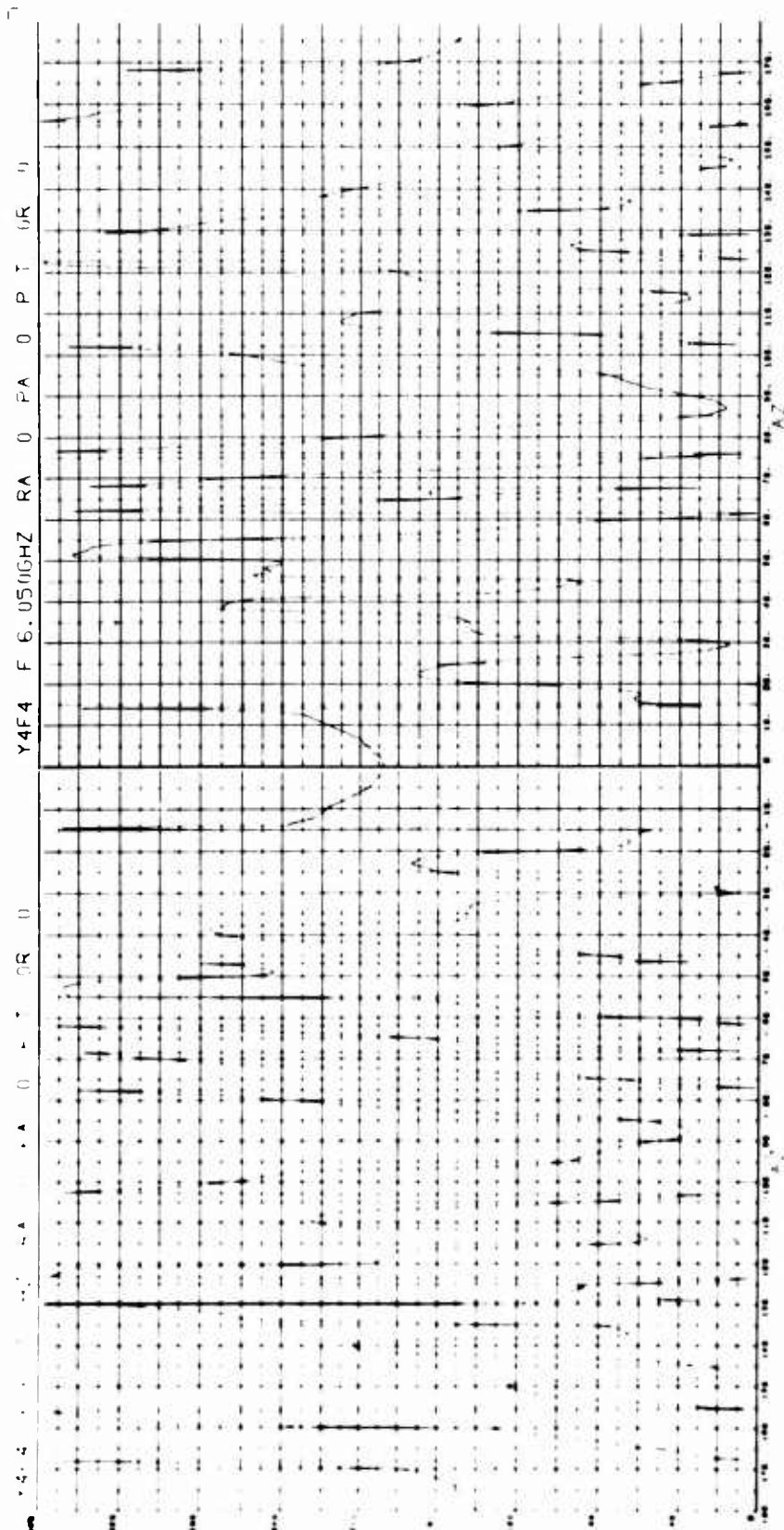
BISTATIC ANGLE = 10.25 DEGREES

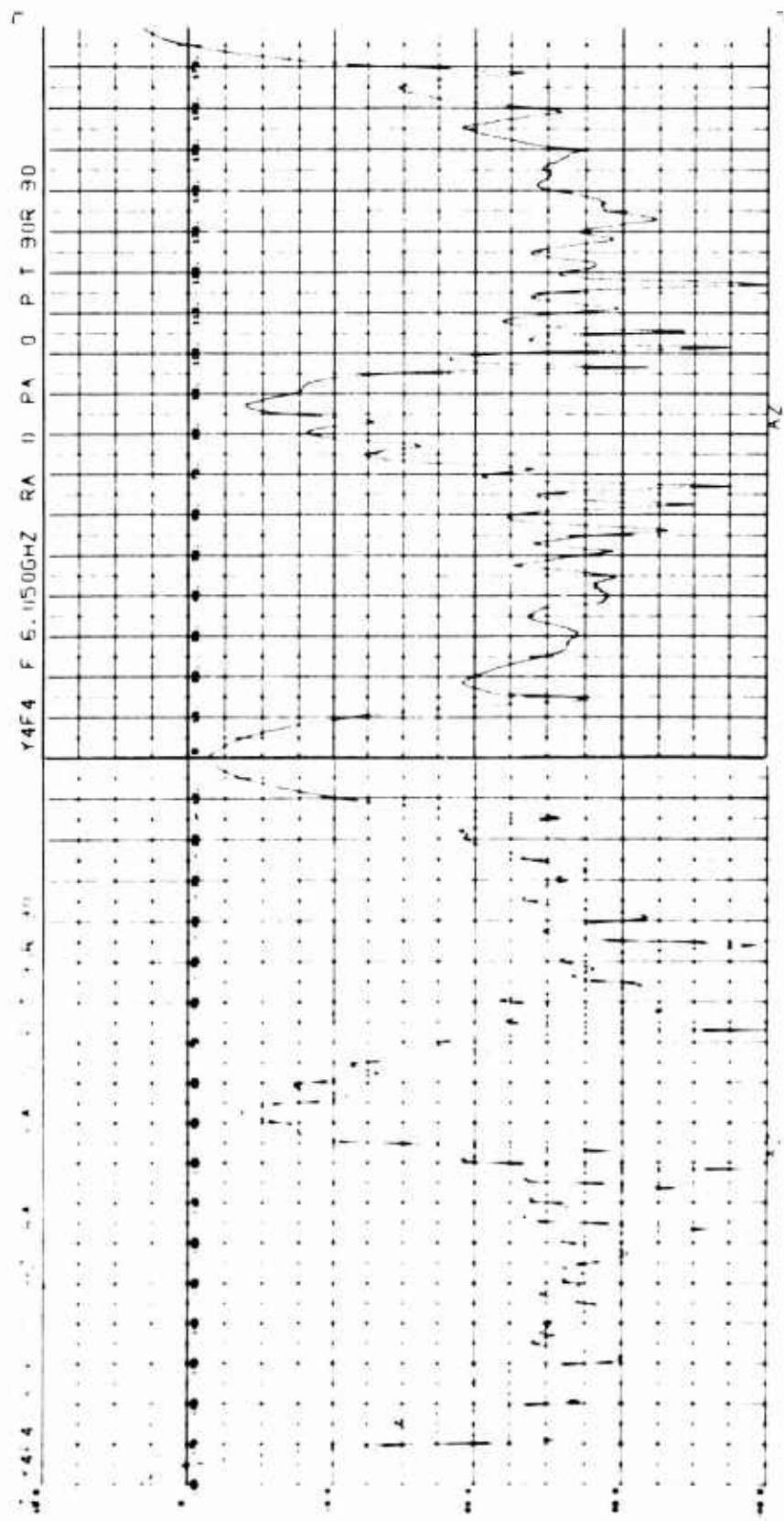


BISTATIC ANGLE = 10.25 DEGREES

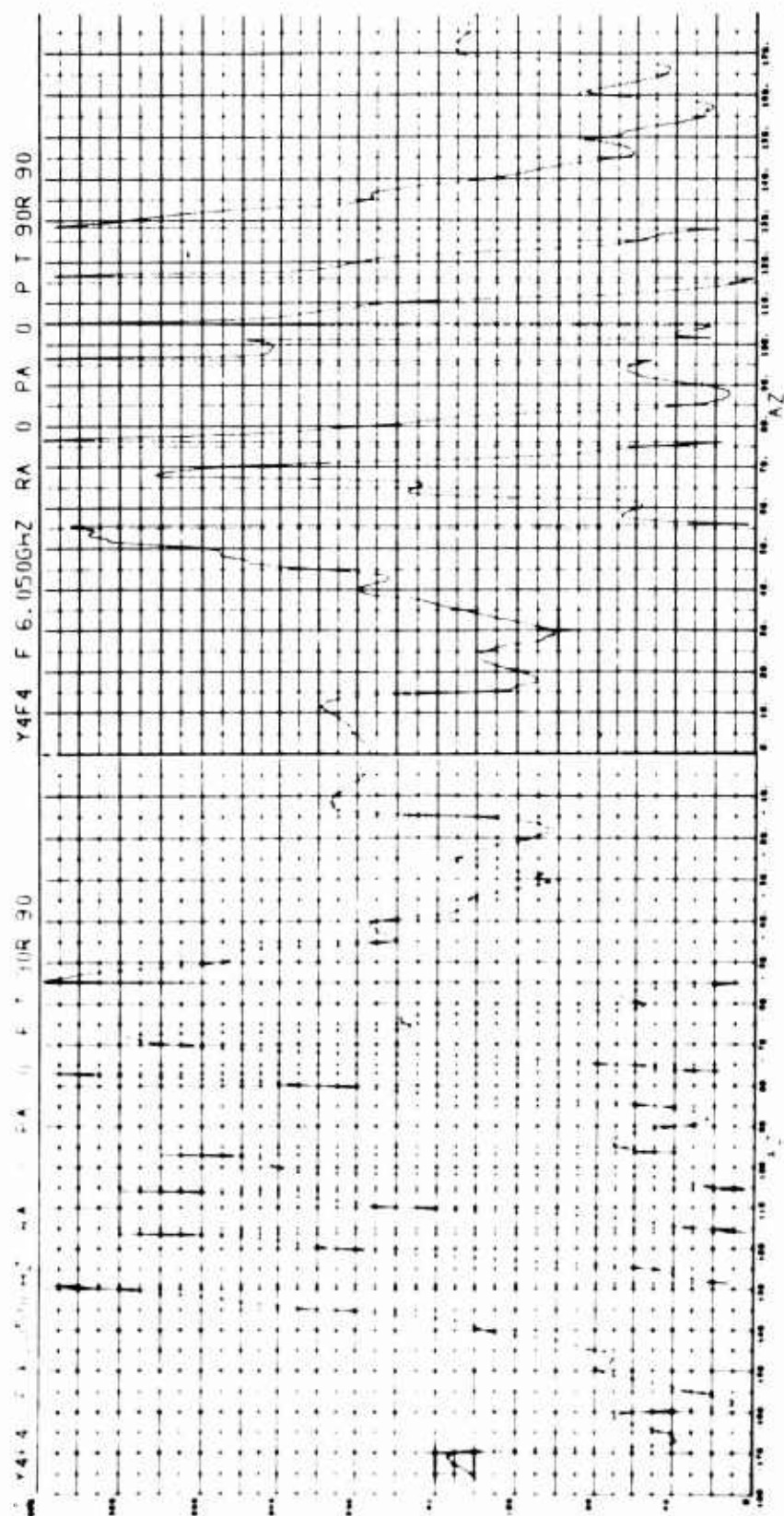


BISTATIC ANGLE = 30.0 DEGREES

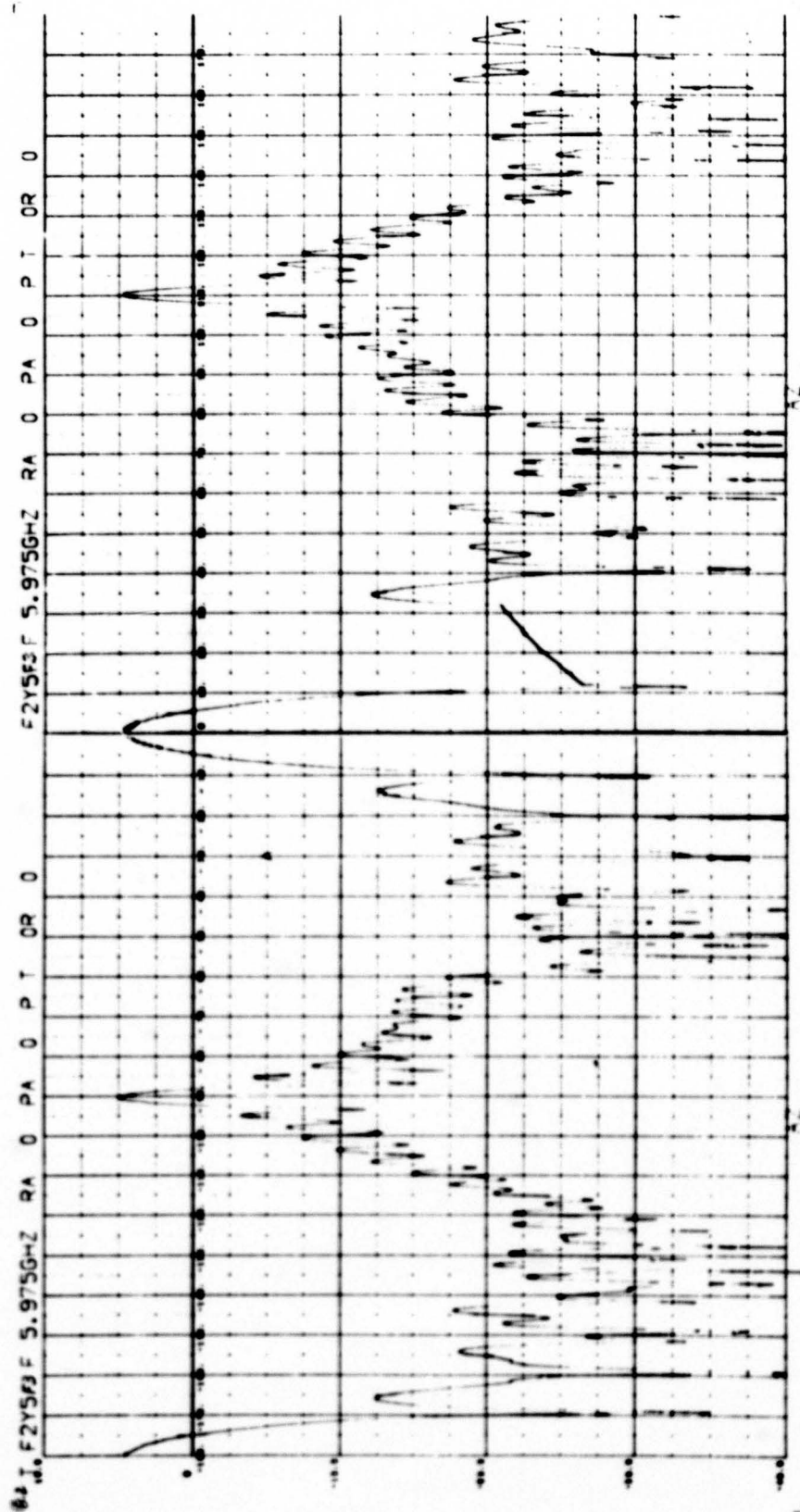


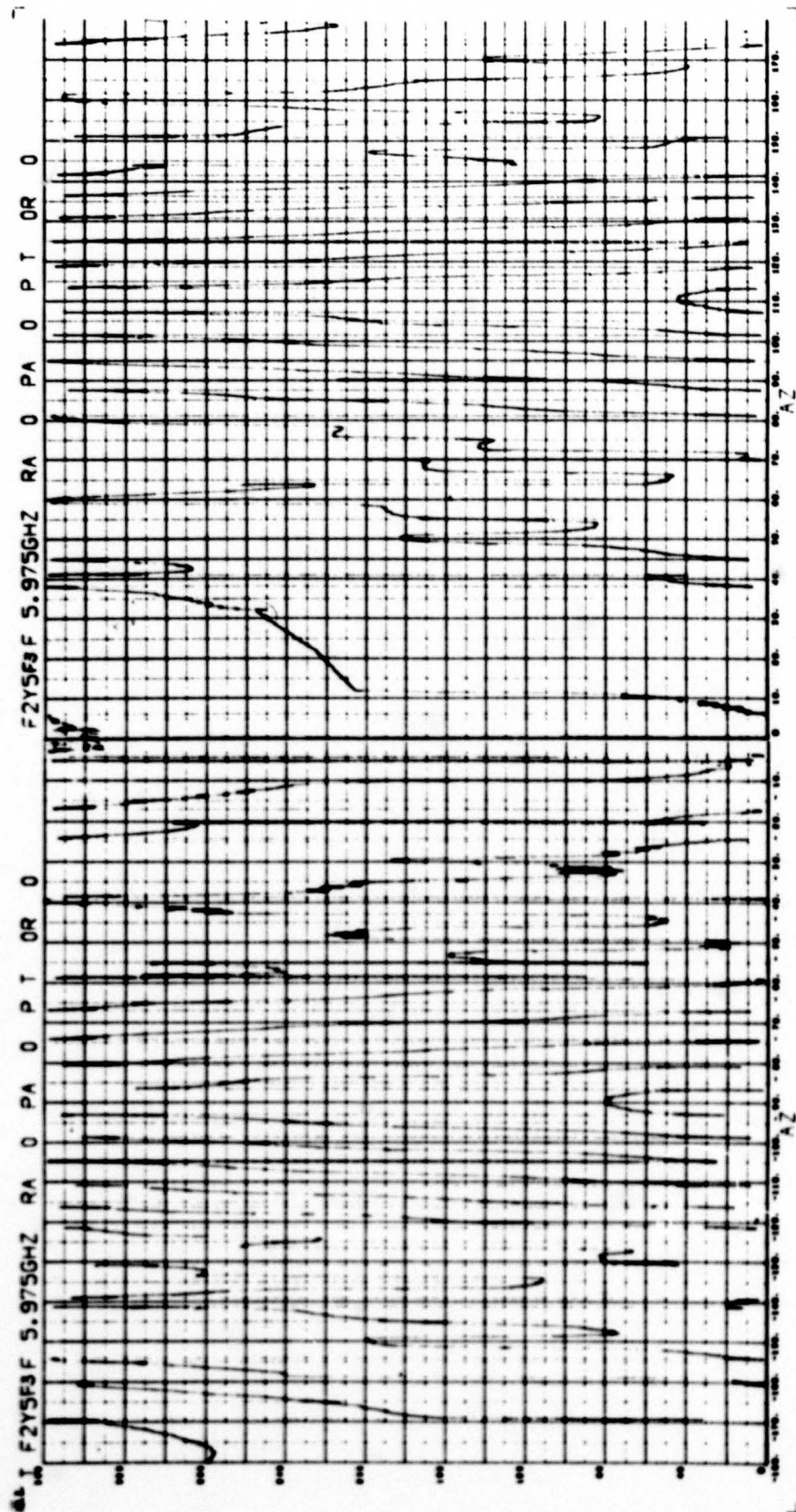


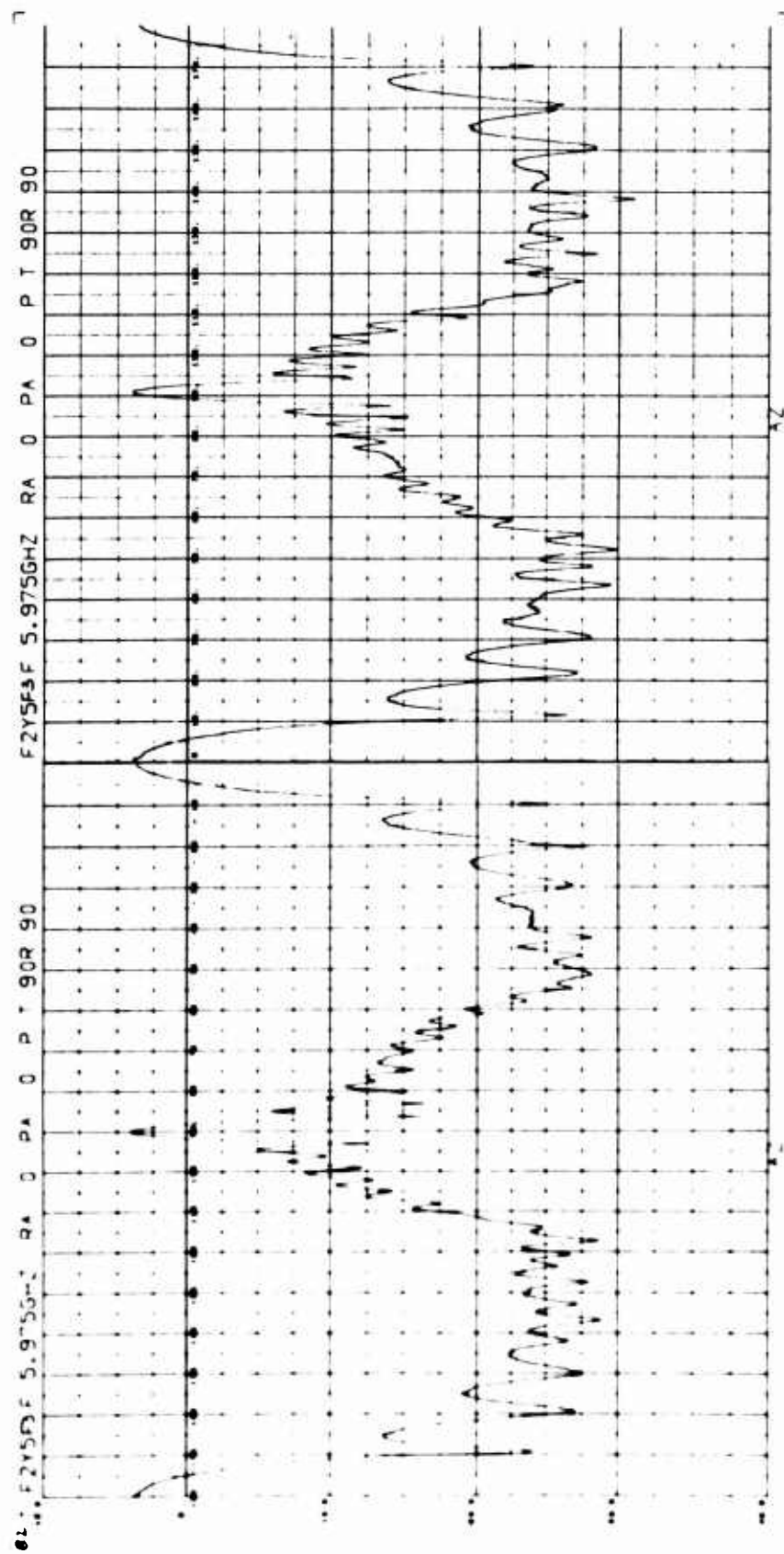
BISTATIC ANGLE = 30.0 DEGREES

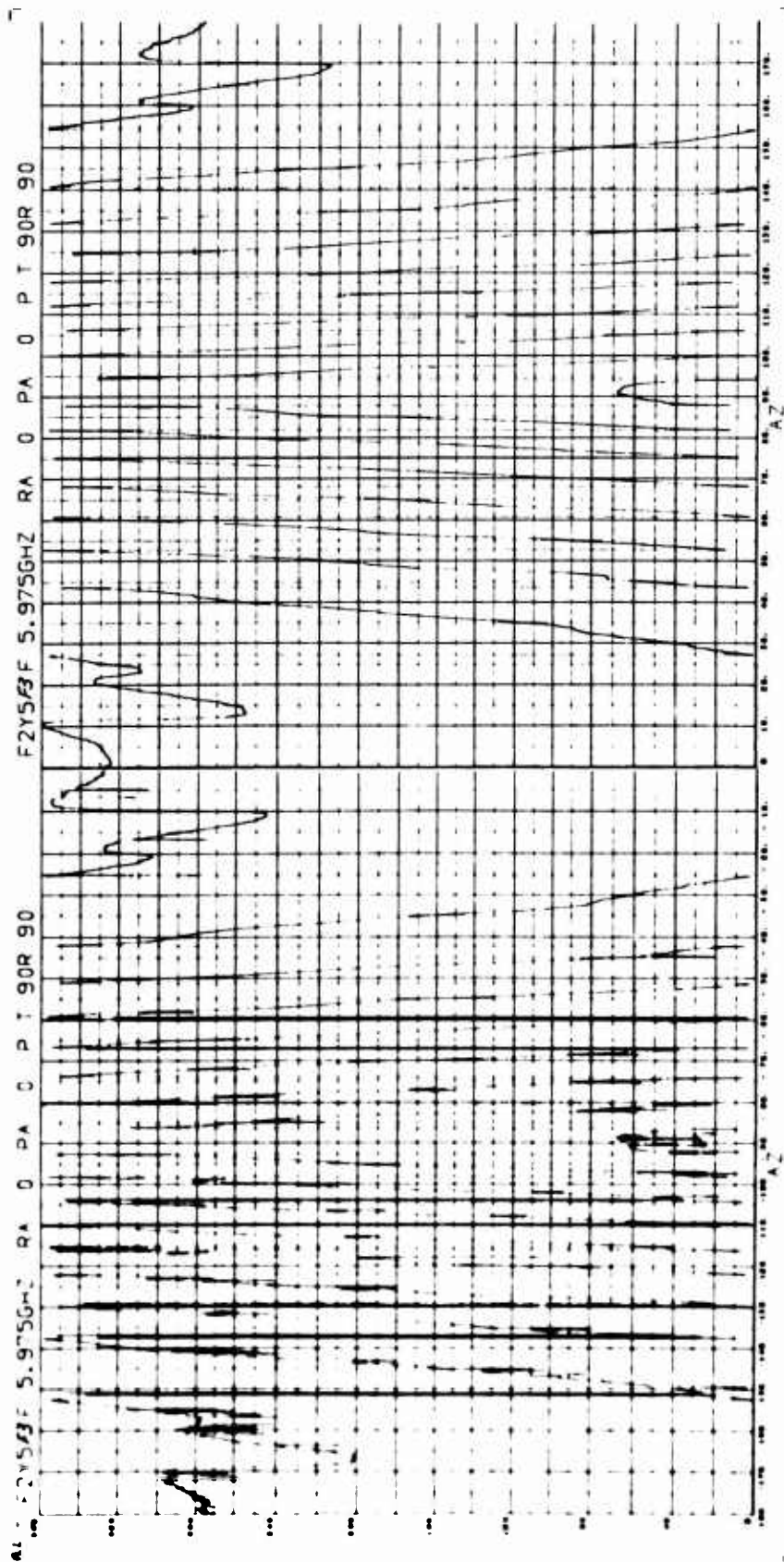


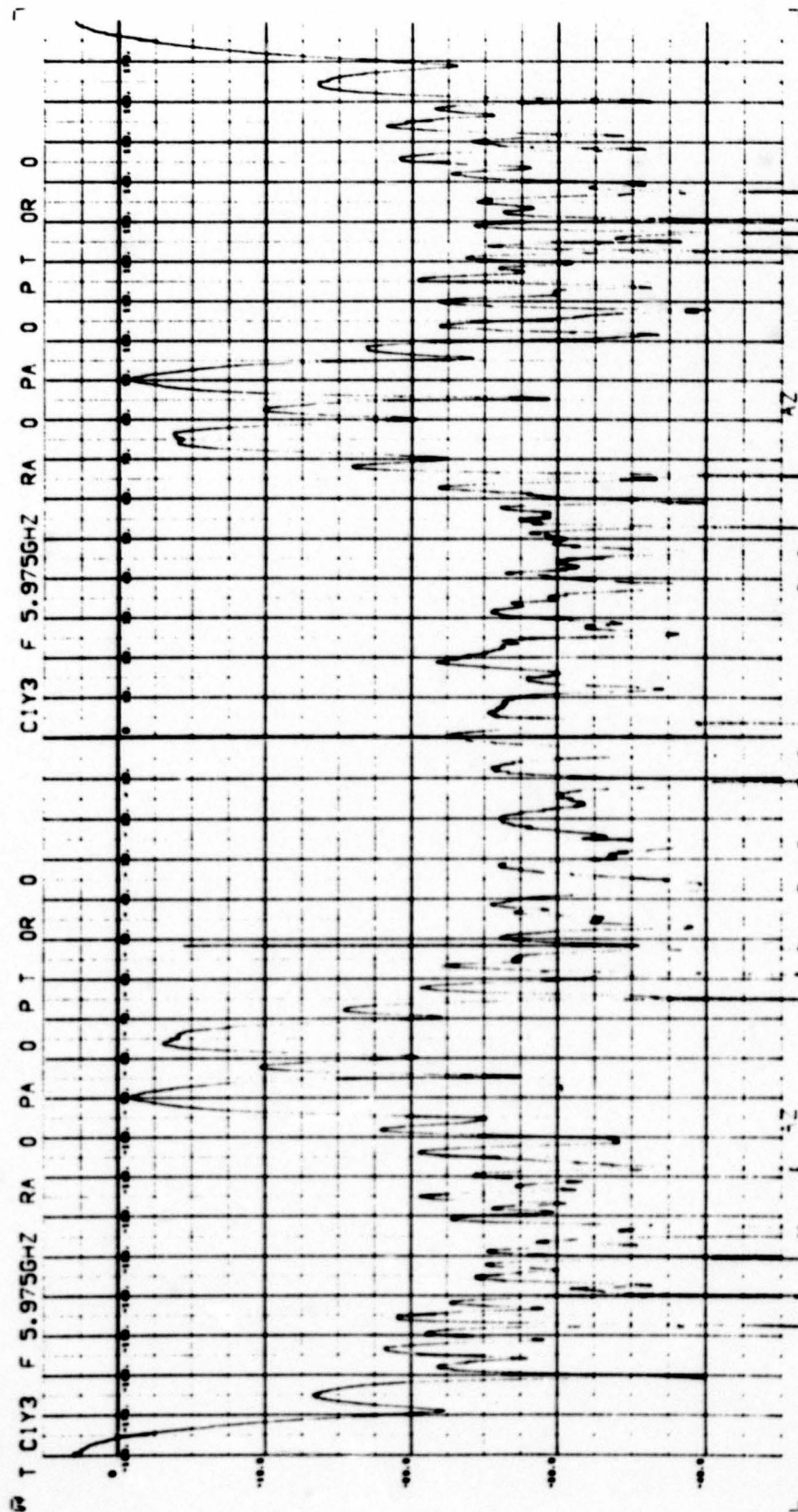
BISTATIC ANGLE = 30.0 DEGREES

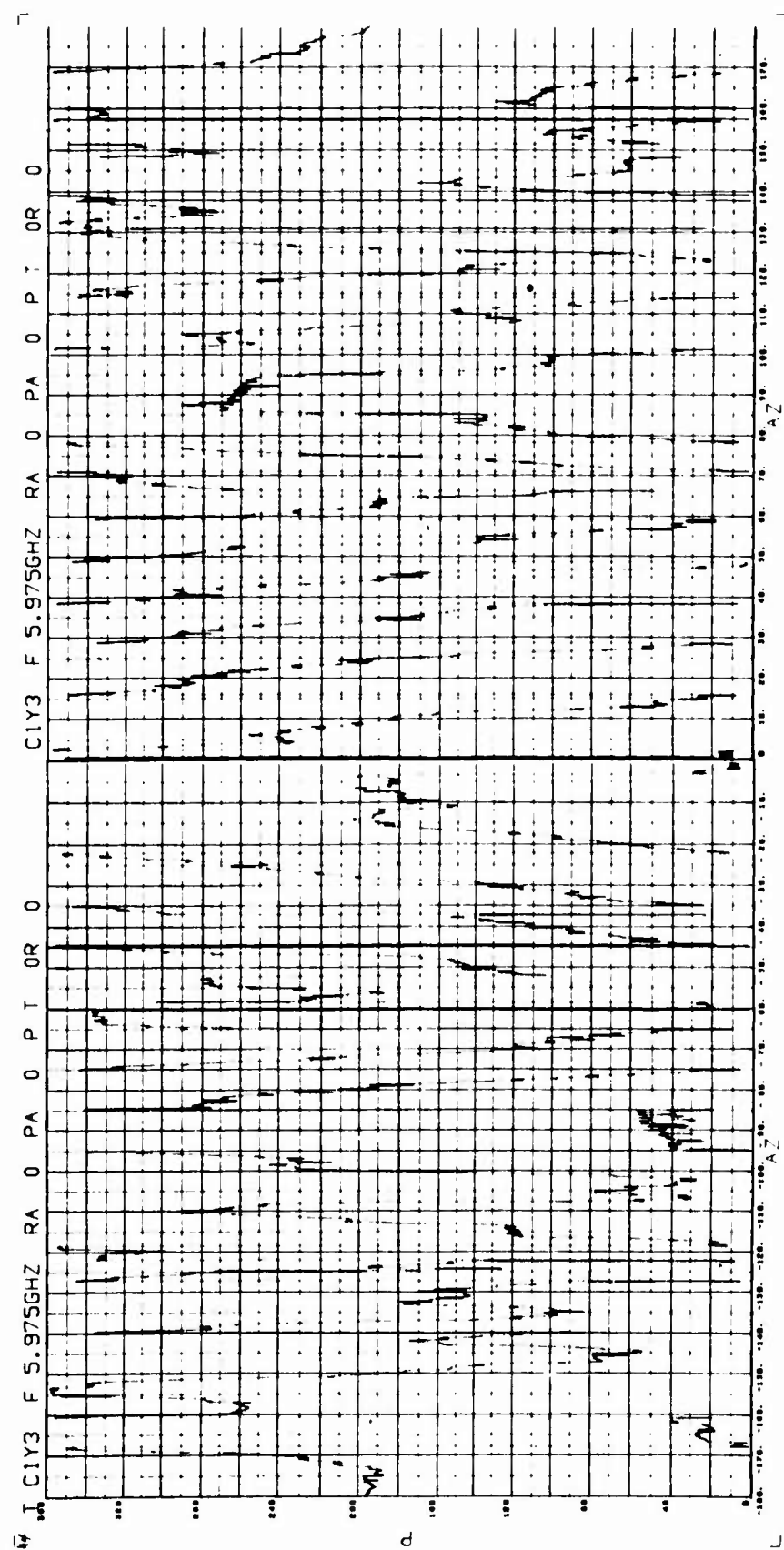


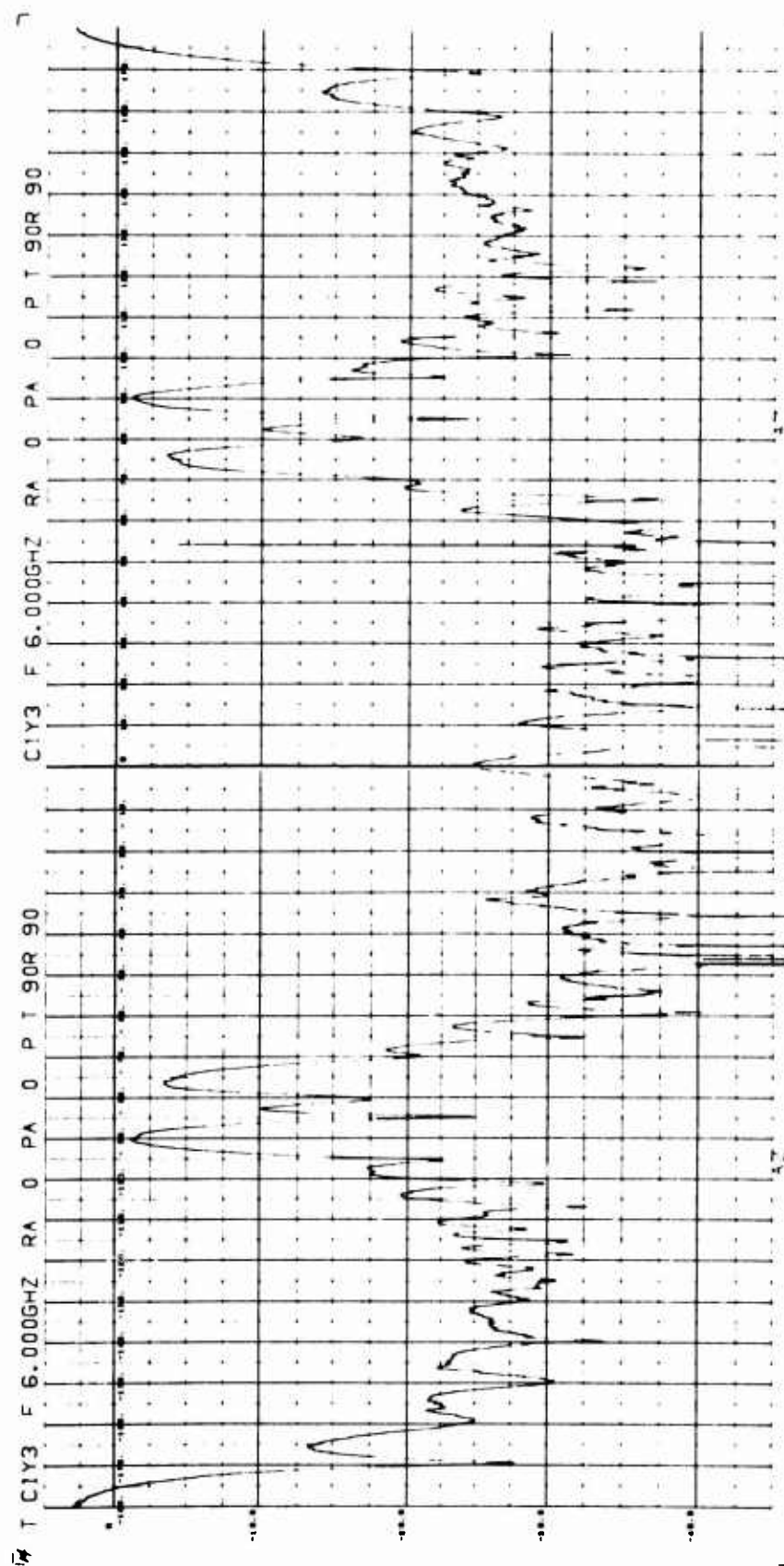


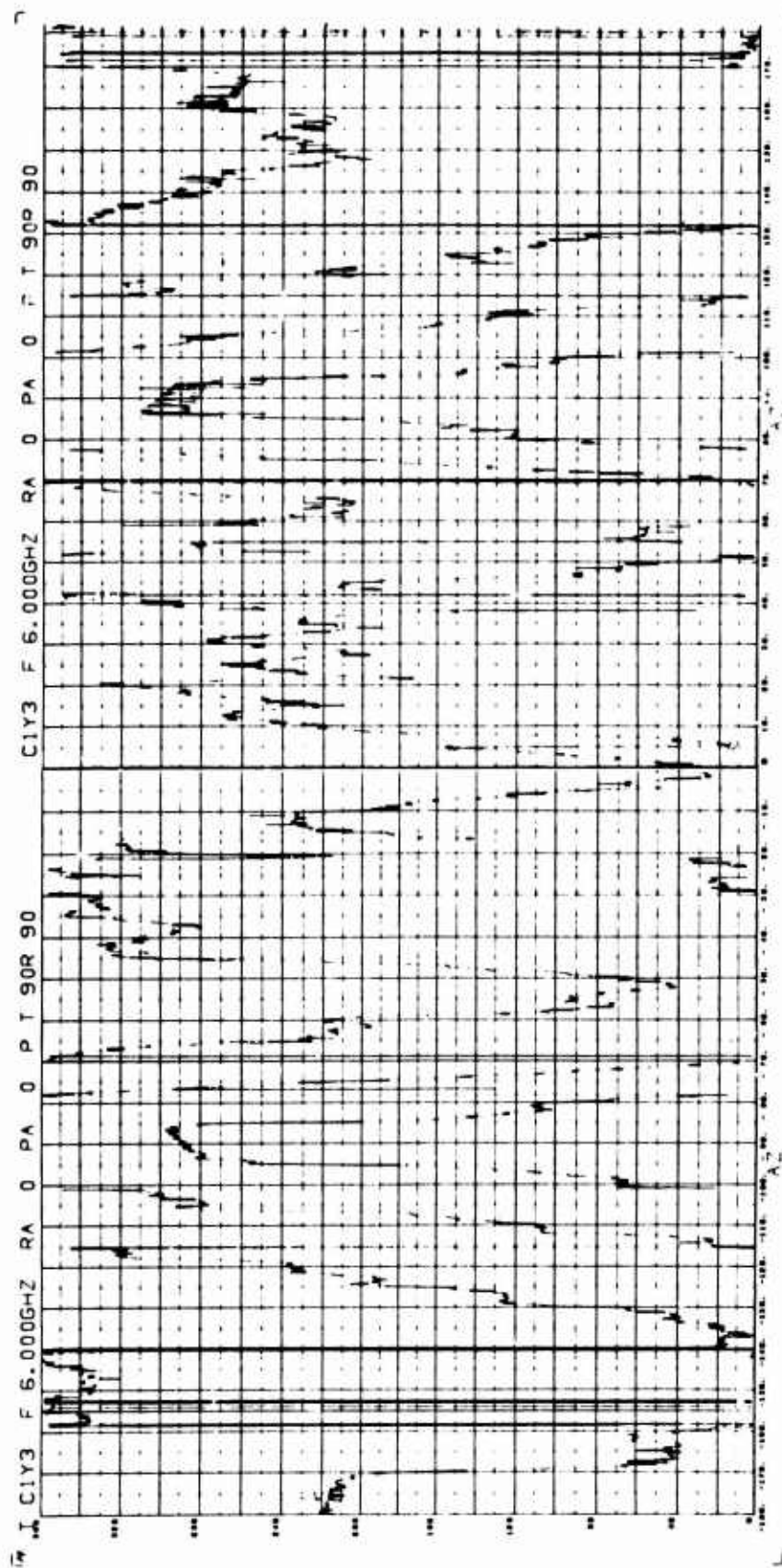


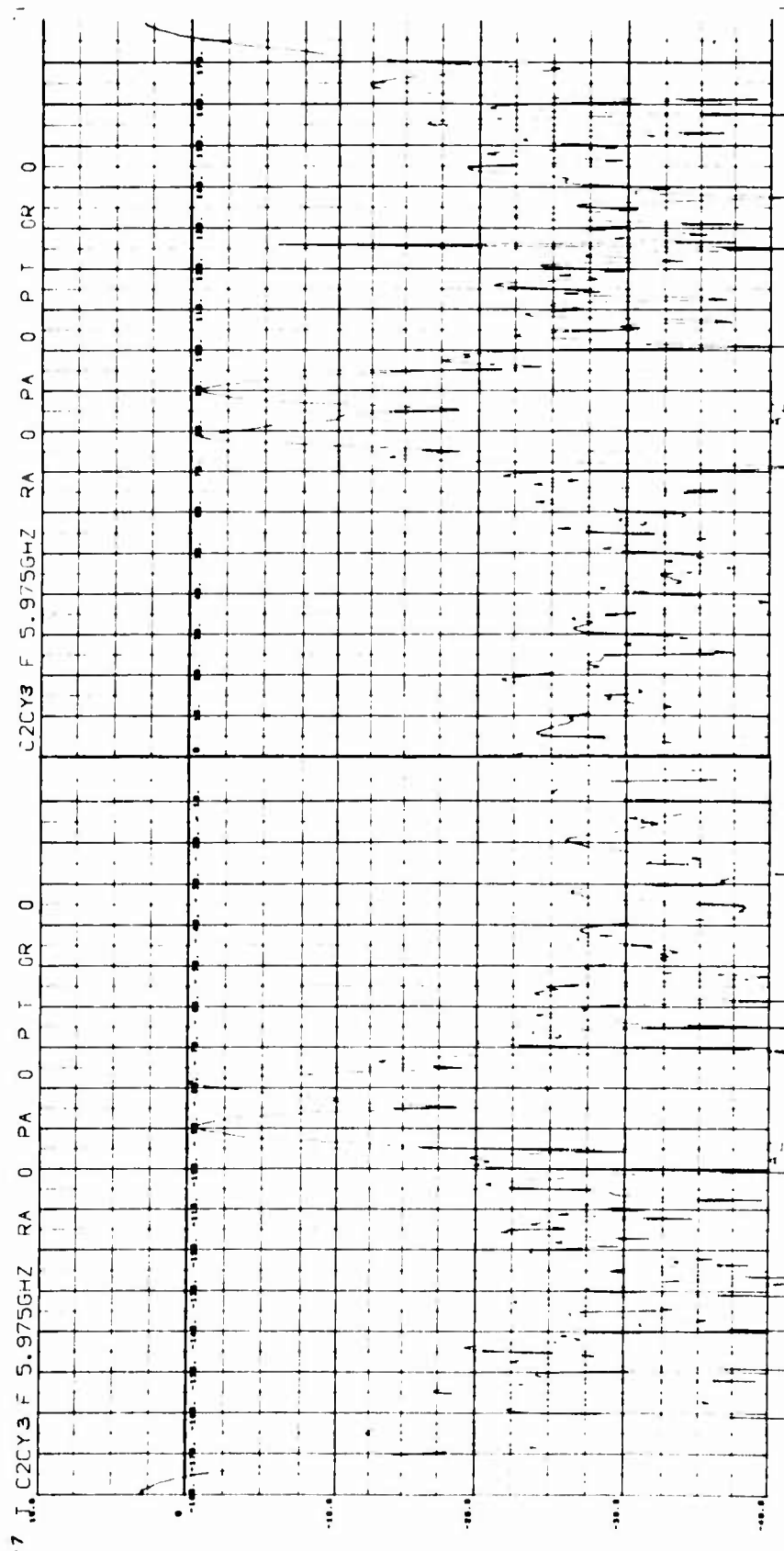


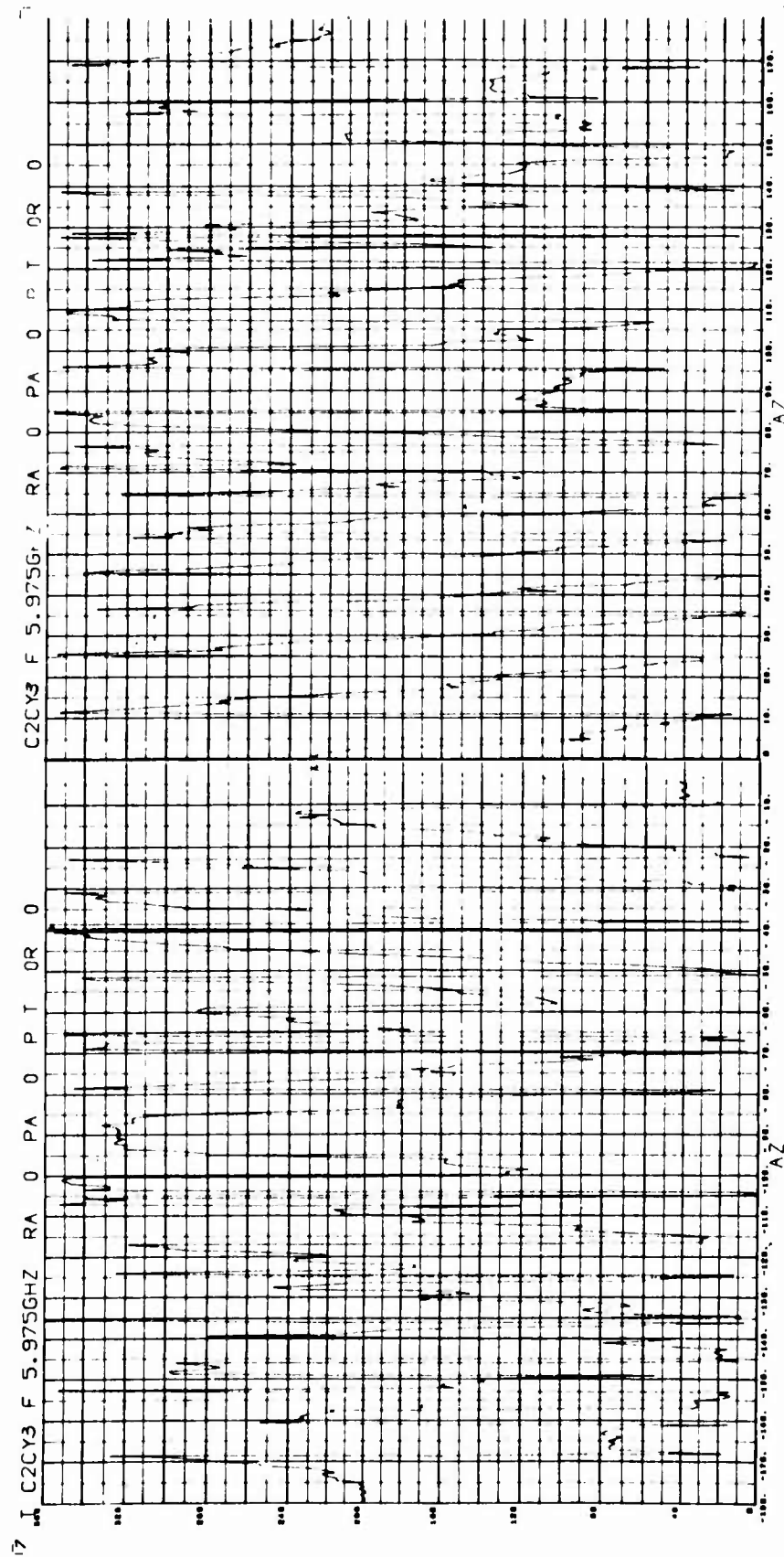


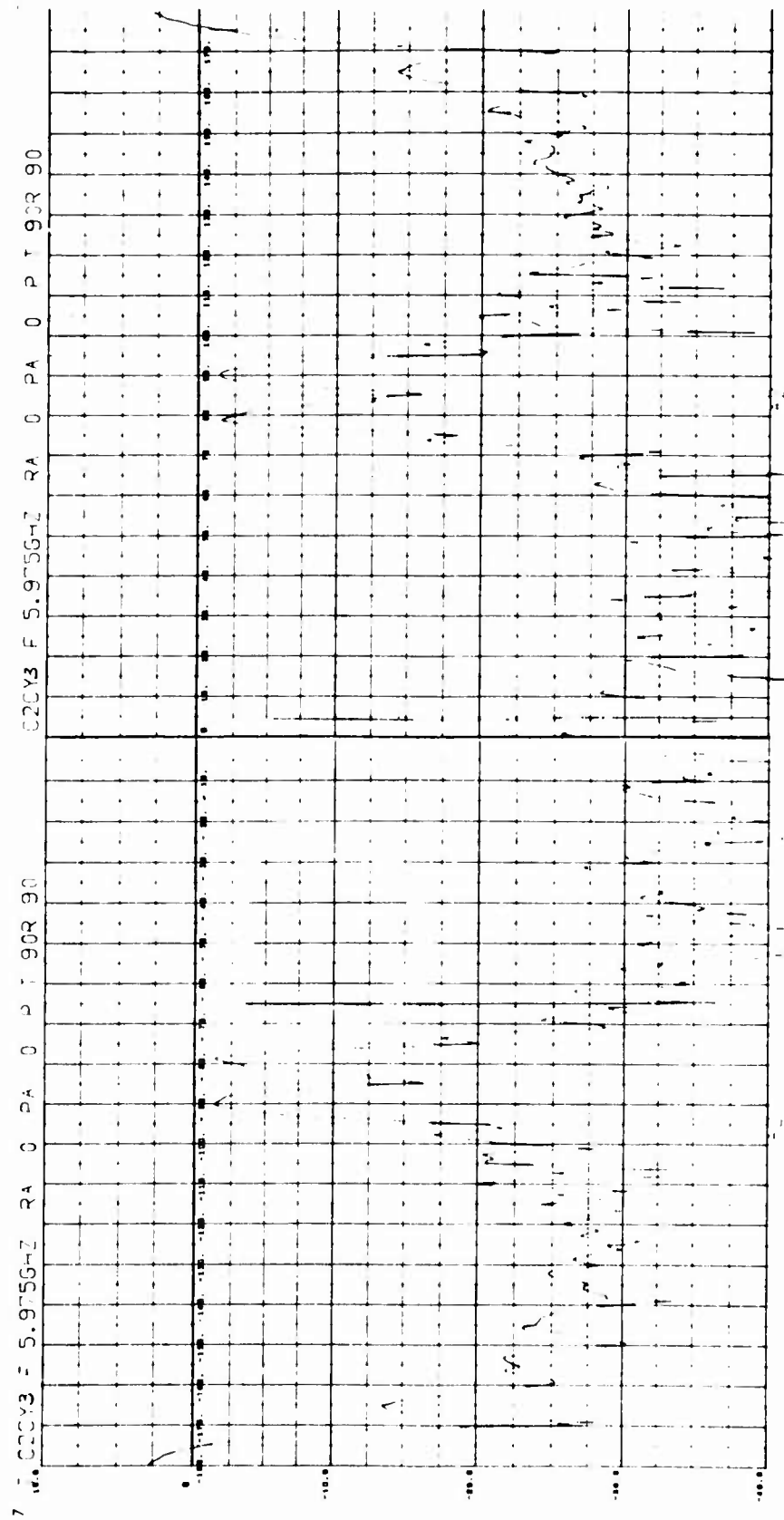


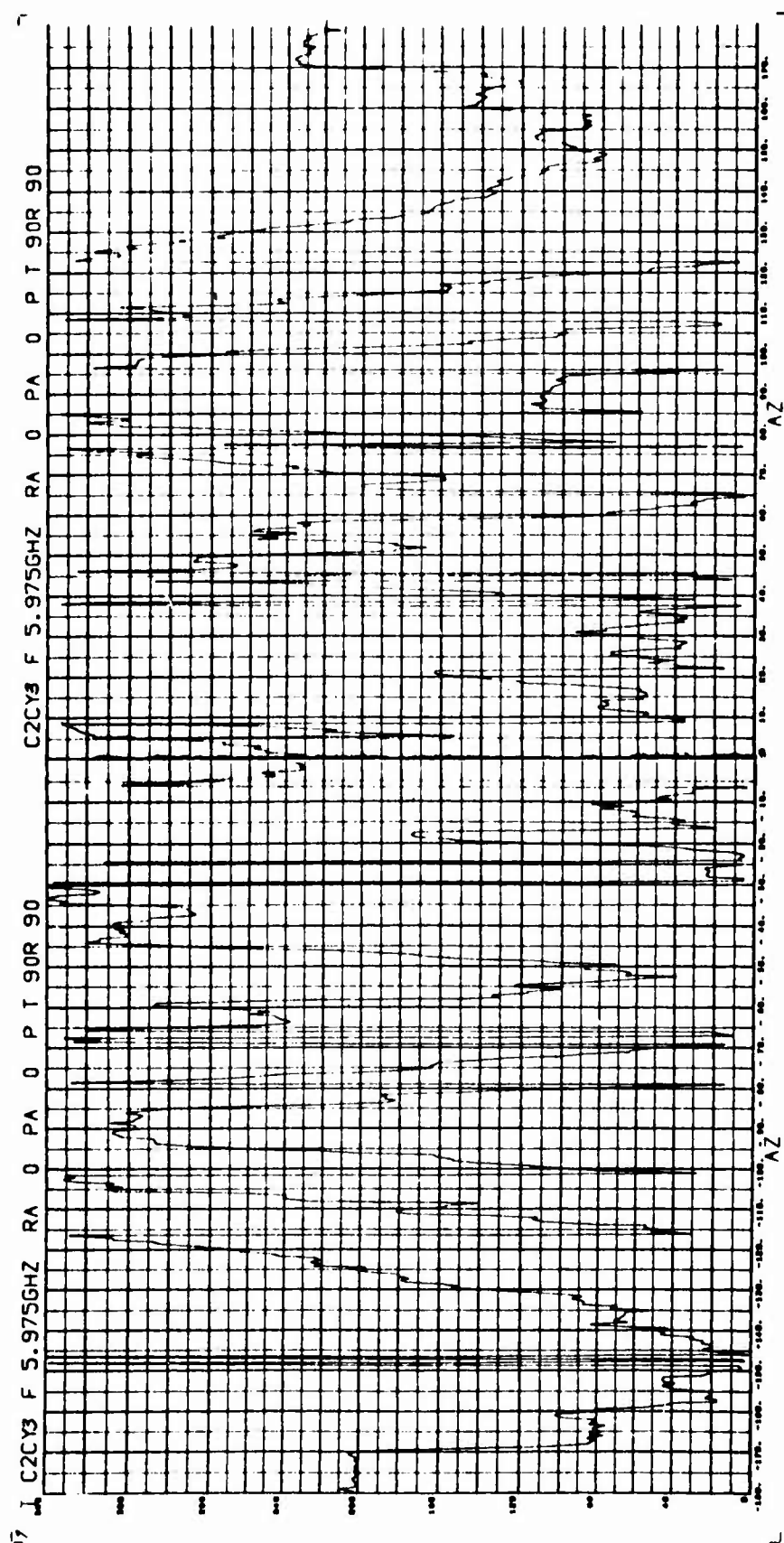


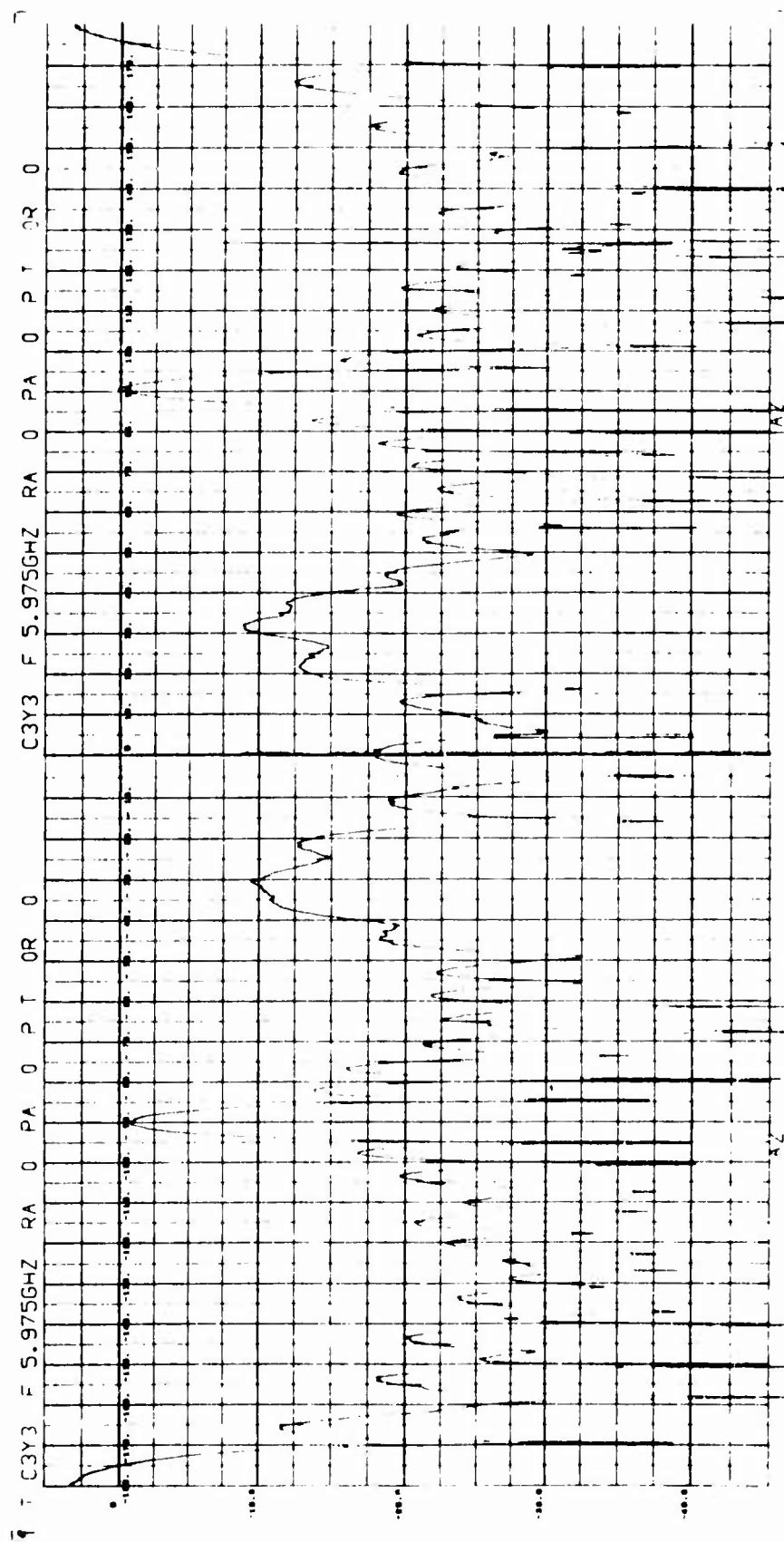


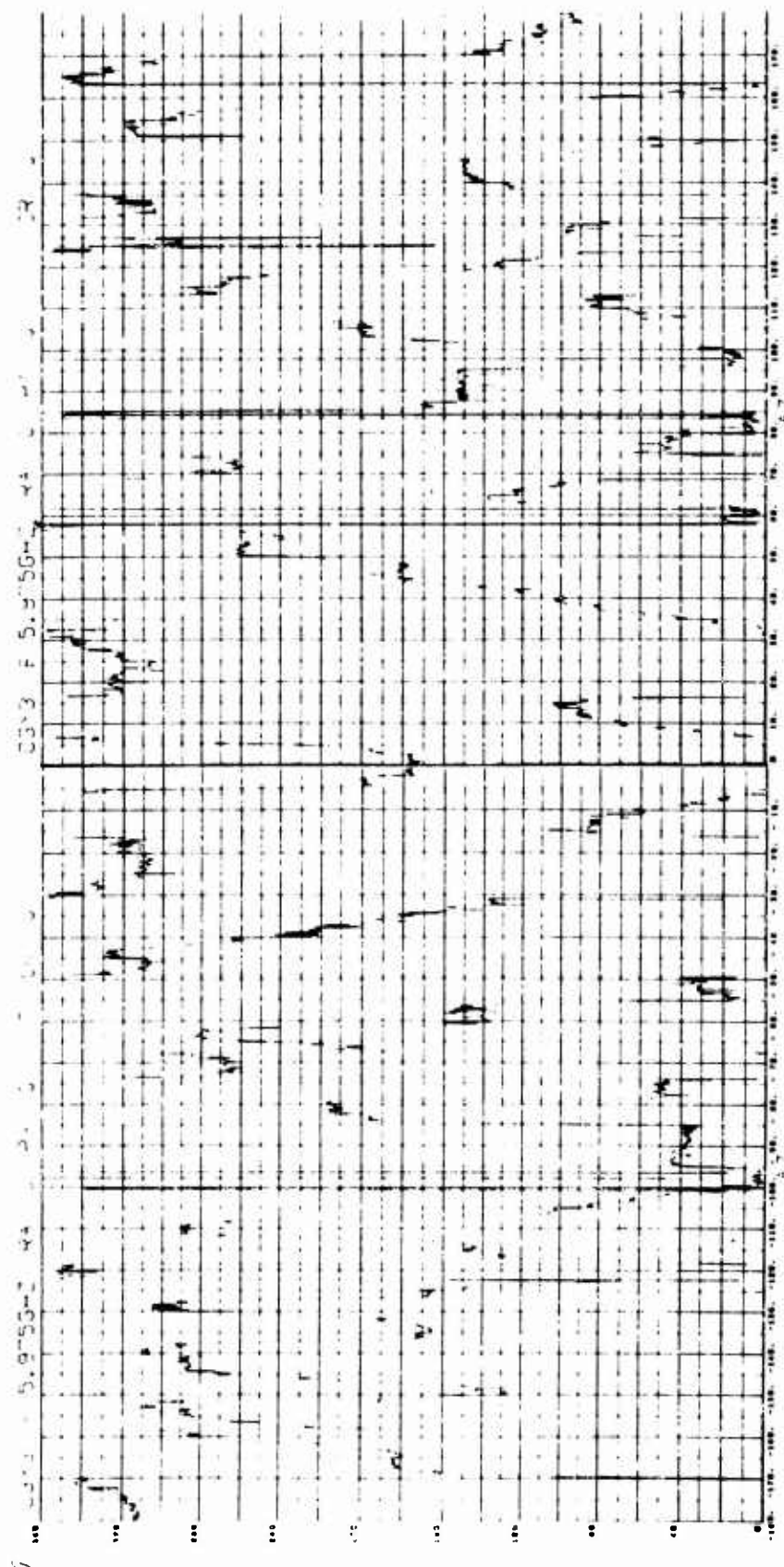


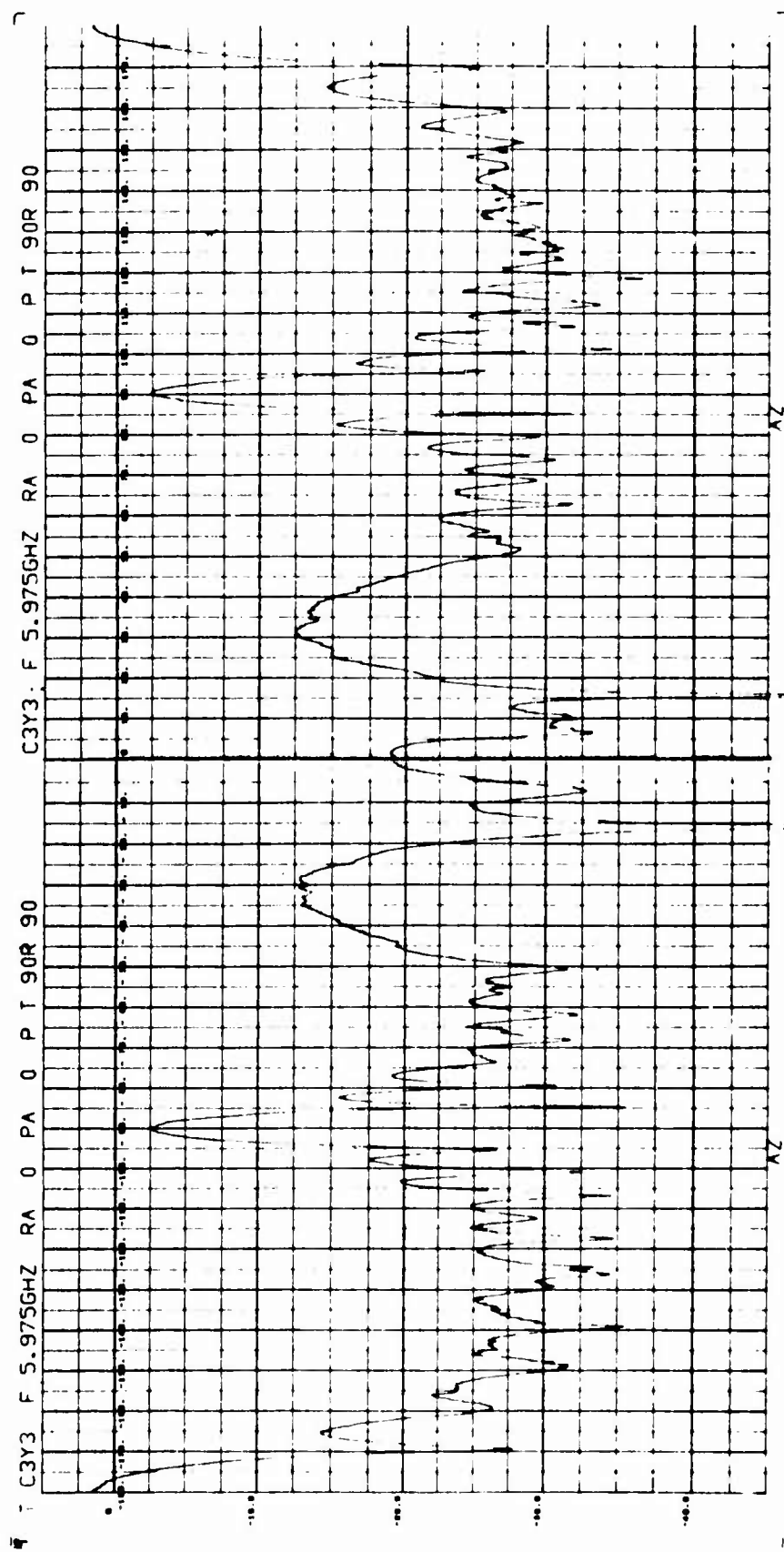


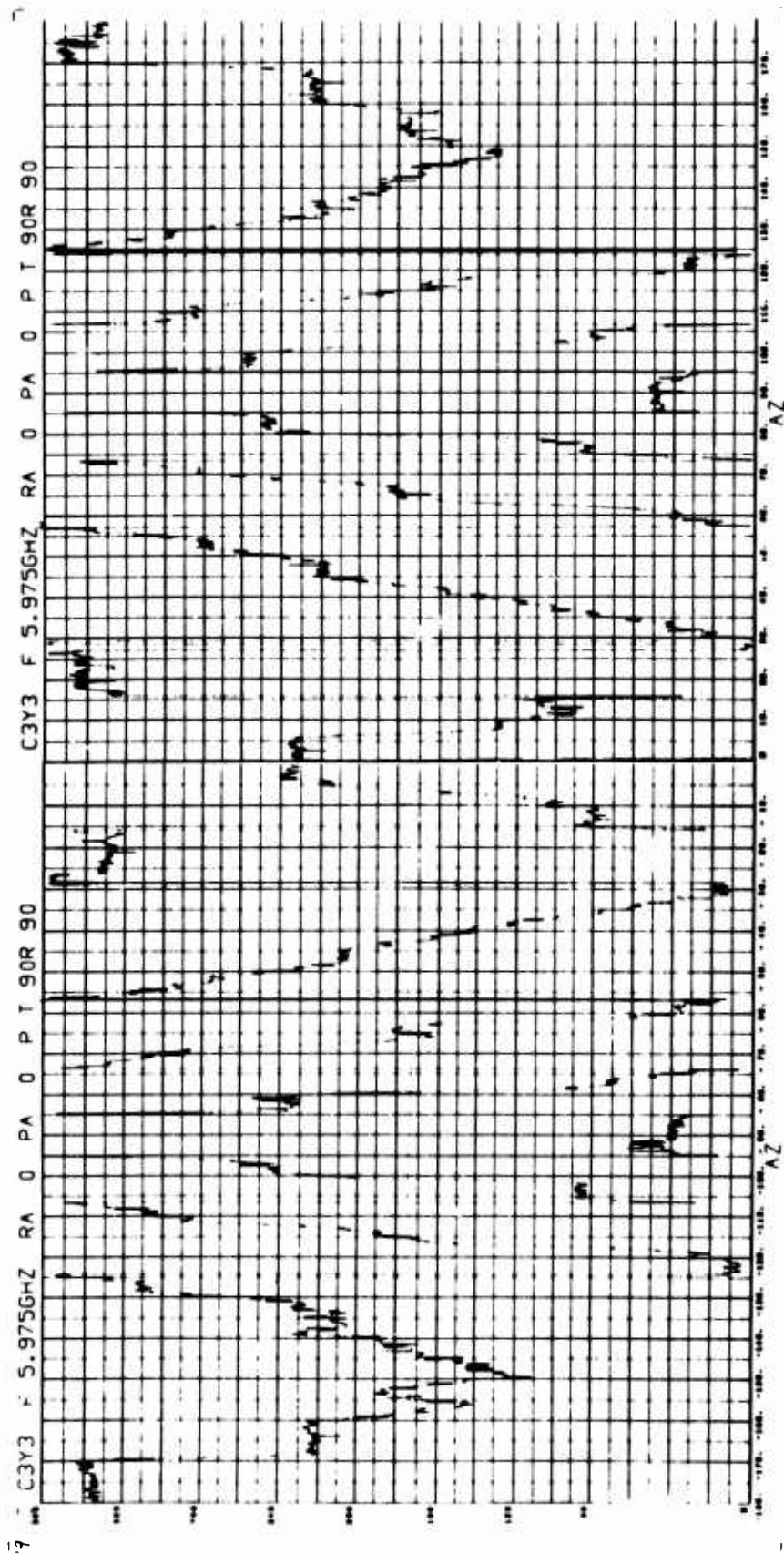


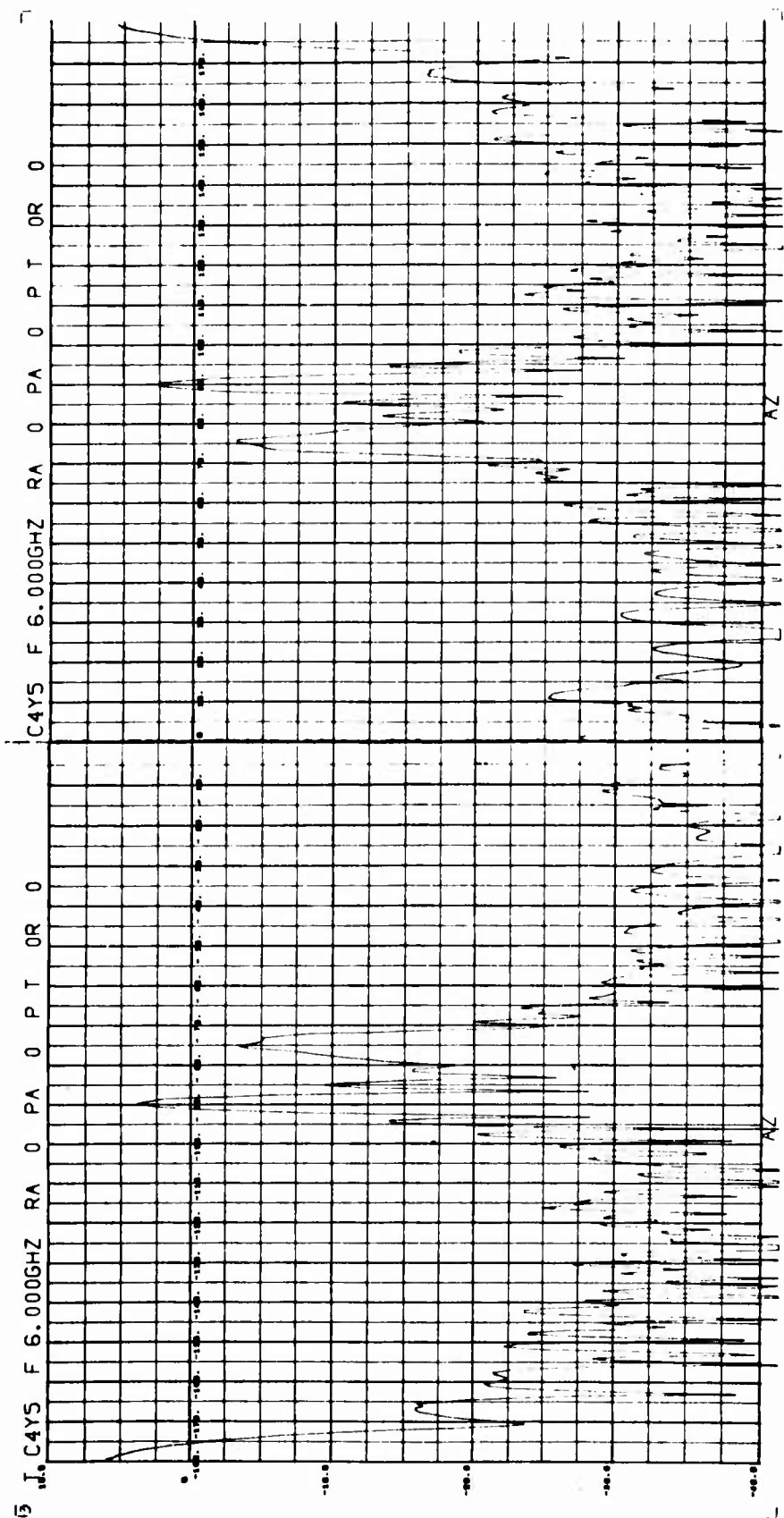


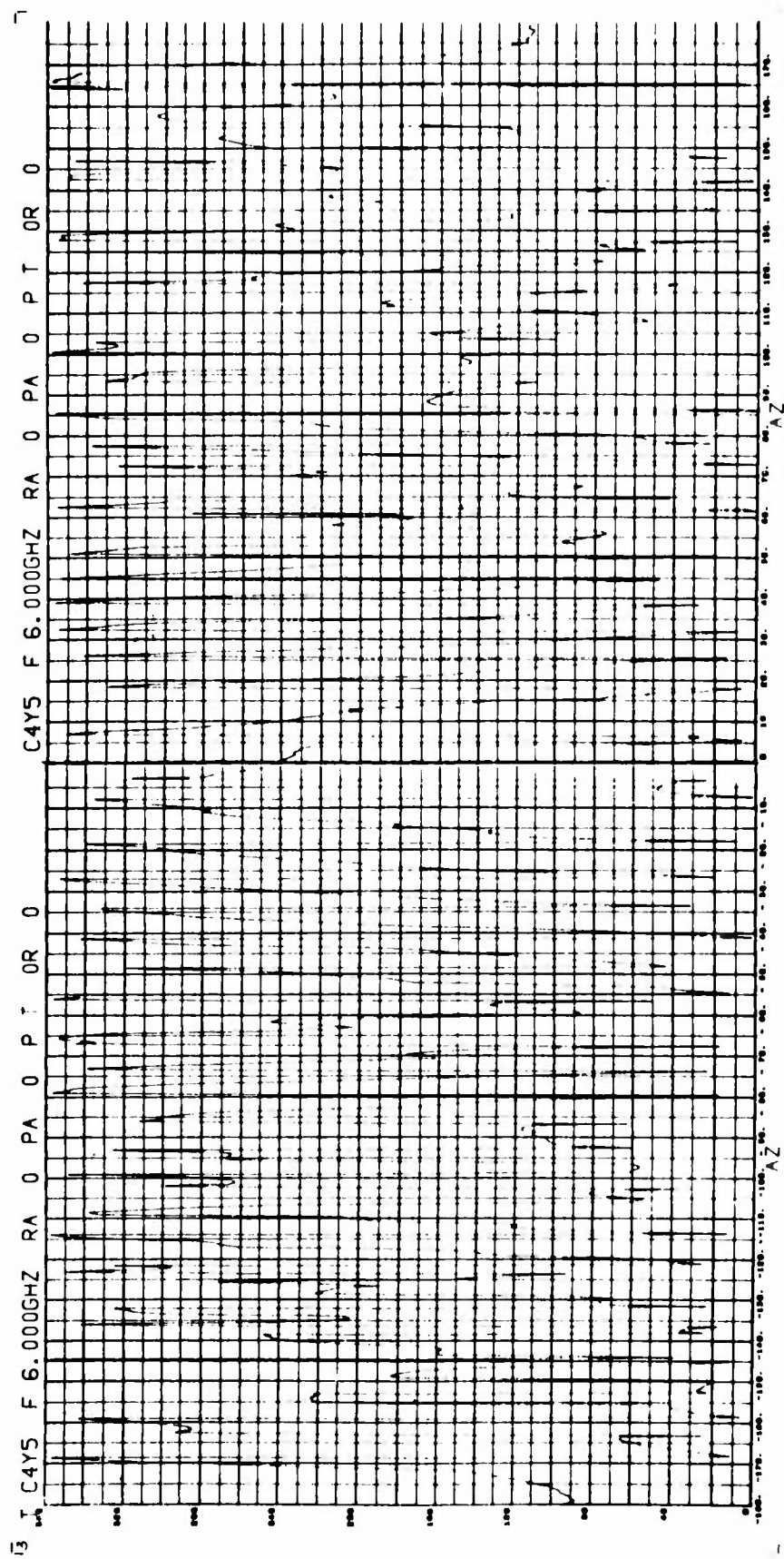


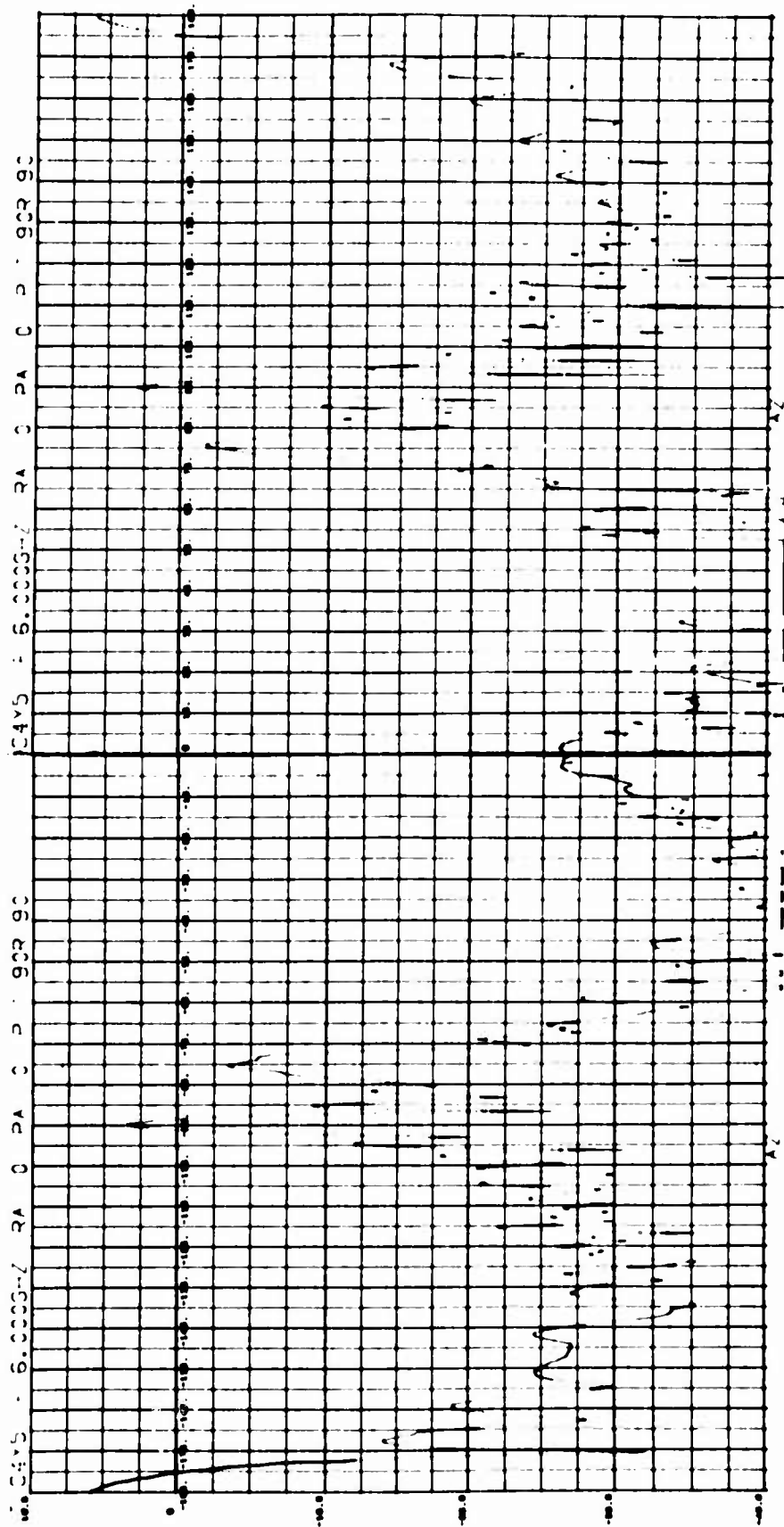


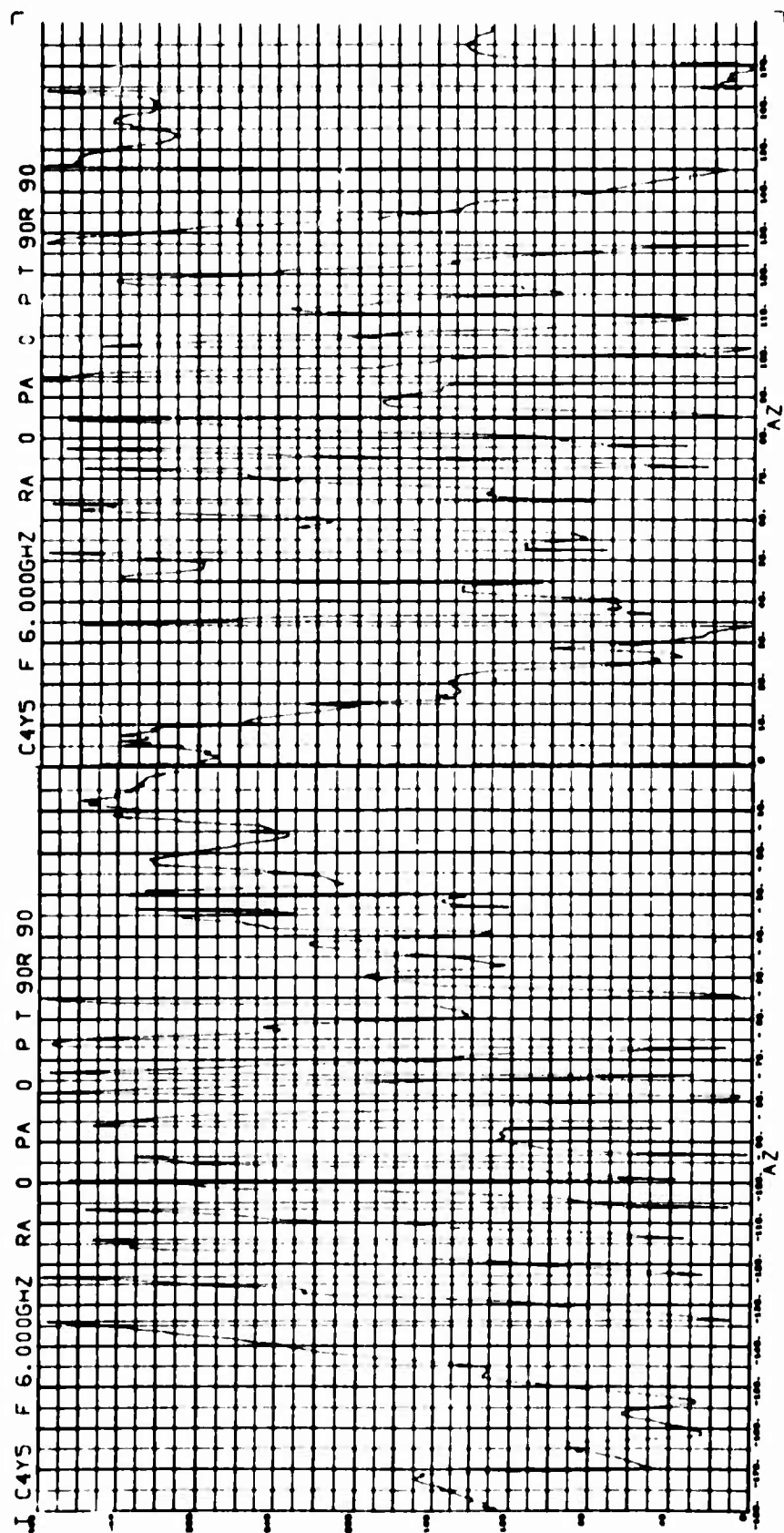


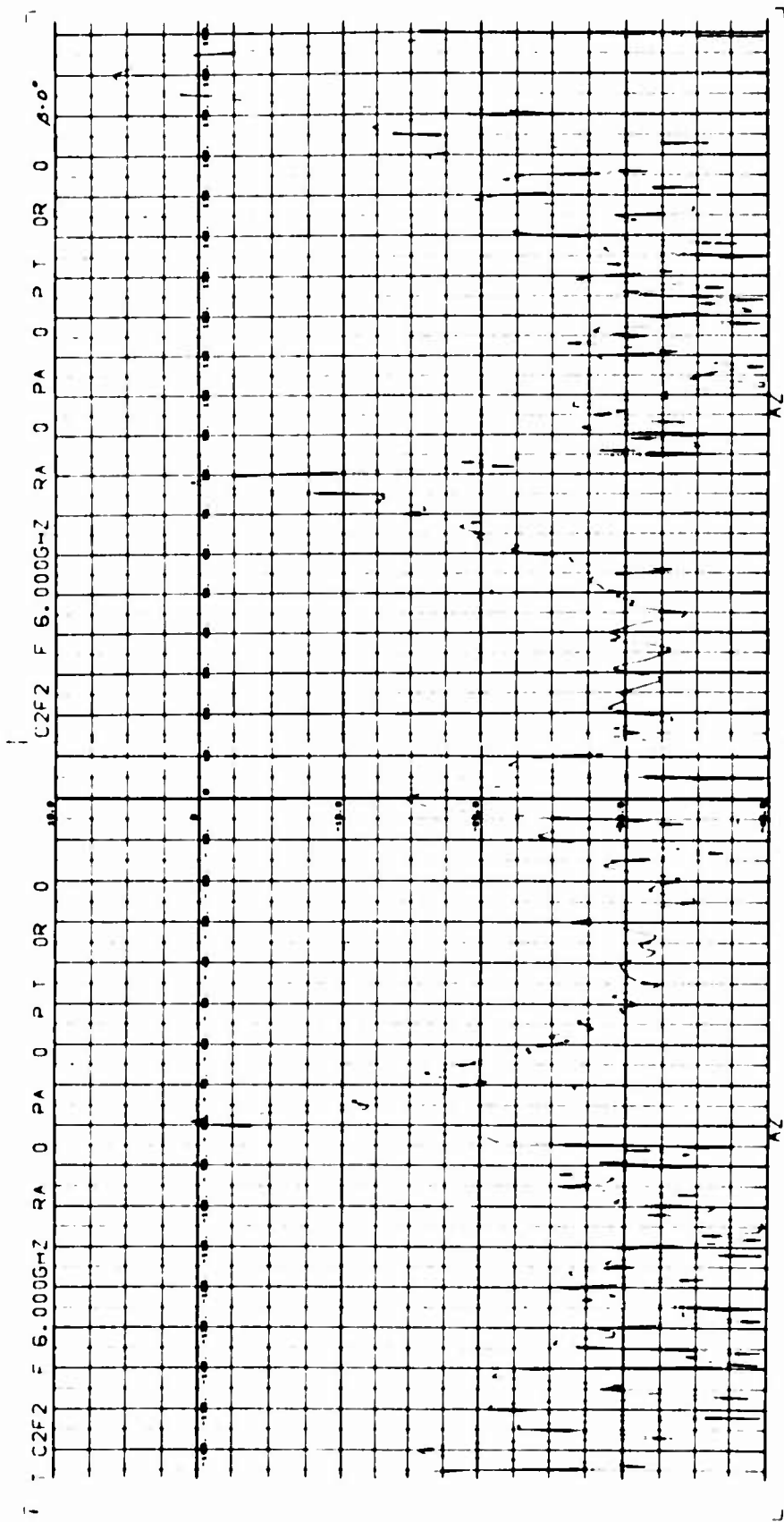


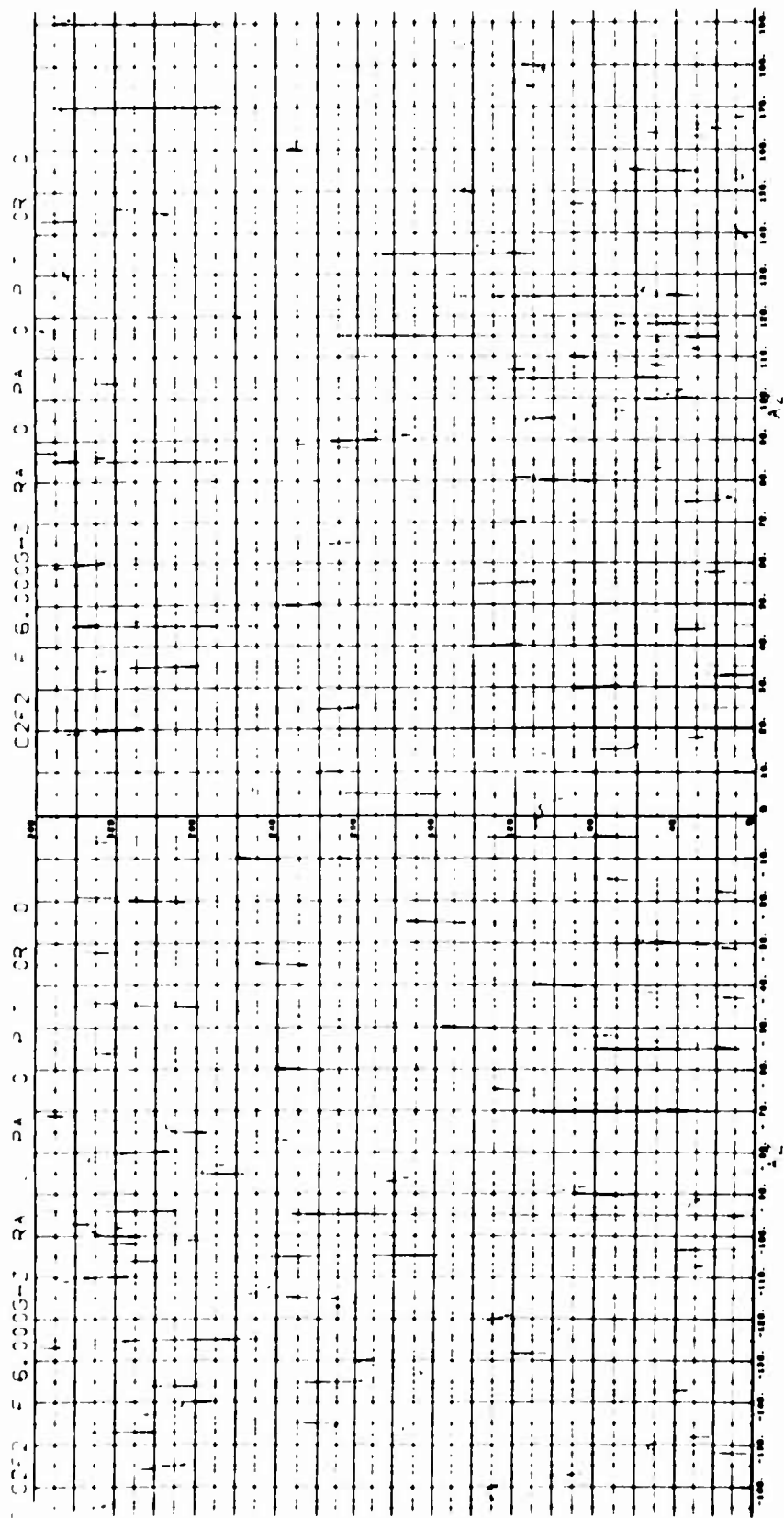


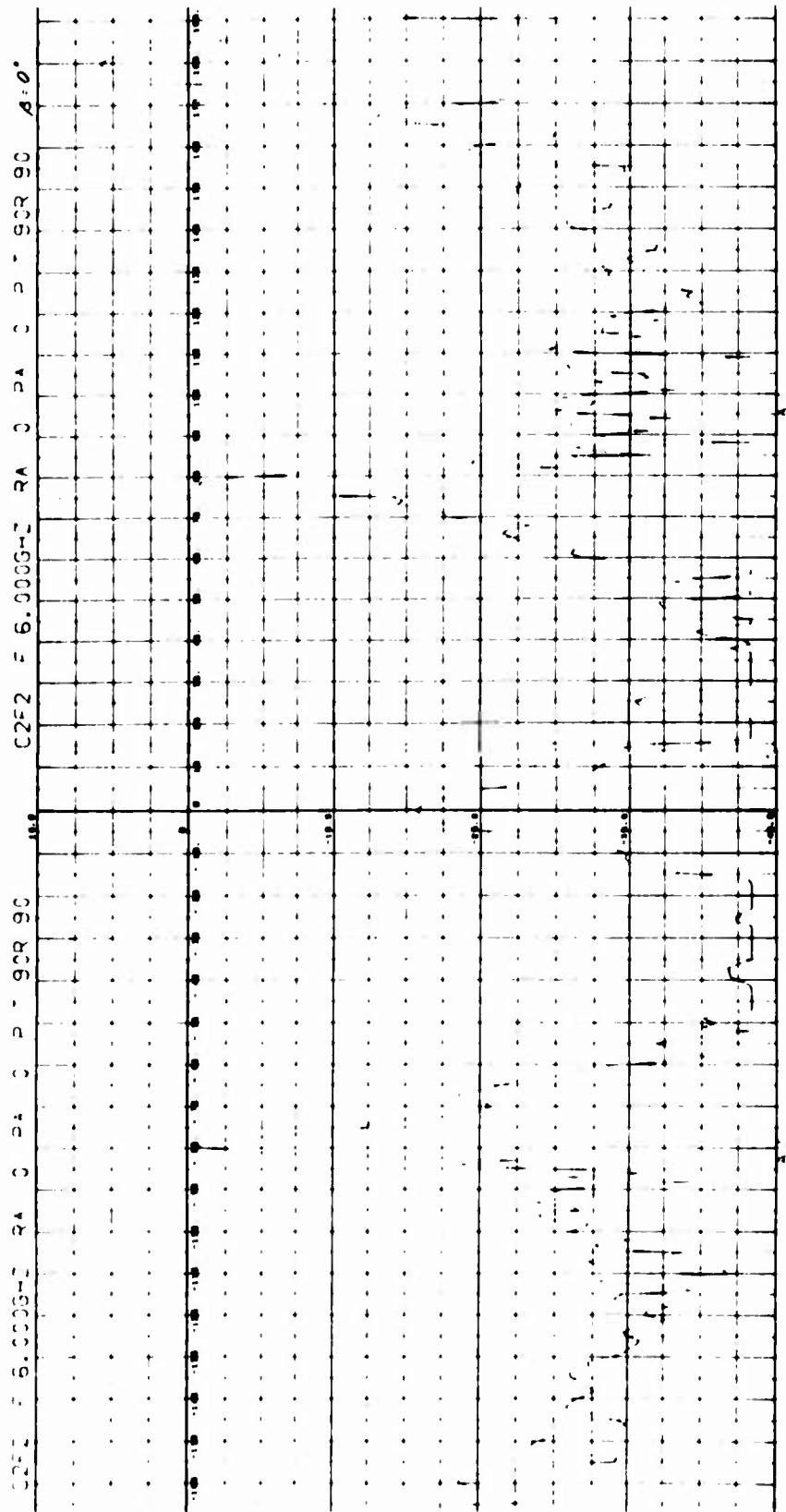


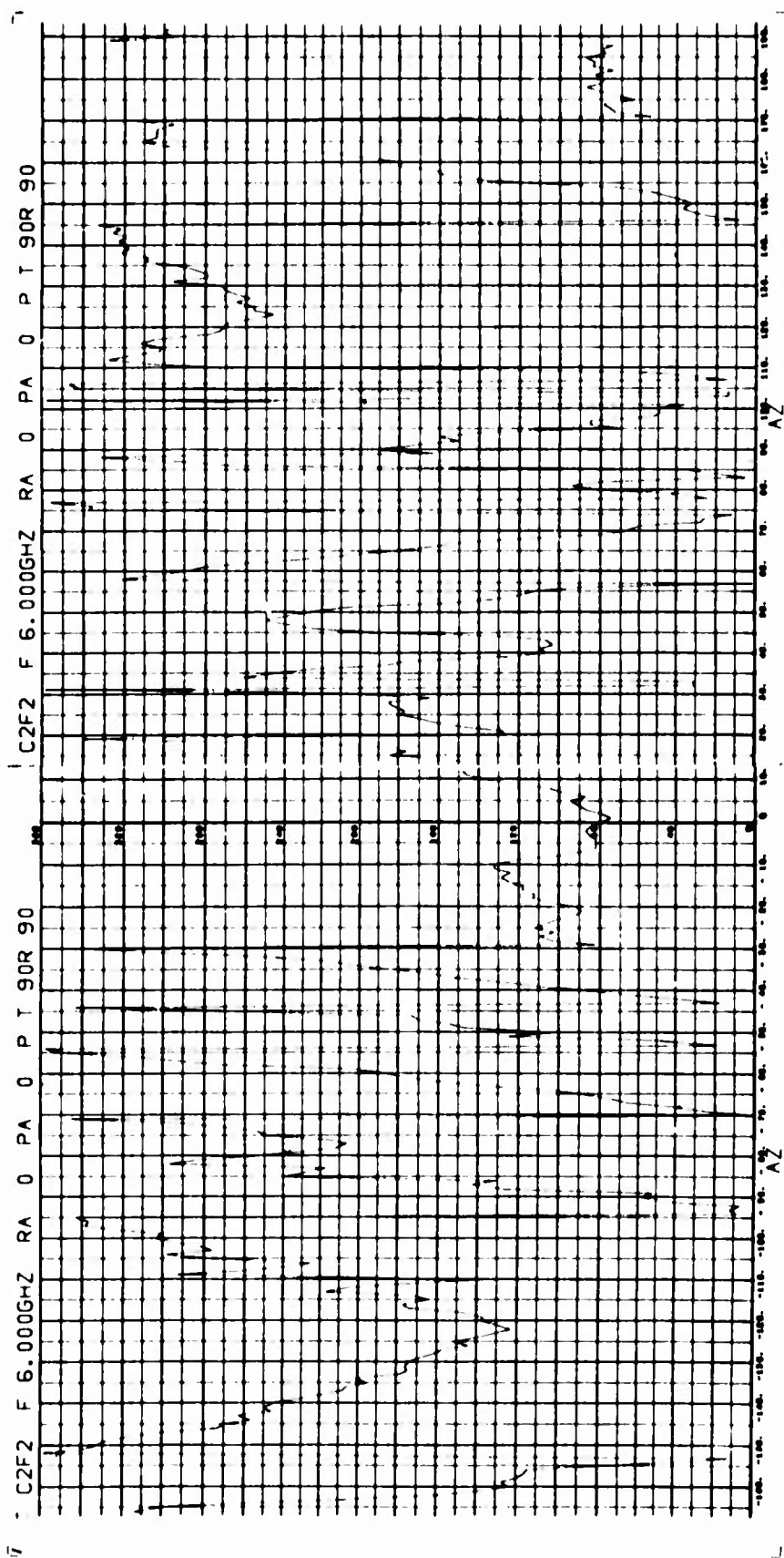


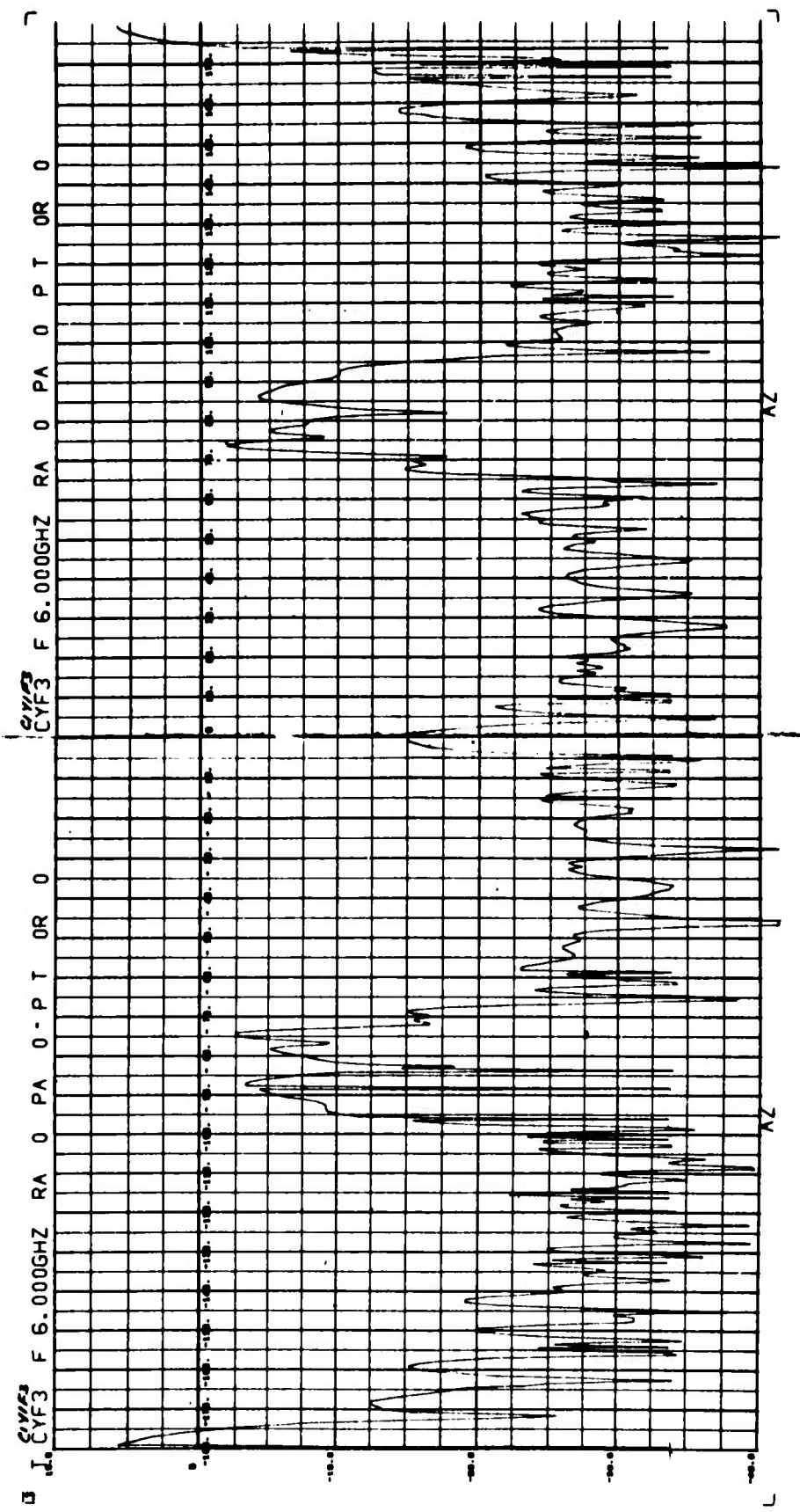


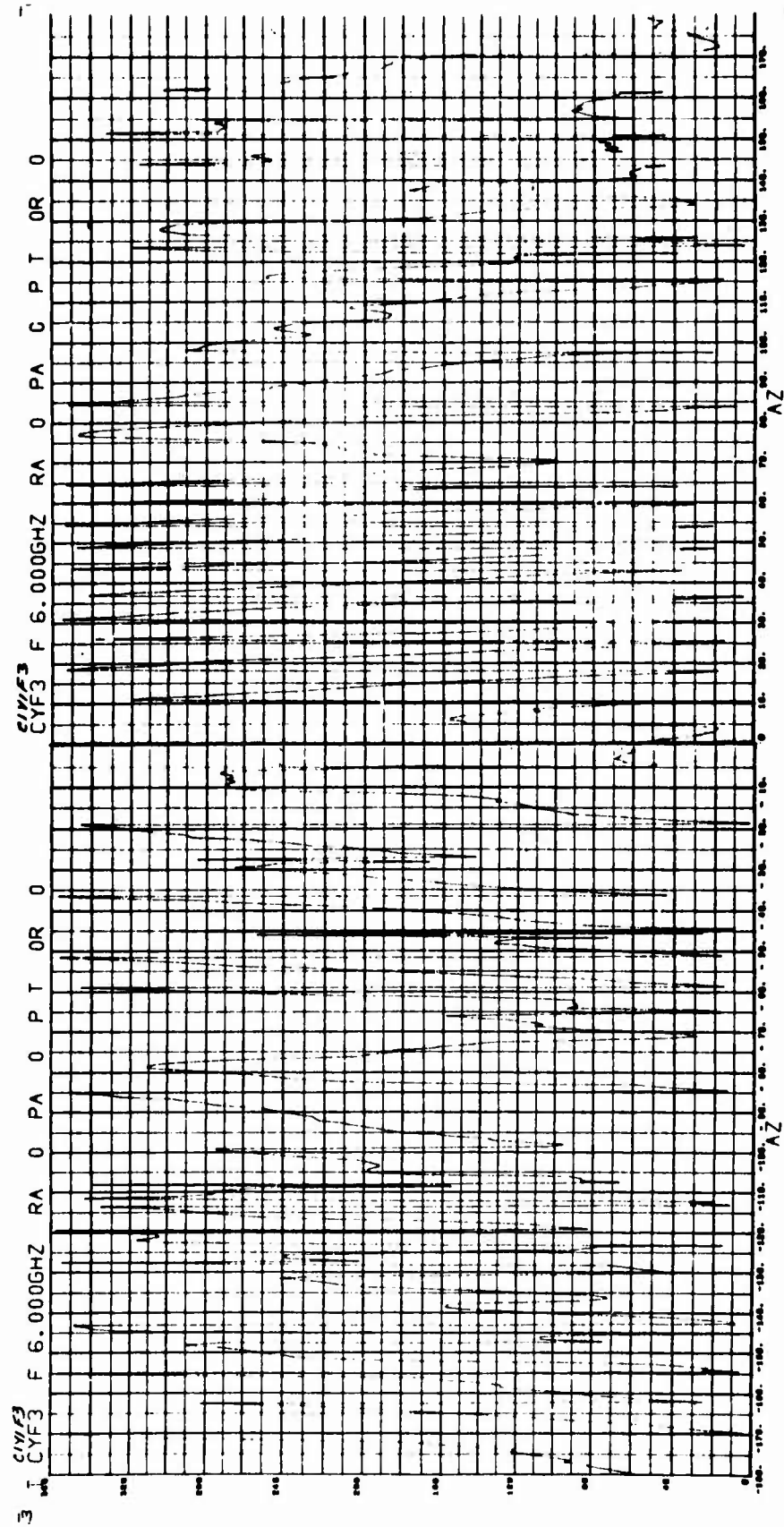


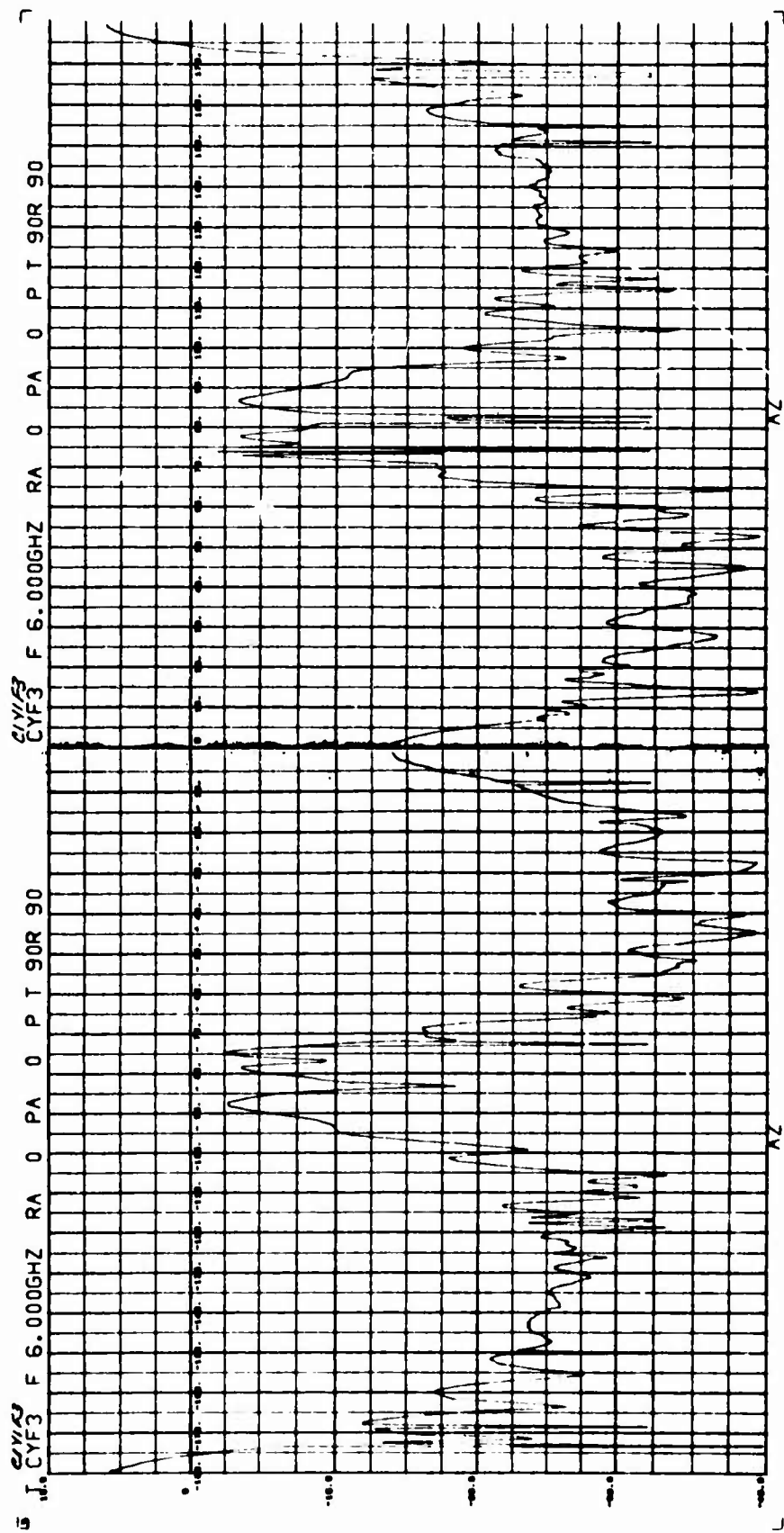


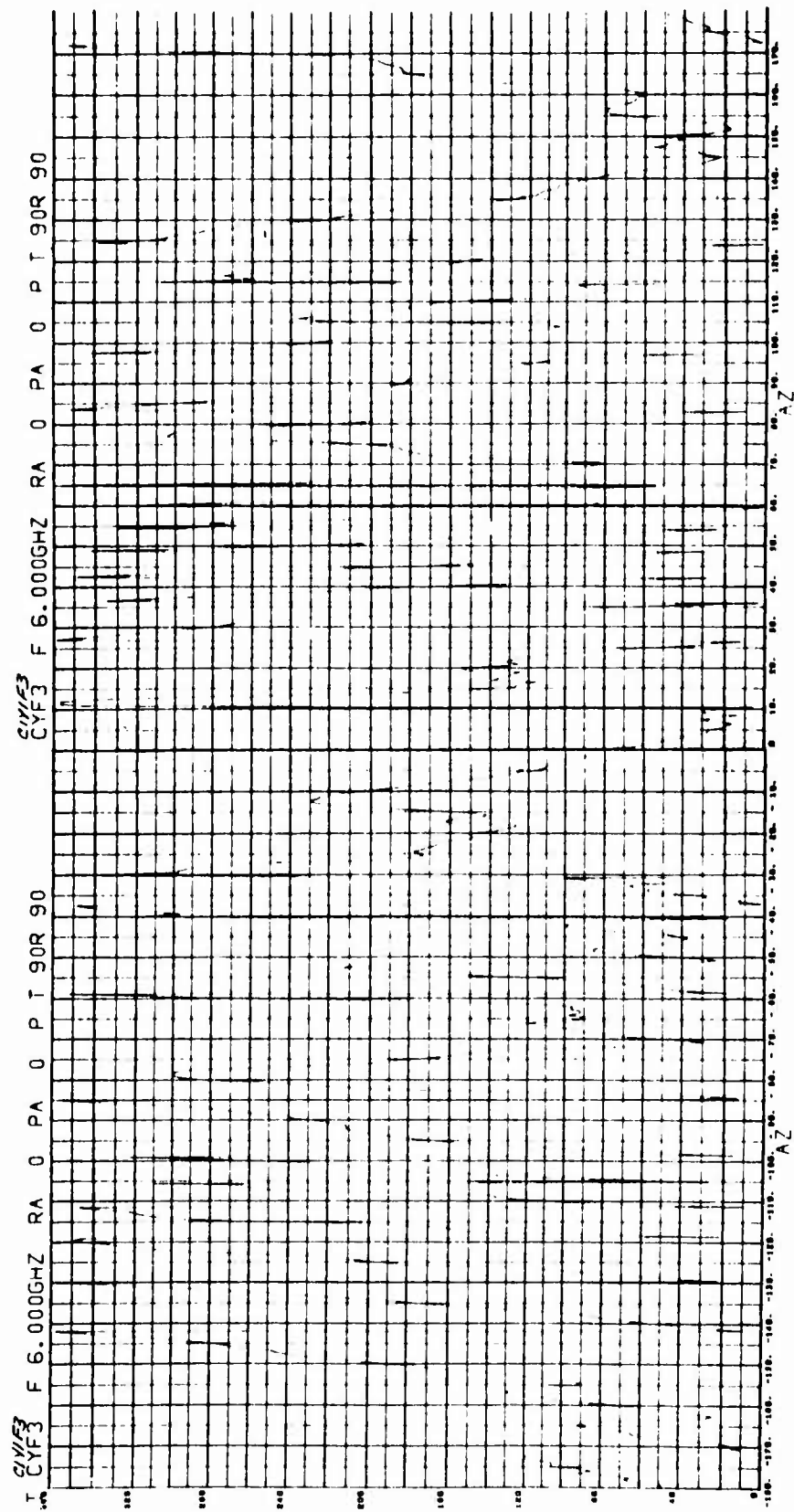


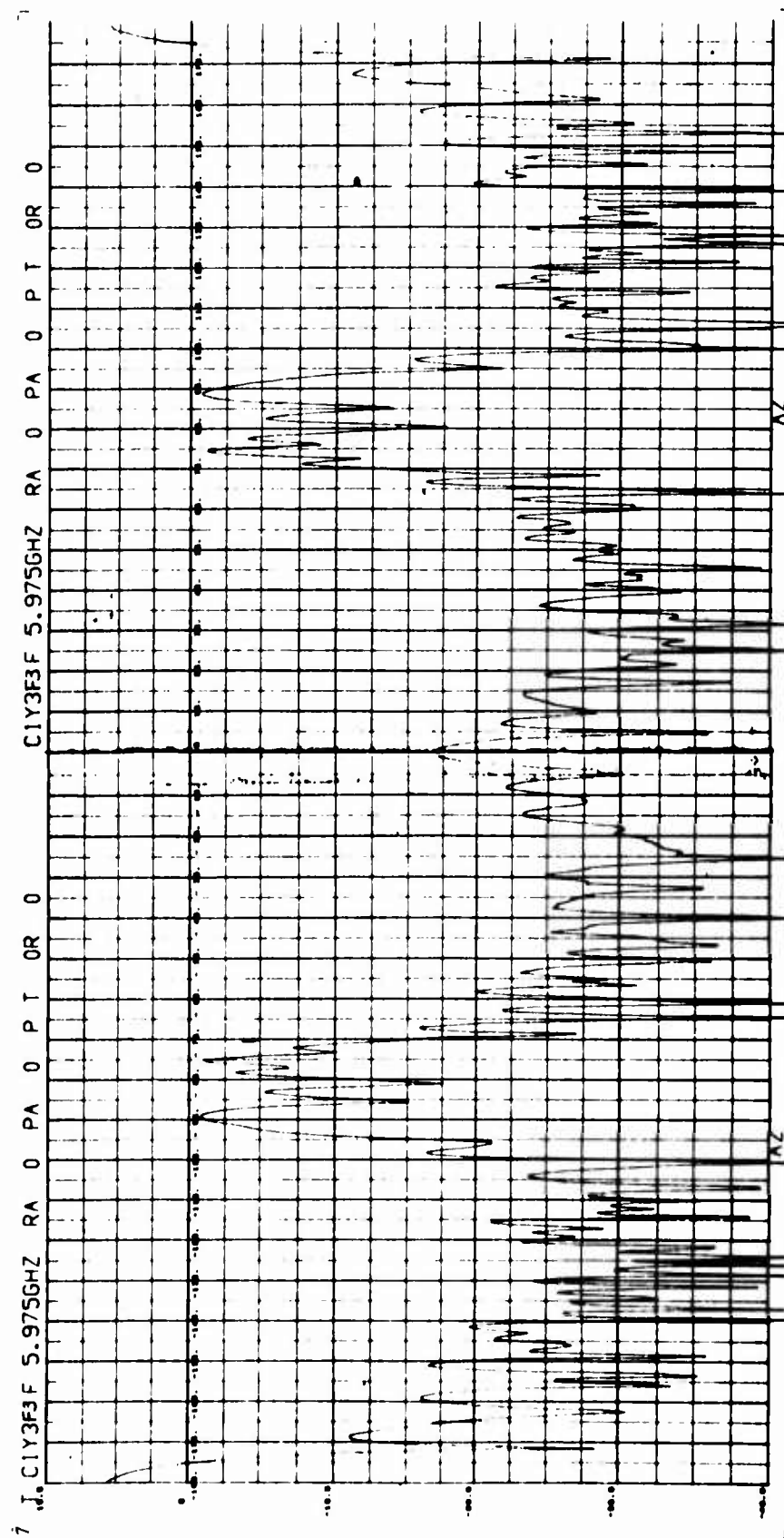


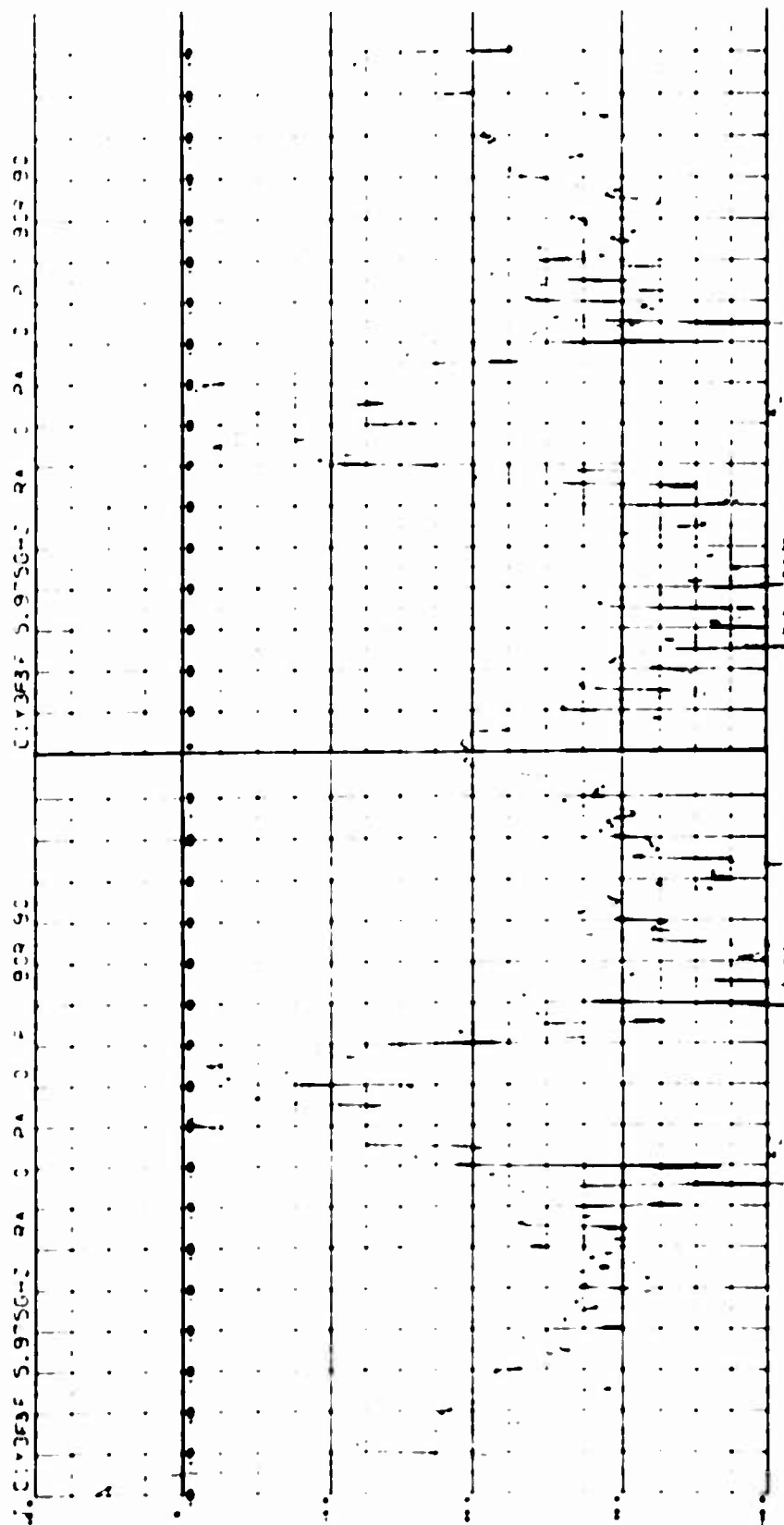


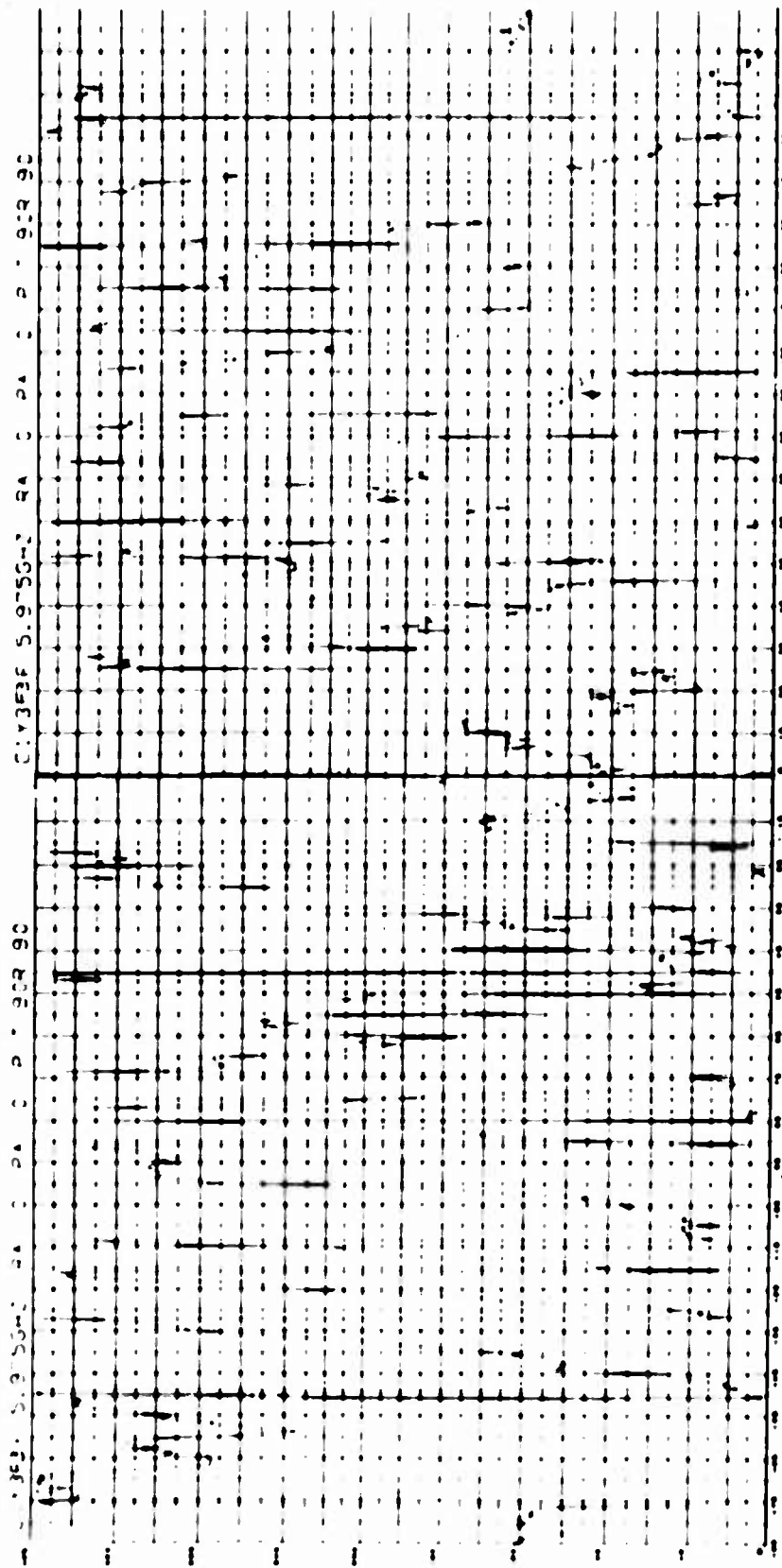


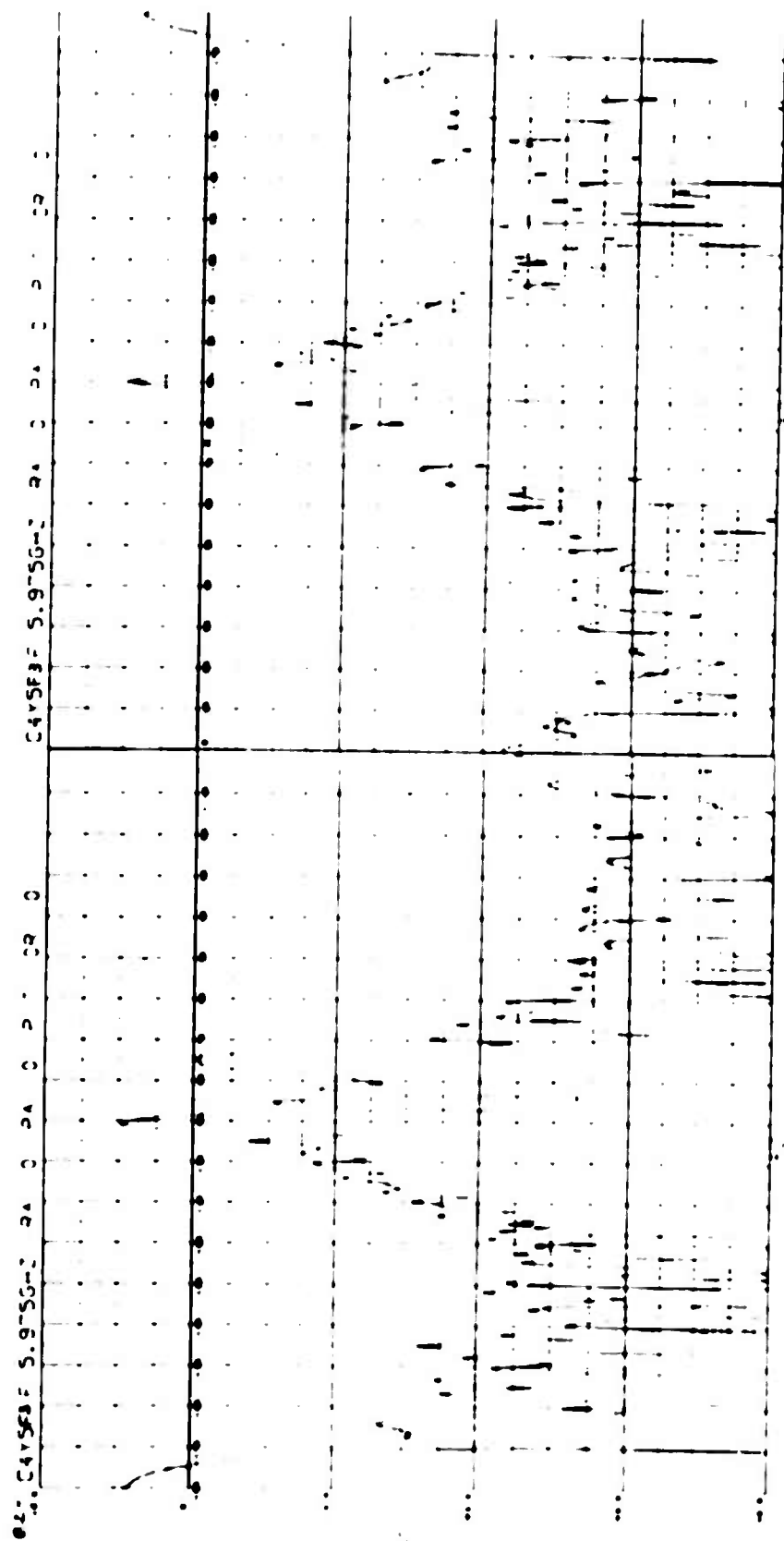


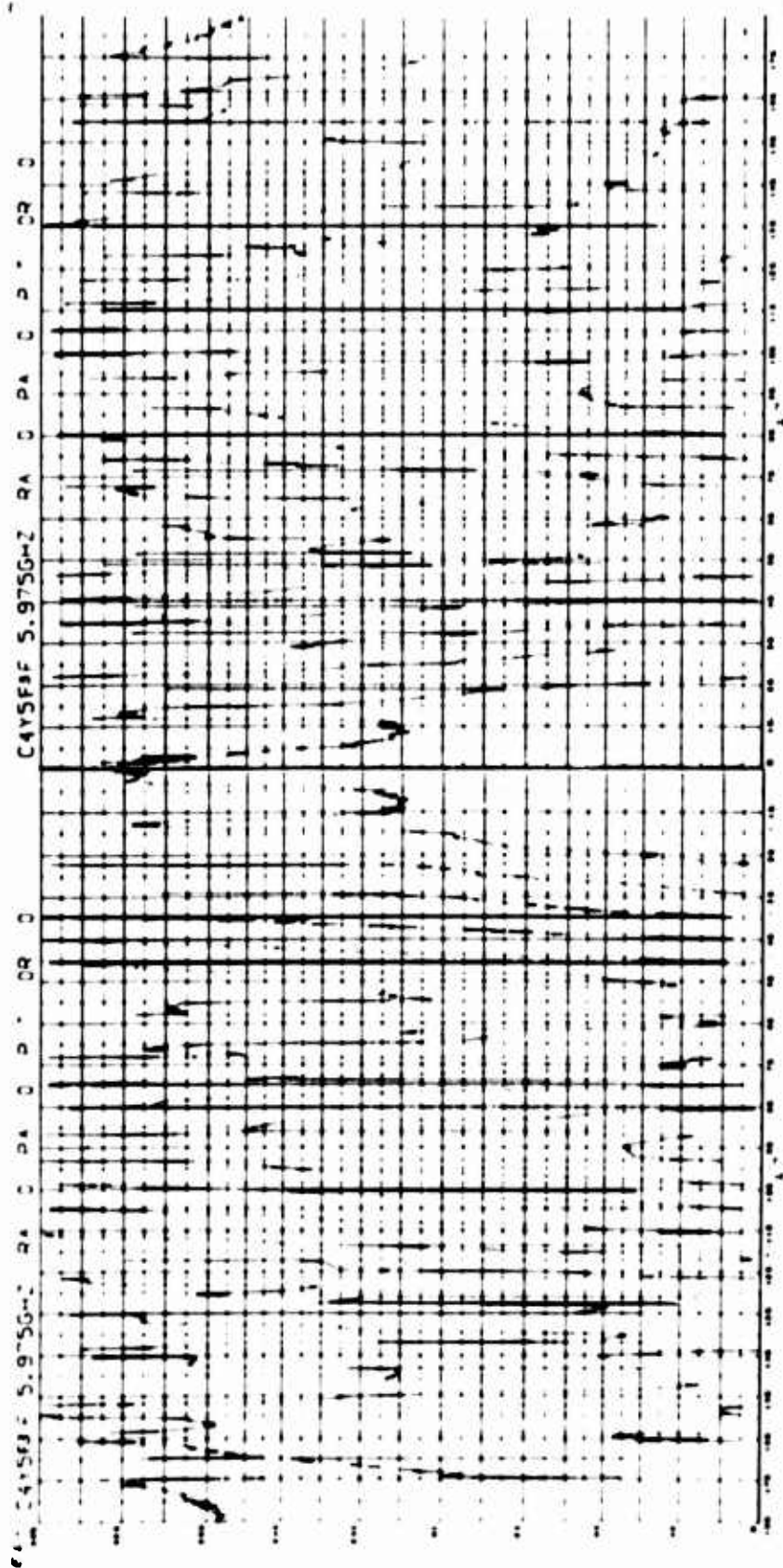




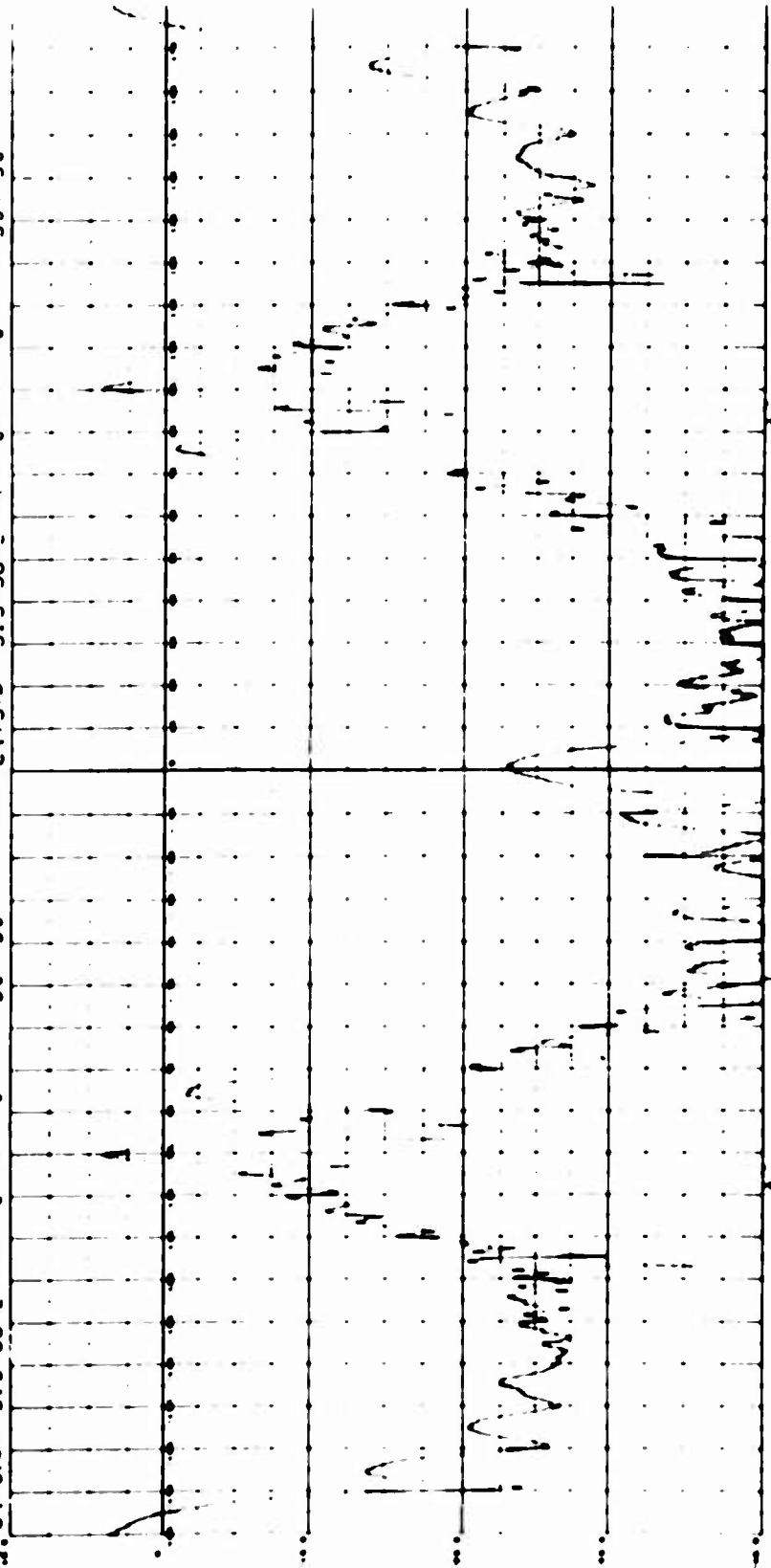


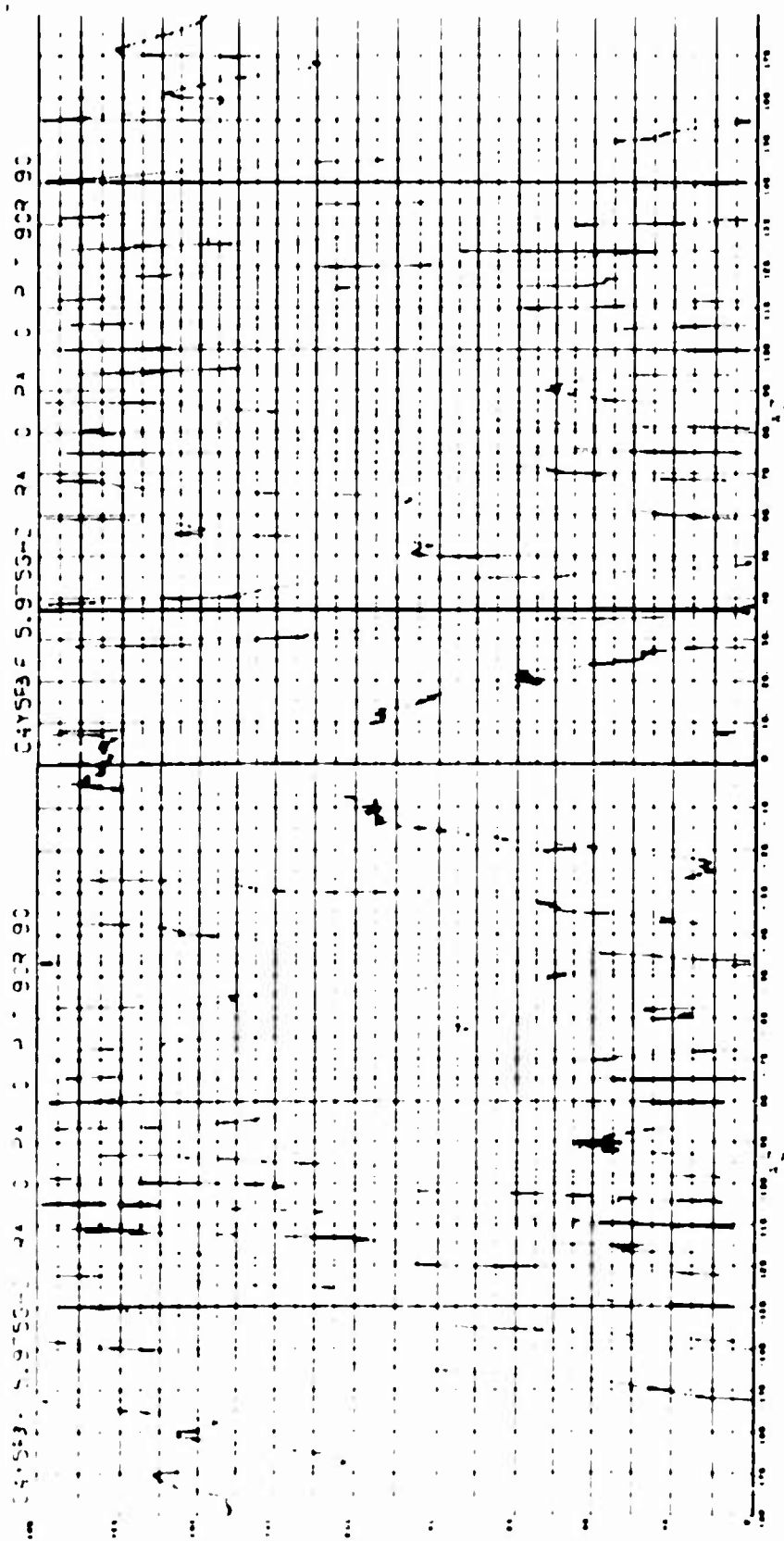


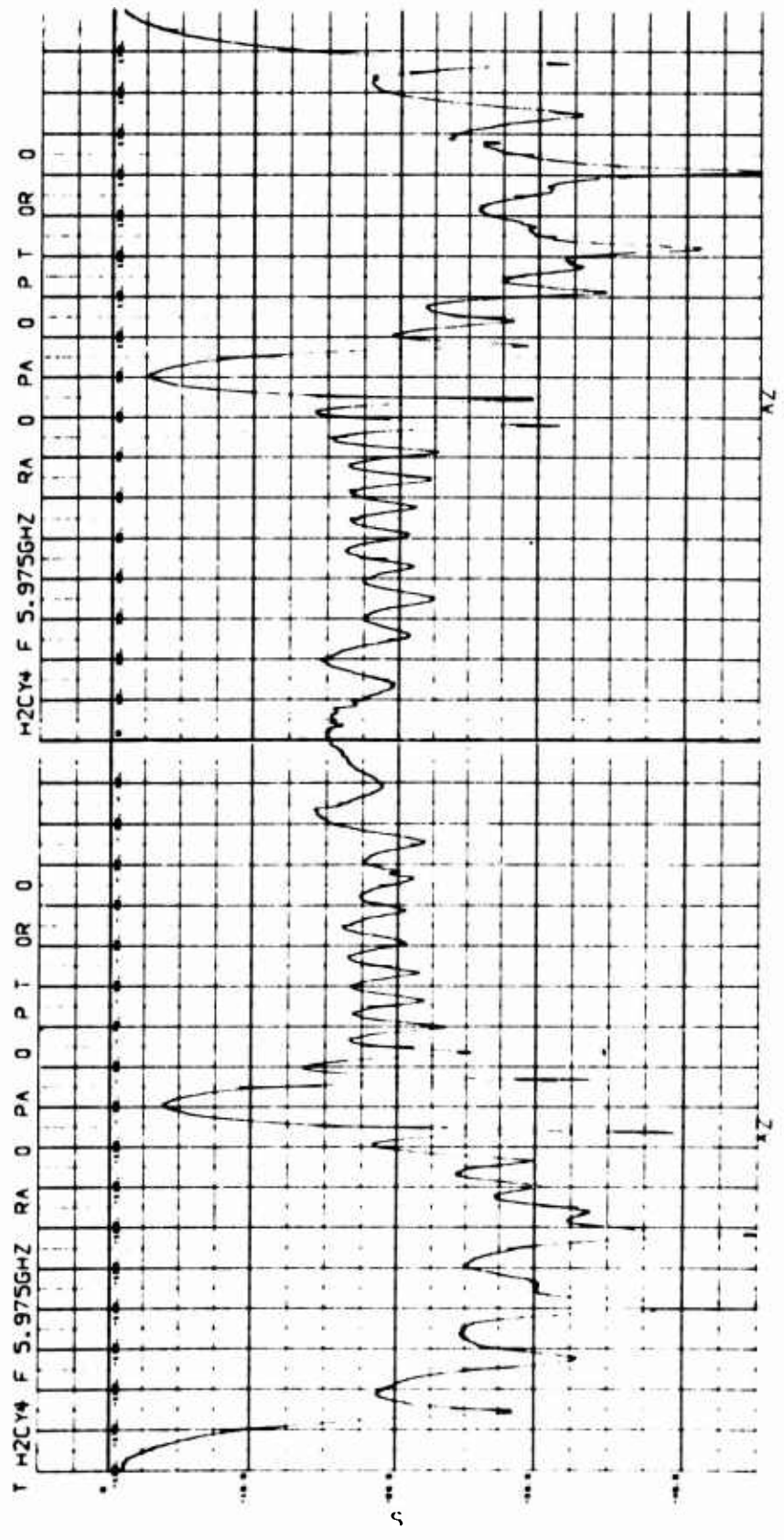


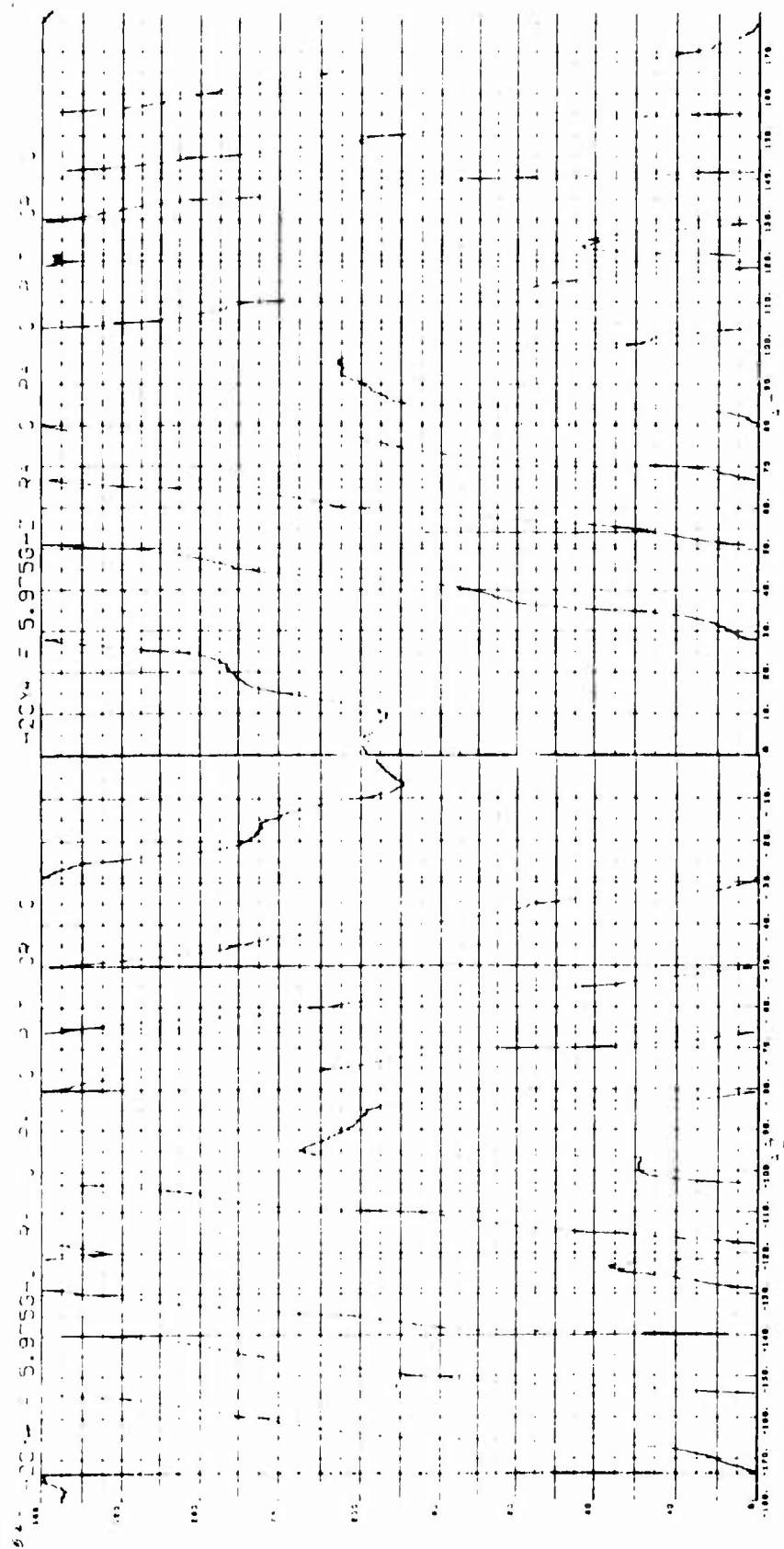


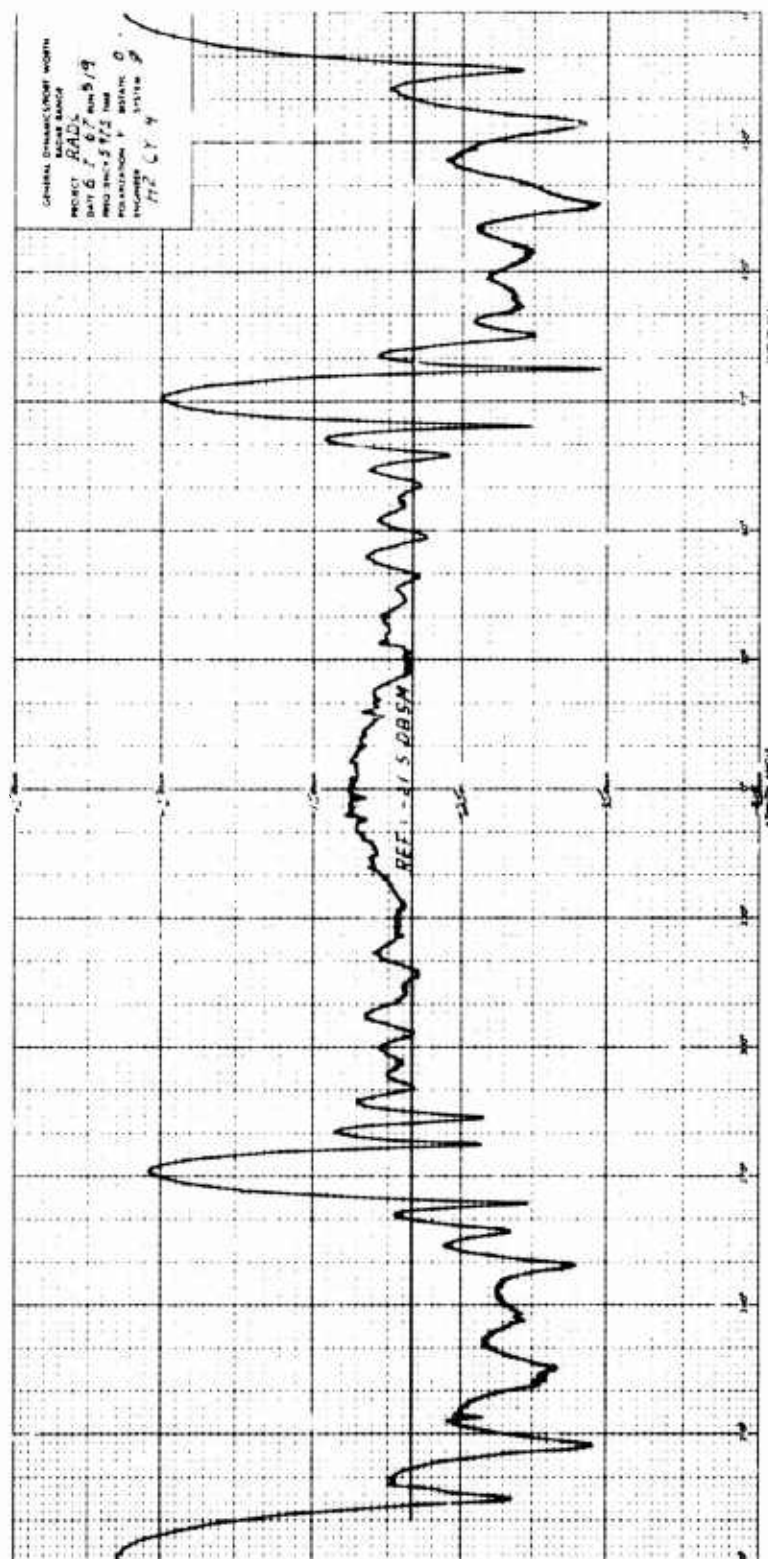
21. C4YSR0F S.975G-2 RA 0 PA 0 P 90R 90 C4YSR0F S.975G-2 RA 0 PA 0 P 90R 90

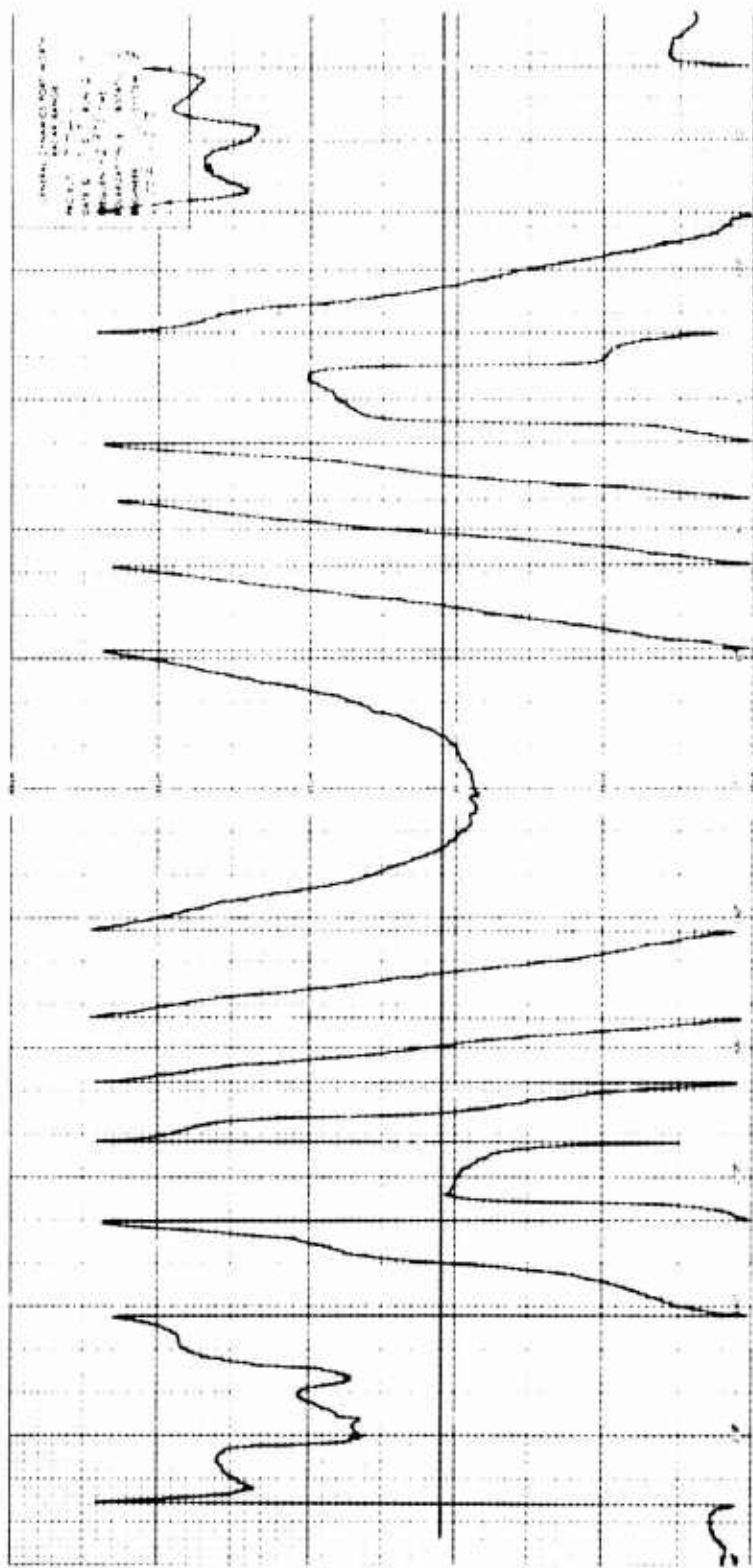


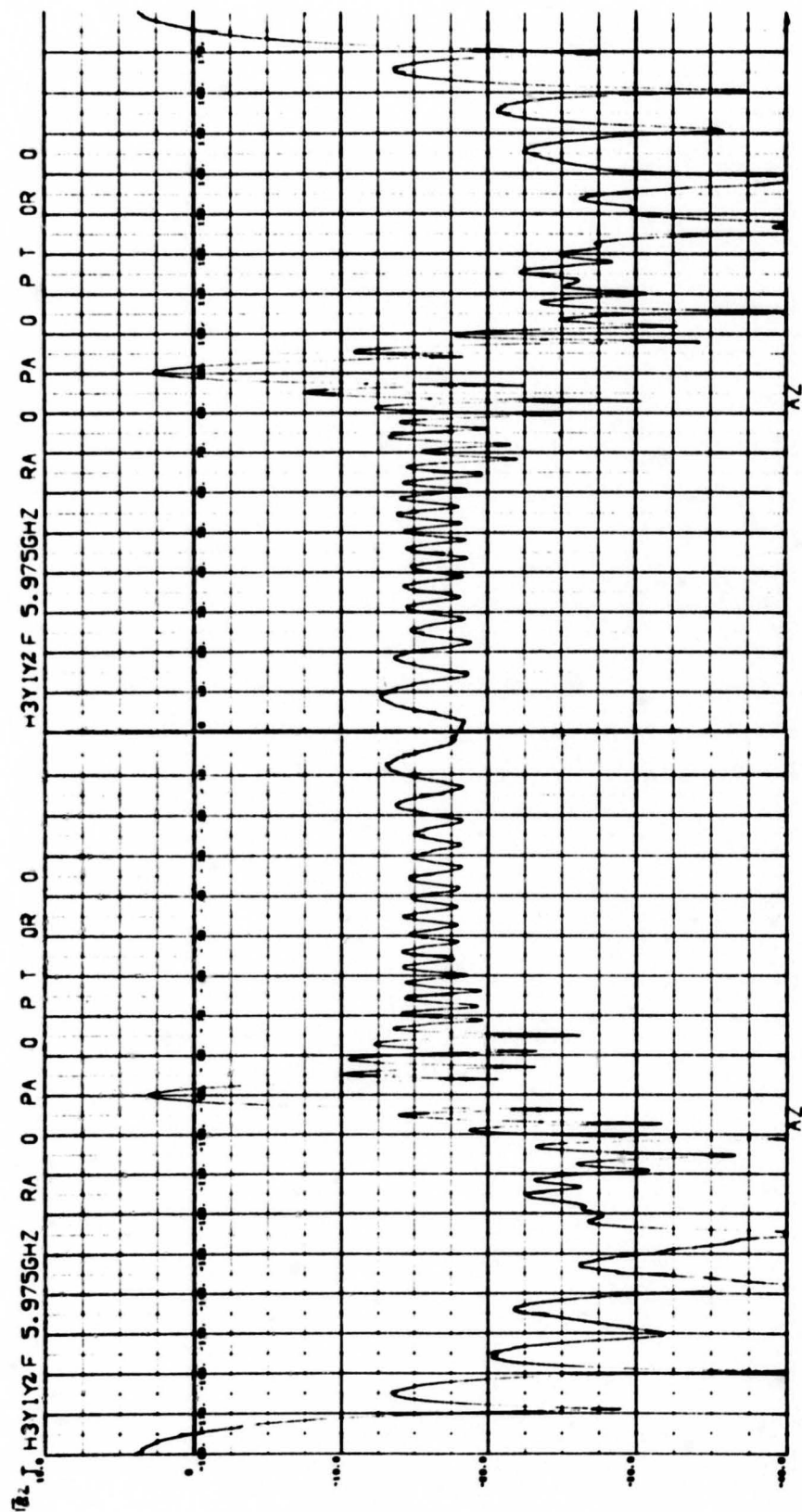


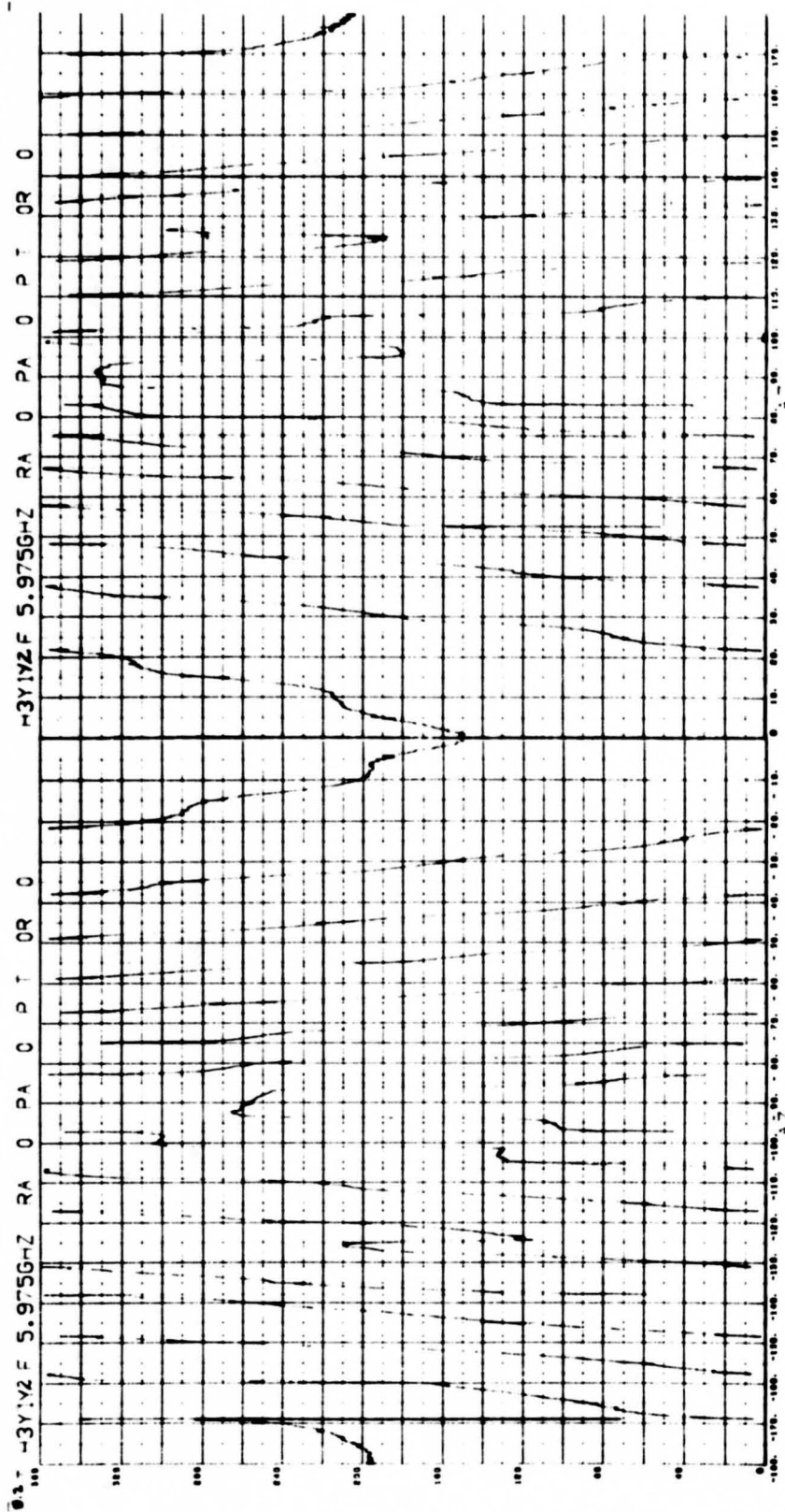


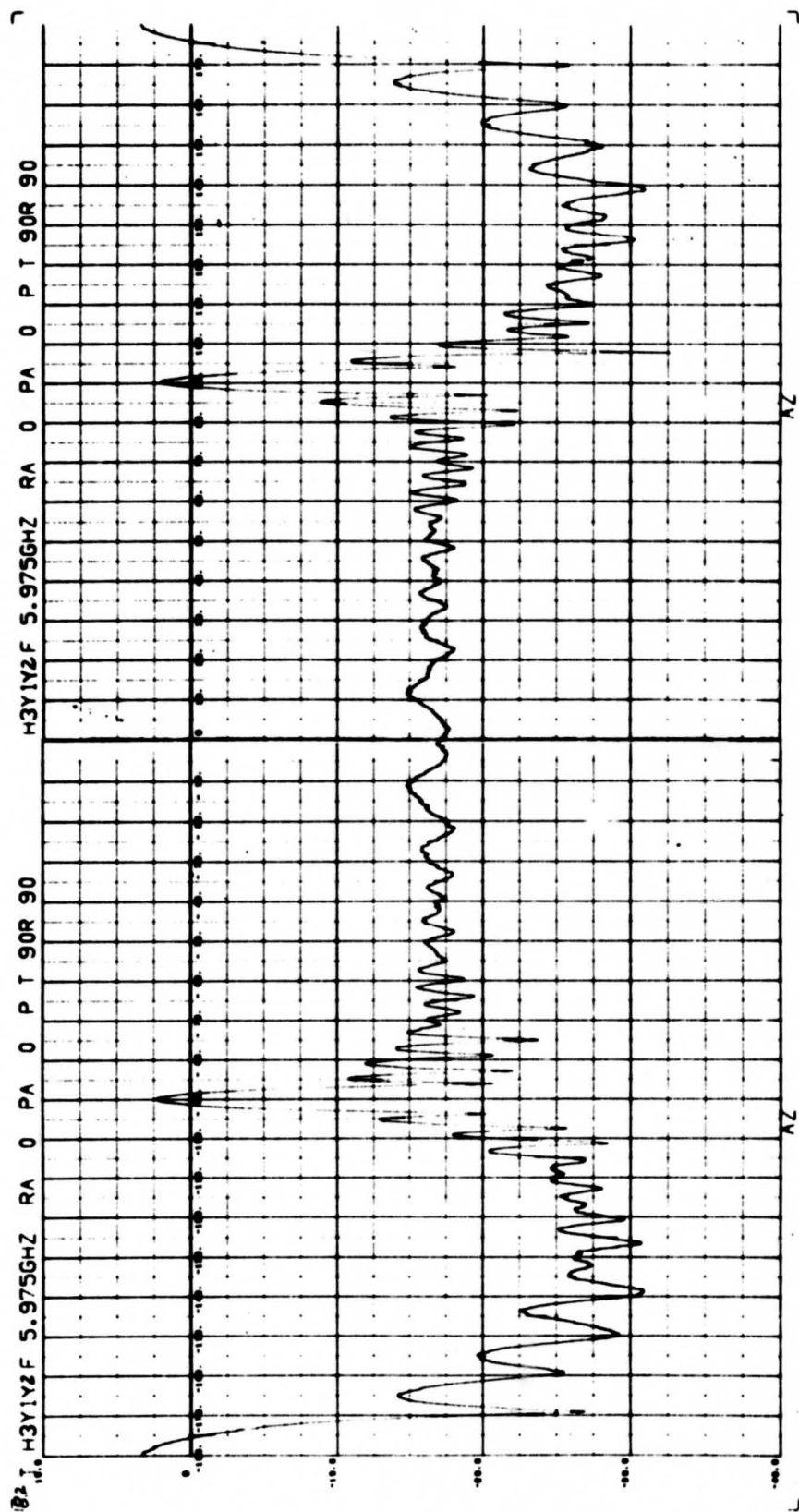


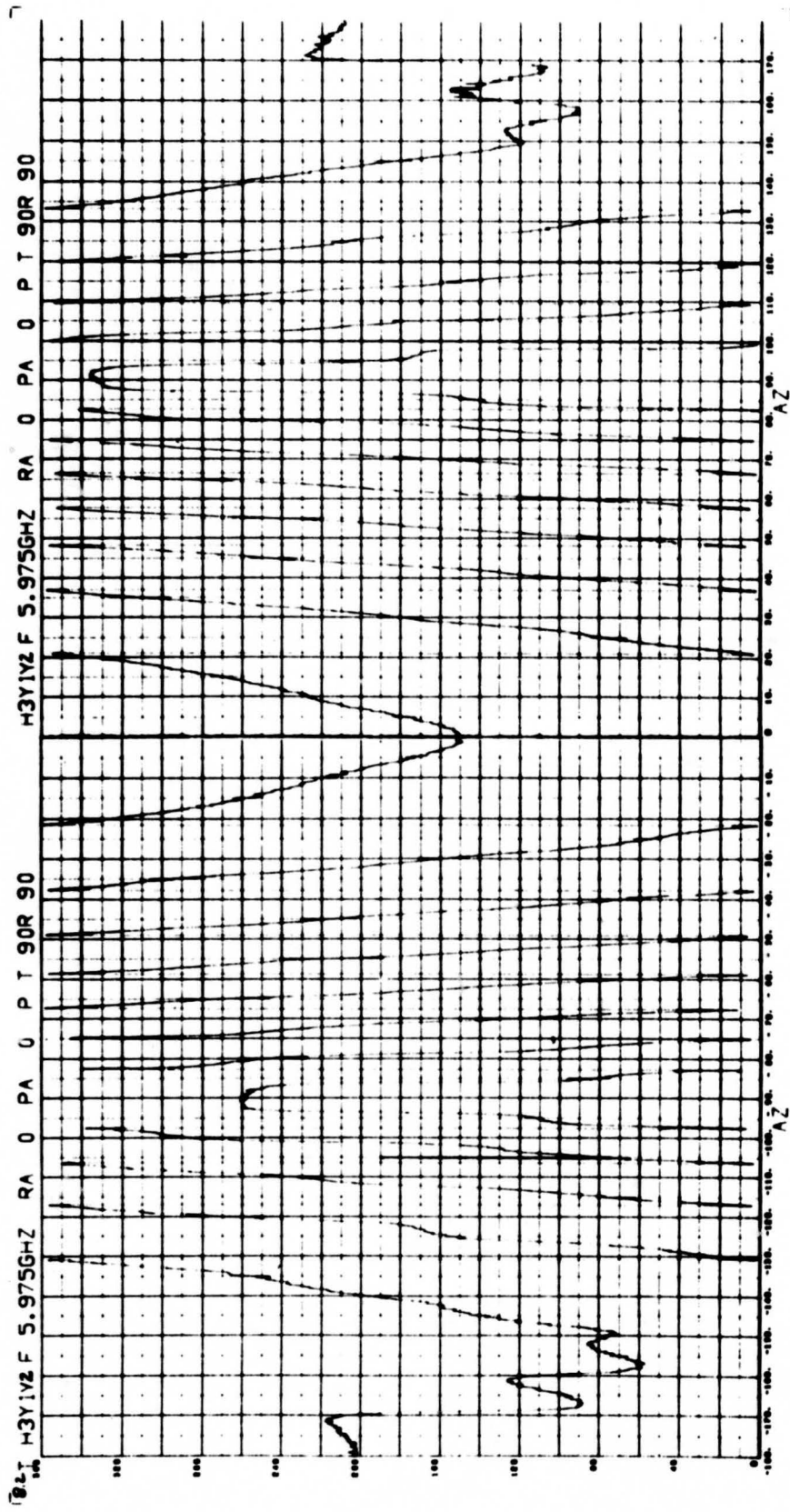


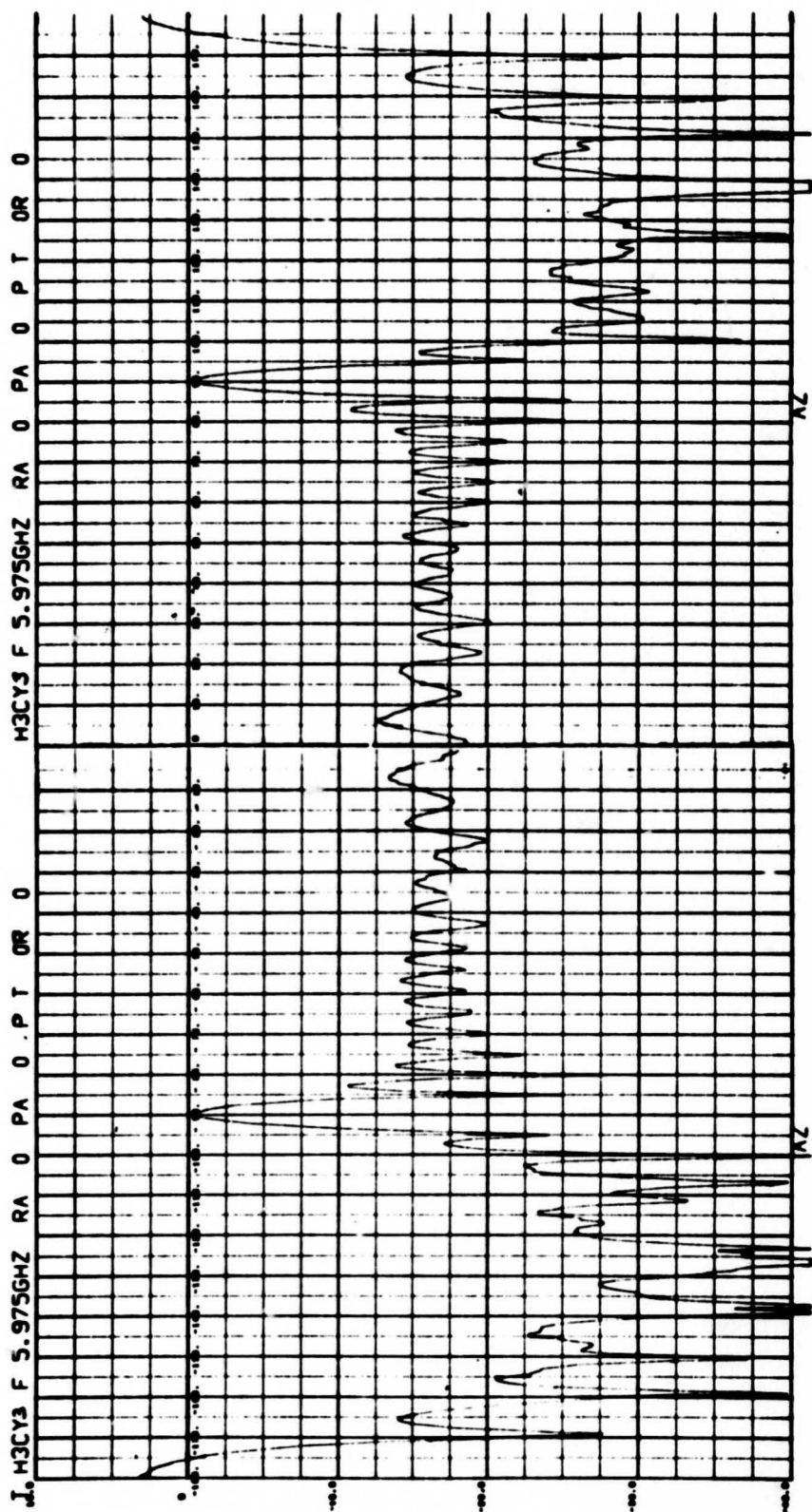


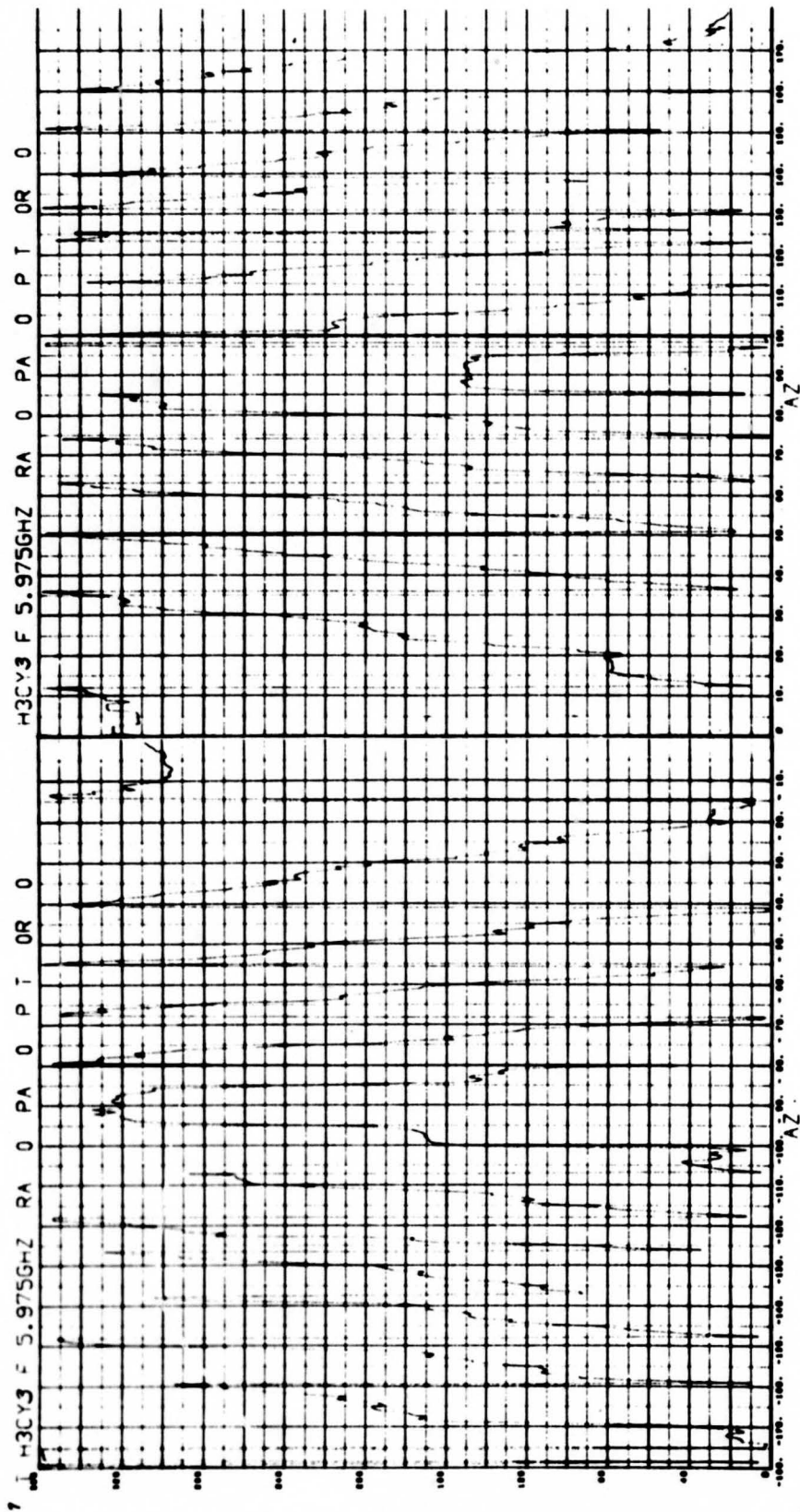


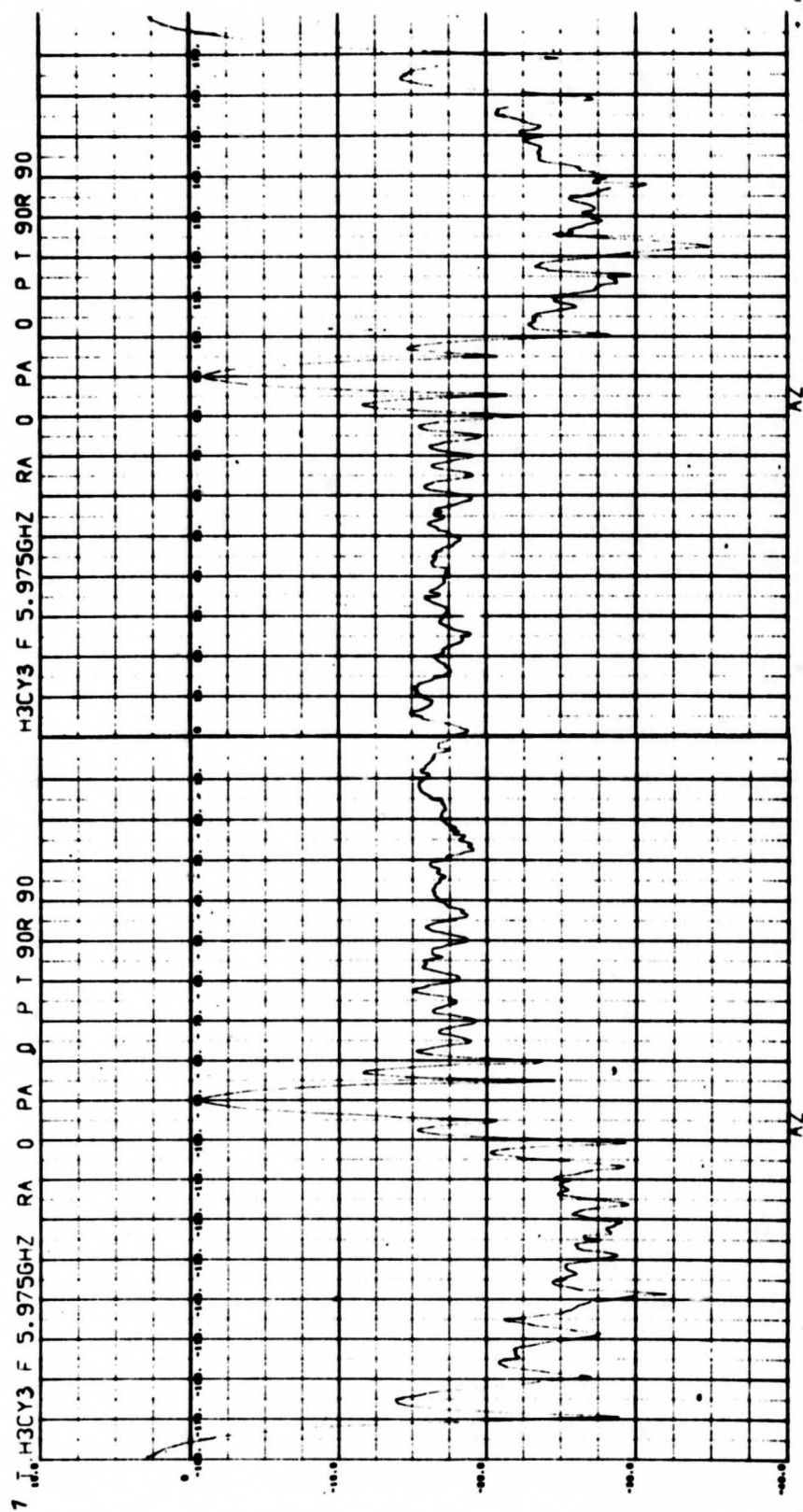


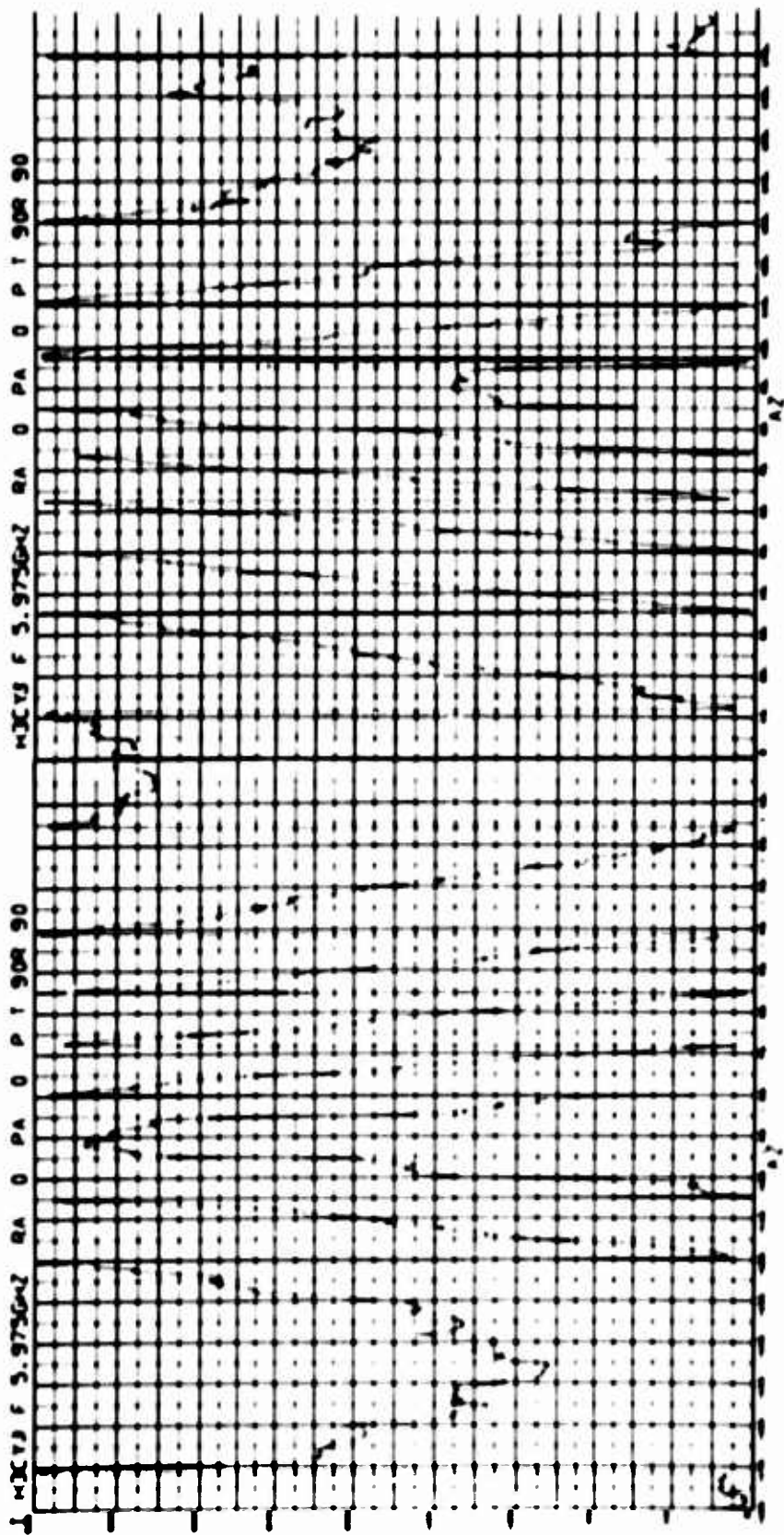


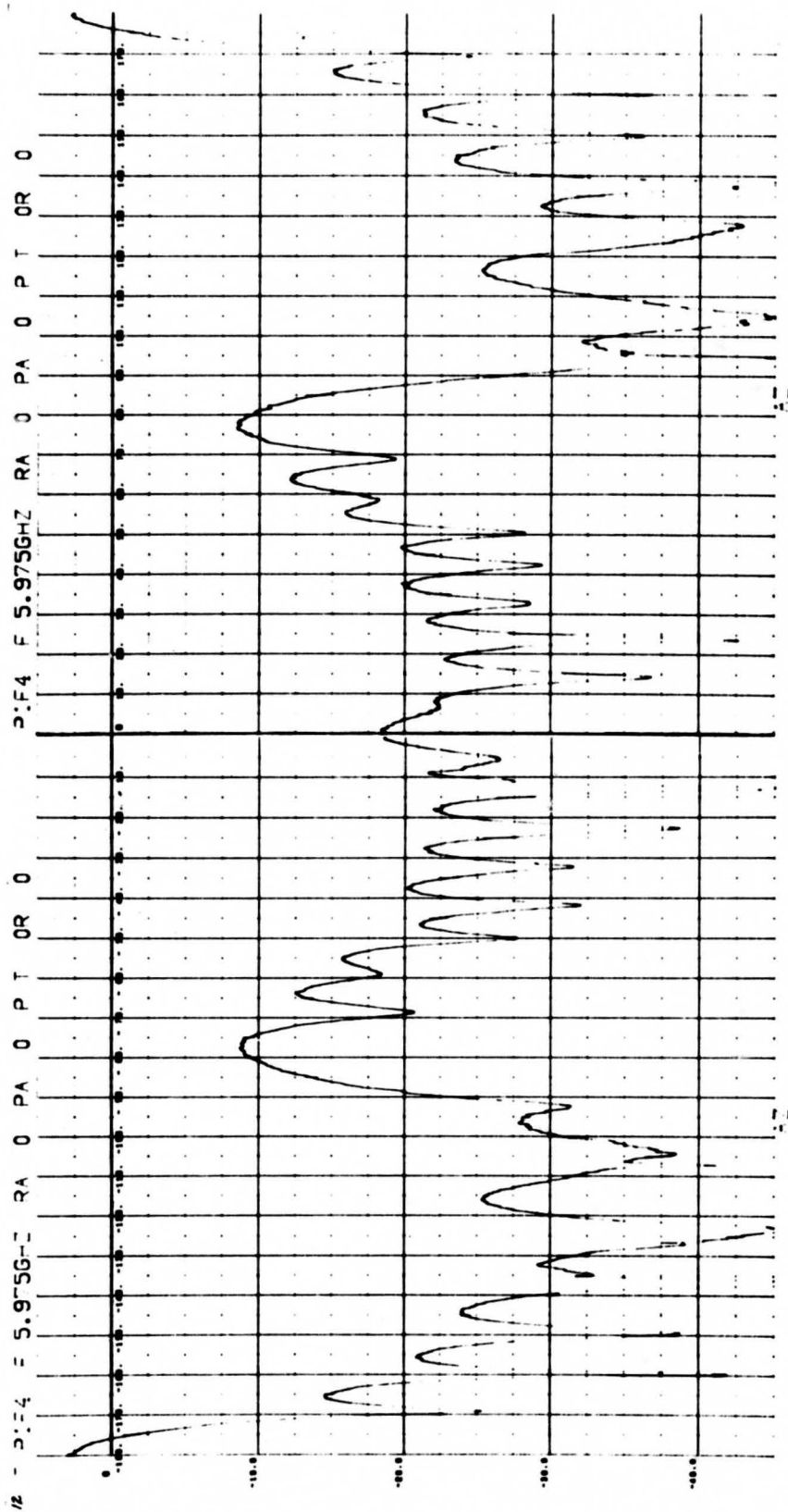


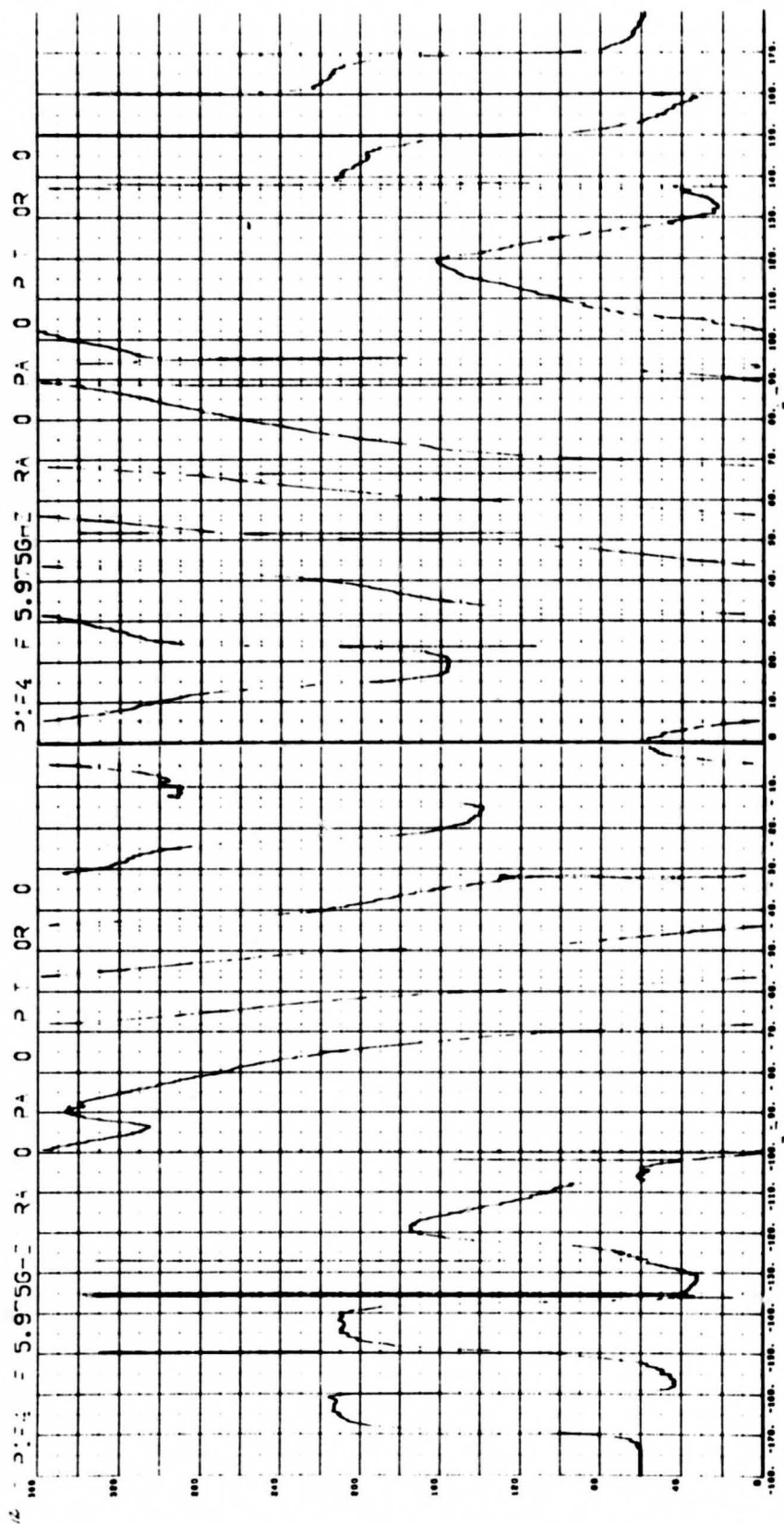


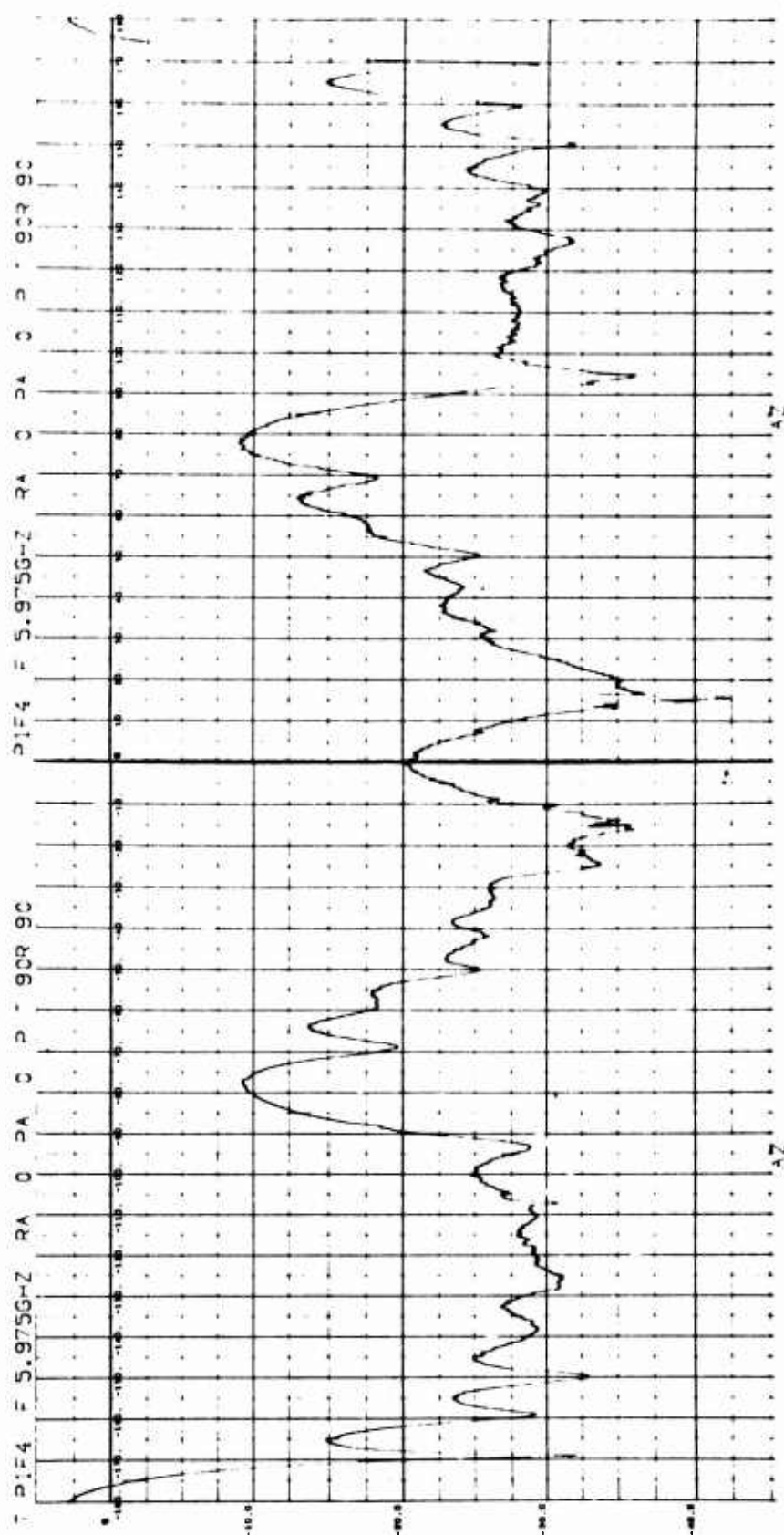


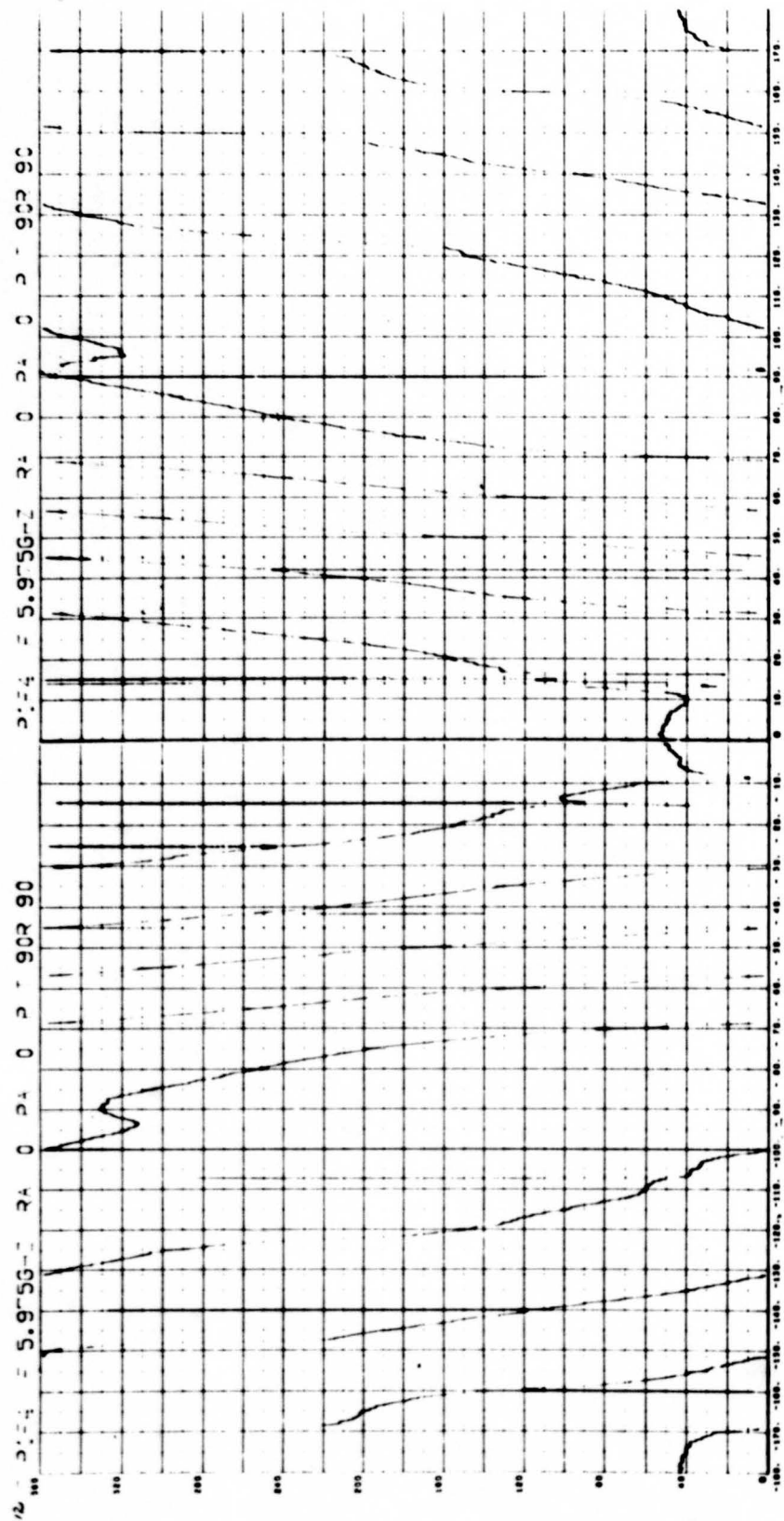


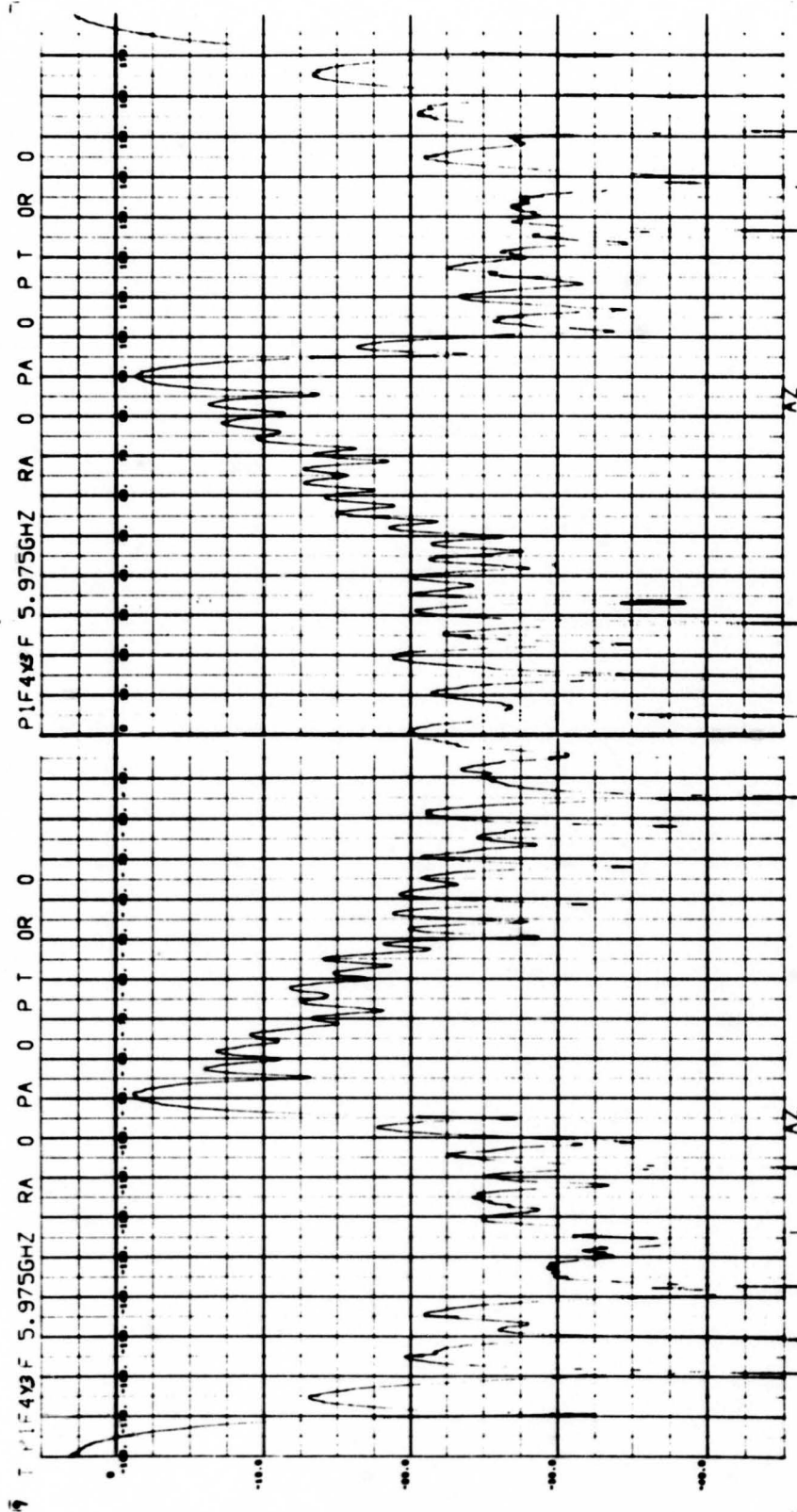


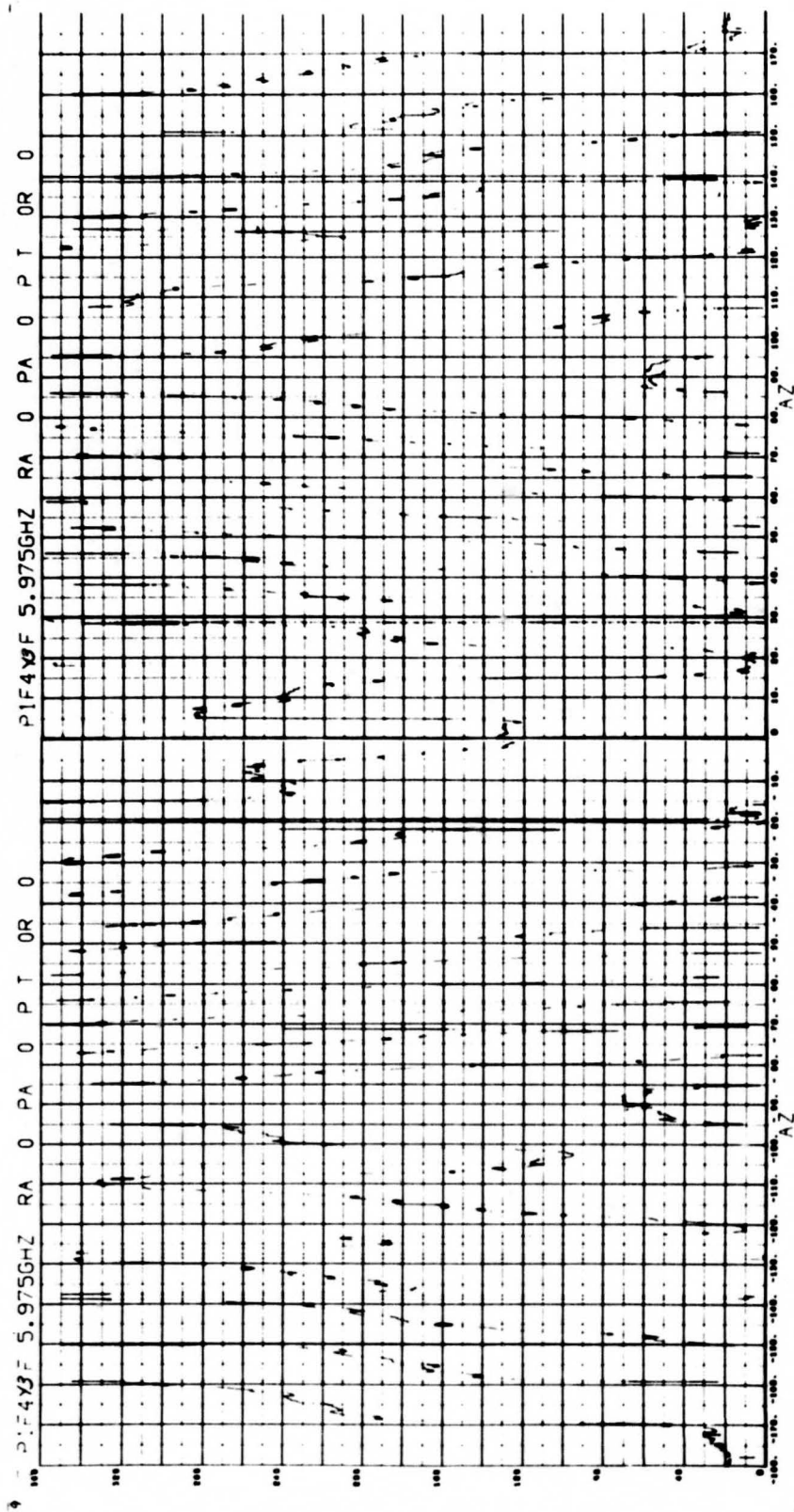


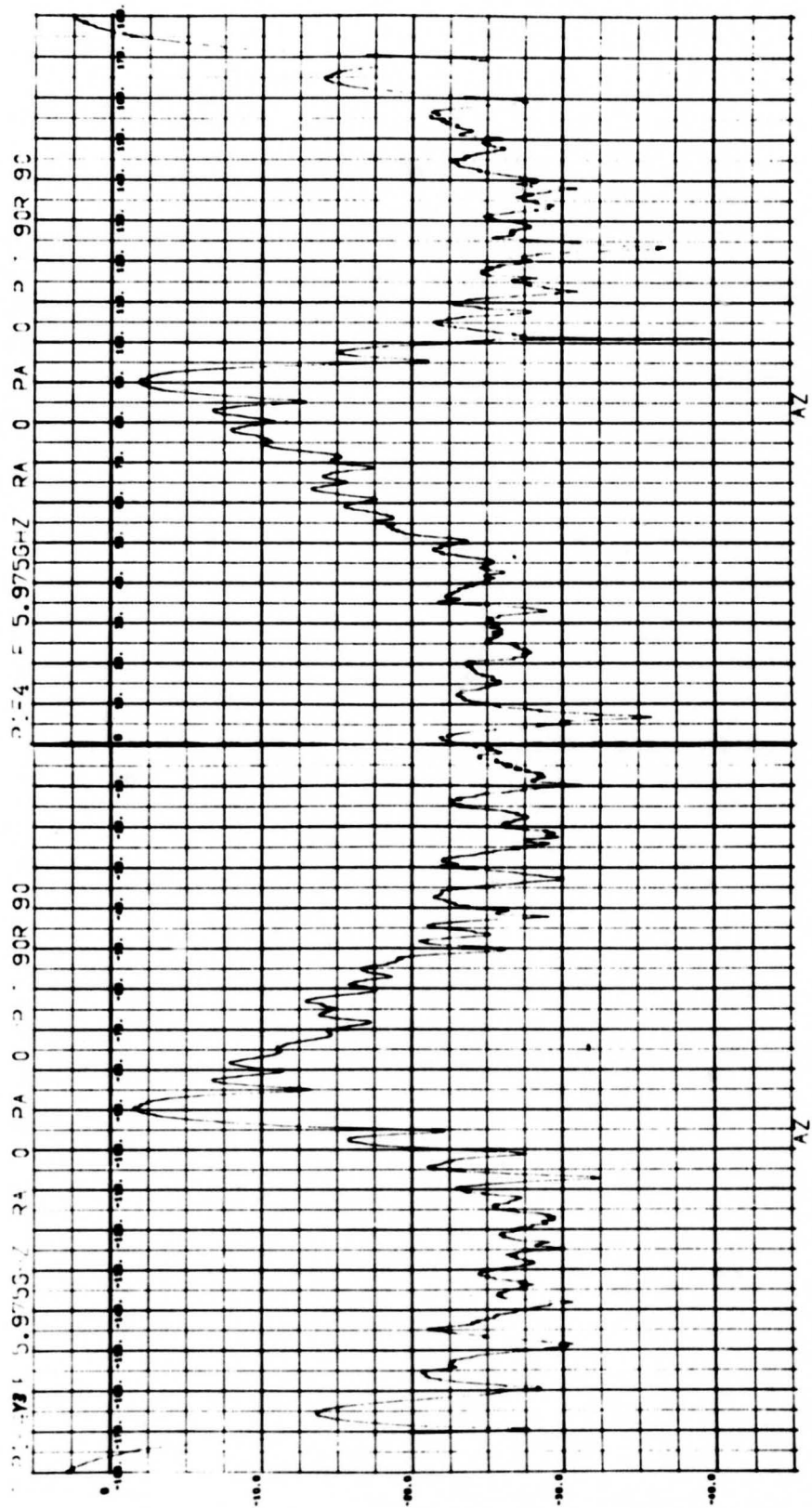


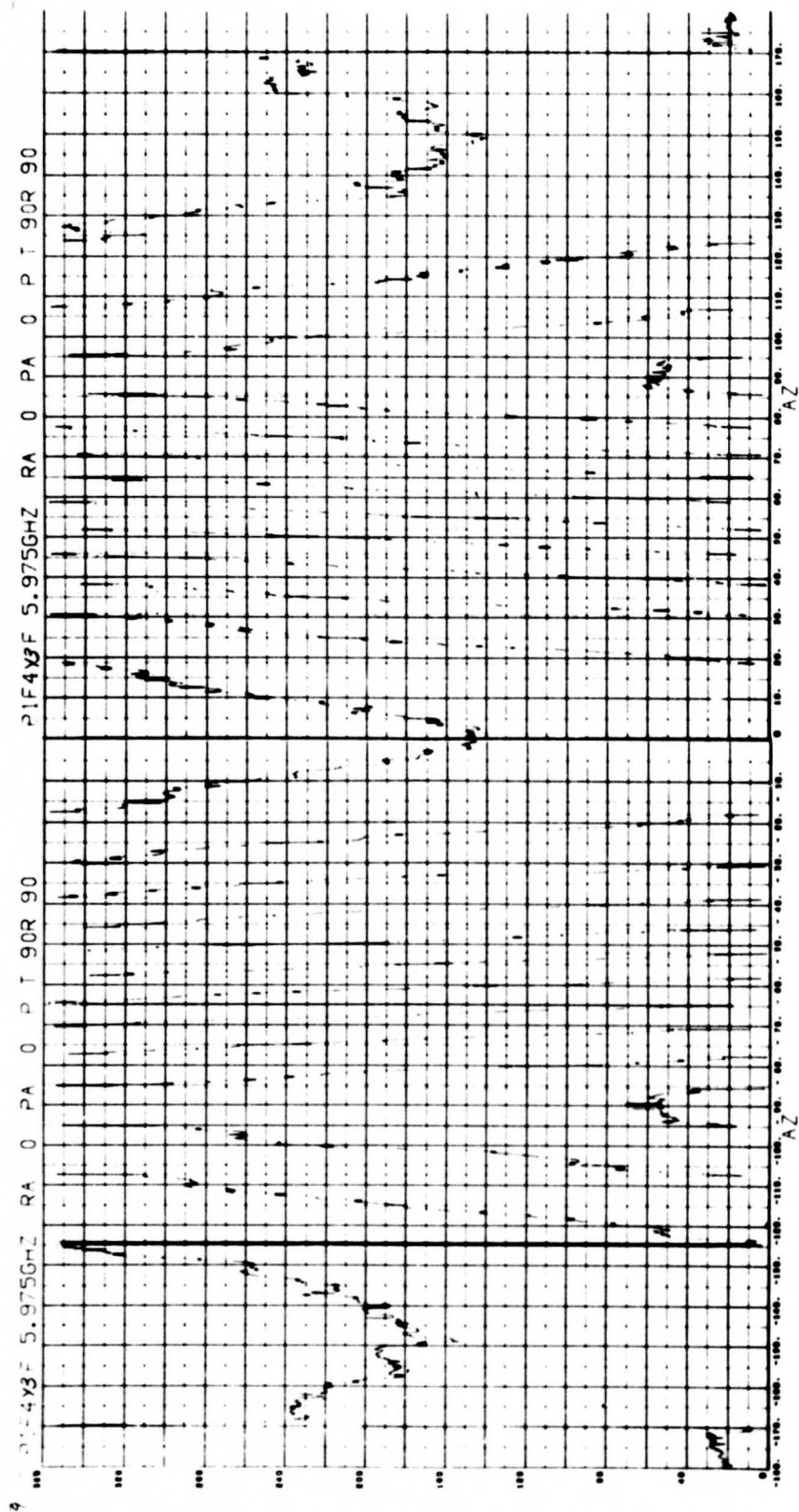


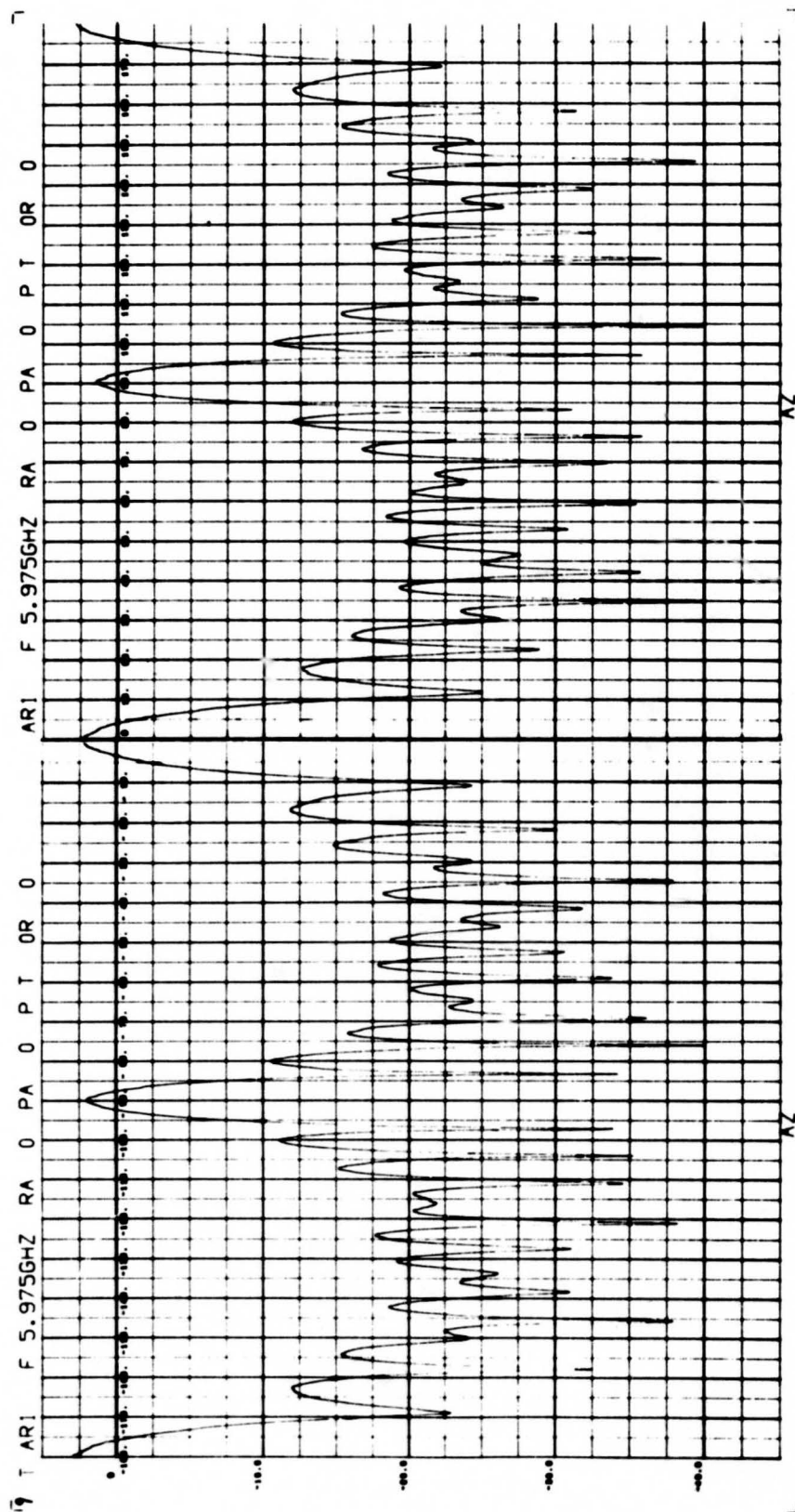


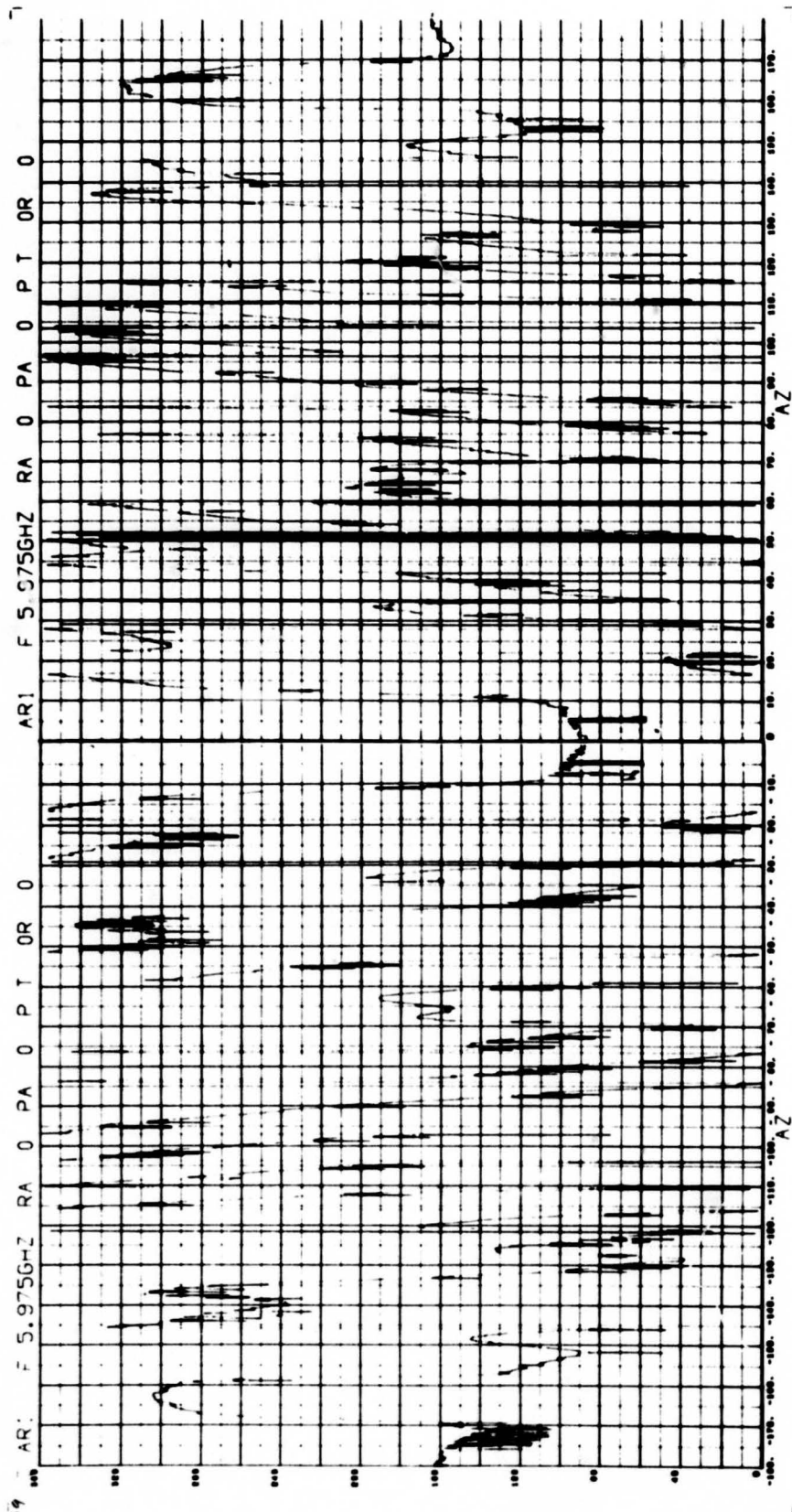


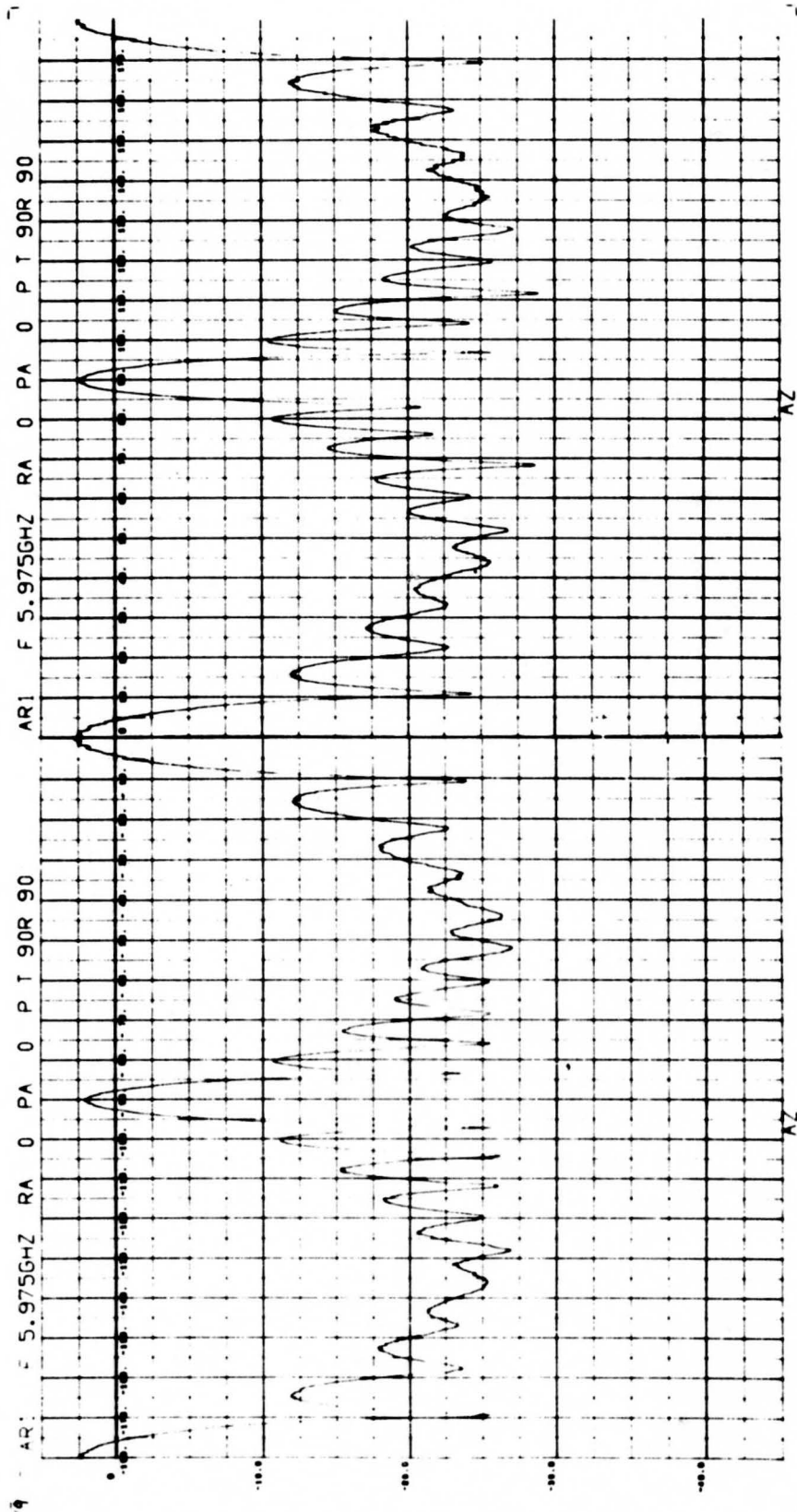


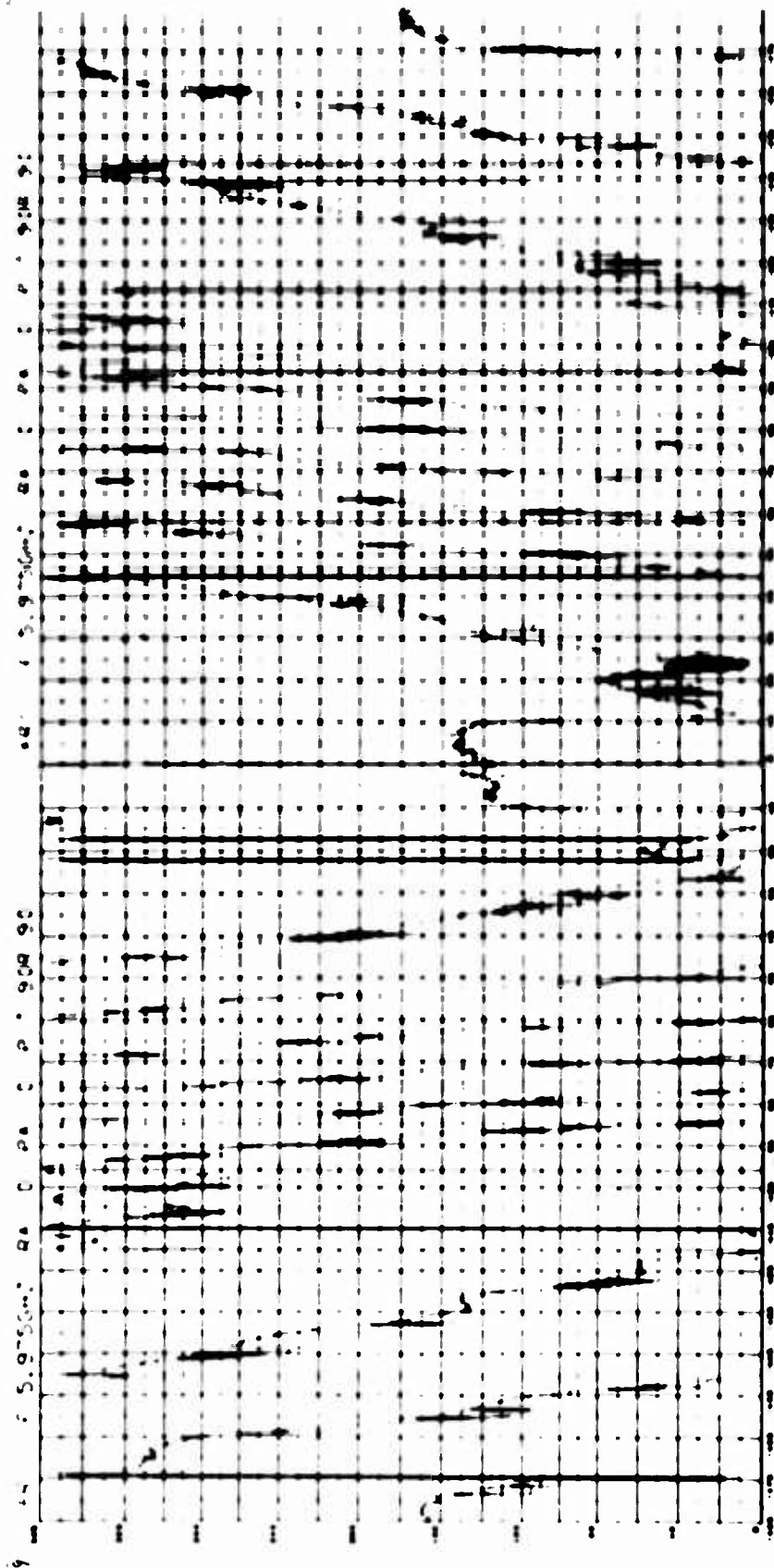


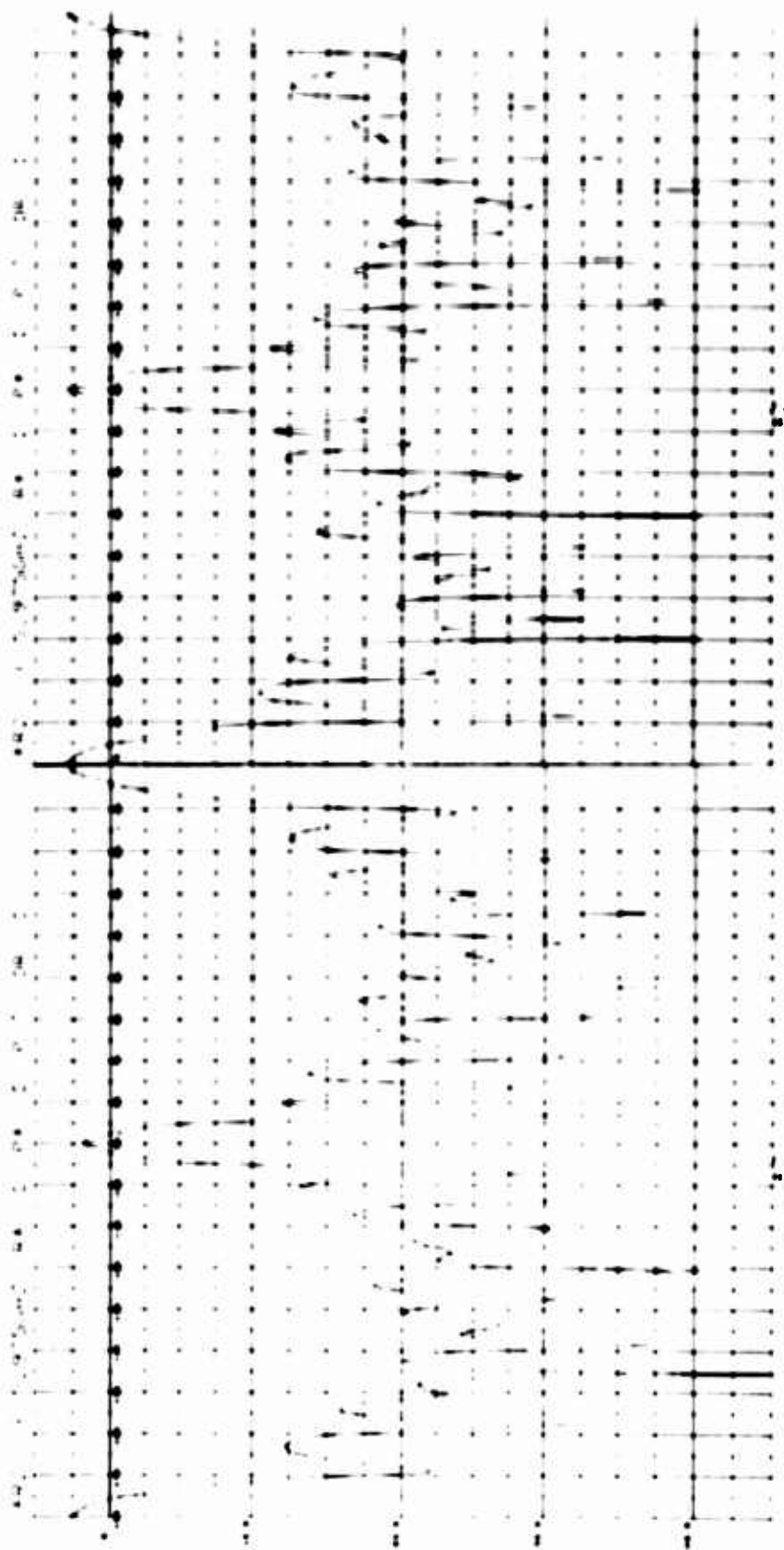


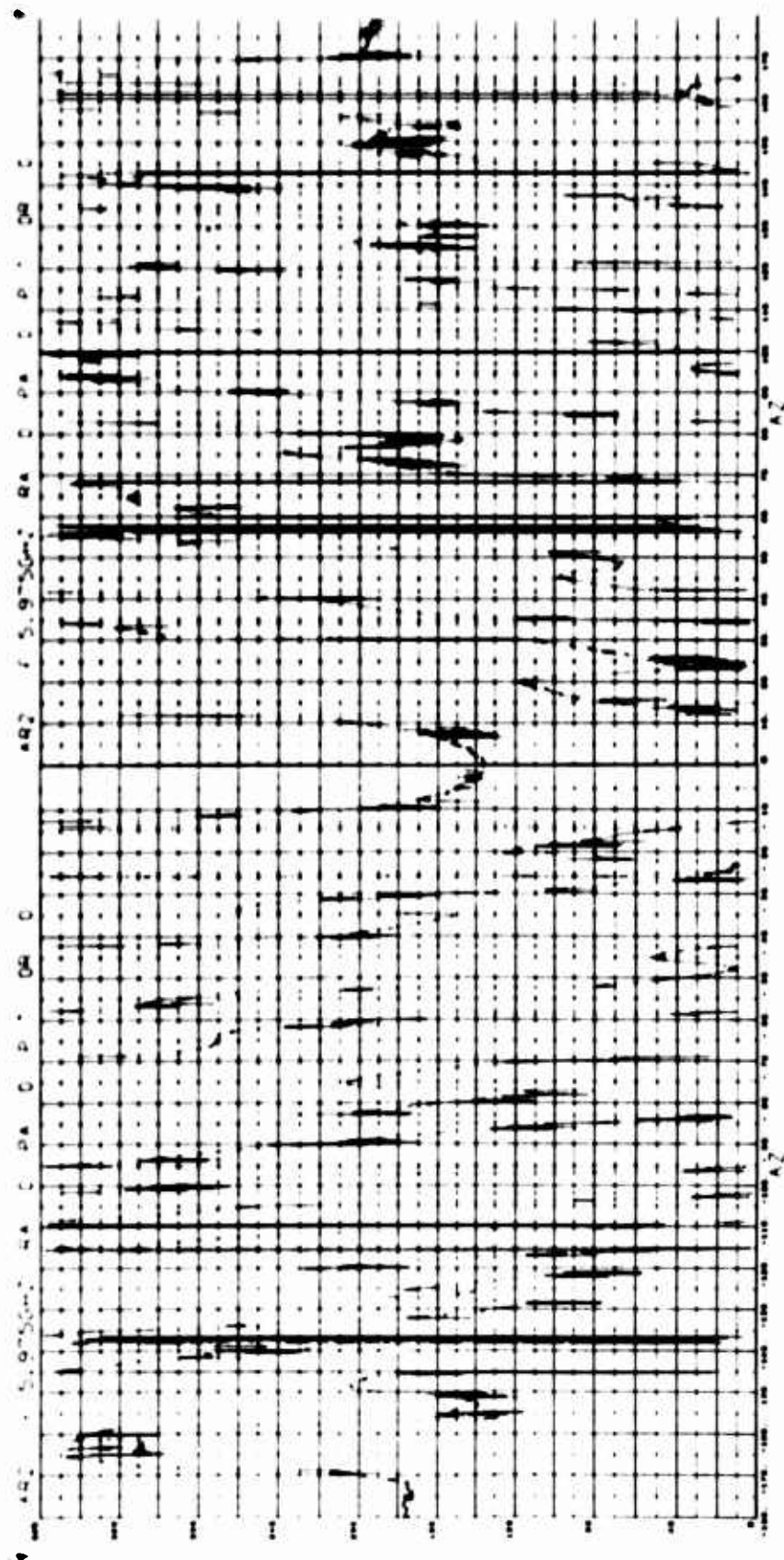


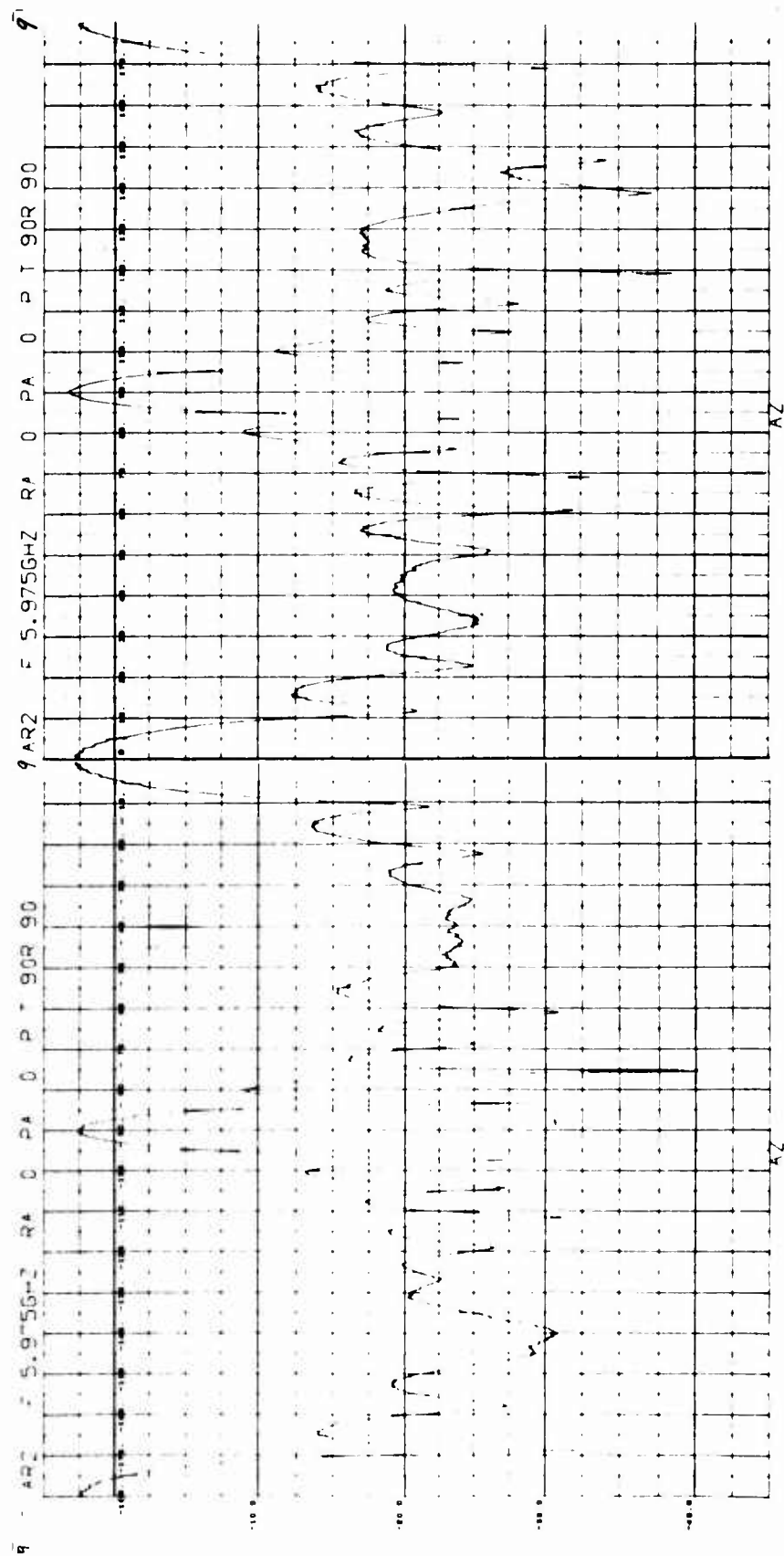


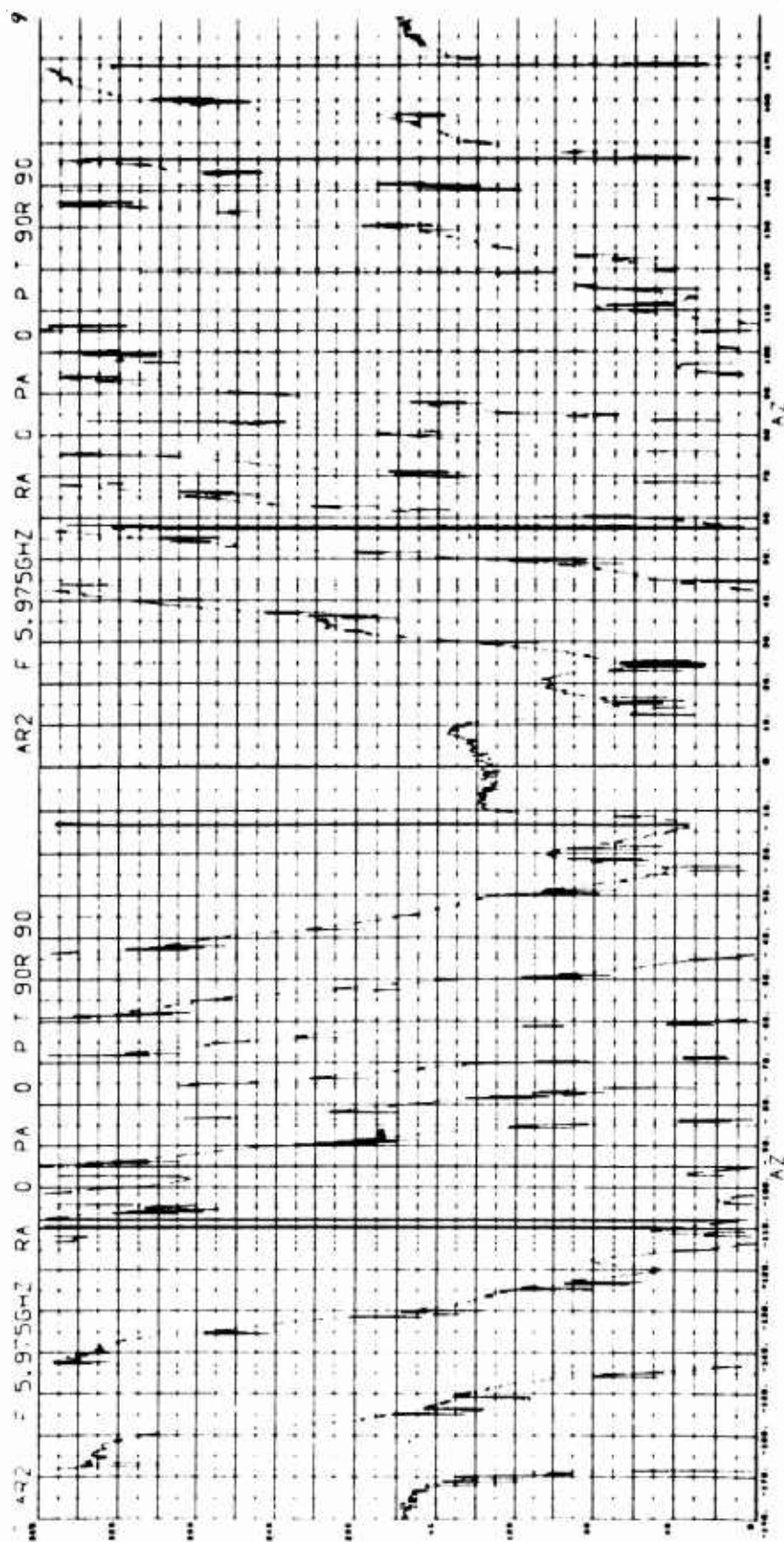


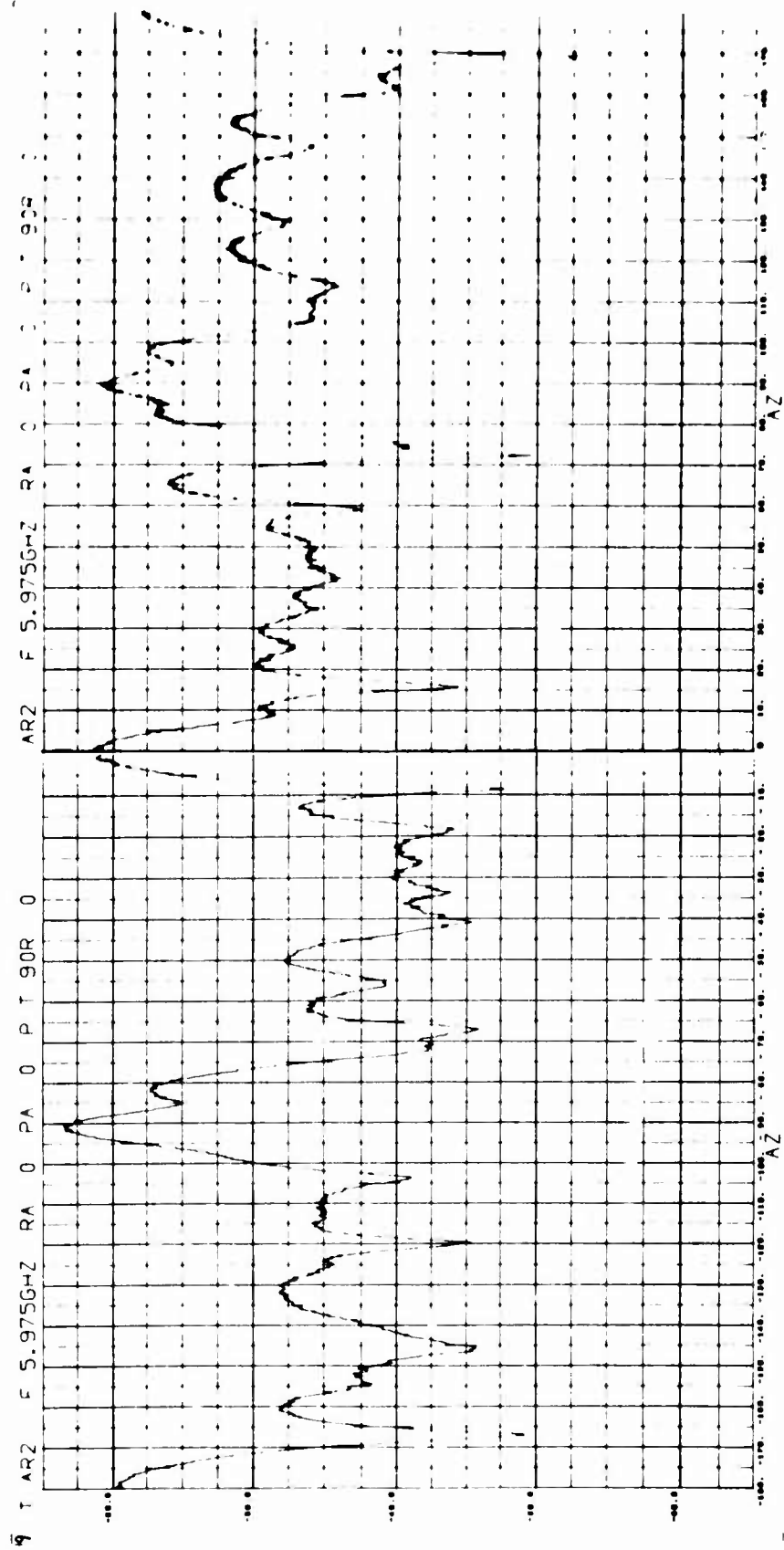


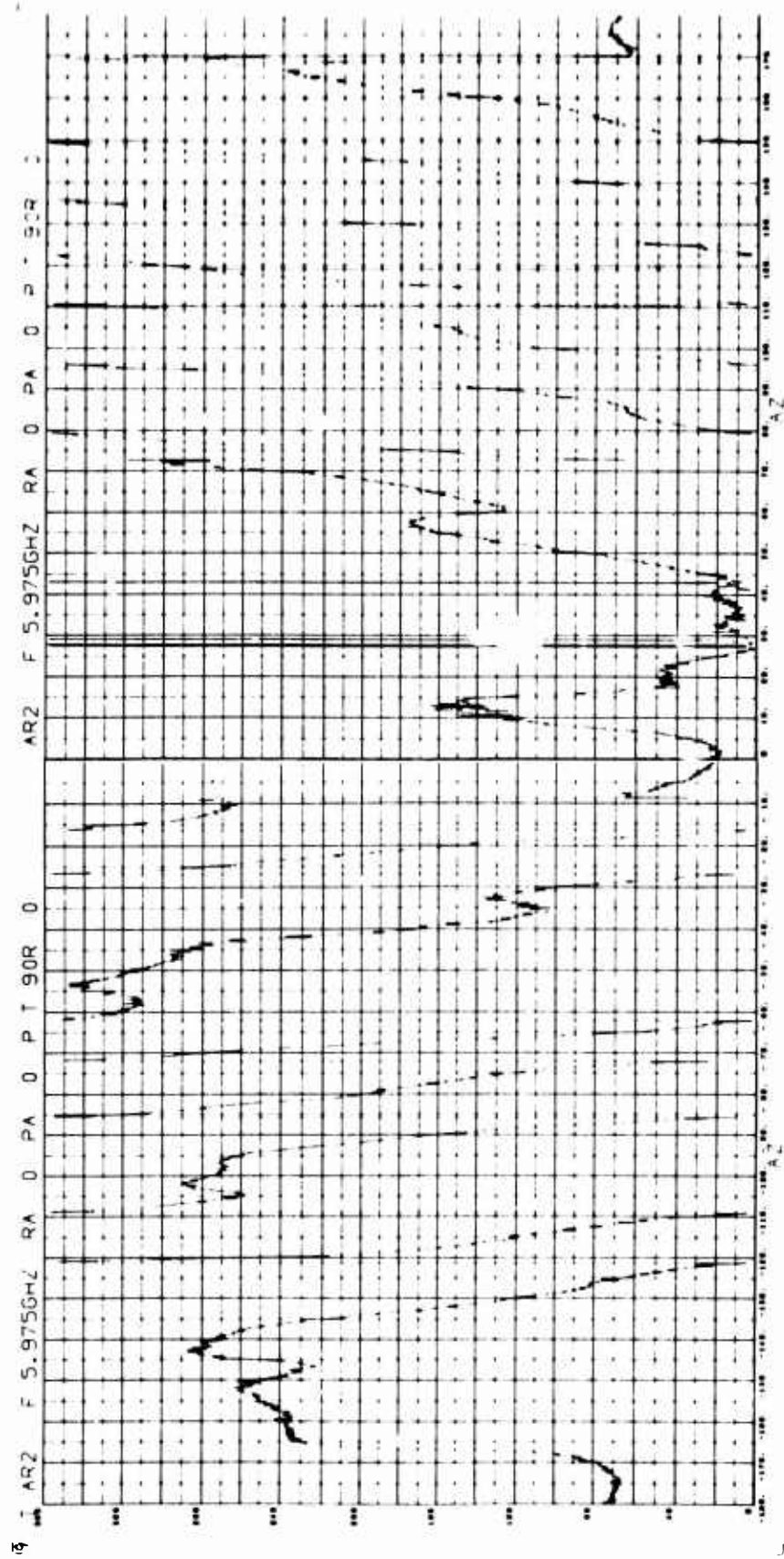


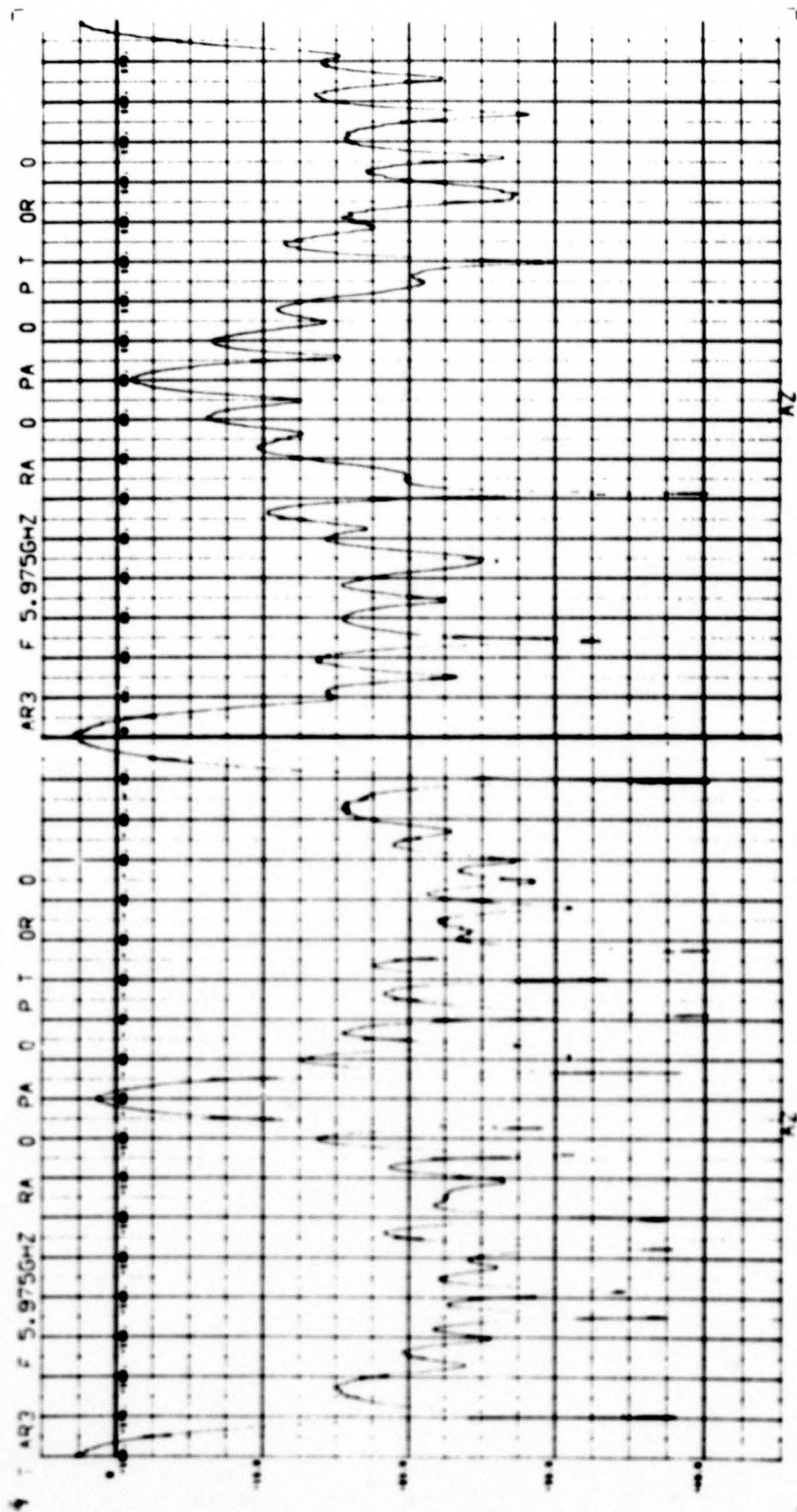


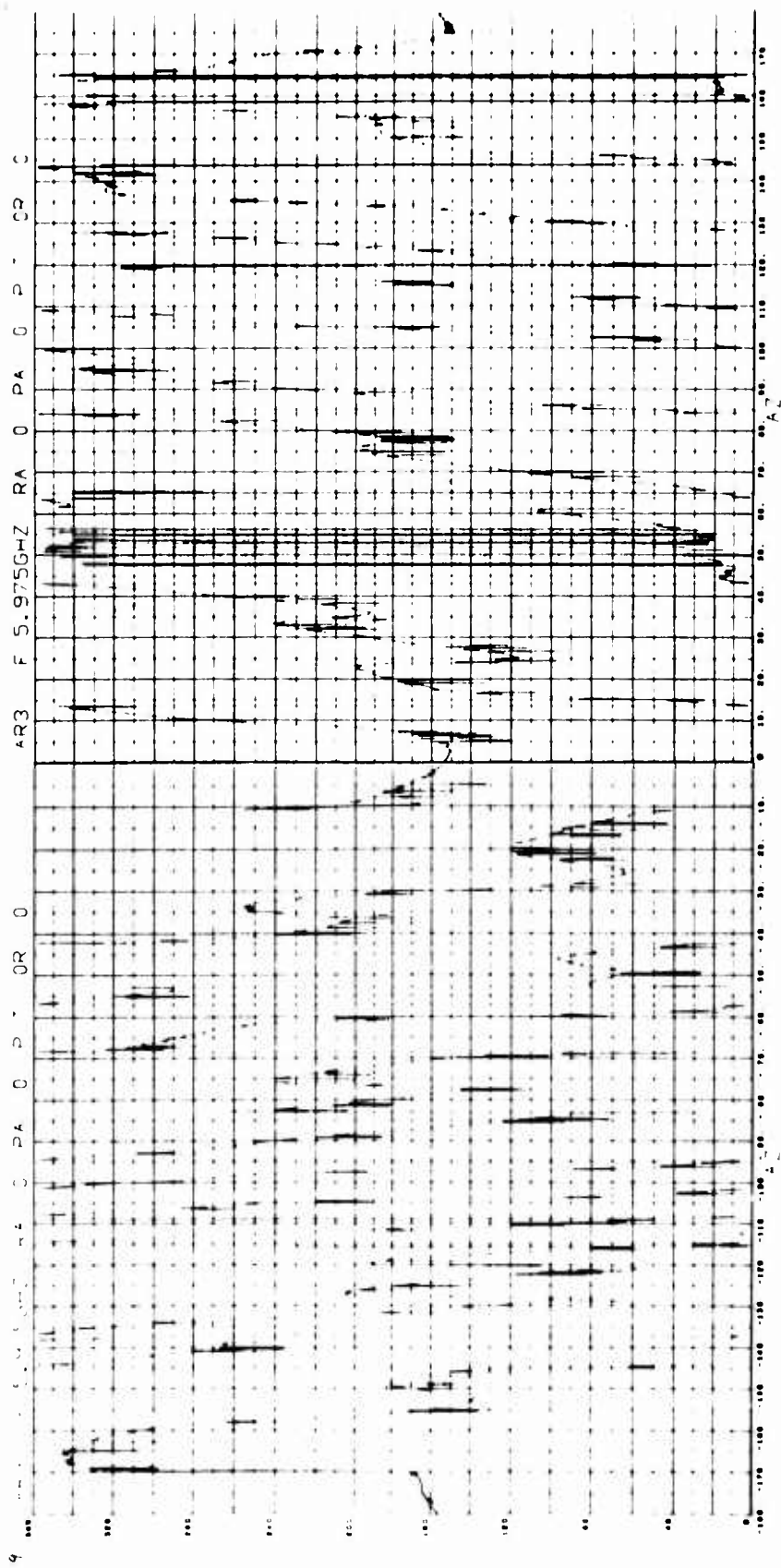


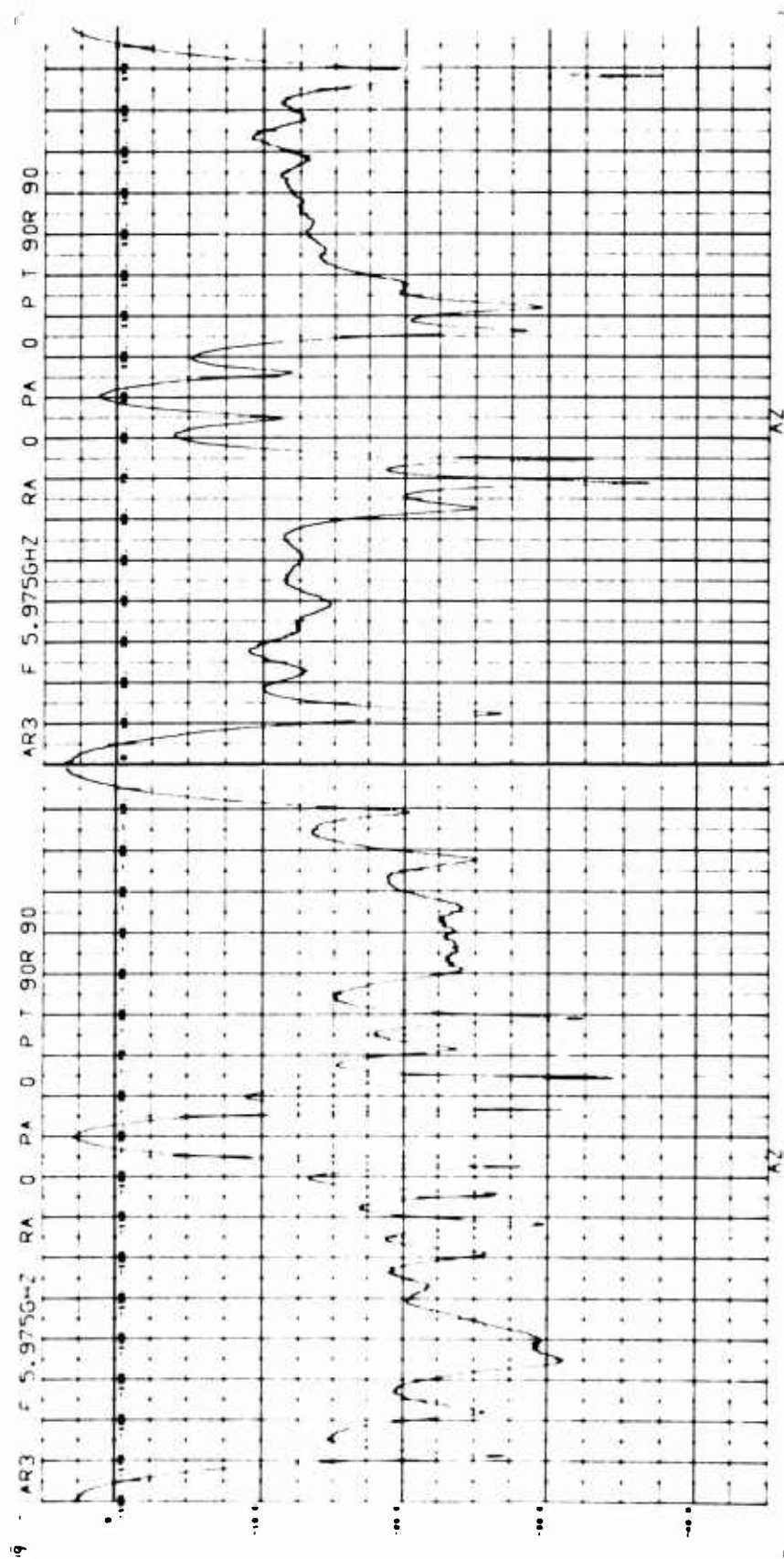


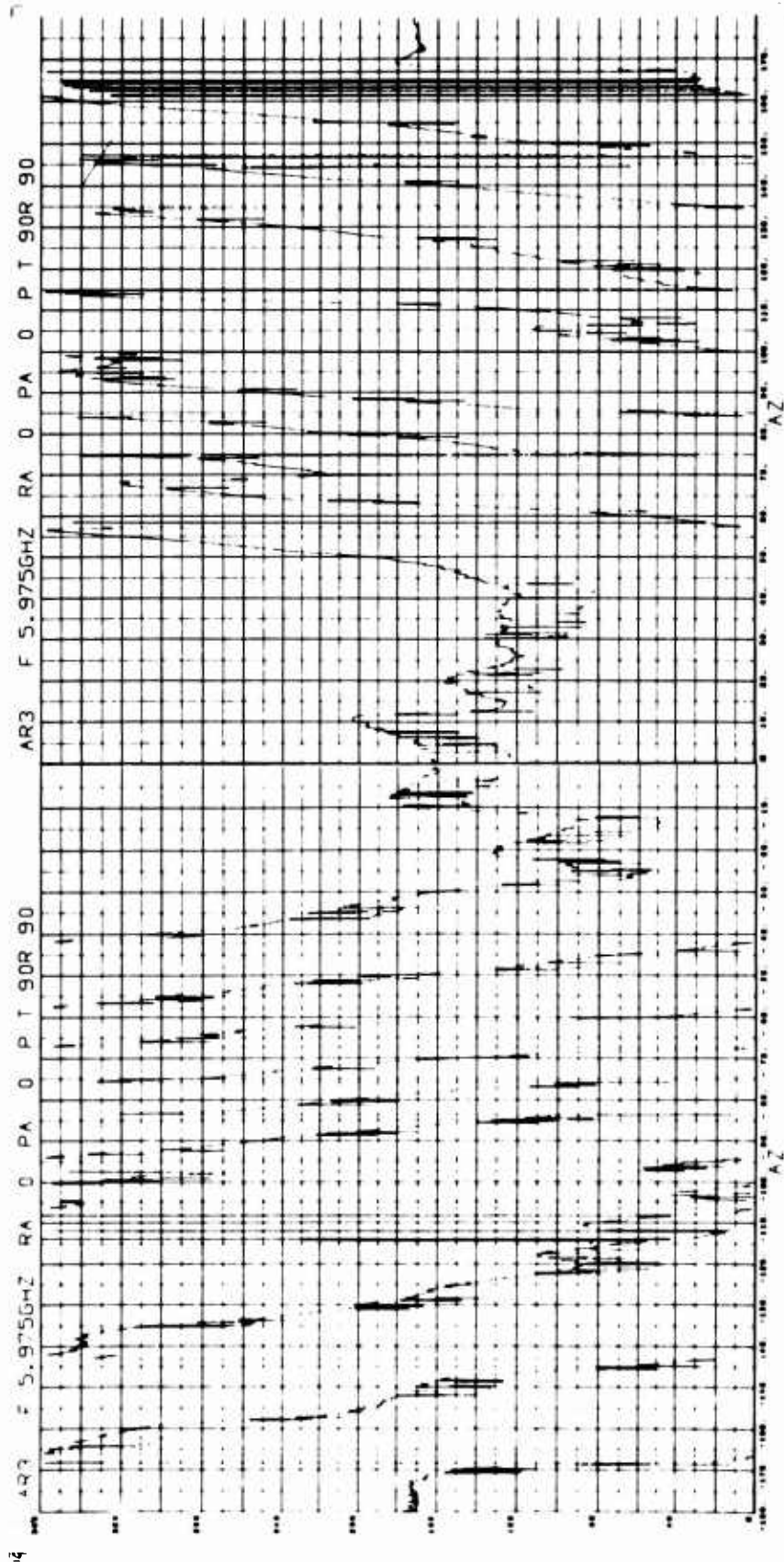


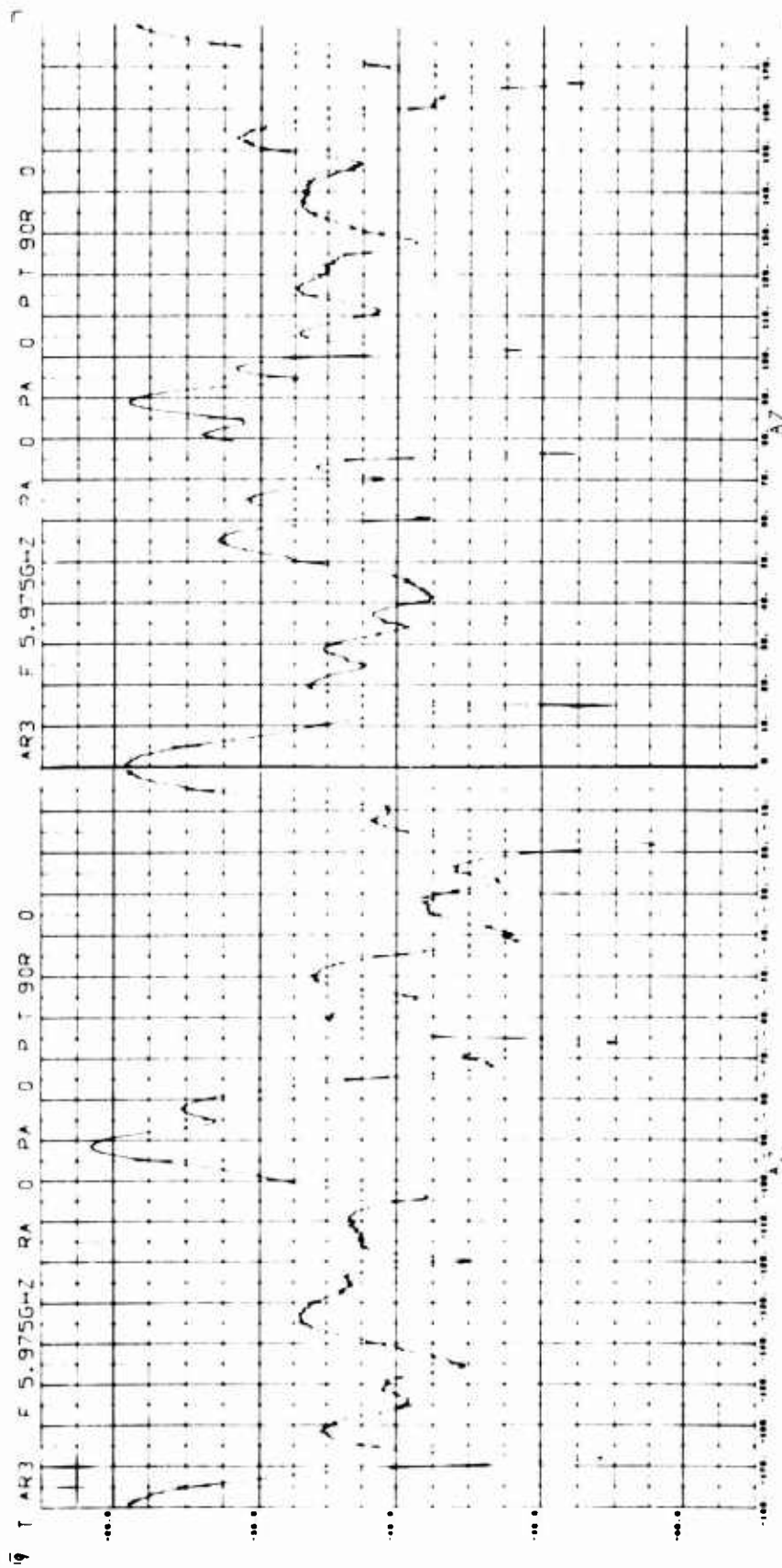












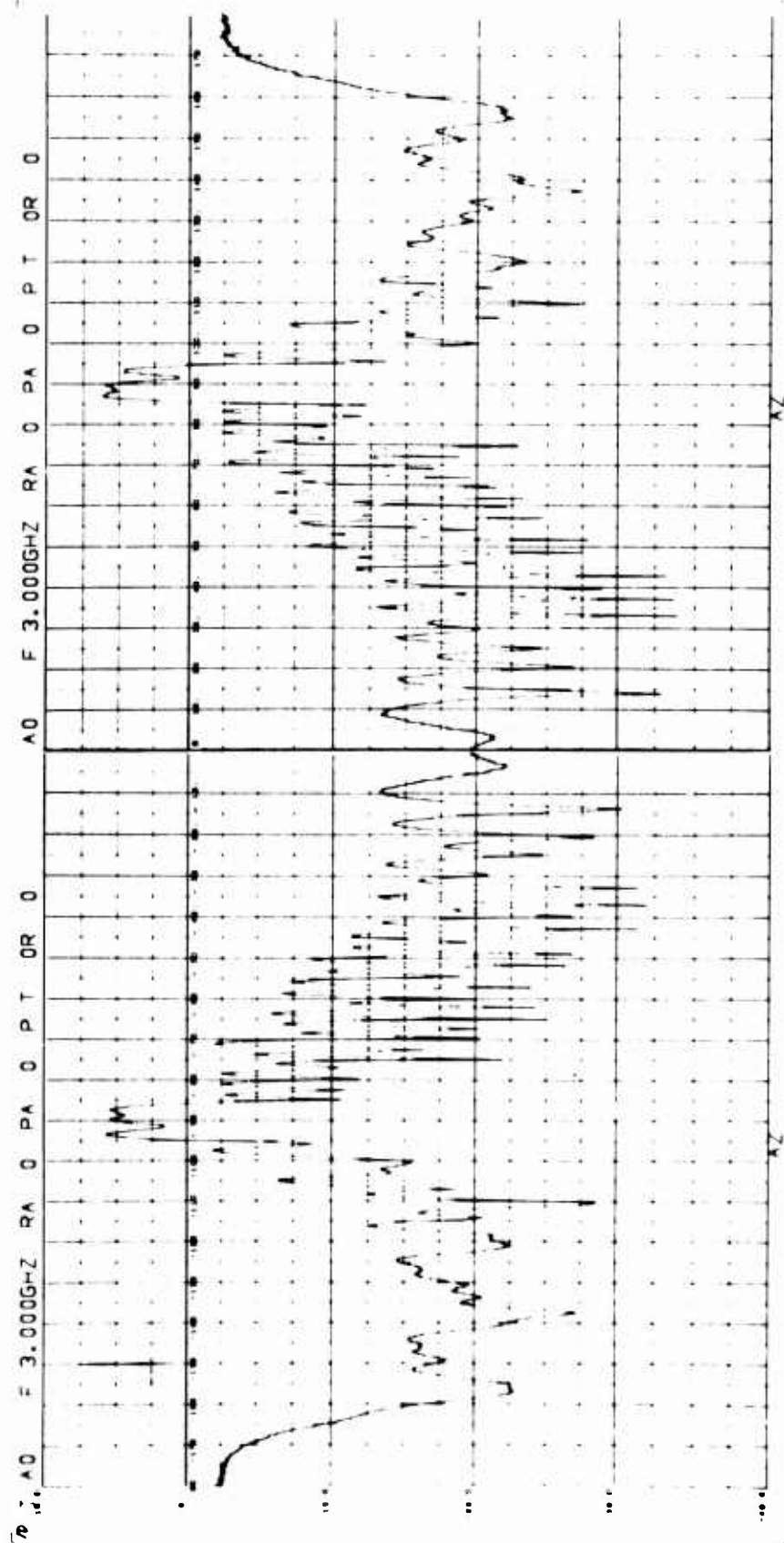
3.2.3 Smooth Aerospace Vehicles

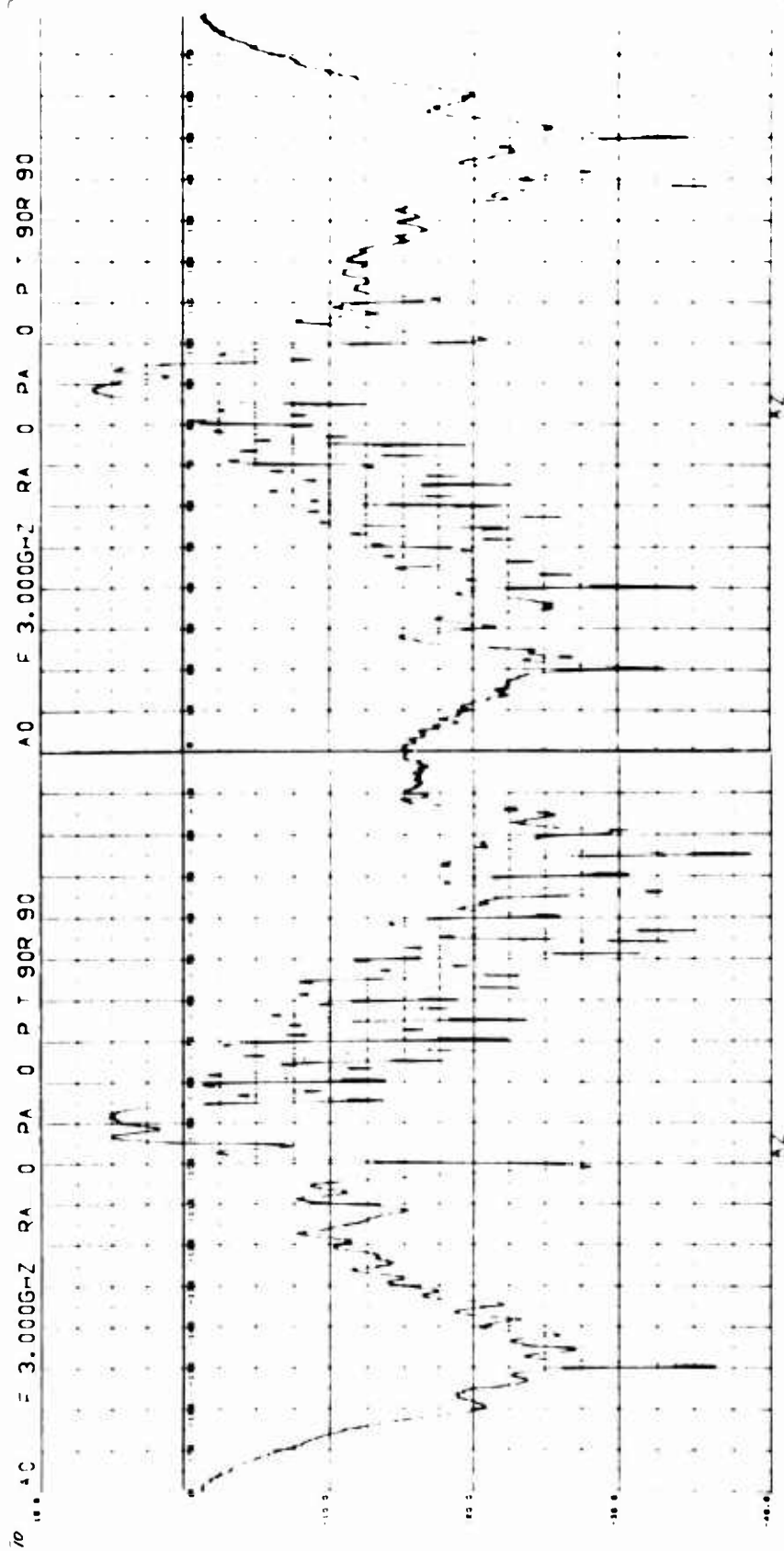
The smooth aerospace vehicles listed in Table 3-4 were constructed by use of the generic shapes described in Table 3-2.

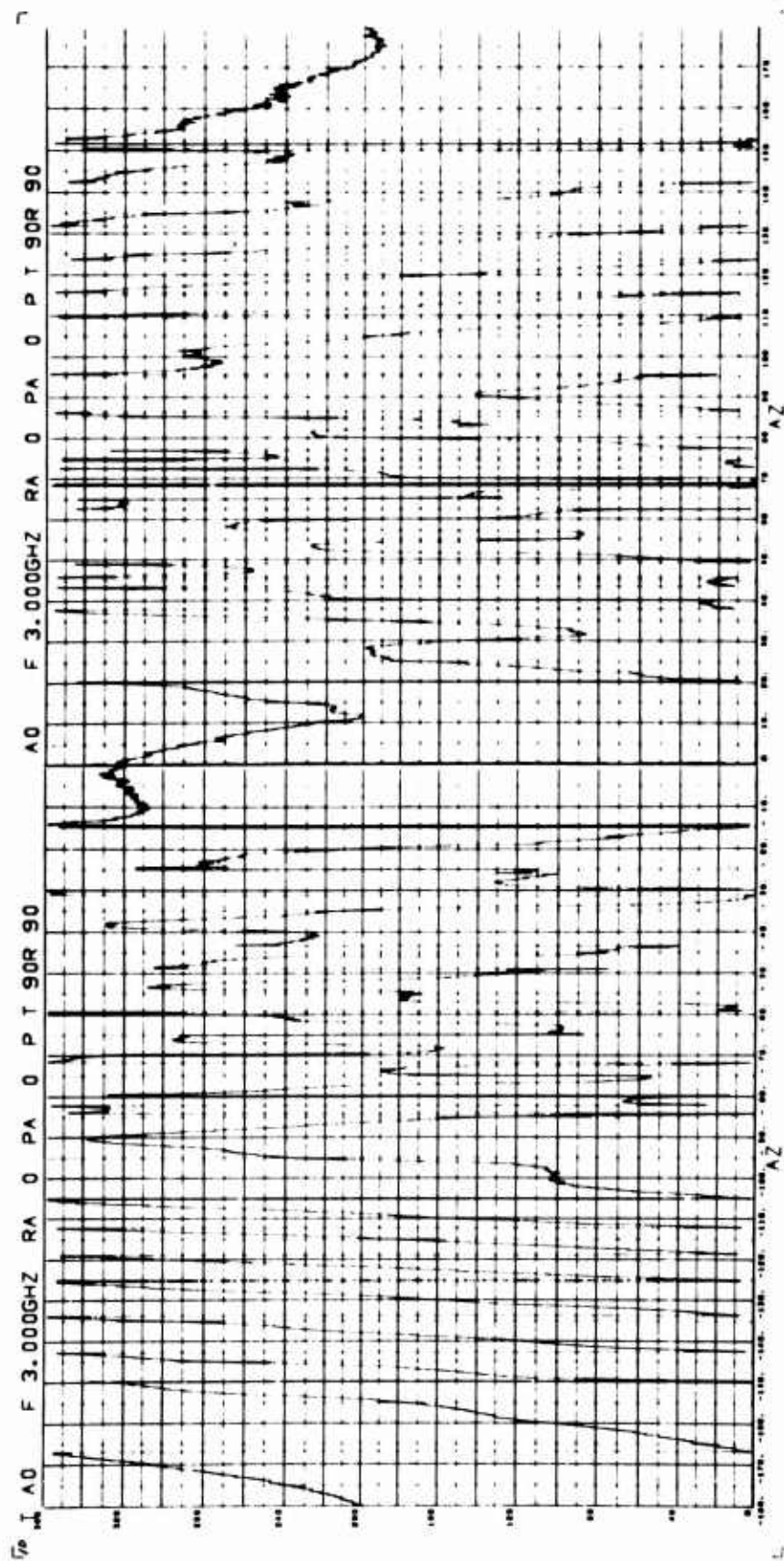
Table 3-4

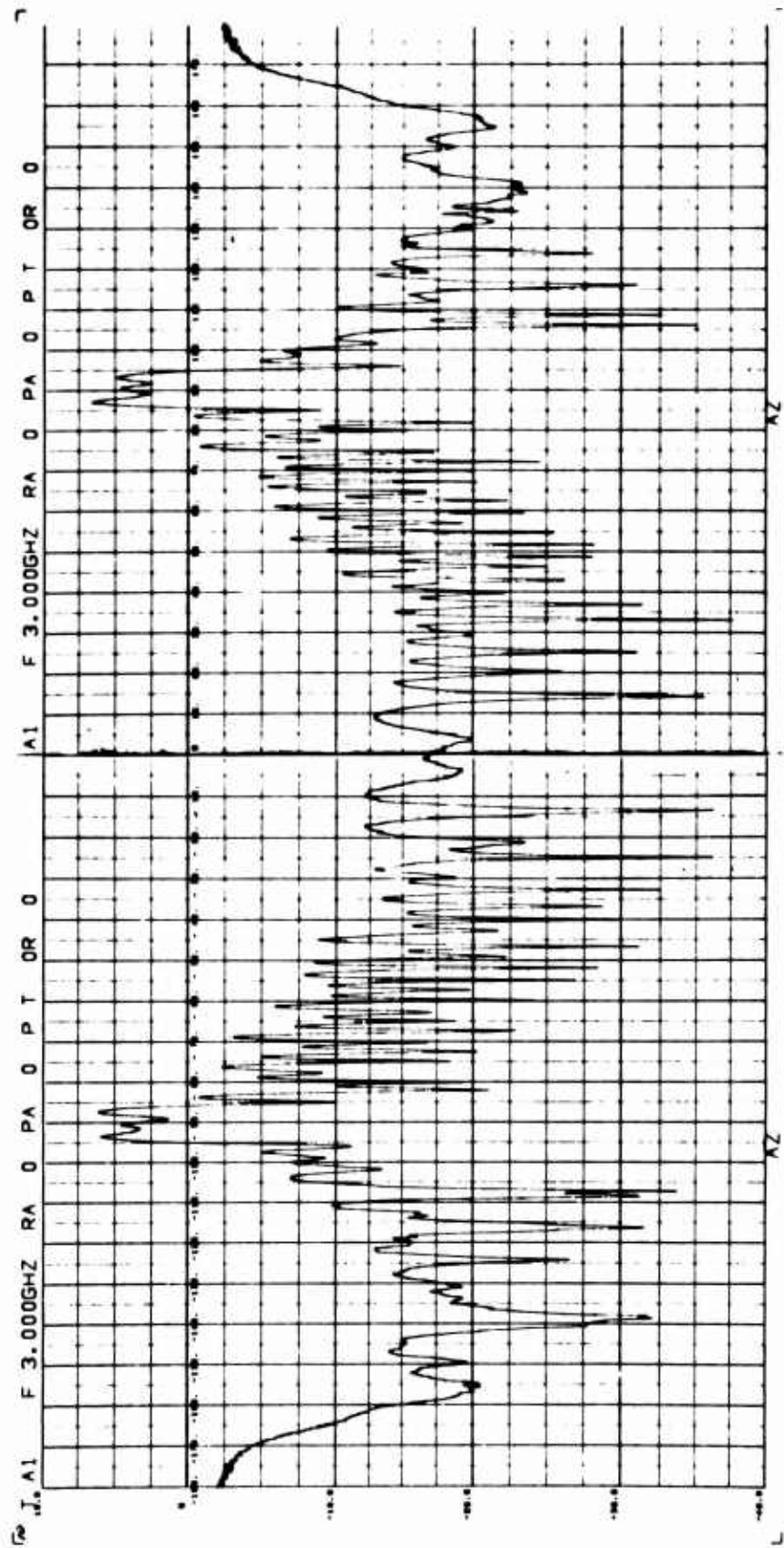
SMOOTH AEROSPACE VEHICLE MEASUREMENTS

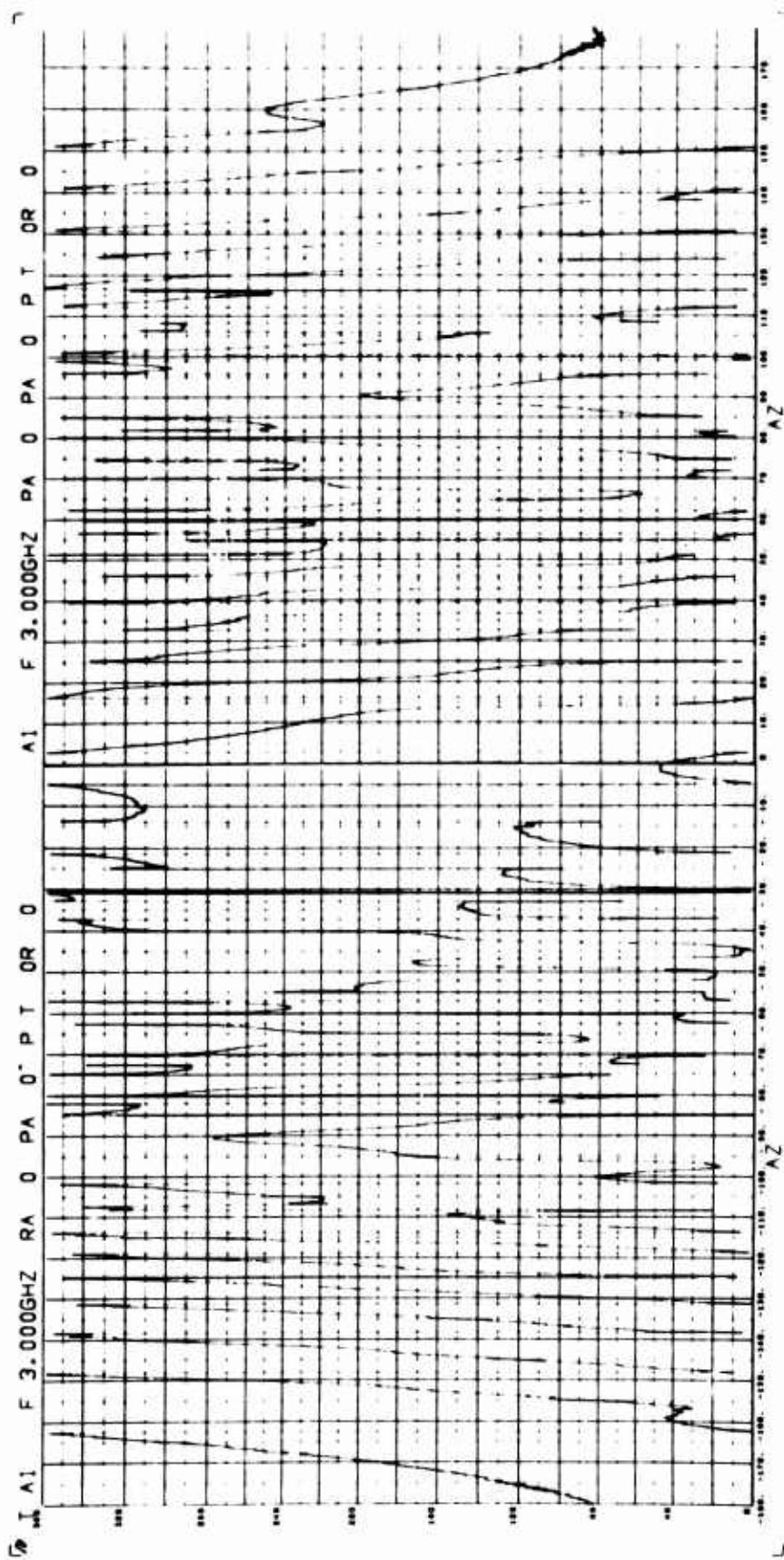
VEHICLE	MAXIMUM DIAMETER Inches	MAXIMUM LENGTH Inches	MEASUREMENT FREQUENCY GHz	BISTATIC ANGLE Degrees
SMOOTH AEROSPACE VEHICLE A0	7.500	53.237	3.0	0
SMOOTH AEROSPACE VEHICLE A1	7.500	53.239	3.0	0
SMOOTH AEROSPACE VEHICLE A2	7.500	55.488	6.0	0
SMOOTH AEROSPACE VEHICLE A3	7.500	47.620	3.0	0
			6.0	0

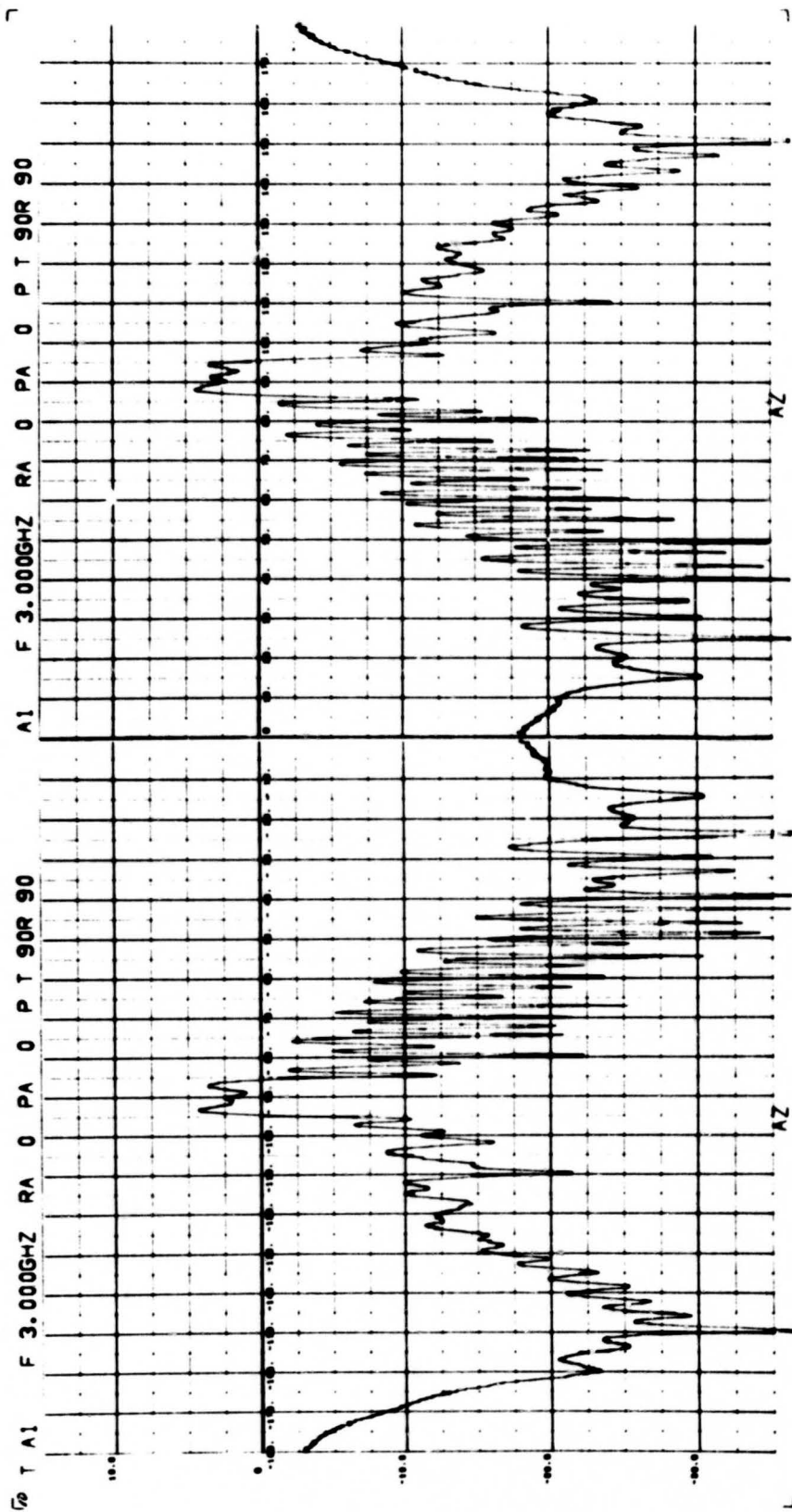


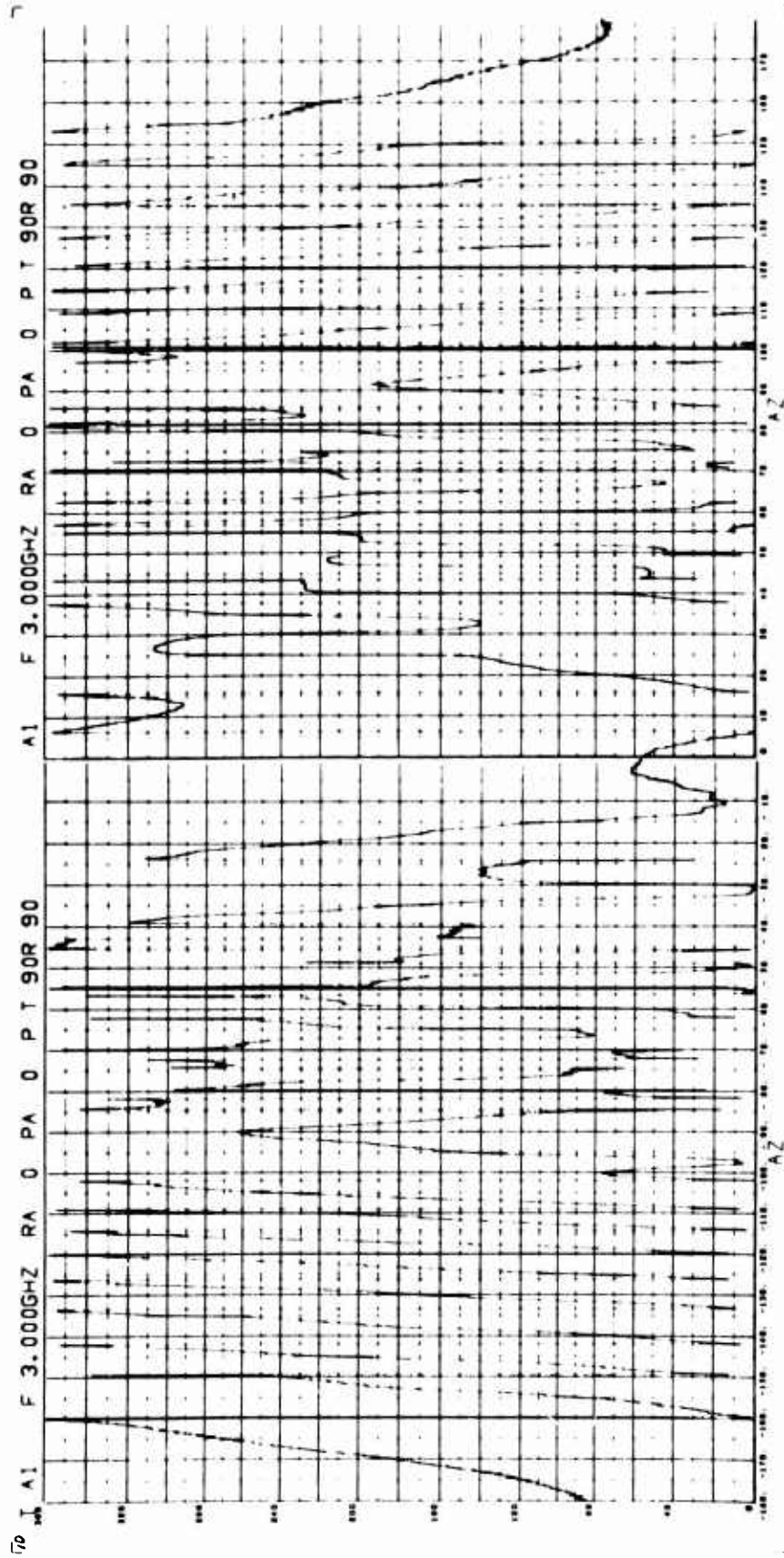


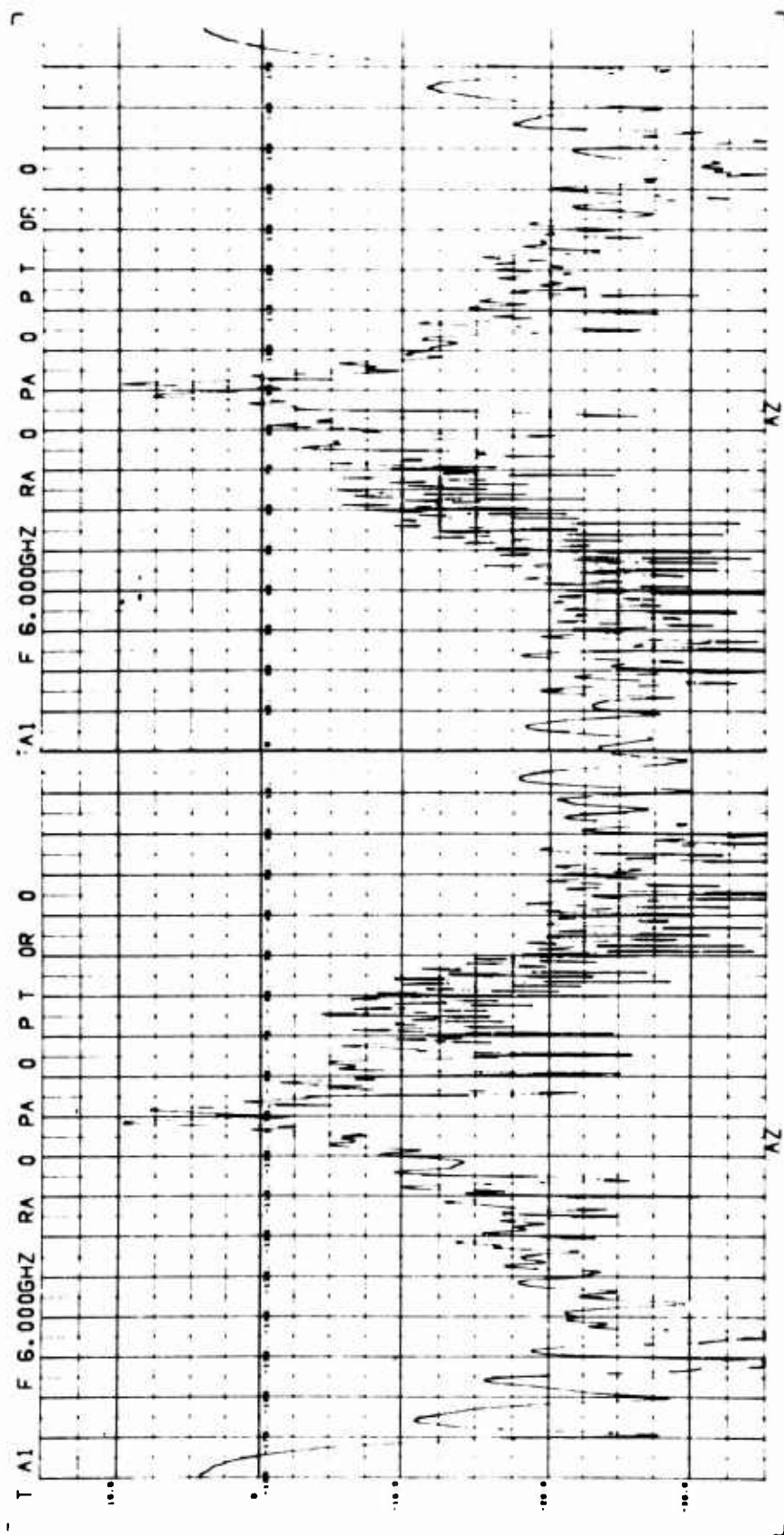


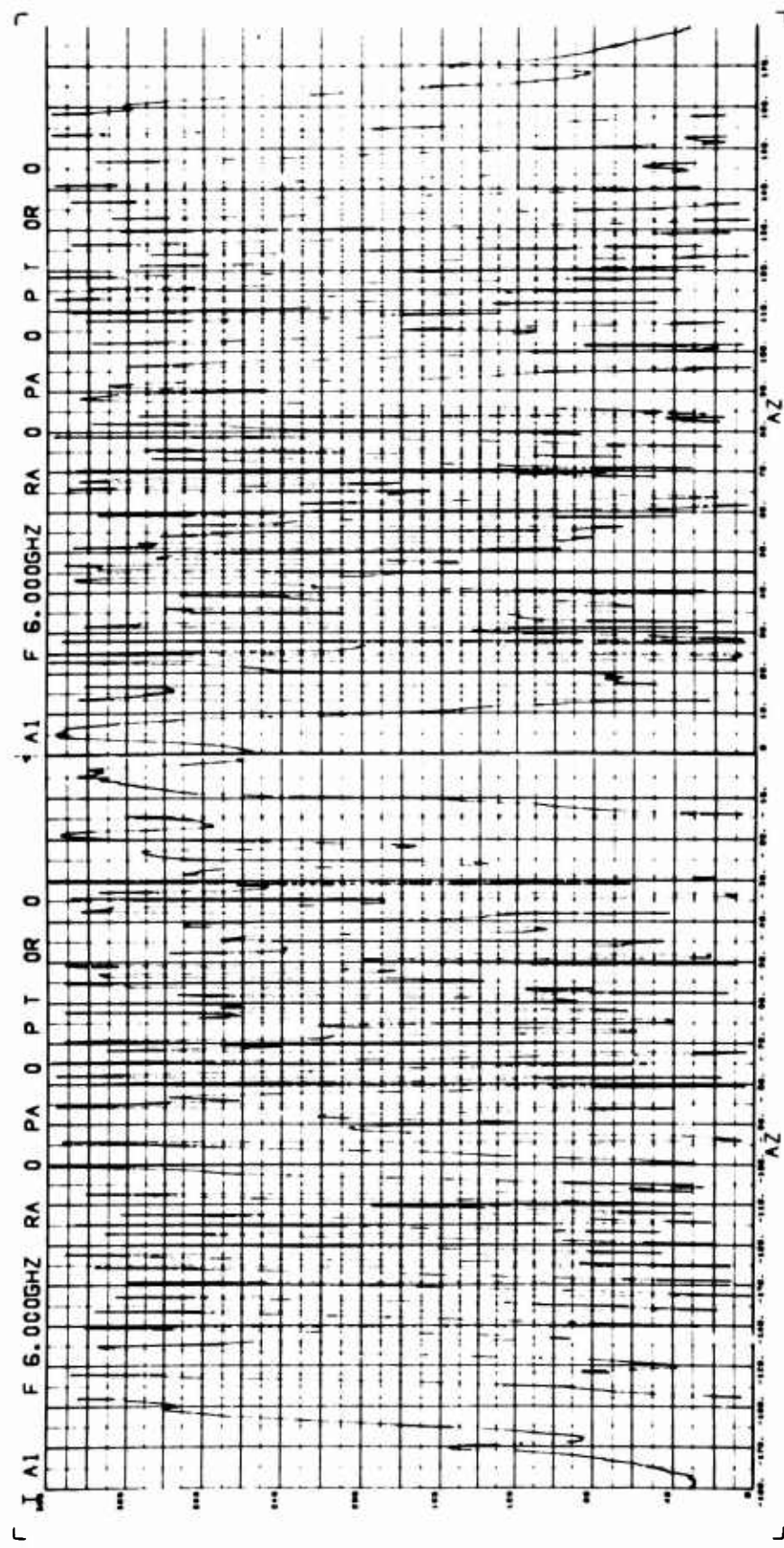


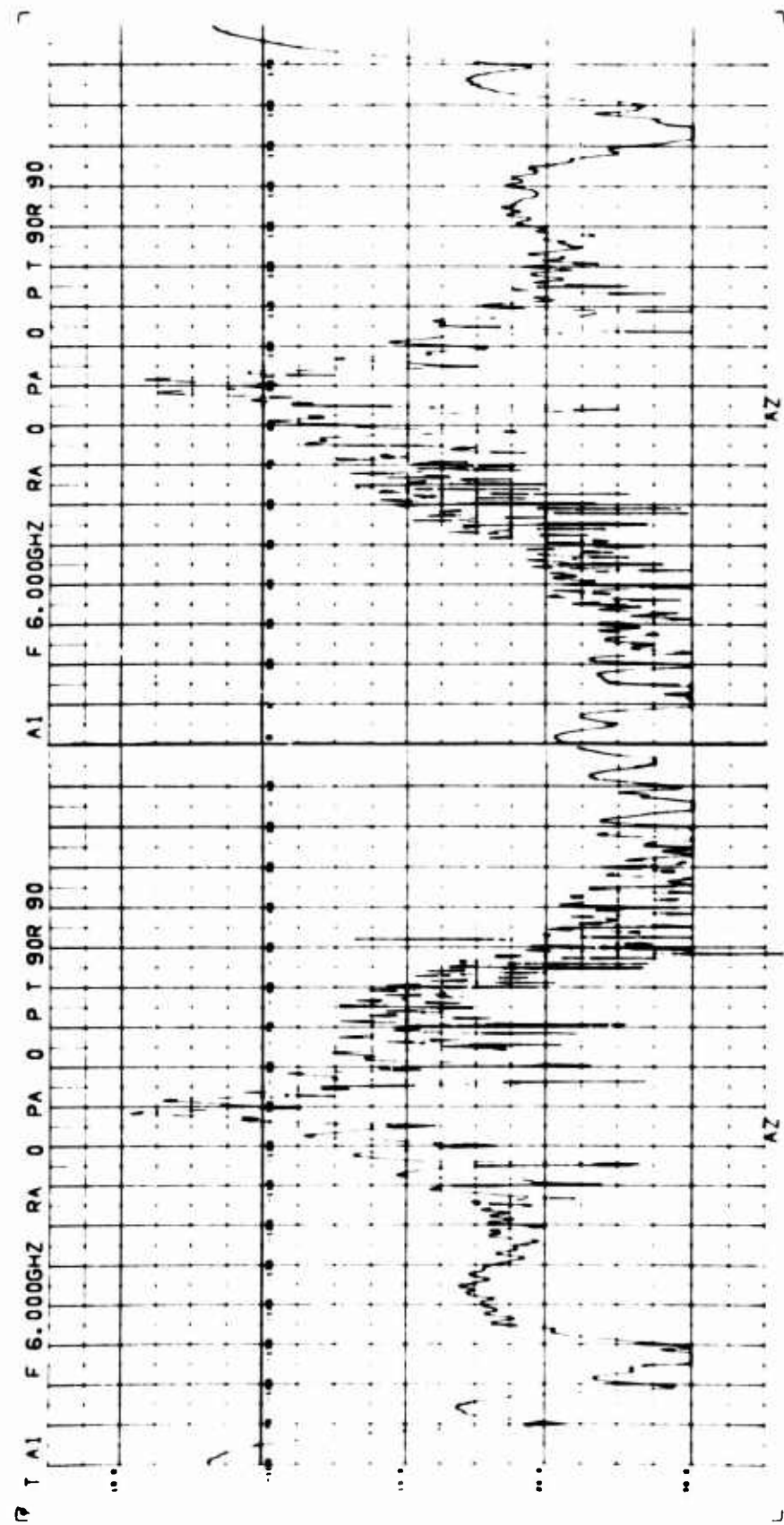


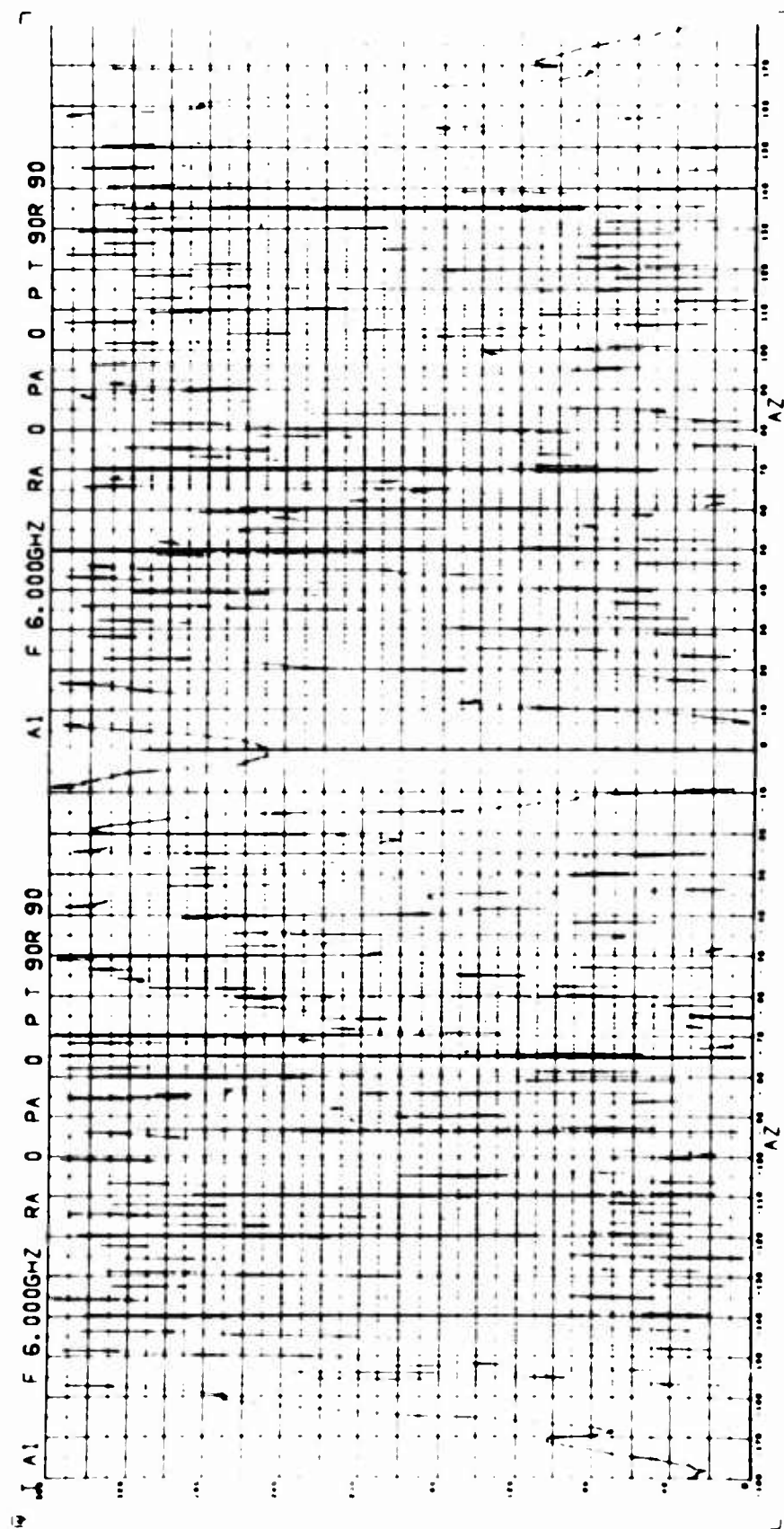


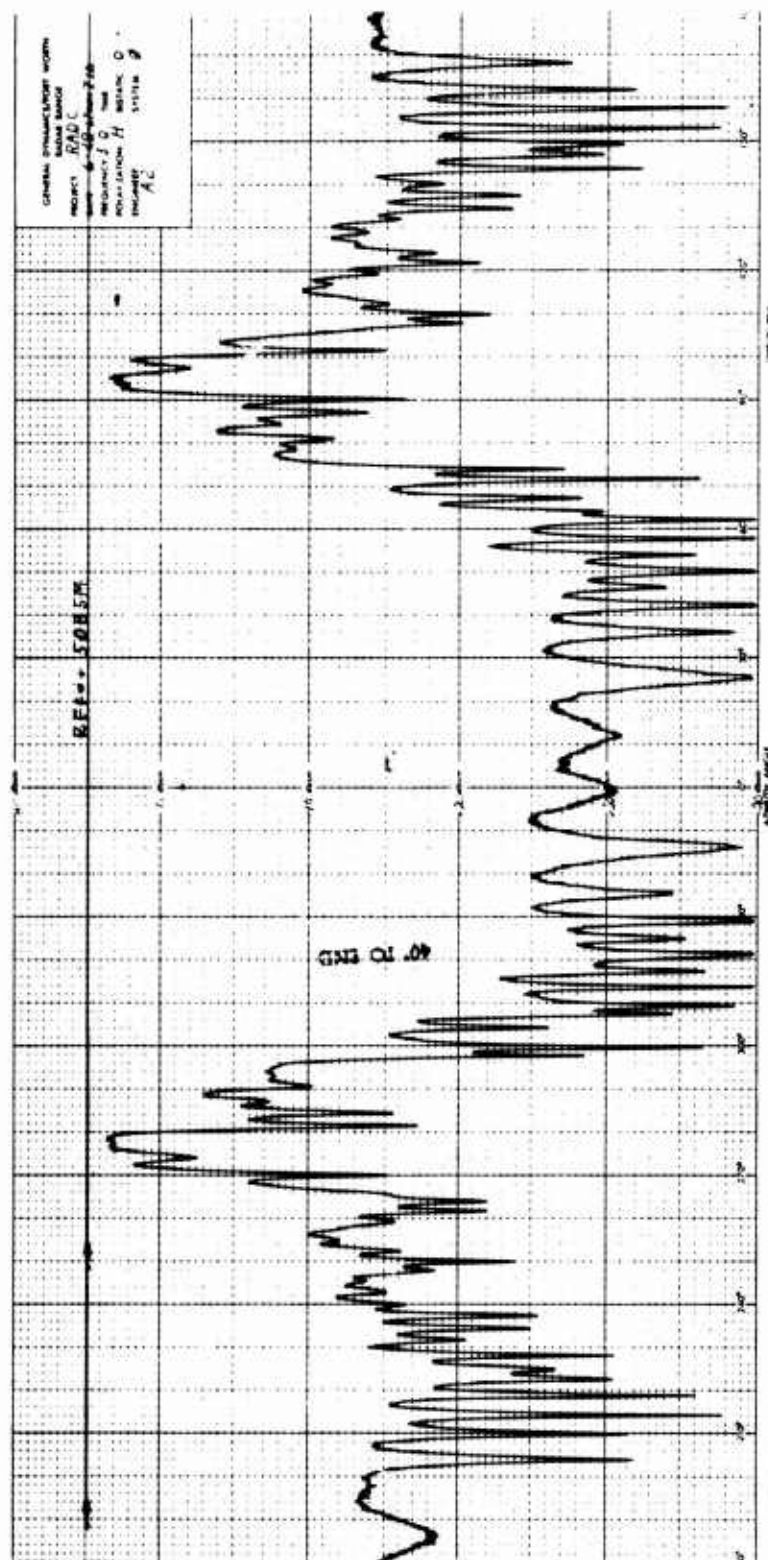


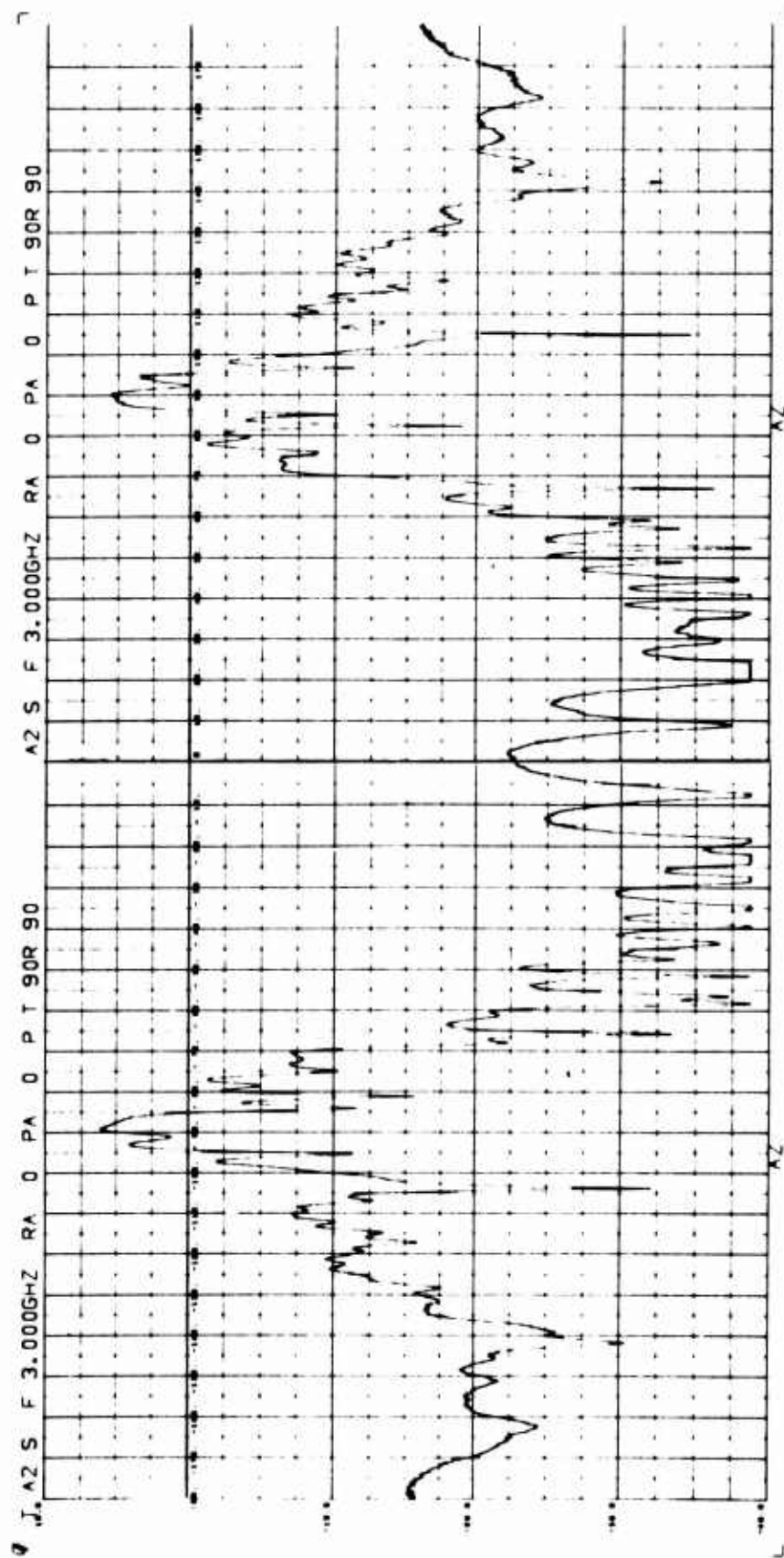


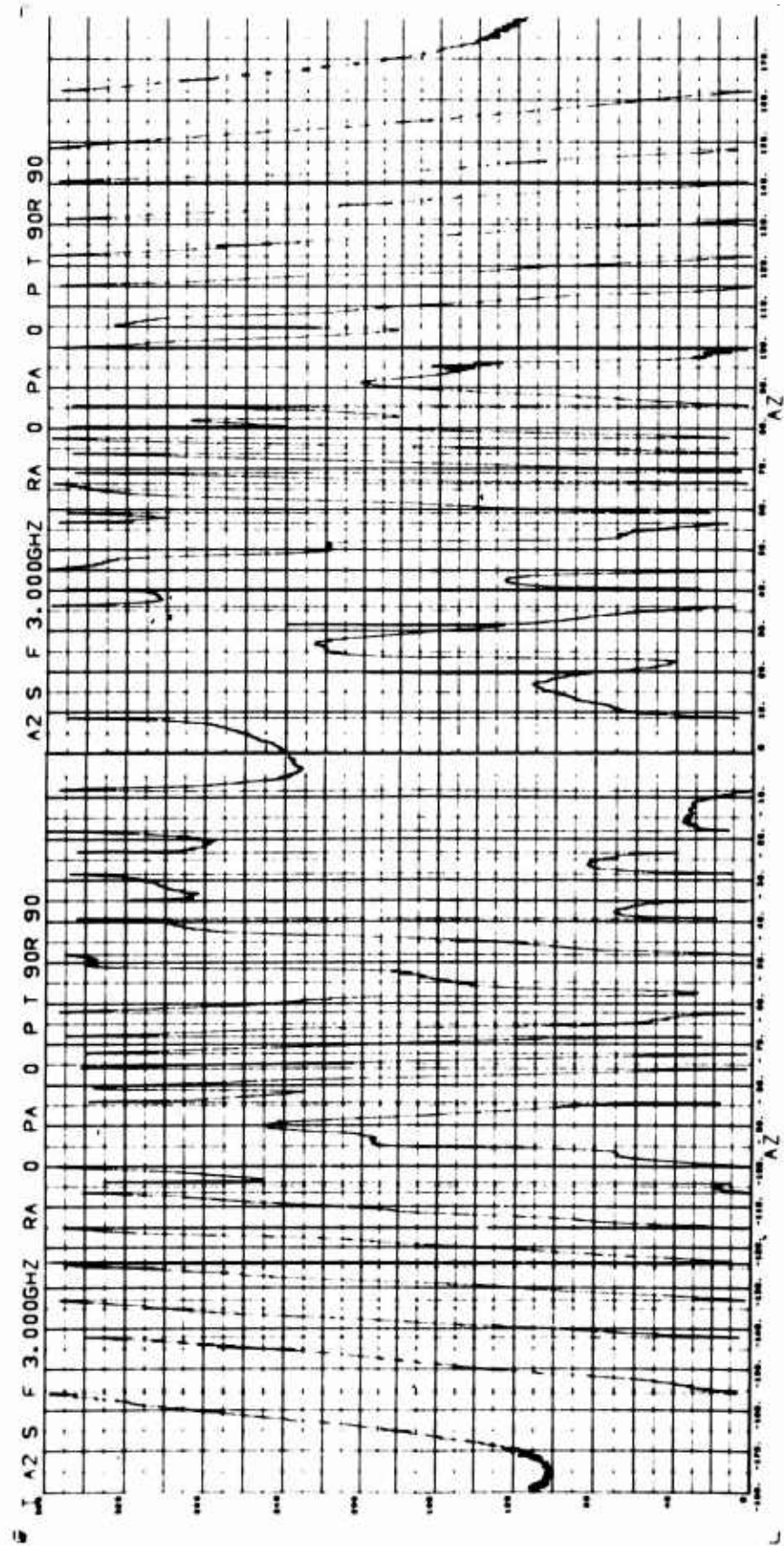


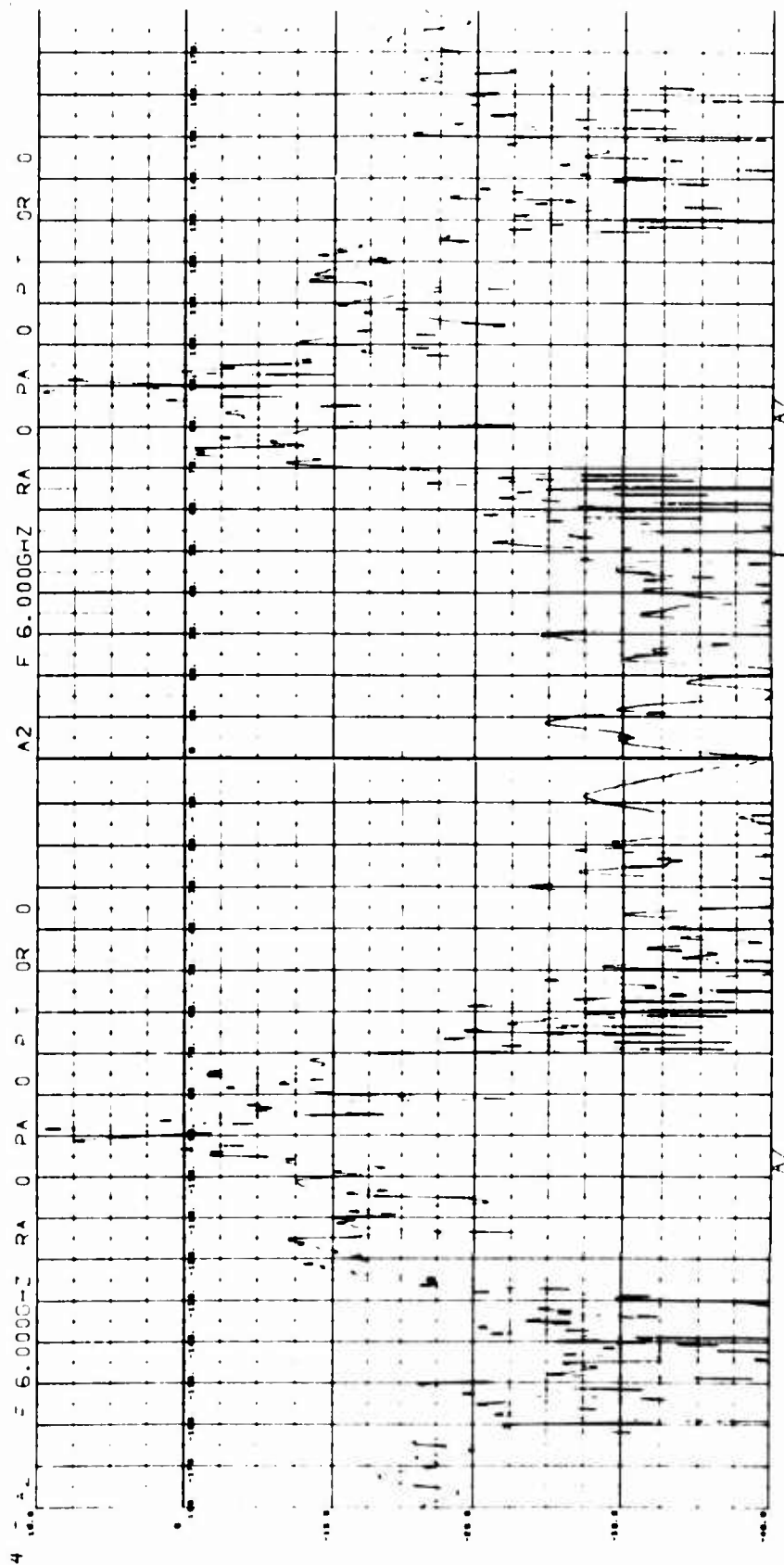


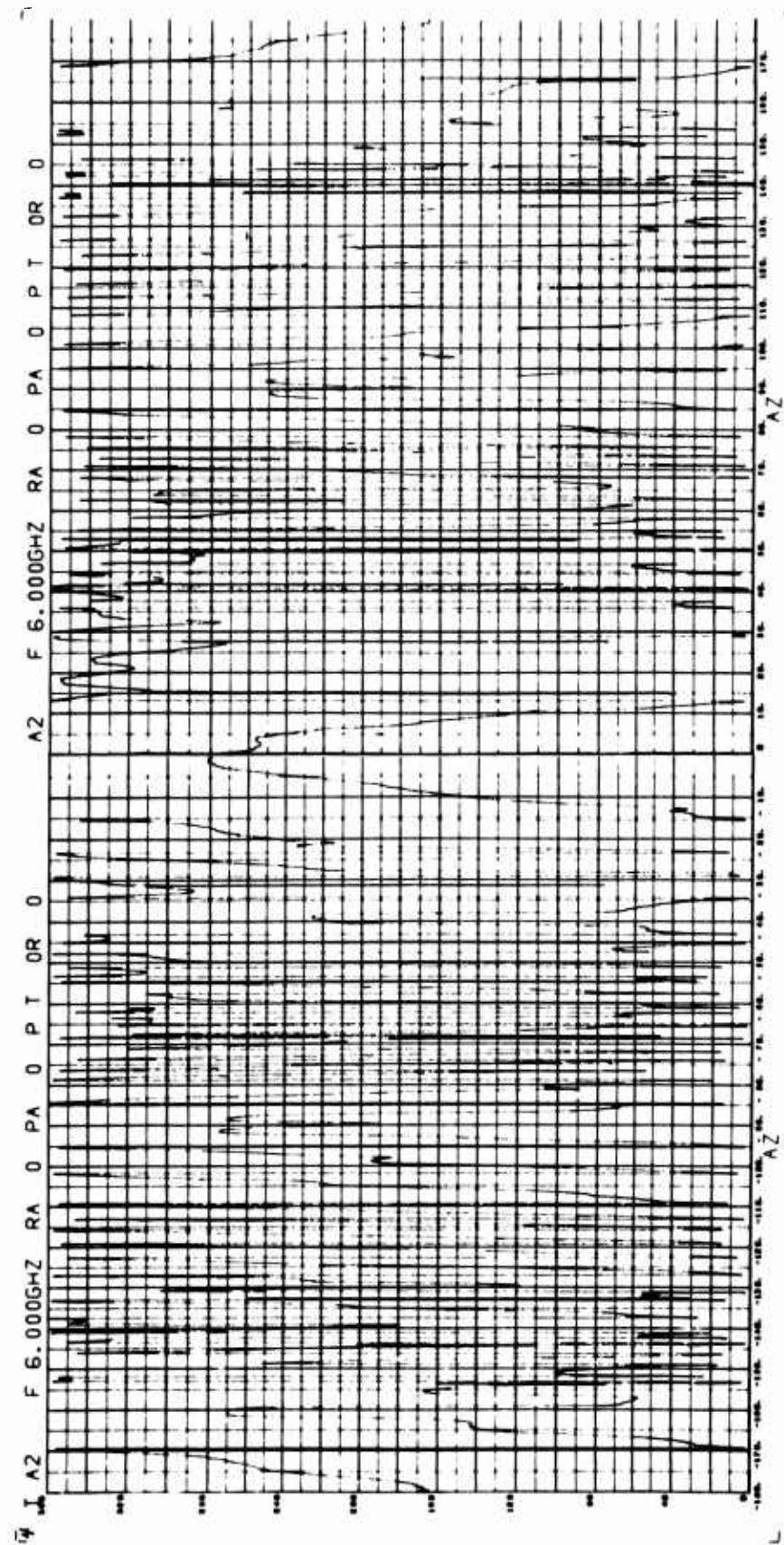


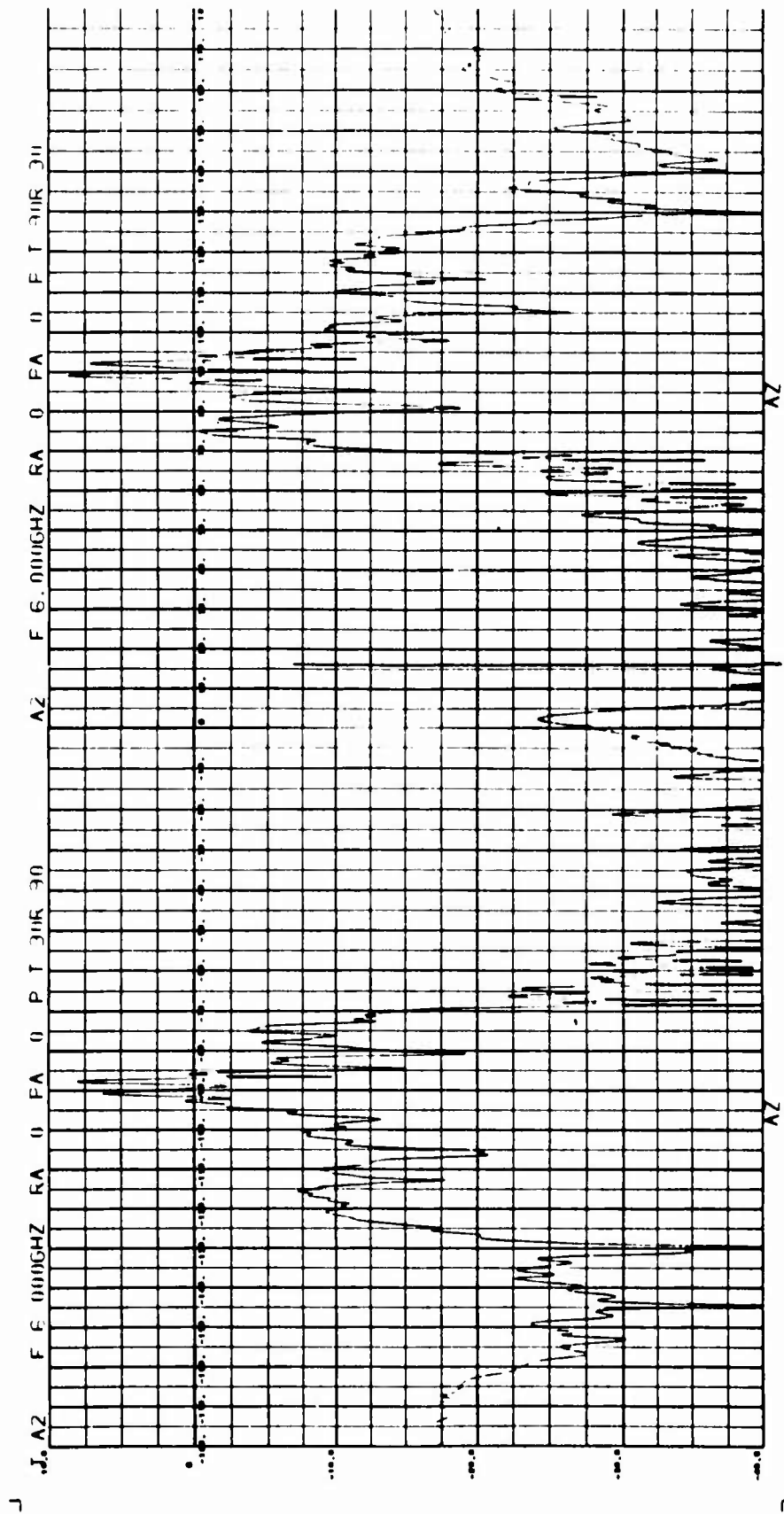


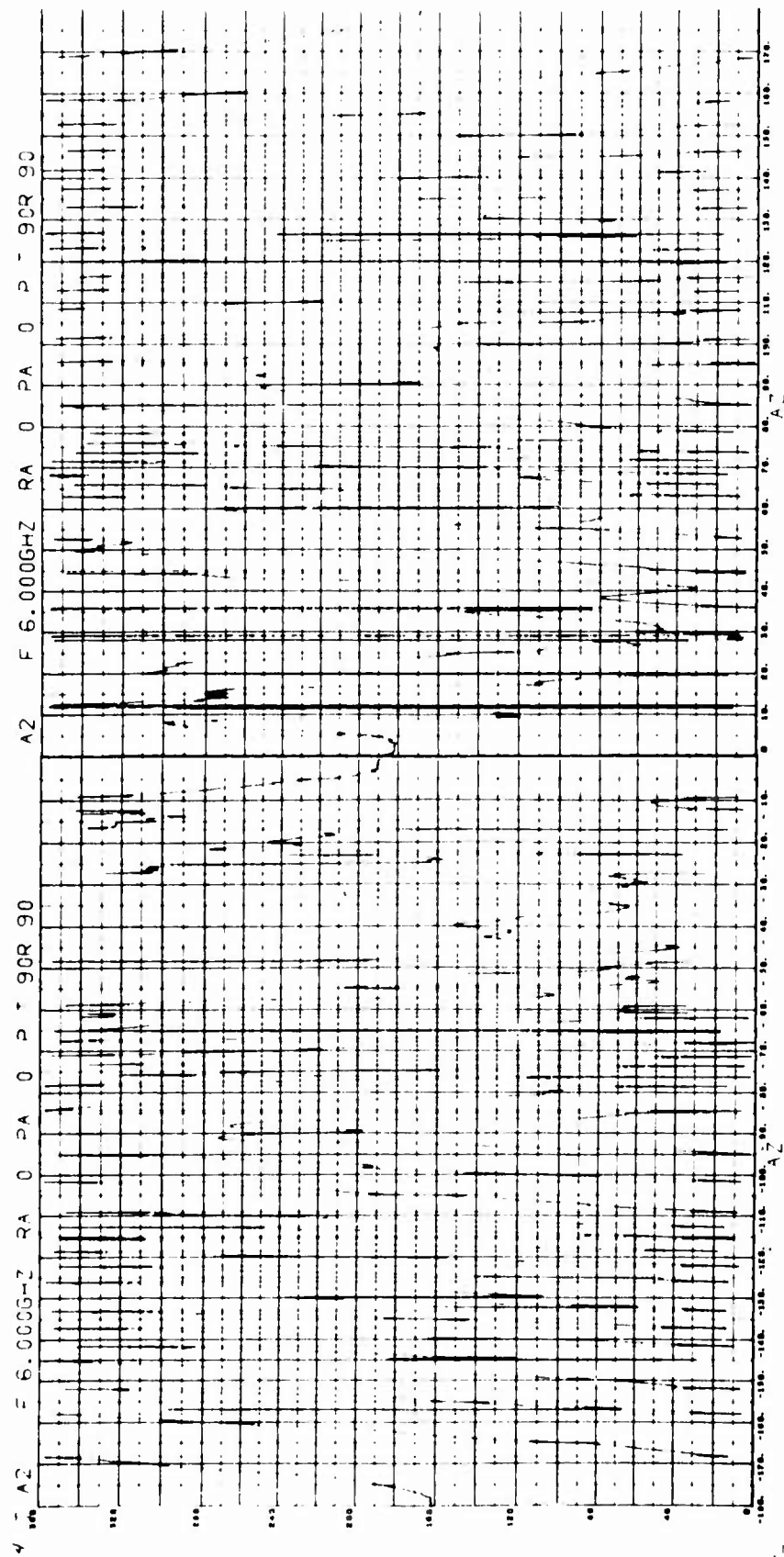


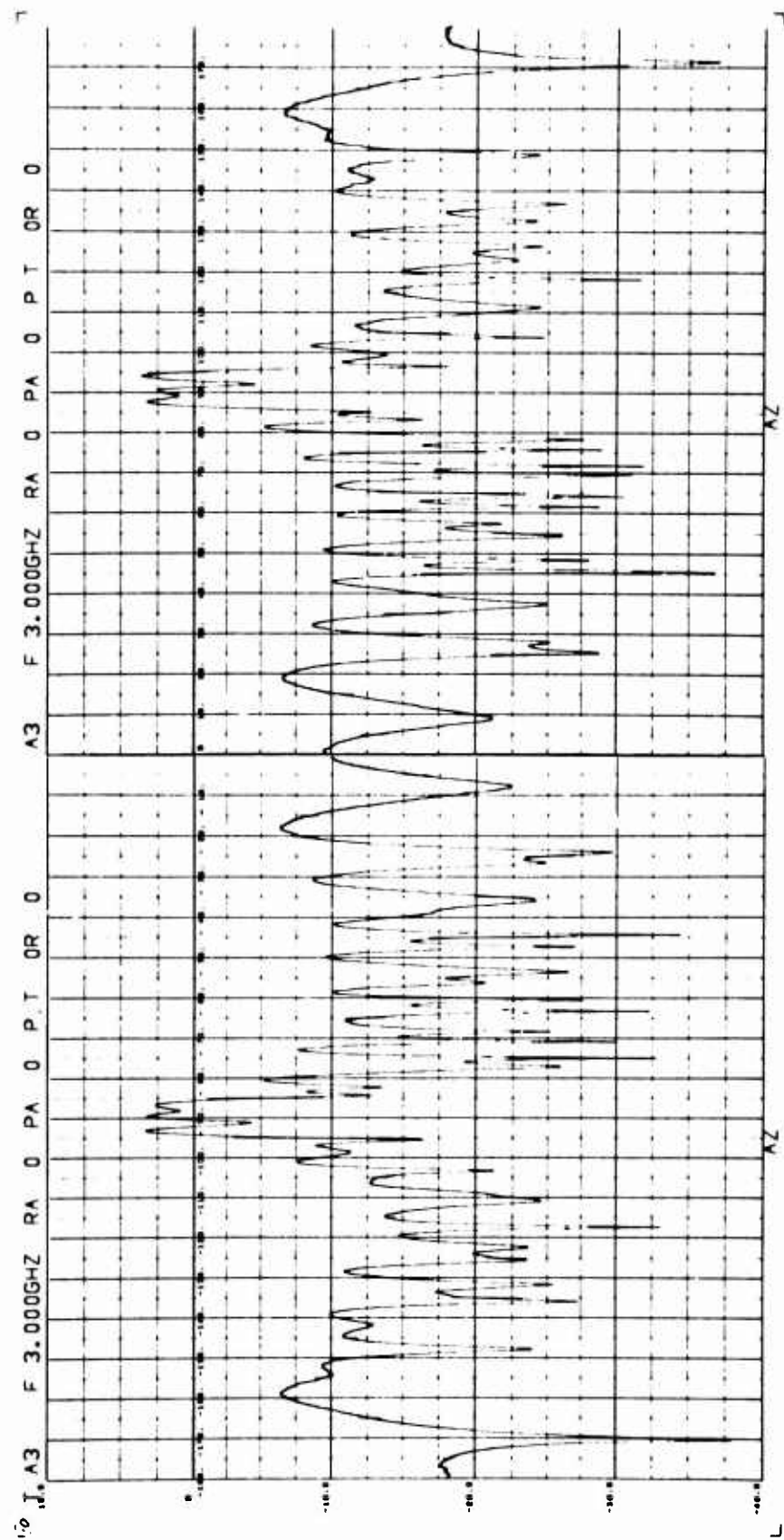


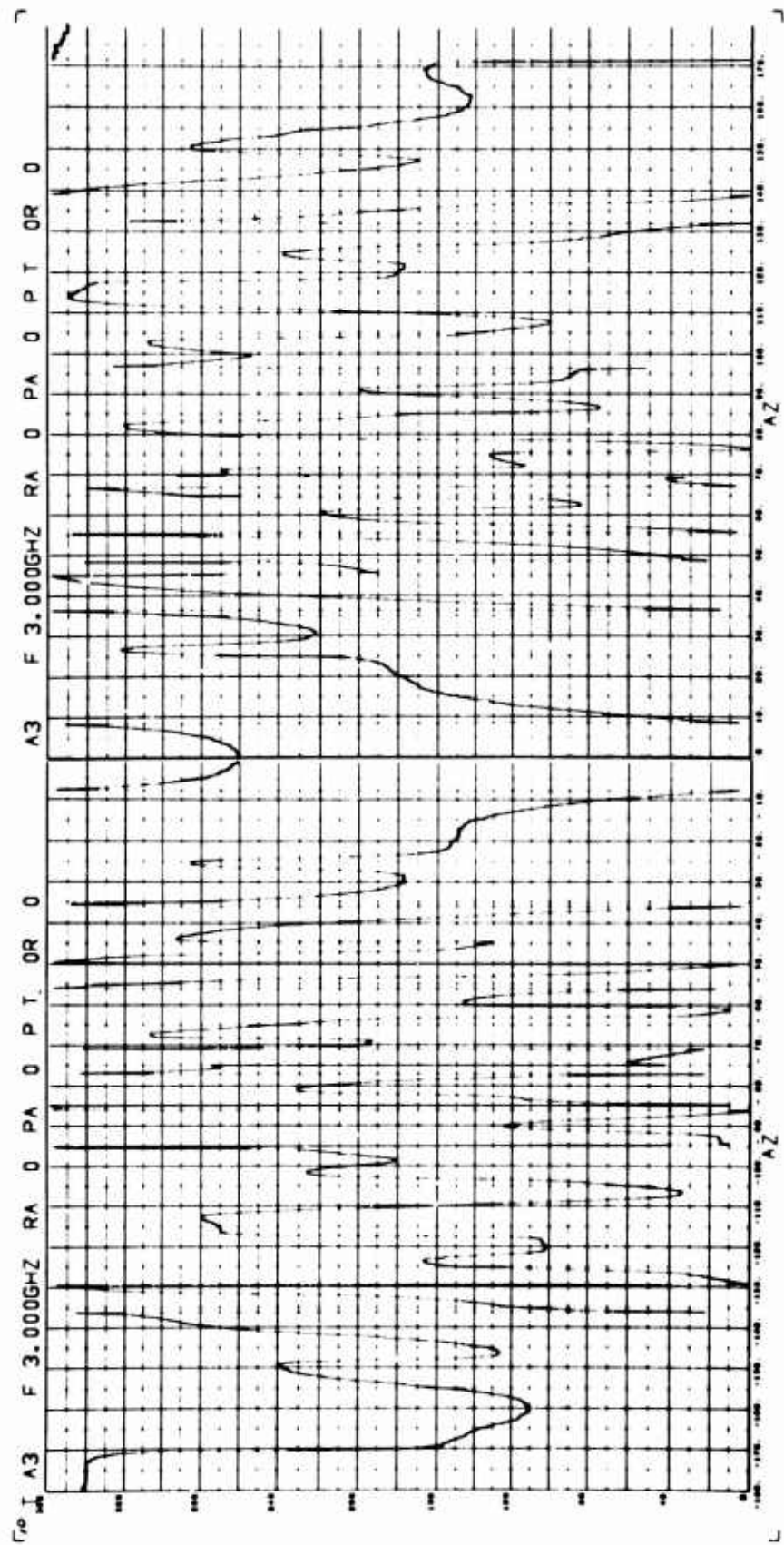


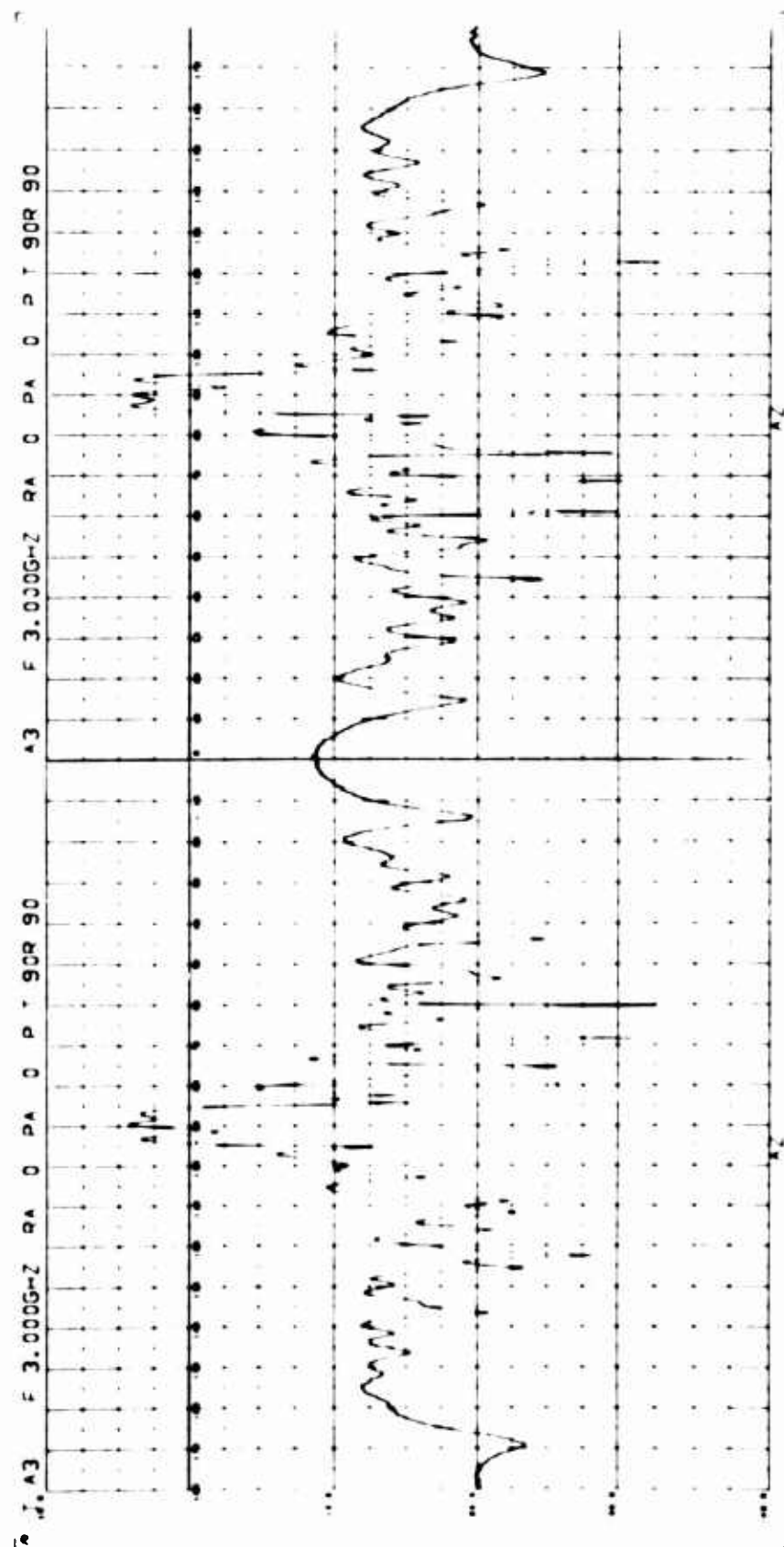


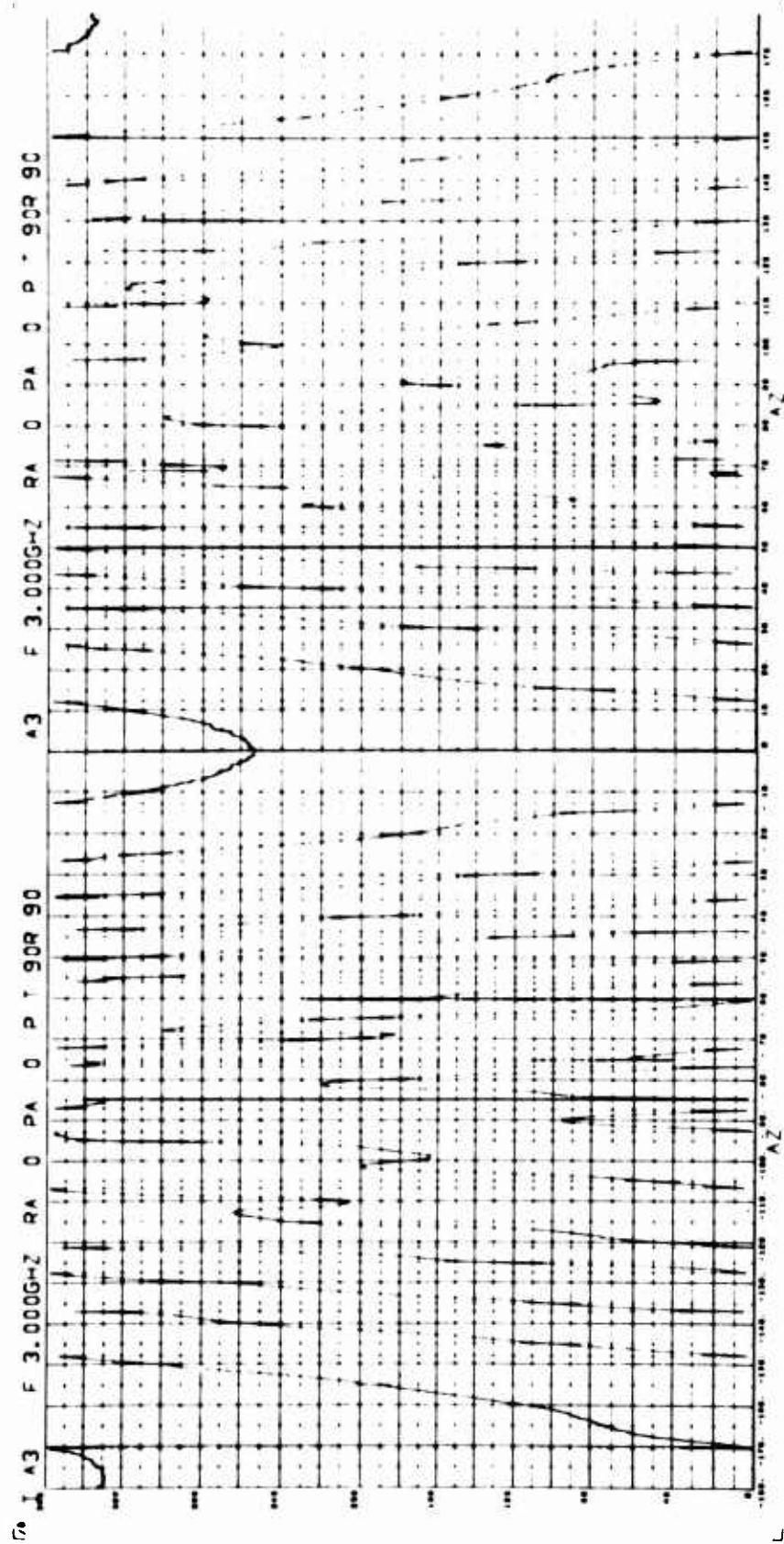


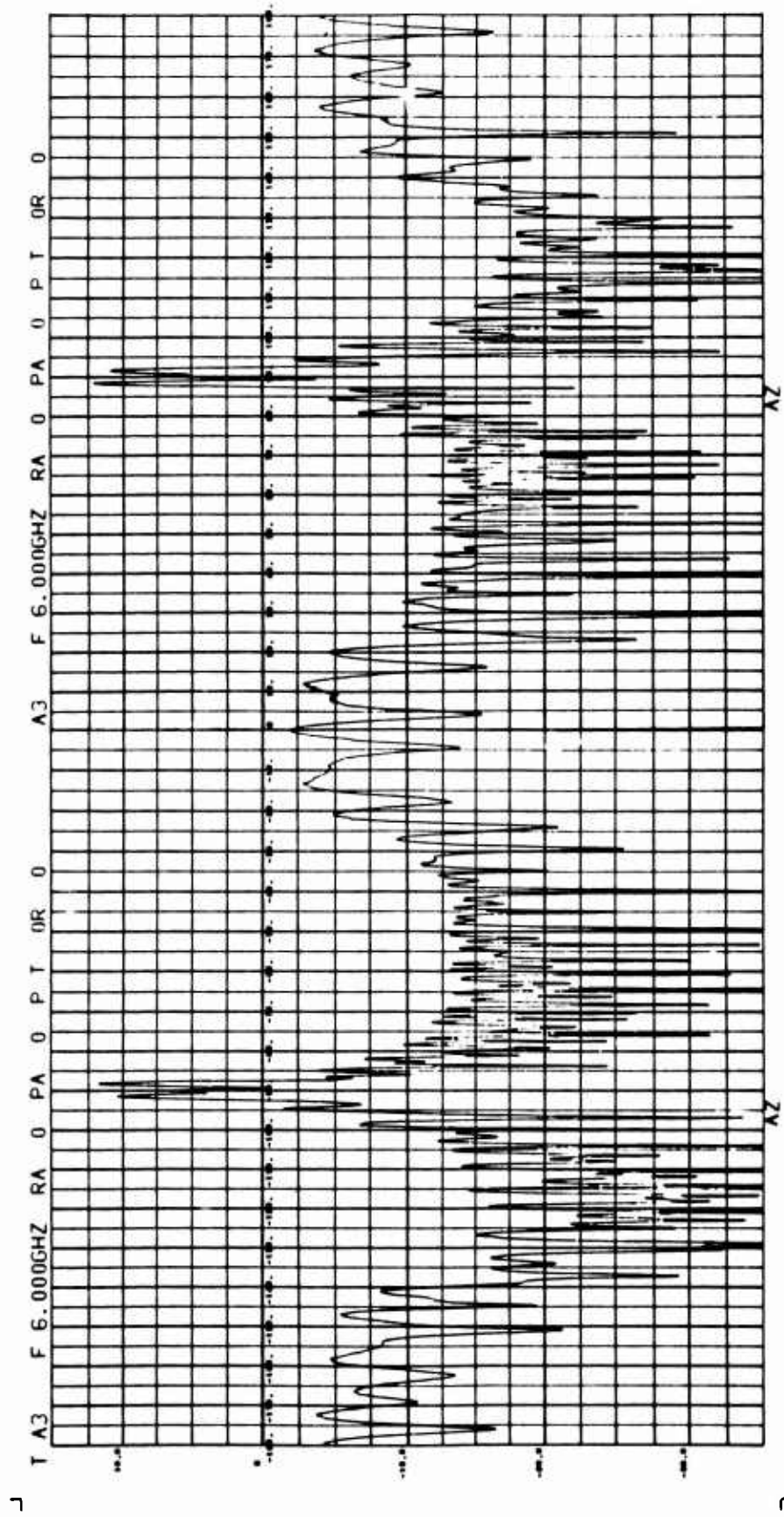


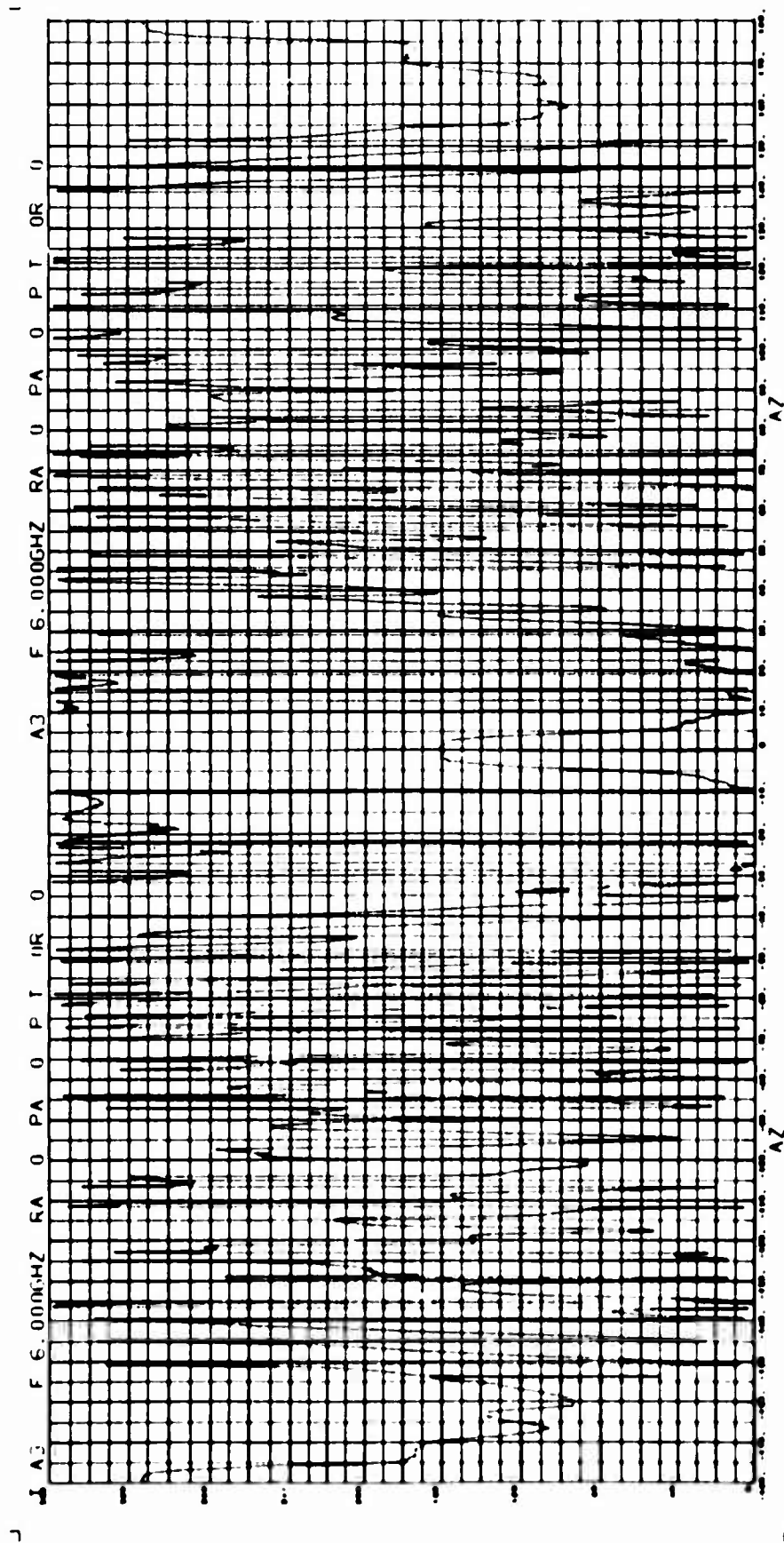


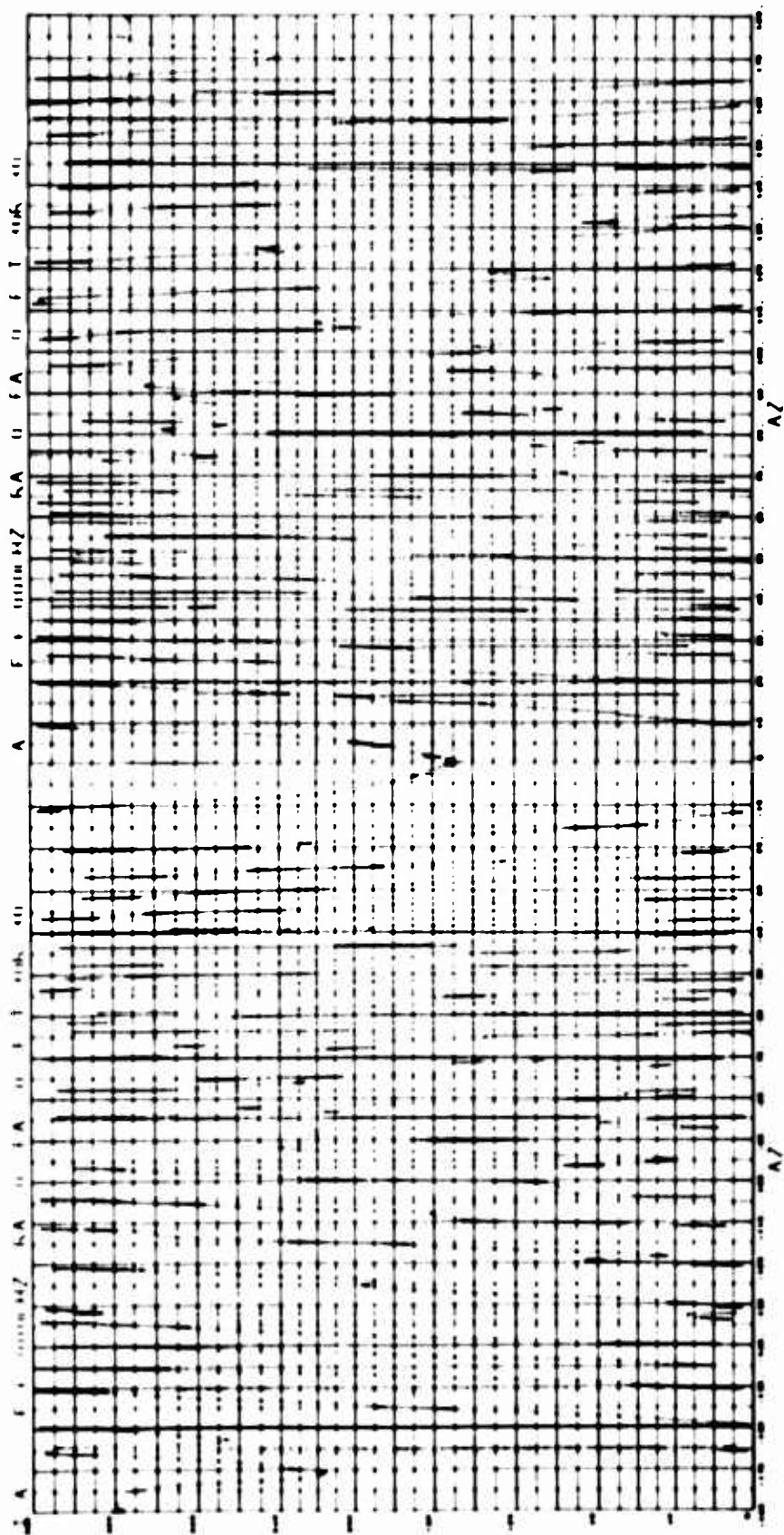












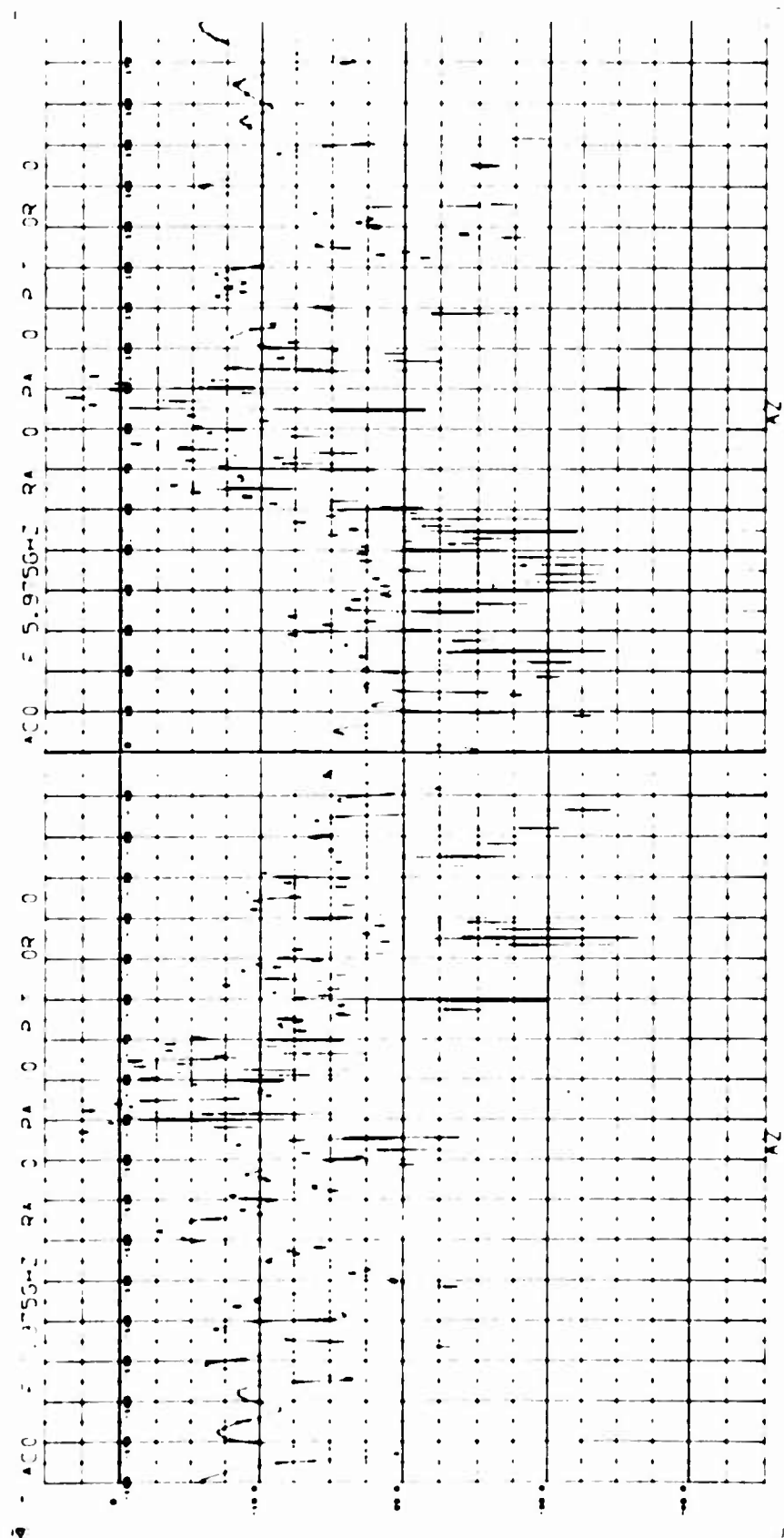
3.2.4 Complex Aerospace Vehicles

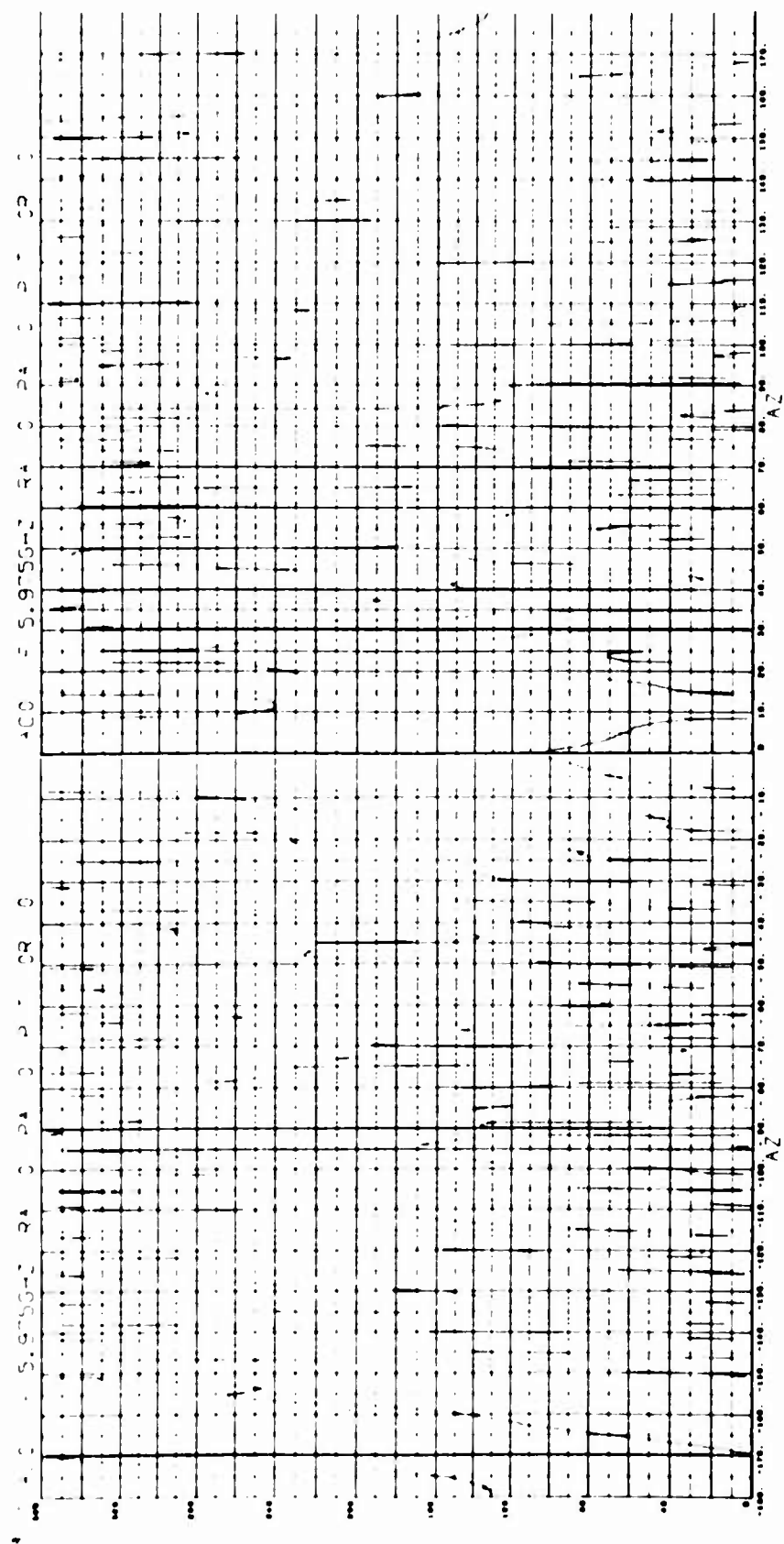
The complex aerospace vehicles described in this paragraph were similar in construction to the smooth aerospace vehicles, with the exception of the use of protuberances which were used to produce varying degrees of asymmetry in the vehicles. Complex aerospace models AC4 and AC5 were, in fact, bodies of rotational symmetry; Model AC3 contained two orthogonal planes of symmetry, Model AC2 contained a single plane of symmetry, and Models AC0 and AC1, contained no planes of symmetry. Data was obtained by using the VH polarization condition in the case of Models AC0, AC1 and AC2, and AC3. Pertinent radar parameters associated with these measurements are described in Table 3-5.

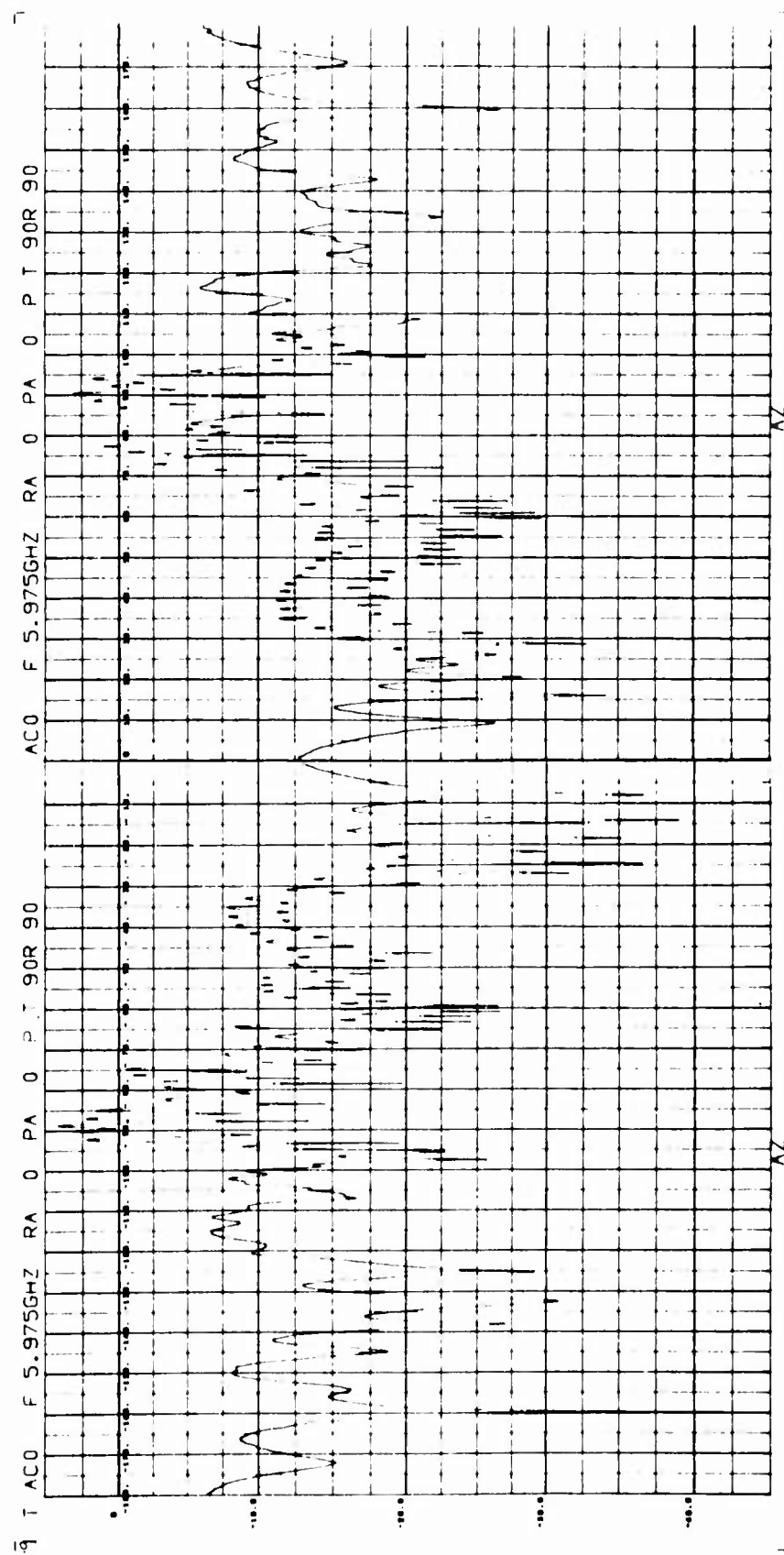
Table 3-5

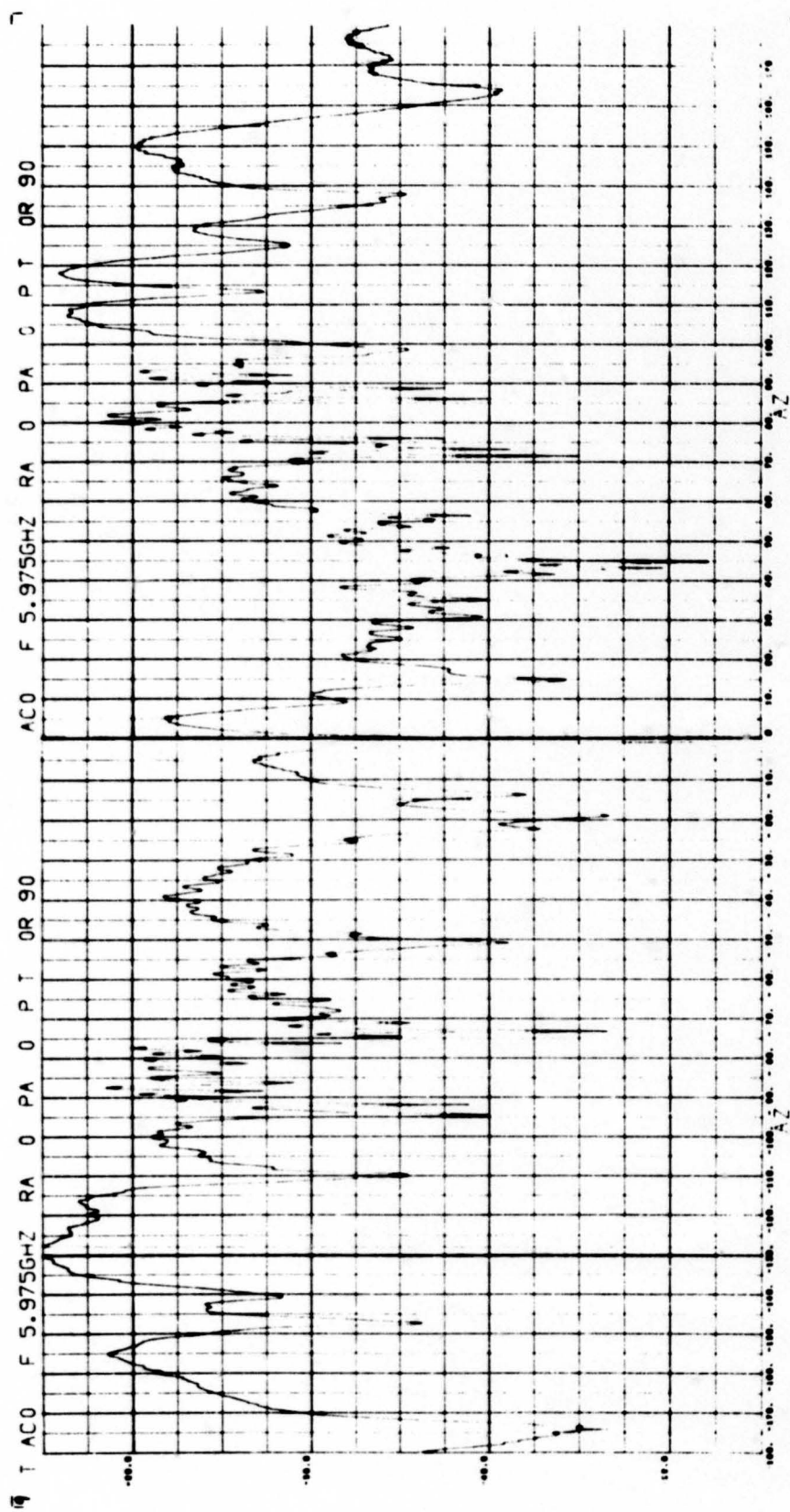
COMPLEX AEROSPACE VEHICLE MEASUREMENTS

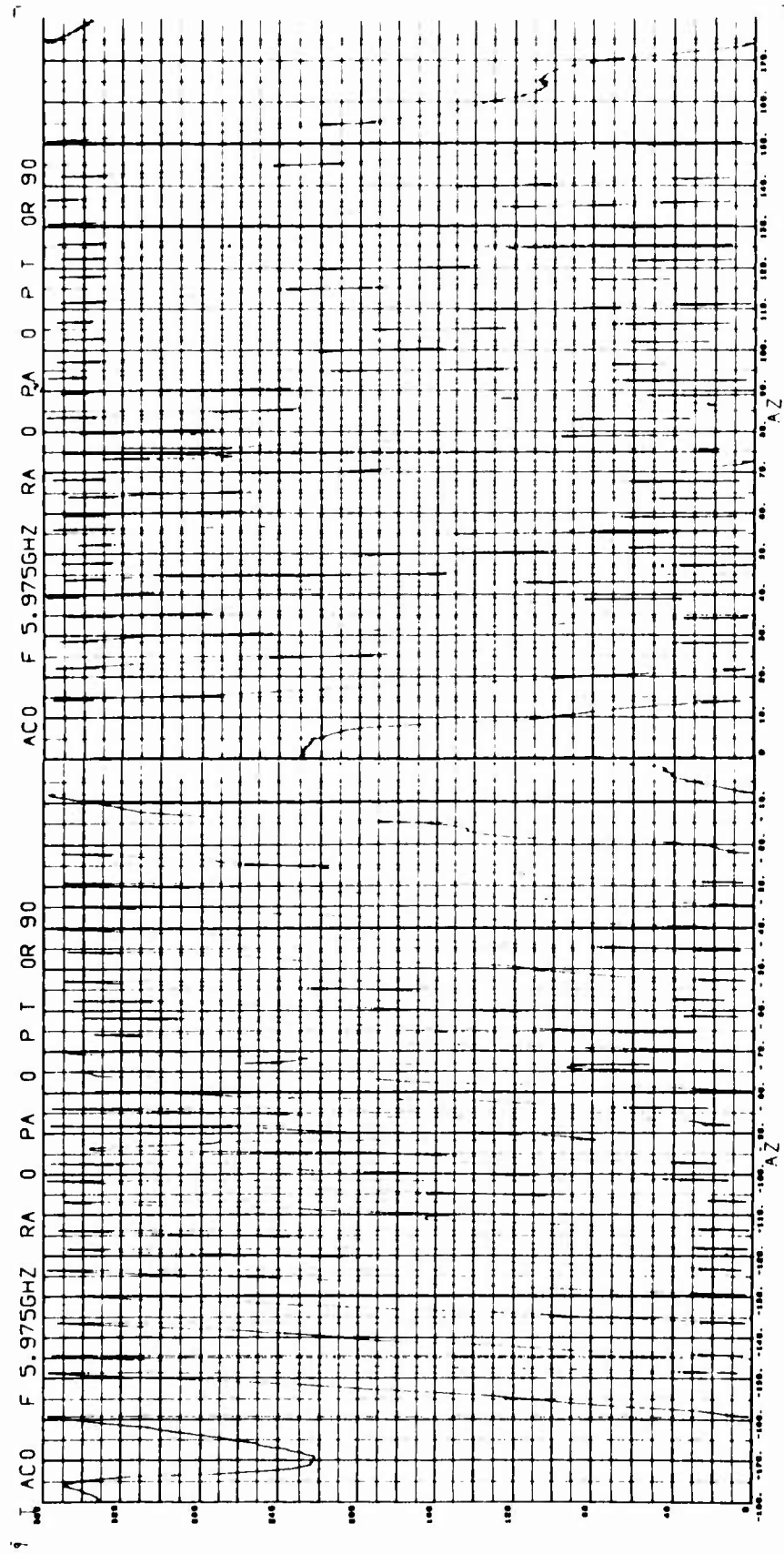
VEHICLE	MAXIMUM DIAMETER Inches	MAXIMUM LENGTH Inches	MEASUREMENT FREQUENCY GHz	BISTATIC ANGLE Degrees
COMPLEX AEROSPACE VEHICLE AC0			5.975	0
COMPLEX AEROSPACE VEHICLE AC1	7.500	52.924	5.975	0
COMPLEX AEROSPACE VEHICLE AC2	7.500	52.924	5.975	0
COMPLEX AEROSPACE VEHICLE AC3	7.500	52.924	5.975	0
COMPLEX AEROSPACE VEHICLE AC4	7.500	53.237	5.975	0
COMPLEX AEROSPACE VEHICLE AC5	7.500	53.237	5.975	0

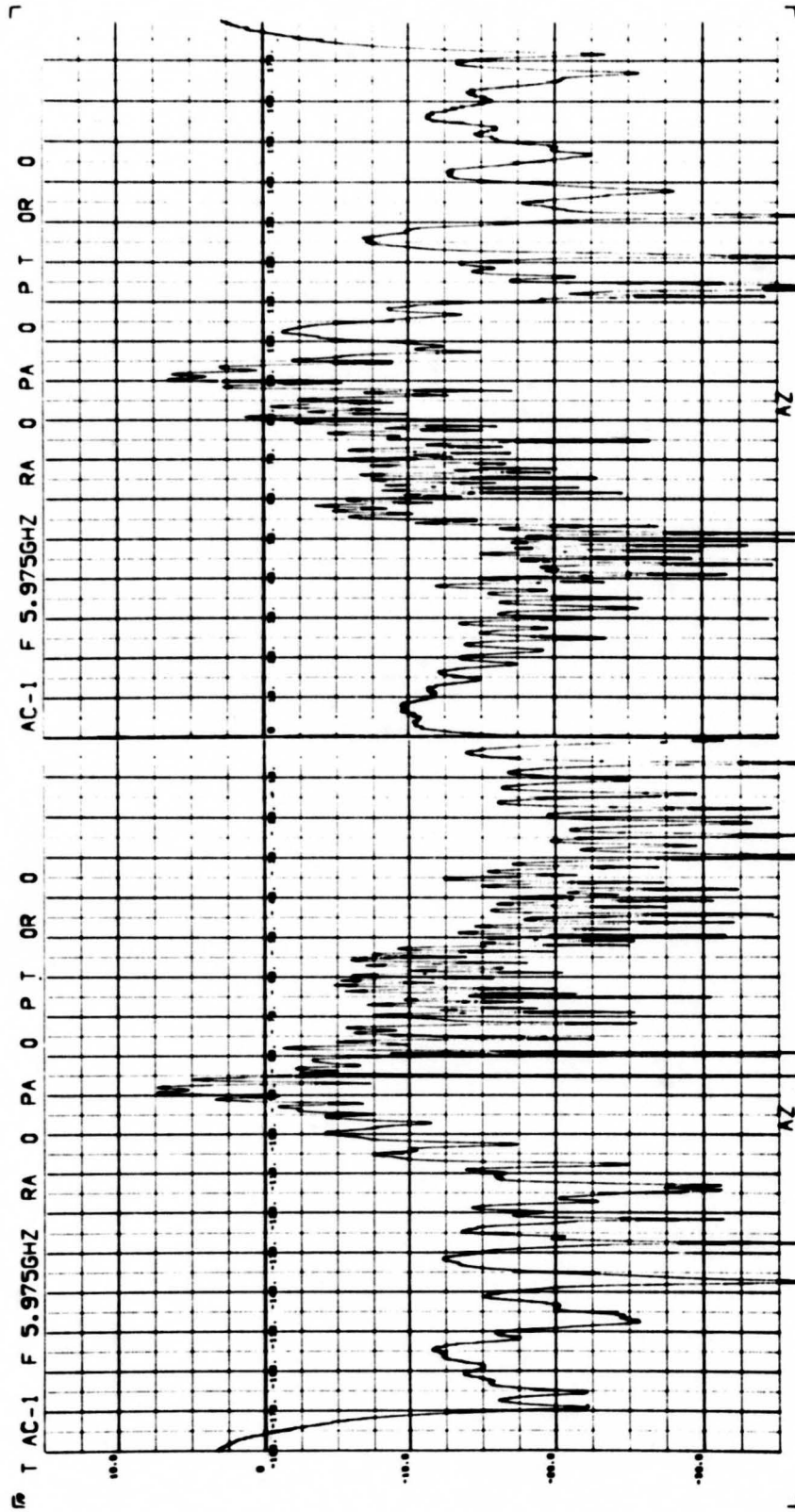


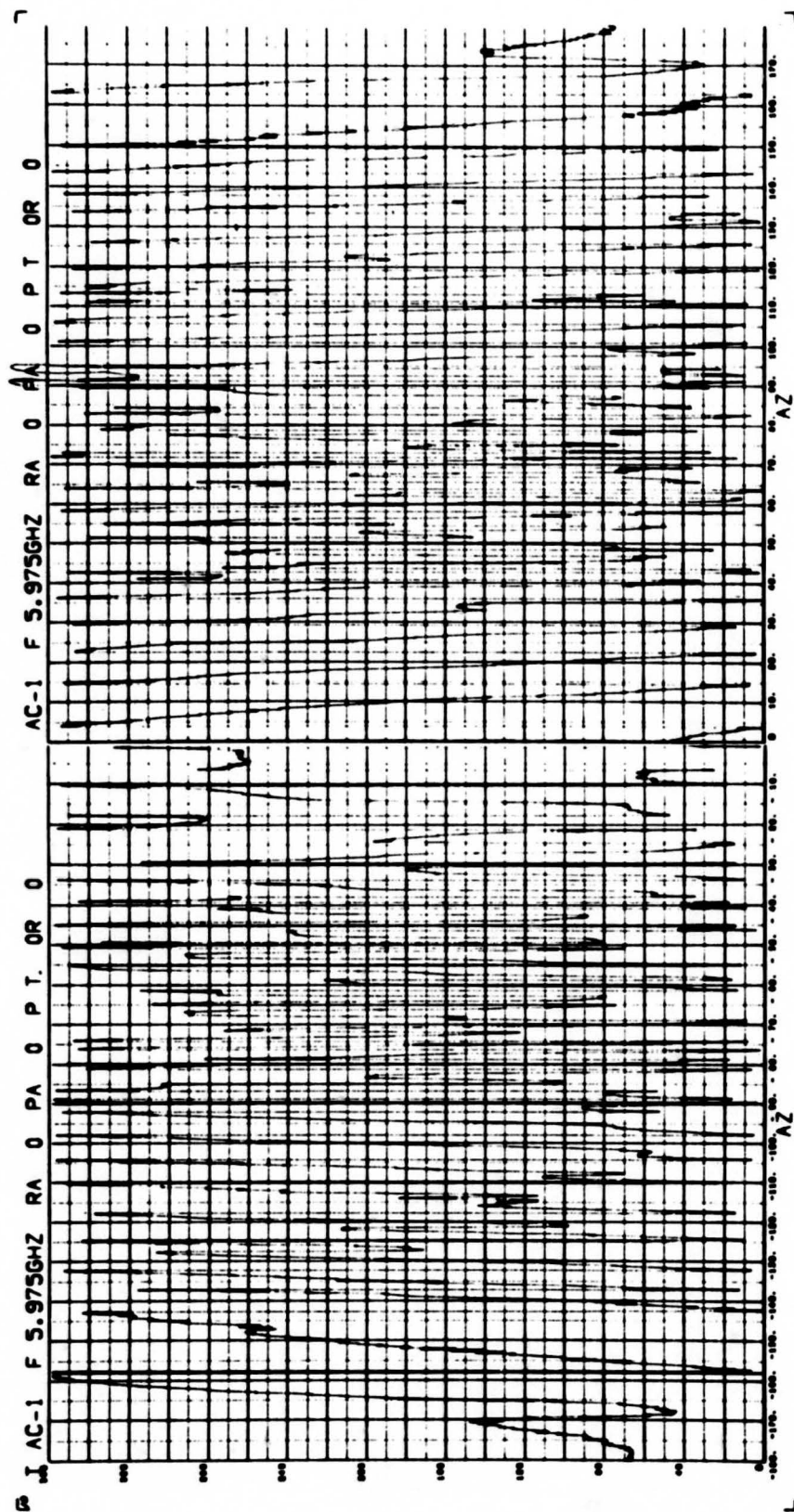


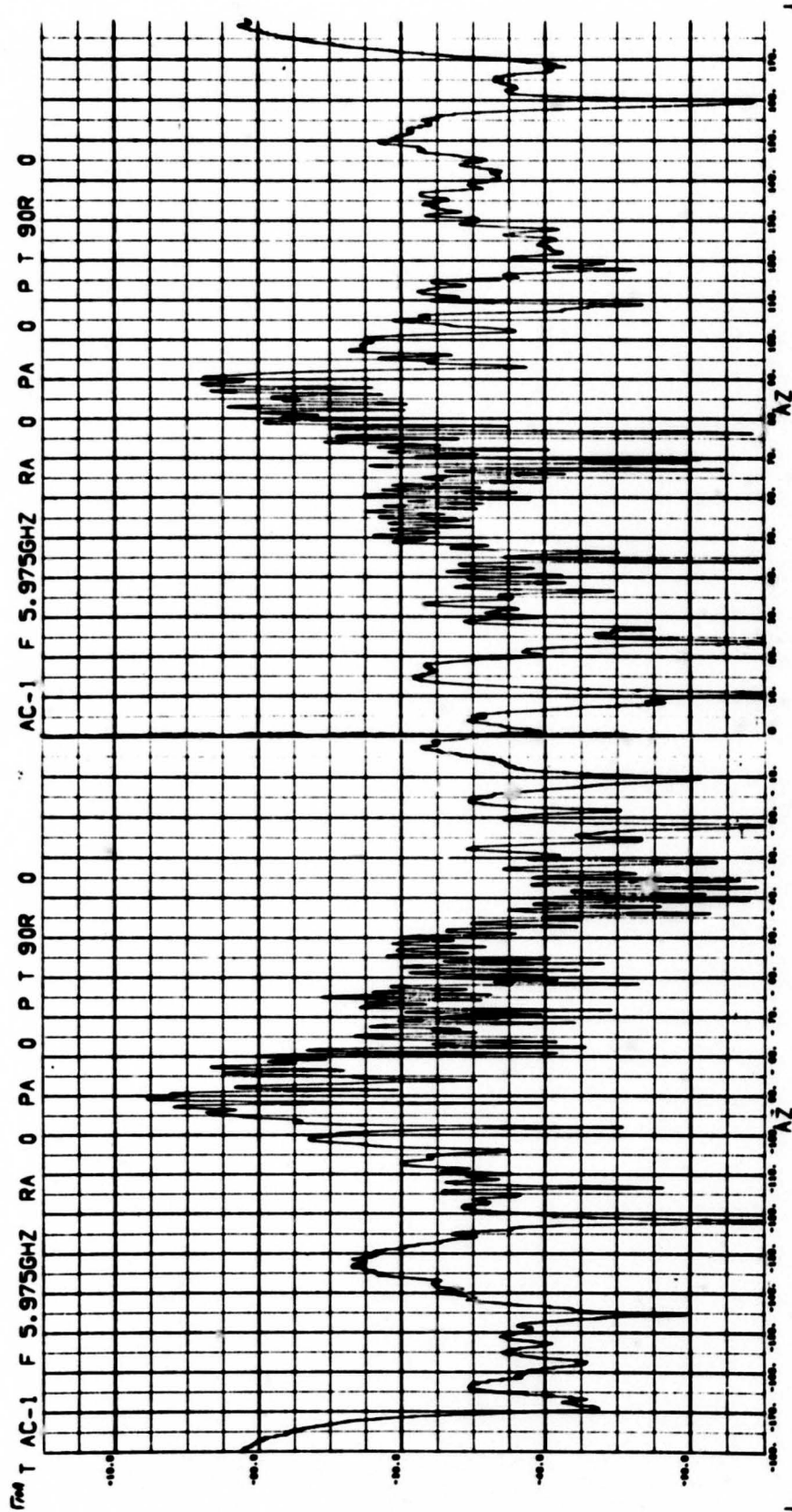


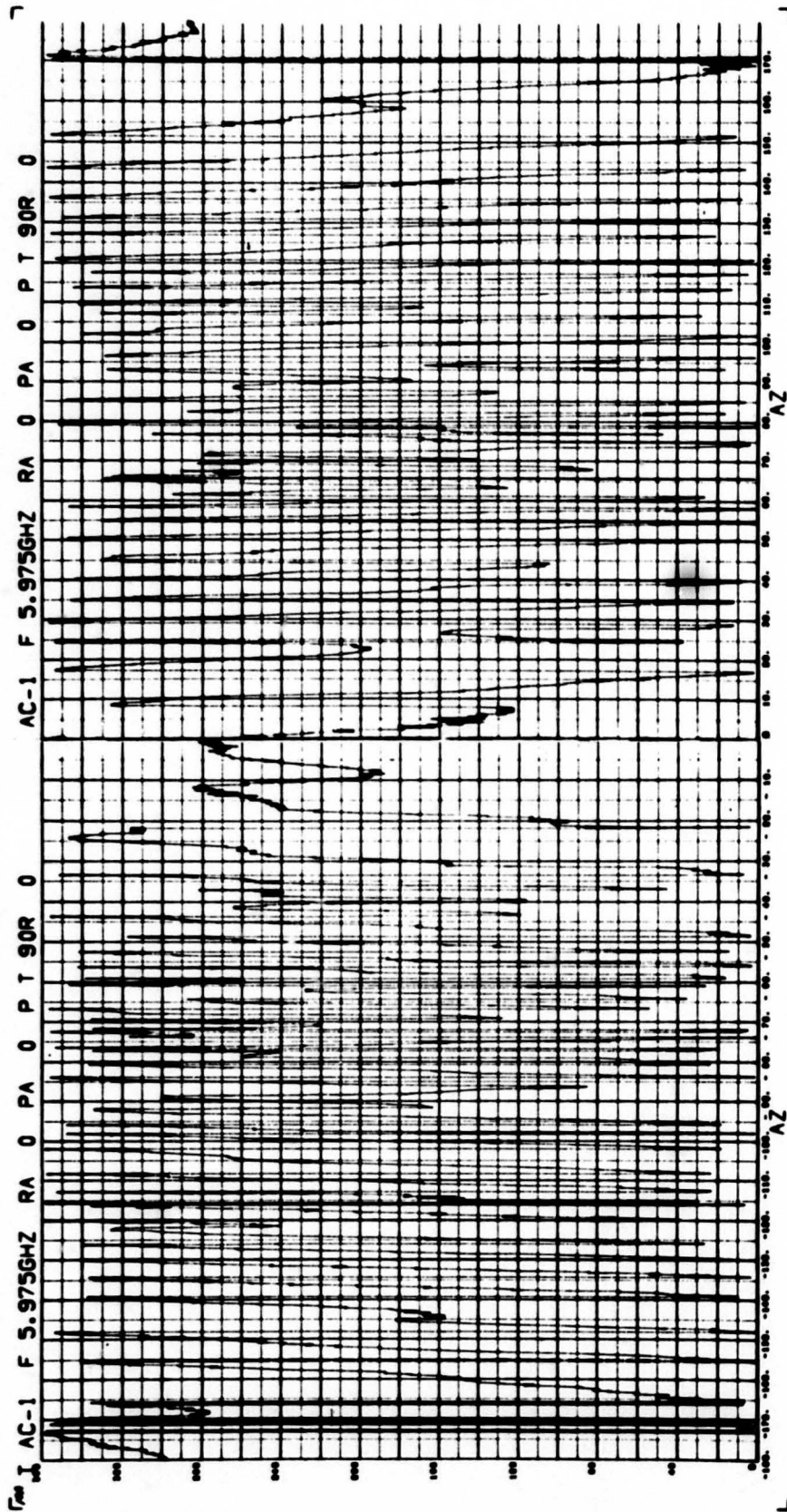


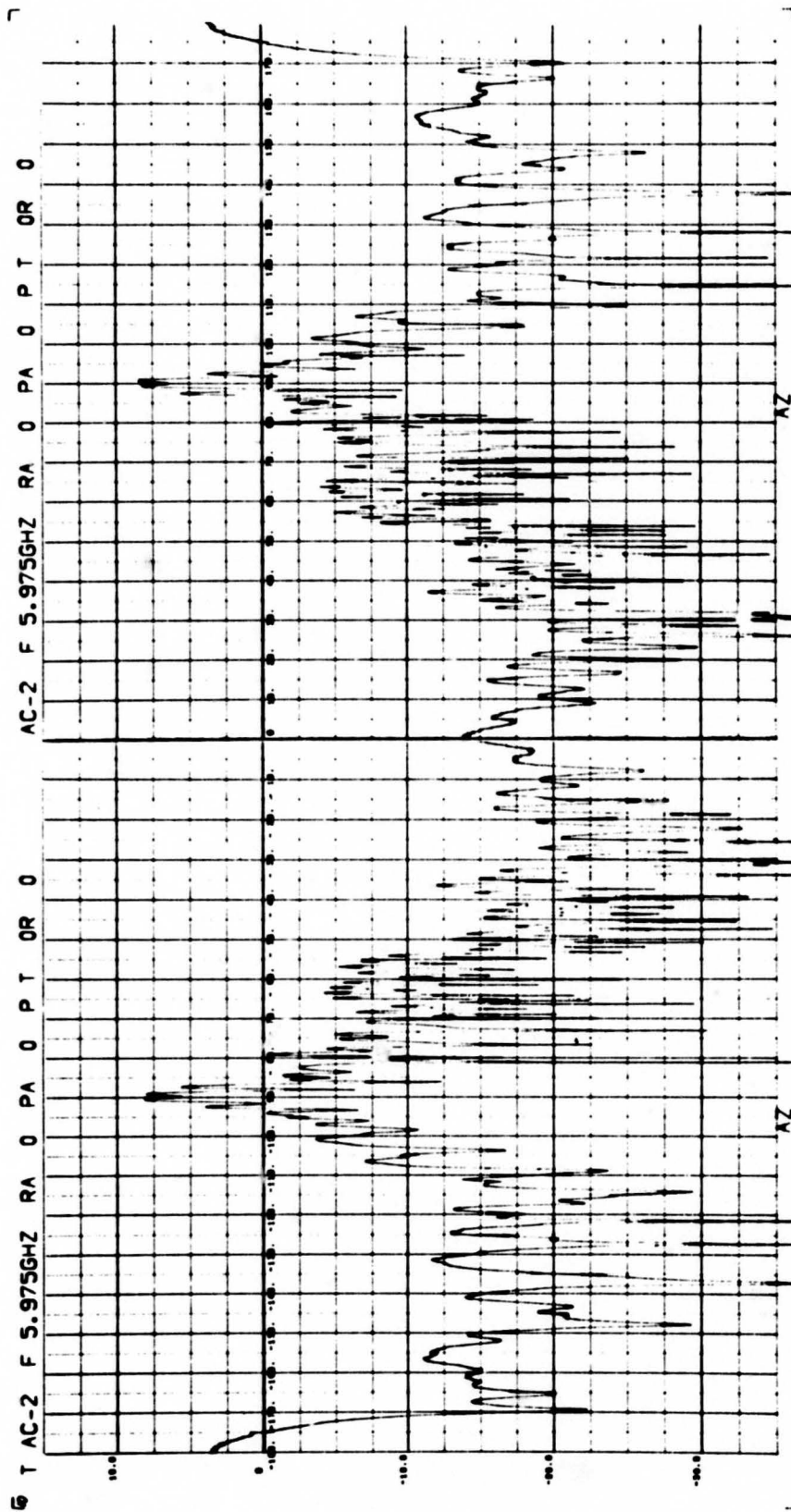


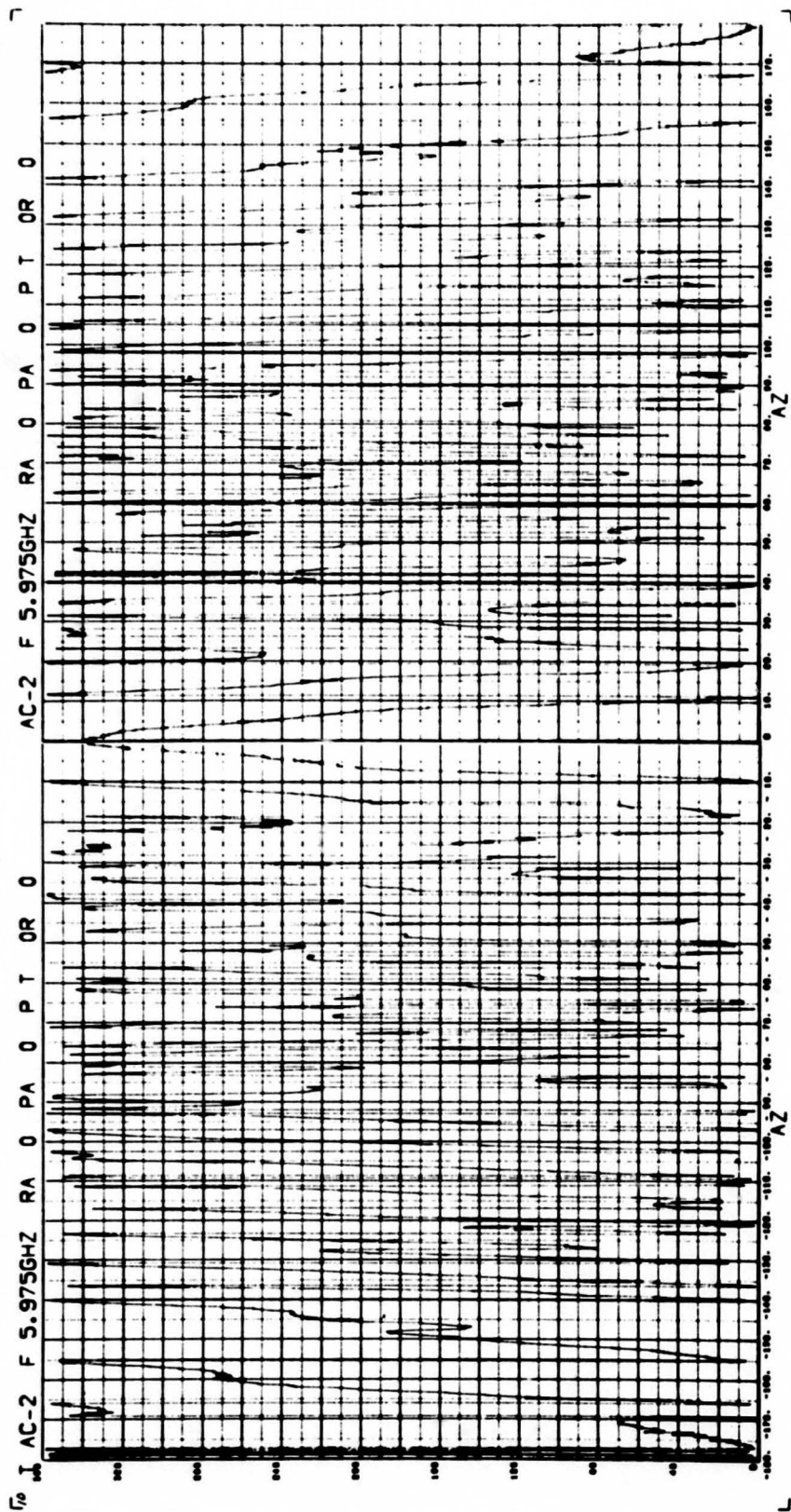


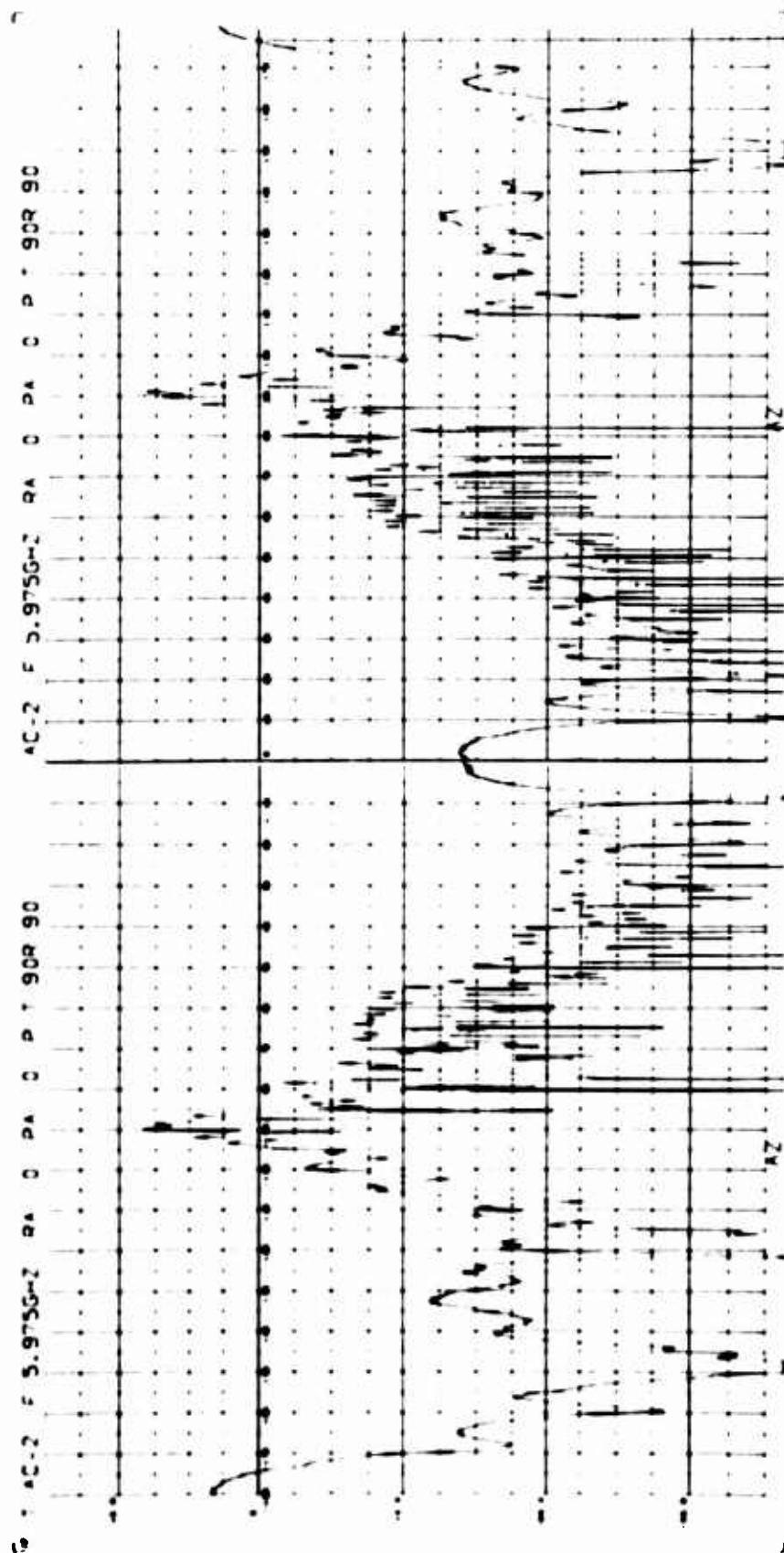


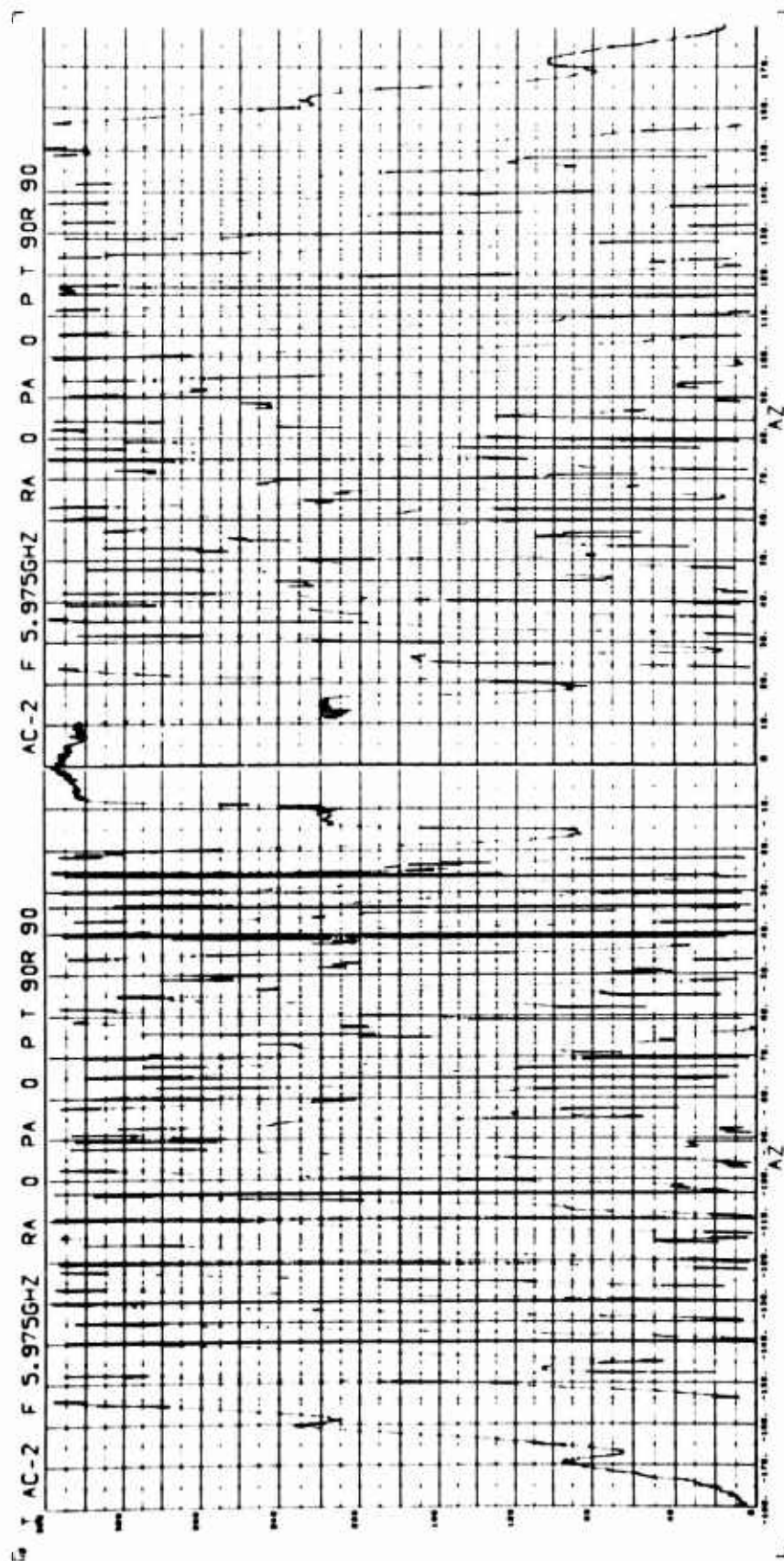


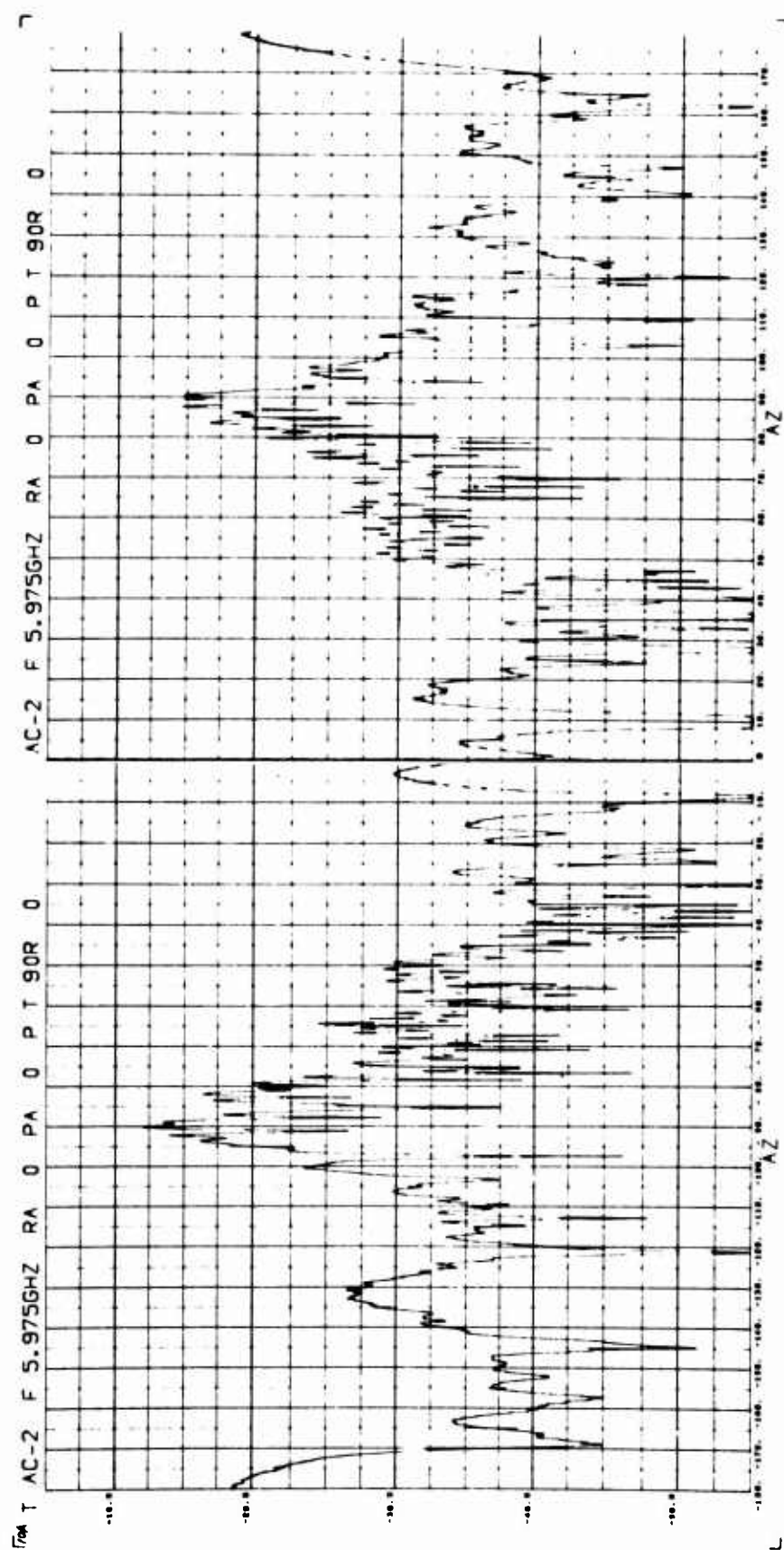


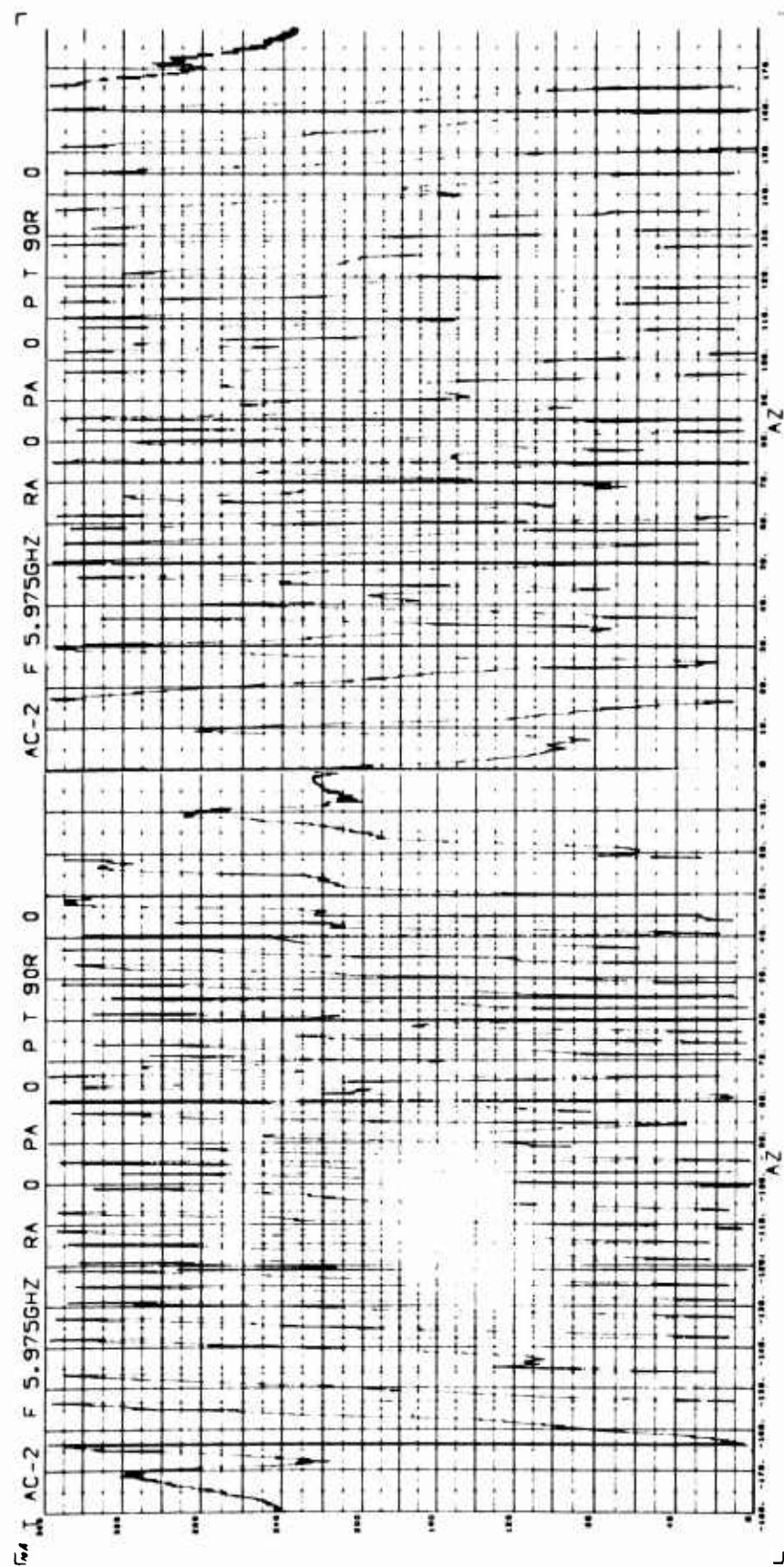


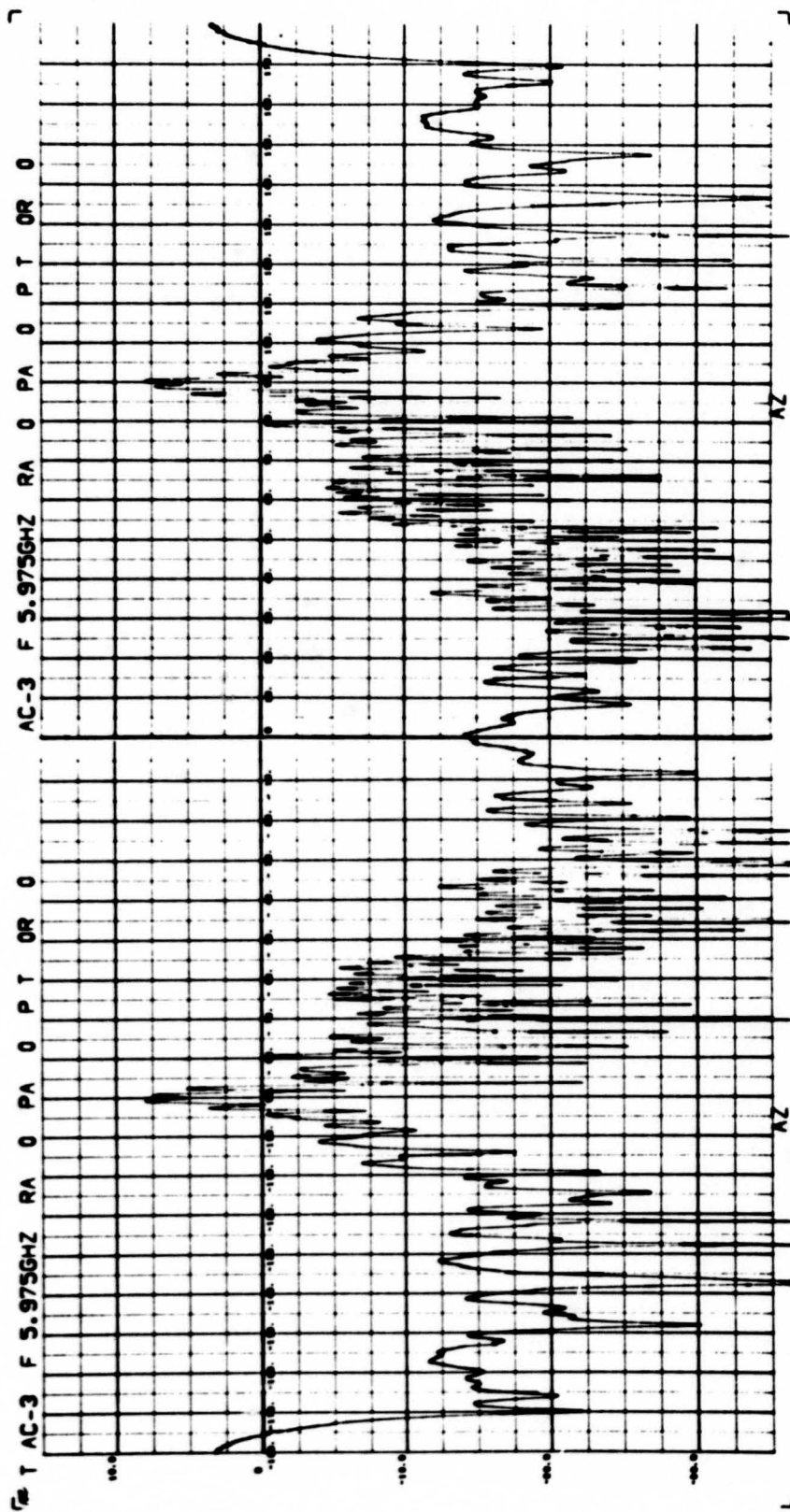


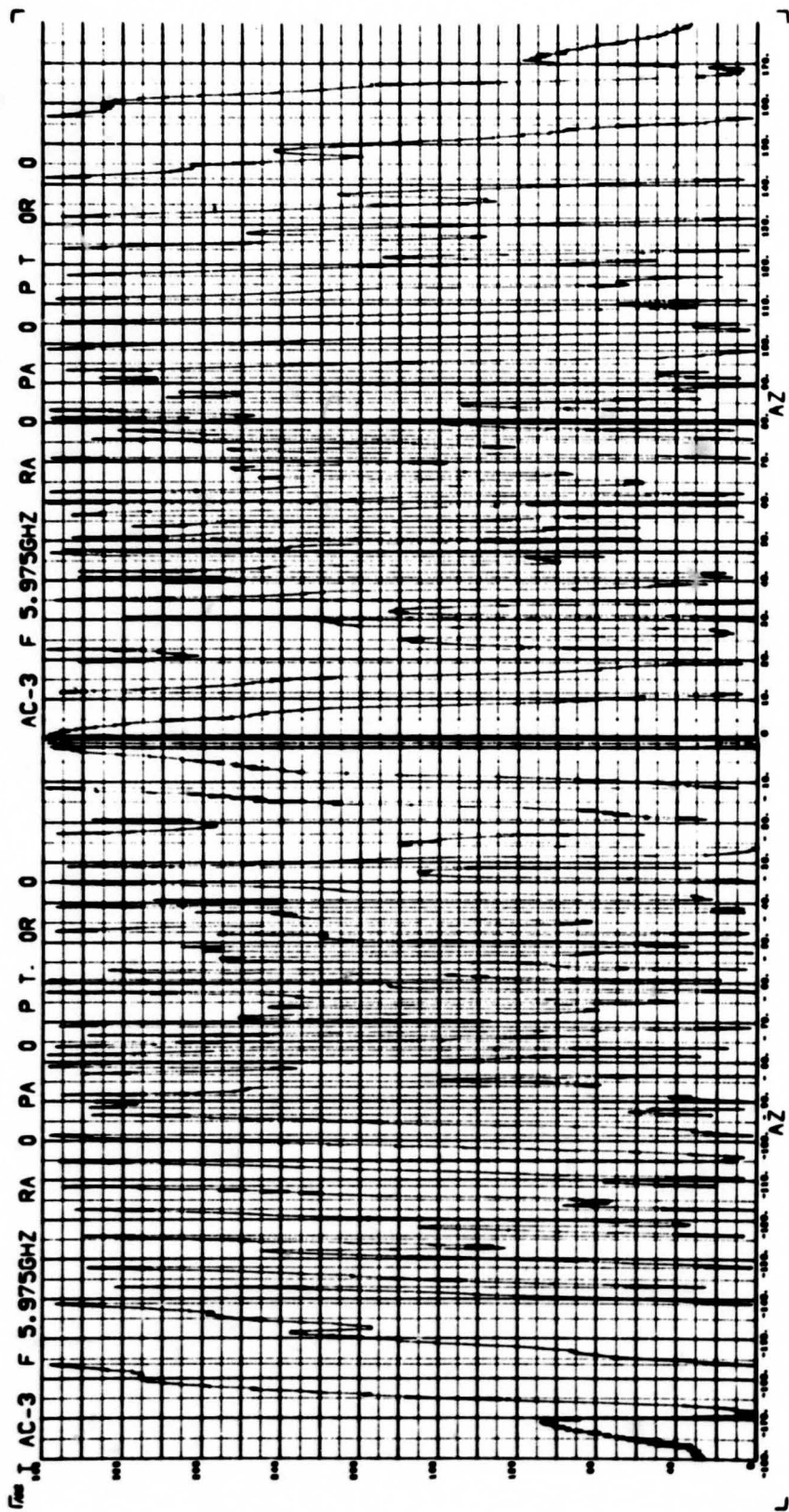


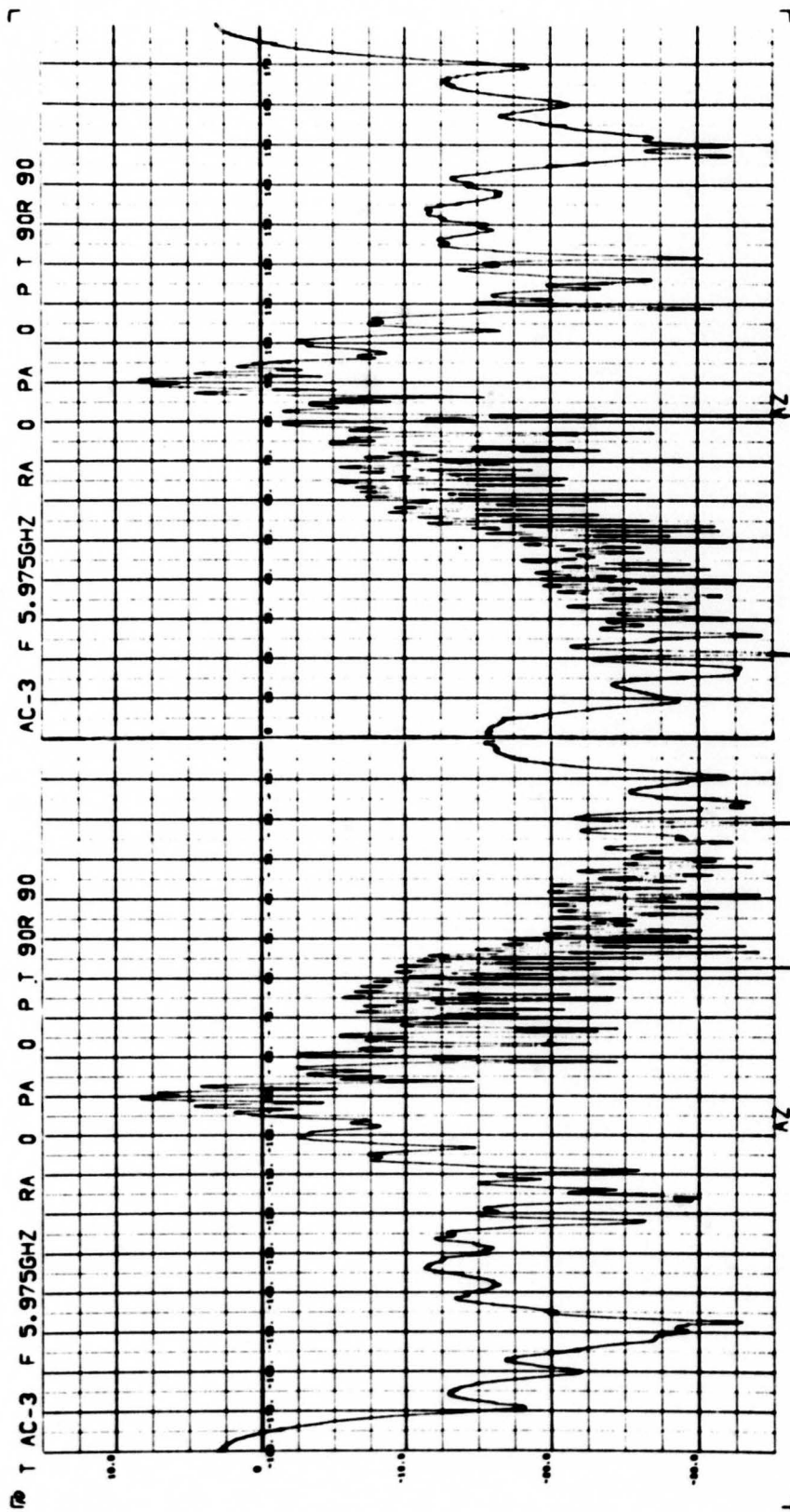


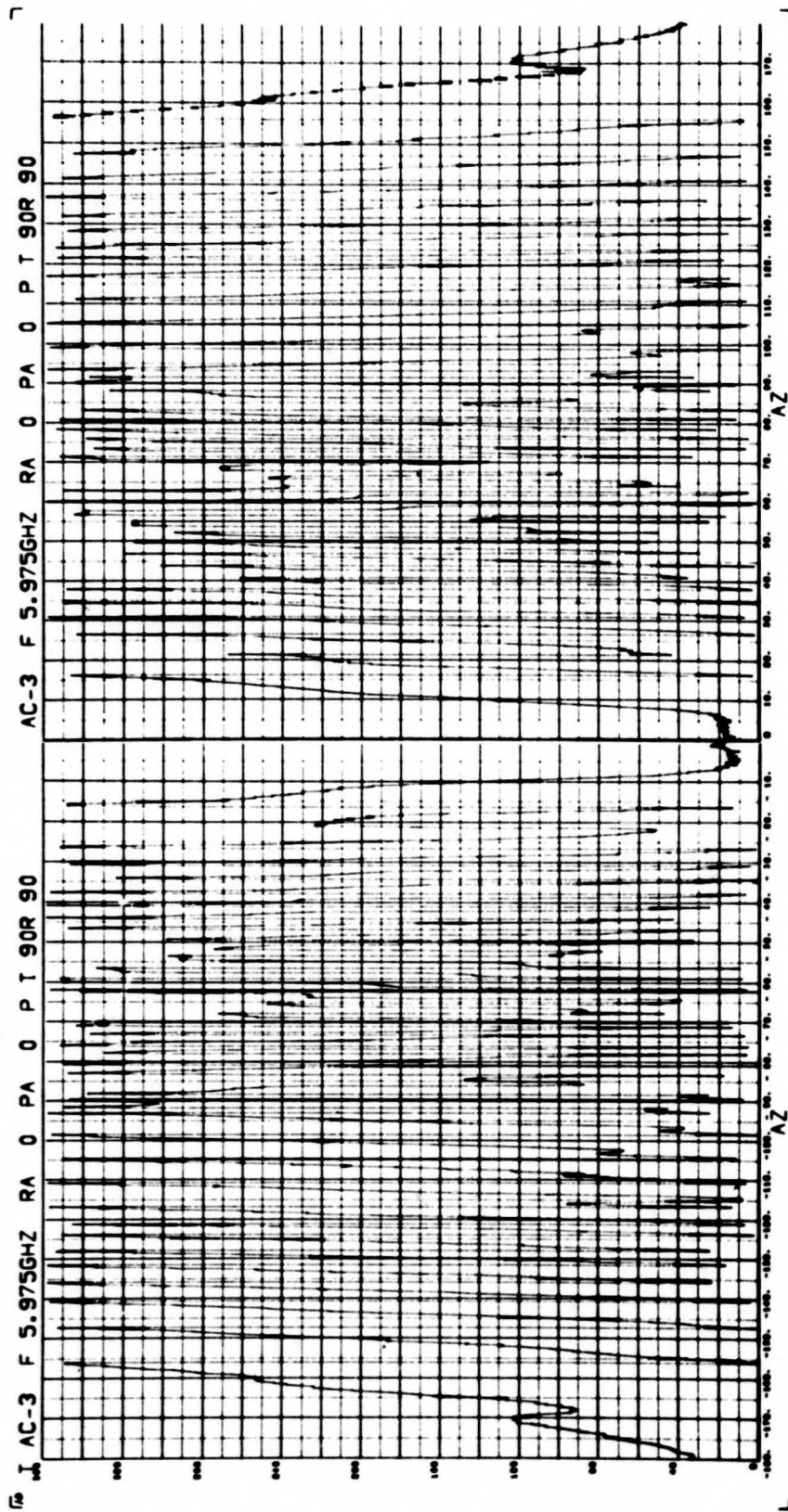




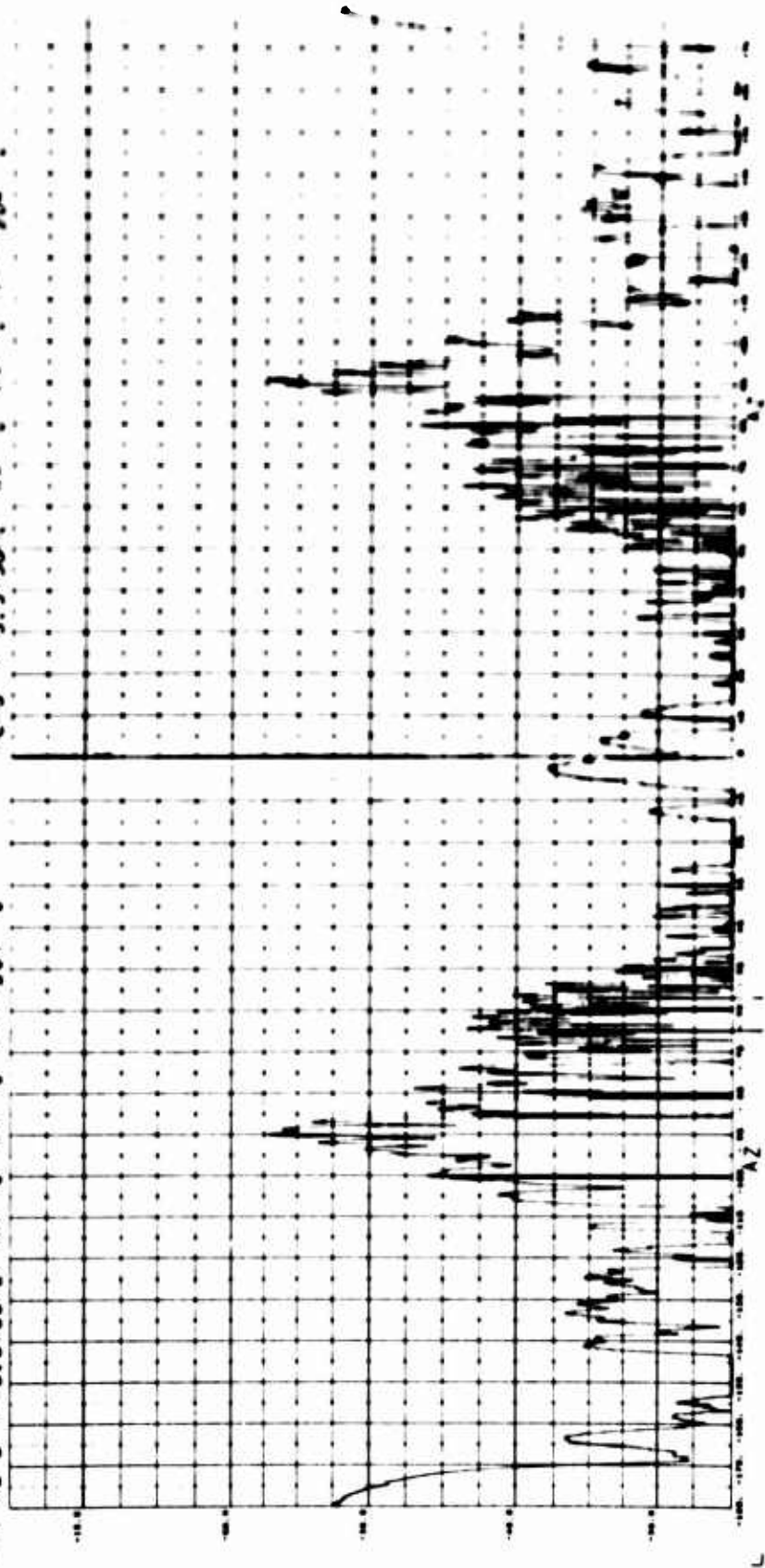


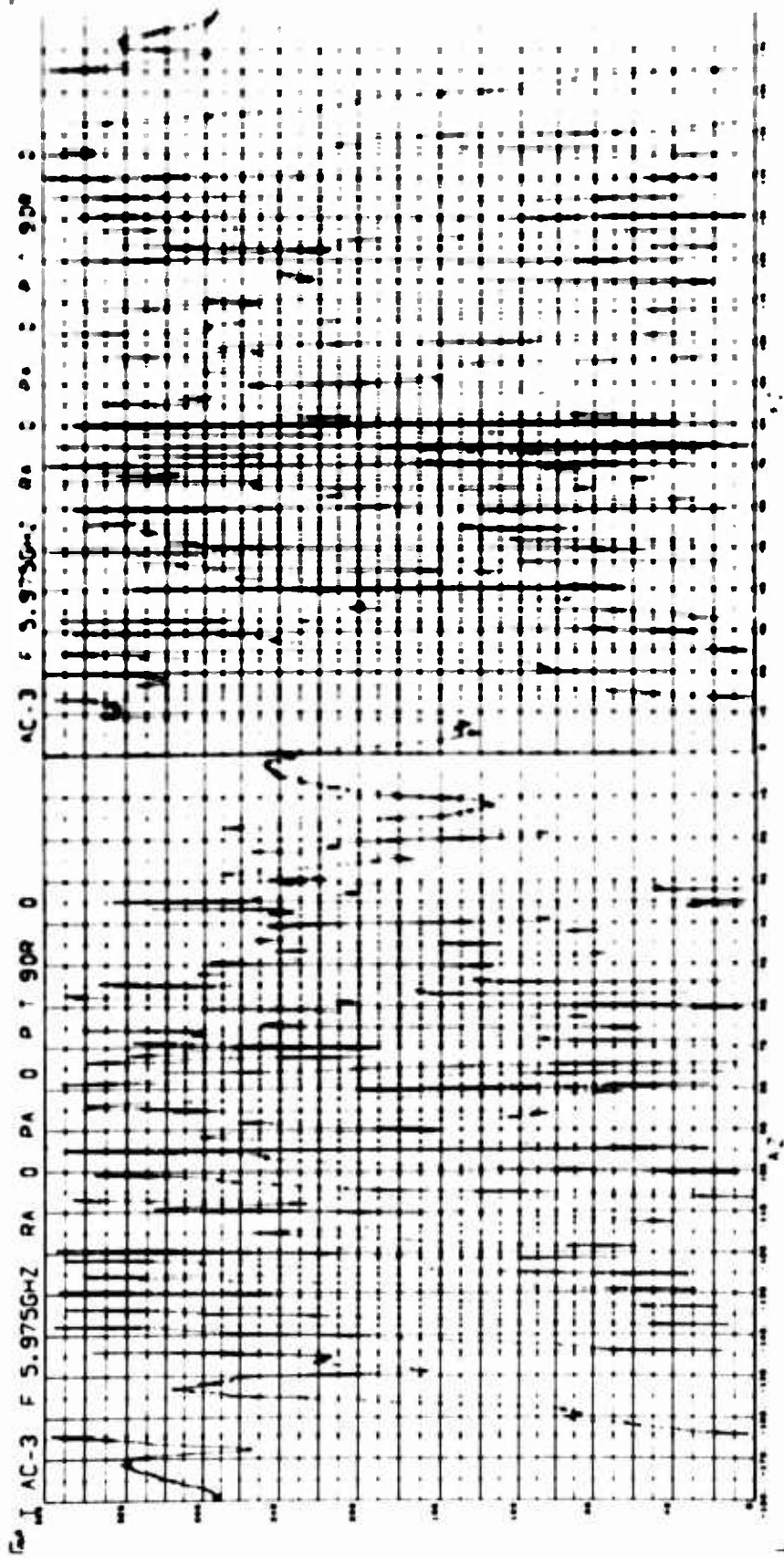




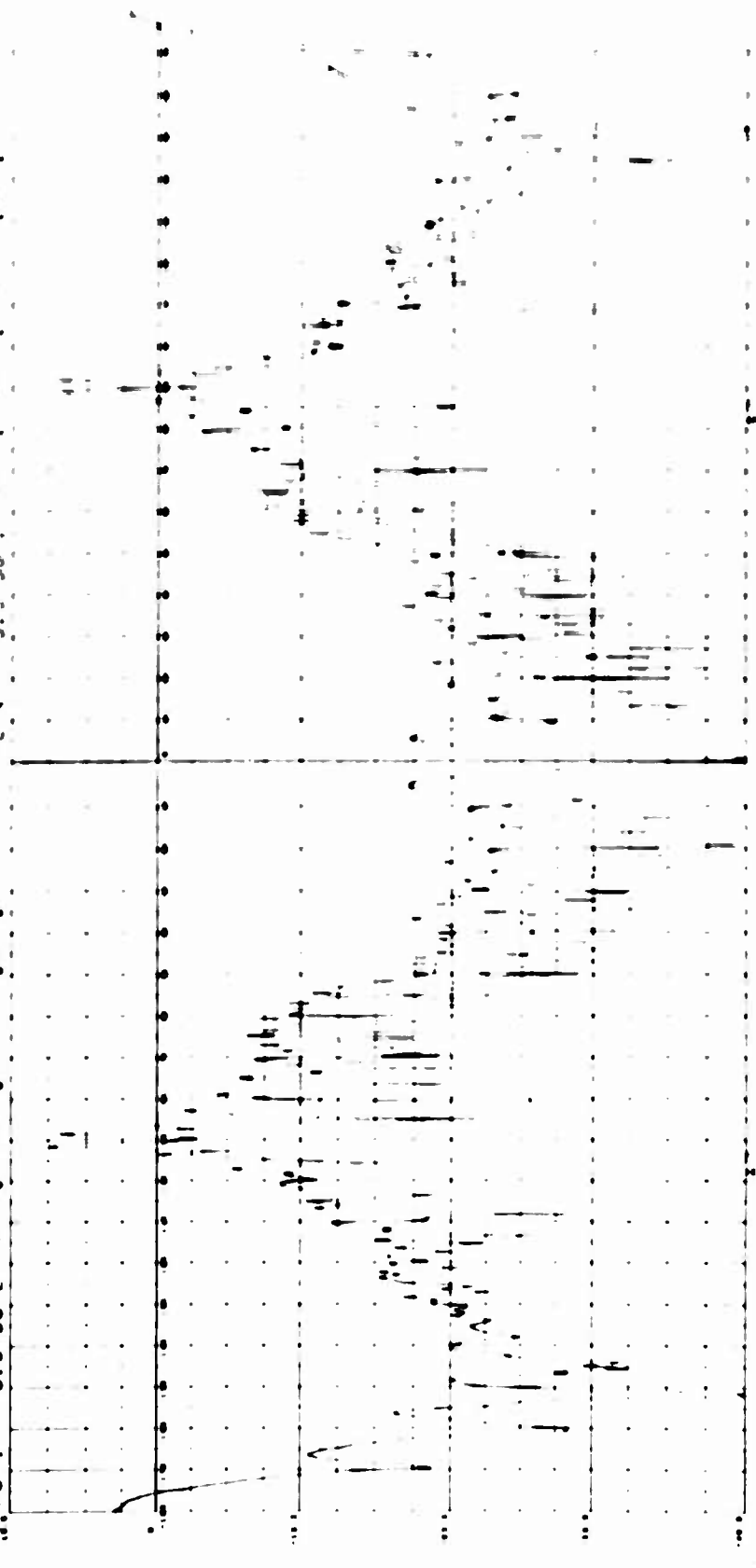


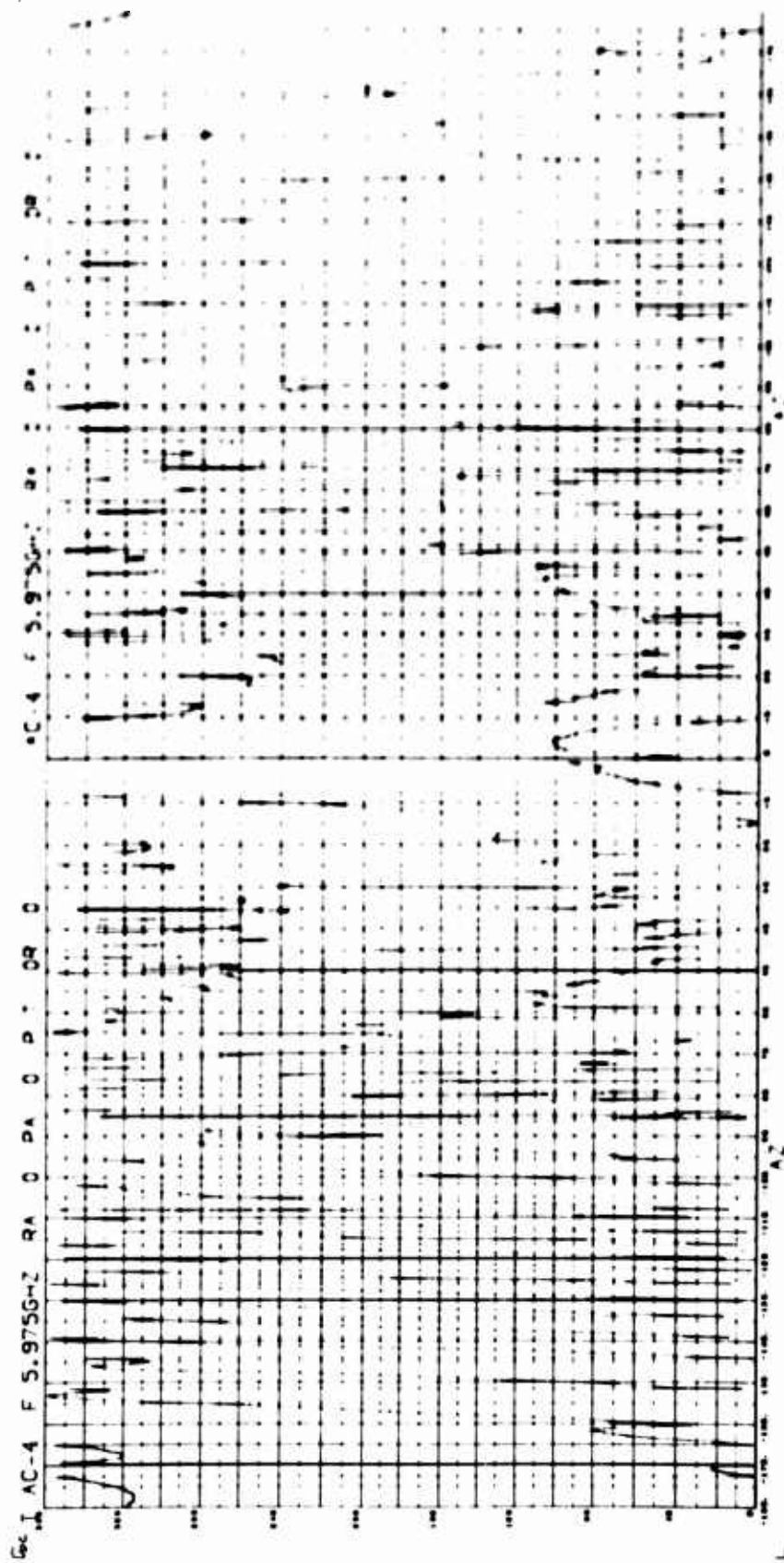
T AC-3 F 5.975GHZ RA 0 PA 0 P T 909 0 AC-3 F 5.975GHZ RA 0 PA 0 P T 909 0

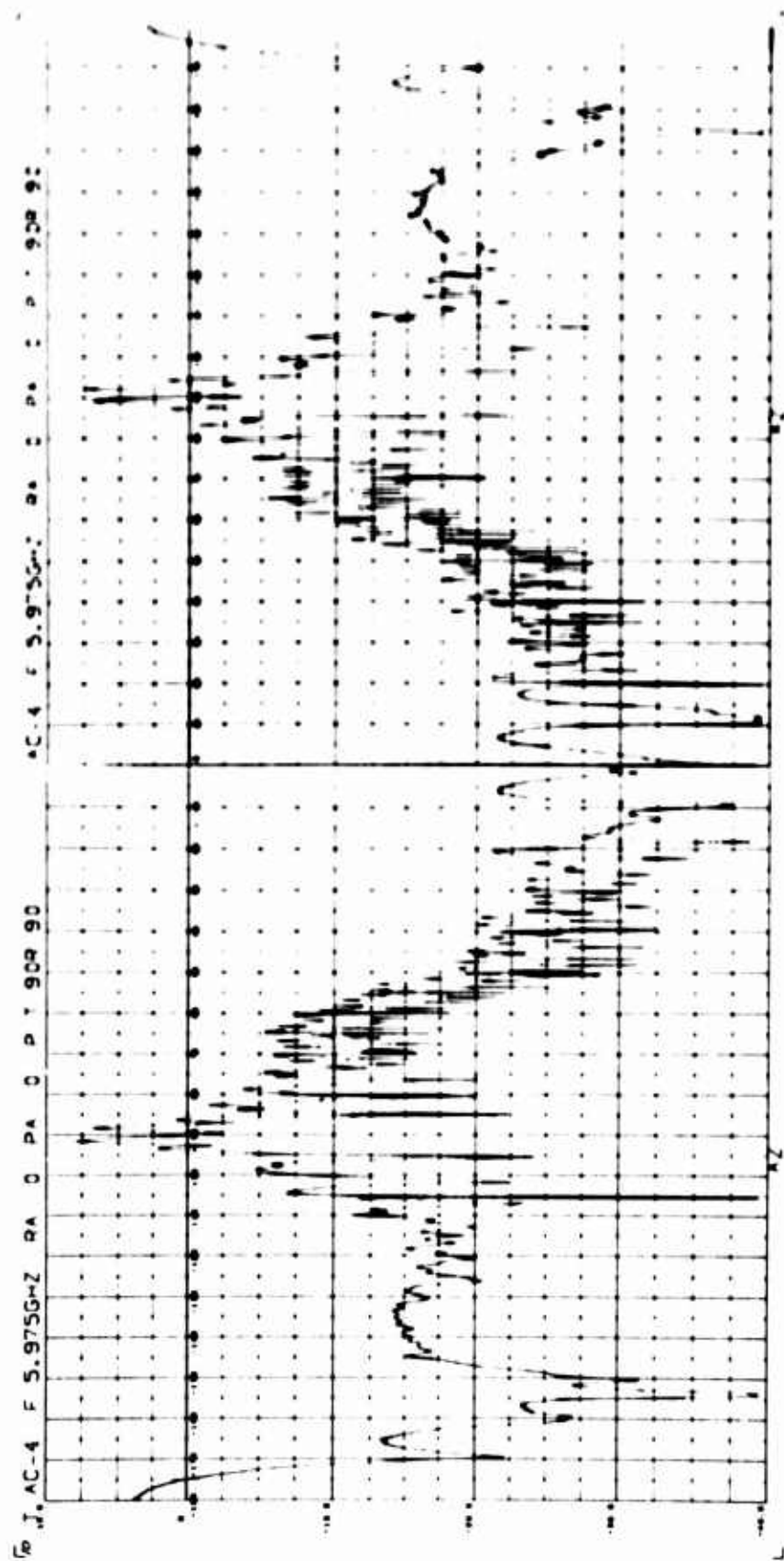


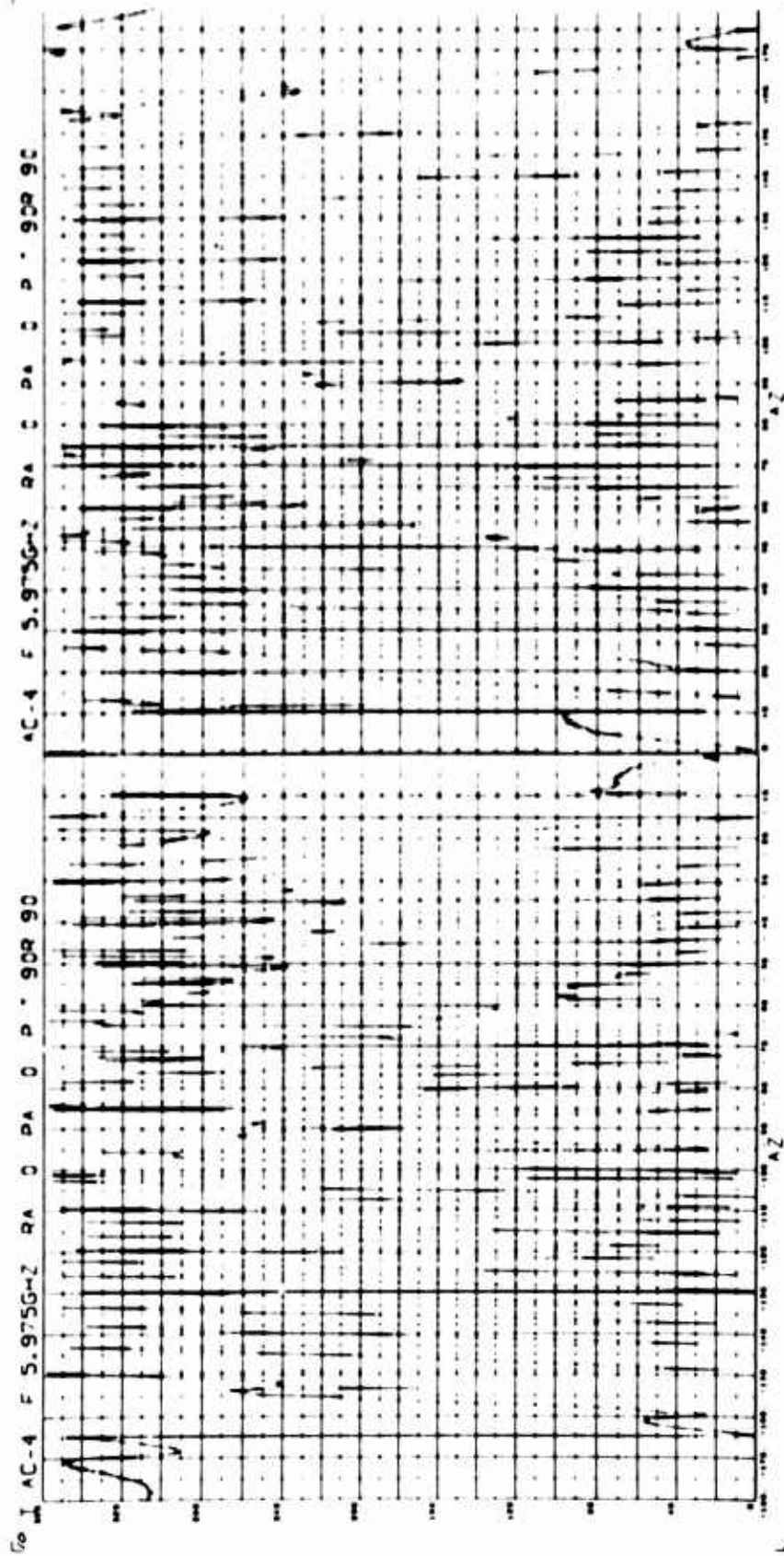


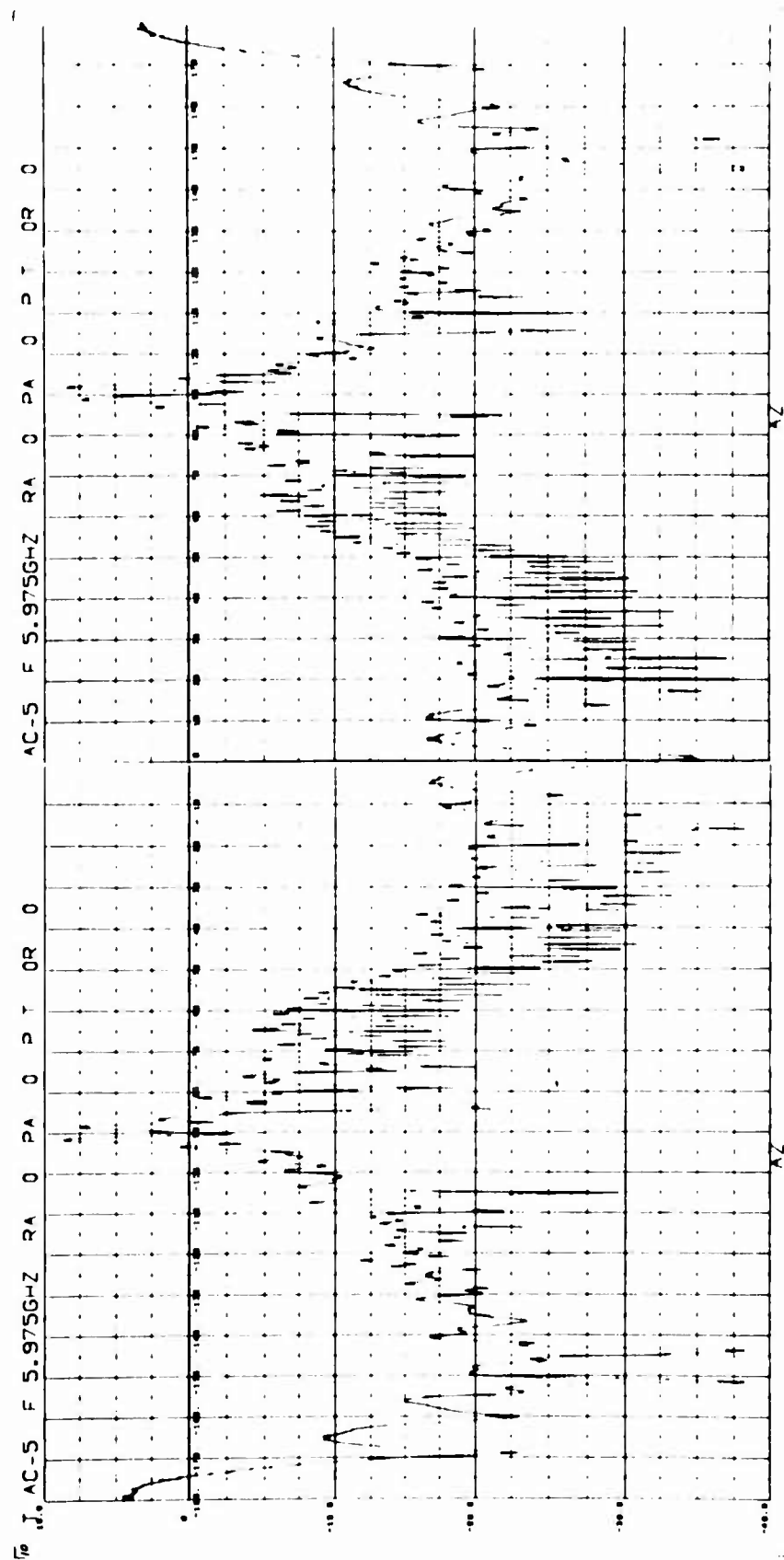
02 J, AC-4 F 5.9"SG-2 RA 0 PA 0 P 0 02 0
 02 4 0.9"SG-2 RA 0 PA 0 P 0 02 0

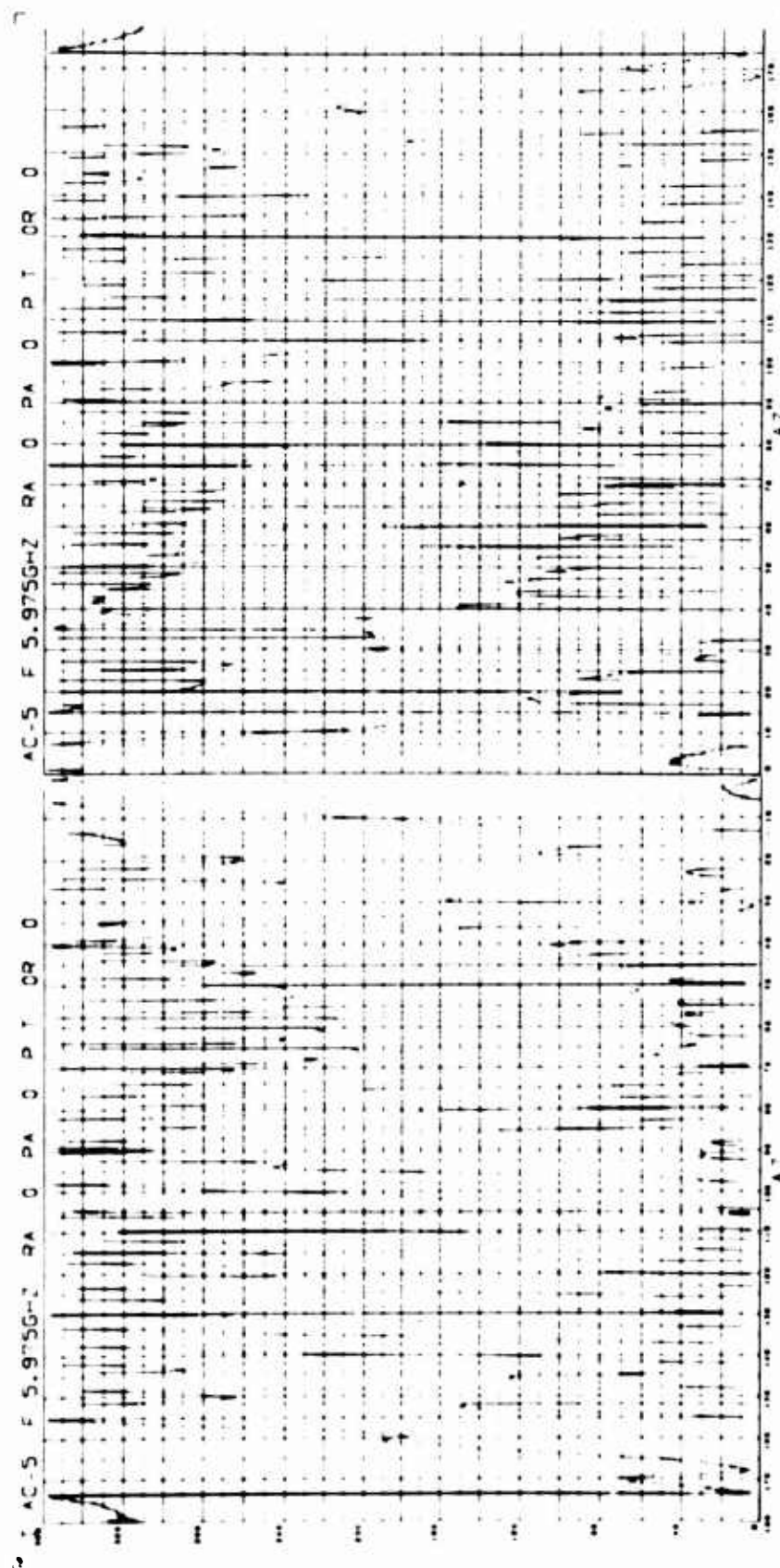


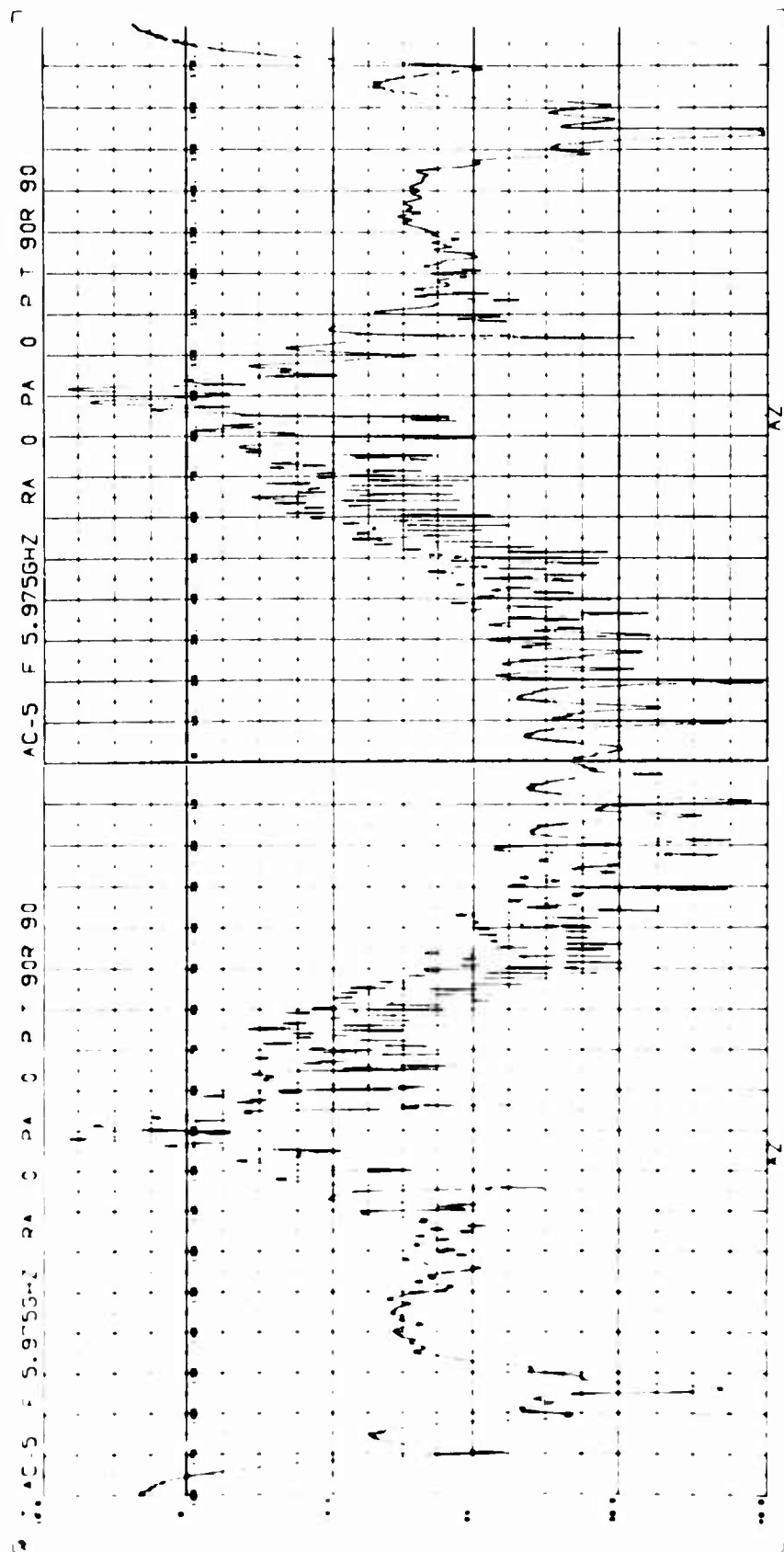


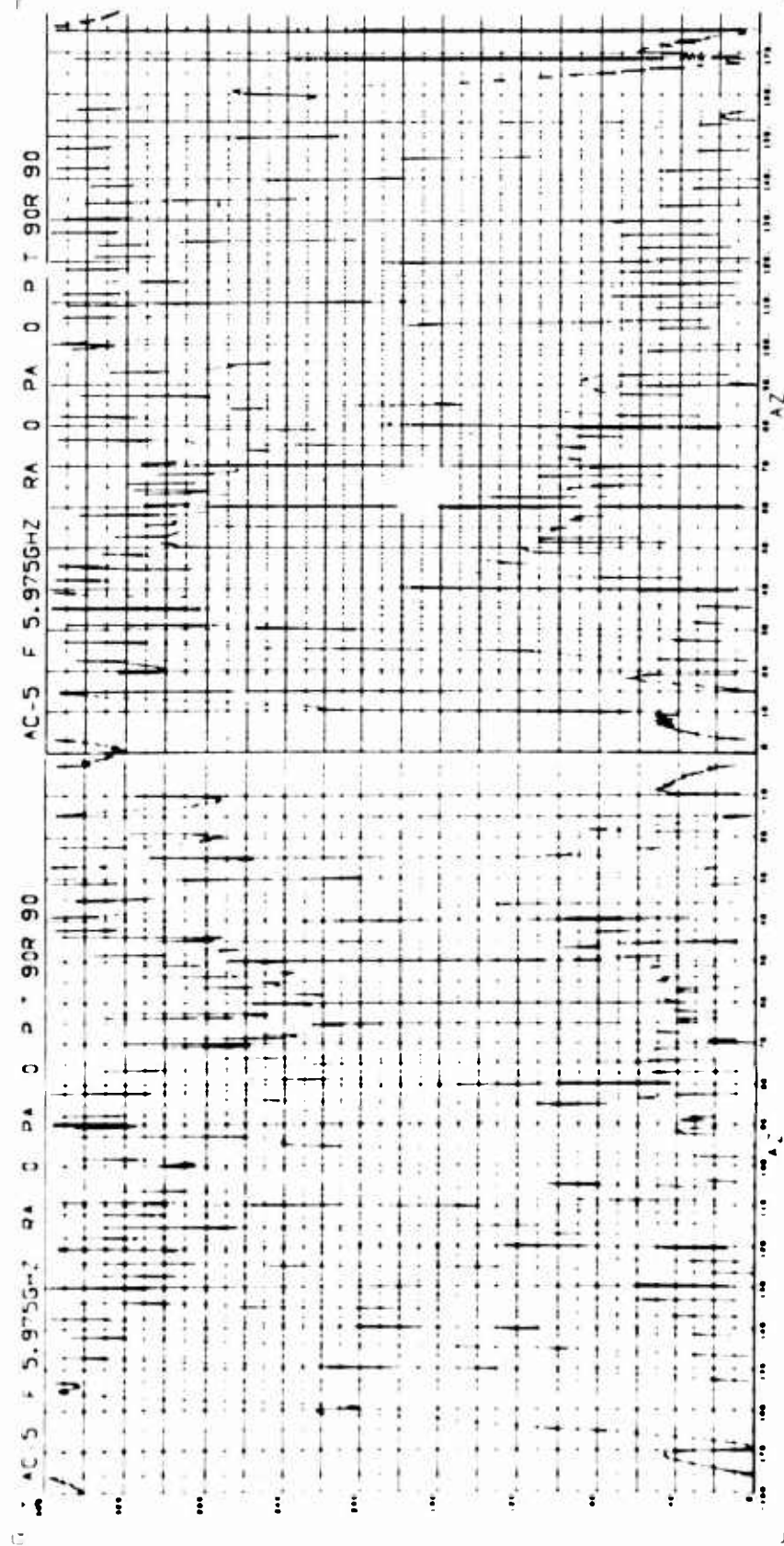












3.2.5 Scientific Satellite Vehicles

Two vehicle models which are representative of scientific satellites were measured at both S- and C-band. These measurements are described in Table 3-6. Figure 3-4 contains photographs of the models used to obtain this data.

Table 3-6

SCIENTIFIC SATELLITE MEASUREMENTS

VEHICLE	DESIGNATION	MAXIMUM DIAMETER Inches	MINIMUM DIAMETER Inches	MAXIMUM LENGTH Inches	MEASUREMENT FREQUENCY GHz	BISTATIC ANGLE Degrees
SCIENTIFIC SATELLITE X1	H3F1CR1H2	6.320	1.500	15.636	3.0 5.95	0 0
SCIENTIFIC SATELLITE X2	C3F1CR1AR2CR2H3	6.320	1.500	20.660	3.0 5.95	0 0

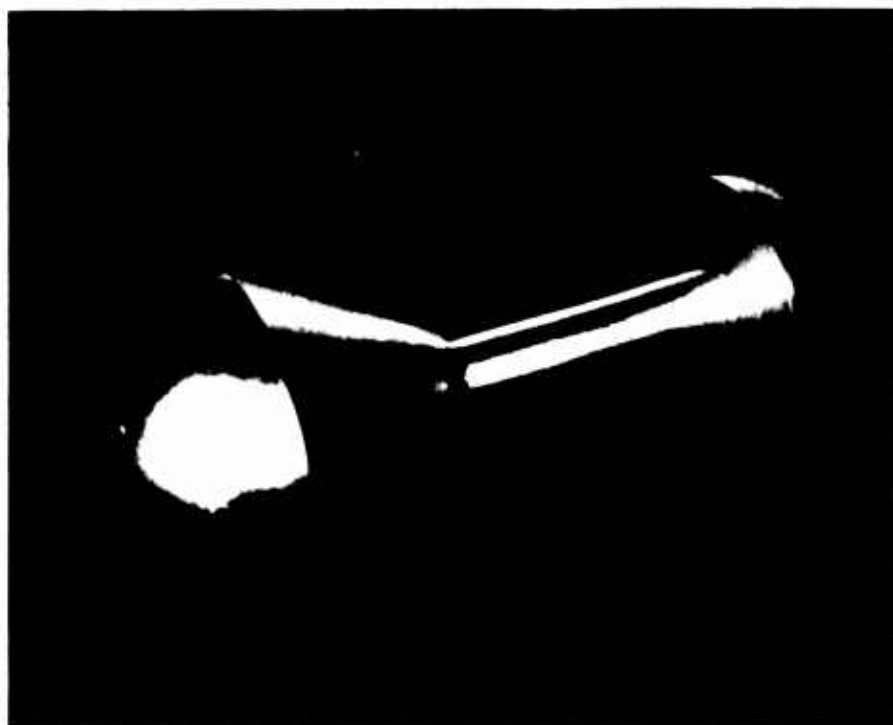
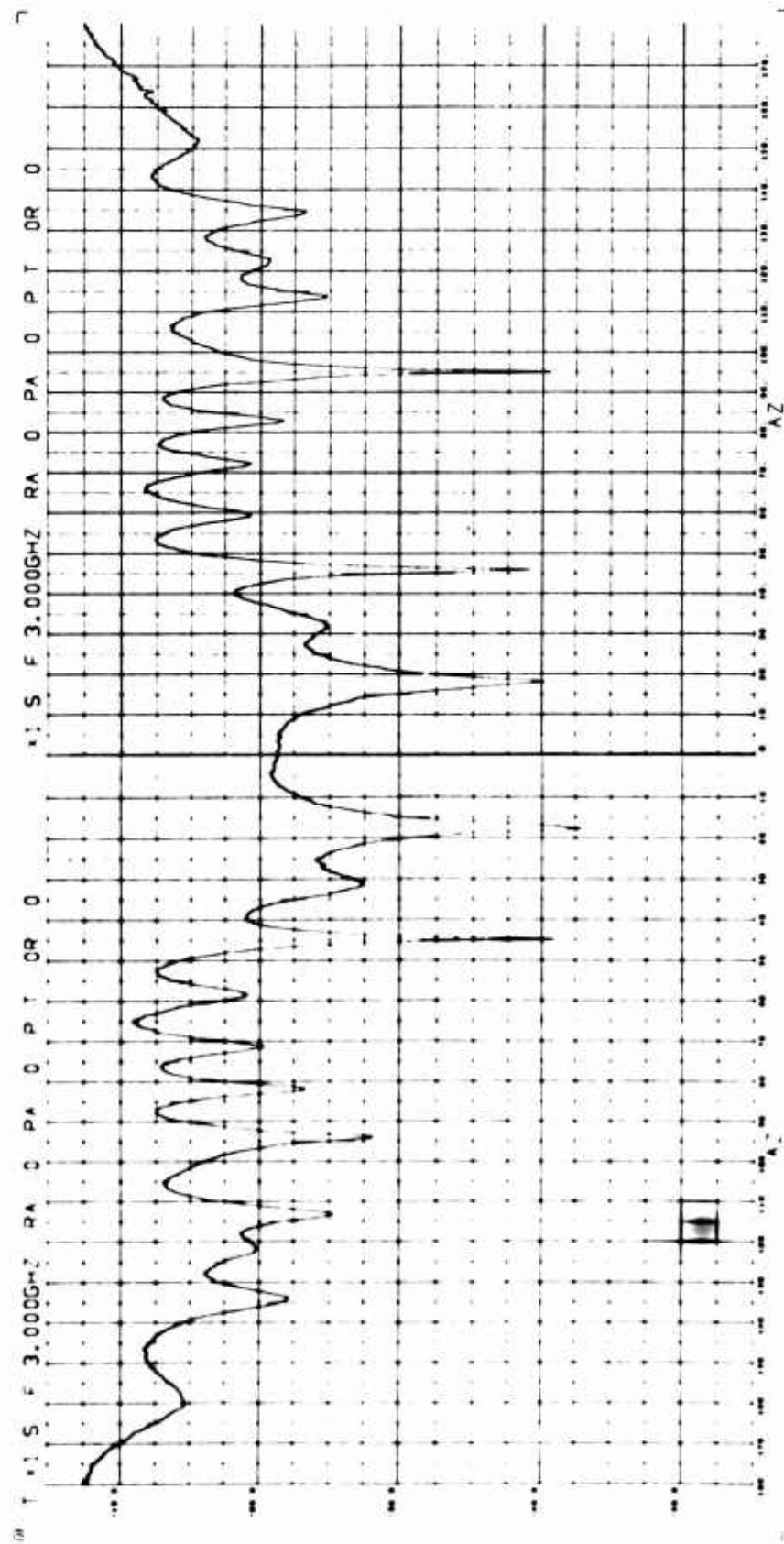
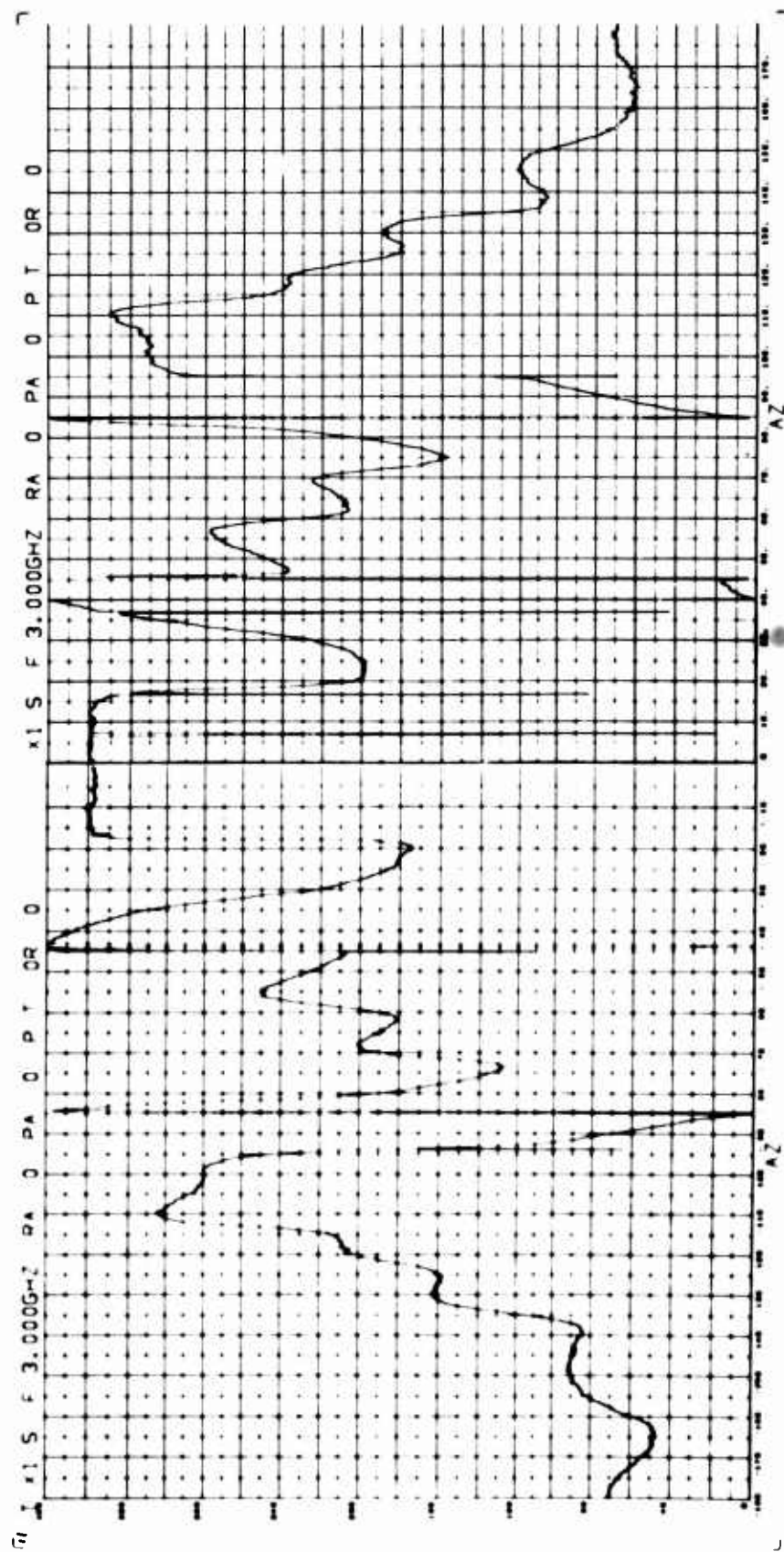
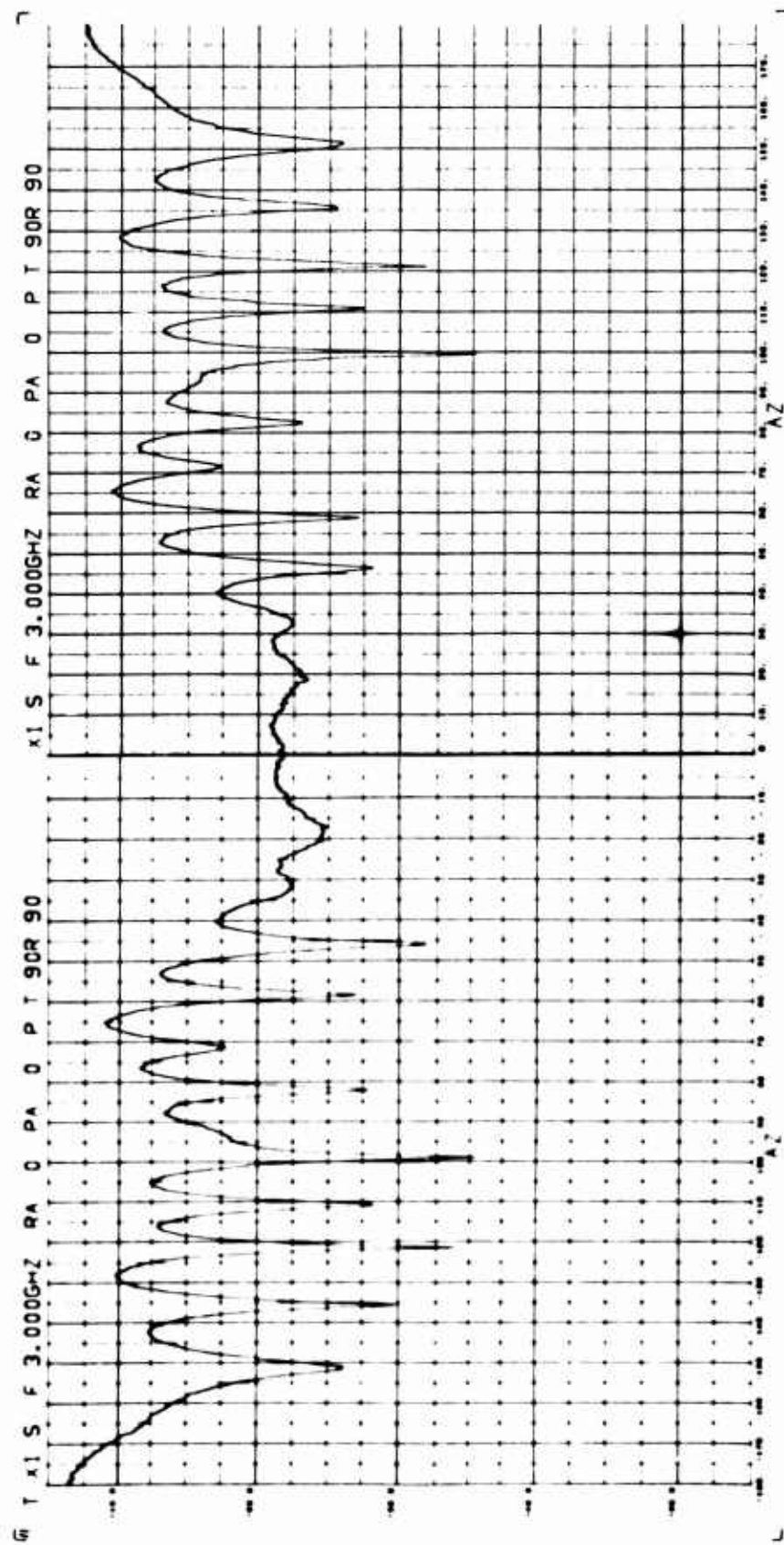
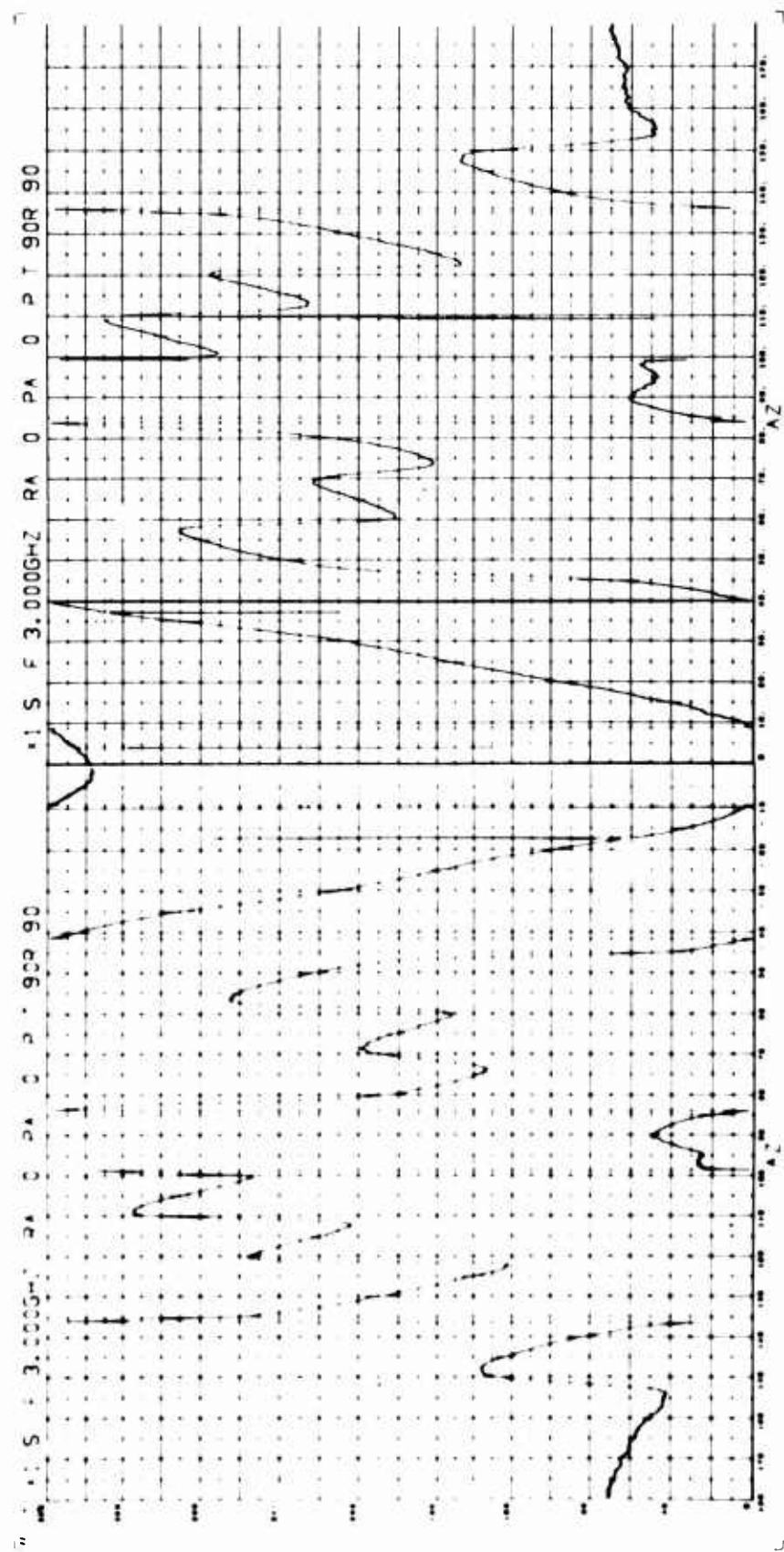


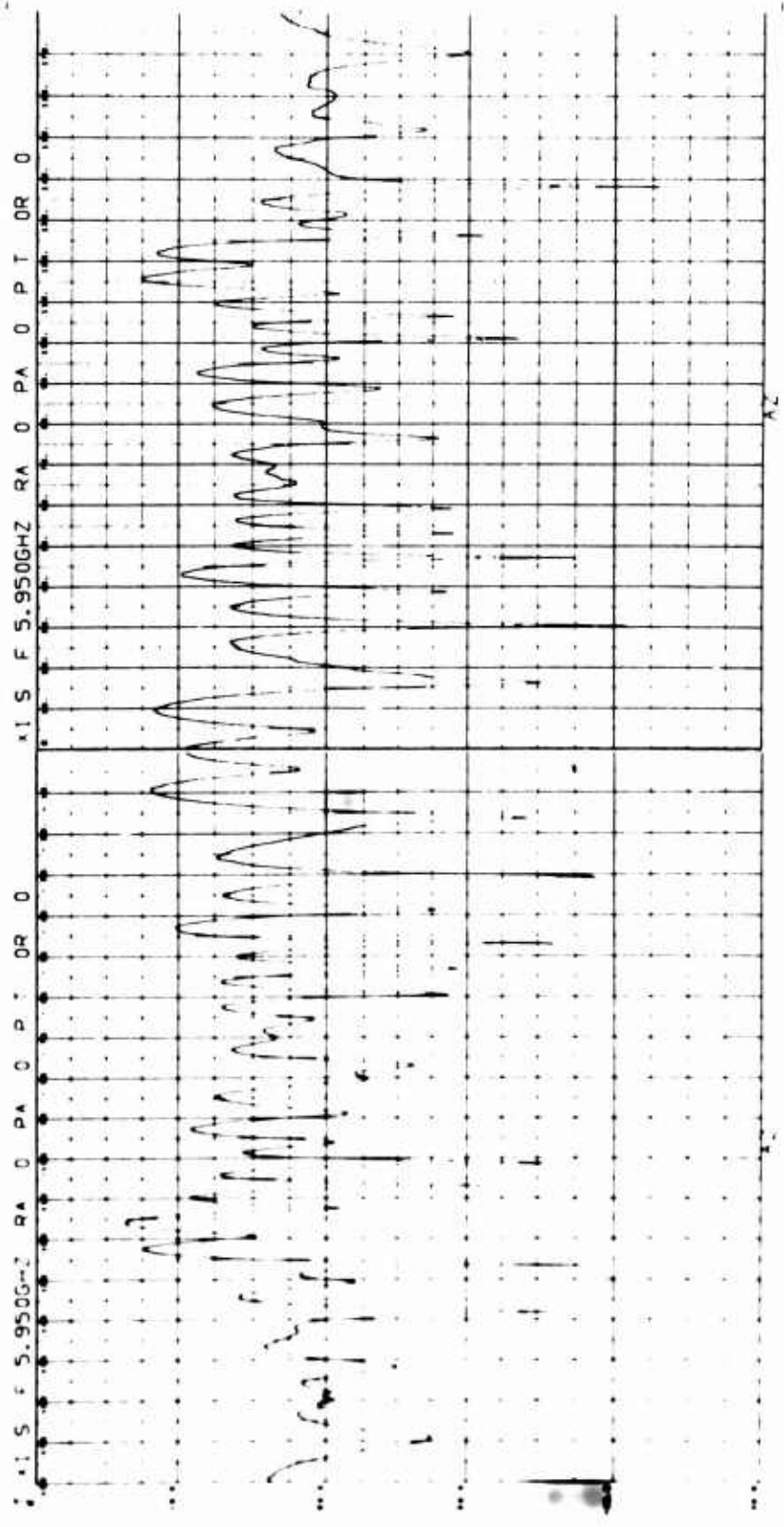
Fig. 3-4 SCIENTIFIC SATELLITE MODELS

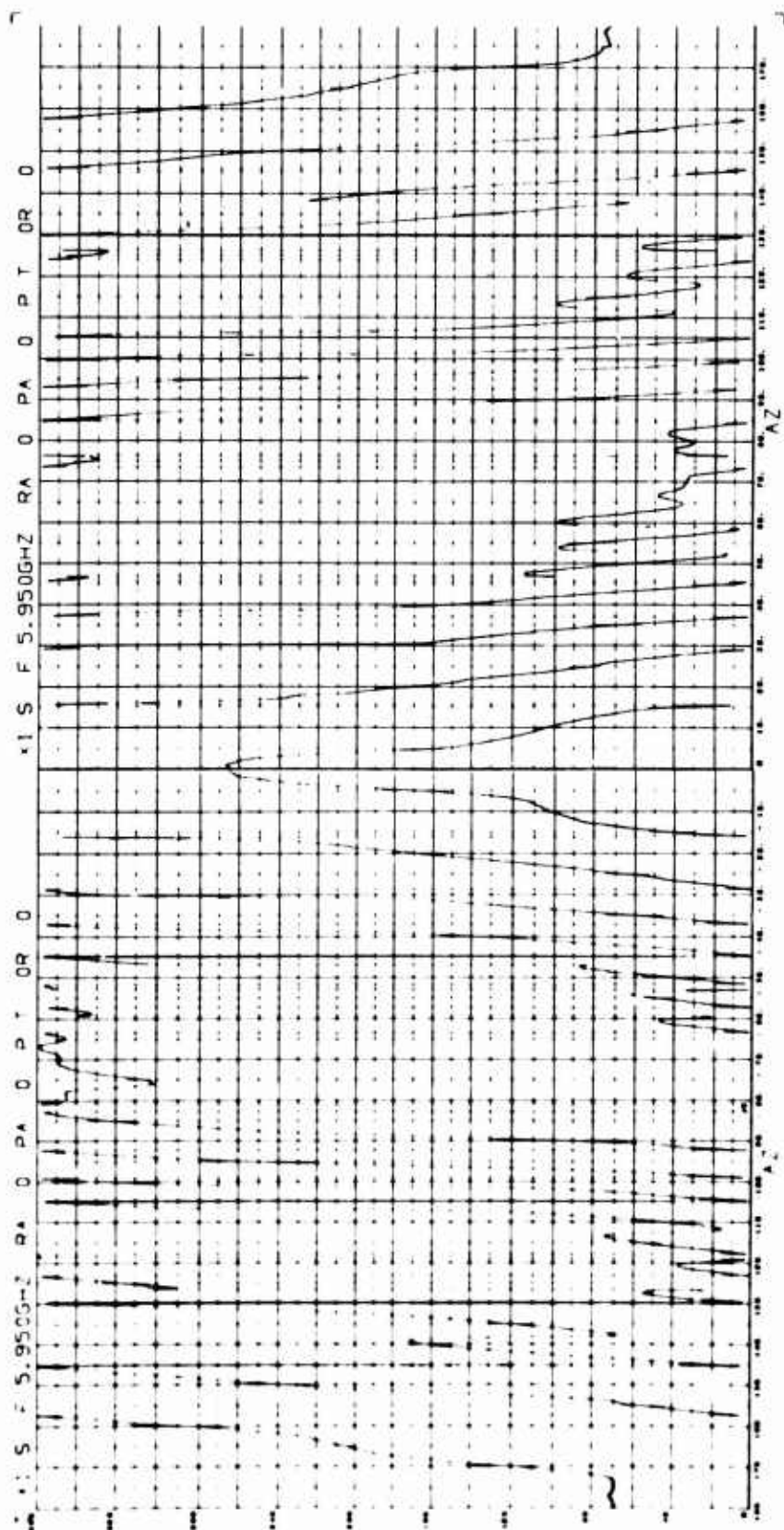


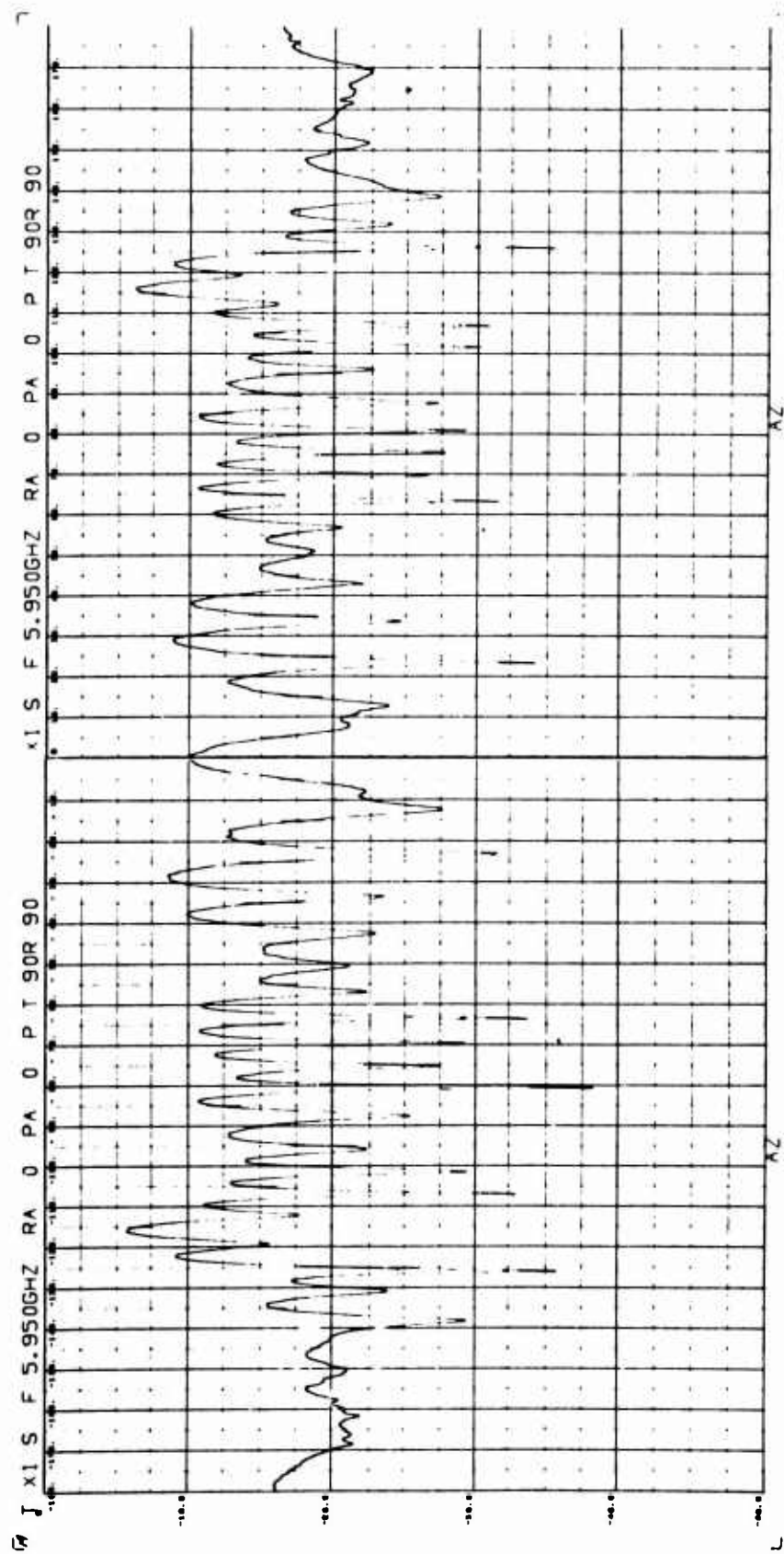


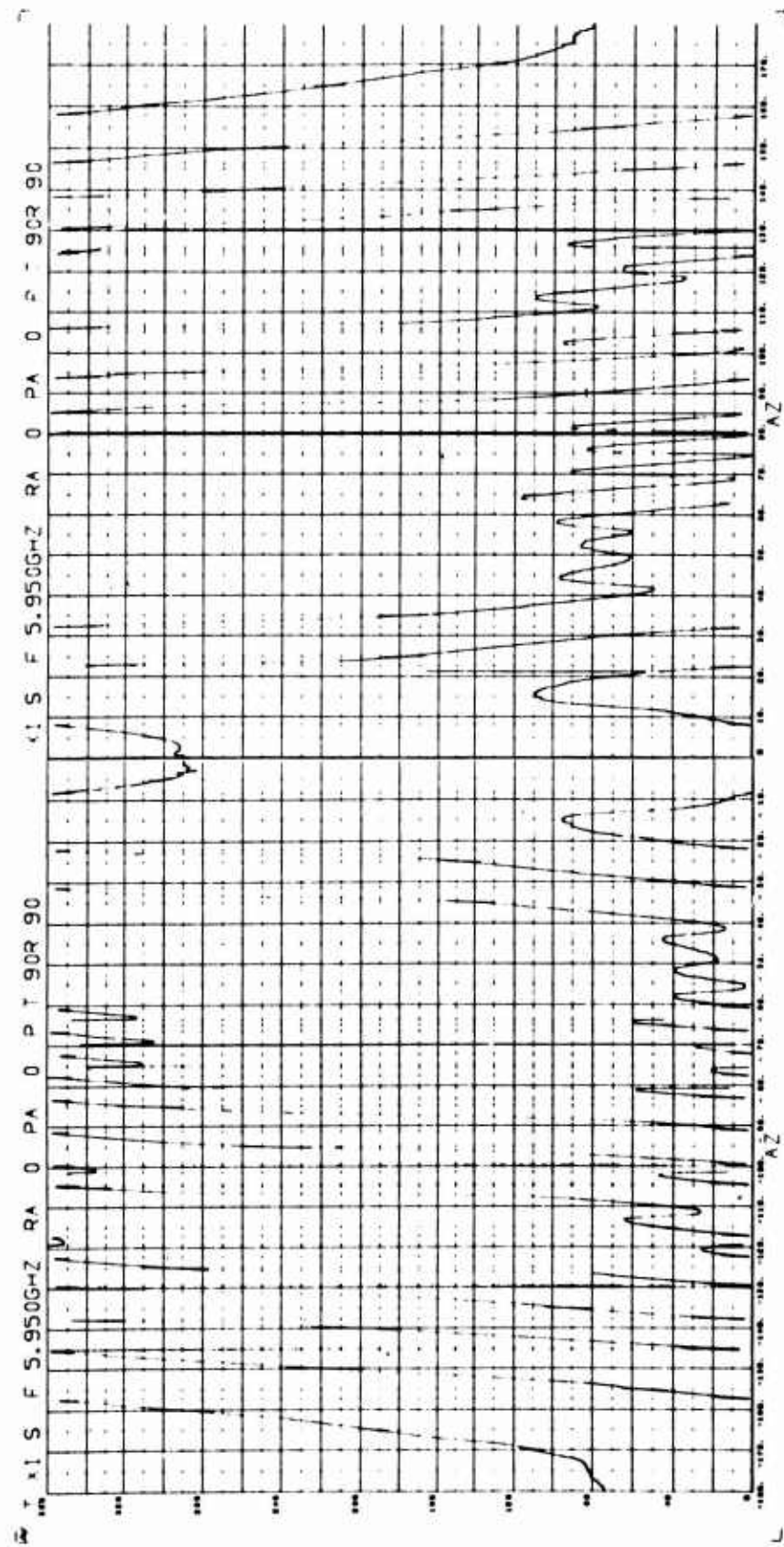


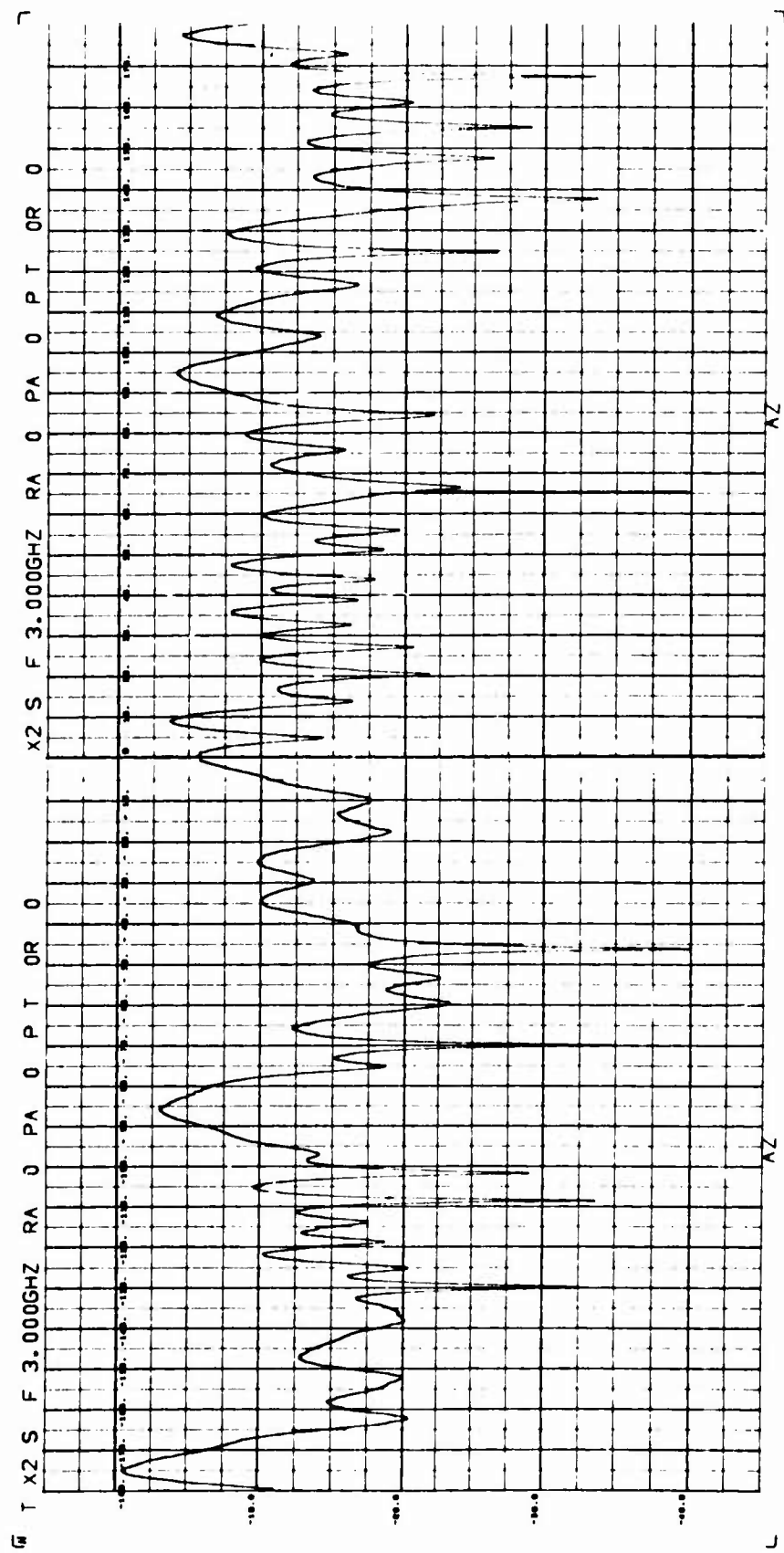


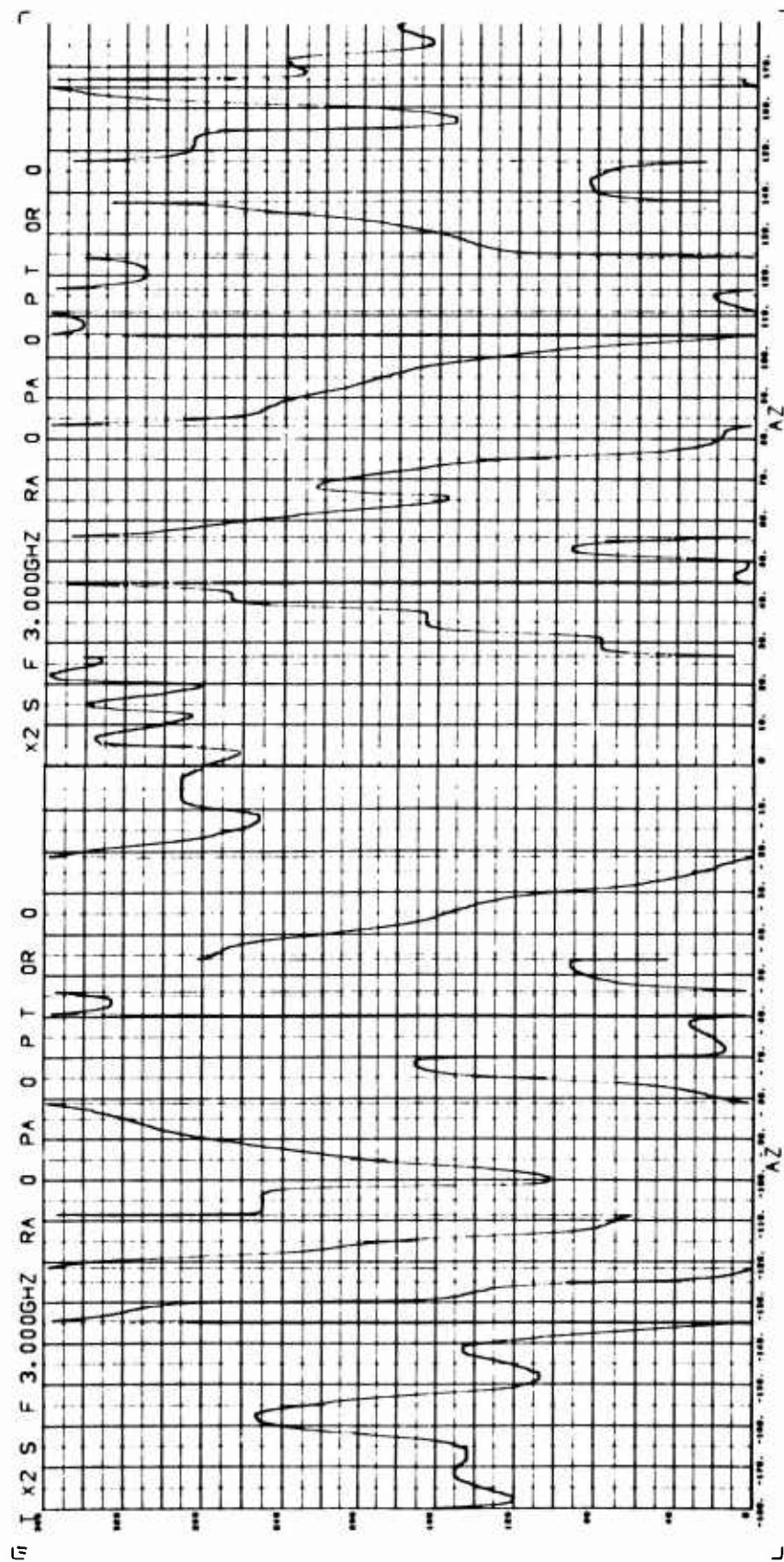


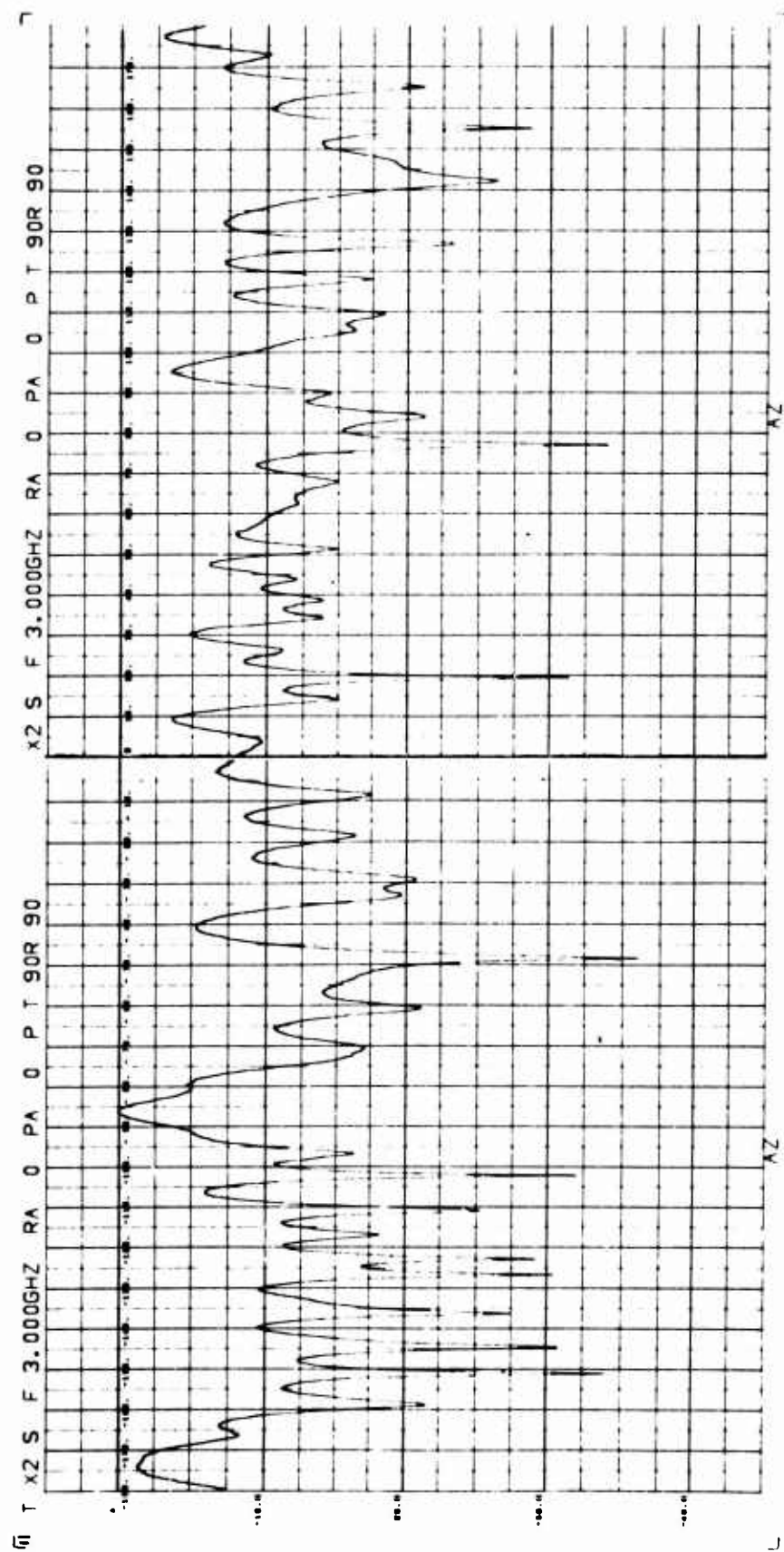


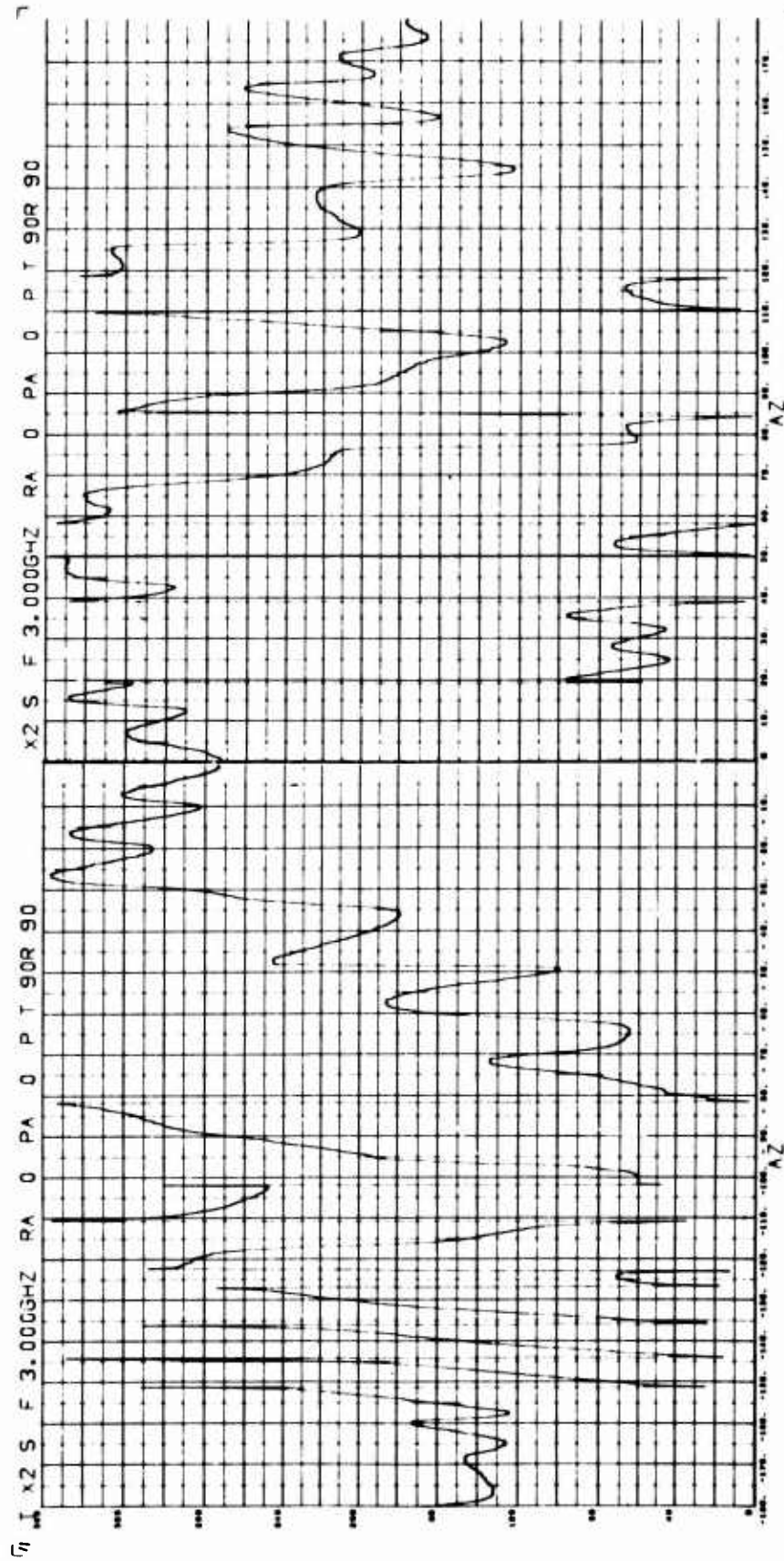


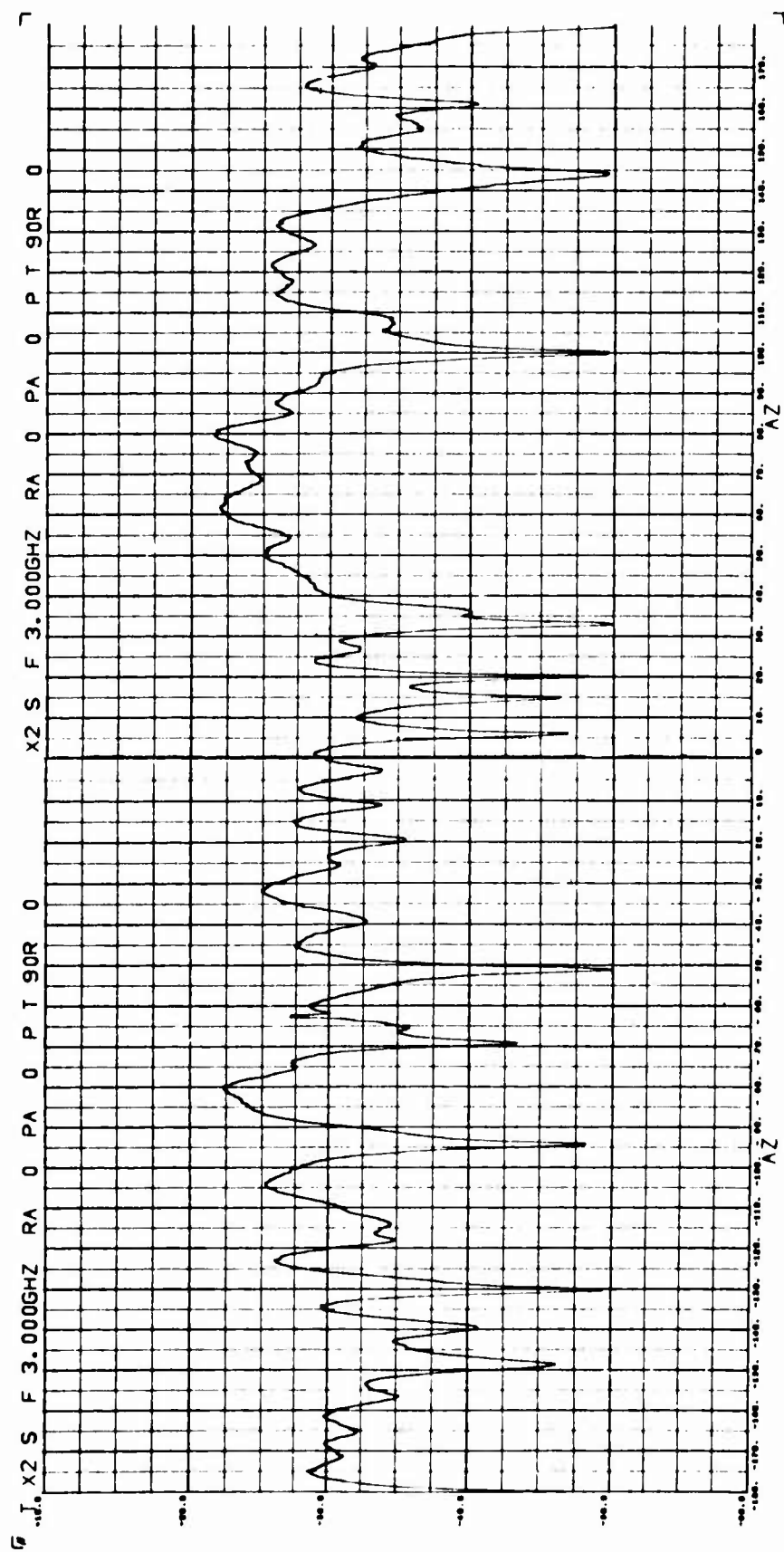


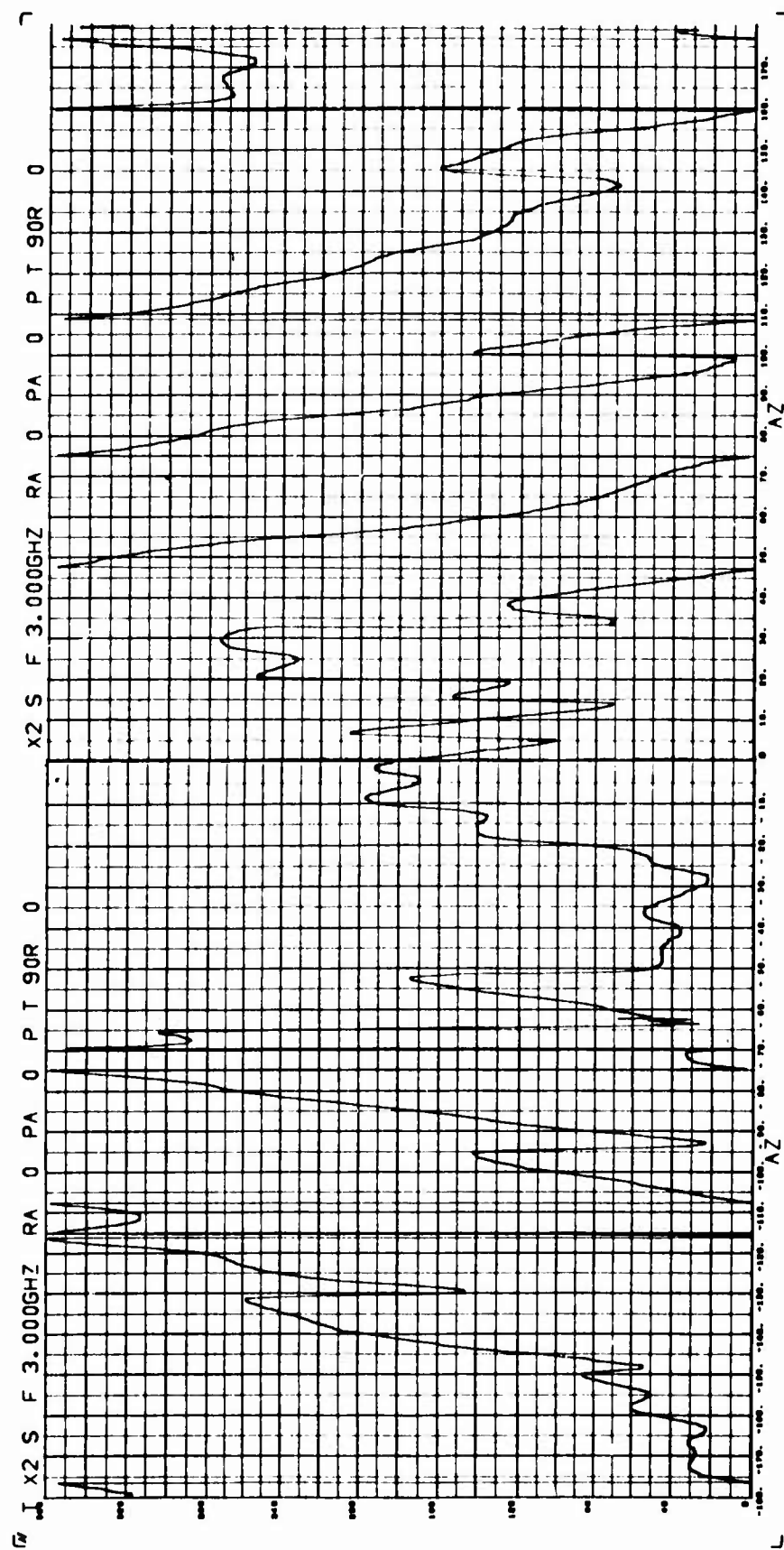


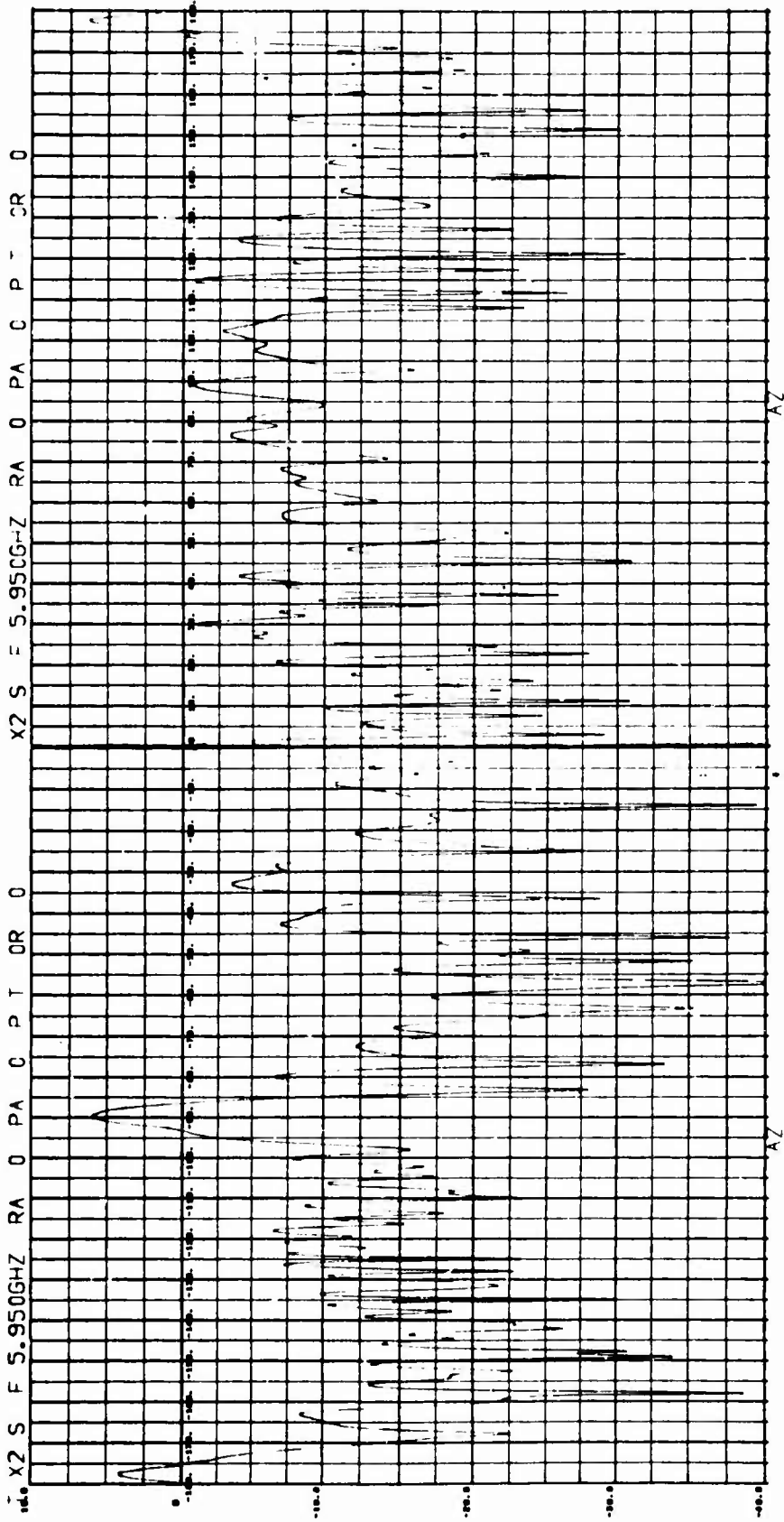


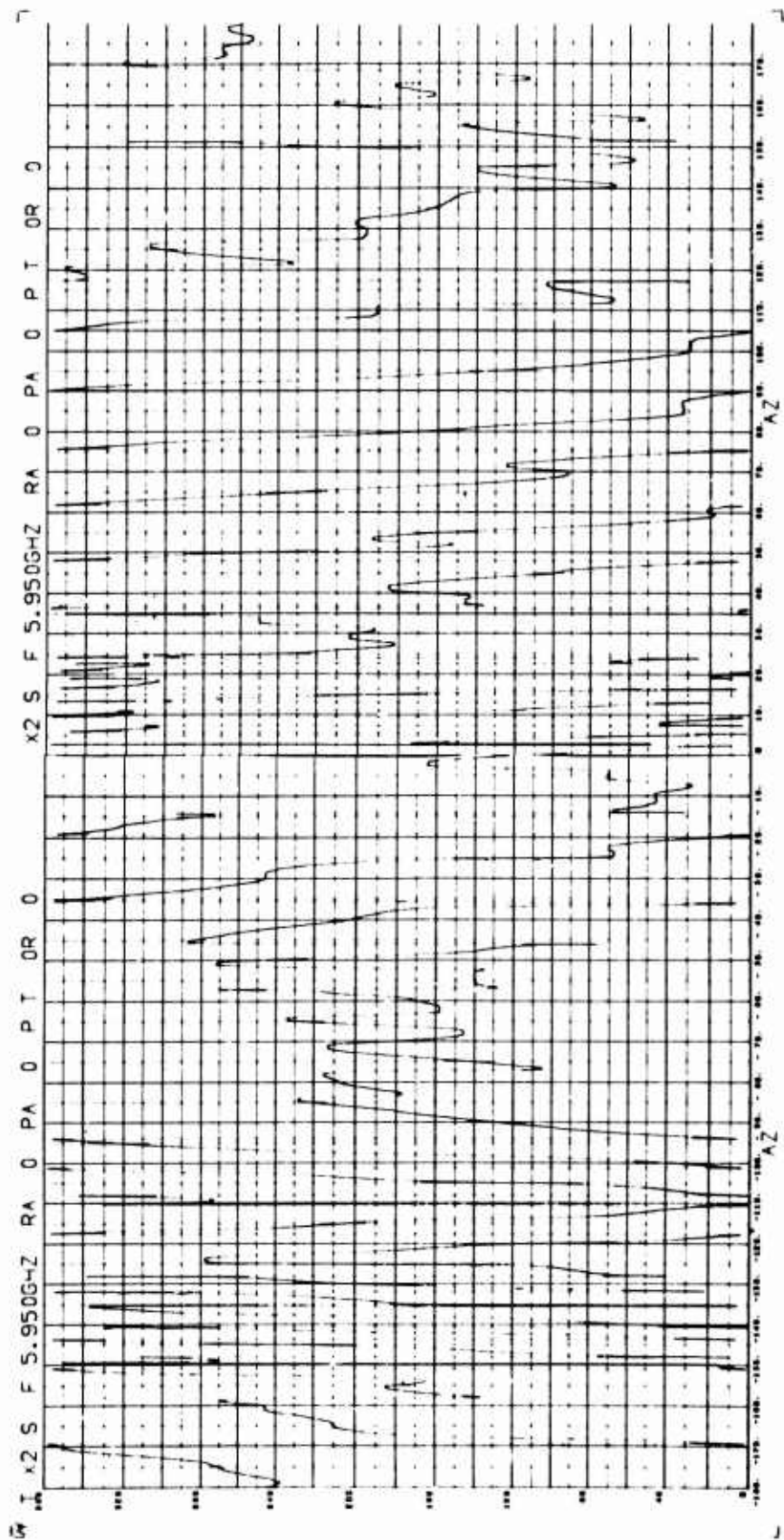


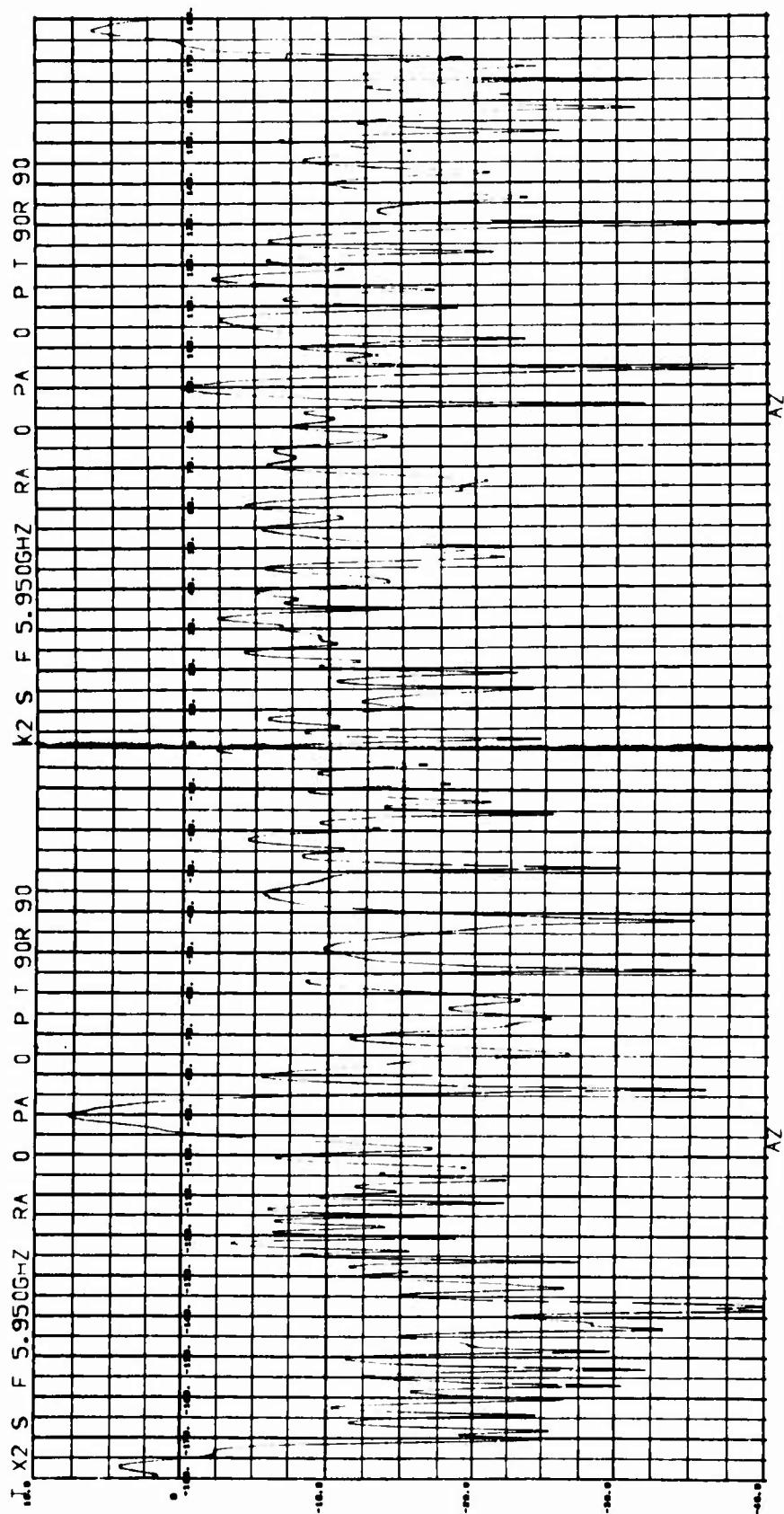


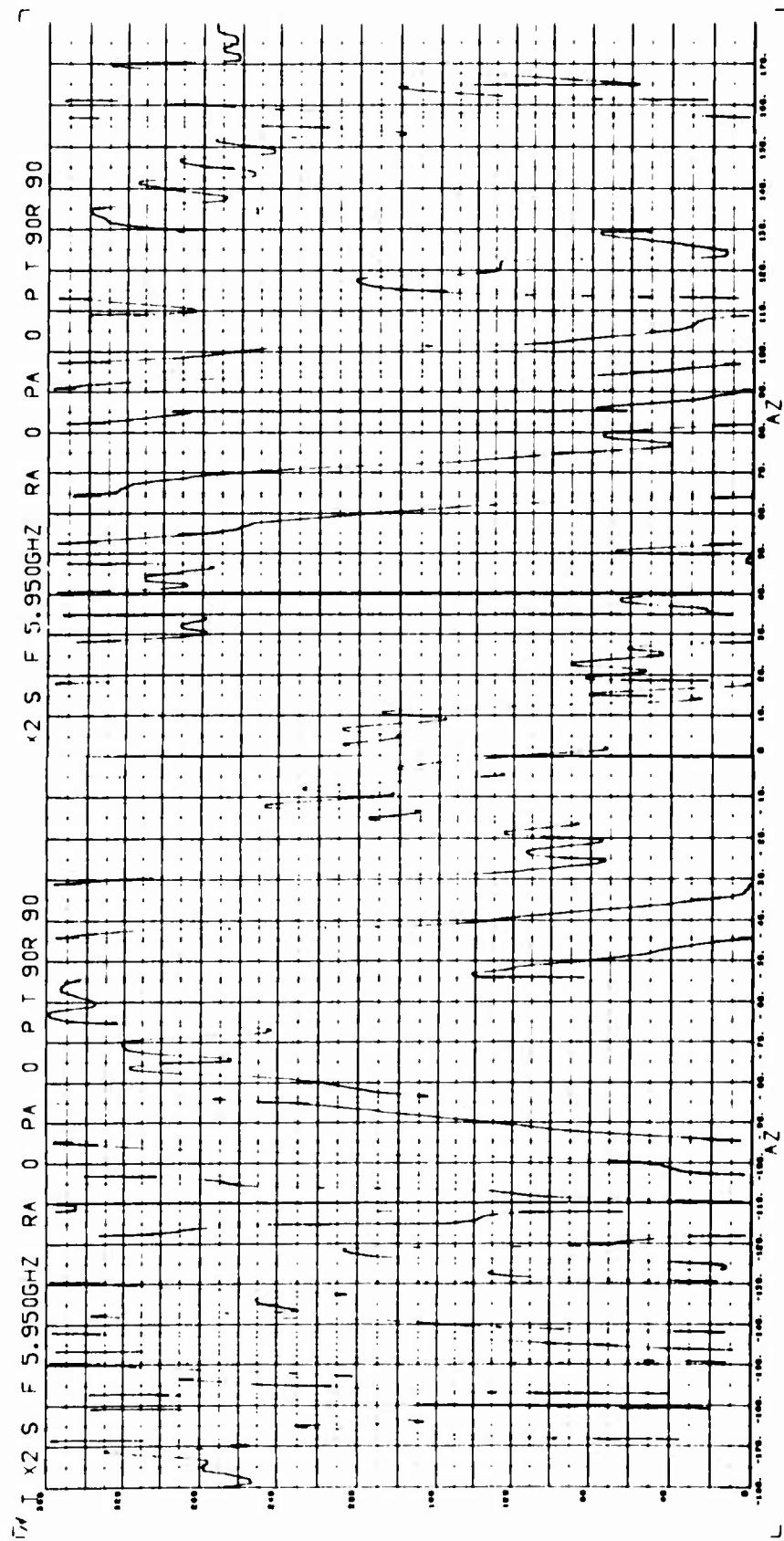


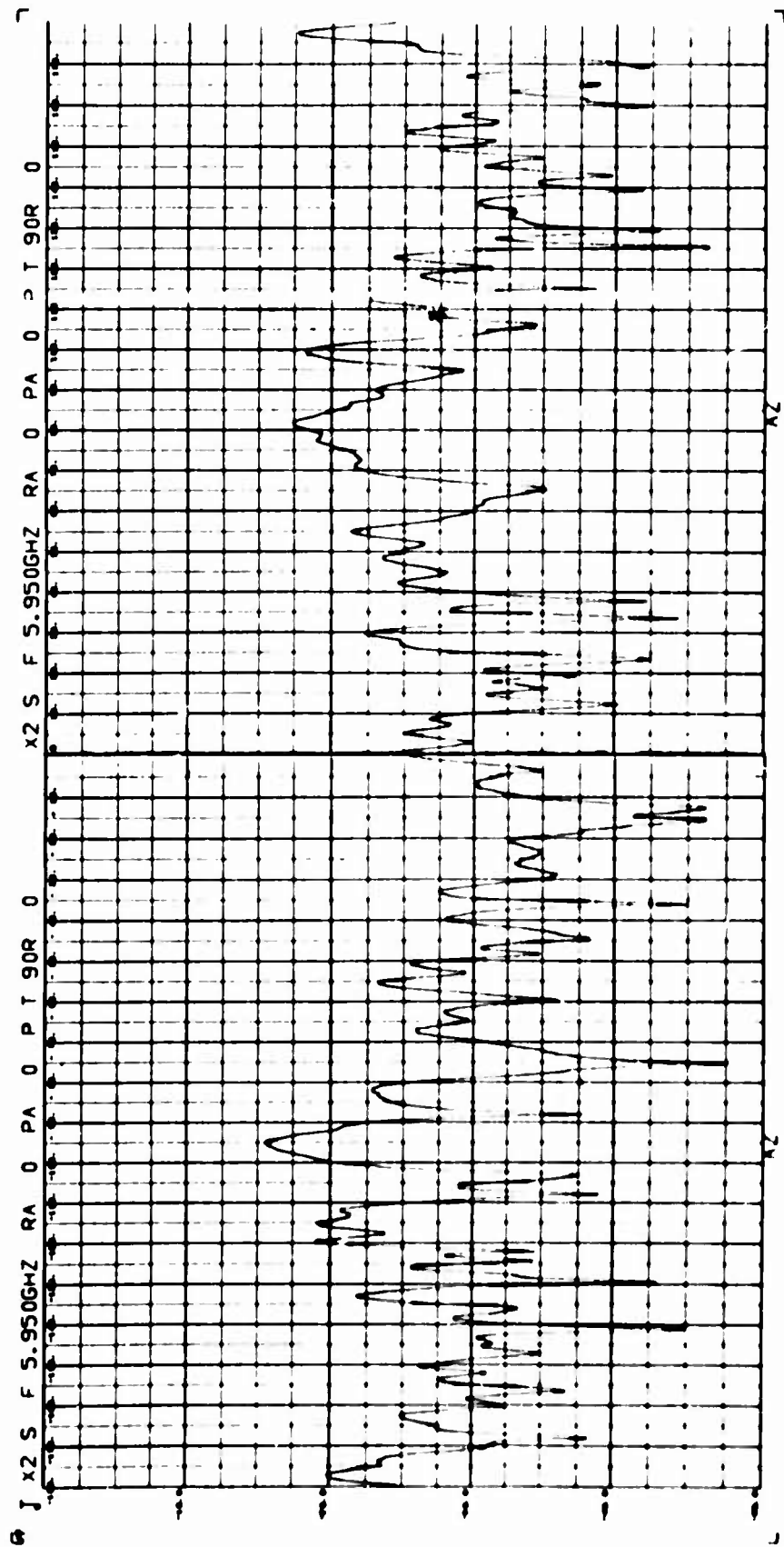


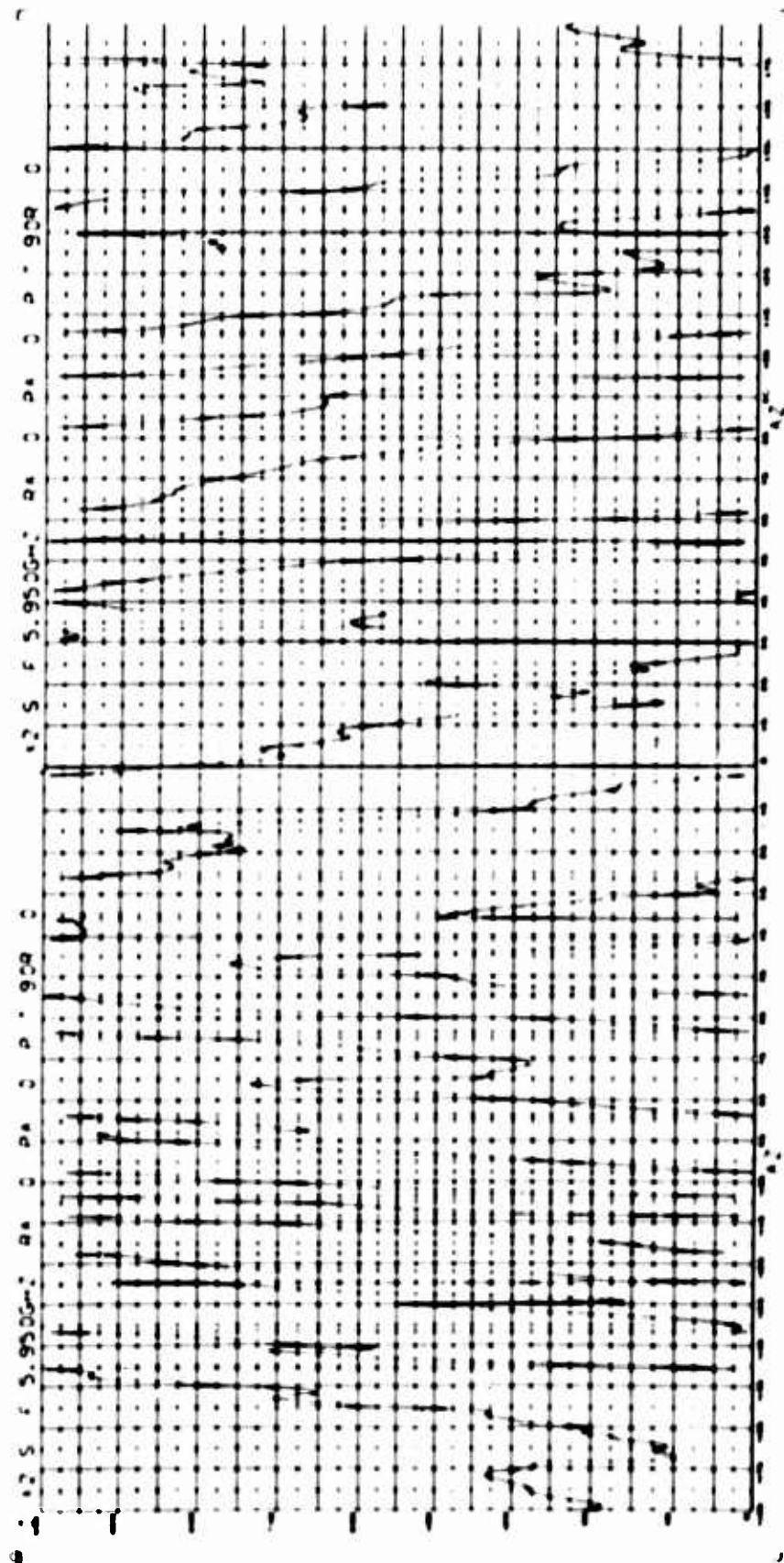












SECTION 4

SUMMARY

The feasibility of making absolute phase measurements at C-band using a variety of target vehicles has been well demonstrated by this program. The calibration techniques necessary in obtaining such measurements have been demonstrated to be within the state-of-the-art when utilized in conjunction with a high quality phase coherent radar.

The model measurement data presented herein provide a comprehensive set of experimental data for use in the analysis of various radar scattering phenomena. Investigations of interest include those concerned with target coupling, the monostatic-bistatic relationships, the behavior of the target phase center as a function of rotation, and the validation of analytical models for computing scattering parameters.

These data were obtained using vehicle models whose body motion during measurement consisted of pure spin at a constant spin rate. Although this represents a very limited range of the body motion parameters which are possible for an orbital vehicle, these data may still provide information useful to Space Object Identification (SOI). For example,

the use of data on generic surfaces in a direct comparison basis with data from unknown vehicles may result in significant identification information when applicable pattern recognition techniques are applied. Visual correlation of the vehicle geometry with the respective measured patterns should also provide a great deal of useful information for use by signature analysts.

The application of these data is further enhanced by the availability of the target scattering matrix. Use of the scattering matrix in conjunction with a single degree of rotation (spin) allows one to simulate a large spectrum of the body motion characteristics of actual vehicles. Introduction of a nonlinear spin-time relation into such a simulation would provide a realistic set of signatures for vehicles exhibiting orbital motion.

REFERENCES

1. "Investigation of Scattering Principles, Volume I," General Dynamics Report FZE-791, 15 August 1968.
2. "Investigation of Scattering Principles, Volume III, Analytical Investigation," General Dynamics Report FZE-793, 20 July 1968.
3. "Investigation of Scattering Principles, Volume IV, Inverse Scattering Analysis," General Dynamics Report FZE-794, 15 August 1968 (SECRET REPORT).
4. An Analysis of the Scattering Matrix Measurements Capabilities of a Ground Plane Radar Cross-Section Range, Technical Documentary Report No. RADC-TDR-64-317, Rome Air Development Center, Rome, New York (June, 1964).
AD NO. 605519,

UNCLASSIFIED

Security Classification

DOCUMENT CONTROL DATA - R & D		
Security Classification of title, body of abstract and indexing annotation must be entered when the overall report is classified		
1. ORIGINATING ACTIVITY (Corporate author)		20. REPORT SECURITY CLASSIFICATION
General Dynamics, Fort Worth Division P.O. Box 748 Fort Worth, Texas 76101		Unclassified
		21. GROUP
		N/A
2. REPORT TITLE		
Investigation of Scattering Principles; Volume II, Scattering Matrix Measurements		
3. DESCRIPTIVE NOTES (Type of report and inclusive dates)		
Final		
4. AUTHOR (First name, middle initial, last name)		
Dr. George W. Gruver		
5. REPORT DATE	16. TOTAL NO. OF PAGES	18. NO. OF REFS
May 1969	357	4
6. CONTRACT OR GRANT NO.	19. ORIGINATOR'S REPORT NUMBER(S)	
F30602-67-C-0074	FZE-792	
7. PROJECT NO.	20. OTHER REPORT NO(S) (Any other numbers that may be assigned this report)	
6512	RADC-TR-68-340, Volume II	
8. Task No:		
651207		
9. DISTRIBUTION STATEMENT		
This document is subject to special export controls and each transmittal to foreign governments, foreign nationals or representatives thereto may be made only with prior approval of RADC (EMASS), Griffiss AFB, NY 13440.		
11. SUPPLEMENTARY NOTES		12. SPONSORING MILITARY ACTIVITY
Project Engineer: John C. Cleary AC 315 330-2118		Rome Air Development Center (EMASS) Griffiss Air Force Base, New York 13440
13. ABSTRACT		
<p>The objective of this effort was to establish and apply the mechanics of radar scattering from complex objects in terms of actual measurement data and the resulting empirically derived mathematical relationships. Volume I contains a summary of each task as well as detailed documentation on the experimental and superposition investigations. Volume II contains the radar range measurement data used in the experimental portion of the effort. Volume III contains the results of the analytical investigation, which uses geometric diffraction theory to predict radar cross section and scattering phase. Volume IV contains the potential military applications and results of the inverse scattering investigation.</p>		

DD FORM 1473

UNCLASSIFIED

Security Classification

UNCLASSIFIED
Security Classification

14	KEY WORDS	LINK A		LINK B		LINK C	
		ROLE	WT	ROLE	WT	ROLE	WT
	Scattering Matrix Measurements Radar Range Radar Target Long Pulse Short Pulse Statistical Analysis Statistical Signature Analysis Equivalence Class						

UNCLASSIFIED
Security Classification